

# frontiers RESEARCH TOPICS



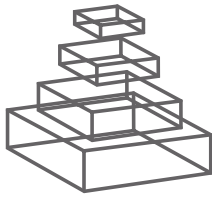
## THE METABOLIC PATHWAYS AND ENVIRONMENTAL CONTROLS OF HYDROCARBON BIODEGRADATION IN MARINE ECOSYSTEMS

Topic Editors

Joel E. Kostka, Andreas P. Teske,  
Samantha B. Joye and Ian Head



**frontiers in**  
**MICROBIOLOGY**



## FRONTIERS COPYRIGHT STATEMENT

© Copyright 2007-2014  
Frontiers Media SA.  
All rights reserved.

All content included on this site, such as text, graphics, logos, button icons, images, video/audio clips, downloads, data compilations and software, is the property of or is licensed to Frontiers Media SA ("Frontiers") or its licensees and/or subcontractors. The copyright in the text of individual articles is the property of their respective authors, subject to a license granted to Frontiers.

The compilation of articles constituting this e-book, wherever published, as well as the compilation of all other content on this site, is the exclusive property of Frontiers. For the conditions for downloading and copying of e-books from Frontiers' website, please see the Terms for Website Use. If purchasing Frontiers e-books from other websites or sources, the conditions of the website concerned apply.

Images and graphics not forming part of user-contributed materials may not be downloaded or copied without permission.

Individual articles may be downloaded and reproduced in accordance with the principles of the CC-BY licence subject to any copyright or other notices. They may not be re-sold as an e-book.

As author or other contributor you grant a CC-BY licence to others to reproduce your articles, including any graphics and third-party materials supplied by you, in accordance with the Conditions for Website Use and subject to any copyright notices which you include in connection with your articles and materials.

All copyright, and all rights therein, are protected by national and international copyright laws.

The above represents a summary only. For the full conditions see the Conditions for Authors and the Conditions for Website Use.

**ISSN** 1664-8714

**ISBN** 978-2-88919-346-2

**DOI** 10.3389/978-2-88919-346-2

## ABOUT FRONTIERS

Frontiers is more than just an open-access publisher of scholarly articles: it is a pioneering approach to the world of academia, radically improving the way scholarly research is managed. The grand vision of Frontiers is a world where all people have an equal opportunity to seek, share and generate knowledge. Frontiers provides immediate and permanent online open access to all its publications, but this alone is not enough to realize our grand goals.

## FRONTIERS JOURNAL SERIES

The Frontiers Journal Series is a multi-tier and interdisciplinary set of open-access, online journals, promising a paradigm shift from the current review, selection and dissemination processes in academic publishing.

All Frontiers journals are driven by researchers for researchers; therefore, they constitute a service to the scholarly community. At the same time, the Frontiers Journal Series operates on a revolutionary invention, the tiered publishing system, initially addressing specific communities of scholars, and gradually climbing up to broader public understanding, thus serving the interests of the lay society, too.

## DEDICATION TO QUALITY

Each Frontiers article is a landmark of the highest quality, thanks to genuinely collaborative interactions between authors and review editors, who include some of the world's best academicians. Research must be certified by peers before entering a stream of knowledge that may eventually reach the public - and shape society; therefore, Frontiers only applies the most rigorous and unbiased reviews.

Frontiers revolutionizes research publishing by freely delivering the most outstanding research, evaluated with no bias from both the academic and social point of view.

By applying the most advanced information technologies, Frontiers is catapulting scholarly publishing into a new generation.

## WHAT ARE FRONTIERS RESEARCH TOPICS?

Frontiers Research Topics are very popular trademarks of the Frontiers Journals Series: they are collections of at least ten articles, all centered on a particular subject. With their unique mix of varied contributions from Original Research to Review Articles, Frontiers Research Topics unify the most influential researchers, the latest key findings and historical advances in a hot research area!

Find out more on how to host your own Frontiers Research Topic or contribute to one as an author by contacting the Frontiers Editorial Office: [researchtopics@frontiersin.org](mailto:researchtopics@frontiersin.org)

# THE METABOLIC PATHWAYS AND ENVIRONMENTAL CONTROLS OF HYDROCARBON BIODEGRADATION IN MARINE ECOSYSTEMS

Topic Editors:

**Joel E. Kostka**, Georgia Institute of Technology, USA

**Andreas P. Teske**, University of North Carolina, Chapel Hill, USA

**Samantha B. Joye**, University of Georgia, USA

**Ian Head**, Newcastle University, UK



Heavily oiled beach sands from cores collected at Elmers Beach, Louisiana, in June of 2010. Elmers Beach was among the shoreline sites which were most heavily impacted by the Deepwater Horizon oil spill in the Gulf of Mexico. See Lamendella et al. (2014, Vol. 5, article 130) for further information.

Biodegradation mediated by indigenous microbial communities is the ultimate fate of the majority of oil hydrocarbon that enters the marine environment. The aim of this Research Topic is to highlight recent advances in our knowledge of the pathways and controls of microbially-catalyzed hydrocarbon degradation in marine ecosystems, with emphasis on the response of microbial communities to the Deepwater Horizon oil spill in the Gulf of Mexico. In this Research Topic, we encouraged original research and reviews on the ecology of hydrocarbon-degrading bacteria, the rates and mechanisms of biodegradation, and the bioremediation of discharged oil under situ as well as near in situ conditions.

# Table of Contents

- 05    *The Metabolic Pathways and Environmental Controls of Hydrocarbon Biodegradation in Marine Ecosystems***  
Joel E. Kostka, Andreas Teske, Samantha B. Joye and Ian M. Head
- 08    *Alkane Hydroxylase Gene (alkB) Phylotype Composition and Diversity in Northern Gulf of Mexico Bacterioplankton***  
Conor Blake Smith, Bradley B. Tolar, James T. Hollibaugh and Gary M. King
- 16    *Assessment of the Deepwater Horizon Oil Spill Impact on Gulf Coast Microbial Communities***  
Regina Lamendella, Steven Strutt, Sharon E. Borglin, Romy Chakraborty, Neslihan Tas, Olivia U. Mason, Jenni Hultman, Emmanuel Prestat, Terry C. Hazen and Janet Jansson
- 29    *Single-Cell Genomics Reveals Features of a Colwellia Species that was Dominant During the Deepwater Horizon Oil Spill***  
Olivia Mason, James Han, Tanja Woyke and Janet K. Jansson
- 37    *The Microbial Nitrogen Cycling Potential is Impacted by Polyaromatic Hydrocarbon Pollution of Marine Sediments***  
Nicole M. Scott, Matthias Hess, Nick J. Bouskill, Olivia U. Mason, Janet K. Jansson and Jack A. Gilbert
- 45    *Biodegradation of MC252 Oil in Oil:sand Aggregates in a Coastal Headland Beach Environment***  
Vijaikrishnah Elango, Marilany Urbano, Kendall R. Lemelle and John H. Pardue
- 56    *The Polycyclic Aromatic Hydrocarbon Degradation Potential of Gulf of Mexico Native Coastal Microbial Communities After the Deepwater Horizon Oil Spill***  
Anthony D. Kappell, Yin Wei, Ryan J. Newton, Joy D. Van Nostrand, Jizhong Zhou, Sandra L. McLellan and Krassimira R. Hristova
- 69    *Natural Oil Slicks Fuel Surface Water Microbial Activities in the Northern Gulf of Mexico***  
Kai Zier vogel, Nigel D'souza, Julia Sweet, Beizahn Yan and Uta Passow
- 79    *A Survey of Deepwater Horizon (DWH) Oil-Degrading Bacteria From the Eastern Oyster Biome and its Surrounding Environment***  
Jesse c.Thomas, IV, Denis Wafula, Ashvini Chauhan, Stefan J. Green, Richard Gragg and Charles Jagoe
- 91    *Marine Coastal Sediments Microbial Hydrocarbon Degradation Processes: Contribution of Experimental Ecology in the Omics'era***  
Cristiana Cravo-Laureau and Robert Duran

- 99 Toward Quantitative Understanding on Microbial Community Structure and Functioning: A Modeling-Centered Approach Using Degradation of Marine Oil Spills as Example**  
Wilfred F. M. Roling and Peter M. van Bodegom
- 111 Geomicrobiological Linkages Between Short-Chain Alkane Consumption and Sulfate Reduction Rates in Seep Sediments**  
Arpita Bose, Daniel R. Rogers, Melissa M Adams, Samantha B. Joye and Peter R. Girguis
- 124 Kinetic Parameters for Nutrient Enhanced Crude Oil Biodegradation in Intertidal Marine Sediments**  
Arvind K. Singh, Angela Sherry, Neil D. Gray, D. Martin Jones, Bernard F. J. Bowler and Ian M. Head
- 137 Volatile Hydrocarbons Inhibit Methanogenic Crude Oil Degradation**  
Angela Sherry, Russell J. Grant, Carolyn M. Aitken, Martin Jones, Ian M. Head and Neil D. Gray
- 146 Effective Bioremediation Strategy for Rapid in Situ Cleanup of Anoxic Marine Sediments in Mesocosm Oil Spill Simulation**  
Maria Genovese, Francesca Crisafi, Renata Denaro, Simone Cappello, Daniela Russo, Rosario Calogero, Santina Santisi, Maurizio Catalfamo, Alfonso Modica, Francesco Smedile, Lucrezia Genovese, Peter N. Golyshin, Laura Giuliano and Michail M. Yakimov
- 160 Anaerobic Hydrocarbon and Fatty Acid Metabolism by Syntrophic Bacteria and their Impact on Carbon Steel Corrosion**  
Christopher N. Lyles, Huynh M. Le, William Howard Beasley, Michael J. McInerney and Joseph M. Suflita
- 172 DNA-Based Stable Isotope Probing Coupled with Cultivation Methods Implicates Methylphaga in Hydrocarbon Degradation**  
Sara Mishamandani, Tony Gutierrez and Michael D. Aitken
- 181 Evaluation of the Biodegradation of Alaska North Slope Oil in Microcosms Using the Biodegradation Model BIOB**  
Jagadish Torlapati and Michel Boufadel



# The metabolic pathways and environmental controls of hydrocarbon biodegradation in marine ecosystems

**Joel E. Kostka<sup>1\*</sup>, Andreas P. Teske<sup>2</sup>, Samantha B. Joye<sup>3</sup> and Ian M. Head<sup>4</sup>**

<sup>1</sup> School of Biology and Earth and Atmospheric Sciences, Georgia Institute of Technology, Atlanta, GA, USA

<sup>2</sup> Department of Marine Sciences, University of North Carolina, Chapel Hill, NC, USA

<sup>3</sup> Department of Marine Sciences, University of Georgia, Athens, GA, USA

<sup>4</sup> School of Civil Engineering and Geosciences, Newcastle University, Newcastle upon Tyne, UK

\*Correspondence: joel.kostka@biology.gatech.edu

**Edited by:**

Jonathan P. Zehr, University of California, Santa Cruz, USA

**Reviewed by:**

Levente Bodrossy, CSIRO Marine and Atmospheric Research, Australia

Stefan Bertilsson, Uppsala University, Sweden

**Keywords:** Deepwater Horizon, biodegradation, Gulf of Mexico, hydrocarbon, oil spill, bacteria, microbial communities, Metagenomics

Hydrocarbon-degrading microorganisms are ubiquitous in the world's oceans (Head et al., 2006; Yakimov et al., 2007), and biodegradation mediated by indigenous microbial communities is the ultimate fate of the majority of oil hydrocarbon that enters the marine environment (Leahy and Colwell, 1990; Prince, 2010; Atlas and Hazen, 2011). In response to the natural complexity of hydrocarbon compounds found in petroleum deposits, diverse marine microorganisms have evolved with an equal complexity of metabolic pathways to take advantage of hydrocarbons as a rich carbon and energy source. To minimize the environmental impact of oil spills and to optimize the environmental benefits of biodegradation, it is essential to uncover the metabolic potential of hydrocarbon-degrading bacteria and to address the factors that limit microbially-catalyzed biodegradation *in situ*.

Microbial community structure and diversity likely defines the metabolic potential of oil-degrading communities (Head et al., 2006). Thus, it is critical to understand the relationships between microbial community structure and the metabolic activity of hydrocarbon-degrading microbial groups. Much progress has been made to determine the response of specific microbial taxa to oil discharge in marine environments impacted by oil spills or natural seeps. However, the majority of studies of hydrocarbon-degrading microorganisms have been conducted in laboratory cultures, and our ability to understand and predict the dynamics of *in situ* microbial communities responding to environmental stimuli such as the presence of oil hydrocarbons remains in its infancy (Prosser et al., 2007).

*In situ* characterization of hydrocarbon-degrading microbial communities was hampered until recently by practical limitations of molecular biology techniques in phylogenetic resolution and depth of coverage (Gilbert and Dupont, 2011; Jansson et al., 2012). Advances in next generation sequencing technologies and the use of stable isotope tracers have greatly improved our ability to interrogate the phylogenetic and functional diversity of hydrocarbon-degrading microorganisms in the field. The development and application of omics approaches

have led to the characterization of novel biochemical pathways of biogeochemical significance. This Research Topic focuses on investigations that utilize the latest molecular and biogeochemical techniques, (including high throughput sequencing, isotope tracers, and omic approaches) to render a predictive understanding of the biogeochemical processes and metabolic pathways that in turn regulate the impacts and biodegradation of petroleum hydrocarbons released into the marine environment.

The Deepwater Horizon (DWH) blowout that occurred in the Gulf of Mexico in 2010 is distinguished as the largest accidental marine oil spill in history (Atlas and Hazen, 2011), and the DWH spill represents the first major event in which next-generation sequencing approaches have been applied to illustrate with high resolution the dramatic changes in the abundance, structure, and metabolic potential of microbial communities in oil-impacted marine ecosystems (Joye et al., 2014; King et al., 2014). In the first 8 articles of this Research Topic, the latest microbiological and biogeochemical approaches are employed to interrogate the diversity, metabolic potential, and environmental forcings of hydrocarbon-degrading microbial communities in response to oil discharged during the DWH blowout. Smith et al. (2013) provide insight into the potential for alkane degradation by prespill or indigenous bacterioplankton in the northern Gulf of Mexico using high-throughput analysis of genes encoding alkane hydroxylase, alkB, one of the best known molecular marker genes for hydrocarbon degradation. In Mason et al. (2014), the metabolic potential of *Colwellia*, a bacterium detected in high abundance in Gulf waters impacted by the DWH spill, is determined using single-cell genomics. A series of papers then describes the impacts of Macondo oil (released from the DWH discharge) on the community structure and metabolic function of benthic microbial communities using omics techniques (Kappell et al., 2014; Lamendella et al., 2014; Scott et al., 2014; Thomas et al., 2014). Biodegradation and the impacts of Macondo oil are then assessed using geochemical methods in studies of the nearshore water

column (Ziervogel et al., 2014) and sediments (Elango et al., 2014).

A major theme of this special issue is to bridge laboratory-based studies of biodegradation to those conducted in the field. Cravo-Laureau and Duran (2014) review how mesocosm experiments have been used to dissect hydrocarbon degradation mechanisms by somewhat reducing environmental complexity and serving as a transition between the lab and the field. Röling and van Bodegom (2014) further posit how observations of oil degradation potential at the cellular level could be scaled to the community as well as ecosystem level using systems biology and omics-based approaches.

Although biodegradation was shown to be successful in naturally remediating oil contamination associated with several spills that impacted marine shorelines (Head et al., 2006; Prince, 2010; Atlas and Hazen, 2011), much remains to be learned about the environmental controls of hydrocarbon degradation in marine sediments. Five papers in this issue evaluate the environmental conditions (oxygen availability, nutrient levels, oil chemistry) controlling biodegradation in sediments with experimental and modeling approaches. Under aerobic conditions, Singh et al. (2014) study the kinetic parameters of crude oil-degrading microbial communities in response to nutrient and oil loading in beach sand microcosms. High nutrient levels are shown to select for members of the hydrocarbonoclastic genus, *Alcanivorax*, while selecting against aromatic-degrading *Cycloclasticus* sp. Bose et al., 2013) quantify oxidation rates of short chain alkanes under sulfate-reducing conditions and explore the use of stable C isotopes to trace biodegradation activity in microcosms of cold seep sediments. Sherry et al. (2014) show that the composition of the crude oil itself may play a critical role as volatile hydrocarbons inhibit biodegradation under methanogenic conditions. Capping and *in situ* aeration are shown to effectively remediate and detoxify buried oil in anaerobic marine sediments by Genovese et al. (2014). Torlapati and Boufadel (2014) present a numerical model that employs genetic algorithms to predict biodegradation kinetics for oil entrapped in sediments.

Finally, two papers in this issue explore the mechanisms of hydrocarbon degradation using novel cultivation methods under aerobic and anaerobic conditions. Mishamandani et al. (2014) use stable isotope probing to reveal that the aerobic methylotroph, *Methylophaga*, is capable of growth on alkanes as the sole source of carbon and energy. Lyles et al. (2014) investigate the linkages between the metabolism of hydrocarbon-degrading syntrophs and steel corrosion in electrochemical cells designed to simulate oil production systems.

By closely coupling cutting-edge microbiological (omics) and biogeochemical (stable isotope tracers) methods, the dynamics and selection of microbial populations responding to the chemical evolution of oil hydrocarbons has just begun to be revealed in marine ecosystems. In general, observations made from studies carried out before the advent of next generation sequencing technologies have been supported by recent work. Moreover, the challenge remains to definitively link the structure and function of hydrocarbon-degrading microbial groups to improve predictive models of biodegradation.

## ACKNOWLEDGMENTS

Research and the preparation of this manuscript were made possible by grants from BP/The Gulf of Mexico Research Initiative (GOMRI) to the Deep-C Consortium (#SA 12-12, GoMRI-008) and the ECOGIG consortium as well as the EU Kill-Spill consortium. For GRIIDC dataset IDs we refer to the contributed papers in this Frontiers Research Topic.

## REFERENCES

- Atlas, R. M., and Hazen, T. C. (2011). Oil biodegradation and bioremediation: a tale of the two worst spills in U.S. *Environ. Sci. Technol.* 45, 6709–6715. doi: 10.1021/es2013227
- Bose, A., Rogers, D. R., Adams, M. M., Joye, S. B., and Girguis, P. R. (2013). Geomicrobiological linkages between short-chain alkane consumption and sulfate reduction rates in seep sediments. *Front. Microbiol.* 4:386. doi: 10.3389/fmicb.2013.00386
- Cravo-Laureau, C., and Duran, R. (2014). Marine coastal sediments microbial hydrocarbon degradation processes: contribution of experimental ecology in the omics' era. *Front. Microbiol.* 5:39. doi: 10.3389/fmicb.2014.00039
- Elango, V., Urbano, M., Lemelle, K. R., and Pardue, J. H. (2014). Biodegradation of MC252 oil in oil:sand aggregates in a coastal headland beach environment. *Front. Microbiol.* 5:161. doi: 10.3389/fmicb.2014.00161
- Genovese, M., Crisafi, F., Denaro, R., Cappello, S., Russo, D., Calogero, R., et al. (2014). Effective bioremediation strategy for rapid *in situ* cleanup of anoxic marine sediments in mesocosm oil spill simulation. *Front Microbiol.* 5:162. doi: 10.3389/fmicb.2014.00162
- Gilbert, J. A., and Dupont, C. L. (2011). Microbial Metagenomics: beyond the Genome. *Ann. Rev. Mar. Sci.* 3, 347–371. doi: 10.1146/annurev-marine-120709-142811
- Head, I. M., Jones, D. M., and Röling, W. F. M. (2006). Marine microorganisms make a meal of oil. *Nat. Rev. Microbiol.* 4, 173–182. doi: 10.1038/nrmicro1348
- Jansson, J. K., Neufeld, J. D., Moran, M. A., and Gilbert, J. A. (2012). Omics for understanding microbial functional dynamics. *Environ. Microbiol.* 14, 1–3. doi: 10.1111/j.1462-2920.2011.02518.x
- Joye, S. B., Teske, A. P., and Kostka, J. E. (2014). Microbial dynamics following the Macondo oil well blowout across Gulf of Mexico environments. *BioScience* 1–21. doi: 10.1093/biosci/biu121
- Kappell, A. D., Wei, Y., Newton, R. J., Van Nostrand, J. D., Zhou, J., McLellan, S. L., et al. (2014). The polycyclic aromatic hydrocarbon degradation potential of Gulf of Mexico native coastal microbial communities after the deep-water horizon oil spill. *Front. Microbiol.* 5:205. doi: 10.3389/fmicb.2014.00205
- King, G. M., Kostka, J. E., Hazen, T., and Sobecky, P. (2014). Microbial Responses to the deepwater horizon oil spill: from coastal wetlands to the deep sea. *Annu. Rev. Mar. Sci.* 7, 1–18. doi: 10.1146/annurev-marine-010814-015543
- Lamendella, R., Strutt, S., Borglin, S., Chakraborty, R., Tas, N., Mason, O., et al. (2014). Assessment of the deepwater horizon oil spill impact on gulf coast microbial communities. *Front. Microbiol.* 5:130. doi: 10.3389/fmicb.2014.00130
- Leahy, J. G., and Colwell, R. R. (1990). Microbial degradation of hydrocarbons in the environment. *Microbiol. Rev.* 54, 305–315.
- Lyles, C. N., Lee, H. M., Beasley, W. H., McInerney, M. J., and Suflita, J. M. (2014). Anaerobic hydrocarbon and fatty acid metabolism by syntrophic bacteria and their impact on carbon steel corrosion. *Front. Microbiol.* 5:114. doi: 10.3389/fmicb.2014.00114
- Mason, O., Han, J., Woyke, T., and Jansson, J. K. (2014). Single-cell genomics reveals features of a *Colwellia* species that was dominant during the deep-water horizon oil spill. *Front. Microbiol.* 5:332. doi: 10.3389/fmicb.2014.00332
- Mishamandani, S., Gutierrez, T., and Aitken, M. D. (2014). DNA-based stable isotope probing coupled with cultivation methods implicates *Methylophaga* in hydrocarbon degradation. *Front. Microbiol.* 5:76. doi: 10.3389/fmicb.2014.00076
- Prince, R. C. (2010). “Bioremediation of marine oil spills Chapter 16,” in: *Handbook of Hydrocarbon and Lipid Microbiology*, ed K. N. Timmis (Berlin; Heidelberg: Springer-Verlag), 2618–2626.

- Prosser, J. I., Bohannan, B. J. M., Curtis, T. P., Ellis, R. J., Firestone, M. K., Freckleton, R. P., et al. (2007). The role of ecological theory in microbial ecology. *Nat. Rev. Microbiol.* 5, 384–392. doi: 10.1038/nrmicro1643
- Röling, W. F. M., and van Bodegom, P. M. (2014). Toward a quantitative understanding on microbial community structure and functioning: a modeling-centered approach using degradation of marine oil spills as example. *Front. Microbiol.* 5:125. doi: 10.3389/fmicb.2014.00125
- Scott, N. M., Hess, M., Bouskill, N. J., Mason, O. U., Jansson, J. K., and Gilbert, J. A. (2014). The microbial nitrogen cycling potential is impacted by polycyclic aromatic hydrocarbon pollution of marine sediments. *Front. Microbiol.* 5:108. doi: 10.3389/fmicb.2014.00108
- Sherry, A., Grant, R. J., Aitken, C. M., Jones, D. M., Head, I. M., and Gray, N. D. (2014). Volatile hydrocarbons inhibit methanogenic crude oil degradation. *Front. Microbiol.* 5:131. doi: 10.3389/fmicb.2014.00131
- Singh, A. K., Sherry, A., Gray, N. D., Jones, D. M., Bowler, B. F. J., and Head, I. M. (2014). Kinetic parameters for nutrient enhanced crude oil biodegradation in intertidal marine sediments. *Front. Microbiol.* 5:160. doi: 10.3389/fmicb.2014.00160
- Smith, C. B., Tolar, B. B., Hollibaugh, J. T., and King, G. M. (2013). Alkane hydroxylase gene (*alkB*) phylotype composition and diversity in northern Gulf of Mexico bacterioplankton. *Front. Microbiol.* 4:370. doi: 10.3389/fmicb.2013.00370
- Thomas J. C. IV., Wafula, D., Chauhan, A., Green, S. J., Gragg, R., and Jagoe, C. (2014). A survey of deepwater horizon (DWH) oil-degrading bacteria from the eastern oyster biome and its surrounding environment. *Front. Microbiol.* 5:149. doi: 10.3389/fmicb.2014.00149
- Torlapati, J., and Boufadel, M. C. (2014). Evaluation of the biodegradation of Alaska North Slope oil in microcosms using the biodegradation model BIOB. *Front. Microbiol.* 5:212. doi: 10.3389/fmicb.2014.00212
- Yakimov, M. M., Timmis, K. N., and Golyshin, P. N. (2007). Obligate oil-degrading marine bacteria. *Curr. Opin. Biotechnol.* 18, 257–266. doi: 10.1016/j.copbio.2007.04.006
- Ziervogel, K., D'Souza, N., Sweet, J., Yan, B., and Passow, U. (2014). Natural oil slicks fuel surface water microbial activities in the northern Gulf of Mexico. *Front. Microbiol.* 5:188. doi: 10.3389/fmicb.2014.00188

**Conflict of Interest Statement:** The authors declare that the research was conducted in the absence of any commercial or financial relationships that could be construed as a potential conflict of interest.

*Received: 04 August 2014; accepted: 19 August 2014; published online: 04 September 2014.*

*Citation: Kostka JE, Teske AP, Joye SB and Head IM (2014) The metabolic pathways and environmental controls of hydrocarbon biodegradation in marine ecosystems. *Front. Microbiol.* 5:471. doi: 10.3389/fmicb.2014.00471*

*This article was submitted to Aquatic Microbiology, a section of the journal Frontiers in Microbiology.*

*Copyright © 2014 Kostka, Teske, Joye and Head. This is an open-access article distributed under the terms of the Creative Commons Attribution License (CC BY). The use, distribution or reproduction in other forums is permitted, provided the original author(s) or licensor are credited and that the original publication in this journal is cited, in accordance with accepted academic practice. No use, distribution or reproduction is permitted which does not comply with these terms.*



# Alkane hydroxylase gene (*alkB*) phylotype composition and diversity in northern Gulf of Mexico bacterioplankton

Conor B. Smith<sup>1†</sup>, Bradley B. Tolar<sup>2</sup>, James T. Hollibaugh<sup>2</sup> and Gary M. King<sup>1‡\*</sup>

<sup>1</sup> Department of Biological Sciences, Louisiana State University, Baton Rouge, LA, USA

<sup>2</sup> Department of Marine Studies, University of Georgia, Athens, GA, USA

**Edited by:**

Joel E. Kostka, Georgia Institute of Technology, USA

**Reviewed by:**

Matthew Schrenk, East Carolina University, USA

Xiu-Lan Chen, Shandong University, China

**\*Correspondence:**

Gary M. King, Department of Biological Sciences, Louisiana State University, Baton Rouge, LA 70803, 225 578 1901, USA

e-mail: gkingme@gmail.com

<sup>†</sup>These authors have contributed equally to this work.

Natural and anthropogenic activities introduce alkanes into marine systems where they are degraded by alkane hydroxylases expressed by phylogenetically diverse bacteria. Partial sequences for *alkB*, one of the structural genes of alkane hydroxylase, have been used to assess the composition of alkane-degrading communities, and to determine their responses to hydrocarbon inputs. We present here the first spatially extensive analysis of *alkB* in bacterioplankton of the northern Gulf of Mexico (nGoM), a region that experiences numerous hydrocarbon inputs. We have analyzed 401 partial *alkB* gene sequences amplified from genomic extracts collected during March 2010 from 17 water column samples that included surface waters and bathypelagic depths. Previous analyses of 16S rRNA gene sequences for these and related samples have shown that nGoM bacterial community composition and structure stratify strongly with depth, with distinctly different communities above and below 100 m. Although we hypothesized that *alkB* gene sequences would exhibit a similar pattern, PCA analyses of operational protein units (OPU) indicated that community composition did not vary consistently with depth or other major physical-chemical variables. We observed 22 distinct OPUs, one of which was ubiquitous and accounted for 57% of all sequences. This OPU clustered with AlkB sequences from known hydrocarbon oxidizers (e.g., *Alcanivorax* and *Marinobacter*). Some OPUs could not be associated with known alkane degraders, however, and perhaps represent novel hydrocarbon-oxidizing populations or genes. These results indicate that the capacity for alkane hydrolysis occurs widely in the nGoM, but that alkane degrader diversity varies substantially among sites and responds differently than bulk communities to physical-chemical variables.

**Keywords:** alkane hydroxylases, AlkB, bacterioplankton, diversity, Gulf of Mexico

## INTRODUCTION

Alkanes enter marine environments from many natural and anthropogenic sources (Head et al., 2006; Hu et al., 2009). Natural sources include phytoplankton and bacteria (Blumer et al., 1971; Youngblood and Blumer, 1975; Dunahay et al., 1996) and fluxes from hydrocarbon seeps associated with petroleum reservoirs (Hornafius et al., 1999; Seewald, 2003; Sassen et al., 2004). These natural sources undoubtedly account for the capacity of many bacteria to degrade alkanes. However, concerns about petroleum spills, not natural hydrocarbon occurrences, are largely responsible for research on the distribution, diversity and activities of alkane-degrading bacteria (Vomberg and Klinner, 2000; Röling et al., 2002; Sei et al., 2003; van Beilen et al., 2003; Kloos et al., 2006; Teramoto et al., 2009; Berthe-Corti and Nachtkamp, 2010; Hazen et al., 2010; Lu et al., 2012; Rivers et al., 2013).

Several different enzyme systems that vary in substrate chain length and reaction mechanism initiate bacterial *n*-alkane catabolism (van Beilen and Funhoff, 2007). The particulate (or membrane-associated) non-heme iron alkane hydroxylases (alkane 1-monoxygenases) oxidize substrates with chain lengths  $\geq C_5-C_{16}$ . These “alkB” hydroxylases are widely distributed among bacteria (Vomberg and Klinner, 2000; van Beilen

et al., 2003; Liu and Shao, 2005; Liu et al., 2007; van Beilen and Funhoff, 2007; Wasmund et al., 2009). They are encoded by three genes, *alkB* for the catalytically active alkane hydroxylase, and *alkG* and *alkT* for rubredoxin and rubredoxin reductase, respectively, (Cappelletti et al., 2011). Though they are variable overall, *alkB* gene sequences contain sufficient conservation for the design of broad spectrum PCR primers, which yield amplicons that contain diagnostic histidine motifs (Kloos et al., 2006). *AlkB* sequence conservation has been exploited in a variety of molecular ecological studies to assess the distribution and diversity of alkane degraders in hydrocarbon-contaminated soils and sediments (van Beilen et al., 2003; Harayama et al., 2004; Kloos et al., 2006; van Beilen and Funhoff, 2007). However, surprisingly few studies have explored alkane degraders in marine systems (Wasmund et al., 2009; Wang et al., 2010a).

Wasmund et al. (2009) analyzed *alkB* diversity in genomic extracts obtained from hydrocarbon seep-associated sediments in the Timor Sea. They observed numerous novel sequences, many of which were related to, but distinct from known alkane oxidizers within the  $\gamma$ -Proteobacteria and Actinobacteria. Diversity was greater in sediments from shallower depths (<100 m) than deeper depths (>400 m), and *alkB* gene copy numbers were elevated in

sediments nearest hydrocarbon seeps. Guibert et al. (2012) analyzed alkane degraders in intertidal and shallow sub-Antarctic coastal sediments, and like Wasmund et al. (2009) observed novel phylotypes that appeared to represent a temperature-selected community. In addition, they identified *alkB* phylotypes that were proposed as biomarkers for Antarctic alkane degradation. In contrast, Païssé et al. (2011) found no clear relationship between *alkB* expression and hydrocarbon contamination in sediments from coastal Berre lagoon that were chronically polluted by hydrocarbons. However, this study only investigated polluted sediments, so its relevance for unpolluted systems is uncertain.

Thus far, analyses of alkane degraders in the water column have mostly involved culture-based studies supplemented with determinations of isolate *alkB* sequences (e.g., Wang et al., 2010a; Choi and Cho, 2013), although Wang et al. (2010b) also showed that *alkB* gene abundance ranged from  $3 \times 10^3$  l<sup>-1</sup> to  $3 \times 10^5$  l<sup>-1</sup> in surface waters around Xiamen Island. In addition, Lu et al. (2012) have used gene probes (GeoChip) to show that relative to uncontaminated waters, *alkB* genes were enriched in the hydrocarbon plume of the Macondo well oil spill. Lu et al. (2012) also attributed *alkB* sequences in the plume to various Proteobacteria (e.g., *Bdellovibrio*, *Roseobacter*, and *Rhodospirillum*), Firmicutes, and Actinobacteria (e.g., *Gordonia* and *Rhodococcus*), including rather enigmatically the obligate mammalian pathogens, *Mycobacterium bovis* and *M. tuberculosis*; representatives of *Alcanivorax* were either undetectable or present in low abundances.

While clearly informative, these studies have not included spatially extensive analyses of *alkB* distribution and diversity, or comparative analyses of patterns for *alkB* and other genetic markers, e.g., 16S rRNA genes. Thus, it is unclear whether alkane-degrading communities as defined by *alkB* are structured similarly to bulk bacterioplankton communities in unpolluted systems, or whether they respond to different variables. To help address this uncertainty, we have analyzed *alkB* gene sequences derived from clone libraries prepared from genomic extracts of bacterioplankton samples distributed across the northern Gulf of Mexico (nGoM) shelf at depths from 2 m to 1700 m. We have previously used a pyrosequencing-based analysis of 16S rRNA genes from the same and additional samples to characterize nGoM bacterioplankton diversity (King et al., 2013). Results from the latter study indicated that composition was stratified by depth, and that known alkane-degrading genera (especially members of the  $\gamma$ -Proteobacteria) occurred throughout the water column. Therefore, we hypothesized that patterns for *alkB* composition and diversity would mirror those for 16S rRNA genes, and for  $\gamma$ -Proteobacteria and Actinobacteria in particular.

## MATERIALS AND METHODS

### SAMPLE COLLECTION AND *ALKB* ANALYSIS

Bacterioplankton DNA was collected during the March 2010 R/V Cape Hatteras cruise GC-5 ( $30^{\circ} 07' N$ ,  $088^{\circ} 02' W$  to  $27^{\circ} 39' N$ ,  $093^{\circ} 39' W$ ) as described in greater detail by King et al. (2013) and Tolar et al. (2013). Genomic DNA was extracted from bacterioplankton collected by filtering about 1 liter of sea-water through 0.2  $\mu$ m filters. DNA extracts were used for *alkB* PCR in reactions containing 12.1  $\mu$ L of PCR grade water, 2.5  $\mu$ L

10X High Fidelity PCR buffer (Invitrogen), 0.2  $\mu$ L 25 mM dNTP mixture, 1  $\mu$ L 50 mM MgSO<sub>4</sub>, 5  $\mu$ L 5X bovine serum albumin (Promega), 1.5  $\mu$ L each of 10 mM stocks of forward and reverse primers, 0.2  $\mu$ L Platinum Taq DNA Polymerase High Fidelity (Invitrogen), and 1  $\mu$ L template DNA. The primers used were *alkB*-1f 5'-AAYACNGCNCAYGARCTNGGNAYAA and *alkB*-1r 5'-GCRTGRTGRTCNGARTGNCGYTG (Kloos et al., 2006). The PCR program consisted of an initial denaturation step (94°C, 3 min), followed by 26 cycles of 94°C (1 min), 61°C (1 min), 68°C (45 s), with a final extension of 10 min at 68°C. Amplicons were visualized by electrophoresis on 0.8% agarose gels. Bands of the correct size were excised from the gels, and DNA was extracted from the gel slices with a Zymoclean gel DNA recovery Kit (Zymo Research) according to the manufacturer's instructions. DNA concentrations of the cleaned reactions were determined using a Nanodrop spectrophotometer.

Cloning reactions were carried out using a CloneJET PCR cloning kit according to the manufacturer's instructions. Three (3)  $\mu$ L of ligation mix was added to 25  $\mu$ L Genlantis SmartCells and incubated on ice for 30 min before heat shock at 42°C for 45 s. Room temperature SOC medium (125  $\mu$ L) was added and the cells were incubated at 37°C for 1 h while shaking at 225 rpm. Cells were plated on LB plates containing ampicillin, and colonies (at least 30 per sample) were picked for screening after overnight incubation at 37°C. Picked colonies were added to PCR reactions containing 10.5  $\mu$ L PCR grade water, 12.5  $\mu$ L Promega GoTaq® Green Master Mix, and 1  $\mu$ L each of F pJET primer and R pJET primer from 10  $\mu$ M stocks. The PCR program consisted of an initial denaturation step (95°C, 3 min), followed by 30 cycles of 94°C (30 s), 60°C (30 s), 72°C (90 s), with a final extension of 10 min at 72°C. Amplicons were visualized by electrophoresis on a 1% agarose gel and purified with UltraClean PCR Clean-up kits (MoBio, Folsom, CA) according to the manufacturer's instructions and then sequenced bi-directionally at the LSU Genomics Facility.

## DATA ANALYSIS

*AlkB* clone sequences and reference sequences downloaded from the FunGene *alkB* database were aligned with ClustalW (Larkin et al., 2007) and adjusted manually as needed. Clone sequences were screened for the presence of two diagnostic histidine-containing motifs (HNXXHH and HSDHH) that contribute to the *alkB* protein active site. Sequences with both motifs were retained; sequences lacking a motif were retained if they were substantially similar to other sequences, and otherwise at least 150 residues in length. Sequences not meeting these criteria were eliminated from further consideration. After manually adjusting the alignment, a maximum likelihood phylogenetic tree was created using MEGA ver. 5.05 (Tamura et al., 2011) with 100 bootstrap replications. A distance matrix of clone sequences was prepared using Phylip (Felsenstein, 1989) as input for the Mothur platform (Schloss et al., 2009), which grouped the *alkB* sequences into OPUs using a distance cutoff of 0.20 (Wasmund et al., 2009; Guibert et al., 2012). Mothur was used to determine relative abundance of *alkB* OPUs and to compare distributions among sites. Statistical analyses of *alkB* data were carried out using Mothur and R (R Development Core Team., 2008).

## ACCESSION NUMBERS

Sequences have been deposited in GenBank with accession numbers KF163175-KF613575.

## RESULTS AND DISCUSSION

A total of 508 clone sequences were obtained from 17 samples representing 9 stations and 14 depths with approximately equal numbers of clones from each. However, after curating the sequences the total number of validated *alkB* gene clones was reduced to 401. Rarefaction analysis indicated OPU “discovery” for each of the libraries was saturated or nearly saturated. Samples from two sites, A6-2 m and F6-2 m, were excluded from additional statistical analyses because the numbers of validated clone sequences (8 and 2, respectively) were too few for meaningful comparisons. Although both of these sites harbored *alkB*-containing populations based on results from a prior survey of 16S rRNA genes (King et al., 2013), they appeared to be dominated by taxa that contained divergent genes that were nonetheless amplified with *alkB* primers. The resulting PCR products contained the HSDHH motif, but lacked HNXXH and otherwise differed substantially from all other validated sequences. The function of these genes is unknown, and could not be inferred from BLAST analysis.

Two additional samples from station A6 (20 m and 1700 m), and one from station D5 (2 m), did not yield *alkB* amplicons at all, in spite of repeated efforts. Reasons for amplification failure with these samples are unclear, since a separate study (King et al., 2013) showed that they each yielded 16S rRNA gene amplicons, including sequences assigned to known alkane-degrading genera (e.g., *Alcanivorax*; King et al., 2013) that were also observed in other samples based on both 16S rRNA and *alkB* gene sequences. Although *alkB* concentrations in the three negative samples might be at or below detection by our PCR protocol, the total amounts of DNA used in each of the PCR reactions was similar, and there is no *a priori* reason to expect substantial variation in relative *alkB* concentrations among samples from similar locations or depths. It also seems unlikely that phylotypes not susceptible to amplification dominated the *alkB*-containing communities in the negative samples. Thus, the lack of amplicons for A6-2 m, A6-1700 m and D5-2 m remains enigmatic.

## OPU ABUNDANCE AND CLASSIFICATION

Sequences from the 17 positive samples were clustered into 22 OPUs using a distance cutoff of 0.20. Guibert et al. (2012) used a cutoff of 0.20 and reported 30 OPUs from 202 clones pooled from 5 libraries obtained during an analysis of coastal sub-Antarctic sediments. Wasmund et al. (2009) reported even greater richness (53 OPUs) from 246 clones from Timor Sea sediments, also pooled from 5 libraries and based on a cutoff of 0.20.

The lower AlkB OPU richness for nGoM bacterioplankton relative to Timor Sea and sub-Antarctic sediment samples (Wasmund et al., 2009; Guibert et al., 2012) is consistent with patterns observed for bacterioplankton and sediment communities as a whole, since the latter typically support greater richness than the former based on 16S rRNA gene sequence analyses (Kemp and Aller, 2004). The difference between bacterioplankton and sediment AlkB OPU richness might simply reflect differences in the number of cells extracted for analysis, since even small sediment

masses can support much larger communities than the water column. In addition (or alternatively), lower habitat diversity in the water column might select for fewer hydrocarbon-oxidizing phylotypes. Whether or not these differences in richness affect responses to hydrocarbon inputs is uncertain.

Two of the AlkB OPUs identified in this study included reference sequences derived from known alkane degraders. OPU 1, which represented 57.4% of all the AlkB clones (Table 1, Figure 1), included reference sequences from *Alcanivorax borkumensis* SK2, *A. borkumensis* S12-4, *A. dieselolei* S10-17, *Marinobacter aquaeoli* VT8, and *Marinobacter* sp. S17-4. Several of these isolates (*A. borkumensis* S12-4, *A. dieselolei* S10-17, and *Marinobacter* sp. S17-4) were obtained by Wang et al. (2010a) from surface waters of the tropical and sub-tropical southern Atlantic Ocean, while *M. aquaeoli* VT8 was isolated from an offshore oil well in coastal southern Vietnam (Huu et al., 1999). *A. borkumensis* SK2 was isolated from sediments off the northwest coast of Germany (Yakimov et al., 1998).

OPU 3, which accounted for 9.2% of all clones (Table 1, Figure 1), contained reference sequences from *M. aderens* HP15, *M. hydrocarbonoclasticus* S17-4, and *Marinobacter* sp. P1-14D. *M. aderens* HP15 was isolated from Wadden Sea diatom aggregates in surface waters (Kaeppel et al., 2012), and *M. hydrocarbonoclasticus* S17-4 was isolated from tropical and sub-tropical southern Atlantic Ocean surface waters (Wang et al., 2010a). Thus, two OPUs that collectively accounted for two-thirds all the nGoM AlkB sequences were closely related to widely distributed *Alcanivorax* and *Marinobacter* isolates.

**Table 1 | Incidence by sampling site and depth of OPUs detected at 3 or more sampling locations.**

Site	OPU							
	01	02	03	04	05	06	09	11
A6-2 m	7	1	0	0	0	0	0	0
A6-80 m	20	0	3	0	1	0	0	0
A6-160 m	18	0	1	3	1	0	0	0
A6-350 m	26	0	0	0	4	0	0	0
A6-700 m	0	23	1	0	0	2	0	0
B4-530 m	28	1	0	0	0	0	0	0
B5-450 m	3	7	6	0	0	1	0	0
D3-68 m	9	0	5	0	7	0	0	0
D5-50 m	11	0	1	0	8	0	2	1
D5-100 m	10	0	0	10	0	0	1	0
D5-450 m	11	0	1	11	0	0	0	1
D5-900 m	24	7	1	0	0	0	0	0
E2-6 m	20	0	0	0	0	0	0	0
F6-2 m	2	0	0	0	0	0	0	0
H6-45 m	10	0	9	0	0	0	1	0
H6-280 m	4	3	9	1	0	4	0	1
MR1-2 m	27	0	0	0	0	0	0	0
Pooled	230	42	37	25	21	7	4	3

OPUs 1 and 3 included reference sequences from *Alcanivorax* and *Marinobacter* (see text). OPUs 2, 6, 9 and 11 were associated with Proteobacteria, and OPUs 4 and 5 were unclassified.

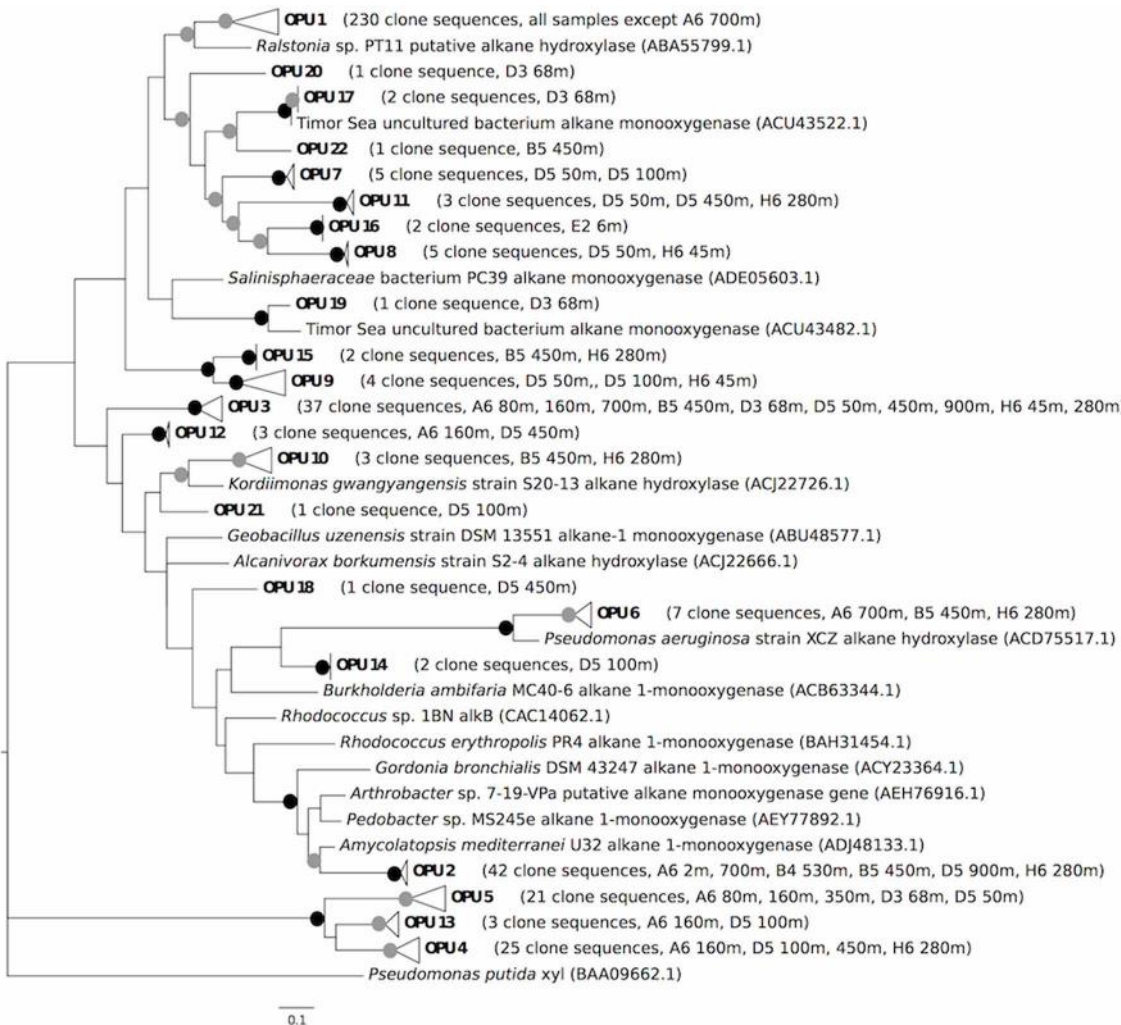


**FIGURE 1 | Maximum likelihood tree comparing putative *alkB* amino acid sequences from this study with reference *alkB* sequences obtained from other studies.** Bootstrap values from 100 resamplings are indicated with black circles for values of 95–100% and gray circles for values of 50–94%. OPUs were determined using a distance cutoff of 0.20 (80% sequence similarity). OPU 1 clusters with the following reference sequences: *Alcanivorax borkumensis* SK2 alkane 1-monoxygenase (CAL18155.1), *Alcanivorax borkumensis* S12-4 alkane hydroxylase (ACJ22702.1), *Alcanivorax*

dieselolei S10-17 alkane hydroxylase (ACJ22698.1), *Marinobacter aquaeolei* VT8 alkane 1-monooxygenase (ABM17541.1), and *Marinobacter* sp. S17-4 putative alkane monooxygenase (ACT31523.1). OPU 3 clusters with *Marinobacter adhaerens* HP15 alkane 1-monooxygenase (ADP98338.1), *Marinobacter hydrocarbonoclasticus* S17-4 alkane hydroxylase (ACJ22716.1), and *Marinobacter* sp. P1-14D alkane hydroxylase (ACS91348.1). The tree was rooted with a xylene monooxygenase amino acid sequence from *Pseudomonas putida* (Hara et al., 2004).

An additional 85 clone sequences that formed 17 OPUs were distributed among polyphyletic clades comprised of sequences from Actinobacteria, Gammaproteobacteria, and Firmicutes (**Figure 1**). These 17 OPUs appeared to represent novel phylogenotypes, some of which were associated with, but distinct from, novel phylogenotypes from the Timor Sea (Wasmund et al., 2009). However, the lack of congruence between 16S rRNA and *alkB* gene phylogenies (Jurelevicius et al., 2013), and the apparent mobility of *alkB* (van Beilen et al., 2001, 2003, 2005; Smits et al., 2002; Wang et al., 2010b), precluded more specific inferences about OPU affiliations. Irrespective of their phylogeny, however, these unclassified OPUs have not been observed in other AlkB clone libraries (e.g., Wasmund et al., 2009; Guibert et al., 2012).

This suggests that the nGoM supports a few widely distributed and dominant alkane degraders along with less abundant, more geographically constrained populations.

A relatively small number of clones (49, 12.2% of the total) forming 3 OPUs (4, 5 and 13) could not be assigned to phyla even tentatively (**Figure 1**). Sequences of these clones contained the signature AlkB histidine motifs, but their divergence might indicate altered substrate ranges relative to other AlkB proteins, or even different functions. Regardless, these OPUs appear unique to the nGoM.

Of the classified AlkB sequences identified in this study, the most abundant were associated with Gammaproteobacteria, and an *Alcanivorax-Marinobacter* OPU in particular (Figures 1, 2).

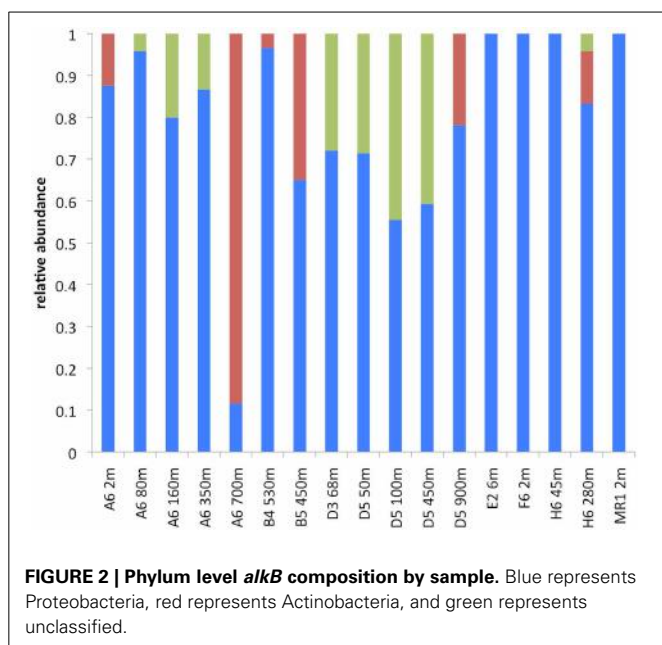


**Table 1**). Gammaproteobacterial AlkB has also been reported as the dominant phylotype in analyses of Timor Sea sediments and surface waters near Xiamen Island (Wasmund et al., 2009; Wang et al., 2010b). In addition, Hazen et al. (2010) noted that hydrocarbon-oxidizing Gammaproteobacteria, albeit not *Alcanivorax*, dominated microbial communities in the Macondo well oil plume. Thus, Gammaproteobacteria appear to dominate the hydrocarbon oxidizers in many natural marine systems as well as those exposed to chronic or acute hydrocarbon inputs. In contrast, soils appear to harbor more diverse alkane-degrading communities, with a predominance of Actinobacteria (e.g., Jurelevicius et al., 2013).

#### OPU DISTRIBUTION

*Alcanivorax*-like AlkB sequences in the dominant OPU 1 were detected in all samples but A6-700 m, even though this sample contained *Alcanivorax* 16S rRNA based on results from a previous analysis (King et al., 2013 and Figure 3). At this site, *Alcanivorax* *alkB* genes might have been at or near detection limits for our PCR conditions, since 16S rRNA gene sequences attributed to *Alcanivorax* accounted for only 0.07% of the total reads. In contrast, *Alcanivorax*-like *alkB* gene sequences were observed in 7 samples (A6-2 m, D5-50 m, D5-100 m, D5-450 m, E6-2 m, F6-2 m, and MR1-2 m) where *Alcanivorax* 16S rRNA genes were not detected (Figure 3). The lack of concordance between *Alcanivorax* 16S rRNA and *Alcanivorax*-like *alkB* gene sequences at these sites might be explained by the presence of *Alcanivorax*-like *alkB* genes in taxa other than *Alcanivorax* (e.g., *Marinobacter*). More generally, there was no significant correlation between the relative abundance of *Alcanivorax*-like *alkB* sequences and the relative abundance of *Alcanivorax* 16S rRNA gene sequences (Figure 3).

PCA analysis showed that the composition of AlkB OPU assemblages did not vary consistently with depth or sampling station (Figure 4A), since there were no coherent clusters with

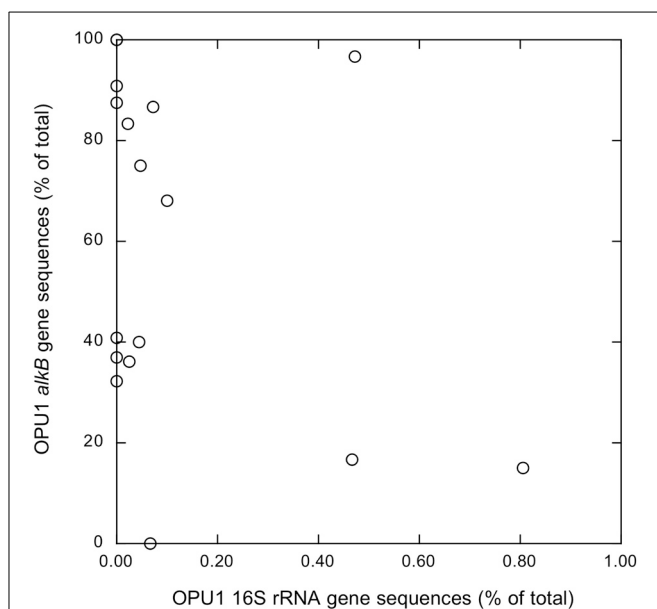
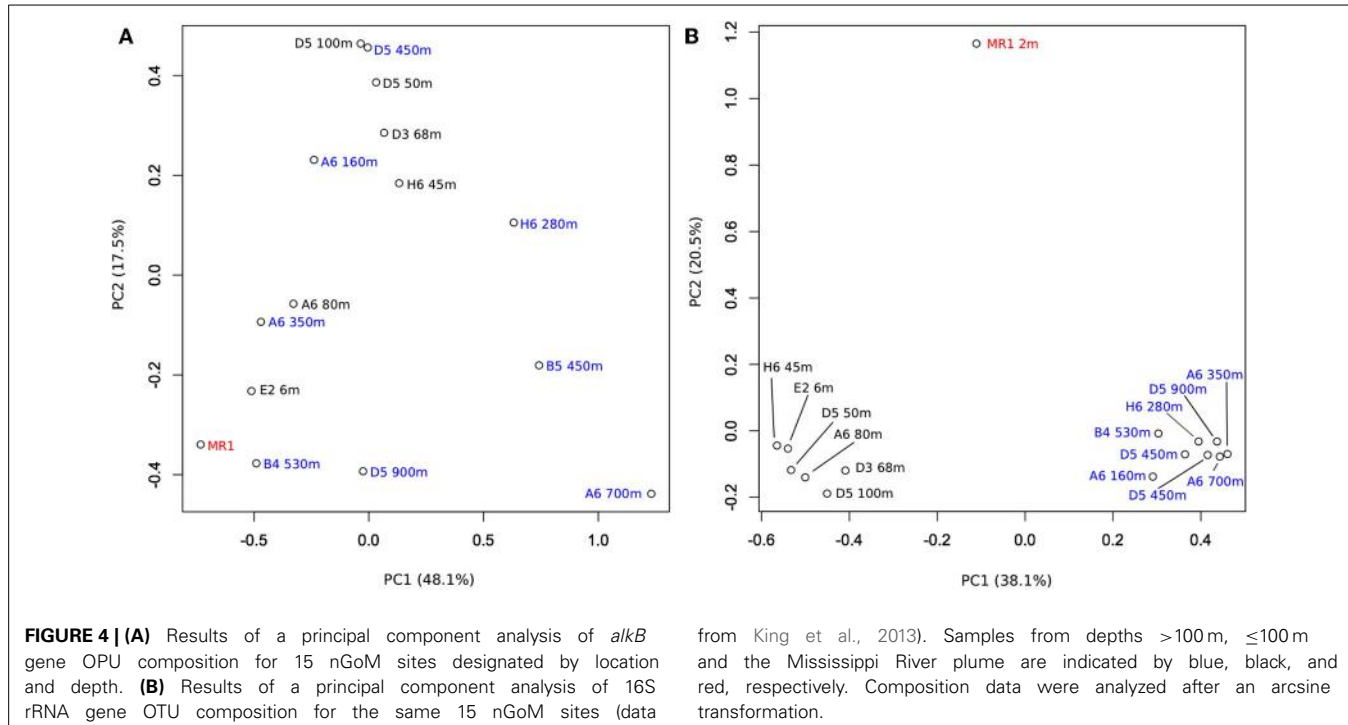


**FIGURE 3 | *Alcanivorax*-like *alkB* gene sequence relative abundances as a function of *Alcanivorax* 16S rRNA gene sequence relative abundances; *alkB* results from this study, 16S rRNA results taken from King et al. (2013).**

separation on axes 1 or 2. These results were consistent with inferences from a similarity plot constructed using the structure-based  $\theta_{YC}$  calculator (SI Figure 1), which also indicated that AlkB OPUs were not clustered by location or depth. Similarly, results from a canonical correlation analysis (CCorA) revealed no consistent relationships among OPUs and depth (SI Figure 2), or several other physical-chemical variables available for the samples (e.g., salinity, fluorescence, beam attenuation (a measure of particle density), dissolved oxygen, pH and temperature). Removing the most abundant OPUs from the PCA analysis (OPU1 and OPU3) resulted in a cluster of shallow water samples ( $\leq 100$  m depth) that included one deeper water sample (A6-350 m); the remaining deep-water samples were dispersed across both axes (SI Figure 3). This suggests that the less abundant OPUs in surface waters might form similar assemblages across sites, but that variability in the more abundant OPUs obscures patterns.

Results similar to those for a PCA with all AlkB OPUs were obtained from a PCA analysis of the relative abundances in each sample of 16S rRNA gene sequences for *Alcanivorax*, *Marinobacter*, *Pseudomonas*, *Hydrocarboniphaga*, and *Kordiimonas*, the primary alkane-oxidizing reference taxa with which some of the clone sequences were identified (and SI Figure 4 and King et al., 2013). The distribution of these taxa did not vary consistently with depth. In contrast, PCA analysis of 16S rRNA gene sequences for the bulk bacterioplankton communities in these same samples showed that they separated distinctly by depth (Figure 4B) as previously reported for a larger set of nGoM samples (King et al., 2013; Tolar et al., 2013).

These results collectively indicate that the composition of nGoM alkane-degrading communities varies in response to as yet unidentified biological or abiological factors that do not change



consistently with sample depth. This pattern differs from that for bulk bacterioplankton, the composition of which appears to be governed by depth-dependent variables (King et al., 2013; Tolar et al., 2013). In particular, the relative abundance of nGoM Gammaproteobacteria, which constitute the majority of classifiable alkane degraders based on 16S rRNA gene and *alkB* sequences, depends strongly on depth (King et al., 2013).

However, a greater relative abundance of Gammaproteobacteria does not necessarily imply a greater abundance of alkane degraders, since there was limited, albeit significant, positive correlation between the two ( $r = 0.518$ ,  $p = 0.033$ ; SI Figure 5). For example, Gammaproteobacteria at D5-900 m constituted >40% of the total bacterial community (King et al., 2013), yet only 0.1% of this community was identified as alkane degraders. In contrast, samples from A6-160 m, A6-350 m, A6-700 m, B5-450 m, and H6-45 m harbored greater relative abundances of alkane degraders, but lower relative abundances of Gammaproteobacteria (King et al., 2013).

#### INDICES OF *AlkB* DIVERSITY

Statistical measures of diversity (e.g., Chao1, ACE, Shannon and Inverse Simpson's indices, and evenness indices) also did not vary consistently with depth or sampling station (Figure 5, SI Table 1). Values for the Shannon index, for example, fell between 0.0 (MR1-2 m, 1 OPU) and 1.79, but there were no systematic differences among samples. Likewise, there were no systematic differences among samples for other diversity indices. In this respect, spatial trends for *AlkB* diversity were comparable to those for bulk nGoM bacterioplankton based on 16S rRNA gene sequences; diversity metrics for the latter also did not vary with depth or geographic location on the shelf (King et al., 2013).

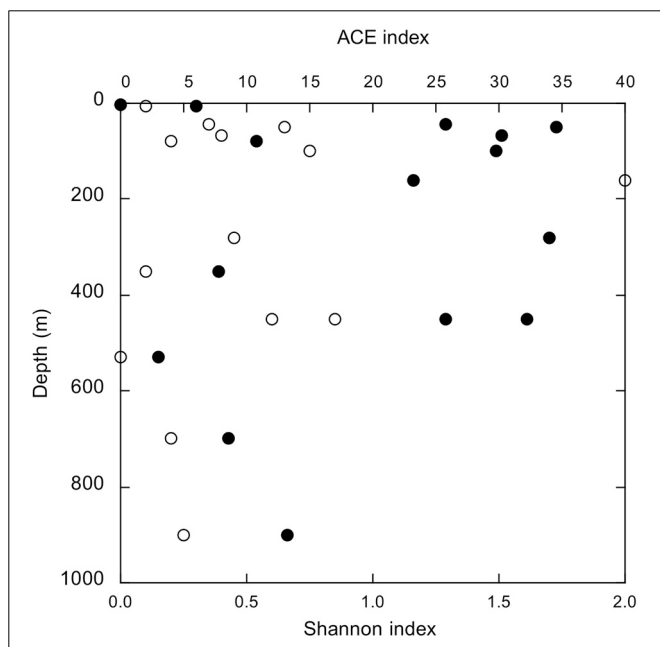


**FIGURE 5 |** *AlkB* diversity indices as a function of depth; open symbols, ACE index and closed symbols, Shannon index.

The absence of spatial patterns in nGoM *alkB* gene sequence diversity suggests that at least during the sampling period (March, 2010), assembly of alkane-degrading communities depended on a common mechanism (e.g., neutral assembly; Emerson and Gillespie, 2008) irrespective of local conditions. A different pattern might emerge, however, during summer stratification and

the establishment of hypoxia in surface waters. Changes in substrate availability and quality, temperature and dissolved oxygen could enrich specific members of surface but not deeper communities resulting in more distinct spatial patterns. Data from the Macondo Well oil plume also indicate that the introduction of hydrocarbons from spills or natural sources can create bloom conditions that alter both richness (Hazen et al., 2010; Valentine et al., 2010) and evenness (Lu et al., 2012; Rivers et al., 2013).

## SUMMARY AND CONCLUSIONS

In summary, results from *alkB* gene sequence analyses show that community structure (composition, richness and diversity) of nGoM alkane-degrading bacteria varies among sites independently of depth and location. The absence of vertical structure contrasts with distinct patterns observed for bulk bacterioplankton communities, but is consistent with the distribution of alkane-degrading genera identified by 16S rRNA gene sequences. Two OPUs, one including *Alcanivorax borkumensis*-like AlkB sequences and a second comprised of *Marinobacter*-like AlkB sequences, accounted for nearly two-thirds of all sequences; the former was widely distributed. In contrast to marine sediment AlkB, nGoM bacterioplankton AlkB appeared OPU-depauperate, and only a small percentage of sequences were not identifiable as Proteobacteria or Actinobacteria. Inconsistencies between AlkB distribution and the distribution of 16S rRNA gene sequences attributable to alkane degraders suggest that both markers may be needed to assess the composition and structure of hydrocarbon-oxidizing communities.

## ACKNOWLEDGMENTS

This work was supported partially by GoMRI-LSU and the National Science Foundation (OCE-0943278 and ANT-0838996 to James T. Hollibaugh). We thank C. Judd for technical support. We thank L. Powers for assistance with sample collection and CTD data processing. We thank the crew of the R/V *Cape Hatteras* and scientists from the Gulf Carbon 5 cruise who provided data, especially C. Fichot, W.-J. Cai, and W.-J. Huang. Funding for Gulf Carbon was from NSF awards OCE-0752110 (W.-J. Cai) and OCE-0752254 (S. Lohrenz).

## SUPPLEMENTARY MATERIAL

The Supplementary Material for this article can be found online at: <http://www.frontiersin.org/journal/10.3389/fmicb.2013.00370/abstract>

**SI Figure 1 | Dendrogram of similarities among communities based on the structure-based  $\theta_{YC}$  calculator for *alkB* OPU compositions.**

**SI Figure 2 | Canonical correlation analysis of OPU distributions among samples (Y1) and correlations with environmental variables for each sample (Y2).** Environmental data from King et al. (2013).

**SI Figure 3 | Results of a principal component analysis of *alkB* gene OPU composition for 15 nGoM sites designated by location and depth as in Figure 4A, but after removal of the two most abundant OPUs: 1 and 3.**

**SI Figure 4 | Results of a principal component analysis of the distribution among sites of alkane-degrading bacterial genera inferred from 16S rRNA sequence analyses.** Relative abundance data for 16S gene sequence OTUs were calculated using a normalized value of 362 sequences per site.

Samples from depths >100 m, ≤100 m and the Mississippi River plume are indicated by blue, black, and red, respectively. The alkane-degrading genera included *Alcanivorax*, *Marinobacter*, *Pseudomonas*, *Hydrocarbonophaga*, and *Kordiimonas*. Composition data were analyzed after an arcsine transformation.

**SI Figure 5 | Relative abundance of gammaproteobacterial alkane-degrading genera identified on the basis of 16S rRNA gene sequences for the sites used in this study as a function of the relative abundance of all gammaproteobacteria in the same samples.** Data from King et al. (2013).

**SI Table 1 | Diversity statistics calculated with Mothur.**  $S_{obs}$ , observed richness; C1, Chao1; H', Shannon index; 1/D, inverse Simpson's index; Cov, coverage. Values in parentheses represent 95% lower and upper confidence limits, respectively, for C1, ACE, H', and 1/D. Because each OPU may be present at multiple sites the sum of  $S_{obs}$  at all sites is not equal to the pooled value for  $S_{obs}$ .

## REFERENCES

- Berthe-Corti, L., and Nachtkamp, M. (2010). "Bacterial communities in hydrocarbon-contaminated marine coastal environments," in *Handbook of Hydrocarbon and Lipid Microbiology*, ed K.N. Timmis (Heidelberg: Springer-Verlag), 2350–2359.
- Blumer, M., Guillard, R. R. L., and Chase, T. (1971). Hydrocarbons of marine phytoplankton. *Mar. Biol.* 8, 183–189. doi: 10.1007/BF00355214
- Cappelletti, M., Fedi, S., Frascari, D., Ohtake, H., Turner, R. J., and Zannoni, D. (2011). Analyses of both the *alkB* gene transcriptional start site and *alkB* promoter-inducing properties of *Rhodococcus* sp. strain BCPI grown on n-alkanes. *Appl. Environ. Microbiol.* 77, 1619–1627. doi: 10.1128/AEM.01987-10
- Choi, A., and Cho, J. C. (2013). *Thalassolituus marinus* sp. nov., a hydrocarbon-utilizing marine bacterium. *Int. J. Syst. Evol. Microbiol.* 63, 2234–2238. doi: 10.1099/ijss.0.046383-0
- Dunahay, T. G., Jarvis, E. E., Dais, S. S., and Roessler, P. G. (1996). "Manipulation of microalgal lipid production using genetic engineering," in *Seventeenth Symposium on Biotechnology for Fuels and Chemicals* (New York, NY: Humana Press), 223–231.
- Emerson, B. C., and Gillespie, R. G. (2008). Phylogenetic analysis of community assembly and structure over space and time. *Trends Ecol. Evol.* 23, 619–630. doi: 10.1016/j.tree.2008.07.005
- Felsenstein, J. (1989). PHYLIP - (Phylogeny interface package) version 3.2. *Cladistics* 5, 164–166.
- Guibert, L. M., Loviso, C. L., Marcos, M. S., Commendatore, M. G., Dionisi, H. M., and Lozada, M. (2012). Alkane biodegradation genes from chronically polluted subantarctic coastal sediments and their shifts in response to oil exposure. *Microp. Ecol.* 64, 605–616. doi: 10.1007/s00248-012-0051-9
- Hara, A., Baik, S., Syutsubo, K., Misawa, N., Smits, T. H. M., van Beilen, J. B., et al. (2004). Cloning and functional analysis of *alkB* genes in *Alcanivorax borkumensis* SK2. *Environ. Microbiol.* 6, 191–197. doi: 10.1046/j.1462-2920.2003.00550.x
- Harayama, S., Kasai, Y., and Hara, A. (2004). Microbial communities in oil-contaminated seawater. *Curr. Opin. Biotechnol.* 15, 205–214. doi: 10.1016/j.copbio.2004.04.002
- Hazen, T. C., Dubinsky, E. A., DeSantis, T. Z., Andersen, G. L., Piceno, Y. M., Singh, N., et al. (2010). Deep-sea oil plume enriches indigenous oil-degrading bacteria. *Science* 330, 204–208. doi: 10.1126/science.1195979
- Head, I. M., Jones, D. M., and Roling, W. F. M. (2006). Marine microorganisms make a meal of oil. *Nature* 4, 173–182. doi: 10.1038/nrmicro1348
- Hornafius, J., Quigley, D., and Luyendyk, B. (1999). The world's most spectacular marine hydrocarbon seeps (Coal Oil Point, Santa Barbara Channel, California): quantification of emissions. *J. Geophys. Res. Oceans* 104, 20703–20711. doi: 10.1029/1999JC900148
- Hu, L., Guo, Z., Feng, J., Yang, Z., and Fang, M. (2009). Distributions and sources of bulk OM and aliphatic hydrocarbons in the surface sediments of the Bohai Sea, China. *Mar. Chem.* 113, 197–211. doi: 10.1016/j.marchem.2009.02.001
- Huu, N. B., Denner, E. B. M., Ha, D. T. C., Wanner, G., and Stan-Lotter, H. (1999). *Marinobacter aquaeolei* sp. nov., a halophilic bacterium isolated from

- a Vietnamese oil-producing well. *Int. J. Syst. Evol. Microbiol.* 49, 367–375. doi: 10.1099/00207713-49-2-367
- Jurelevicius, D., Alvarez, V. M., Peixoto, R., Rosado, A. S., and Seldin, L. (2013). The use of a combination of *alkB* primers to better characterize the distribution of alkane-degrading bacteria. *PLoS ONE* 8:e66565. doi: 10.1371/journal.pone.0066565
- Kaeppele, E., Gärdes, A., Seebah, S., Grossart, H.-P., and Ullrich, M. S. (2012). *Marinobacter adherens* sp. nov., isolated from marine aggregates formed by the diatom *Thalassiosira weissflogii*. *Int. J. Syst. Evol. Microbiol.* 62, 124–128. doi: 10.1099/ijss.0.030189-0
- Kemp, P. F., and Aller, J. Y. (2004). Bacterial diversity in aquatic and other environments: what 16S rDNA libraries can tell us. *FEMS Microbiol. Ecol.* 47, 161–177. doi: 10.1016/S0168-6496(03)00257-5
- King, G. M., Smith, C. B., Tolar, B., and Hollibaugh, J. T. (2013). Analysis of composition and structure of bacterioplankton communities in the northern Gulf of Mexico. *Front. Microbiol.* 3:438. doi: 10.3389/fmicb.2012.00438
- Kloos, K., Munch, J. C., and Schloter, M. (2006). A new method for the detection of alkane-monooxygenase homologous genes (*alkB*) in soils based on PCR hybridization. *J. Microbiol. Meth.* 66, 486–496. doi: 10.1016/j.mimet.2006.01.014
- Larkin, M. A., Blackshields, G., Brown, N. P., Chenna, R., McGgettigan, P. A., McWilliam, H., et al. (2007). ClustalW and ClustalX version 2. *Bioinformatics* 23, 2947–2948. doi: 10.1093/bioinformatics/btm404
- Liu, Z., Lozupone, C., Hamady, M., Bushman, F. D., and Knight, R. (2007). Short pyrosequencing reads suffice for accurate microbial community analysis. *Nucleic Acids Res.* 35, e120. doi: 10.1093/nar/gkm541
- Liu, C., and Shao, Z. (2005). *Alcanivorax dieselolei* sp. nov., a novel alkane-degrading bacterium isolated from sea water and deep-sea sediment. *Int. J. Syst. Evol. Microbiol.* 55, 1181–1186. doi: 10.1099/ijss.0.63443-0
- Lu, Z., Deng, Y., Van Nostrand, J. D., He, Z., Voordeckers, J., Zhou, A., et al. (2012). Microbial gene functions enriched in the Deepwater Horizon deep-sea oil plume. *ISME J.* 6, 451–460. doi: 10.1038/ismej.2011.91
- Païssé, S., Duran, R., Coulon, F., and Goñi-Urriza, M. (2011). Are alkane hydroxylase genes (*alkB*) relevant to assess petroleum bioremediation processes in chronically polluted coastal sediments? *Appl. Microbiol. Biotechnol.* 92, 835–844. doi: 10.1007/s00253-011-3381-5
- R Development Core Team. (2008). *R: A Language and Environment for Statistical Computing*. Vienna: R Foundation for Statistical Computing. ISBN 3-900051-07-0. Available online at: <http://www.R-project.org>.
- Rivers, A. R., Sharma, S., Tringe, S. G., Martin, J., Joye, S. B., and Moran, M. A. (2013). Transcriptional response of bathypelagic marine bacterioplankton to the Deepwater Horizon oil spill. *ISME J.* 7, 2315–2329. doi: 10.1038/ismej.2013.129
- Röling, W. F., Milner, M. G., Jones, D. M., Lee, K., Daniel, F., Swannell, R. J., et al. (2002). Robust hydrocarbon degradation and dynamics of bacterial communities during nutrient-enhanced oil spill bioremediation. *Appl. Environ. Microbiol.* 68, 5537–5548. doi: 10.1128/AEM.68.11.5537-5548.2002
- Sassen, R., Roberts, H. H., Carney, R., Milkove, A. V., DeFreitas, D. A., Lanoil, B., et al. (2004). Free hydrocarbon gas, gas hydrate, and authigenic minerals in chemosynthetic communities of the northern Gulf of Mexico continental slope: relation to microbial processes. *Chem. Geol.* 205, 195–217. doi: 10.1016/j.chemgeo.2003.12.032
- Schloss, P. D., Westcott, S. L., Ryabin, T., Hall, J. R., Hartmann, M., Hollister, E. B., et al. (2009). Introducing mothur: open-source, platform-independent, community-supported software for describing and comparing microbial communities. *Appl. Environ. Microbiol.* 75, 7537–41. doi: 10.1128/AEM.01541-09
- Seewald, J. (2003). Organic–inorganic interactions in petroleum-producing sedimentary basins. *Nature* 426, 327–333. doi: 10.1038/nature02132
- Sei, K., Sugimoto, Y., Mori, K., Maki, H., and Kohno, T. (2003). Monitoring of alkane-degrading bacteria in a sea-water microcosm during crude oil degradation by polymerase chain reaction based on alkane-catabolic genes. *Environ. Microbiol.* 5, 517–522. doi: 10.1046/j.1462-2920.2003.00447.x
- Smits, T. H. M., Balada, S. B., Witholt, B., and van Beilen, J. B. (2002). Functional analysis of alkane hydroxylases from Gram-negative and Gram-positive bacteria. *J. Bacteriol.* 184, 1733–1742. doi: 10.1128/JB.184.6.1733-1742.2002
- Tamura, K., Peterson, D., Peterson, N., Stecher, G., Nei, M., and Kumar, S. (2011). MEGA5: molecular evolutionary genetics analysis using maximum likelihood, evolutionary distance, and maximum parsimony methods. *Mol. Biol. Evol.* 28, 2731–2739. doi: 10.1093/molbev/msr121
- Teramoto, M., Suzuki, M., Okazaki, F., Hatmanti, A., and Harayama, S. (2009). Oceanobacter-related bacteria are important for the degradation of petroleum aliphatic hydrocarbons in the tropical marine environment. *Microbiology* 155, 3362–3370. doi: 10.1099/mic.0.030411-0
- Tolar, B., King, G. M., and Hollibaugh, J. T. (2013). An analysis of Thaumarchaeota populations from the northern Gulf of Mexico. *Front. Microbiol.* 4:72. doi: 10.3389/fmicb.2013.00072
- Valentine, D. L., Kessler, J. D., Redmond, M. C., Mendes, S. D., Heintz, M. B., Farwell, C., et al. (2010). Propane respiration jump-starts microbial response to a deep oil spill. *Science* 330, 208–211. doi: 10.1126/science.1196830
- van Beilen, J. B., and Funhoff, E. G. (2007). Alkane hydroxylases involved in microbial alkane degradation. *Appl. Microbiol. Biotechnol.* 74, 13–21. doi: 10.1007/s00253-006-0748-0
- van Beilen, J. B., Li, Z., Duetz, W. A., Smits, T. H. M., and Witholt, B. (2003). Diversity of alkane hydroxylase systems in the environment. *Oil Gas Sci. Technol.* 58, 427–440. doi: 10.2516/ogst:2003026
- van Beilen, J. B., Panke, S., Lucchini, S., Franchini, A. G., Röthlisberger, M., and Witholt, B. (2001). Analysis of *Pseudomonas putida* alkane-degradation gene clusters and flanking insertion sequences: evolution and regulation of the *alk* genes. *Microbiology* 147, 1621–1630.
- van Beilen, J. B., Smiths, T. H. M., Roos, F. F., Brunner, T., Balada, S. B., Röthlisberger, M., et al. (2005). Identification of an amino acid position that determines the substrate range of integral membrane alkane hydroxylases. *J. Bact.* 187, 85–91. doi: 10.1128/JB.187.1.85-91.2005
- Vomberg, A., and Klinner, U. (2000). Distribution of *alkB* genes within n-alkane-degrading bacteria. *J. Appl. Microbiol.* 89, 339–348. doi: 10.1046/j.1365-2672.2000.01121.x
- Wang, L., Wang, W., Lai, Q., and Shao, Z. (2010a). Gene diversity of CYP153A and *AlkB* alkane hydroxylases in oil-degrading bacteria isolated from the Atlantic Ocean. *Environ. Microbiol.* 12, 1230–1242. doi: 10.1111/j.1462-2920.2010.02165.x
- Wang, W., Wang, L., and Shao, Z. (2010b). Diversity and abundance of oil-degrading bacteria and alkane hydroxylase (*alkB*) genes in the subtropical seawater of Xiamen Island. *Microb. Ecol.* 60, 429–439. doi: 10.1007/s00248-010-9724-4
- Wasmund, K., Burns, K. A., Kurtböke, I., and Bourne, D. G. (2009). Novel alkane hydroxylase gene (*alkB*) diversity in sediments associated with hydrocarbon seeps in the Timor Sea, Australia. *Appl. Environ. Microbiol.* 75, 7391–7398. doi: 10.1128/AEM.01370-09
- Yakimov, M. M., Golyshev, P. N., Lang, S., Moore, E. R. B., Abraham, W., Lünsdorf, H., et al. (1998). *Alcanivorax borkumensis* gen. nov., sp. nov., a new, hydrocarbon-degrading and surfactant-producing marine bacterium. *Int. J. Syst. Bacteriol.* 48, 339–348. doi: 10.1099/00207713-48-2-339
- Youngblood, W. W., and Blumer, M. (1975). Polycyclic aromatic hydrocarbons in the environment: homologous series in soils and recent marine sediments. *Geochim. Cosmochim. Acta* 39, 1303–1314. doi: 10.1016/0016-7037(75)90137-4

**Conflict of Interest Statement:** The authors declare that the research was conducted in the absence of any commercial or financial relationships that could be construed as a potential conflict of interest.

Received: 02 September 2013; accepted: 20 November 2013; published online: 12 December 2013.

Citation: Smith CB, Tolar BB, Hollibaugh JT and King GM (2013) Alkane hydroxylase gene (*alkB*) phylotype composition and diversity in northern Gulf of Mexico bacterioplankton. *Front. Microbiol.* 4:370. doi: 10.3389/fmicb.2013.00370

This article was submitted to Aquatic Microbiology, a section of the journal Frontiers in Microbiology.

Copyright © 2013 Smith, Tolar, Hollibaugh and King. This is an open-access article distributed under the terms of the Creative Commons Attribution License (CC BY). The use, distribution or reproduction in other forums is permitted, provided the original author(s) or licensor are credited and that the original publication in this journal is cited, in accordance with accepted academic practice. No use, distribution or reproduction is permitted which does not comply with these terms.



# Assessment of the Deepwater Horizon oil spill impact on Gulf coast microbial communities

**Regina Lamendella<sup>1,2\*</sup>, Steven Strutt<sup>2</sup>, Sharon Borglin<sup>1</sup>, Romy Chakraborty<sup>1</sup>, Neslihan Tas<sup>1</sup>, Olivia U. Mason<sup>1,3</sup>, Jenni Hultman<sup>1,4</sup>, Emmanuel Prestat<sup>1</sup>, Terry C. Hazen<sup>1,5,6</sup> and Janet K. Jansson<sup>1,7</sup>**

<sup>1</sup> Lawrence Berkeley National Laboratory, Earth Sciences Division, Ecology Department, Berkeley, CA, USA

<sup>2</sup> Biology Department, Juniata College, Huntingdon, PA, USA

<sup>3</sup> Department of Earth, Ocean and Atmospheric Science, Florida State University, Tallahassee, FL, USA

<sup>4</sup> Department of Food Hygiene and Environmental Health, University of Helsinki, Helsinki, Finland

<sup>5</sup> Department of Civil and Environmental Engineering, University of Tennessee, Knoxville, TN, USA

<sup>6</sup> Oak Ridge National Laboratory, Biosciences Division, Oak Ridge, TN, USA

<sup>7</sup> Department of Energy, Joint Genome Institute, Walnut Creek, CA, USA

**Edited by:**

Joel E. Kostka, Georgia Institute of Technology, USA

**Reviewed by:**

Peter Golyshin, Bangor University, UK

Kostas Konstantinidis, Georgia Institute of Technology, USA

**\*Correspondence:**

Regina Lamendella, Lawrence Berkeley National Laboratory, Earth Sciences Division, Ecology Department, 1 Cyclotron Road, Berkeley, CA 94720, USA  
e-mail: jrjansson@lbl.gov

One of the major environmental concerns of the Deepwater Horizon oil spill in the Gulf of Mexico was the ecological impact of the oil that reached shorelines of the Gulf Coast. Here we investigated the impact of the oil on the microbial composition in beach samples collected in June 2010 along a heavily impacted shoreline near Grand Isle, Louisiana. Successional changes in the microbial community structure due to the oil contamination were determined by deep sequencing of 16S rRNA genes. Metatranscriptomics was used to determine expression of functional genes involved in hydrocarbon degradation processes. In addition, potential hydrocarbon-degrading Bacteria were obtained in culture. The 16S data revealed that highly contaminated samples had higher abundances of *Alpha*- and *Gammaproteobacteria* sequences. Successional changes in these classes were observed over time, during which the oil was partially degraded. The metatranscriptome data revealed that PAH, n-alkane, and toluene degradation genes were expressed in the contaminated samples, with high homology to genes from *Alteromonadales*, *Rhodobacterales*, and *Pseudomonales*. Notably, *Marinobacter* (*Gammaproteobacteria*) had the highest representation of expressed genes in the samples. A *Marinobacter* isolated from this beach was shown to have potential for transformation of hydrocarbons in incubation experiments with oil obtained from the Mississippi Canyon Block 252 (MC252) well; collected during the Deepwater Horizon spill. The combined data revealed a response of the beach microbial community to oil contaminants, including prevalence of Bacteria endowed with the functional capacity to degrade oil.

**Keywords:** hydrocarbons, 16S rRNA gene, metatranscriptomics, oil spill, microbial communities

## INTRODUCTION

The Deepwater Horizon oil spill was the largest accidental marine oil spill in the history of the oil industry, spewing an estimated 4.1 million barrels of crude oil into the Gulf of Mexico (Zukunft, 2010). In addition, 1.84 million gallons of chemical dispersants were applied to assist in oil dispersal (The Federal Intragency Solutions Group: Oil Budget Calculator Science and Engineering Team, 2010). Physical barriers, direct collection from the well-head, skimming, and burning were also implemented in order to mitigate the effects of the spill. Despite significant efforts to protect hundreds of miles of beaches, wetlands, and estuaries from oil, it began washing up on the Gulf Coast by early May 2010 (OSAT-2, 2011). Most recent estimates indicate that up to 22% of the 4.1 million barrels of oil was either trapped under the surface of the water as sheen, carried on the water surface as conglomeration tar (Lubchenco et al., 2010; Kimes et al., 2013), or deposited onto surface sediments (US Coast Guard, USGS, and NOAA, 2010; Mason et al., 2014). Some of the oil washed ashore

where it was either collected or became entrained in sand and sediments. The contamination of beach ecosystems raised considerable concern due to the potential for detrimental environmental and economic impacts in the Gulf region (McCrea-Strub et al., 2011; Sumaila et al., 2012).

Initial research studies of the Gulf oil spill mainly focused on the fate of the oil in the water column. These studies highlighted the significant contribution of microorganisms toward the degradation of oil in a deep-sea hydrocarbon plume (Camilli et al., 2010; Hazen et al., 2010; Valentine et al., 2010, 2012; Redmond and Valentine, 2011; Baetur et al., 2012; Mason et al., 2012), and in particular a rapid response of members of the *Gammaproteobacteria* to hydrocarbon inputs. Specifically, there was an initial increase in relative abundance of members of the *Oceanospirillales* (Hazen et al., 2010; Redmond and Valentine, 2011; Mason et al., 2012), followed by members of the genera *Colwellia* and *Cycloclasticus* during later sampling periods (Redmond and Valentine, 2011; Valentine et al., 2012; Dubinsky et al., 2013).

Comparably less is known about the fate of the oil that reached the shore during the Deepwater Horizon spill. One study by Kostka et al. (2011) investigated the impact of the oil on beach samples collected several months after the spill occurred (July and September 2010) at municipal Pensacola Beach, Florida. By 16S rRNA gene sequencing, the authors found that the spill had a significant impact on the abundance and community composition of indigenous bacteria in beach sand with increases in many members of the *Alpha*- and *Gammaproteobacteria*, including some well-known hydrocarbon degraders (*Alcanivorax* and *Marinobacter*) (Yakimov et al., 1998; Alonso-Gutiérrez et al., 2009). In the same study, several proteobacterial isolates, capable of growth on oil as their sole carbon source, were obtained from the contaminated samples (Kostka et al., 2011).

Here we aimed to determine the response of indigenous beach microbial communities to the oil that washed ashore early in the spill history. We focused our efforts on Elmers's Beach, Grand Isle, LA. This location was one of the most heavily oiled beaches in the Gulf, where oil began washing up onto the beach in early May 2010 (OSAT-2, 2011). A total of 153 oil contaminated and uncontaminated samples were collected at three time points in June 2010, while the oil continued to accumulate on the beach. The well was finally capped on July 15, 2010 and declared sealed on September 19, 2010.

We performed targeted 16S rRNA gene sequencing and total RNA sequencing (metatranscriptomics) to determine the composition of the microbial community, as well as to elucidate which members were actively degrading hydrocarbons in oiled samples. In addition, we isolated putative MC252 oil degrading microorganisms and studied their potential for hydrocarbon degradation. This study revealed a succession in the microbial community structure on the beach during early time points in the Deepwater Horizon oil spill. This study also represents the first use of metatranscriptome data to highlight the expression of genes involved in hydrocarbon transformations in a coastline community.

## MATERIALS AND METHODS

### SAMPLE COLLECTION

Beach sand cores were collected on Elmer's Beach (29.1782853, -90.0684072) at three time points on 03/06/2010 ( $n = 7$ ), 21/06/2010 ( $n = 7$ ), and 29/06/2010 ( $n = 3$ ). Sand cores (10–20 cm deep) were taken by manual insertion of 40 cm long polybutyrate plastic liners into the sand. The cores were taken from locations submerged in the water close to the waterline, at the waterline, and inland. To circumvent potential contamination from the polybutyrate liners, each sand core was sub-cored using a 25 mm diameter sterile copper pipe, and sectioned into 3 cm depth intervals. Additionally, tar-like samples found on the surface of the beach ( $n = 24$ ) were collected at each sampling period by aseptically scraping approximately 2–10 g into sterile 50 mL conical tubes. All samples were kept on ice in the field and were maintained at 4°C until further processing. Detailed information about all the samples, relating to location, date, core depth, and hydrocarbon composition can be found in Supplemental Table S1.

### ACRIDINE ORANGE DIRECT COUNTS

Approximately 1 g of each sample was homogenized and diluted in 1X PBS. Samples were filtered through a 0.2  $\mu$ m pore size black polycarbonate membrane (Whatman International Ltd., Piscataway, NJ). Filtered cells were stained with 25 mg/mL acridine orange for 2 min in the dark. Unbound acridine orange was filtered through the membrane with 10 mL filter sterilized 1X PBS (Sigma Aldrich Corp., St. Louis, MI) and the rinsed membrane was mounted on a slide for microscopy. Cells were imaged with a FITC filter on a Zeiss Axioskop (Carl Zeiss, Inc., Germany).

### PETROLEUM HYDROCARBON CONCENTRATIONS

Total petroleum hydrocarbon (TPH) concentrations were determined using previously published procedures (Hazen et al., 2010) with the following modifications: 500  $\mu$ L of chloroform were added to 500 mg of sample and then vortexed thoroughly, shaken for 2 min and sonicated for 2 min. The samples were incubated at room temperature for 1 h, centrifuged at 2,000 rpm for 5 min, and 50  $\mu$ L of the extract was removed for analysis on an Agilent 6890N GC/FID (Santa Clara, CA). The GC was operated with an injector temperature of 250°C and detector temperature of 300°C, following a temperature program of 50°C for 2 min, ramped by 5°C/min until reaching 300°C and subsequently held for 15 min. TPH were quantified by integrating all the peaks from 20 to 60 min and comparing to oil standards (0–200 mg/L) obtained from the Macondo source well during the Deepwater Horizon spill.

PAH and alkane compound analysis was completed on the Agilent 6890N equipped with a 5972 mass selective detector and operated in SIM/SCAN mode. The injection temperature was 250°C, detector temperature was 300°C, and column used was 60 m Agilent HP-1 MS with a flow rate of 2 mL/min. The oven temperature program included a 50°C hold for 3 min ramped to 300°C at 4°C/min with a final 10 min hold at 300°C. Compound identification was determined from selective ion monitoring coupled with comparison to known standards and compound spectra in the NIST 08 MS library. Biomarker profiles were obtained by running the same samples in SIM mode targeting ions 191 for hopanes and 217 for steranes. Monitoring these ions has been widely used for oil source identification and degree of biodegradation (Venosa et al., 1997; Volkman et al., 1983; Greenwood and Georges, 1999; Hauser et al., 1999; Rosenbauer et al., 2010) and was utilized here to compare oil biomarker fingerprint to oil from the MC 252 source oil (Macondo crude). A proxy for biodegradation within the samples was calculated using the depletion of C<sub>25</sub> with respect to C<sub>17</sub> and the ratio of branched to aliphatic alkanes.

### DNA EXTRACTION

Samples were extracted in duplicate using a modified Miller DNA extraction method (Miller et al., 1999). Approximately 0.5 g of each sample was placed into an FT500-ND Pulse Tube (Pressure BioSciences, Inc., USA). 300  $\mu$ L of Miller phosphate buffer and 300  $\mu$ L of Miller SDS lysis buffer were added and mixed. 600  $\mu$ L phenol:chloroform:isoamyl alcohol (25:24:1) were then added, and the tubes were subjected to 25 cycles of 35,000 psi for 10 s and ambient pressure for 10 s, to improve cell lysis. The mixture was transferred to a Lysing Matrix E tube (MP Biomedicals,

Solon, OH) and subjected to bead-beating at 5.5 m/s for 45 s in a FastPrep (MP Biomedicals, Solon, OH) instrument. The tubes were centrifuged at 16,000 × g for 5 min at 4°C and 540 µL of supernatant was transferred to a 2 mL tube with addition of an equal volume of chloroform. Tubes were mixed and then centrifuged at 10,000 × g for 5 min, after which 400 µL of the aqueous phase was transferred to another tube and 2 volumes of Solution S3 (MoBio, Carlsbad, CA) were added and mixed by inversion. The subsequent clean-up methods were based on the MoBio Soil DNA extraction kit according to the manufacturer's instructions. Samples were recovered in 60 µL 10 mM Tris and stored at -20°C.

#### COMMUNITY PROFILING AND STATISTICAL METHODS

Small subunit (SSU) rRNA gene sequences were amplified from duplicate DNA extractions using the primer pair 926f/1392r as previously described (Kunin et al., 2010). The reverse primer included a 5 bp barcode for multiplexing of samples during sequencing. Emulsion PCR and sequencing of the PCR amplicons was performed at DOE's Joint Genome Institute following manufacturer's instructions for the Roche 454 GS FLX Titanium technology, with the exception that the final dilution was 1e-8 (Allgaier et al., 2010).

Sequence reads were submitted to the PyroTagger computational pipeline (Kunin and Hugenholtz, 2010) where the reads were quality filtered, trimmed, dereplicated and clustered at 97% sequence identity. OTU tables generated from Pyrotagger were then imported into the QIIME pipeline (Caporaso et al., 2010) for further analyses. The number of sequence reads in each sample varied, therefore, the dataset was rarified. Alpha diversity calculations were performed on rarified data.

Multivariate community analysis was performed within PCORD 5 software (McCune et al., 2002) using normalized OTU data (family-level and OTU level). OTUs found in less than two samples were removed. Outliers were removed from the dataset using PCORD 5 with a cutoff of two standard deviations. The Bray-Curtis distance measure was used for non-metric multidimensional scaling (nMDS). Pearson correlation coefficients were calculated for metadata variables and each axis of the nMDS.

#### RNA EXTRACTION, AMPLIFICATION, AND SEQUENCING

Total RNA was extracted from three of the oil contaminated samples as previously described (Kasai et al., 2001) and amplified using the Message Amp II-Bacteria Kit (Ambion, Austin, TX) following the manufacturer's instructions. First strand synthesis of cDNA from the resulting antisense RNA was carried out with the SuperScript III First Strand Synthesis System (Invitrogen, Carlsbad, CA). The SuperScript Double-Stranded cDNA Synthesis Kit (Invitrogen, Carlsbad, CA) was used to synthesize double stranded cDNA. cDNA was purified using a QIAquick PCR purification kit (Qiagen, Valencia, CA) and poly(A) tails were removed by digesting purified DNA with *Bpm*I for 3 h at 37°C. Digested cDNA was purified with QIAquick PCR purification kit (Qiagen, Valencia, CA). RNA was prepared for sequencing using the Illumina Truseq kit following the manufacturer's guidelines. Each library was sequenced on one lane of the Illumina HiSeq platform using the 150 bp Paired-end technology

resulting in a total of 57 Gb of sequence data for all three samples.

#### METATRANSCRIPTOMICS DATA ANALYSIS

Raw Illumina sequence reads from each of three surface-contaminated samples (one from each sampling date) were trimmed using the CLC Genomics Workbench v5.0.1 with a quality score limit of 0.05. Phred quality scores (Q) were imported into the genomics workbench, where they were converted to error probabilities, using  $p_{\text{error}} = 10^{Q/-10}$  and were trimmed using a limit of 0.05 as described in the CLC Workbench Manual (<http://www.clcbio.com>).

Sequences shorter than 50 bp in length and all adapter sequences were removed. To characterize the active microbial community members, unassembled reads were searched against the Greengenes (DeSantis et al., 2006) database of 16S rRNA genes using BLASTn with a bit score cutoff of >100.

Transcript profiles from each sample were determined by first subjecting trimmed unassembled reads from each sample to ORF calling using Prodigal (Hyatt et al., 2010). Resulting ORFs were compared to a translated in-house hydrocarbon gene database using BLASTp. This database was constructed using all KEGG genes involved in hydrocarbon degradation from the KEGG database (Kanehisa and Goto, 2000). For the resulting BLAST outputs, the highest bit score was selected (min bit score >40). Metatranscriptome data from each sample were normalized to RecA expression levels. A pairwise statistical comparison of the BLAST analyses was carried out using STAMP (Parks and Beiko, 2010) using a two-sided Chi-square test (with Yates correction) statistic with the DP: Asymptotic-CC confidence interval method and the Bonferroni multiple test correction. A p-value of < 0.05 was used with a double effect size filter (difference between proportions effect size < 1.00 and a ratio of proportions effect size < 2.00. The metatranscriptome from the June 29 sampling date yielded an insufficient number of transcripts after quality filtering, thus subsequent analyses of the metatranscriptome data focused on the June 3 and June 21 samples.

Paired-end Illumina reads from each of the June 3 and June 21 samples were assembled using the *De Novo* Assembly Tool within the CLC Genomics Workbench at a word size of 20 and a bubble size of 50. Reads were scaffolded onto the contigs, which were submitted to MG-RAST (Meyer et al., 2008) for annotation. In MG-RAST, functional tables were generated for each sample against the KO annotation database, using default parameters (1e-5 maximum e-value cutoff, 60% minimum sequence identity, and 15 bp of minimum alignment length). To determine which organisms express genes involved in hydrocarbon degradation, contigs for each enzyme mapping to a xenobiotic pathway were annotated against the M5NR database for best-hit organismal classification using the default parameters. Using default parameters for the best-hit classification tool in MG-RAST, contigs were annotated against the Greengenes database to further assess presence of microbial community members through 16S rRNA transcripts. Recruitment plots were generated using a maximum e-value cutoff of 1e-3 and a log<sub>2</sub> abundance scale. Contigs mapping to xenobiotic pathways were rarefied to a depth of 20,000 annotated contigs each. Xenobiotic degradation maps annotated

using Kegg Orthology (KO) were downloaded from the KEGG server in KGML format and manually colored using the KGML editor (Klukas and Schreiber, 2007). Charts were generated from the Krona template (Ondov et al., 2011).

Assembled data are publicly available in the MG-RAST database under project ID 7309. Raw reads were submitted to NCBI's sequence read archive under project ID SUB442498.

### ENRICHMENTS AND ISOLATIONS

Bacteria were isolated from sand cores and contaminated beach samples after incubation under aerobic conditions with 100 ppm Macondo oil (MC 252) in either Marine broth medium (Difco), Minimal marine medium (Baelum et al., 2012) or Synthetic minimal marine medium. Synthetic Minimal marine medium was prepared as follows: For 1 L, autoclaved separately 850 mL of 20 g NaCl, 0.67 g KCl, 10 mL each of mineral and vitamin mixes (Coates et al., 1995), 100 mL of 30 mM phosphate buffer (pH 7.5), and added to 50 mL of 10.1 MgCl<sub>2</sub>.6H<sub>2</sub>O + 1.52 g CaCl<sub>2</sub>. 2 H<sub>2</sub>O. Enrichments that resulted in an increase in turbidity, in addition to an increase in cell number by microscopic observations, were transferred periodically into fresh media. After 3–4 transfers, colonies were obtained by plating on the respective agar plates and were incubated for 1 week. Isolates were obtained from single colonies and incubated aerobically in modified Synthetic Seawater medium with 100 ppm MC252 oil as the sole carbon source. Within a few days, the oil initially observed as a thin layer floating on top disappeared with a concurrent increase in cell number. At this point, DNA was extracted from the cultures using the MoBio UltraClean Microbial DNA Isolation Kit (MoBio Inc, Carlsbad, CA). PCR amplification was conducted using universal bacterial 16S rRNA gene primers 27F and 1492R in 50  $\mu$ l reactions, with a final concentration of 0.025 unit/ $\mu$ l Taq, 0.2 mM dNTPs, 15 ng of DNA template, and 0.04  $\mu$ M primer. Initial denaturation was at 95°C for 180 s, followed by 25 cycles of melting at 95°C for 30 s, annealing at 54°C for 30 s, extension at 72°C for 60 s. This was followed by a final extension of 10 min at 72°C and samples were held at 4°C on completion of amplification. Verified 16S amplicons were purified using the procedure provided in the MoBio Ultraclean PCR Clean-up kit (MoBio, Carlsbad, CA). Samples were sequenced using the Applied Biosystems ABI 3730XL DNA Analyzers with the BigDye Terminator V3.1 Cycle Sequencing Kit (Applied Biosystems, Carlsbad, CA), according to the manufacturer's instructions.

### OIL DEGRADATION WITH ISOLATES

Different selective minimal media were prepared to test individual isolates for their ability to degrade oil, since the isolates belonged to different genera and had different nutritional requirements. *Marinobacter* isolate 33 was grown in MC252 oil amended with minimal marine media. *Roseobacter* isolate 36 was grown in modified Sistrom's Minimal Medium (Sistrom, 1962). Oil degradation experiments were set up in 30 mL of respective media amended with 20 ppm MC252 oil and 0.1 ppm COREXIT 9500, inoculated with the respective bacterial cultures, and incubated at room temperature in the dark. The inoculant was grown in the respective minimal medium amended with 0.1% Yeast extract to promote biomass. Prior to inoculation, cells were pelleted and washed in

phosphate buffer (pH 7.5) to remove any carry over of media constituents. Heat killed cells (autoclaved) were used as negative controls, by 10% inoculation into experimental bottles containing oil and media.

At periodic intervals during the incubations, experimental bottles were sacrificed for hydrocarbon analyses to determine the extent of oil degradation. All glassware used in extraction and analyses was muffled at 500°C for 4 h prior to use. To extract hydrocarbons, the entire culture volume (30 ml) was transferred from the experimental bottles to a 50 mL glass culture tube with a Teflon-lined lid. The empty bottles were extracted three times with 2 mL of chloroform (BDH, ACS grade) to assay hydrocarbons sorbed to the glass and the rinses were added to the 50 mL tube. This mixture was vortexed for 1 min and extracted for 1 h, after which they were re-vortexed and centrifuged at 2000 rpm for 15 min to aid the separation of the chloroform from the aqueous media layer. The chloroform layer was removed with a glass pipette into a GC vial and analyzed as described above.

## RESULTS

### STATE OF THE SAMPLING SITE

On June 3, 2010, the sampling site was almost completely covered to the tidal berm with viscous oil. Seawater washing up on the shore contained large, amorphous globules of oil. On June 21, 2010, the beach no longer contained visible globules of oil and the surface of the sampling site was no longer covered in oil. Instead, the oil present was in the form of small dried globules, less than 2 cm in diameter. By June 29, 2010, oil and oil mixed with foam were evident at the sampling site. The beach surface was rust in color and a light sheen of oil was noted on the seawater surface.

### CHEMICAL ANALYSIS

The hydrocarbon profiles of the beached oil and contaminated sand core samples showed a clear correspondence to the MC252 oil (Supplemental Figure. S1). Total petroleum hydrocarbons (TPH) ranged from 0 mg/kg to 2072 mg/kg. Several components in the oil decreased over time and were significantly depleted by June 21 and June 29 sampling dates. Specifically, there was a depletion of shorter alkanes ( $C_{17}$ – $C_{20}$ ) and a corresponding higher relative amount of longer chain alkanes ( $>C_{20}$ ) and branched alkanes. Cluster analysis of hydrocarbons revealed a clustering of the samples according to the level of hydrocarbon contamination (Supplemental Figure. S2). PAHs were detected in more than one third of the contaminated samples. Three-ring PAHs including, fluorene, anthracene, and phenanthracene and four-ring PAHs, including chrysene and pyrene, were highest in concentration of the measured PAH compounds, while naphthalene and other two-ring compounds were present in lower amounts and were nearly completely depleted in the less contaminated and uncontaminated samples from all time points (Supplemental Figure S2).

### MICROBIAL COMMUNITY ANALYSES

Cell counts ranged from  $10^5$  cells  $g^{-1}$  in uncontaminated samples to more than  $10^7$  cells  $g^{-1}$  in highly contaminated, beached oil samples and this difference was significant (*t*-test;  $p = 2.97 \times 10^{-5}$ ). Therefore, there was a significant increase in microbial cell

density as a result of the hydrocarbon influx on the beach, as previously reported by (Kostka et al., 2011).

We retrieved  $>1.6$  million non-chimeric, quality filtered 16S rRNA gene sequences from a total of 153 oiled and uncontaminated samples, yielding more than 11,000 sequences per sample. The sequence data were dominated by OTUs corresponding to *Alpha-* and *Gammaproteobacteria* (Figure 1). Several OTUs that were abundant in the oil-contaminated samples corresponded to taxa with members known to degrade hydrocarbons, including *Rhodobacteraceae*, *Alteromonadaceae*, *Pseudomonadaceae*, *Chromatiaceae*, *Alcanivoraceae*, and other families within the *Oceanospirillales*. Samples with the highest concentrations of hydrocarbons had higher relative abundances of *Alphaproteobacteria* (Figure 1).

Non-metric multidimensional scaling (nMDS) analysis revealed a pronounced response of the microbial community to oil contamination (Figure 2). Samples with high TPH concentrations clustered separately from less contaminated samples (Pearson correlation to Axis 1;  $r = 0.971$ ). In addition, the TPH concentration was inversely related to several alpha diversity measures (Figure 2 and Supplemental Figure S3). Co-inertia analyses revealed that the microbial communities differed significantly between the two types of contaminated samples: beached oil and oil-contaminated sand ( $p$ -value  $< 0.001$ ). The beached-oil samples also clustered separately by time (Pearson correlation to Axis 1;  $r = 0.869$ ), suggesting temporal shifts in the microbial community as a response to the oil spill (Figure 2B and Supplemental Table S2). The depletion in TPH was also positively correlated with time of sampling for all of the contaminated samples. Shifts in the microbial community aligned with continuous disappearance of hydrocarbons during the sampling period (Supplemental Table S2 and Table S3). Several PAHs and aliphatic hydrocarbon components were among the highest factors that correlated to Axis 2 on the nMDS plots (Figure 2C and Supplemental Table S3). Pearson correlations

revealed that *Rhodobacteraceae* and *Alteromonadaceae* were most highly correlated with hydrocarbon concentrations in the contaminated samples (Supplemental Table S4) with genus and species-specific differences within sand and beached oil matrices. For example, sequences with closest homology to *Rhodobacter* sp., *Jannachia* sp., and *Marinobacter luteoensis* had the highest correlation to beached oil samples (Supplemental Table S5), while *Ruegeria* sp., *Jannachia* sp., *Alishewanella baltica*, and *Pseudomonas pachastrella* correlated with contaminated sand samples (Supplemental Table S6). Of these highest correlating OTUs, the *Marinobacter* and *Pseudomonas* genera were the most prevalent and abundant OTUs in the dataset, comprising up to 7 and 4% of the total community, respectively. It should also be noted, that microbial community composition and hydrocarbon profiles were highly correlated (Mantel test;  $t > 0$ ,  $p = 0.00000$ ,  $r = 0.6104$ ).

## METATRANSCRIPTOMICS OF OIL CONTAMINATED SAMPLES

In order to assess which hydrocarbon degradation genes were expressed, we studied the metatranscriptomic profiles of representative heavily oiled samples. Approximately 380 million paired end sequences (57 Gb) were retrieved from three beached oil samples, one from each sampling date (June 3, June 21, June 29). Our goal was to determine what types of genes were expressed in the beach community as a whole in response to heavy oil contamination. We found that 40–67% of the quality filtered reads contained ribosomal RNA genes, which was not surprising considering rRNA depletion was not applied to these samples prior to sequencing, given the low RNA yields. When analyzing which taxa were most prevalent in the rRNA from the metatranscriptomes, we saw similar trends to the 16S rRNA microbial community analysis. Metatranscriptome data matching the Greengenes SSU database were dominated by the proteobacteria (74%), more specifically the *Alteromonadales* (30%), *Oceanospirillales* (11%), and the *Rhodobacterales* (8%). Further,

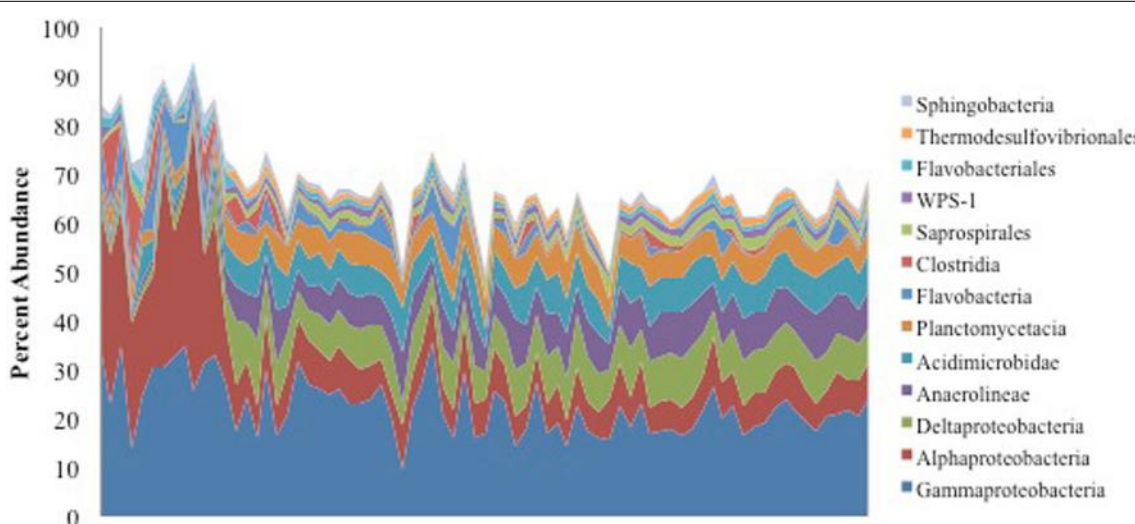


**FIGURE 1 |** Percent abundance of the 13 most abundant bacterial classes using 16S rRNA gene sequences. Samples are ordered from highest to lowest TPH concentration, left to right.

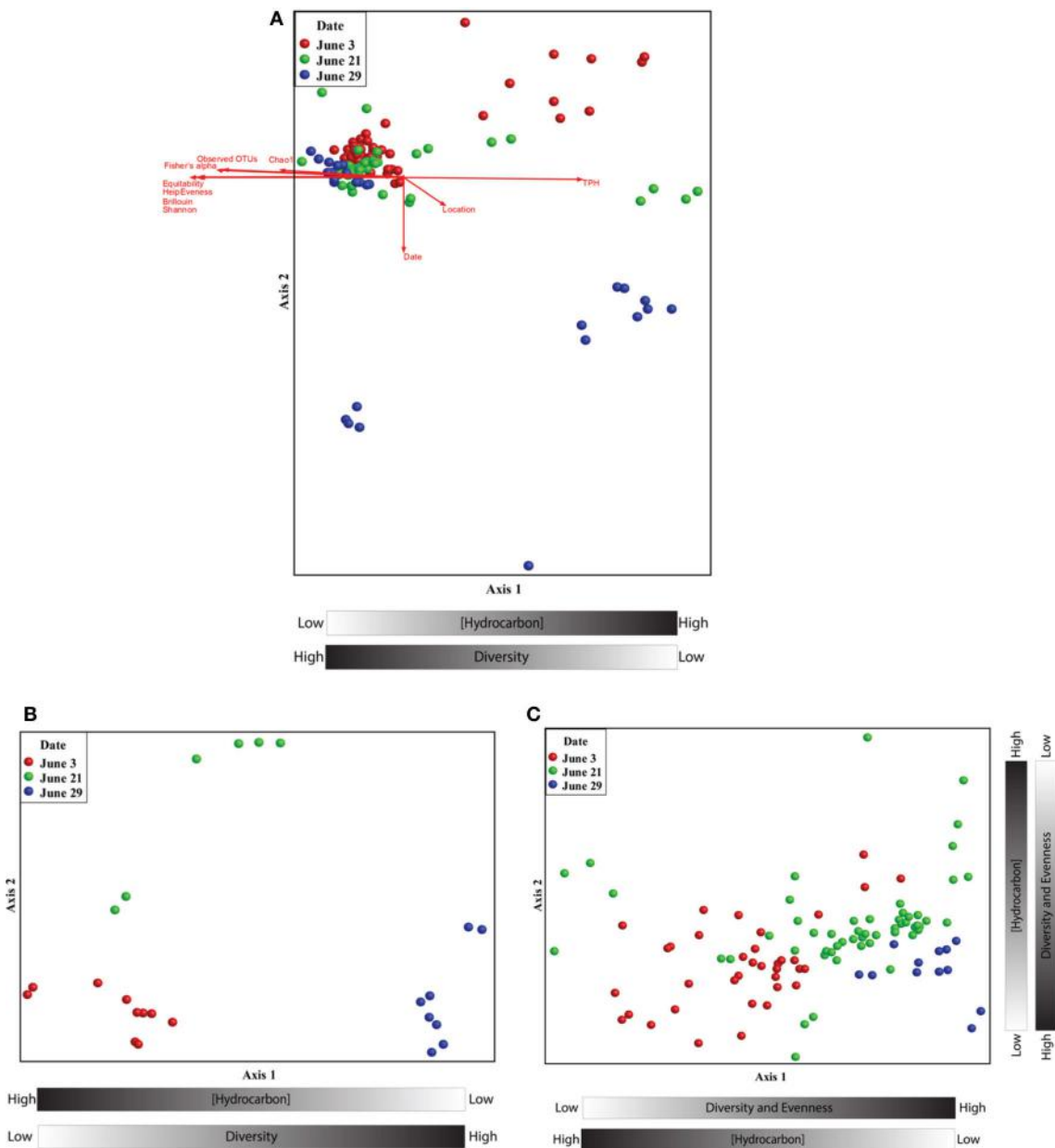


**FIGURE 2 | (A)** Non-metric multidimensional scaling ordination of beached oil and sand samples based on the relative abundance pyrotag sequences assigned to family-level taxonomy. The ordination plot was rotated to maximize the degree of correlation with the total petroleum hydrocarbon variable. A two dimensional solution was found and the final stress was 0.023. **(B)** Non-metric multidimensional scaling ordinations of beached oil based on the relative abundance pyrotag sequences assigned to family-level

taxonomy. The ordination plot was rotated to maximize the degree of correlation with the time variable. A two dimensional solution was found and the final stress was 0.039. **(C)** Non-metric multidimensional scaling ordinations of sand samples based on the relative abundance pyrotag sequences assigned to family-level taxonomy. The ordination plot was rotated to maximize the degree of correlation with the time variable. A two dimensional solution was found and the final stress was 0.086.

we found that when the metatranscriptome data were compared to the SSU Greengenes database, 19.2% of sequences annotated at the genus level matched to *Marinobacter*.

Even though the samples were dominated by ribosomal genes, more than 100 million of the quality filtered reads were available for functional gene annotation. Nearly 17 million of these reads matched to the hydrocarbon gene database. A total of 3553

different matches to the hydrocarbon database were retrieved from the metatranscriptomics data with an average of 2357 reads mapping to each hit. Comparison of the unassembled data to the hydrocarbon gene database revealed that enzymes involved in degradation of a variety of hydrocarbons, including PAHs were expressed; including a variety of monooxygenases and dioxygenases, and those involved in converting PAHs to dihydrodiols

(Supplemental Table S7). Genes involved in the pathway for gentisate and substituted gentisate degradation were also expressed. Gentisate is a central metabolite in the aerobic biodegradation of both simple and complex aromatic hydrocarbons.

Two of the metatranscriptomes were assembled (those from the June 3 and June 21 sampling dates) yielding approximately 350,000 and 150,000 contigs (>150 bp), respectively, (Supplemental Table S8) and the assemblies were also screened for hydrocarbon degradation genes. When the metatranscriptomes were searched for matches to reference genomes in the MG-RAST database, *Marinobacter aquaeolei* strain VT8 was the closest match (94% average identity) (Figure 3). The most abundant xenobiotic degradation transcripts and overall functional transcripts matching to this strain were cyclohexanone monooxygenase, naphthal-2-methylsuccinyl-CoA dehydrogenase, naphthal-2-methylsuccinyl-CoA dehydrogenase, 3-hydroxyacyl-CoA dehydrogenase/ enoyl-CoA hydratase, and a succinate dehydrogenase complex (Table 1). Genes involved in motility were amongst the most abundant features of all contigs mapping to *M. aquaeolei* and included the CheA signal transduction histidine kinase involved in chemotaxis signaling and a flagellar hook-associated 2 domain-containing protein (Table 1).

Besides *M. aquaeolei*, xenobiotic degradation transcripts mapped to several other *Proteobacteria* isolates in the MG-RAST database. For example, transcripts matched to PAH (Figure 4), *n*-alkane (Supplementary Figure S4A), and toluene degradation

genes, matching to sequenced organisms in the *Pseudomonadales*, *Burkholderiales*, and *Alteromonadales*. Additionally, PAH (Figure 4), toluene, and benzoate pathways (Supplemental Figure S4B) mapped to members of the *Rhodobacterales* and toluene and benzoate metabolism transcripts mapped to *Rhizobiales*. It should be noted, that comparing metatranscriptomic data to KEGG pathways and organisms does not ascribe a complete pathway to a particular organism.

### ISOLATION OF OIL DEGRADING STRAINS FROM THE CONTAMINATED BEACH SAMPLES

Enrichment with oil-contaminated samples from the sampling location resulted in isolation of 18 unique bacterial strains belonging almost entirely to the *Gammaproteobacteria*. 16S rRNA gene sequencing revealed that almost half of the isolates shared highest sequence homology to members of the *Pseudomonadales*, including *Pseudomonas stutzeri*, *Pseudomonas pachastrella*, and *Pseudomonas alcaligenes* (Table 2). Three isolates belonging to the *Marinobacter* genus were retrieved from the more contaminated samples. Isolates having >99% sequence homology to known *Alcanivorax*, *Vibrio*, *Rheinheimera*, and *Bacillus* sp. were also retrieved from these samples. Most of the isolates were halophilic, Gram-negative organisms, and showed the potential for degrading the MC252 oil.

Because of their high relative abundance in the 16S rRNA gene data in contaminated samples, two representative isolates, 33 (*Marinobacter* spp.) and 36 (*Roseobacter* spp.) were selected for their ability to grow using MC252 as the carbon source. Total hydrocarbons were extracted at selected time points and straight chain alkanes and PAHs (Figure 5) were depleted during the

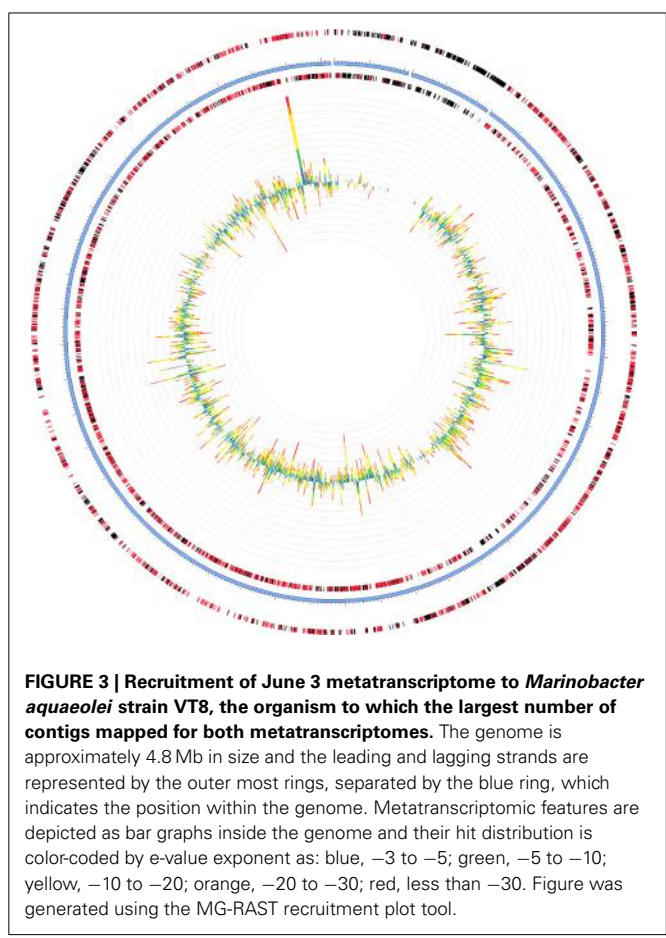


**Table 1 | Top xenobiotic and overall metatranscriptomic functions mapping to *Marinobacter aquaeolei*.**

Function	Relative abundance June 3*	Relative abundance June 21*
<b>XENOBIOTIC</b>		
Cyclohexanone monooxygenase	0.382	0.114
Naphthal-2-methylsuccinyl-CoA dehydrogenase	0.318	0.795
Glutathione S-transferase	0.255	0.000
3-hydroxyacyl-CoA dehydrogenase / enoyl-CoA hydratase	0.191	0.568
Succinate dehydrogenase	0.085	0.455
<b>OVERALL</b>		
CheA signal transduction histidine kinase	0.806	0.450
Flagellar hook-associated 2 domain-containing protein	0.467	0.340
Elongation factor Tu	0.042	1.023
Tetratricopeptide TPR_4	0.361	0.909

\*Relative abundances are percentages of total reads mapping to *Marinobacter aquaeolei*.

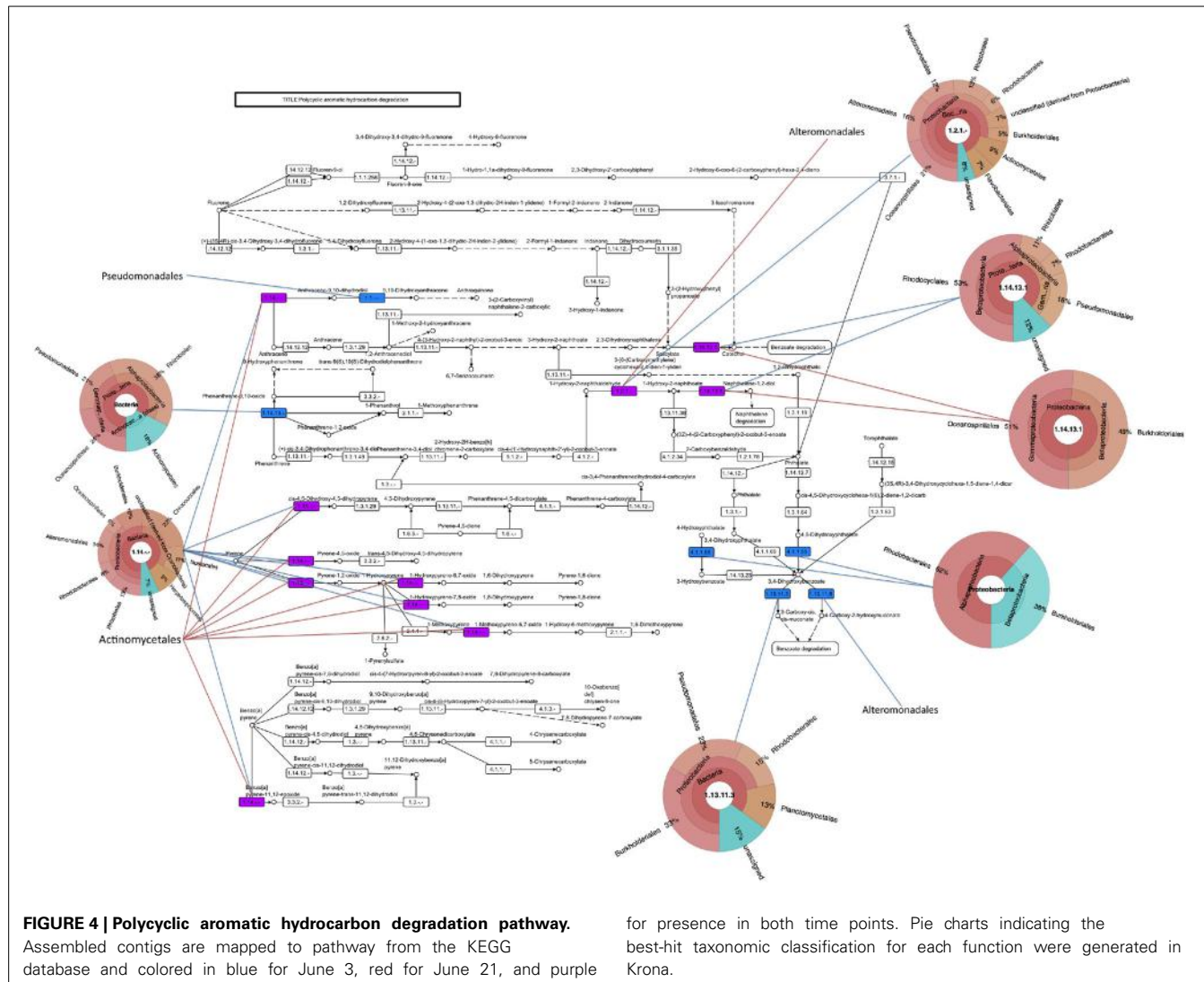


**FIGURE 4 | Polycyclic aromatic hydrocarbon degradation pathway.**

Assembled contigs are mapped to pathway from the KEGG database and colored in blue for June 3, red for June 21, and purple

for presence in both time points. Pie charts indicating the best-fit taxonomic classification for each function were generated in Krona.

incubations for both cultures, although longer alkanes (C25 and longer) persisted after 15 and 20 days of incubation, respectively (Supplemental Figure S5). It should be noted that the MC252 source oil used in the incubations was already depleted in the lighter hydrocarbons at the start of the incubation (Supplemental Figure S6).

## DISCUSSION

Macondo oil from the Deepwater Horizon oil spill that reached the shore of Elmer's Beach caused shifts in the indigenous microbial communities in the beach sand toward a hydrocarbon-degrading consortium. This observation is consistent with previous studies that have assessed the impact of oil spills on coastline microbial communities (Kasai et al., 2001; Maruyama et al., 2003; Medina-Bellver et al., 2005; Alonso-Gutiérrez et al., 2009; Vila et al., 2010; Kostka et al., 2011). Kostka et al. (2011) also reported that highly contaminated samples exhibited higher bacterial cell densities than uncontaminated samples, and that there was a significant reduction in bacterial diversity associated with oil contamination. Here, we found that the contaminated samples collected

from Elmer's Beach were generally dominated by *Alpha-* and *Gammaproteobacteria* (Figure 1) with up to 60% of the total microbial community being members of the *Alphaproteobacteria*. Other studies in the water column similarly reported a short-term shift of microbial communities toward specific members of the *Gammaproteobacteria* as an immediate response to crude oil inputs, which were then succeeded within 1 month by members of the *Alphaproteobacteria* (Abed et al., 2002; Röling et al., 2002; Hernandez-Raquet et al., 2006; Hazen et al., 2010; Redmond and Valentine, 2011; Valentine et al., 2012; Dubinsky et al., 2013).

Microbial community analysis revealed increases in the abundance of the *Rhodobacteraceae* and *Alteromonadaceae* in both the beached surface oil and contaminated beach sand samples. Therefore the different contaminated samples collected from the beach shared a similar bacterial community composition at the family level and exhibited parallel temporal successional changes in bacterial community structures driven by hydrocarbon inputs. During the first two sampling points, members of the *Alteromonadaceae*, with high sequence identity to *Marinobacter luteoensis*, were very abundant in samples with high

**Table 2 | Cultured Isolates retrieved from beached oil and contaminated beach sands.**

Isolate number	Sample source	Phylogenetic order	Closest relative in greengenes 16S rRNA gene database (accession no)	Similarity (%)
2	Sand	Vibrionales	<i>Vibrio</i> sp. str. QY102 (AY174868.1)	99.86
3	Sand	Pseudomonadales	<i>Pseudomonas</i> sp. MOLA 58 (AM990833.1)	99.64
4	Sand	Vibrionales	<i>Vibrio</i> sp. str. QY102 (AY174868.1)	99.79
8	Sand	Vibrionales	<i>Vibrio</i> sp. str. QY102 (AY174868.1)	99.79
11	Sand	Alteromonadales	<i>Marinobacter</i> sp. str. Libra (AY734434.1) or <i>Marinobacter hydrocarbonoclasticus</i> str. JL795 (EF512720.1)	99.93
12	Sand	Pseudomonadales	<i>Pseudomonas pachastrella</i> str. PTG4-14 (EU603457.1)	97.14
14	Sand	Pseudomonadales	<i>Pseudomonas</i> sp. Da2 (AY570696.1)	99.43
16	Sand	Pseudomonadales	<i>Pseudomonas stutzeri</i> str. A1501 (NC_009434.1)	100
18	Sand	Bacillales	<i>Bacillus</i> sp. str. NRRL B-14911 (AAOX01000059.1)	99.72
19	Sand	Pseudomonadales	<i>Pseudomonas pseudoalcaligenes</i> str. 14 (AB276371.1)	99.86
23	Sand	Chromatiales	<i>Rheinheimera</i> sp. 97(2010) str. 97 (HM059656.1)	99.64
25	Sand	Alteromonadales	<i>Marinobacter</i> sp. str. Libra (AY734434.1) or <i>Marinobacter hydrocarbonoclasticus</i> str. JL795 (EF512720.1)	99.79
26	Sand	Pseudomonadales	<i>Pseudomonas pseudoalcaligenes</i> str. 14 (AB276371.1)	98.58
31	Beached oil	Oceanospirillales	<i>Alcanivorax</i> sp. str. Abu-1 (AB053129.1)	99.64
32	Beached oil	Pseudomonadales	<i>Pseudomonas</i> sp. str. BJQ-B3 (FJ600357.1)	94.52
33	Beached oil	Alteromonadales	<i>Marinobacter</i> sp. Str. NT N31 (AB166980.1)	98.32
35	Beached oil	Rhodobacterales	<i>Citreicella thiooxidans</i> str. 2PR57-8 (EU440958.1)	99.77
36	Beached oil	Rhodobacterales	<i>Roseobacter</i> sp. str. 49Xb1 (EU090129.1)	99.93

TPH concentrations. Members of the *Marinobacter* genus have previously been shown to be capable of degradation of both alkanes and PAH compounds with some isolates growing on single PAHs as their sole carbon source (Huu et al., 1999; Cohen, 2002; Shieh et al., 2003; Nicholson and Fathepure, 2004; Gerdes et al., 2005; Márquez and Ventosa, 2005; Brito et al., 2006; Gu et al., 2007; Cui et al., 2008; Rosano-Hernández and Fernández-Linares, 2009; Vila et al., 2010; Wu et al., 2010; Dos Santos et al., 2011). Here we also successfully isolated *Marinobacter* strains from contaminated beach samples, which were capable of growth on MC252 oil as their sole carbon source. Several previous studies have reported the role of *Marinobacter* in degradation of oil (Gerdes et al., 2005; Vila et al., 2010; Kostka et al., 2011). The potential biodegradation of oil by these isolates at ambient temperature further supports their potential for natural biodegradation of oil *in situ* (Figure 5). However, it should be noted that further work is needed to determine the exact nature of the hydrocarbon transformations that occurred during the incubations and whether they were mineralized or transformed to other metabolites.

Several bacterial taxa within the *Rhodobacteraceae* were abundant in the highly contaminated samples. The *Rhodobacteraceae* are metabolically and ecologically diverse, comprised of photoheterotrophs that can grow, either, photoautotropically or chemotrophically, as well as chemoorganotrophs, fermenters, and methylotrophs. Several members of the *Rhodobacteraceae* have previously been identified in oil polluted soils and marine environments and in fact have been shown to dominate oil polluted environments of the North Sea (Brakstad and Lødeng, 2005) and Southeast Asia (Harwati et al., 2008, 2009a,b). A few studies have demonstrated that the addition of photosynthetic bacteria to

oil-polluted wastewater and soil triggers an increase in the abundance of hydrocarbon-oxidizing bacteria and thus enhances the rate of oil degradation (Martínez-Alonso et al., 2004; Llirós et al., 2008). Additionally, our cultivation-based experiments revealed that one representative of the *Rhodobacteraceae*, *Roseobacter* isolate 36, was also able to grow on MC252 as its sole carbon source. Overall, our data suggested oil degradation on the surface of beach sand that is exposed to light may have been promoted naturally by increases in photosynthetic populations.

Additionally many *Pseudomonas* species, having highest sequence homology to *P. pachastrella*, were abundant in our 16S rRNA gene and cultivation experiments. Incidentally, similar pseudomonas strains were enriched from beach sands in the aftermath of both the Prestige oil spill in Northwestern Spain (Mulet et al., 2011) and other contaminated coastal sites during the Deepwater Horizon spill (Kostka et al., 2011) and these strains were shown to be central to the biodegradation of both aliphatic and aromatic hydrocarbons. Additionally, members of the *Alcanivorax* were abundant in the oil contaminated samples, corroborating previous 16S rRNA-based studies (Kasai et al., 2002; Kostka et al., 2011; Chakraborty et al., 2012).

Metatranscriptome analyses revealed that members of the *Alpha-* and *Gammaproteobacteria* were active in hydrocarbon degradation. This is the first study to determine functional genes involved in hydrocarbon degradation that were expressed in beach samples during the Deepwater Horizon spill. This study highlighted that metatranscriptomic data mapped to hydrocarbon degrading genes, including those involved in PAH, benzoate, and *n*-alkane degradation from *Alteromonadales*, *Pseudomonas*, and *Rhodobacterales* genomes. Data also mapped to other hydrocarbon degradation genes, including monooxygenases,

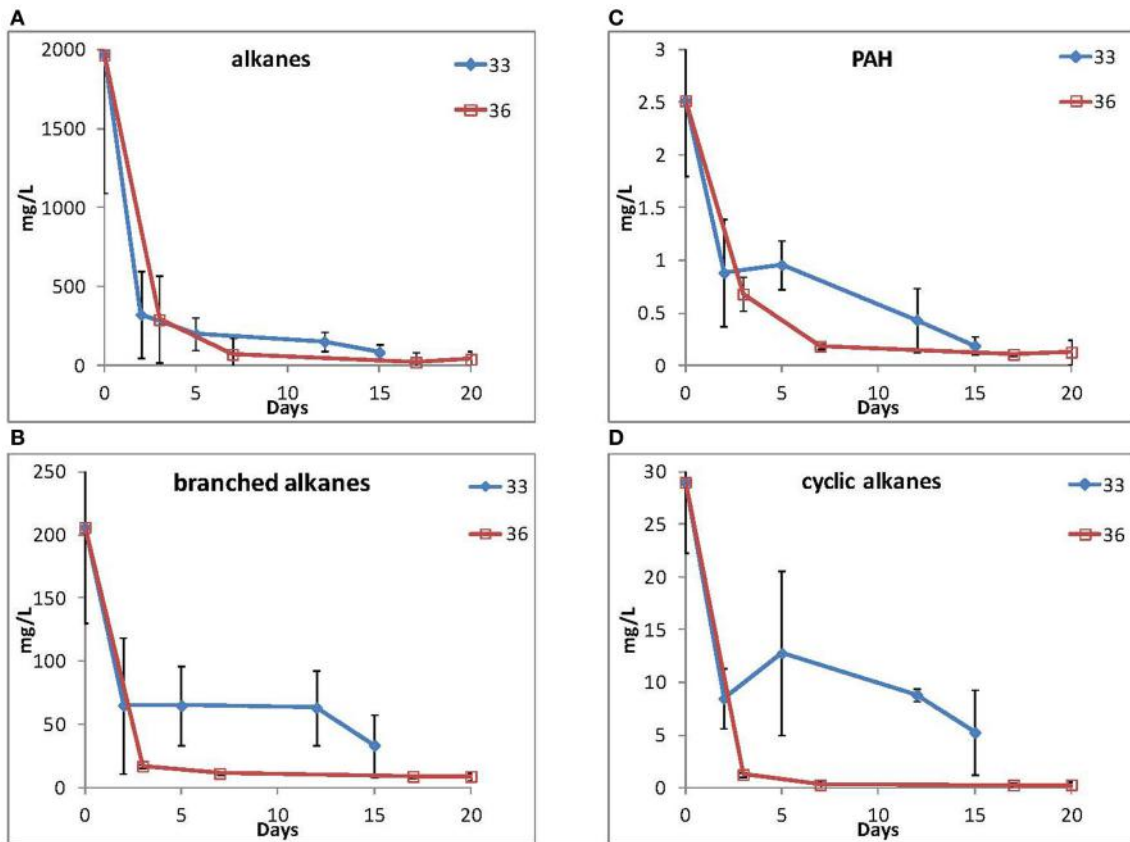


**FIGURE 5 |** Loss of (A) straight alkanes, (B) branched alkanes, (C) PAHs, and (D) cyclic alkanes during incubation by isolate 33 (*Marinobacter spp.*) and isolate 36 (*Roseobacter spp.*).

dioxygenases, dehydrogenases, and hydratases, from members of these microbial classes. While this analysis doesn't necessarily ascribe a complete pathway to a particular organism, these results suggest that not only are these microorganisms abundant in the beach microbial community as suggested by the 16S rRNA gene data, but they may also play an active role in hydrocarbon degradation.

*Marinobacter aquaeolei* strain VT8 was the bacterium in the reference genome database that had the highest abundance of expressed genes in the oil contaminated samples, including those for cyclohexanone monooxygenase and naphthalyl-2-methylsuccinyl-CoA dehydrogenase. In addition, transcripts for genes involved in chemotaxis and cellular motility mapped to *Marinobacter* suggesting that there was an active response to the hydrocarbon contamination in the beach communities, similar to the response observed for *Oceanospirillales* that were detected in the deep-sea plume (Mason et al., 2012). The high levels of gene expression observed for *Marinobacter* in the beach metatranscriptome data was supported by the finding that members of this genus were also enriched in the 16S rRNA data. In addition, we successfully isolated a representative of *Marinobacter* from the contaminated beach samples and demonstrated the ability of the isolate to degrade MC252 oil. These data suggest that *Marinobacter* may have played a key role in degradation of the

oil that reached the coast during the Deepwater Horizon oil spill.

## CONCLUSIONS

During the Deepwater Horizon oil spill, MC252 oil originating from the Macondo well reached the coastline and Elmer's Beach was heavily impacted by the oil in June 2010, during which time we collected samples. Oil deposited on the shore appeared to cause a shift in the community structure toward a hydrocarbonoclastic consortia, as 16S rRNA gene sequencing demonstrated a diverse array of known petroleum hydrocarbon degrading microorganisms in these samples. Interestingly, several OTUs representative of previously described oil-degrading phototrophs were abundant in the heavily oiled samples from the first two sampling periods and these were succeeded by a diverse array of other potential oil-degrading bacteria. Metatranscriptome profiling revealed that members of the *Alpha-* and *Gammaproteobacteria* expressed genes for hydrocarbon degradation in the contaminated samples, suggesting that they played a key role in potential degradation processes. Of note, *Marinobacter* were abundant members of the community in the oil-contaminated samples and expressed genes for degradation of hydrocarbons. Compared to other oil spills that have impacted shorelines, such as the *Prestige* oil spill that occurred in

a cold pristine habitat, the disappearance of MC252 oil seemed more rapid. This difference in microbial response could be due to differences in temperatures between the two sites as well as differences in other environmental variables, including previous exposure to oil spills. Overall, this study of the microbial community response on the Gulf shoreline may assist in the understanding of microbial proxies for oil contamination in similar coastal ecosystems.

## AUTHOR CONTRIBUTIONS

Regina Lamendella, Janet K. Jansson, and Terry C. Hazen were responsible for study conception and design. Regina Lamendella, Steven Strutt, and Janet K. Jansson were responsible for manuscript preparation. Sharon Borglin was responsible for chemical analyses. Romy Chakraborty was responsible for cultivation experiments. Regina Lamendella and Jenni Hultman were responsible for 16S RNA gene and metatranscriptomics experiments. Regina Lamendella, Steven Strutt, Olivia U. Mason, Emmanuel Prestat, and Neslihan Tas were responsible for bioinformatics and biostatistical analyses.

## ACKNOWLEDGMENTS

This work was supported by a subcontract from the University of California at Berkeley, Energy Biosciences Institute to Lawrence Berkeley National Laboratory under its U.S. Department of Energy contract DE-AC02-05CH11231. The Energy Biosciences Institute to UC Berkeley is supported by a grant from British Petroleum. We acknowledge support from Theresa Pollard, Yvette Piceno and Dominique Joyner with ordering, and transportation of supplies and samples to and from the field.

## SUPPLEMENTARY MATERIAL

The Supplementary Material for this article can be found online at: <http://www.frontiersin.org/journal/10.3389/fmicb.2014.00130/abstract>

## REFERENCES

- Abed, R. M. M., Safi, N. M. D., Köster, J., Beer, D. de, El-Nahhal, Y., Rullkötter, J. et al. (2002). Microbial diversity of a Heavily polluted microbial mat and its community changes following degradation of petroleum compounds. *Appl. Environ. Microbiol.* 68, 1674–1683. doi: 10.1128/AEM.68.4.1674-1683.2002
- Allgaier, M., Reddy, A., Park, J. I., Ivanova, N., D'haeseleer, P., Lowry, S. et al. (2010). Targeted discovery of glycoside hydrolases from a switchgrass-adapted compost community. *PLoS ONE* 5:e8812. doi: 10.1371/journal.pone.0008812
- Alonso-Gutiérrez, J., Figueras, A., Albaiges, J., Jiménez, N., Viñas, M., Solanas, A. M., et al. (2009). Bacterial communities from shoreline environments (Costa da Morte, Northwestern Spain) affected by the prestige oil spill. *Appl. Environ. Microbiol.* 75, 3407–3418. doi: 10.1128/AEM.01776-08
- Baelum, J., Borglin, S., Chakraborty, R., Fortney, J. L., Lamendella, R., Mason, O. U., et al. (2012). Deep-sea bacteria enriched by oil and dispersant from the Deepwater Horizon spill. *Environ. Microbiol.* 14, 2405–2416. doi: 10.1111/j.1462-2920.2012.02780.x
- Brakstad, O. G., and Lødeng, A. G. G. (2005). Microbial diversity during biodegradation of crude oil in seawater from the North Sea. *Microb. Ecol.* 49, 94–103. doi: 10.1007/s00248-003-0225-6
- Brito, E. M. S., Guyoneaud, R., Goñi-Urriza, M., Ranchou-Peyruse, A., Verbaere, A., Crapez, M. A. C., et al. (2006). Characterization of hydrocarbonoclastic bacterial communities from mangrove sediments in Guanabara Bay, Brazil. *Res. Microbiol.* 157, 752–762. doi: 10.1016/j.resmic.2006.03.005
- Camilli, R., Reddy, C. M., Yoerger, D. R., Van Mooy, B. A. S., Jakuba, M. V., Kinsey, J. C., et al. (2010). Tracking hydrocarbon plume transport and biodegradation at deepwater horizon. *Science* 330, 201–204. doi: 10.1126/science.1195223
- Caporaso, J. G., Kuczynski, J., Stombaugh, J., Bittinger, K., Bushman, F. D., Costello, E. K., et al. (2010). QIIME allows analysis of high-throughput community sequencing data. *Nat. Methods* 7, 335–336. doi: 10.1038/nmeth.f.303
- Chakraborty, R., Borglin, S. E., Dubinsky, E. A., Andersen, G. L., and Hazen, T. C. (2012). Microbial Response to the MC-252 Oil and Corexit 9500 in the Gulf of Mexico. *Front. Microbiol.* 3:357. doi: 10.3389/fmicb.2012.00357
- Coates, J. D., Lonergan, D. J., Philips, E. J. P., Jenter, H., and Lovley, D. R. (1995). *Desulfuromonas palmitatis* sp. nov., a marine dissimilatory Fe(III) reducer that can oxidize long-chain fatty acids. *Arch. Microbiol.* 164, 406–413. doi: 10.1007/BF0259738
- Cohen, Y. (2002). Bioremediation of oil by marine microbial mats. *Int. Microbiol.* Off. J. Span. Soc. Microbiol.
- Cui, Z., Lai, Q., Dong, C., and Shao, Z. (2008). Biodiversity of polycyclic aromatic hydrocarbon-degrading bacteria from deep sea sediments of the Middle Atlantic Ridge. *Environ. Microbiol.* 10, 2138–2149. doi: 10.1111/j.1462-2920.2008.01637.x
- DeSantis, T. Z., Hugenholtz, P., Larsen, N., Rojas, M., Brodie, E. L., Keller, K., et al. (2006). Greengenes, a Chimera-Checked 16S rRNA gene database and workbench compatible with ARB. *Appl. Environ. Microbiol.* 72, 5069–5072. doi: 10.1128/AEM.03006-05
- Dos Santos, H. F., Cury, J. C., do Carmo, F. L., dos Santos, A. L., Tiedje, J., van Elsas, J. D., et al. (2011). Mangrove bacterial diversity and the impact of oil contamination revealed by pyrosequencing: bacterial proxies for oil pollution. *PLoS ONE* 6:e16943. doi: 10.1371/journal.pone.0016943
- Dubinsky, E. A., Conrad, M. E., Chakraborty, R., Bill, M., Borglin, S. E., Hollibaugh, J. T., et al. (2013). Succession of hydrocarbon-degrading bacteria in the aftermath of the deepwater horizon oil spill in the Gulf of Mexico. *Environ. Sci. Technol.* 47, 10860–10867. doi: 10.1021/es401676y
- Gerdes, B., Brinkmeyer, R., Dieckmann, G., and Helmke, E. (2005). Influence of crude oil on changes of bacterial communities in Arctic sea-ice. *FEMS Microbiol. Ecol.* 53, 129–139. doi: 10.1016/j.femsec.2004.11.010
- Greenwood, P. F., and Georges, S. C. (1999). Mass spectral characteristics of C19 and C20 tricyclic terpanes detected in Latrobe tasmanite oil shale. *Eur. Mass Spectrom.* 5, 221–230. doi: 10.1255/ejms.278
- Gu, J., Cai, H., Yu, S.-L., Qu, R., Yin, B., Guo, Y.-F., et al. (2007). *Marinobacter gudaonensis* sp. nov., isolated from an oil-polluted saline soil in a Chinese oilfield. *Int. J. Syst. Evol. Microbiol.* 57, 250–254. doi: 10.1099/ij.s.0.64522-0
- Harwati, T. U., Kasai, Y., Kodama, Y., Susilaningsih, D., and Watanabe, K. (2008). *Tranquillimonas alkalinivorans* gen. nov., sp. nov., an alkane-degrading bacterium isolated from Semarang Port in Indonesia. *Int. J. Syst. Evol. Microbiol.* 58, 2118–2121. doi: 10.1099/ij.s.0.65817-0
- Harwati, T. U., Kasai, Y., Kodama, Y., Susilaningsih, D., and Watanabe, K. (2009a). *Tropicibacter naphthalenivorans* gen. nov., sp. nov., a polycyclic aromatic hydrocarbon-degrading bacterium isolated from Semarang Port in Indonesia. *Int. J. Syst. Evol. Microbiol.* 59, 392–396. doi: 10.1099/ij.s.0.65821-0
- Harwati, T. U., Kasai, Y., Kodama, Y., Susilaningsih, D., and Watanabe, K. (2009b). *Tropicimonas isoalkanivorans* gen. nov., sp. nov., a branched-alkane-degrading bacterium isolated from Semarang Port in Indonesia. *Int. J. Syst. Evol. Microbiol.* 59, 388–391. doi: 10.1099/ij.s.0.65822-0
- Hauser, A., Dashti, H., and Khan, Z. H. (1999). Identification of biomarker compounds in selected Kuwait crude oils. *Fuel* 78, 1483–1488. doi: 10.1016/S0016-2361(99)00075-7
- Hazen, T. C., Dubinsky, E. A., DeSantis, T. Z., Andersen, G. L., Piceno, Y. M., Singh, N., et al. (2010). Deep-sea oil plume enriches indigenous oil-degrading bacteria. *Science* 330, 204–208. doi: 10.1126/science.1195979
- Hernandez-Raquet, G., Budzinski, H., Caumette, P., Dabert, P., Le Ménach, K., Muyzer, G., et al. (2006). Molecular diversity studies of bacterial communities of oil polluted microbial mats from the Etang de Berre (France). *FEMS Microbiol. Ecol.* 58, 550–562. doi: 10.1111/j.1574-6941.2006.00187.x
- Huu, N. B., Denner, E. B., Ha, D. T., Wanner, G., and Stan-Lotter, H. (1999). *Marinobacter aquaeolei* sp. nov., a halophilic bacterium isolated from a Vietnamese oil-producing well. *Int. J. Syst. Bacteriol.* 49(Pt 2), 367–375.
- Hyatt, D., Chen, G.-L., LoCascio, P. F., Land, M. L., Larimer, F. W., and Hauser, L. J. (2010). Prodigal: prokaryotic gene recognition and translation initiation site identification. *BMC Bioinformatics* 11:119. doi: 10.1186/1471-2105-11-119

- Kanehisa, M., and Goto, S. (2000). KEGG: kyoto encyclopedia of genes and genomes. *Nucleic Acids Res.* 28, 27–30. doi: 10.1093/nar/28.1.27
- Kasai, Y., Kishira, H., Sasaki, T., Syutsubo, K., Watanabe, K., and Harayama, S. (2002). Predominant growth of Alcanivorax strains in oil-contaminated and nutrient-supplemented sea water. *Environ. Microbiol.* 4, 141–147. doi: 10.1046/j.1462-2920.2002.00275.x
- Kasai, Y., Kishira, H., Syutsubo, K., and Harayama, S. (2001). Molecular detection of marine bacterial populations on beaches contaminated by the Nakhodka tanker oil-spill accident. *Environ. Microbiol.* 3, 246–255. doi: 10.1046/j.1462-2920.2001.00185.x
- Kimes, N. E., Callaghan, A. V., Aktas, D. F., Smith, W. L., Sunner, J., Golding, B., et al. (2013). Metagenomic analysis and metabolite profiling of deep-sea sediments from the Gulf of Mexico following the Deepwater Horizon oil spill. *Front. Microbiol.* 4:50. doi: 10.3389/fmicb.2013.00050
- Klukas, C., and Schreiber, F. (2007). Dynamic exploration and editing of KEGG pathway diagrams. *Bioinformatics* 23, 344–350. doi: 10.1093/bioinformatics/btl611
- Kostka, J. E., Prakash, O., Overholt, W. A., Green, S. J., Freyer, G., Canion, A., et al. (2011). Hydrocarbon-degrading bacteria and the bacterial community response in Gulf of Mexico beach sands impacted by the deepwater horizon oil spill. *Appl. Environ. Microbiol.* 77, 7962–7974. doi: 10.1128/AEM.05402-11
- Kunin, V., and Hugenholtz, P. (2010). PyroTagger: a fast, accurate pipeline for analysis of rRNA amplicon pyrosequence data. *Open J.* 1, 1–8. Available online at: [http://www.theopenjournal.org/toj\\_articles/1](http://www.theopenjournal.org/toj_articles/1)
- Kunin, V., Engelbrektson, A., Ochman, H., and Hugenholtz, P. (2010). Wrinkles in the rare biosphere: pyrosequencing errors can lead to artificial inflation of diversity estimates. *Environ. Microbiol.* 12, 118–123. doi: 10.1111/j.1462-2920.2009.02051.x
- Llirós, M., Gajú, N., de Oteyza, T. G., Grimalt, J. O., Esteve, I., and Martínez-Alonso, M. (2008). Microcosm experiments of oil degradation by microbial mats. II. The changes in microbial species. *Sci. Total Environ.* 393, 39–49. doi: 10.1016/j.scitotenv.2007.11.034
- Lubchenco, J., McNutt, M., Lehr, B., Sogge, M., Miller, M., Hammond, S., et al. (2010). Deepwater Horizon/BP Oil Budget: What Happened to the Oil? Available online at: [http://www.noaanews.noaa.gov/stories2010/PDFs/OilBudget\\_description\\_%2083final.pdf](http://www.noaanews.noaa.gov/stories2010/PDFs/OilBudget_description_%2083final.pdf)
- Márquez, M. C., and Ventosa, A. (2005). *Marinobacter hydrocarbonoclasticus* Gauthier et al. 1992 and *Marinobacter aquaeolei* Nguyen et al. 1999 are heterotypic synonyms. *Int. J. Syst. Evol. Microbiol.* 55, 1349–1351. doi: 10.1099/ijss.0.63591-0
- Martínez-Alonso, M., de Oteyza, T. G., Llirós, M., Munill, X., Muyzer, G., Esteve, I., et al. (2004). Diversity shifts and crude oil transformation in polluted microbial mat microcosms. *Ophelia* 58, 205–216. doi: 10.1080/00785236.2004.10410228
- Maruyama, A., Ishiwata, H., Kitamura, K., Sunamura, M., Fujita, T., Matsuo, M., et al. (2003). Dynamics of microbial populations and strong selection for *Cycloclasticus pugettii* following the Nakhodka oil spill. *Microb. Ecol.* 46, 442–453. doi: 10.1007/s00248-002-3010-z
- Mason, O. U., Hazen, T. C., Borglin, S., Chain, P. S. G., Dubinsky, E. A., Fortney, J. L., et al. (2012). Metagenome, metatranscriptome and single-cell sequencing reveal microbial response to Deepwater Horizon oil spill. *ISME J.* 6, 1715–1727. doi: 10.1038/ismej.2012.59
- Mason, O. U., Scott, N. M., Gonzalez, A., Robbins-Pianka, A., Bælum, J., Kimbrel, J., et al. (2014). Metagenomics reveals sediment microbial community response to Deepwater Horizon oil spill. *ISME J.* doi: 10.1038/ismej.2013.254. [Epub ahead of print].
- McCrea-Strub, A., Kleisner, K., Sumaila, U. R., Swartz, W., Watson, R., Zeller, D., et al. (2011). Potential impact of the Deepwater Horizon oil spill on commercial fisheries in the Gulf of Mexico. *Fisheries* 36, 332–336. doi: 10.1080/03632415.2011.589334
- McCune, B., Grace, J. B., and Urban, D. L. (2002). *Analysis of Ecological Communities*. Corvallis, OR: MjM Software Design.
- Medina-Bellver, J. I., Marín, P., Delgado, A., Rodríguez-Sánchez, A., Reyes, E., Ramos, J. L., et al. (2005). Evidence for *in situ* crude oil biodegradation after the prestige oil spill. *Environ. Microbiol.* 7, 773–779. doi: 10.1111/j.1462-2920.2005.00742.x
- Meyer, F., Paarmann, D., D'Souza, M., Olson, R., Glass, E. M., Kubal, M., et al. (2008). The metagenomics RAST server – a public resource for the automatic phylogenetic and functional analysis of metagenomes. *BMC Bioinformatics* 9:386. doi: 10.1186/1471-2105-9-386
- Miller, D. N., Bryant, J. E., Madsen, E. L., and Ghiorse, W. C. (1999). Evaluation and optimization of DNA Extraction and purification procedures for soil and sediment samples. *Appl. Environ. Microbiol.* 65, 4715–4724.
- Mulet, M., David, Z., Nogales, B., Bosch, R., Lalucat, J., and García-Valdés, E. (2011). Pseudomonas diversity in crude-oil-contaminated intertidal sand samples obtained after the prestige oil spill. *Appl. Environ. Microbiol.* 77, 1076–1085. doi: 10.1128/AEM.01741-10
- Nicholson, C. A., and Fathepure, B. Z. (2004). Biodegradation of benzene by halophilic and halotolerant bacteria under aerobic conditions. *Appl. Environ. Microbiol.* 70, 1222–1225. doi: 10.1128/AEM.70.2.1222-1225.2004
- Ondov, B. D., Bergman, N. H., and Phillippy, A. M. (2011). Interactive metagenomic visualization in a Web browser. *BMC Bioinformatics* 12:385. doi: 10.1186/1471-2105-12-385
- OSAT-2. (2011). *Summary Report for Fate and Effects of Remnant Oil in the Beach Environment*. Operational Science Advisory Team, Deepwater Horizon MC252. Prepared for Federal On-Scene Coordinator. Available online at: [http://www.dep.state.fl.us/deepwaterhorizon/files2/osat\\_2\\_report\\_\\_10feb.pdf](http://www.dep.state.fl.us/deepwaterhorizon/files2/osat_2_report__10feb.pdf)
- Parks, D. H., and Beiko, R. G. (2010). Identifying biologically relevant differences between metagenomic communities. *Bioinforma. Oxf. Engl.* 26, 715–721. doi: 10.1093/bioinformatics/btq041
- Redmond, M. C., and Valentine, D. L. (2011). Natural gas and temperature structure a microbial community response to the Deepwater Horizon oil spill. *Proc. Natl. Acad. Sci. U.S.A.* doi: 10.1073/pnas.110875610
- Röling, W. F. M., Milner, M. G., Jones, D. M., Lee, K., Daniel, F., Swannell, R. J. P., et al. (2002). Robust hydrocarbon degradation and dynamics of bacterial communities during nutrient-enhanced oil spill bioremediation. *Appl. Environ. Microbiol.* 68, 5537–5548. doi: 10.1128/AEM.68.11.5537-5548.2002
- Rosano-Hernández, M. C., and Fernández-Linares, L. C. (2009). Bacterial diversity of marine seeps in the southeastern Gulf of Mexico. *Pak. J. Biol. Sci.* 12, 683–689. doi: 10.3923/pjbs.2009.683.689
- Rosenbauer, R. J., Campbell, P. L., Lam, A., Lorenson, T. D., Hostettler, F. D., Thomas, B., et al. (2010). *Reconnaissance of Macondo-1 Well Oil in Sediment and Tarballs from the Northern Gulf of Mexico shoreline, Texas to Florida*. United States Geological Survey. Available online at: <http://pubs.usgs.gov/of/2010/1290/>
- Shieh, W. Y., Jean, W. D., Lin, Y.-T., and Tseng, M. (2003). *Marinobacter luteoensis* sp. nov., a thermotolerant marine bacterium isolated from a coastal hot spring in Lutao, Taiwan. *Can. J. Microbiol.* 49, 244–252. doi: 10.1139/w03-032
- Sistrom, W. R. (1962). The Kinetics of the Synthesis of Photopigments in Rhodopseudomonas sphaeroides. *J. Gen. Microbiol.* 28, 607–616. doi: 10.1099/00221287-28-4-607
- Sumaila, U. R., Cisneros-Montemayor, A. M., Dyck, A., Huang, L., Cheung, W., Jacquet, J., et al. (2012). Impact of the Deepwater Horizon well blowout on the economics of US Gulf fisheries. *Can. J. Fish. Aquat. Sci.* 69, 499–510. doi: 10.1139/f2011-171
- The Federal Intragency Solutions Group: Oil Budget Calculator Science and Engineering Team (2010). *Oil Budget Calculator Deepwater Horizon*.
- US Coast Guard, USGS, and NOAA. (2010). *Deepwater Horizon MC252 Gulf Incident Oil Budget*. Available online at: <http://www.usgs.gov/foia/budget/08-02-2010.Deepwater%20Horizon%20Oil%20Budget.pdf>
- Valentine, D. L., Kessler, J. D., Redmond, M. C., Mendes, S. D., Heintz, M. B., Farwell, C., et al. (2010). Propane respiration jump-starts microbial response to a deep oil spill. *Science* 330, 208–211. doi: 10.1126/science.1196830
- Valentine, D. L., Mezic, I., Macesic, S., Crnjarić-Zic, N., Ivic, S., Hogan, P. J., et al. (2012). Dynamic autoinoculation and the microbial ecology of a deep water hydrocarbon eruption. *Proc. Natl. Acad. Sci. U.S.A.* 109, 20286–20291. doi: 10.1073/pnas.1108820109
- Venosa, A. D., Suidan, M. T., King, D., and Wrenn, B. A. (1997). Use of hopane as a conservative biomarker for monitoring the bioremediation effectiveness of crude oil contaminating a sandy beach. *J. Ind. Microbiol. Biotechnol.* 18, 131–139. doi: 10.1038/sj.jim.2900304
- Vila, J., María Nieto, J., Mertens, J., Springael, D., and Grifoll, M. (2010). Microbial community structure of a heavy fuel oil-degrading marine consortium: linking microbial dynamics with polycyclic aromatic hydrocarbon utilization. *FEMS Microbiol. Ecol.* 73, 349–362. doi: 10.1111/j.1574-6941.2010.00902.x
- Volkman, J. K., Alexander, R., Kagi, R. I., and Rullkötter, J. (1983). GC-MS characterisation of C27 and C28 triterpanes in sediments and petroleum. *Geochim. Cosmochim. Acta* 47, 1033–1040. doi: 10.1016/0016-7037(83)90233-8

- Wu, C., Wang, X., and Shao, Z. (2010). Diversity of oil-degrading bacteria isolated from the Indian Ocean sea surface. *Wei Sheng Wu Xue Bao* 50, 1218–1225.
- Yakimov, M. M., Golyshin, P. N., Lang, S., Moore, E. R., Abraham, W. R., Lünsdorf, H., et al. (1998). *Alcanivorax borkumensis* gen. nov., sp. nov., a new, hydrocarbon-degrading and surfactant-producing marine bacterium. *Int. J. Syst. Bacteriol.* 48(Pt 2), 339–348. doi: 10.1099/00207713-48-2-339
- Zukunft, P. (2010). *Summary Report for Sub-Sea and Sub-Surface Oil and Disperion Detection: Sampling and Monitoring*. Available online at: [http://www.restorethegulf.gov/sites/default/files/documents/pdf/OSAT\\_Report\\_FINAL\\_17DEC.pdf](http://www.restorethegulf.gov/sites/default/files/documents/pdf/OSAT_Report_FINAL_17DEC.pdf)

**Conflict of Interest Statement:** The authors declare that the research was conducted in the absence of any commercial or financial relationships that could be construed as a potential conflict of interest.

Received: 20 November 2013; accepted: 13 March 2014; published online: 03 April 2014.

Citation: Lamendella R, Strutt S, Borglin S, Chakraborty R, Tas N, Mason OU, Hultman J, Prestat E, Hazen TC and Jansson JK (2014) Assessment of the Deepwater Horizon oil spill impact on Gulf coast microbial communities. *Front. Microbiol.* 5:130. doi: 10.3389/fmicb.2014.00130

This article was submitted to Virology, a section of the journal *Frontiers in Microbiology*.

Copyright © 2014 Lamendella, Strutt, Borglin, Chakraborty, Tas, Mason, Hultman, Prestat, Hazen and Jansson. This is an open-access article distributed under the terms of the Creative Commons Attribution License (CC BY). The use, distribution or reproduction in other forums is permitted, provided the original author(s) or licensor are credited and that the original publication in this journal is cited, in accordance with accepted academic practice. No use, distribution or reproduction is permitted which does not comply with these terms.



# Single-cell genomics reveals features of a *Colwellia* species that was dominant during the Deepwater Horizon oil spill

Olivia U. Mason<sup>1\*</sup>, James Han<sup>2</sup>, Tanja Woyke<sup>2</sup> and Janet K. Jansson<sup>3,4\*</sup>

<sup>1</sup> Department of Earth, Ocean and Atmospheric Science, Florida State University, Tallahassee, FL, USA

<sup>2</sup> Department of Energy Joint Genome Institute, Walnut Creek, CA, USA

<sup>3</sup> Lawrence Berkeley National Laboratory, Earth Sciences Division, Ecology Department, Berkeley, CA, USA

<sup>4</sup> Department of Plant and Microbial Biology, University of California, Berkeley, CA, USA

**Edited by:**

Ian M. Head, Newcastle University, UK

**Reviewed by:**

Vanessa Karel Michelou, University of Hawaii, USA

Kasper Urup Kjeldsen, Aarhus University, Denmark

**\*Correspondence:**

Olivia U. Mason, Department of Earth, Ocean and Atmospheric Science, Florida State University, 117 N Woodward Avenue, Rogers Building Rm. 307, Tallahassee, FL, USA

e-mail: omason@fsu.edu;

Janet K. Jansson, 1 Cyclotron Road, Berkeley, CA, USA

e-mail: jrjansson@lbl.gov

During the Deepwater Horizon (DWH) oil spill in the Gulf of Mexico a deep-sea hydrocarbon plume developed resulting in a rapid succession of bacteria. *Colwellia* eventually supplanted *Oceanospirillales*, which dominated the plume early in the spill. These successional changes may have resulted, in part, from the changing composition and abundance of hydrocarbons over time. *Colwellia* abundance peaked when gaseous and simple aromatic hydrocarbons increased, yet the metabolic pathway used by *Colwellia* in hydrocarbon disposition is unknown. Here we used single-cell genomics to gain insights into the genome properties of a *Colwellia* enriched during the DWH deep-sea plume. A single amplified genome (SAG) of a *Colwellia* cell isolated from a DWH plume, closely related (avg. 98% 16S rRNA gene similarity) to other plume *Colwellia*, was sequenced and annotated. The SAG was similar to the sequenced isolate *Colwellia psychrerythraea* 34H (84% avg. nucleotide identity). Both had genes for denitrification, chemotaxis, and motility, adaptations to cold environments and a suite of nutrient acquisition genes. The *Colwellia* SAG may be capable of gaseous and aromatic hydrocarbon degradation, which contrasts with a DWH plume *Oceanospirillales* SAG which encoded non-gaseous *n*-alkane and cycloalkane degradation pathways. The disparate hydrocarbon degradation pathways are consistent with hydrocarbons that were abundant at different times in the deep-sea plume; first, non-gaseous *n*-alkanes and cycloalkanes that could be degraded by *Oceanospirillales*, followed by gaseous, and simple aromatic hydrocarbons that may have been degraded by *Colwellia*. These insights into the genomic properties of a *Colwellia* species, which were supported by existing metagenomic sequence data from the plume and DWH contaminated sediments, help further our understanding of the successional changes in the dominant microbial players in the plume over the course of the DWH spill.

**Keywords:** DWH oil spill, *Colwellia*, single-cell genomics, deep-sea plume, hydrocarbon degradation, bacteria

## INTRODUCTION

The Deepwater Horizon (DWH) oil spill from April to July 2010 was unprecedented due to the extreme depth (1500 m below sea-level; mbsl) and low temperature (4°C), at which it took place. *Colwellia* species bloomed in the deep-sea hydrocarbon plume, that formed at 1100 mbsl, in early June, 2010 (Valentine et al., 2010; Redmond and Valentine, 2012) after partial capture of the oil began (Dubinsky et al., 2013). At this time the unmitigated flow of oil ceased, and cycloalkanes and non-gaseous *n*-alkanes, which were dominant until that point, decreased in concentration (Dubinsky et al., 2013). Concomitantly, the concentration of natural gases and simple aromatics increased (Dubinsky et al., 2013). The change in hydrocarbon composition and abundance resulting from partial capture was mirrored by differences in microbial community composition, with a shift in dominance of *Oceanospirillales* to *Colwellia* (Dubinsky et al., 2013). Mason et al. (2012) analyzed *Oceanospirillales* single amplified genomes (SAG) from the deep-sea plume and reported the genome encoded

pathways for cyclohexane and non-gaseous *n*-alkane degradation. These data helped to explain the dominance of *Oceanospirillales* when cycloalkanes and non-gaseous *n*-alkanes were abundant, and its subsequent decline when these hydrocarbon constituents decreased. The later appearance of *Colwellia* in the spill history could be due to its ability to degrade other hydrocarbon constituents in the oil. Microcosm experiments established that *Colwellia* species were capable of degrading hydrocarbons originating from the oil spill at 4°C (Baelum et al., 2012; Redmond and Valentine, 2012). Specifically, Redmond and Valentine (2012) reported that *Colwellia* species from the deep-sea plume incorporated labeled ethane, propane, and benzene. The ability to degrade ethane and propane, for example, provides clues as to why *Colwellia* appears to have increased in abundance when the concentration of these and other gases increased in June 2010.

Hydrocarbon degradation by cultured *Colwellia* has not previously been reported (e.g., Bowman et al., 1997; Methé et al.,

2005). For example, *Colwellia psychrerythraea* 34H, cultivated from Arctic marine sediments, is psychrophilic, with optimal growth at  $-1^{\circ}\text{C}$  to  $10^{\circ}\text{C}$  (Huston, 2003) was not reported to degrade hydrocarbons. The genome of *C. psychrerythraea* provides insights into the adaptations that enable it to be active at such low temperatures, such as changes to cell membrane fluidity and the use of compounds that provide cryotolerance (Methé et al., 2005). Further, this genome provides a platform for comparison to *Colwellia* that were enriched during the DWH oil spill. Although the possible role of *C. psychrerythraea* in bioremediation by aromatic, or C<sub>1</sub> contaminant degradation was inferred, the specific contaminants and the pathways catalyzing these reactions have not yet been elucidated (Methé et al., 2005). Thus it remains unresolved as to how *Colwellia* species that were identified during the DWH spill are capable of growth with ethane, propane, and benzene (Redmond and Valentine, 2012), polycyclic aromatic hydrocarbons (PAH) (Gutierrez et al., 2013), or MC252 crude oil constituents (Baelum et al., 2012). Here our aim was to use single-cell genomics to gain a better understanding of the genomic properties of a deep-sea *Colwellia* species that enabled it to bloom during the oil spill. Specifically, we present a genome analysis of a *Colwellia* single-cell isolated directly from the deep-sea plume described in Hazen et al. (2010) and Mason et al. (2012).

## MATERIALS AND METHODS

### SINGLE-CELL SORTING, WHOLE-GENOME AMPLIFICATION, AND SCREENING

Cells were collected following the clean sorting procedures detailed by Rodrigue et al. (2009). Briefly, single cells from the proximal plume water sample, collected on May 29, 2010 from 1207 mbsl (described in Mason et al., 2012), were sorted by the Cytopeia Influx Cell Sorter (BD Biosciences, Franklin Lakes, NJ) into three 96-well plates containing 3  $\mu\text{l}$  of ultraviolet-treated TE. The cells were stained with SYBR Green I (Invitrogen, Carlsbad, CA) and illuminated by a 488-nm laser (Coherent Inc., Santa Clara, CA). As described by Woyke et al. (2011) the sorting window was based on the size determined by side scatter and green fluorescence (531/40 bp filter). Single cells were lysed for 20 min at room temperature using alkaline solution from the Repli-G UltraFast Mini Kit (Qiagen, Valencia, CA) according to the manufacturer's instructions. After neutralization, the samples were amplified using the RepliPHI Phi29 reagents (Epicenter Biotechnologies, Madison, WI). Each 50- $\mu\text{l}$  reaction contained Phi29 Reaction Buffer (1  $\times$  final concentration), 50  $\mu\text{M}$  random hexamers with the phosphorothioate bonds between the last two nucleotides at the 3' end (IDT, Coralville, IA), 0.4 mM dNTP, 5% DMSO (Sigma, St Louis, MO), 10 mM DTT (Sigma), 100 U Phi29 and 0.5 mM Syto 13 (Invitrogen). A mastermix of multiple displacement amplification (MDA) reagents minus the Syto 13 sufficient for a 96-well plate was ultraviolet-treated for 60 min for decontamination. Syto 13 was then added to the mastermix, which was added to the single cells for real-time MDA on the Roche LightCycler 480 for 17 h at  $30^{\circ}\text{C}$ . All steps of single-cell handling and amplification were performed under most stringent conditions to reduce the introduction of contamination. Single-cell MDA products were screened using Sanger sequencing

of 16S rRNA gene amplicons derived from each MDA product. Two single-cell MDA products were identified as *Colwellia*, one of which was selected for shotgun sequencing and analysis based on the clean appearance of the 16S rRNA gene Sanger sequencing electropherogram.

### SINGLE-CELL ILLUMINA SEQUENCING, QUALITY CONTROL, AND ASSEMBLY

Single-cell amplified DNA of *Colwellia* was used to generate normalized, indexed Illumina libraries. Briefly, 3  $\mu\text{g}$  of MDA product was sheared using the Covaris E210 (Covaris, Woburn, MA) with the following protocol: 10% duty cycle, intensity 5 and 200 cycles per burst for 6 min per sample. The fragmented DNA was purified using QIAquick columns (Qiagen) according to the manufacturer's instructions. The sheared DNA was end-repaired, A-tailed and ligated to the Illumina adaptors according to the Illumina standard paired-end protocol. The ligation product was purified using AMPure SPRI beads, then underwent normalization using the Duplex-Specific Nuclease Kit (Axxora, San Diego, CA). The normalized libraries were then amplified by PCR for 12 cycles using a set of two indexed primers and the library pool was sequenced on one lane of an Illumina HiSeq 2000 sequencer according to the manufacturer's protocols (run mode 2  $\times$  76 bp). To ensure that the single-amplified genome was free of contamination, the Illumina sequence data was quality controlled using GC content and blast analysis (for details, see supplemental material).

### BIOINFORMATICS

The 16S rRNA gene sequence of the *Colwellia* SAG was compared to 16S rRNA gene datasets in plume samples and stable isotope probing (SIP) experiments (Valentine et al., 2010; Mason et al., 2012; Redmond and Valentine, 2012). SAG reads were assembled using SPAdes 2.4.0 (Bankevich et al., 2012) with the following parameters: -sc -careful -m 40 -12. The single copy gene analysis was carried out according to Rinke et al. (2013). Unassembled metagenome and metatranscriptome reads from deep-sea plume samples presented by Mason et al. (2012) (available at <http://mason.eoas.fsu.edu>) and metagenome reads from surface sediments (<http://mason.eoas.fsu.edu> and MG-RAST IDs 4510162.3-4510175.3), several of which were contaminated during the DWH spill (Mason et al., 2014), were mapped against the assembled *Colwellia* SAG using Bowtie2 (Langmead and Salzberg, 2012) with default parameters. The SAG assembly was annotated using CAMERA 2.0 (Sun et al., 2011). The reads that went into the SAG assembly were compared to *C. psychrerythraea* (Methé et al., 2005) using PAUDA (Huson and Xie, 2014), with a bit score of  $\geq 40$  serving as the cutoff. JSpecies (Richter and Rosselló-Móra, 2009) was used to compute the average nucleotide identity between the *Colwellia* SAG assembly and *C. psychrerythraea*. The average was computed by using values greater than 70%. The lowest observed value that was used in the calculation was 70.34% and the highest was 100%. Additionally, the reads that went into the *Colwellia* SAG assembly were also compared to a database of genes involved in hydrocarbon degradation (bit score of  $\geq 40$  cutoff), similar to the methodology described by Mason et al. (2012) with PAUDA (Huson and Xie, 2014). Last, the *Colwellia* SAG

assembly was compared (blastx) to gene products of the BMO operon of *Thauera butanivorans* (NCBI locus AY093933). Contigs with *bmoR* were also compared to the non-redundant protein sequences (nr) in GenBank using blastx. The *Colwellia* SAG raw reads and assembly are available at: <http://mason.eoas.fsu.edu>, as are the *Oceanospirillales* SAG reads and assemblies from Mason et al. (2012).

## RESULTS AND DISCUSSION

### GENOMIC FEATURES

More than 38 million reads, representing 587X coverage were obtained (assuming a genome size of 5.0 Mb). The *Colwellia* SAG assembly resulted in 141 contigs with a total assembly size of 1.3 Mb. The estimated genome recovery was 30%, based on single-copy gene analysis (Supplementary Table 1). Average G + C content was 37.5% (Supplementary Results), compared to 37.9% for *C. psychrerythraea* (Methé et al., 2005). A total of 1163 open reading frame(s) were identified. In the assembled *Colwellia* SAG 11 rRNA operons and 8 tRNAs were present. All annotated COGs (CAMERA) of the *Colwellia* SAG assembly are shown in Supplementary Table 2. The average nucleotide identity when comparing the *Colwellia* SAG to *C. psychrerythraea* was 84%.

### SAG TAXONOMY

The SAG selected for Illumina sequencing, *Colwellia* SAG HUGN, was closely related to *C. psychrerythraea* based on its 16S rRNA gene sequence (99% similar). This clade also includes highly similar *Colwellia* sequences retrieved from the DWH plume (average 98%; Valentine et al., 2010; Mason et al., 2012) and by stable isotope probing analysis (97–99%; Redmond and Valentine, 2012) (Figure 1). Although the SAG was very similar to the *Colwellia* sequences identified *in situ* in the plume sample, *Colwellia* was not abundant early in the spill history at the time the sample was obtained (Mason et al., 2012). The SAG was also highly similar to *Colwellia* species found in the June 2010 plume samples

(Figure 1), in which *Colwellia* had a relative abundance of >60% of the community (Valentine et al., 2010).

### HYDROCARBON DEGRADATION

The most frequently observed genes in the reads that went into the *Colwellia* SAG assembly were aldehyde dehydrogenase, alcohol dehydrogenase, enoyl-CoA hydratase, *bmoR*, 2-hydroxymuconic semialdehyde dehydrogenase and 4-cresol dehydrogenase. Generally, these genes could be part of several different metabolic pathways, but the observed *bmoR*, which was highly similar (avg. similarity was 74%) to that of *Pseudomonas butanovora* [subsequently renamed *Thauera butanivorans* (Dubbels et al., 2009)] suggested that it may play a similar functional role in the *Colwellia* species described here. *T. butanivorans* (Dubbels et al., 2009), isolated from activated sludge from an oil refining plant (Takahashi, 1980), is able to grow on C<sub>2</sub>–C<sub>9</sub> alkanes (Dubbels et al., 2009) using the following pathway: Butane (BMO) → 1-Butanol (alcohol dehydrogenase) → Butyraldehyde (aldehyde dehydrogenase) → Butyric Acid (further metabolized as fatty acid) (Arp, 1999). Although a butane monooxygenase was not identified in the *Colwellia* SAG presented here, *T. butanivorans*' *bmoR*, which encodes a transcriptional regulator (BmoR) for BMO, and is located upstream of the BMO operon (Kurth et al., 2008), was identified (Figure 2). A total of 758 raw reads were annotated as *bmoR* in the SAG using blastx. The average similarity was 74% to *T. butanivorans* *bmoR* (bit score ≥ 40). In a separate analysis this *bmoR* was also compared to the assembled SAG. When carrying out blastx analysis of the contigs compared to *bmoR* the percent similarity ranged from 33–42%, with a high bit score average of 172. We acknowledge that similarities in this range are low in terms of a reliable annotation as *bmoR*. The discrepancy in the % similarity is likely due to methodological differences (short, unassembled 76 bp reads compared to contigs). Further, the GC content of the contigs upon which *bmoR* was identified was 38%, which is identical to the GC content for the entire SAG assembly (38%). The presence of

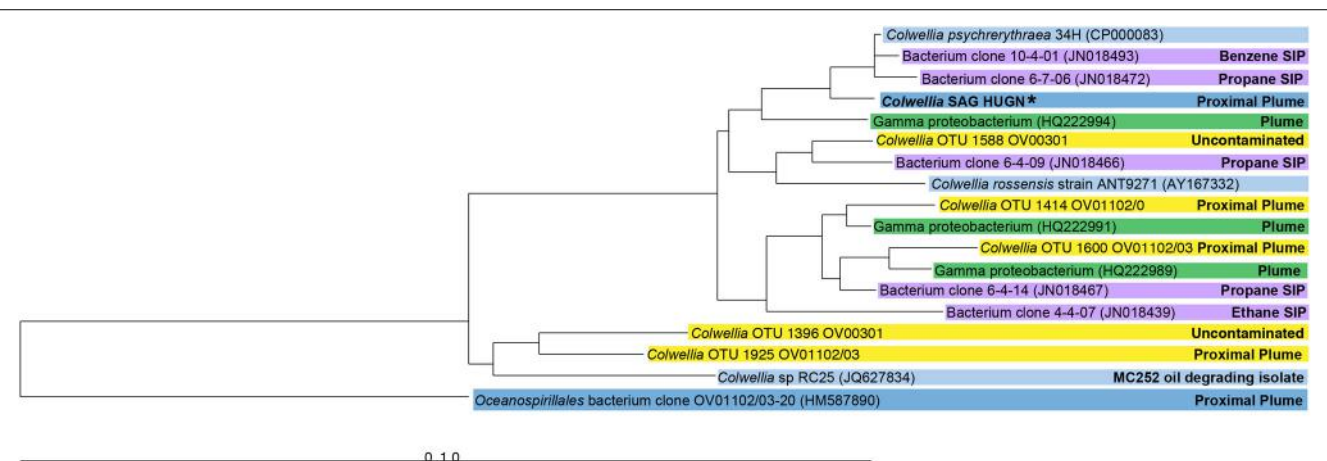
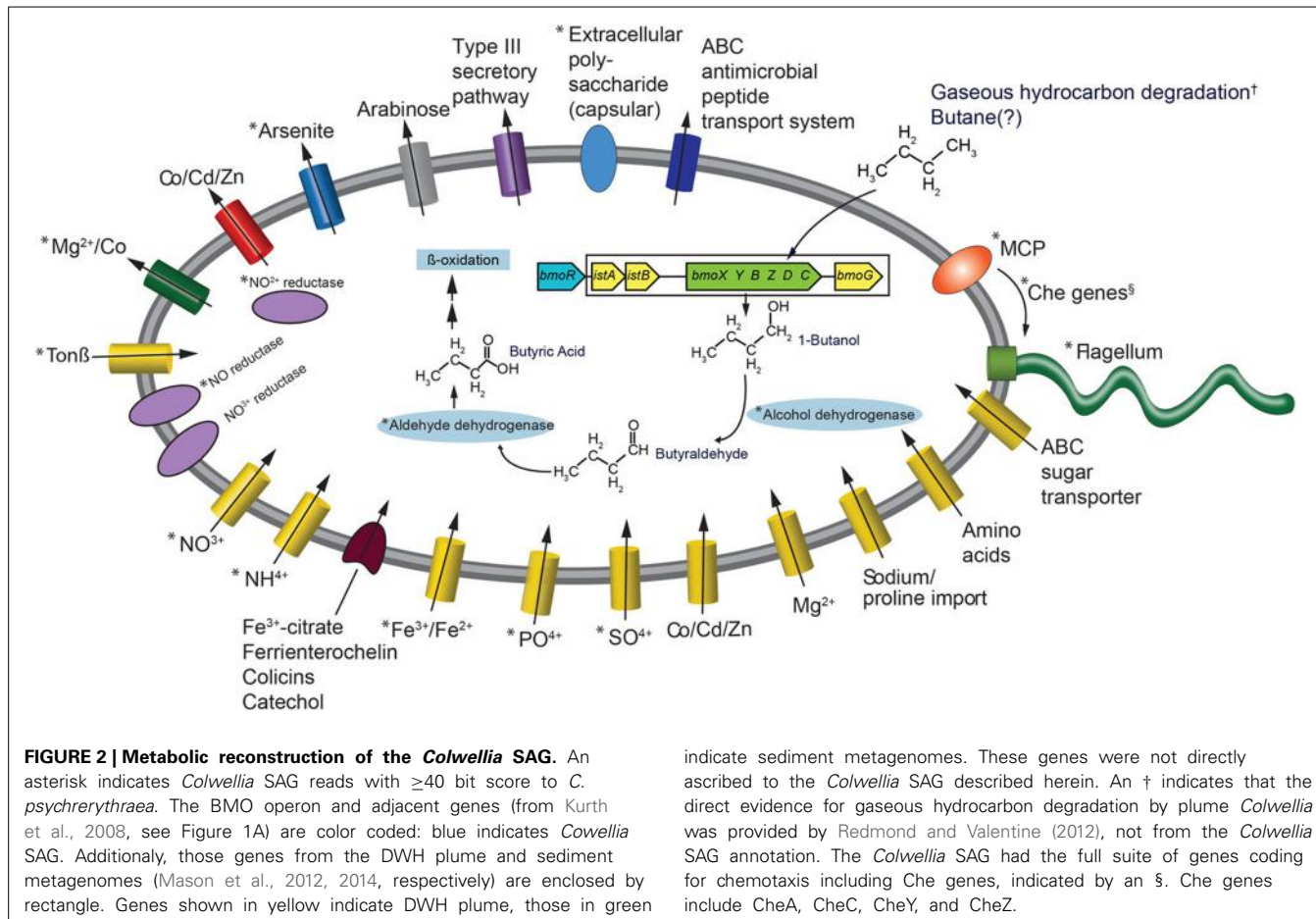


**FIGURE 1 |** Neighbor-joining phylogenetic tree of 16S rRNA genes of the *Colwellia* SAG and close relatives. Sequences from a particular study are highlighted with the same color. Information about the

environment from which a particular microorganism was found is indicated in the figure. The *Colwellia* SAG is in bold text and indicated by an asterisk.



*bmoR*, similar to *T. butanivorans*, in the *Colwellia* SAG, is not however, diagnostic for presence of the BMO operon. The remaining metabolic pathway used by *T. butanivorans* in butane oxidation was encoded in the SAG (Figure 2) and was highly similar ( $\geq 40$  bit score) to that of *C. psychrerythraea*. *C. psychrerythraea* does not have a butane monooxygenase thus has a paraphyletic lineage with the *Colwellia* SAG.

The lack of a butane monooxygenase in the SAG may indicate that it, does not, in fact have that metabolic capability. Alternatively, it may be due to insufficient coverage of the genome (30% complete) of the *Colwellia* SAG. To test this hypothesis, we turned to metagenomes from the plume ( $\sim 0.03$  Tb of sequence data) and from sediments ( $\sim 1$  Tb of sequence data), several of which were highly contaminated by the DWH spill (Mason et al., 2012 and 2014, respectively). Although the relative abundance of *Colwellia* in the DWH plume, from which the single cell was retrieved, was low (1–2%) (Mason et al., 2012), the same *bmoR* gene was identified in metagenomes from the plume, as were several additional *T. butanivorans* genes involved in butane oxidation (bit score of  $\geq 40$ ) (Figure 2). However, no butane monooxygenase was recovered in the DWH plume metagenomes. In sediment samples, *Colwellia* had a high relative abundance of 6% in the more contaminated samples (Mason et al., 2014). The higher abundance of *Colwellia* in contaminated sediments (Mason et al.,

2014) compared to the deep-sea plume may have resulted in better coverage of *Colwellia*. In the resulting sediment metagenomes, *bmoR*, *bmoG*, *istA*, and *istB* were identified, all of which had a bit score of  $\geq 40$ , as was the alpha subunit of butane monooxygenase (*bmoX*) (Figure 2). The metagenomic data, particularly in surface sediments, suggested that gaseous hydrocarbon degradation via butane monooxygenase was a plausible pathway for degrading DWH hydrocarbon constituents, however this pathway was not directly linked to *Colwellia*.

Direct evidence for gaseous hydrocarbon degradation by DWH plume *Colwellia*, which were closely related to the *Colwellia* SAG described herein, was provided by Redmond and Valentine (2012) who used SIP to examine the uptake of methane, ethane, and propane. They reported that *Colwellia* enriched from the plume was responsible for the bulk of  $^{13}\text{C}$  labeled propane and ethane uptake, but also showed, to a far lesser extent uptake of methane by *Colwellia*, consistent with the properties of *T. butanivorans* BMO (Cooley et al., 2009). The putative hydrocarbon degradation pathways discussed above help to resolve several aspects of the microbial response to the oil spill that hitherto were unclear. Specifically, the BMO of *T. butanivorans* is highly efficient at discriminating against methane when grown on  $\geq \text{C}_2$  alkanes (Cooley et al., 2009). At the time *Colwellia* was abundant in mid-June 2010 (Valentine et al., 2010; Redmond and Valentine, 2012),

Valentine et al. (2010) reported that, despite the abundance of methane input to the deep-sea during the spill (Joye et al., 2011), propane, ethane (and perhaps butane) fueled microbial respiration. These findings suggested that *Colwellia* was likely involved in degrading gaseous hydrocarbons, but not methane (Valentine et al., 2010), which was substantiated by the aforementioned SIP experiments.

In addition to gaseous hydrocarbon degradation Redmond and Valentine (2012) also reported that *Colwellia* enriched in the DWH plume incorporated benzene in SIP experiments. In the *Colwellia* SAG 4-cresol dehydrogenase (EC 1.17.99.1) and 2-hydroxymuconic semialdehyde dehydrogenase (EC 1.2.1.85) both of which are involved in degradation of several aromatics (e.g., benzene by *Pseudomonas putida* according to Reardon et al., 2000), were identified. These were also identified in the water column and sediment metagenomes. Together, these data support the uptake of aromatics by plume *Colwellia* as reported by Redmond and Valentine (2012).

## NITROGEN

Previously we reported that nitrate was significantly lower in plume samples from which the *Colwellia* SAG was isolated compared to non-plume samples (*p*-value 0.003) (Hazen et al., 2010). One hypothesis is that nitrate was consumed as an electron acceptor during hydrocarbon degradation. As the previously sequenced *C. psychrerythraea* strain was reported to have genes coding for denitrification (Methé et al., 2005), we sought to determine whether the *Colwellia* SAG also possessed the genetic capacity for denitrification. First, a direct comparison was made between *C. psychrerythraea* and unassembled reads from the *Colwellia* SAG that went into the final assembly. This comparison revealed a high sequence similarity ( $\geq 40$  bit score) of genes involved in denitrification in both the *Colwellia* SAG and *C. psychrerythraea* (Figure 2). For example, *C. psychrerythraea*'s nitrate permease (GI71146856), nitrite reductases (small and large sub-units; GI71146751 and GI71143641), nitric-oxide reductase (GI71148260 and GI71144846) and an anaerobic nitric-oxide reductase transcription regulator (GI71282073) were present in the SAG (Figure 2).

Although many genes in the denitrification pathway were common between the *Colwellia* SAG and *C. psychrerythraea*, there were differences. For example, nitrate reduction appears to be encoded by different genes. In the *Colwellia* SAG reduction of nitrate could be carried out via a nitrate/TMAO reductase (COG3005) and a periplasmic nitrate reductase system, NapE component (COG4459). Further an uncharacterized protein involved in response to nitric oxide was present in the SAG (COG3213). The *Colwellia* SAG lacked a nitrous-oxide reductase gene, which may be an artifact of an incomplete genome for the *Colwellia* SAG. It is, however, plausible that the SAG does in fact lack the capability to reduce nitrous oxide. Given the importance of nitrous oxide as a greenhouse gas (Wuebbles, 2009), further elucidating the role of *Colwellia* in denitrifying processes and end-products is necessary, particularly in the context of an unprecedented ecosystem perturbation, such as the DWH oil spill.

## IRON

Baelum et al. (2012) tested the hypothesis put forth by Hazen et al. (2010), that iron could have limited microbial growth, in microcosm experiments with MC252 crude oil. The results suggested that iron limitation resulted in floc formation of which *Colwellia* was the most abundant microorganism. They also reported that in the first 20 days of incubation, lower growth, and hydrocarbon degradation rates were observed, although the total amount of oil degraded after 20 days was the same as in microcosms with sufficient iron. Further, Joung and Shiller (2013) reported that iron concentrations in the plume compared to non-plume samples indicate an enhanced microbial iron demand. This suggests that in the deep-sea plume, at least initially, iron could have affected both the growth and degradation rate of hydrocarbons by *Colwellia*, although is unlikely that iron concentrations were a growth-limiting factor nor a factor in the total amount of hydrocarbons degraded during the spill (Joung and Shiller, 2013).

To better understand *Colwellia*'s iron acquisition strategy we first compared the *Colwellia* SAG to *C. psychrerythraea*, followed by direct annotation of *Colwellia* SAG contigs using CAMERA. Similar to *C. psychrerythraea* the *Colwellia* SAG lacked genes for siderophore production. Yet, highly similar genes when comparing the two ( $\geq 40$  bit score) were found for iron transport and uptake (Figure 2). Iron(III) ABC transporter proteins (GIs 71277892 and 71143632) and ferrous iron transport proteins (GIs 71144726 and 71143643) were identified, yet the two genomes had different genes coding for interactions with siderophore complexes (Figure 2). Annotation of the *Colwellia* SAG assembly with CAMERA revealed the genome encoded functions involved in iron acquisition, including an outer membrane receptor for the siderophore-iron complex ferrienterochelin (Lundrigan and Kadner, 1986) (COG4771), and an outer membrane receptor for Fe<sup>3+</sup>-dicitrate (COG4772) (Figure 2). Other functions involved in iron transport were also annotated (COGs 0370, 1629, and 1918) (Figure 2). Taken together, the data suggested that the *Colwellia* SAG could have been at a physiological disadvantage if it was, in fact, unable to synthesize siderophores. Conceivably, *Colwellia* could have relied on scavenging siderophores produced by other microorganisms in the plume for remediating iron limitation. Although we acknowledge that missing genes for siderophore production could be due to the incompleteness of the *Colwellia* SAG, *C. psychrerythraea* also lacks the ability to produce siderophores.

## FLOC FORMATION

The *C. psychrerythraea* genome encodes a capsular polysaccharide biosynthesis protein (GI71145258), as does the *Colwellia* SAG (Figure 2). Polysaccharide capsules are found on the cell surface of many bacteria and are involved in, among other processes, adherence of one bacterium to another (Roberts, 1996). Further, *C. psychrerythraea*'s putative polysaccharide biosynthesis glycosyltransferase, which likely functions in extracellular polysaccharide biosynthesis (Methé et al., 2005), was identified in the *Colwellia* SAG. As discussed above, Baelum et al. (2012) observed flocs largely comprised of *Colwellia* that formed under iron limiting conditions in microcosms incubated with MC252 oil. Our

findings provide preliminary evidence for a plausible mechanism by which cells could have aggregated together in the face of nutrient, and particularly, iron limitation in the deep-sea plume.

### CHEMOTAXIS AND MOTILITY

A full suite of genes involved in signal transduction, chemotaxis, and motility were present in the *Colwellia* SAG (Figure 2), many of which were highly similar to *C. psychrerythraea*. For example *C. psychrerythraea*'s chemotaxis proteins CheA, CheY, and CheZ, numerous methyl-accepting chemotaxis proteins (MCP) and the full suite of genes coding for flagellum synthesis and operation were observed in the *Colwellia* SAG. Parales et al. (2000) reported that several strains of bacteria exhibited a chemotactic response to benzene and toluene and suggested MCPs were involved. More direct evidence was provided regarding the role of MCPs in the ability of *Pseudomonas putida* to detect naphthalene (Grimm and Harwood, 1999). Given the suite of genes, including MCP, encoded in the *Colwellia* SAG, it is plausible that the *Colwellia* SAG was able to sense and move toward a chemo-attractant, such as degradable hydrocarbons that accumulated in the deep-sea plume during the DWH spill.

### ADAPTATION TO COLD TEMPERATURES

Direct comparison of the SAG to the *C. psychrerythraea* genome revealed shared genomic features ( $\geq 40$  bit score similarity) thought to be involved in adaptation to life at cold temperatures; for example a *C. psychrerythraea* fatty acid cis/trans isomerase, which would allow the cell to alter the ratio of cis- to trans-esterified fatty acids in phospholipids (Methé et al., 2005). The ability to increase cis-isomerization, could enhance membrane fluidity at low temperatures (Methé et al., 2005), which would be an important adaption to life at low temperatures. Further, *C. psychrerythraea*'s putative 3-oxoacyl-(acyl-carrier-protein) reductase and putative 3-oxoacyl-(acyl-carrier-protein) synthase III, which serve key roles in fatty acid and phospholipid biosynthesis (Methé et al., 2005), were identified in the SAG, and could also play a role regulating membrane fluidity at cold temperatures (Russell, 1997).

### BIOSYNTHESIS OF COMPATIBLE SOLUTES

The *Colwellia* SAG had genes coding for choline dehydrogenase and betaine aldehyde dehydrogenase, which were highly similar ( $\geq 40$  bit score) to those of *C. psychrerythraea*. In the genome sequence of the psychrophilic hydrocarbon degrader, *Oleispira antarctica* these were the two mechanisms for biosynthesis of compatible solutes (Kube et al., 2013). Choline dehydrogenase and betaine aldehyde dehydrogenase are involved in catalyzing the reaction that leads to synthesis of the osmolyte betaine (Kube et al., 2013). Genes coding for choline dehydrogenase, and others, were suggested to be involved in synthesis of betaine, which was cited as an osmoprotectant, and also a cryoprotectant in *C. psychrerythraea* (Methé et al., 2005). The dual functionality of an osmoprotectant and cryoprotectant in *Colwellia* would be an important adaptation for the *Colwellia* SAG to life in the low temperature, deep-sea marine environment.

### COMPARISON OF DWH DEEP-SEA PLUME *COLWELLIA* SAG TO *OCEANOSPIRILLALES* SAG

Mason et al. (2012) presented an annotated *Oceanospirillales* SAG that was isolated from the proximal plume sample (OV01102/03 in Hazen et al., 2010) from which the *Colwellia* SAG presented herein was also isolated. *Oceanospirillales* had a higher relative abundance in the proximal plume sample compared to *Colwellia* (16S rRNA gene sequence relative abundance was 81% vs. 1% percent, respectively) (Mason et al., 2012). Thus most of the genes and transcripts from the proximal plume sample were thought to derive from *Oceanospirillales* and the role that *Colwellia* played in oil disposition has been largely unexplored. Comparison of the SAGs revealed several differences; namely the dominant hydrocarbon pathways, iron acquisition strategies, and respiration capabilities. First, the *Oceanospirillales* genome encoded cyclohexane degradation by an alkane monooxygenase (Mason et al., 2012), also recently identified in the genome sequence of the closely related *Oleispira antarctica* (Kube et al., 2013). As discussed above, the *Colwellia* SAG encoded *bmoR*, 4-cresol dehydrogenase and 2-hydroxymuconic semialdehyde dehydrogenase, the latter of which are involved in degradation of several aromatics. Thus, the hydrocarbon constituents potentially degraded by these two gammaproteobacteria, that increased in abundance in the plume, are disparate. Second, the ability to synthesize siderophores to acquire iron, which may have affected hydrocarbon respiration rates early on (but was not likely limiting) by the microbial community in the deep-sea plume during the oil spill, would have given the dominant *Oceanospirillales* a competitive advantage over *Colwellia*. As discussed above, the *Colwellia* described here may have been able to scavenge siderophores produced by other microorganisms, perhaps those of *Oceanospirillales*, to acquire iron. Finally, the genome of *Oceanospirillales* did not encode a pathway for denitrification, in contrast to the *Colwellia* presented here. Therefore, when faced with reduced oxygen concentrations *Colwellia* could have continued to carry out respiration, while *Oceanospirillales* may not have been able to do so.

### COMPARISON OF DWH DEEP-SEA PLUME METAGENOMES AND METATRANSCRIPTOMES AND SEDIMENT METAGENOMES TO THE *COLWELLIA* SAG

Mason et al. (2012) reported relative abundances of 1–2% of *Colwellia* in metagenomes from the proximal plume closest to the DWH wellhead (1.8 km away) and at a more distant location, referred to as the distal plume (10.8 km away), collected May 26–June 2, 2010. Of these metagenome sequence reads 0.30% mapped to the *Colwellia* SAG. To determine if the *Colwellia* SAG was active in the deep-sea plume, 5S, 16S, and 23S rRNA sequences were subtracted from the plume metatranscriptomes. These reads were then mapped against the assembled *Colwellia* SAG. Comparison of the *Colwellia* SAG to proximal plume station metatranscriptome sequences revealed that 0.20% of the metatranscriptome reads mapped to the single-cell assembly. Fewer metatranscriptome reads from the distal station mapped to the *Colwellia* SAG (0.01%). Thus a representative of plume *Colwellia* may have been actively degrading gaseous and simple aromatic hydrocarbons, albeit at low levels, in late May 2010, when these hydrocarbons were less abundant. In contrast Rivers et al. (2013)

reported that 16% of their metatranscriptome reads from two DWH plume stations (6–8 km from the wellhead, collected May 26–June 3, 2010; at the same time we sampled) mapped to *C. psychrerythraea*, although these authors used blastx while we used Bowtie2. Further, the abundance of *Colwellia* was significantly higher in Rivers et al. (2013; see **Figure 1B** for abundance) 16S rRNA gene survey as compared to the samples presented in Mason et al. (2012).

Previously, we characterized the microbial community in 64 surface sediment samples, which had varying degrees of hydrocarbon contamination from the DWH spill (Mason et al., 2014). As discussed above, *Colwellia* was up to 6% (relative abundance) of the microbial community in these sediments, particularly those with the highest hydrocarbon concentrations (Mason et al., 2014). From these samples 14 were selected for metagenomic sequencing. Of these 14 samples, 7 were determined *a priori* to exceed the Environmental Protection Agency (EPA)'s PAH benchmarks for aquatic life. The *Colwellia* SAG assembly was mapped to the sediment metagenomes with 0.25–0.04% of reads mapping. The most SAG reads mapped to 6 of the 7 samples that exceeded the EPA's PAH benchmarks. These results are similar to the plume metagenome and indicate that the *Colwellia* SAG sequenced was represented in both the water column and sediments that were contaminated during the DWH spill.

## CONCLUSION

Analyses of the microbial community response to the oil spill revealed a clear story of microbial succession, however, few detailed descriptions of the cellular physiology of the indigenous microbes that responded to the hydrocarbon inputs have been presented. Herein we describe several aspects of a *Colwellia* single-cell genome that furthers our understanding of the potential role that *Colwellia* played during microbial succession in the deep-sea hydrocarbon plume that formed during the DWH spill. At the time that *Colwellia* was most abundant in the plume, methane was highly abundant but largely not degraded in favor of other gaseous hydrocarbons. This could have been due to the genetic capacity of the *Colwellia* to preferentially degrade gaseous hydrocarbons at the expense of methane, if it does, in fact, have a butane monooxygenase. Additionally, genes involved in BTEX degradation in the *Colwellia* SAG were identified. These preliminary findings may help to resolve the simultaneous increase in *Colwellia* abundance when these hydrocarbon compounds accumulated in the plume. The *Colwellia* SAG was captured in metagenomes from the water column and surface sediments that were contaminated by the DWH spill. In addition, both *Oceanospirillales* and *Colwellia* SAGs possessed genes for chemotaxis and motility, suggesting that this is an advantage for rapid response to hydrocarbon inputs in the deep-sea. We also provide preliminary evidence that the *Colwellia* species described herein may have been able to produce polysaccharides for floc production that corresponds to the high abundance of flocs in microcosms under iron limited conditions as reported by Baelum et al. (2012). This could represent a novel property enabling *Colwellia* to cope with conditions of low iron concentrations, but further experiments are necessary to confirm this hypothesis.

## AUTHOR CONTRIBUTIONS

Olivia U. Mason participated in the research cruise during which the deep-sea plume sample for single-cell isolation and sequencing was obtained. Olivia U. Mason carried out bioinformatics analyses and wrote the manuscript. James Han carried out bioinformatics analyses and helped write the manuscript. Tanja Woyke carried out single-cell genome isolation and sequencing and helped write the manuscript. Janet K. Jansson conceived the experimental design and helped write the manuscript.

## ACKNOWLEDGMENTS

This work was supported by a subcontract from the University of California at Berkeley, Energy Biosciences Institute (EBI) to Lawrence Berkeley National Laboratory under its U.S. Department of Energy contract DE-AC02-05CH11231. We would like to thank the captain and crew of the R/V Ocean Veritas.

## SUPPLEMENTARY MATERIAL

The Supplementary Material for this article can be found online at: <http://www.frontiersin.org/journal/10.3389/fmicb.2014.00332/abstract>

## REFERENCES

- Arp, D. J. (1999). Butane metabolism by butane-grown “*Pseudomonas butanovora*.” *Microbiology* 145, 1173–1180. doi: 10.1099/13500872-145-5-1173
- Baelum, J., Borglin, S., Chakraborty, R., Fortney, J. L., Lamendella, R., Mason, O. U., et al. (2012). Deep-sea bacteria enriched by oil and dispersant from the Deepwater Horizon spill. *Environ. Microbiol.* 14, 2405–2416. doi: 10.1111/j.1462-2920.2012.02780.x
- Bankevich, A., Nurk, S., Antipov, D., Gurevich, A. A., Dvorkin, M., Kulikov, A. S., et al. (2012). SPAdes: a new genome assembly algorithm and its applications to single-cell sequencing. *J. Comput. Biol.* 19, 455–477. doi: 10.1089/cmb.2012.0021
- Bowman, J. P., Gosink, J. J., McCammon, S. A., Skerratt, H., Lewis, T. E., Nichols, D. S., et al. (1997). *Colwellia demingiae* sp. nov., *Colwellia hornerae* sp. nov., *Colwellia rossensis* sp. nov. and *Colwellia psychrotropica* sp. nov.: psychrophilic Antarctic species with the ability to synthesize docosahexaenoic acid (22:ω6). *Int. J. Syst. Bacteriol.* 48, 1171–1180. doi: 10.1099/00207713-48-4-1171
- Cooley, R. B., Dubbels, B. L., Sayavedra-Soto, L. A., Bottomley, P. J., and Arp, D. J. (2009). Kinetic characterization of the soluble butane monooxygenase from *Thauera butanivorans*, formerly “*Pseudomonas butanovora*.” *Microbiology* 155, 2086–2096. doi: 10.1099/mic.0.028175-0
- Dubbels, B. L., Sayavedra-Soto, L. A., Bottomley, P. J., and Arp, D. J. (2009). *Thauera butanivorans* sp. nov., a C2–C9 alkane-oxidizing bacterium previously referred to as “*Pseudomonas butanovora*.” *Int. J. Syst. Evol. Microbiol.* 59, 1576–8. doi: 10.1099/ijss.0.000638-0
- Dubinsky, E. A., Conrad, M. E., Chakraborty, R., Bill, M., Borglin, S. E., Hollibaugh, J. T., et al. (2013). Succession of hydrocarbon-degrading bacteria in the aftermath of the deepwater horizon oil spill in the gulf of Mexico. *Environ. Sci. Technol.* 47, 10860–10867. doi: 10.1021/es401676y
- Grimm, A. C., and Harwood, C. S. (1999). NahY, a catabolic plasmid-encoded receptor required for chemotaxis of *pseudomonas putida* to the aromatic hydrocarbon naphthalene. *J. Bacteriol.* 181, 3310.
- Gutierrez, T., Singleton, D. R., Berry, D., Yang, T., Aitken, M. D., and Teske, A. (2013). Hydrocarbon-degrading bacteria enriched by the Deepwater Horizon oil spill identified by cultivation and DNA-SIP. *ISME J.* 7, 2091–2104. doi: 10.1038/ismej.2013.98
- Hazen, T. C., Dubinsky, E. A., DeSantis, T. Z., Andersen, G. L., Piceno, Y. M., Singh, N., et al. (2010). Deep-sea oil plume enriches indigenous oil-degrading bacteria. *Science* 330, 204–208. doi: 10.1126/science.1195979
- Huson, D. H., and Xie, C. (2014). A poor man's BLASTX - high-throughput metagenomic protein database search using PAUDA. *Bioinformatics* 30, 38–39. doi: 10.1093/bioinformatics/btt254

- Huston, A. L. (2003). *Bacterial Adaptation to the Cold: in situ Activities of Extracellular Enzymes in the North Water Polynya and Characterization of a Cold-Active Aminopeptidase from Colwellia Psychrerythraea Strain 34H*. Ph.D. thesis, Seattle, WA: University of Washington.
- Joung, D., and Shiller, A. M. (2013). Trace element distributions in the water column near the Deepwater Horizon well blowout. *Environ. Sci. Technol.* 47, 2161–2168. doi: 10.1021/es303167p
- Joye, S. B., MacDonald, I. R., Leifer, I., and Asper, V. (2011). Magnitude and oxidation potential of hydrocarbon gases released from the BP oil well blowout. *Nat. Geosci.* 4, 160–164. doi: 10.1038/ngeo1067
- Kube, M., Chernikova, T. N., Al-Ramahi, Y., Beloqui, A., Lopez-Cortez, N., Guazzaroni, M.-E., et al. (2013). Genome sequence and functional genomic analysis of the oil-degrading bacterium *Oleispira antarctica*. *Nat. Commun.* 4, 2156. doi: 10.1038/ncomms3156
- Kurth, E. G., Doughty, D. M., Bottomley, P. J., Arp, D. J., and Sayavedra-Soto, L. A. (2008). Involvement of BmoR and BmoG in n-alkane metabolism in “*Pseudomonas butanovora*.” *Microbiology* 154, 139–147. doi: 10.1099/mic.0.2007/012724-0
- Langmead, B., and Salzberg, S. L. (2012). Fast gapped-read alignment with Bowtie 2. *Nat. Methods* 9, 357–359. doi: 10.1038/nmeth.1923
- Lundrigan, M. D., and Kadner, R. J. (1986). Nucleotide sequence of the gene for the ferrienterochelin receptor FepA in *Escherichia coli*. Homology among outer membrane receptors that interact with TonB. *J. Biol. Chem.* 261, 10797–10801.
- Mason, O. U., Hazen, T. C., Borglin, S., Chain, P. S. G., Dubinsky, E. A., Fortney, J. L., et al. (2012). Metagenome, metatranscriptome and single-cell sequencing reveal microbial response to Deepwater Horizon oil spill. *ISME J.* 6, 1715–1727. doi: 10.1038/ismej.2012.59
- Mason, O. U., Scott, N. M., Gonzalez, A., Robbins-Pianka, A., Bælum, J., Kimbrel, J., et al. (2014). Metagenomics reveals sediment microbial community response to Deepwater Horizon oil spill. *ISME J.* 8, 1464–1475. doi: 10.1038/ismej.2013.254
- Methé, B. A., Nelson, K. E., Deming, J. W., Momen, B., Melamud, E., Zhang, X., et al. (2005). The psychrophilic lifestyle as revealed by the genome sequence of *Colwellia psychrerythraea* 34H through genomic and proteomic analyses. *Proc. Natl. Acad. Sci. U.S.A.* 102, 10913–10918. doi: 10.1073/pnas.0504766102
- Parales, R. E., Ditty, J. L., and Harwood, C. S. (2000). Toluene-Degrading bacteria are chemotactic toward the environmental pollutants benzene, toluene, and trichloroethylene. *Appl. Environ. Microbiol.* 66, 4098. doi: 10.1128/AEM.66.9.4098-4104.20
- Reardon, K. F., Mosteller, D. C., and Bull Rogers, J. D. (2000). Biodegradation kinetics of benzene, toluene, and phenol as single and mixed substrates for *Pseudomonas putida* F1. *Biotechnol. Bioeng.* 69, 385–400. doi: 10.1002/1097-0290(20000820)69:4<385::AID-BIT5>3.0.CO;2-Q
- Redmond, M. C., and Valentine, D. L. (2012). Natural gas and temperature structured a microbial community response to the Deepwater Horizon oil spill. *Proc. Natl. Acad. Sci. U.S.A.* 109, 20292–20297. doi: 10.1073/pnas.1108756108
- Richter, M., and Rosselló-Móra, R. (2009). Shifting the genomic gold standard for the prokaryotic species definition. *Proc. Natl. Acad. Sci. U.S.A.* 106, 19126–19131. doi: 10.1073/pnas.0906412106
- Rinke, C., Schwientek, P., Sczyrba, A., Ivanova, N. N., Anderson, I. J., Cheng, J.-F., et al. (2013). Insights into the phylogeny and coding potential of microbial dark matter. *Nature* 499, 431–437. doi: 10.1038/nature12352
- Rivers, A. R., Sharma, S., Tringe, S. G., Martin, J., Joye, S. B., and Moran, M. A. (2013). Transcriptional response of bathypelagic marine bacterioplankton to the Deepwater Horizon oil spill. *ISME J.* 7, 2315–2329. doi: 10.1038/ismej.2013.129
- Roberts, I. S. (1996). The biochemistry and genetics of capsular polysaccharide production in bacteria. *Annu. Rev. Microbiol.* 50, 285–315. doi: 10.1146/annurev.micro.50.1.285
- Rodrigue, S., Malmstrom, R. R., Berlin, A. M., Birren, B. W., Henn, M. R., and Chisholm, S. W. (2009). Whole genome amplification and *de novo* assembly of single bacterial cells. *PLoS ONE* 4:e6864. doi: 10.1371/journal.pone.0006864
- Russell, N. J. (1997). Psychrophilic bacteria—molecular adaptations of membrane lipids. *Comp. Biochem. Physiol. A Physiol.* 118, 489–493. doi: 10.1016/S0300-9629(97)87354-9
- Sun, S., Chen, J., Li, W., Altintas, I., Lin, A., Peltier, S., et al. (2011). Community cyberinfrastructure for Advanced Microbial Ecology Research and Analysis: the CAMERA resource. *Nucleic Acids Res.* 39, D546–D551. doi: 10.1093/nar/gkq1102
- Takahashi, J. (1980). Production of intracellular protein from n-butane by *Pseudomonas butanovora* sp. nov. *Adv. Appl. Microbiol.* 26, 117–128.
- Valentine, D. L., Kessler, J. D., Redmond, M. C., Mendes, S. D., Heintz, M. B., Farwell, C., et al. (2010). Propane respiration jump-starts microbial response to a deep oil spill. *Science* 330, 208–211. doi: 10.1126/science.1196830
- Woyke, T., Sczyrba, A., Lee, J., Rinke, C., Tighe, D., Clingenpeel, S., et al. (2011). Decontamination of MDA reagents for single cell whole genome amplification. *PLoS ONE* 6:e26161. doi: 10.1371/journal.pone.0026161
- Wuebbles, D. J. (2009). Atmosphere. Nitrous oxide: no laughing matter. *Science* 326, 56–57. doi: 10.1126/science.1179571

**Conflict of Interest Statement:** The authors declare that the research was conducted in the absence of any commercial or financial relationships that could be construed as a potential conflict of interest.

Received: 01 November 2013; accepted: 16 June 2014; published online: 08 July 2014.

Citation: Mason OU, Han J, Woyke T and Jansson JK (2014) Single-cell genomics reveals features of a *Colwellia* species that was dominant during the Deepwater Horizon oil spill. *Front. Microbiol.* 5:332. doi: 10.3389/fmicb.2014.00332

This article was submitted to Aquatic Microbiology, a section of the journal *Frontiers in Microbiology*.

Copyright © 2014 Mason, Han, Woyke and Jansson. This is an open-access article distributed under the terms of the Creative Commons Attribution License (CC BY). The use, distribution or reproduction in other forums is permitted, provided the original author(s) or licensor are credited and that the original publication in this journal is cited, in accordance with accepted academic practice. No use, distribution or reproduction is permitted which does not comply with these terms.



# The microbial nitrogen cycling potential is impacted by polycyclic aromatic hydrocarbon pollution of marine sediments

**Nicole M. Scott<sup>1,2\*</sup>, Matthias Hess<sup>3,4</sup>, Nick J. Bouskill<sup>5</sup>, Olivia U. Mason<sup>6</sup>, Janet K. Jansson<sup>5</sup> and Jack A. Gilbert<sup>1,2</sup>**

<sup>1</sup> Institute of Genomic and Systems Biology, Argonne National Laboratory, Lemont, IL, USA

<sup>2</sup> Department of Ecology and Evolutionary Biology, University of Chicago, Chicago, IL, USA

<sup>3</sup> Energy and Efficiency Division, Chemical and Biological Process Development Group, Pacific Northwest National Laboratory, Richland, WA, USA

<sup>4</sup> Systems Microbiology and Biotechnology Group, Washington State University, Richland, WA, USA

<sup>5</sup> Ecology Department, Earth Sciences Division, Lawrence Berkeley National Laboratory, Berkeley, CA, USA

<sup>6</sup> Earth, Ocean and Atmospheric Science, Florida State University, Tallahassee, FL, USA

**Edited by:**

Andreas Teske, University of North Carolina at Chapel Hill, USA

**Reviewed by:**

Mike L. Dyall-Smith, Charles Sturt University, Australia

David Gregory Weissbrodt, ETH Zürich and Eawag, Switzerland

**\*Correspondence:**

Nicole M. Scott, Department of Ecology and Evolutionary Biology, University of Chicago, 1101 E. 57th Street Chicago, IL 360637 USA  
e-mail: nicolescott1@gmail.com

During hydrocarbon exposure, the composition and functional dynamics of marine microbial communities are altered, favoring bacteria that can utilize this rich carbon source. Initial exposure of high levels of hydrocarbons in aerobic surface sediments can enrich growth of heterotrophic microorganisms having hydrocarbon degradation capacity. As a result, there can be a localized reduction in oxygen potential within the surface layer of marine sediments causing anaerobic zones. We hypothesized that increasing exposure to elevated hydrocarbon concentrations would positively correlate with an increase in denitrification processes and the net accumulation of dinitrogen. This hypothesis was tested by comparing the relative abundance of genes associated with nitrogen metabolism and nitrogen cycling identified in 6 metagenomes from sediments contaminated by polycyclic aromatic hydrocarbons from the Deepwater Horizon (DWH) oil spill in the Gulf of Mexico, and 3 metagenomes from sediments associated with natural oil seeps in the Santa Barbara Channel. An additional 8 metagenomes from uncontaminated sediments from the Gulf of Mexico were analyzed for comparison. We predicted relative changes in metabolite turnover as a function of the differential microbial gene abundances, which showed predicted accumulation of metabolites associated with denitrification processes, including anammox, in the contaminated samples compared to uncontaminated sediments, with the magnitude of this change being positively correlated to the hydrocarbon concentration and exposure duration. These data highlight the potential impact of hydrocarbon inputs on N cycling processes in marine sediments and provide information relevant for system scale models of nitrogen metabolism in affected ecosystems.

**Keywords:** nitrogen cycling, marine sediments, denitrification, microbial ecology, metagenomics, deepwater horizon oil spill, oil contamination, oil seeps

## INTRODUCTION

Petroleum hydrocarbon spills considerably alter the composition and functional dynamics of marine microbial communities (Hazen et al., 2010; Gutierrez et al., 2013). Ultimately, microorganisms that can respond to complex hydrocarbon mixtures are preferentially enriched by hydrocarbons provided during an oil spill; growing from small natural seed populations (Röling et al., 2002, 2004). A number of studies have demonstrated changes in the spatiotemporal ecology of microbial communities in the presence of oil contamination (Bordenave et al., 2007; Païssé et al., 2008; Hazen et al., 2010; Bælum et al., 2012; Lu et al., 2012; Mason et al., 2012), which has concomitant impacts on microbially-mediated biogeochemistry (Atlas, 1991). Proliferation of heterotrophs in the presence of hydrocarbons as the sole electron donor can result in the rapid depletion of oxygen in the ecosystem through aerobic respiration (Riser-Roberts, 1992).

One potential limiting factor for hydrocarbon degradation in marine sediments is nitrogen availability (Herbert, 1999). Marine sediments are a key location for global nitrogen cycling (Engström et al., 2009; Lam and Kuypers, 2011; Hamme and Emerson, 2013), because they provide both a physical location for organic matter remineralization through ammonification, and also an anoxic environment for denitrification processes (Laverock et al., 2011). At the water-sediment interface, ammonium generated through organic matter remineralization, is converted to nitrite and then nitrate by nitrification (Henriksen and Kemp, 1988). Available nitrite or nitrate may diffuse to the water column or be consumed in various biotic reactions depending on oxygen availability. Under oxygen limited conditions, deeper within the sediment, nitrate may be reduced via dissimilatory nitrate reduction to ammonium (DNRA), which can be anaerobically oxidized, with nitrite, to dinitrogen, through anammox processes, also the experimental evidence for this mechanism remains limited

(Brandes et al., 2007; Kalvelage et al., 2011). It has been estimated that dinitrogen production in deep benthic sediments (1000–3000 m) is responsible for ~7–16% of the total nitrogen loss in the marine ecosystem (Engström et al., 2009).

How oil contamination affects nitrogen cycling processes *in situ* is still not well understood (Deni and Penninckx, 1999; Bell et al., 2011; Trimmer et al., 2013). Although petroleum oil is typically rich in nitrogen, most of it is bound in aromatic heterocyclic compounds whose carbon to nitrogen bonds are difficult to break (Snyder, 1970). Thus, bioremediation of oil contamination often requires the addition of inorganic nutrients including nitrogen, phosphorus, and/or iron, to increase enzyme activity (Brook et al., 2001; Head et al., 2006; Bell et al., 2011). In the case of high carbon and low nitrogen environments, there is evidence of increased diazotrophy within microbial communities (Karl et al., 2002), although this has rarely been observed in the presence of hydrocarbons despite nitrogen limiting conditions (Laguerre et al., 1987; Eckford et al., 2002; Musat et al., 2006). A more recent study exploring the relationship between microbial nitrogen cycling dynamics and oil contamination found evidence of DNRA being coupled to nitrogen cycling in a suboxic hydrocarbon contaminated subsurface well (Yagi et al., 2010).

A number of studies have evaluated how well the relative abundance of genes encoding nitrogen metabolic enzymes correlate with biogeochemical measurements of N metabolism. For instance, the abundance of *nirS*, *nrfA*, *narG*, and *napA* genes involved in nitrite and nitrate reduction significantly predicted the rates of denitrification and DNRA in the Colne estuary (Dong et al., 2009). However, *nirK*, another nitrite reduction gene, has been shown to be a poor predictor of functional traits relevant for denitrification (Salles et al., 2012). The metabolic pathways themselves are a network of interactions, so we hypothesize that the non-linear relationship between gene abundance and metabolite turnover is best evaluated as a function of compound changes in the relative abundance of many different related genes, rather than any single gene abundance. Predicted relative metabolic turnover (PRMT) quantifies relative changes in the metabolic potential as a network of predicted metabolic reactions inferred from the relative abundance of genes annotated from a metagenome (Larsen et al., 2011). Each predicted metabolite is then a function of the predicted enzymes and their “metabolic community of reactions” rather than simply the relative abundance of just the single gene that codes for the enzyme responsible for the metabolism. PRMT has previously been used to accurately predict seasonal variation in metabolites in marine surface waters (Larsen et al., 2011).

Here we hypothesize that increasing exposure to elevated hydrocarbon concentrations will positively correlate with predicted metabolic shifts toward denitrification in anaerobic zones in sediments. This is based on the premise that previously challenged and constantly exposed hydrocarbon samples are more likely to be “primed” for hydrocarbon response (Deni and Penninckx, 1999; Labb   et al., 2007; Taketani et al., 2010). To test this hypothesis we analyzed metagenomic sequence data from 17 sediment samples from the Gulf of Mexico and the Santa Barbara Channel, which represent sites with short term exposure to oil contamination [those from the Deepwater Horizon (DWH) oil

spill], sites with a long history of exposure to hydrocarbons (those from the natural oil seeps), and sites unaffected by hydrocarbon contamination.

## MATERIALS AND METHODS

### DATA

Data were downloaded from MG-RAST (Meyer et al., 2008) including the DWH spill project (MGRAST IDs: 4510162.3-4510175.3) and the natural oil seeps study (MGRAST IDs: 4537092.3-4537094.3), which were all annotated using SEED, with a maximum *e*-value of  $1 \times 10^{-3}$ , a minimum identity of 50%, and minimum identity cutoff of 15. Data was also annotated in MG-RAST using Hierarchical Classification subsystems with a maximum *e*-value cutoff of  $10^{-5}$ , minimum percent identity cutoff of 60%, and a minimum alignment length cutoff of 15; this data was used for looking at functional annotations for gene abundances. For the samples collected from the Gulf of Mexico during the DWH spill, 6 of the samples were from oil-contaminated sites (hereafter referred to as DWH oil spill samples), and 8 samples were from uncontaminated sites (hereafter referred to as uncontaminated samples). This grouping was based on whether the samples clustered based on the normalized gene abundances, and additionally based on whether they exceeded ( $>1.0$  polycyclic aromatic hydrocarbon [PAH] index) or did not exceed EPA ( $\leq 1$  PAH index) BPA benchmarks for hydrocarbon pollution (Mason et al., 2014) (for more information about how the EPA aquatic benchmarks are calculated please see <http://www.epa.gov/bpspill/water-benchmarks.html#dblstar>). The Santa Barbara channel oil seep samples included depth, latitude and longitude, and collection date as contextual metadata. This data is summarized in Supplementary Table 1. The Gulf of Mexico samples (Mason et al., 2014) had these contextual metadata in addition to total petroleum hydrocarbons (TPH), polycyclic aromatic hydrocarbons (PAH), dissolved-phosphate (PO<sub>4</sub>-P), dissolved nitrate (NO<sub>3</sub>-N), total ammonia nitrogen (NH<sub>3</sub>-N and NH<sub>4</sub>-N), dissolved inorganic nitrogen (DIN; NH<sub>3</sub>-N and NH<sub>4</sub>-N), total nitrogen (NH<sub>3</sub>/NH<sub>4</sub>-N, NO<sub>3</sub>/NO<sub>2</sub>-N, and organic nitrogen), total sulfur (S), and total carbon (C). A complete metadata table for the Gulf of Mexico samples is given in Supplementary Table 1 of Mason et al. (2014). For more information about sample collection and the context of these samples please see Hawley et al. (2014), Mason et al. (2014). These values were normalized and log<sub>2</sub> transformed before analysis was performed.

### ANALYSIS

The oil seep samples had genetic sequences that annotated to 131 nitrogen metabolism genes that were not present in any of the Gulf samples. Thus for gene annotations, SEED Subsystems-based functional (level 2) annotations were summed and then standardized as a function of total reads within each sample. Predicted Metabolic Turnover Analysis (PRMT) (Larsen et al., 2011) was used to evaluate the community metabolic potential between samples as a function of microbial community gene abundances. PRMT transforms annotated enzyme abundances by a weighted matrix of all possible reactions including those enzymes, their reactions, and associated metabolites as annotated by KEGG (Ogata et al., 1999). Enzyme commission (EC)

abundances were gathered from the SEED Subsystems L3 tables, quantile normalized and then  $\log_2$  transformed before analysis. The EC abundances were compared to a “reference,” which in this analysis was an average of all samples. Positive PRMT score values represent the consumption of a particular metabolite, and negative scores represent the accumulation or production of a particular metabolite. For the nitrogen metabolism pathway (KEGG map00910), the PRMT scores were summed to give either a “net” positive or negative PRMT value. The “net difference” or “pathway flow” was found by adding the net positive and net negative values for PRMT scores for each metabolite in the pathway per sample. For comparisons of sample scores, Kruskal-Wallis rank sum tests were used. Hierarchical annotation for gene abundances were also quantile normalized and  $\log_2$  transformed. A principal component analysis was performed on the quantile normalized and  $\log_2$  transformed hierarchical abundances, removing those genes completely absent in the Gulf of Mexico dataset. To pull out hydrazine related gene sequences, bowtie 1.0.0 (Langmead et al., 2009) was used to align reads to custom index of hydrazine hydratase related sequences downloaded from NCBI (Benson et al., 2013). Then we used reads per kilobase per million (RPKM), quantile normalization, and a  $\log_2$  transformation to normalize the hydrazine hydratase related gene abundances. Pearson correlation coefficients (corr) were used where cited. 10,000 permutations were used to assess empirical  $p$ -values.

## RESULTS

The contaminated sediments from the Gulf of Mexico were exposed to hydrocarbon contamination from the DWH spill for between 3 and 5 months at the time they were collected. By contrast, the natural oil seeps from the Santa Barbara Channel were estimated to be exposed to hydrocarbons for more than 11,000 years (Hornafius et al., 1999). To the best of our knowledge the uncontaminated sediments from the Gulf of Mexico had not recently been exposed to the amounts of hydrocarbon contamination caused by the DWH Oil spill, although historical presence of temporary natural oil seeps nearby cannot be ruled out (Kvenvolden and Cooper, 2003). The metagenomic data were all generated using the HiSeq2000 platform, with a minimum of 36,851,796 reads and a maximum of 86,321,188 reads per metagenome, with read lengths of  $\sim 150$  bp.

### OIL SEEP SAMPLES MAINTAINED A GREATER DIVERSITY OF GENES ASSOCIATED WITH NITROGEN METABOLISM

Oil seep samples had sequences that annotated to 131 nitrogen metabolism genes; these genes were not present in the samples from the Gulf of Mexico (oil spill and uncontaminated sites). Of the 11 SEED level 2 annotations within nitrogen metabolism, 4 were present only in the oil seep samples- these included amide cluster with urea and nitrile hydratase functions, cyanate hydrolysis, citric oxide synthase, and nitrilase.

### NITROGEN METABOLISM GENES SHOWED DIFFERENTIAL RELATIVE ABUNDANCES BETWEEN THE 3 DIFFERENT SAMPLE GROUPS

Anammox pathway specific genes related to hydrazine production (an intermediate of the anammox reaction pathway) were not

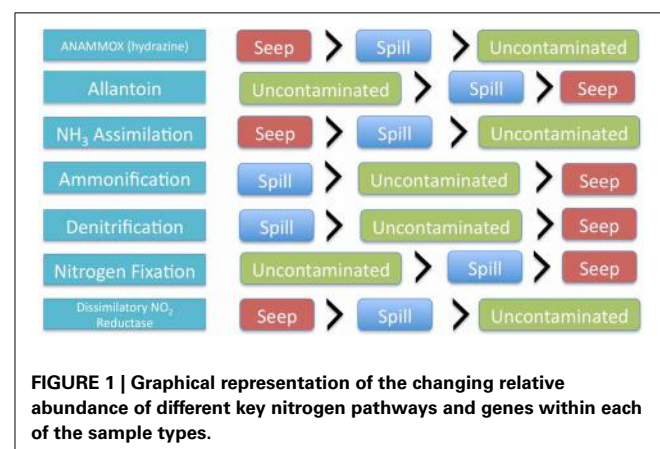
significantly different between oil seep, oil spill and uncontaminated samples; however they trended toward higher abundance in oil seep samples, followed by oil spill samples and uncontaminated samples. Interestingly, nitrosative stress, was found only in the petroleum-contaminated groups (both oil spill and oil seep), and is involved in response to nitric oxide accumulation (Ridnour et al., 2004). Coincidentally, nitric oxide is predicted to be accumulated by the PRMT analysis (Table 2). Interestingly, only 3 of the 11 SEED level 2 nitrogen pathway annotations showed a significantly different relative abundance between sample types, including dissimilatory nitrite reductase, nitrate and nitrite ammonification, and nitrogen fixation (Table 1, Figure 1).

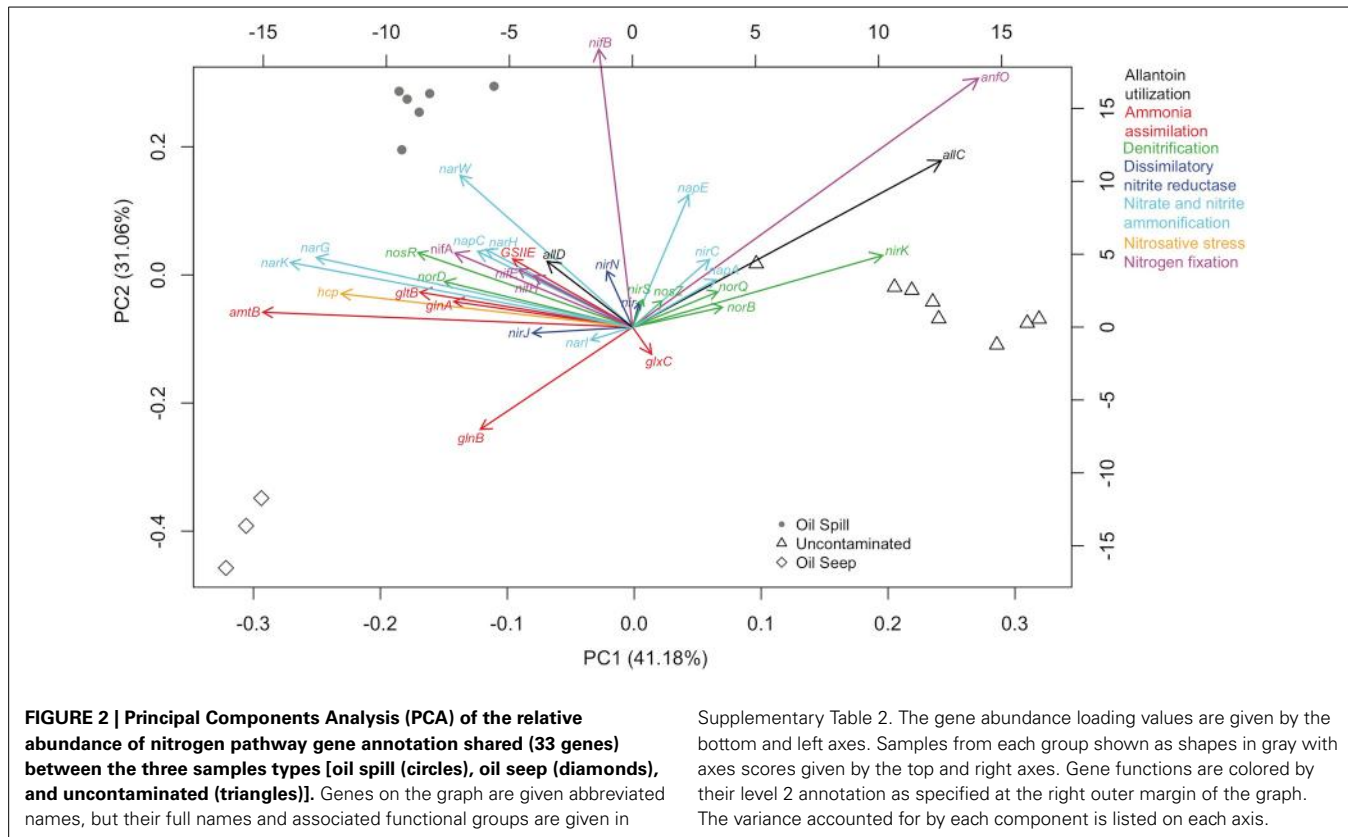
A principal component analysis was performed using only the 33 genes that were present across all sample types, with the SEED level 2 hierarchical gene annotation used to demonstrate which genes showed the greatest differentiation between sample types (Figure 2). The first two principal components account for 72.78% of the variance, and while the variance and the distribution of the sample types was due to multiple factors, the influence of key genes in differentiation of sample types was evident. For example, an abundance of nitrogen regulatory protein P-II (*glnB*) in seep samples, respiratory nitrate reductase (alpha, beta, delta, and gamma chain; *narG*, *narH*, *narW* and *narI*,

**Table 1 | Average proportion of reads annotation to each SEED subsystems-based functional annotation (level 2) function from nitrogen metabolism with their standard deviations in parentheses.**

	Oil seep	Oil spill	Uncontaminated
Allantoin utilization	0.034 (0.008)	0.082 (0.024)	0.232 (0.123)
Ammonia assimilation	0.44 (0.007)	0.313 (0.029)	0.272 (0.227)
Denitrification	0.107 (0.031)	0.122 (0.010)	0.111 (0.034)
Dissimilatory nitrite reductase*	0.059 (0.005)	0.019 (0.006)	0.016 (0.010)
Nitrate and nitrite ammonification*	0.206 (0.021)	0.299 (0.016)	0.215 (0.074)
Nitrogen fixation*	0.055 (0.025)	0.136 (0.013)	0.153 (0.056)

\* $p$ -value < 0.05.





respectively) and nitrogenase (alpha and beta chain; *nifA* and *nifB*, respectively) in DWH spill samples, and Cu-nitrite reductase (*nirK*), AnFO protein (*anfO*), and allantoate amidohydrolase (*allC*) in uncontaminated sediments played a considerable role in the differentiation of the 3 sample types (Figure 2).

#### THE PREDICTED RELATIVE TURNOVER FOR NITROGEN METABOLITES WAS SIGNIFICANTLY DIFFERENT BETWEEN THE 3 GROUPS

The relative abundance of individual key genes showed differential responses (Figures 1, 2) across the gradient of hydrocarbon exposure time (seep > DWH spill > uncontaminated); therefore PRMT was used to infer how these differential relative abundances could be combined to predict relative metabolite turnover for the different nitrogen pathways. The KEGG nitrogen metabolism reference pathway includes 21 metabolites. The PRMT scores were used to infer whether these metabolites were relatively consumed or accumulated in each group; the PRMT score is positive if the metabolite is being consumed, and negative if it is being accumulated, with the magnitude an indication of the relative level of this metabolism. The overall “pathway flow” (the difference between predicted “net consumption” and “net production” for all metabolites in a pathway) was positive for the three sample types. A positive net pathway flow suggests that overall more nitrogen metabolites were being consumed than accumulated. The difference in “pathway flow” between the sample types was not significantly different; however, the highest “pathway flow” score was found in the oil seeps (PRMT “net difference” score [ $\text{PRMT}_{\text{diff}}$ ] = 11.35),

followed by the DWH spill samples ( $\text{PRMT}_{\text{diff}} = 10.77$ ) and uncontaminated sediments ( $\text{PRMT}_{\text{diff}} = 9.56$ ). When the average “net accumulation” (negative PRMT) scores were summed per group, the difference between sample types was significantly different ( $p = 0.02$ ) and 2-fold higher in the oil seep samples (PRMT “net production” [ $\text{PRMT}_p$ ] = -14.39) compared to the DWH spill ( $\text{PRMT}_p = -8.08$ ) and uncontaminated sediments ( $\text{PRMT}_p = -7.15$ ). For the specific metabolites in the pathway, there were also numerous significant differences between sample types (Table 2). Specifically, nitrate was predicted to be significantly more consumed in the oil seep (mean = 5.1,  $SD = 2.73$ ) and DWH spill samples (mean = 2.98,  $SD = 3.41$ ), compared to uncontaminated sediments, where it was predicted to be more significantly accumulated (mean = -0.75,  $SD = 0.73$ ;  $p$ -value < 0.01). Meanwhile, nitrite was predicted to be significantly more accumulated in the oil seep (mean = -3.28,  $SD = 0.64$ ) and DWH spill samples (mean = -1.99,  $SD = 1.67$ ), while being relatively consumed in the uncontaminated sediments (mean = 0.37,  $SD = 0.58$ ;  $p$ -value < 0.01). Genes annotating to nitrosative stress were only found in the hydrocarbon contaminated sediments, which is supported by the prediction that nitric oxide was significantly more accumulated in both the oil seep (mean = -2.3,  $SD = 1.27$ ) and oil spill (mean = -1.1,  $SD = 0.31$ ) compared to the uncontaminated sediments where it was relatively consumed (mean = 0.45,  $SD = 0.61$ ). There was also a relative increase in the consumption of ammonia in the oil seep group, although this difference was not statistically significant (Table 1). In addition, nitrile was predicted to be significantly consumed

**Table 2 | Nitrogen metabolism associated metabolites' mean (and standard deviation in parentheses) PRMT scores.**

Metabolite	Oil Seep (N = 3)	Oil Spill (N = 6)	Uncontaminated (N = 8)
NH <sub>3</sub>	0.41 (0.08)	-0.11 (0.31)	-0.27 (0.67)
Nitrite**	-3.28 (0.64)	-1.99 (1.67)	0.37 (0.58)
Carbamoyl phosphate*	0.047 (0.32)	-1.28 (0.36)	-1.1 (0.43)
Nitrate**	5.1 (2.73)	2.98 (3.41)	-0.75 (0.73)
Formamide**	2.59 (0.6)	1.84 (0.52)	-0.69 (0.79)
Nitric oxide**	-2.3 (1.27)	-1.11 (0.31)	0.45 (0.61)
Nitrogen**	0.42 (2.11)	-0.75 (0.62)	3.88 (2.88)
Nitrile***	2.11 (0.59)	0.72 (0.14)	-0.34 (0.33)
Nitrous oxide*	-0.86 (1.57)	0.29 (0.17)	-0.13 (0.14)
alpha-amino acid	0.39 (0.12)	0.45 (0.33)	0.33 (0.54)
L-aspartate**	1.36 (0.52)	0.46 (0.71)	-0.76 (0.44)
L-glutamine*	0.57 (0.07)	0.07 (0.08)	-0.11 (0.07)
CO <sub>2</sub> *	-0.4 (0.21)	-0.08 (0.46)	0.45 (0.54)
L-glutamate	-0.38 (0.11)	-0.39 (0.21)	-0.11 (0.51)
Glycine*	0.23 (0.13)	0.8 (0.41)	-0.001 (0.56)
Formate	-1.26 (0.66)	-0.31 (0.57)	-0.45 (0.94)
L-asparagine	-0.65 (0.64)	-0.26 (0.59)	0.58 (2.38)
Hydroxylamine	0.61 (3.21)	-0.66 (1.99)	-0.32 (1.20)
Amide	0.28 (0.54)	0.88 (0.74)	0.45 (0.62)
Amine	1.93 (0.35)	1.76 (1.24)	0.23 (1.35)
Cyclic amidines	0.39 (0.36)	0.29 (0.06)	1.03 (1.63)

\*p-value < 0.05, \*\*p-value < 0.01, \*\*\*p-value < 0.001.

Positive values denote consumption and negative values denote accumulation of the metabolite.

(*p*-value < 0.001) in the oil seep (mean = 2.11, SD = 0.59) and the DWH spill samples (0.72, SD = 0.14), while being relatively accumulated in the uncontaminated sediments (mean = -0.34, SD = 0.33).

#### PRMT SCORES FOR NITROGEN PATHWAY METABOLITES SHOW SIGNIFICANT CORRELATIONS WITH IN SITU BIOGEOCHEMICAL MEASUREMENTS BETWEEN OIL SPILL AND UNCONTAMINATED SEDIMENT SAMPLES IN THE GULF OF MEXICO

The samples collected from the Gulf of Mexico were analyzed in more detail for significant correlations to the available biochemical data (Mason et al., 2014). PRMT scores for dinitrogen showed a significant positive correlation with measured concentrations of *in situ* total nitrogen (*p* < 0.05, corr = 0.55). In addition, a number of the other PRMT scores had significant correlations with total sulfur, total carbon, total nitrogen, dissolved nitrate, total ammonium, dissolved inorganic nitrogen, and dissolved phosphate (Table 3). The PRMT scores for nitrite had a significant negative correlation with total carbon (*p* < 0.01, corr = -0.58), which suggests that when there is more carbon there is a significant accumulation of nitrite. In addition, L-aspartate had a significant correlation (*p* < 0.05, corr = 0.53) with total hydrocarbon concentration.

## DISCUSSION

Here we present evidence of the impact of oil contamination, including comparisons of short-term vs. long-term duration of exposure, on nitrogen metabolism in marine sediments. Oil contaminated and uncontaminated sediment samples collected after the DWH spill in the Gulf of Mexico were compared to samples collected from natural oil seeps from the Santa Barbara Channel. Genes and pathways involved in the nitrogen cycle were annotated from metagenomic sequencing data and used to explore differences in the relative abundance of specific genes and to predict relative nitrogen metabolite turnover potential between the 3 sample types. These sample types come from disparate regions (e.g., Gulf of Mexico vs. Santa Barbara Channel), thus numerous other geochemical and physical factors could have played a role in the observed trends in nitrogen metabolism between these environments. However, this study suggests that the selective pressure of oil contamination contributes a significant role toward shaping the functional diversity of these community processes. In addition, we expand on an analysis of metagenome data (Mason et al., 2014) and show that this analysis can be useful for exploring the impacts of hydrocarbon contamination on nitrogen cycling in other contaminated environments.

Studies of the relative abundances of specific genes may not be the best way to study complex, multi-branching metabolic pathways. To overcome this limitation, we used PRMT to better capture the emergent property of the multiphasic gene abundance profiles that make up a metabolic pathway. The PRMT approach captures the relative metabolic changes across an observed assemblage of genes, and therefore the relative abundances of genes and their corresponding metabolic pathways are taken in proportion to each other (Larsen et al., 2011). The predicted "net pathway flow" suggests that overall more nitrogen metabolites were consumed in each sample type than were accumulated, with this value being greatest in the oil seep samples. While this might seem to infer a system mass balance bias, as the data used for predictions is static, these inferences cannot be used to infer mass potential. For those metabolites that are predicted to be accumulated, there was a two-fold increase in the oil seep samples compared to DWH spill and uncontaminated sediment samples. In addition, the specific metabolites that were predicted to accumulate in the contaminated samples were different from those in the uncontaminated samples, which may represent shifts in nitrogen cycling processes in sediments exposed to hydrocarbon saturation.

The metabolites that were significantly different between the three groups, i.e., nitrate, nitrite, and nitric oxide had a common trend in which the oil seep samples had the highest consumption and accumulation, followed by the DWH spill samples, and finally the uncontaminated samples, where the values were often close to 0; suggesting that the pathways involved in consumption and accumulation of nitrogen were balanced. Dinitrogen was an exception in that the uncontaminated sediments had a three-fold higher predicted consumption than in the contaminated samples. This was supported by the relative abundance of genes involved in diazotrophy (nitrogen fixation), which were most abundant in uncontaminated sediments.

**Table 3 | Pearson correlations of metadata from 14 metagenome samples (Mason et al., 2014) with predicted relative nitrogen metabolite PRMT scores and their associated *p*-values.**

	Total hydrocarbons	Total sulfur	Total carbon	Total nitrogen	Dissolved nitrate	Total ammonium	DIN	Dissolved phosphate	Sum of PAH
NH <sub>3</sub>	-0.02	-0.01	0.21	-0.45	0.11	0.10	0.08	0.002	-0.04
Nitrite	-0.45	-0.66**	-0.58**	0.07	-0.48	-0.49	-0.52	-0.28	-0.37
Carbamoyl phosphate	-0.001	0.04	-0.42	0.41	-0.37	-0.19	-0.22	-0.29	0.07
Nitrate	0.42	0.64**	0.55*	0.02	0.45	0.48	0.50	0.26	0.39
Formamide	0.47	0.41	0.78***	-0.45	0.57*	0.44	0.49	0.45	0.33
Nitric oxide	-0.45	-0.47	-0.67**	0.34	-0.49	-0.42	-0.47	-0.32	-0.37
Nitrogen	-0.19	-0.21	-0.46	0.55*	-0.11	-0.45	-0.41	-0.34	-0.20
Nitrile	0.43	0.46	0.72**	-0.46	0.49	0.52*	0.54*	0.45	0.30
Nitrous oxide	0.44	0.44	0.57*	-0.41	0.51	0.49	0.51	0.57*	0.33
alpha-Amino acid	0.19	0.24	0.05	0.28	-0.09	-0.09	-0.09	-0.07	0.16
L-aspartate	0.53*	0.39	0.66**	-0.16	0.52*	0.23	0.29	0.29	0.47
L-glutamine	-0.40	-0.06	-0.13	-0.005	-0.21	0.04	0.002	-0.33	-0.39
CO <sub>2</sub>	0.10	0.13	-0.42	0.50	-0.29	-0.35	-0.40	-0.28	0.13
L-glutamate	0.36	0.19	0.49	-0.46	0.45	0.38	0.45	0.44	0.21
Glycine	0.47	0.51	0.56*	0.08	0.58*	0.28	0.33	0.37	0.45
Formate	0.17	-0.08	0.37	0.04	0.58*	0.001	0.11	0.29	0.23
L-asparagine	-0.08	-0.15	-0.24	0.28	-0.07	-0.15	-0.11	-0.11	0.002
Hydroxylamine	-0.37	0.05	-0.15	0.11	0.33	0.33	0.39	0.15	-0.56
Amide	0.43	0.71**	0.32	0.42	0.33	0.30	0.34	0.19	0.41
Amine	0.29	0.07	0.48	-0.04	0.22	0.07	0.09	0.18	0.43
Cyclic amidines	0.05	-0.19	-0.33	0.39	-0.14	-0.33	-0.31	-0.05	0.14

\**p*-value < 0.05, \*\**p*-value < 0.01, \*\*\**p*-value < 0.001.

The sum of predicted metabolite turnover scores for all nitrogen metabolism pathways evidenced an increase in denitrification processes either through canonical denitrification or anammox, as nitrite and nitric oxide were predicted to significantly accumulate and nitrate was predicted to be consumed by microbial metabolism in contaminated samples. It is more likely that this evidence could be interpreted as relating to canonical denitrification, despite the relatively higher abundance of anammox pathway specific genes related to hydrazine production and ammonium assimilation in seep and spill compared to uncontaminated samples.

The oil spill sediments from the Gulf of Mexico were collected ~3 months after the Deepwater Horizon's Macondo well was capped, thus giving them an active exposure time between 3 and 5 months, if we assume the absence of natural oil seeps near these sites. By contrast, the oil seep samples from the Santa Barbara Channel were actively exposed to petroleum for more than 11,000 years (Hornafius et al., 1999) and samples were taken directly from the seep head. The difference in the time of exposure to hydrocarbon pollution in the oil-contaminated sediments could thus account for differences in the predicted turnover of nitrogen metabolites. Additionally, significant differences in the composition of the oil from both sites (Hornafius et al., 1999; Reddy et al., 2011), may also have influenced the observed compositional differences the microbial communities (Hawley et al., 2014; Mason et al., 2014). Depth of sample collection from the two different environments may also have affected nitrogen cycling

as shown in several studies (Engström et al., 2009; Trimmer et al., 2013), however, this trend is probably due to differences in the physicochemical properties of different sites, as has been shown for sites at different distances from shore (Herbert, 1999; Dalsgaard et al., 2005; Zhu et al., 2010). Despite these geographic, depth, and oil composition differences, there were surprising similarities in the response of metabolic turnover to hydrocarbon contamination, suggesting that oil contamination results in a predictable metabolic response despite differences in the affected ecosystems. It is suggested that a topic for future research might be using PRMT on genetic data generated from oil exposed laboratory enrichments or environmental samples through time, to aid in unraveling the relationship between nitrogen cycling and microbial oil remediation.

Nitrite consumption showed a significant negative correlation to the concentration of total carbon in the Gulf of Mexico sediments. The decreased availability of reactive carbon and a high concentration of organic carbon in extremely deep benthic environments would favor the dominance of anammox over denitrification (Thamdrup and Dalsgaard, 2002; Engström et al., 2005), which would therefore lead to direct oxidation of ammonia to dinitrogen reducing nitrite consumption. This would however lead to a nitrogen limited environment, which could be supplanted by the oxidation of organic matter by sulfur reducing bacteria (Canfield et al., 2010); this is potentially supported by significant correlations between the concentration of sulfur and the accumulation of nitrate and nitrite.

To summarize, there is evidence from the PRMT analysis for a shift in the metabolic flow of nitrogen to the denitrification pathways, potentially including the anammox pathway, in hydrocarbon-contaminated sediments (both DWH spill and natural oil seep). Changes in metabolites in the anammox pathway were positively correlated with hydrocarbon concentration, although these were not statistically significant, potentially due to the small sample sizes and confounding environmental factors. The relative abundance of genes related to anammox associated hydrazine metabolism were also greatest in the seep samples that were predicted to have been exposed to hydrocarbons for ~11,000 years.

Marine sediments are very important sites for microbially mediated nitrogen transformation, providing a link between organic matter degradation and nutrient regeneration, essentially supporting primary productivity in the oceans. Exploring factors that significantly influence this process are vital for providing relevant data to propagate system scale models of how basin processes, such as nitrogen cycling and primary productivity in marine sediments, can influence regional and global climate.

## ACKNOWLEDGMENTS

This work was supported in part by the US Department of Energy under Contract DE-AC02-06CH11357 and under Contract DE-AC02-05CH11231, and BP/The Gulf of Mexico Research Initiative. The sequence data from the Santa Barbara oils were produced by the US Department of Energy Joint Genome Institute <http://www.jgi.doe.gov/> in collaboration with the user community. We also thank Ali Shojaie for his advice about missing data problems in statistical analyses and Ben Rathbone for analytical discussions.

## SUPPLEMENTARY MATERIAL

The Supplementary Material for this article can be found online at: <http://www.frontiersin.org/journal/10.3389/fmicb.2014.00108/abstract>

## REFERENCES

- Atlas, R. M. (1991). Microbial hydrocarbon degradation—bioremediation of oil spills. *J. Chem. Technol. Biotechnol.* 52, 149–156. doi: 10.1002/jctb.280520202
- Bælum, J., Borglin, S., Chakraborty, R., Fortney, J. L., Lamendella, R., Mason, O. U., et al. (2012). Deep-sea bacteria enriched by oil and dispersant from the Deepwater Horizon spill. *Environ. Microbiol.* 14, 2405–2416. doi: 10.1111/j.1462-2920.2012.02780.x
- Bell, T. H., Yergeau, E., Martineau, C., Juck, D., Whyte, L. G., and Greer, C. W. (2011). Identification of nitrogen-incorporating bacteria in petroleum-contaminated arctic soils by using [15N]DNA-based stable isotope probing and pyrosequencing. *Appl. Environ. Microbiol.* 77, 4163–4171. doi: 10.1128/AEM.00172-11
- Benson, D. A., Cavanaugh, M., Clark, K., Karsch-Mizrachi, I., Lipman, D. J., Ostell, J., et al. (2013). GenBank. *Nucleic Acids Res.* 41, D36–D42. doi: 10.1093/nar/gks1195
- Bordenave, S., Goñi-Urriza, M. S., Caumette, P., and Duran, R. (2007). Effects of heavy fuel oil on the bacterial community structure of a pristine microbial mat. *Appl. Environ. Microbiol.* 73, 6089–6097. doi: 10.1128/AEM.01352-07
- Brandes, J. A., Devol, A. H., and Deutsch, C. (2007). New developments in the marine nitrogen cycle. *Chem. Rev.* 107, 577–589. doi: 10.1021/cr050377t
- Brook, T. R., Stiver, W. H., and Zytner, R. G. (2001). Biodegradation of diesel fuel in soil under various nitrogen addition regimes. *Soil Sediment Contam. Int. J.* 10, 539–553. doi: 10.1080/200115891109428
- Canfield, D. E., Glazer, A. N., and Falkowski, P. G. (2010). The evolution and future of earth's nitrogen cycle. *Science* 330, 192–196. doi: 10.1126/science.1186120
- Dalsgaard, T., Thamdrup, B., and Canfield, D. E. (2005). Anaerobic ammonium oxidation (anammox) in the marine environment. *Res. Microbiol.* 156, 457–464. doi: 10.1016/j.resmic.2005.01.011
- Deni, J., and Penninckx, M. J. (1999). Nitrification and autotrophic nitrifying bacteria in a hydrocarbon-polluted soil. *Appl. Environ. Microbiol.* 65, 4008–4013.
- Dong, L. F., Smith, C. J., Papaspyrou, S., Stott, A., Osborn, A. M., and Nedwell, D. B. (2009). Changes in benthic denitrification, nitrate ammonification, and anammox process rates and nitrate and nitrite reductase gene abundances along an estuarine nutrient gradient (the Colne Estuary, United Kingdom). *Appl. Environ. Microbiol.* 75, 3171–3179. doi: 10.1128/AEM.02511-08
- Eckford, R., Cook, F. D., Saul, D., Aislabie, J., and Foght, J. (2002). Free-living heterotrophic nitrogen-fixing bacteria isolated from fuel-contaminated Antarctic soils. *Appl. Environ. Microbiol.* 68, 5181–5185. doi: 10.1128/AEM.68.10.5181-5185.2002
- Engström, P., Penton, C. R., and Devol, A. H. (2009). Anaerobic ammonium oxidation in deep-sea sediments off the Washington margin. *Limnol. Oceanogr.* 54, 1643–1652. doi: 10.4319/lo.2009.54.5.1643
- Engström, P., Dalsgaard, T., Hulth, S., and Aller, R. C. (2005). Anaerobic ammonium oxidation by nitrite (anammox): implications for N<sub>2</sub> production in coastal marine sediments. *Geochim. Cosmochim. Acta* 69, 2057–2065. doi: 10.1016/j.gca.2004.09.032
- Gutierrez, T., Singleton, D. R., Berry, D., Yang, T., Aitken, M. D., and Teske, A. (2013). Hydrocarbon-degrading bacteria enriched by the Deepwater Horizon oil spill identified by cultivation and DNA-SIP. *ISME J.* 7, 2091–2104. doi: 10.1038/ismej.2013.98
- Hammie, R. C., and Emerson, S. R. (2013). Deep-sea nutrient loss inferred from the marine dissolved N<sub>2</sub>/Ar ratio. *Geophys. Res. Lett.* 40, 1149–1153. doi: 10.1002/grl.50275
- Hawley, E. R., Piao, H., Scott, N. M., Malfatti, S., Pagani, I., Huntemann, M., et al. (2014). Metagenomic analysis of microbial consortium from natural crude oil that seeps into the marine ecosystem offshore Southern California. *Stand. Genomic Sci.* 9, 635–650. doi: 10.4056/sigs.5029016
- Hazen, T. C., Dubinsky, E. A., DeSantis, T. Z., Andersen, G. L., Piceno, Y. M., Singh, N., et al. (2010). Deep-sea oil plume enriches indigenous oil-degrading bacteria. *Science* 330, 204–208. doi: 10.1126/science.1195979
- Head, I. M., Jones, D. M., and Röling, W. F. M. (2006). Marine microorganisms make a meal of oil. *Nat. Rev. Microbiol.* 4, 173–182. doi: 10.1038/nrmicro1348
- Henriksen, K., and Kemp, W. M. (1988). “Nitrification in estuarine and coastal marine sediments: methods, patterns and regulating factors,” in *Nitrogen Cycling in Coastal Marine Environments*, eds T. H. Blackburn and J. Sørensen (Hoboken, NJ: John Wiley and Sons), 207–250.
- Herbert, R. A. (1999). Nitrogen cycling in coastal marine ecosystems. *FEMS Microbiol. Rev.* 23, 563–590. doi: 10.1111/j.1574-6976.1999.tb00414.x
- Hornafius, J. S., Quigley, D., and Luyendyk, B. P. (1999). The world's most spectacular marine hydrocarbon seeps (Coal Oil Point, Santa Barbara Channel, California): quantification of emissions. *J. Geophys. Res. Oceans* 104, 20703–20711. doi: 10.1029/1999JC900148
- Kalvelage, T., Jensen, M. M., Contreras, S., Revsbech, N. P., Lam, P., Günter, M., et al. (2011). Oxygen sensitivity of anammox and coupled N-cycle processes in oxygen minimum zones. *PLoS ONE* 6:e29299. doi: 10.1371/journal.pone.0029299
- Karl, D., Michaels, A., Bergman, B., Capone, D., Carpenter, E., Letelier, R., et al. (2002). Dinitrogen fixation in the world's oceans. *Biogeochemistry* 57–58, 47–98. doi: 10.1023/A:1015798105851
- Kvenvolden, K. A., and Cooper, C. K. (2003). Natural seepage of crude oil into the marine environment. *Geo-Mar. Lett.* 23, 140–146. doi: 10.1007/s00367-003-0135-0
- Labbé, D., Margesin, R., Schinner, F., Whyte, L. G., and Greer, C. W. (2007). Comparative phylogenetic analysis of microbial communities in pristine and hydrocarbon-contaminated Alpine soils. *FEMS Microbiol. Ecol.* 59, 466–475. doi: 10.1111/j.1574-6941.2006.00250.x
- Laguerre, G., Bossand, B., and Bardin, R. (1987). Free-living dinitrogen-fixing bacteria isolated from petroleum refinery oily sludge. *Appl. Environ. Microbiol.* 53, 1674–1678.
- Lam, P., and Kuypers, M. M. M. (2011). Microbial nitrogen cycling processes in oxygen minimum zones. *Annu. Rev. Mar. Sci.* 3, 317–345. doi: 10.1146/annurev-marine-120709-142814

- Langmead, B., Trapnell, C., Pop, M., and Salzberg, S. L. (2009). Ultrafast and memory-efficient alignment of short DNA sequences to the human genome. *Genome Biol.* 10, R25. doi: 10.1186/gb-2009-10-3-r25
- Larsen, P. E., Collart, F. R., Field, D., Meyer, F., Keegan, K. P., Henry, C. S., et al. (2011). Predicted Relative Metabolomic Turnover (PRMT): determining metabolic turnover from a coastal marine metagenomic dataset. *Microb. Inform. Exp.* 1, 4. doi: 10.1186/2042-5783-1-4
- Laverock, B., Gilbert, J. A., Tait, K., Osborn, A. M., and Widdicombe, S. (2011). Bioturbation: impact on the marine nitrogen cycle. *Biochem. Soc. Trans.* 39, 315–320. doi: 10.1042/BST0390315
- Lu, Z., Deng, Y., Van Nostrand, J. D., He, Z., Voordeckers, J., Zhou, A., et al. (2012). Microbial gene functions enriched in the Deepwater Horizon deep-sea oil plume. *ISME J.* 6, 451–460. doi: 10.1038/ismej.2011.91
- Mason, O. U., Hazen, T. C., Borglin, S., Chain, P. S. G., Dubinsky, E. A., Fortney, J. L., et al. (2012). Metagenome, metatranscriptome and single-cell sequencing reveal microbial response to Deepwater Horizon oil spill. *ISME J.* 6, 1715–1727. doi: 10.1038/ismej.2012.59
- Mason, O. U., Scott, N. M., Gonzalez, A., Robbins-Pianka, A., Bælum, J., Kimbrel, J., et al. (2014). Metagenomics reveals sediment microbial community response to Deepwater Horizon oil spill. *ISME J.* doi: 10.1038/ismej.2013.254. [Epub ahead of print].
- Meyer, F., Paarmann, D., D'Souza, M., Olson, R., Glass, E. M., Kubal, M., et al. (2008). The metagenomics RAST server – a public resource for the automatic phylogenetic and functional analysis of metagenomes. *BMC Bioinformatics* 9:386. doi: 10.1186/1471-2105-9-386
- Musat, F., Harder, J., and Widdel, F. (2006). Study of nitrogen fixation in microbial communities of oil-contaminated marine sediment microcosms. *Environ. Microbiol.* 8, 1834–1843. doi: 10.1111/j.1462-2920.2006.01069.x
- Ogata, H., Goto, S., Sato, K., Fujibuchi, W., Bono, H., and Kanehisa, M. (1999). KEGG: Kyoto Encyclopedia of Genes and Genomes. *Nucleic Acids Res.* 27, 29–34. doi: 10.1093/nar/27.1.29
- Païssé, S., Coulon, F., Goñi-Urriza, M., Peperzak, L., McGinity, T. J., and Duran, R. (2008). Structure of bacterial communities along a hydrocarbon contamination gradient in a coastal sediment. *FEMS Microbiol. Ecol.* 66, 295–305. doi: 10.1111/j.1574-6941.2008.00589.x
- Reddy, C. M., Arey, J. S., Seewald, J. S., Sylva, S. P., Lemkau, K. L., Nelson, R. K., et al. (2011). Composition and fate of gas and oil released to the water column during the Deepwater Horizon oil spill. *Proc. Natl. Acad. Sci. U.S.A.* 20229–20234. doi: 10.1073/pnas.1101242108
- Ridnour, L. A., Thomas, D. D., Mancardi, D., Espey, M. G., Miranda, K. M., Paolocci, N., et al. (2004). The chemistry of nitrosative stress induced by nitric oxide and reactive nitrogen oxide species. Putting perspective on stressful biological situations. *Biol. Chem.* 385, 1–10. doi: 10.1515/BC.2004.001
- Riser-Roberts, E. (1992). *Bioremediation of Petroleum Contaminated Sites*. Boca Raton, FL: CRC Press.
- Röling, W. F. M., Milner, M. G., Jones, D. M., Fratetpietro, F., Swannell, R. P. J., Daniel, F., et al. (2004). Bacterial community dynamics and hydrocarbon degradation during a field-scale evaluation of bioremediation on a mudflat beach contaminated with buried oil. *Appl. Environ. Microbiol.* 70, 2603–2613. doi: 10.1128/AEM.70.5.2603-2613.2004
- Röling, W. F. M., Milner, M. G., Jones, D. M., Lee, K., Daniel, F., Swannell, R. J. P., et al. (2002). Robust hydrocarbon degradation and dynamics of bacterial communities during nutrient-enhanced oil spill bioremediation. *Appl. Environ. Microbiol.* 68, 5537–5548. doi: 10.1128/AEM.68.11.5537-5548.2002
- Salles, J. F., Le Roux, X., and Poly, F. (2012). Relating phylogenetic and functional diversity among denitrifiers and quantifying their capacity to predict community functioning. *Front. Microbiol.* 3:209. doi: 10.3389/fmicb.2012.00209
- Snyder, L. R. (1970). Petroleum nitrogen compounds and oxygen compounds. *Acc. Chem. Res.* 3, 290–299. doi: 10.1021/ar50033a002
- Taketani, R. G., Franco, N. O., Rosado, A. S., and van Elsas, J. D. (2010). Microbial community response to a simulated hydrocarbon spill in mangrove sediments. *J. Microbiol.* 48, 7–15. doi: 10.1007/s12275-009-0147-1
- Thamdrup, B., and Dalsgaard, T. (2002). Production of N(2) through anaerobic ammonium oxidation coupled to nitrate reduction in marine sediments. *Appl. Environ. Microbiol.* 68, 1312–1318. doi: 10.1128/AEM.68.3.1312-1318.2002
- Trimmer, M., Engström, P., and Thamdrup, B. (2013). Stark contrast in denitrification and anammox across the deep Norwegian trench in the Skagerrak. *Appl. Environ. Microbiol.* 79, 7381–7389. doi: 10.1128/AEM.01970-13
- Yagi, J. M., Suflita, J. M., Gieg, L. M., DeRito, C. M., Jeon, C.-O., and Madsen, E. L. (2010). Subsurface cycling of nitrogen and anaerobic aromatic hydrocarbon biodegradation revealed by nucleic acid and metabolic biomarkers. *Appl. Environ. Microbiol.* 76, 3124–3134. doi: 10.1128/AEM.00172-10
- Zhu, G., Jetten, M. S. M., Kuschk, P., Ettwig, K. F., and Yin, C. (2010). Potential roles of anaerobic ammonium and methane oxidation in the nitrogen cycle of wetland ecosystems. *Appl. Microbiol. Biotechnol.* 86, 1043–1055. doi: 10.1007/s00253-010-2451-4

**Conflict of Interest Statement:** The authors declare that the research was conducted in the absence of any commercial or financial relationships that could be construed as a potential conflict of interest.

*Received: 22 November 2013; accepted: 03 March 2014; published online: 25 March 2014.*

*Citation: Scott NM, Hess M, Bouskill NJ, Mason OU, Jansson JK and Gilbert JA (2014) The microbial nitrogen cycling potential is impacted by polycyclic aromatic hydrocarbon pollution of marine sediments. Front. Microbiol. 5:108. doi: 10.3389/fmicb.2014.00108*

*This article was submitted to Aquatic Microbiology, a section of the journal Frontiers in Microbiology.*

*Copyright © 2014 Scott, Hess, Bouskill, Mason, Jansson and Gilbert. This is an open-access article distributed under the terms of the Creative Commons Attribution License (CC BY). The use, distribution or reproduction in other forums is permitted, provided the original author(s) or licensor are credited and that the original publication in this journal is cited, in accordance with accepted academic practice. No use, distribution or reproduction is permitted which does not comply with these terms.*



# Biodegradation of MC252 oil in oil:sand aggregates in a coastal headland beach environment

Vijaikrishnah Elango, Marilany Urbano, Kendall R. Lemelle and John H. Pardue \*

Department of Civil and Environmental Engineering, Louisiana State University, Baton Rouge, LA, USA

**Edited by:**

Joel E. Kostka, Georgia Institute of Technology, USA

**Reviewed by:**

David Gregory Weissbrodt, ETH Zürich and Eawag, Switzerland

Christoph Aeppli, Bigelow

Laboratory for Ocean Sciences, USA

Markus Huettel, Florida State University, USA

**\*Correspondence:**

John H. Pardue, Department of Civil and Environmental Engineering, Louisiana State University, 3523

Patrick F. Taylor Hall, Baton Rouge, LA 70803, USA

e-mail: jpardue@lsu.edu

Unique oil:sand aggregates, termed surface residue balls (SRBs), were formed on coastal headland beaches along the northern Gulf of Mexico as emulsified MC252 crude oil mixed with sand following the *Deepwater Horizon* spill event. The objective of this study is to assess the biodegradation potential of crude oil components in these aggregates using multiple lines of evidence on a heavily-impacted coastal headland beach in Louisiana, USA. SRBs were sampled over a 19-month period on the supratidal beach environment with reasonable control over and knowledge of the residence time of the aggregates on the beach surface. Polycyclic aromatic hydrocarbons (PAHs) and alkane concentration ratios were measured including PAH/C30-hopane, C2/C3 phenanthrenes, C2/C3 dibenzothiophenes and alkane/C30-hopane and demonstrated that biodegradation was occurring in SRBs in the supratidal. These biodegradation reactions occurred over time frames relevant to the coastal processes moving SRBs off the beach. In contrast, submerged oil mat samples from the intertidal did not demonstrate chemical changes consistent with biodegradation. Review and analysis of additional biogeochemical parameters suggested the existence of a moisture and nutrient-limited biodegradation regime on the supratidal beach environment. At this location, SRBs possess moisture contents <2% and molar C:N ratios from 131–323, well outside of optimal values for biodegradation in the literature. Despite these limitations, biodegradation of PAHs and alkanes proceeded at relevant rates ( $2\text{--}8 \text{ year}^{-1}$ ) due in part to the presence of degrading populations, i.e., *Mycobacterium* sp., adapted to these conditions. For submerged oil mat samples in the intertidal, an oxygen and salinity-impacted regime is proposed that severely limits biodegradation of alkanes and PAHs in this environment. These results support the hypothesis that SRBs deposited at different locations on the beach have different biogeochemical characteristics (e.g., moisture, salinity, terminal electron acceptors, nutrient, and oil composition) due, in part, to their location on the landscape.

**Keywords:** PAHs, crude oil, beach, *Deepwater Horizon*, biodegradation, alkanes, biogeochemistry

## INTRODUCTION

MC252 oil reaching the shoreline from the *Deepwater Horizon* blowout was primarily in the form of a water-in-oil emulsion. As these emulsions reached sandy beach shorelines, they mixed with sand and shell to produce several unique oil forms including thick agglomerated deposits, termed oil “mats” or “tarmats,” and smaller oil:sand aggregates, termed “surface residue balls” or SRBs. SRBs are typically 0.5–5 cm in diameter (Urbano et al., 2013). The aggregates are stable in that they can be easily handled without breaking and can be transported by waves and currents across the beach. SRBs are often imprecisely referred to as “tar balls” which are solid or semi-solid pieces of weathered oil which wash onto beaches worldwide from natural and anthropogenic sources (Nemirovskaya, 2011; Suneel et al., 2013). Characterization of some of the biogeochemical properties of SRBs has been performed for risk and fate purposes (OSAT-II, 2011; Urbano et al., 2013), but longer-term weathering or biodegradation studies are limited (Aeppli et al., 2012; Hall et al., 2013).

The presence of soil aggregates can inhibit the rate and extent of biodegradation processes of hydrocarbons by a number of mechanisms including pore size exclusion of microbial populations and diffusion limitations on supplies of key nutrients and electron acceptors (Monrozier et al., 1991; Scow and Alexander, 1992; Nocentini and Pinelli, 2001; Nam et al., 2003). The rate of biodegradation is often inversely related to aggregate size (Scow and Alexander, 1992). The SRB aggregates generally have higher porosities (Urbano et al., 2013) than clay aggregates that may mitigate diffusion limitations. However, SRB aggregate structure can provide protection from predation for hydrocarbon-degrading microbial populations and limit desiccation in moisture-limited environments. Larger aggregate sizes with their larger pore structure can create opportunities for biostimulation, i.e., addition of nutrients and oxygen (Chang et al., 2013).

Rate and extent of microbial degradation of crude oil components can be heavily influenced by geochemical parameters including temperature (Mohn and Stewart, 2000; Eriksson et al., 2001; Haritash and Kaushik, 2009), salinity (Kastner et al., 1998; Diaz et al., 2002; Badejo et al., 2013), nutrient content (Dibble and

Bartha, 1979; Chen et al., 2008; Tejeda-Agredano et al., 2011) and the availability of electron acceptors such as oxygen (Tang et al., 2006; Uribe-Jongbloed and Bishop, 2007; Haritash and Kaushik, 2009; Ortega-Calvo and Gschwend, 2010). On beach environments, additions of nutrients and organic matter have enhanced biodegradation rates of MC252 oil (Horel et al., 2012; Mortazavi et al., 2013) confirming previous studies (Bragg et al., 1994; Xu and Obbard, 2003). Background levels of nutrients are important in demonstrating a positive effect for fertilization on crude oil degrading consortia on beaches (Verosa et al., 1996). For crude oil classes of n-alkanes and polycyclic aromatic hydrocarbons (PAHs), optimal geochemical conditions for biodegradation are typically aerobic, low to moderate salinity conditions with sufficient available nitrogen and phosphorus to approximate cellular molar ratios of C:N:P (total carbon:total nitrogen:total phosphorus) of 100:10:1. The goal of this study was to determine and assess the biogeochemical conditions contributing to biodegradation of crude oil components in these coastal systems.

This study focuses on the heavily impacted coastal headland beach system, the Caminada Headlands, which consists of 2 segments, Elmer's Island and Fourchon Beach. This study will couple new oil composition and biogeochemical data with previous measurements on SRBs (Urbano et al., 2013) to make the case for the importance of biodegradation as an important fate process for these aggregates on the coastal headland beach environment. These systems are extremely dynamic, with tropical storms and strong cold fronts reworking the sand. The regularity of these storm events means that surface SRBs are washed away over time frames of months to years. Therefore, weathering reactions need to occur over time scales less than storm-driven transport to be relevant to hydrocarbon fate. Chemical analyses conducted for a suite of alkanes and PAHs on hundreds of SRBs and oil mat samples will be coupled with data on biogeochemical parameters to establish evidence for biodegradation potential. This data will also be used to develop hypotheses on which biogeochemical conditions that may be limiting the rate and extent of biodegradation of crude oil components in these aggregates. This paper provides the biodegradation potential assessment for a larger study on beach fate that has included papers on SRB characterization (Urbano et al., 2013) and the statistical distribution of SRBs on the beach surface (Lemelle et al., 2014).

## METHODS AND MATERIALS

### FIELD SAMPLING

SRBs were sampled from 5 distinct areas on the supratidal portion of the Caminada Headlands beach, 4 sites on Fourchon Beach and 1 site on Elmer's Island (Figure 1). Oil first reached this shoreline beginning on May 20, 2010. Two of the sites on Fourchon Beach, termed the "Zone 3" site and the "Zone 4" site were set aside from clean-up activities from October 2010 through June 2011. The sites were located north of the beach crest in the supratidal zone. SRBs were deposited on these beach segments by 2 tropical events, Hurricane Alex and TS Bonnie, which brought high tide and storm surge to the beach in June and July of 2010, respectively. The 2 sites were inspected daily and were unaffected by high tides, storm surge or cleanup activities during the sampling period: for the Zone 4 site (10/26/10–11/11/2010) and for the Zone 3 site

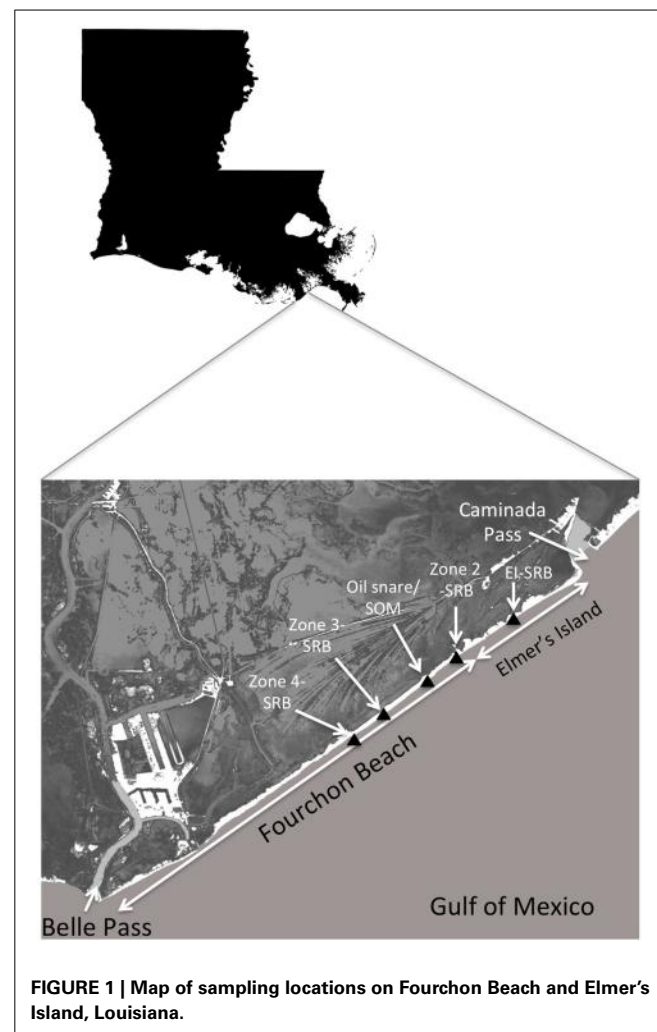


**FIGURE 1 |** Map of sampling locations on Fourchon Beach and Elmer's Island, Louisiana.

(12/15/11–12/21/11). The Zone 3 site was sampled again for SRBs on 5/18/11 after inspection and tidal records revealed that tidal surge did not impact this site from December 2010 to May 2011. SRBs were completely washed off of both sites during TS Lee, whose storm surge impacted the beach in September 2011.

The Zone 3 and Zone 4 sites each consisted of an area  $30.5\text{ m} \times 30.5\text{ m}$  with surface coverage of SRBs ranging from 0.01 to 8.1%. Both sites were sampled using randomized block methods without resampling. Briefly,  $0.9\text{ m} \times 0.9\text{ m}$  sampling areas were selected randomly, photographed, and 2 individual SRBs collected from the surface. In addition, composite SRB samples were obtained by sampling and sieving the top 5 cm of each selected area. Zone 4 was sampled on 10/26/2010 (day 159 since oil reached the shoreline), 11/04/2010 (day 167) and 11/11/2010 (day 174). Zone 3 was sampled on 12/15/2010 (day 208), 12/21/2010 (day 214) and 05/18/2011 (day 362). Information on the statistical surface and size distribution of SRBs is presented in a separate paper (Lemelle et al., 2014).

A third SRB location on Fourchon Beach ( $N 29^{\circ}09.34'$ ,  $W 090^{\circ}06.38'$ ) was sampled on 8/4/2011 (day 439) at an area east of the previous sampling areas in Zone 2. These SRBs were part of a broader characterization study of the biogeochemical

characteristics of the oil:sand aggregates (Urbano et al., 2013). These SRBs were presumed to have reached the supratidal during the same storms as the other 2 Fourchon sites and therefore extend the time frame of weathering an additional 2.5 months from the last samples taken from the Zone 3 site. Like the Zone 3 and Zone 4 sites, SRBs on the surface were completely removed by storm surge during TS Lee in 9/2011.

The fourth sampling location was on the supratidal of Elmer's Island, a segment of the Caminada Headlands beach east of Fourchon Beach. This location had a deposition field of SRBs on the edge of sand dunes at a slightly higher elevation than the beach surface. Sampling details are described in Urbano et al. (2013). These SRBs were not mobilized during TS Lee storm surge in 2011 and therefore allowed sampling of SRBs to continue through May 2012. Representative SRBs were obtained on 10/20/2011 (day 547), 2/9/2012 (day 628) and 5/31/2012 (day 739). Storm surge from Hurricane Isaac in August 2012 removed the remaining SRBs from this location. In total, SRB samples were obtained sequentially from 10/26/10 through 5/31/2012.

A fifth set of samples was obtained immediately after TS Lee in September 2011. These consisted of 2 sample types: submerged oil mat (SOM) samples and oil associated with oil snare, a pom-pom type of oil adsorbent used extensively on these beach during the active spill response. SOMs are larger oil, sand and shell agglomerations that were buried on the beach surface or offshore as a result of storm events described above. TS Lee broke up the subtidal mat and samples were obtained from the beach surface. Snare oil samples were associated with a set of pom-pom adsorbent left behind on the beach during the response and uncovered during TS Lee. These samples are significant since the oil snare was buried in the upper intertidal, where regular inundation of seawater would occur, but without complete submergence. Biogeochemical characteristics of these samples are described in Urbano et al. (2013).

MC252 oil was confirmed using the form of the oil as the identifying feature. The study focused solely on SRBs and SOMs; the oil, sand and shell aggregates that formed as emulsified MC252 mixed with sand and shell in the nearshore environment. These oil forms are unique to this spill in the Caminada Headlands environment. Condensed oil forms from other sources, including tar balls and tar patties, were occasionally observed at much lower frequencies to SRBs and SOMs. However, tar forms are visibly distinct by color, shape, and texture and therefore, were not sampled during the activities described above.

#### PAH AND N-ALKANE ANALYSIS

The SRBs, SOM and oil snare samples were extracted and analyzed for PAH, alkanes and hopane biomarkers. Discrete SRBs, SOM, and oil snare samples were extracted without drying. Composite samples from Zones 3 and 4 sampling sites were dried in a greenhouse for 5–7 days and sieved (30 USA standard testing sieve with 0.60 mm nominal opening) in the laboratory to separate SRBs from the beach sand. Subsamples of approximately 10 g were placed in a 50 mL Teflon tube with 20 mL of acetone/hexane (50:50 v/v) mixture and tumbled at room temperature for 48 h. Repetitive extraction on selected

samples demonstrated less than 10% of oil remains after this step. The tumbled Teflon tubes were centrifuged (Beckman Coulter Avanti J-20 XPI) at 8000 rpm for 10 min and the upper solvent phase in the tube was removed. The solvent was dried over Na<sub>2</sub>SO<sub>4</sub> and further concentrated to a 10 mL volume with a RapidVap N2 evaporation system (Labconco). The solvent extract was analyzed by injecting 1 µL onto a Hewlett Packard 6890N gas chromatograph equipped with HP 6890 series autosampler, DB 5 capillary column (30 m × 0.25 mm × 0.25 µm film) and HP 5973 mass selective detector. The temperature program for analysis was: injector and detector at 300°C and 280°C respectively and the oven temperature program used was: 45°C for 3 min, increased at 6°C/min to 315°C and hold for 15 min. Helium at 5.7 mL/min was used as the carrier gas. Quantitation was done in selected ion monitoring mode using internal standards after calibration with alkane, alkylated PAH and biomarker standards. Daily quality control included blanks and continuing calibration standards for analytes. Precision of the combined extraction and analytical method was within 15% relative standard deviation (RSD), based on replicate analyses.

The following PAHs were quantified: naphthalene (NAPH), C1-naphthalenes (C1-NAPH), C2-naphthalenes (C2-NAPH), acenaphthylene (ACENAPH), acenaphthene (ACE), fluorene (FLU), C3-naphthalenes (C3-NAPH), phenanthrene (PHEN), C1-phenanthrenes (C1-PHEN), C2-fluorennes (C2-FLU), C1-dibenzothiophenes (C1-DiBENZ), fluoranthene (FLUOR), pyrene, C2-phenanthrenes (C2-PHEN), C3-fluorennes (C3-FLU), C2-dibenzothiophenes (C2-DiBENZ), C1-pyrene/fluoranthene, C3-phenanthrenes (C3-PHEN), C3-dibenzothiophenes (C3-DiBENZ), chrysene (CHRYS), C4-phenanthrenes (C4-PHEN), C1-chrysenes (C1-CHRYS), C2-chrysenes (C2-CHRYS), and C3-chrysenes (C3-CHRYS). Total PAHs were computed as the sum of the detected compounds in this list.

The following alkanes were analyzed: decane (C10), undecane (C11), tridecane (C13), tetradecane (C14), pentadecane (C15), hexadecane (C16), heptadecane (C17), pristane, octadecane (C18), n-eicosane (C20), docosane (C22), n-tetracosane (C24), n-hexacosane (C26), n-octacosane (C28), n-tricontane (C30), n-dotricontane (C32), and n-hexatriacontane (C36). 17α(H),21β(H)-hopane (30αβ), hereafter referred to as C30-hopane, was also quantified.

#### NUTRIENT AND MOISTURE CONTENT ANALYSIS

Total C and N were measured on intact SRBs, SOM, and snare oil pieces. Total carbon was measured via combustion and coulometric detection using a modified ASTM D5373 method. Nitrogen was determined on a Thermo Flash EA 1112 analyzer. The N technique utilized was the classical Dumas method, using thermal conductivity detection. The method is described in ASTM D5373 (coal) and ASTM D5291 (petroleum products). Moisture content was determined by loss on drying overnight at 105°C. The moisture content determination did not distinguish between loss of moisture and volatile losses from oil at these temperatures. The absence of alkanes below C15 in these weathered oil samples demonstrates the low volatile content of the oil, however.

## STATISTICAL ANALYSIS AND RATE COMPUTATION

All statistical analyses were done using one and two tailed student *t*-test at 95% confidence interval. First-order rate constants from declines in PAHs and alkanes were calculated using nonlinear regression of data pooled from all the samples from each sampling event.

## RESULTS

### CHEMICAL EVIDENCE FOR SRB BIODEGRADATION POTENTIAL

Concentrations of PAHs and other crude oil components were used to compute ratios that tracked changes in more biodegradable compounds to less biodegradable compounds over time. Two sets of ratios were computed for the aromatic fraction: comparing PAHs to the poorly biodegradable biomarker C30-hopane (Prince et al., 1994) and comparing concentrations of C2-phenanthrenes and C2-dibenzothiophenes to their more alkylated homologues, C3-phenanthrenes and C3-dibenzothiophenes (Michel and Hayes, 1999). These ratios were computed for SRBs on the Caminada Headlands beach over a 19-month interval. Declines in PAHs relative to C30-hopane were observed in the 4 sampling locations on Fourchon Beach and Elmer's Island (**Figure 2**). Total PAH/hopane ratios declined from 7 to 0.5 over this time frame (**Figure 2D**). The dominant PAHs observed were C1-, C2-, C3- and C4-phenanthrenes, C1-, C2- and C3-dibenzothiophenes, chrysene, and C1-chrysene (**Figure 2**). The lower molecular weight naphthalenes, acenaphthylene, acenaphthene, fluorene,

alkylated fluorenes, unsubstituted phenanthrene, and dibenzothiophene were observed at minor levels or below our detection limit of 0.05 mg/kg. By the last sampling event in May 2012, the greatest percentage decrease was observed for C1- and C2-phenanthrenes, followed by C2- and C3-dibenzothiophenes and C3- and C4-phenanthrenes. No apparent change in chrysene and C1-chrysene were observed when the data was normalized to C30-hopane (**Figure 2C**). This is consistent with the lower rate and extent of biodegradation of 4-ring PAHs like chrysenes (Haritash and Kaushik, 2009).

Ratios of C2/C3 phenanthrenes and C2/C3 dibenzothiophenes were computed and compared using a “double ratio” plot that can illustrate temporal changes in PAH composition (**Figure 3**) (Michel and Hayes, 1999). For comparison, the plot includes ratios computed from open ocean samples from near the wellhead taken during the week of 05/09/2010 (Diercks et al., 2010) to contrast the magnitude of the immediate weathering after the spill. SRB datapoints on **Figure 3** represent averages of SRBs sampled in this study from the 4 study sites described above. They show a clear trend of movement toward the origin over time, which occurs as the concentration of the C2 homolog declines with respect to the C3 homolog. This is consistent with biodegradation patterns of these alkylated 3 ring PAHs, not due to physical weathering reactions such as dispersion or volatilization (Wang et al., 1998). One other trends is apparent from this double-ratio plot is the change in the C2/C3 phenanthrenes ratio from samples at sea

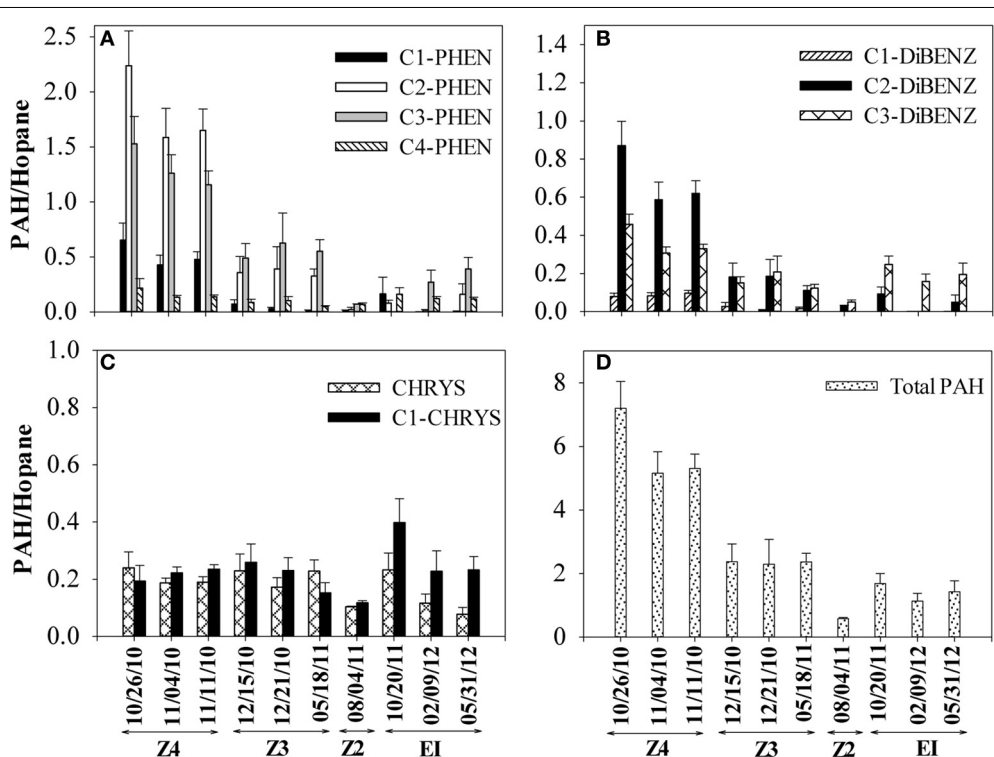


**FIGURE 2 |** Changes in PAH/hopane ratios in SRBs from 4 sampling locations [Fourchon Beach (FB) Zone 4, FB Zone 3, FB Zone 2, and Elmer's Island (EI)] sampled over time. **(A)** C1–C4 phenanthrenes **(B)** C1–C3 dibenzothiophenes, **(C)** chrysene and C1-chrysenes and **(D)** total PAHs. Dates

correspond to the following times since oil reached the shoreline beginning on May 20, 2010: 10/26/2010 (day 159), 11/04/2010 (day 167), 11/11/2010 (day 174), 12/15/2010 (day 208), 12/21/2010 (day 214), 05/18/2011 (day 362), 8/4/2011 (day 439), 10/20/2011 (day 547), 2/9/2012 (day 628) and 5/31/2012 (day 739).

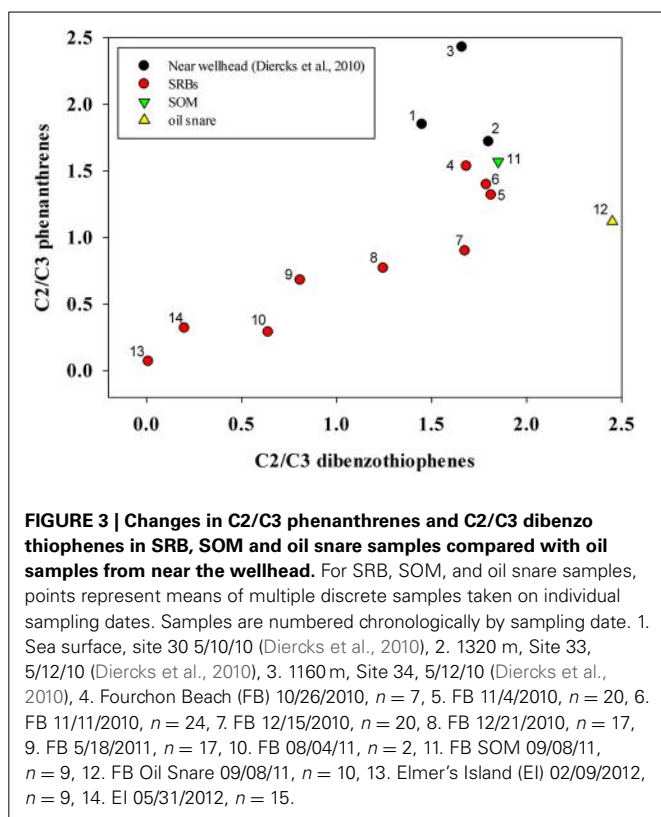


**FIGURE 3 | Changes in C2/C3 phenanthrenes and C2/C3 dibenzothiophenes in SRB, SOM and oil snare samples compared with oil samples from near the wellhead.** For SRB, SOM, and oil snare samples, points represent means of multiple discrete samples taken on individual sampling dates. Samples are numbered chronologically by sampling date. 1. Sea surface, site 30 5/10/10 (Diercks et al., 2010), 2. 1320 m, Site 33, 5/12/10 (Diercks et al., 2010), 3. 1160 m, Site 34, 5/12/10 (Diercks et al., 2010), 4. Fourchon Beach (FB) 10/26/2010,  $n = 7$ , 5. FB 11/4/2010,  $n = 20$ , 6. FB 11/12/2010,  $n = 24$ , 7. FB 12/15/2010,  $n = 20$ , 8. FB 12/21/2010,  $n = 17$ , 9. FB 5/18/2011,  $n = 17$ , 10. FB 08/04/11,  $n = 2$ , 11. FB SOM 09/08/11,  $n = 9$ , 12. FB Oil Snare 09/08/11,  $n = 10$ , 13. Elmer's Island (EI) 02/09/2012,  $n = 9$ , 14. EI 05/31/2012,  $n = 15$ .

and onto the Fourchon Beach shoreline without a corresponding change in the ratio of C2–C3-dibenzothiophenes (Figure 3). Subsequent changes in both ratios in the SRBs on the beach did not show any bias toward phenanthrenes or dibenzothiophenes and both ratios declined approximately equally.

Similar to PAHs, we observed a consistent decrease in alkane/hopane ratios from October 2010 to May 2011 (Figure 4). Between October 2010 and May 2011, the total alkane ratio decreased by approximately 85% (Figure 4D). Alkane/hopane ratios did not decline appreciably in the later Elmer's Island samples and at the end of the sampling period in May 2012, measurable alkanes were still observed in the SRBs. Among alkanes (Figure 4), only C17–C36 alkanes were observed consistently in all of the SRB samples. Lighter alkanes C10–C12 were below our detection limit for all the samples. In total, alkane concentrations were roughly 10x those of the PAHs.

A second set of biodegradation ratios were computed, the ratios of C26–C15, C16 and C17 (Table 1). These ratios have also been used to evaluate loss due to biodegradation (Hazen et al., 2010) on the principle that lower molecular weight alkanes should biodegrade faster than higher molecular weight alkanes. Initially, these ratios (C26/C15, C26/C16, and C26/C17) were two to three orders of magnitude higher than what was observed in MC252 oil and other ocean samples collected immediately after the spill (Hazen et al., 2010) (Table 1). The ratio of C26–C15 consistently decreased during our sampling period and the difference between October 2010 and May 2011 was statistically significant ( $p = 0.003$ ). For the C26/C16 ratio, differences observed between October 2010 and May 2011 sampling events were not

statistically significant ( $p = 0.91$ ). However, C15 and C16 alkanes were close to our detection limit in all our samples and only minor losses were observed during our sampling period. Therefore, the decrease in the ratio was primarily due to decreases observed in C26. The difference in C26/C17 ratio was also not significant between October 2010 and May 2011 sampling events ( $p = 0.67$ ). Elevated ratios in Table 1 suggest the persistence of C26 relative to C15, C16, and C17, which is consistent with other field observations where long chain alkanes were more persistent over short chain alkanes (Venosa et al., 1996; Hazen et al., 2010; Liu et al., 2012) and where slow biodegradation of long chain alkanes was observed in oiled sands (Rodriguez-Blanco et al., 2010; Kostka et al., 2011). Ultimately, two trends from the alkane data in Figure 4 and Table 1 stand out. These are the persistence of some alkanes in the SRBs over the length of the sampling period and the variability in the alkane results between SRBs, which results in the high observed standard deviations in Table 1.

#### RATE CONSTANTS FOR PAHS AND ALKANES IN SRBs

First-order rate constants ( $\text{year}^{-1}$ ) for declines in PAH and alkane concentrations in the SRBs are of the same order of magnitude for most compounds (Table 2). However, the initial concentrations of alkanes in SRBs are an order of magnitude higher than PAHs and therefore, would persist longer in the environment. C1-phenanthrenes, the lowest molecular weight PAHs evaluated for this study, had the highest loss rate and the more alkylated phenanthrenes (C2, C3, and C4) were 48, 25, and 39% lower respectively. Among dibenzothiophenes, C1-dibenzothiophene had the highest loss rate but was only 58% of that for C1-phenanthrene. Chrysene and C1-chrysene weathering rates were the lowest of all the PAHs quantitated in this study consistent with the persistence of heavier molecular weight PAHs. In order to account for the variability observed in the standard error, statistical analysis were performed to determine if the rates were significantly different. The loss rates were statistically different for C3-phenanthrenes ( $p = 0.044$ ), C2-dibenzothiophenes ( $p = 0.048$ ), chrysene ( $p = 0.012$ ) and C1-chrysene ( $p = 0.016$ ), when compared with C1-phenanthrene. However, the loss rates were not statistically different for C2-phenanthrene ( $p = 0.16$ ), C4-phenanthrene ( $p = 0.08$ ), C1-dibenzothiophene ( $p = 0.13$ ), C3-dibenzothiophene when compared to C1-phenanthrene. The ratio of rates of C2/C3 phenanthrenes (1.9) was not statistically different from the ratio of rates of C2/C3 dibenzothiophenes (1.72), which explains the nearly equal change in these ratios in SRBs in Figure 3.

Among alkanes, the rate constants were highest for C17 (6.4  $\text{year}^{-1}$ ) and, while rate constants for C21, C22, C24, and C26 were lower by 2–29%, they were not statistically different ( $p = 0.83$ , 0.78, 0.23, and 0.21 respectively) (Table 2). Compared to C17, rate constants for C18, C28, C30, and C32 alkanes were lower by 47, 41, 36, and 41% respectively and were statistically different ( $p \leq 0.003$ ). The lowest rate constant observed for C36 was only 7% of the rate constant for C17 ( $p < 0.001$ ). In general, the rate constants of longer chain alkanes were smaller than the short chain alkanes, consistent with preferential biodegradation of short chain alkanes. Taken together, the rate constant for total

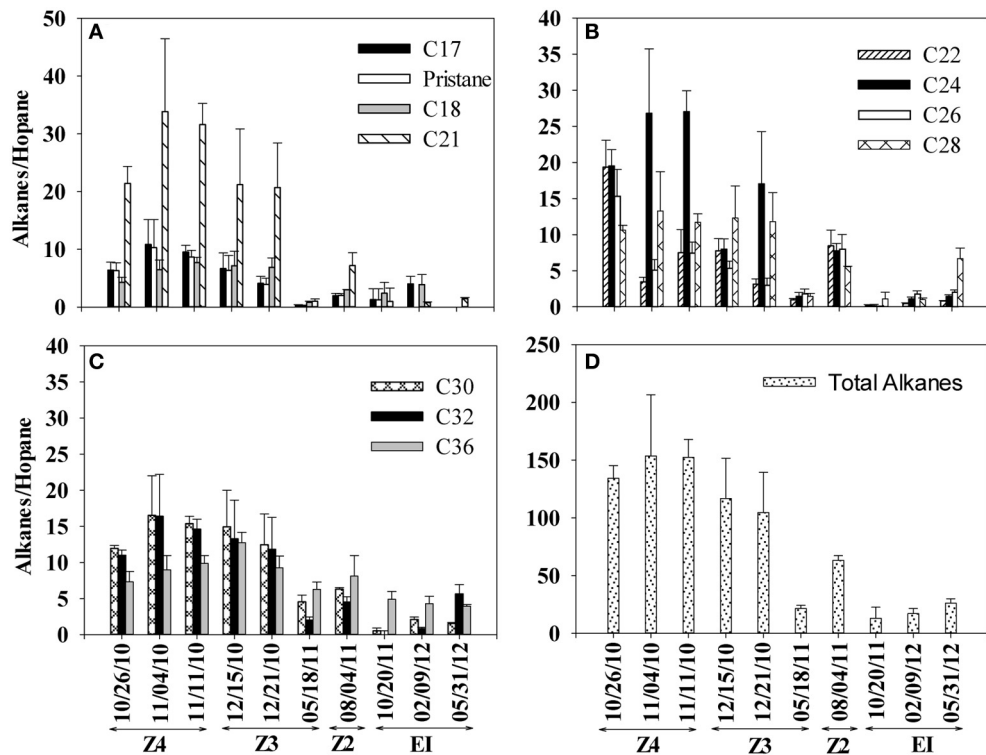


**FIGURE 4 |** Changes in alkane/hopane ratios in SRBs from 4 sampling locations [Fourchon Beach (FB) Zone 4, FB Zone 3, FB Zone 2, and Elmer's Island (EI)] sampled over time. **(A)** C17, pristane, C18, and C21 **(B)** C22, C24, C26, and C28 **(C)** C30, C32, and C36 **(D)** total alkanes. Dates

correspond to the following times since oil reached the shoreline beginning on May 20, 2010: 10/26/2010 (day 159), 11/04/2010 (day 167), 11/11/2010 (day 174), 12/15/2010 (day 208), 12/21/2010 (day 214), 05/18/2011 (day 362), 8/4/2011 (day 439), 10/20/2011 (day 547), 2/9/2012 (day 628) and 5/31/2012 (day 739).

alkanes was similar to the rate constant for total PAHs and they were not statistically different ( $p = 0.38$ ).

#### COMPARING CHEMICAL SIGNATURE OF SUBMERGED OIL MATS, SNARE OIL, AND SRBS

A fifth sampling event, conducted immediately after TS Lee in September 2011, collected two additional categories of samples; pieces of submerged oil mat (SOM) that had been broken up by the storm and distributed on the beach, and oil associated with “snare,” a pom pom-type of oil absorbent consisting of polypropylene strands that occasionally was left on the beach and buried by sand. Biodegradation ratios for the SOM and snare samples are compared with the initial SRB samples (10/26/10) and SRB samples collected from Elmer's Island after the passage of TS Lee in 2011 in **Table 3**. The SOM samples had the highest measured PAHs of all the samples and the total PAH normalized to hopane was  $19 \pm 5.8$ , which is approximately twice the amount observed from 10/26/2010 sampled SRBs (**Table 3**) and an order of magnitude larger than snare samples and SRBs from Elmer's Island. C2-phenanthrene data had similar trends although C2-phenanthrenes were nearly completely depleted in the Elmer's Island samples. Alkanes were highest in the SOM samples and lowest in the Elmer's Island SRBs that were on the beach the longest.

When plotted on the double ratio plot (**Figure 3**), snare oil and SOM samples plotted near the initial SRB samples taken in

October 2010 and the oil sampled immediately after the spill (Diercks et al., 2010). Based on the values from **Figure 3**, SOM samples are similar to the oil that first reached the shoreline, even though they were over a year old. Snare oil samples plotted similar to an unweathered sample, even though results of hopane ratios indicated a much more degraded profile. These samples are in sharp contrast to the SRBs from the supratidal, which showed consistent changes in C2/C3 phenanthrene and dibenzothiophene ratios over time (**Figure 3**).

#### BIOGEOCHEMICAL PARAMETERS

Biogeochemical parameters relevant to the biodegradation of crude oil components in SRBs have been measured in 3 previous studies (OSAT-II, 2011; Urbano et al., 2013; Lemelle et al., 2014). Available chemical, physical and microbial data are summarized in **Table 4**. Review of those parameters identified data gaps that would improve assessments of biodegradation potential of crude oil in SRBs. These included data to compute molar C:N ratios and a more extensive set of measurements of moisture content. %C, %N and moisture content were assessed on a series of SRB and SOM samples from Fourchon Beach and Elmer's Island (**Table 5**).

Moisture contents were all below 2% by weight and those of supratidal SRBs were all below 1%. C:N molar ratios for all samples were larger than 100:1 (**Table 5**). Supratidal SRB C:N ratios ranged from 131 to 323 while SOM ratios were substantially higher (317–474). Intertidal snare oil has the lowest ratio at

**Table 1 | Ratio of C26 to C15, C16 and C17 in SRBs from Fourchon Beach (FB) and Elmer's Island (EI).**

Sample ID	Date	N	C26/C15	C26/C16	C26/C17
FB Zone 4	10/26/2010	7	260 ± 79	86 ± 52	9.8 ± 7.1
FB Zone 4	11/4/2010	20	120 ± 52	170 ± 100	4.7 ± 2.8
FB Zone 4	11/11/2010	24	150 ± 31	93 ± 50	5.6 ± 3.1
FB Zone 3	12/15/2010	20	67 ± 10	41 ± 21	4.5 ± 0.57
FB Zone 3	12/21/2010	17	57 ± 11	85 ± 11	3.8 ± 0.99
FB Zone 3	5/18/2011	17	40 ± 30	75 ± 57	12 ± 1.7
FB Zone 2	08/04/11	2	bdl <sup>a</sup>	bdl	bdl
EI SRB	10/20/11	9	bdl	bdl	bdl
EI SRB	02/09/2012	9	bdl	bdl	bdl
EI SRB	05/31/2012	15	bdl	bdl	bdl
MC252 <sup>b</sup>	5/2010		1.61	0.85	0.56
BM057104 <sup>b,c</sup>	5/2010		3.4	1.8	1.1
BM058104 <sup>b,c</sup>	5/2010		2.84	1.48	0.8

<sup>a</sup>bdl = samples below detection for C15, C16, or C17<sup>b</sup>Hazen et al., 2010.<sup>c</sup>BM057104 and BM058104 are samples collected 10 km away from wellhead.**Table 2 | First-order rate constants for declines in PAH and alkane concentrations from Fourchon Beach and Elmer's Island from 2010–2012.**

PAH	Rate (1/year)	Alkanes	Rate (1/year)
C1-PHEN	8.0 ± 2.4 <sup>a</sup>	C17	6.4 ± 0.24
C2-PHEN	3.8 ± 1.3	C18	3.4 ± 0.68
C3-PHEN	2.0 ± 0.78	C21	6.3 ± 0.38
C4-PHEN	3.1 ± 0.59	C22	6.0 ± 1.4
C1-DIBENZ	4.6 ± 2.5	C24	5.6 ± 0.58
C2-DIBENZ	2.2 ± 0.68	C26	4.6 ± 1.2
C3-DIBENZE	3.8 ± 0.79	C28	3.8 ± 0.48
CHRYS	0.28 ± 0.33	C30	2.3 ± 0.15
C1-CHRYS	0.76 ± 0.19	C32	3.8 ± 0.25
Total PAHs	3.05 ± 0.49	C36	0.46 ± 0.39
		Total alkanes	3.6 ± 0.15

<sup>a</sup>±standard error.

111, consistent with regular washing with Gulf of Mexico seawater with approximately 1 mg N/L of seawater (Urbano et al., 2013).

## DISCUSSION

Changes in SRB PAH/hopane ratios over time (Figure 2) are consistent with a biodegradation process. Declines in hopane ratios for the three-ring PAHs (phenanthrenes and dibenzothiophenes) over time on the beach are in contrast to relatively constant 4-ring chrysene and C1-chrysene hopane ratios. When double-ratio plots are used to track relative biodegradation of the three-ring alkylated PAHs in the supratidal SRBs, a clear pattern of change is observed as C2-PHEN and C2-DIBENZ are degraded preferentially to their C3 alkylated homologues. The extent of MC252 oil components losses observed in Fourchon Beach and Elmer's Island SRBs over 19 months are similar to those observed after 8 years in the Exxon Valdez spill (Michel and Hayes, 1999). Also, the

**Table 3 | Comparison of submerged oil mat (SOM) hopane ratios with SRBs from Fourchon Beach (FB) and Elmer's Island (EI).**

Sample	Date	ΣPAH/hopane	C2-PHEN/hopane	C1-CHRYS/hopane	ΣAlkane/hopane
FB-SRBs	10/26/10	7.2 ± 0.84	2.2 ± 0.3	0.19 ± 0.05	130 ± 11
SOM	9/8/11	19 ± 5.8	4.8 ± 1.5	0.49 ± 0.12	199 ± 27
Oil snare	9/8/11	1.0 ± 0.17	0.11 ± 0.04	0.15 ± 0.03	40 ± 8.8
EI-SRB	10/20/11	1.7 ± 0.31	0.08 ± 0.03	0.39 ± 0.08	13 ± 9.6

profiles of MC252 oil components observed on Fourchon Beach and Elmer's Island are similar to those observed in MC252 oil analyzed from Pensacola, FL beaches (Kostka et al., 2011) and Marsh Point MS marsh samples (Liu et al., 2012). These changes include loss of alkanes <C15 and the alkylated naphthalenes. Patterns of change were similar to those of a biodegradation process not a physical weathering process (Wang et al., 1998), namely the decline of lower alkylated homologues and persistence of higher molecular weight PAHs. Within these SRBs, however, oxygenated residues representing partial biodegradation products of crude oil components were present in significant concentrations (Aeppli et al., 2012) although PAHs may not necessarily be precursors to these byproducts (Hall et al., 2013). Disappearance of the parent PAHs may not result in complete mineralization to CO<sub>2</sub>.

For alkanes, consistent declines in hopane ratios were also observed in SRBs on the beach over time (Figure 4). Initial ratios of C26 to lower molecular weight alkanes (C15–17) were 1–2 orders of magnitude higher than concentrations at sea, suggesting that substantial biodegradation of these alkanes had already occurred prior to our first sampling event on shore. On the beach, ratios declined consistently over time as C26 continued to degrade relative to the low concentrations of C15–C17 remaining in the aggregates. Nevertheless, concentrations of higher molecular weight alkanes persisted in the SRBs, even until the final sampling date. Rate constants, measured from losses of alkanes and PAHs in the SRBs, were of the same order of magnitude as those measured during an experimental oil spill on Delaware Bay, USA (Venosa et al., 1996). Rate constant of PAH loss from the Delaware Bay study were approximately double those of the rates of PAHs measured in SRBs from Fourchon Beach while alkane rates from control treatments were approximately 3 times rates observed in the SRBs.

While biodegradation ratios, relative patterns of PAH and alkane loss and computed rate constants suggests that biodegradation reactions are occurring, is there evidence that hydrocarbon-degrading microbial populations can colonize these aggregates? Previous measurements of eubacterial and sulfate-reducing microbial populations within several SRBs using DGGE revealed several trends (Urbano et al., 2013). SRB microbial populations differed with position on the beach, with populations within supratidal SRBs distinct from intertidal snare oil and SOM samples (Urbano et al., 2013). Specifically, known PAH degrading genera such as *Mycobacterium* (Khan et al., 2002; Uyttebroek et al., 2006) and *Stenotrophomonas* (Juhasz et al., 2000; Papizadeh et al., 2011) comprised significant bands in the supratidal and

**Table 4 | Summary of published biogeochemical parameters of SRBs and submerged oil mat (SOM) samples.**

Parameter	Value	References
Porosity	0.35 (SRBs) 0.07 (SOM)	OSAT-II, 2011; Urbano et al., 2013
Mass	14.5 ± 3.0 g; 5.6 ± 2.3 g (SRBs from 2 locations) 31.3 ± 2.6 g (SOM)	Urbano et al., 2013
Moisture	<0.5% (SRBs)	Urbano et al., 2013
Projected area	106.4 ± 134 mm <sup>2</sup> ; 55.2 ± 113 mm <sup>2</sup> (SRBs from 2 locations)	Lemelle et al., 2014
% Oil	4.2–12.8% (SRBs) 9.4–16.8% (SOMs)	OSAT-II, 2011
N	1.4–2.0 mg/kg (SRBs) (NH <sub>4</sub> <sup>+</sup> ) 7.5 mg/kg (SOM) (NH <sub>4</sub> <sup>+</sup> ) 2 mg/L total N (Grand Isle beach porewater)	OSAT-II, 2011; Urbano et al., 2013
P (orthophosphate)	0.5–0.66 mg/kg (SRBs) 0.29 mg/kg (SOM)	Urbano et al., 2013
Salinity	1.3–1.5 ppt (SRBs) 59.8 ppt (SOM)	Urbano et al., 2013
Sulfate (water-extractable)	148–4.3 mg/kg (SRBs) 6.1 mg/kg (SOM)	Urbano et al., 2013
Oxygen	~220 mM (7 mg/L) after wetting 0–180 mM (0–5.76 mg/L) after 4 days in aerobic seawater 0.4 mg/L in Grand Isle, LA beach porewater	OSAT-II, 2011; Urbano et al., 2013
Microbial populations	Known PAH degraders: <i>Mycobacterium</i> sp. (SRBs)	Urbano et al., 2013

intertidal snare samples, respectively (Urbano et al., 2013). These results compliment microbial community structure analyses in oiled beach sands in Florida (Kostka et al., 2011) that revealed a diverse response, including sequences derived from members of oil-degrading taxa such as *Gammaproteobacteria* (*Alcanivorax*, *Marinobacter*) and *Alphaproteobacteria* (*Rhodobacteraceae*).

Biogeochemical conditions present in SRBs need to be examined critically to develop hypotheses about the rate and extent of observed concentration changes. These may shed insight to data trends including the detection of alkanes in SRBs after over a year and a half on the beach, the persistence of PAHs and alkanes in SOM samples and the relatively high variability in analyses between SRBs, particularly for alkanes. From a review of previously collected data and the values measured in the current study, four biogeochemical parameters are of concern as potentially limiting biodegradation rate and extent. These are moisture content, oxygen concentrations, N concentrations and salinity.

**Table 5 | C:N ratios and moisture content in SRBs, SOM and snare oil from Fourchon Beach (FB) and Elmer's Island (EI).**

Sample	Date sampled	Location	Moisture content (%)	% C	% N	C/N (molar)
<b>SUPRATIDAL SRBs</b>						
A 3-1	8/4/2011	FB	0.99	5.44	0.04	159
A 3-2	8/4/2011	FB	0.81	5.54	0.04	162
Z9-SS	3/1/2011	FB	0.35	5.54	0.02	323
B 14-12 s	5/19/2011	FB	0.35	4.78	0.03	186
EM-5	2/9/2012	EI	0.26	2.25	0.02	131
EM-18B	2/9/2012	EI	0.31	2.72	0.02	159
<b>SUBMERGED OIL MATS</b>						
MAT-1	9/16/2011	FB	1.02	14.19	0.04	414
BC-2	12/15/2011	FB	1.80	8.15	0.03	317
TB12	9/8/2011	FB	0.92	12.18	0.03	474
<b>INTERTIDAL SNARE OIL</b>						
S20	9/8/2011	FB	1.75	6.68	0.07	111

Moisture content of SRBs are very low (<1%) on the supratidal beach environment in periods between rainfall events (Urbano et al., 2013). Additional measurements (Table 5) were conducted for this study and were also very low, ranging from 0.26–1.8%. Supratidal SRBs had lower moisture contents when sampled when compared with SOM or snare oil samples that were regularly inundated (Table 5). SRBs appear to have poor water holding capacities and rely on regular rainfall or tidal inundation to replenish moisture. These sampled water contents are well below concentrations optimal for biodegradation (Dibble and Bartha, 1979; Hejazi and Husain, 2004; Tibbett et al., 2011). These studies maintained water concentrations between 30 and 80% of field capacity, and between 50 and 70% of field capacity for optimal results. For SRBs, measured moisture contents would represent field capacities of between 2 and 9% given our knowledge of porosity, density and volume of typical SRBs. Given the rainfall patterns on the beach and the frequency of storm-driven tides, infrequent periods of wetting would be interspersed with longer drying periods leading to suboptimal moisture concentrations. *Mycobacterium*, observed as one of the prominent bands in the supratidal SRBs, can be adapted to low moisture content and periods of desiccation (Wick et al., 2003; Harland et al., 2008) and this capability may have insured that biodegradation of PAHs continued between rain events on the beach.

*In situ* oxygen measurements are not available in the very limited water in field-sampled SRBs but microelectrode measurements from SOM pieces incubated in the laboratory (Urbano et al., 2013) show that O<sub>2</sub> is at saturation in aggregate porewater immediately after wetting. As the SOM is submerged, however, O<sub>2</sub> is consumed over a several day period to produce a large zone of anaerobiosis within the aggregate. While these measurements are limited, the level of carbon observed in the aggregates, the presence of aerobic hydrocarbon degraders and the porosities observed supports the development of anaerobic conditions. This can help explain relative PAH and alkane persistence in SOM samples. SOM samples had higher alkane/hopane and PAH/hopane ratios than the initial SRB samples, despite

sampling a year later. Because of their position on the beach, these oil forms were consistently submerged and likely anaerobic over the course of their time in the system. While alkanes have been observed to degrade under sulfate-reducing conditions (Caldwell et al., 1998; Townsend et al., 2003), alkane concentrations still persist in these SOM samples. In contrast, the continued biodegradation of these compounds in the SRBs on the supratidal is likely greatly enhanced by the regular wetting by aerobic rainwater followed by drying which limits the formation of anaerobic conditions within the aggregates. *Mycobacterium sp.*, observed in the supratidal SRBs only, is capable of degrading pyrene at O<sub>2</sub> concentrations as low as 3 μM (Fritzsche, 1994), which may allow them to function in that critical time after rewetting when oxygen is being consumed.

Hydrocarbon biodegradation requires a source of nutrients and can be commonly limited by N and P concentrations lower than optimal levels (Dibble and Bartha, 1979). Previous measurements of exchangeable NH<sub>4</sub><sup>+</sup> and soluble NO<sub>2</sub><sup>-</sup>/NO<sub>3</sub><sup>-</sup> in SRBs demonstrated 3 features of N chemistry in the aggregates (Urbano et al., 2013). First, exchangeable ammonium was the dominant labile form of N in the aggregates ranging from 1.39 to 12.6 mg of exchangeable ammonium per kg of SRB. Second, concentrations of N varied with position on the beach with SRBs in the intertidal possessing higher concentrations of N. This is consistent with regular inundation with seawater that contains about 1 mg/L of N at this location. Third, SRBs that were present on the supratidal the longest period of time had the lowest concentrations of N. These data suggest that nutrient content is due to the position of the SRBs on the beach but the form of the nutrients within the aggregate can be influenced by microbial activity.

The previous data (Urbano et al., 2013) does not allow easy computation of absolute amounts of N relative to the carbon, primarily crude oil, present in the aggregates. Therefore, additional SRBs from defined classes (i.e., supratidal SRBs, SOM and snare oil samples) were analyzed for total C and N to make that comparison (**Table 5**). C/N molar ratios, commonly used as a diagnostic variable for hydrocarbon biodegradability, ranged from 111 to 474 in SRBs, SOM and snare oil samples. Molar C/N ratios were well-above optimal values reported for experimental aerobic hydrocarbon biodegradation in crude oil contaminated soils that were approximately 60:1 (Dibble and Bartha, 1979). Is N limiting biodegradation in the SRBs? If we consider literature values for specific PAH degrading populations, optimal molar C:N ratios are much lower. For phenanthrene degradation by *Sphingomonas* in mangrove soils, C:N ratios of 100:1 were optimal (Chen et al., 2008). For 2 important PAH degraders, *Sphingomonas* and *Mycobacterium*, soil slurry experiments showed that biodegradation can proceed under lower nutrient concentrations, C:N of 100:1, even though 100:10 were optimal (Leys et al., 2005). In the SRBs sampled here, C:N ratios are generally 3× higher than those studies. N replenishment is occurring through several mechanisms including deposition of sea spray aerosols (Zhu et al., 2013) and occasional inundation with seawater containing N during storm events. For extended periods, though, SRBs on the beach have whatever N was retained in the aggregate.

Measurements of salinities ranged from hypersaline conditions in intertidal aggregates to low salinities in supratidal aggregates.

Since salinity can be an important inhibitor for PAH consortia (Kastner et al., 1998; Diaz et al., 2002), the apparent ability of rainfall to reduce salinity to low levels may be important in sustaining biodegradation reactions in supratidal SRBs. PAH biodegradation is impacted by salinity and lower salinities (<15 ppt) are often optimal (Chen et al., 2010). A *Mycobacterium* and *Sphingomonas* culture could not grow at salinities above 19 ppt (Leys et al., 2005). SRBs on the supratidal beach environment have low salinities, presumably via washing by rainwater. In contrast, high salinities including hypersaline conditions in the SOM samples are likely contributing to the persistence of these oil forms.

Based on a critical examination of biogeochemical parameters in SRBs and SOM samples, 2 regimes on the beach can be hypothesized with respect to biodegradation; a moisture and nutrient-limited regime on the supratidal and an oxygen and salinity-limited regime in the intertidal. Despite these challenges, biodegradation processes in SRBs occurs at rates and timeframes that are relevant to the coastal transport processes that move them off the beach and into the adjacent mudflats and marshes. In contrast, SOM samples do not appear to be amenable to biodegradation while in the intertidal environment where oxygen limitations and salinity impacts may be inhibitory. Intact mats also have much lower surface areas relative to the SRBs which may contribute to persistence as well. As these mats break up and are deposited on the beach, they represent new oiling very similar to the chemical quality of oil that reached the beach immediately after the spill began. Finally, while PAH and alkanes represent significant components of MC252 that have both aerobic and anaerobic biodegradation potential, it should be emphasized that many other classes of compounds exist in crude oil whose behavior may not be accurately represented by examining these 2 groups alone. The overall decline in C content in the aggregates (**Table 5**) is evidence, however, that additional components of the mixture are degrading.

While the chemical evidence can be explained by biodegradation, what about the other potential weathering processes such as evaporation, dissolution and photo-oxidation? SRB samples were formed from highly weathered oil and significant evaporative (Middlebrook et al., 2012) and dissolution (Reddy et al., 2012) losses had occurred in the water column and on slicks prior to reaching the shoreline. Alkanes less than C15 and lower molecular weight PAHs such as alkylated naphthalenes were essentially absent from the SRBs analyzed in this study. The remaining components have lower vapor pressures and lower solubilities and therefore, are less susceptible to these weathering processes. SRB structure and position on the beach creates mass transfer limitations in the aggregates for these processes. Dissolution of oil components in the aggregates is limited by infrequent wetting events while evaporation is limited by layers of cleaner sand adhering to the oilier core. This structure creates similar limitations for continued photooxidation within SRBs even though this process was likely important at sea (Aeppli et al., 2012; Genuino et al., 2012). Taken together, these data provide a weight of evidence that biodegradation is occurring but not conclusive proof. Only controlled studies that include killed controls can confirm unequivocally that a microbial process is responsible for chemical changes within these unique oil:sand aggregates.

## AUTHOR CONTRIBUTIONS

Vijaikrishnah Elango wrote the first draft of the manuscript and provided day-to-day supervision of study objectives. Marilany Urbano performed biogeochemical analyses, chemical analysis of SOM samples and reviewed biogeochemical data. Kendall R. Lemelle performed chemical analysis of SRB samples. John H. Pardue designed studies, provided oversight and edited final draft of manuscript.

## ACKNOWLEDGMENTS

Funding for the study was provided by Gulf of Mexico Research Initiative and the Edward J. Wisner Donation. Special thanks to F. Travirca III, F. Travirca IV, A. Travirca and A. Travirca, Jr. for field support.

## REFERENCES

- Aeppli, C., Carmichael, C. A., Nelson, R. K., Lemkau, K. L., Graham, W. M., Redmond, M. C., et al. (2012). Oil weathering after the Deepwater Horizon disaster led to the formation of oxygenated residues. *Environ. Sci. Technol.* 46, 8799–8807. doi: 10.1021/es3015138
- Badejo, A. C., Badejo, A. O., Shin, K. H., and Chai, Y. G. (2013). A gene expression study of the activities of aromatic ring-cleavage dioxygenases in *Mycobacterium gilvum* PYR-GCK to changes in salinity and pH during pyrene degradation. *PLoS ONE* 8:e58066. doi: 10.1371/journal.pone.0058066
- Bragg, J. R., Prince, R. C., Harner, E. J., and Atlas, R. M. (1994). Effectiveness of bioremediation for the Exxon Valdez oil spill. *Nature* 368, 413–418. doi: 10.1038/368413a0
- Caldwell, M. E., Garrett, R. M., Prince, R. C., and Sufita, J. M. (1998). Anaerobic biodegradation of long-chain n-Alkanes under sulfate-reducing conditions. *Environ. Sci. Technol.* 32, 2191–2195. doi: 10.1021/es9801083
- Chang, W., Akbari, A., Snelgrove, J., Frigon, D., and Ghoshal, S. (2013). Biodegradation of petroleum hydrocarbons in contaminated clayey soils from a sub-arctic site: the role of aggregate size and microstructure. *Chemosphere* 91, 1620–1626. doi: 10.1016/j.chemosphere.2012.12.058
- Chen, J., Wong, M. H., Wong, Y. S., and Tam, N. F. Y. (2008). Multi-factors on biodegradation kinetics of polycyclic aromatic hydrocarbons (PAHs) by *Sphingomonas* sp a bacterial strain isolated from mangrove sediment. *Mar. Pollut. Bull.* 57, 695–702. doi: 10.1016/j.marpolbul.2008.03.013
- Chen, J. L., Au, K. C., Wong, Y. S., and Tam, N. F. Y. (2010). Using orthogonal design to determine optimal conditions for biodegradation of phenanthrene in mangrove sediment slurry. *J. Hazard. Mater.* 176, 666–671. doi: 10.1016/j.jhazmat.2009.11.083
- Diaz, M. P., Boyd, K. G., Grigson, S. J. W., and Burgess, J. G. (2002). Biodegradation of crude oil across a wide range of salinities by an extremely halotolerant bacterial consortium MPD-M, immobilized onto polypropylene fibers. *Biotechnol. Bioeng.* 79, 145–153. doi: 10.1002/bit.10318
- Dibble, J. T., and Bartha, R. (1979). Effect of environmental parameters on the biodegradation of oil sludge. *Appl. Environ. Microbiol.* 37, 729–739.
- Diercks, A. R., Highsmith, R. C., Asper, V. L., Joung, D. J., Zhou, Z. Z., Guo, L. D., et al. (2010). Characterization of subsurface polycyclic aromatic hydrocarbons at the Deepwater Horizon site. *Geophys. Res. Lett.* 37:L20602. doi: 10.1029/2010GL045046
- Eriksson, M., Ka, J. O., and Mohn, W. W. (2001). Effects of low temperature and freeze-thaw cycles on hydrocarbon biodegradation in Arctic tundra soil. *Appl. Environ. Microbiol.* 67, 5107–5112. doi: 10.1128/AEM.67.11.5107-5112.2001
- Fritzsche, C. (1994). Degradation of pyrene at low defined oxygen concentrations by a *Mycobacterium* sp. *Appl. Environ. Microbiol.* 60, 1687–1689.
- Genuino, H. C., Horvath, D. T., King'ondu, C. K., Hoag, G. E., Collins, J. B., and Suib, S. L. (2012). Effects of visible and UV light on the characteristics and properties of crude oil-in-water (O/W) emulsions. *Photochem. Photobiol. Sci.* 11, 692–702. doi: 10.1039/c2pp05275j
- Hall, G. J., Frysinger, G. S., Aeppli, C., Carmichael, C. A., Gros, J., Lemkau, K. L., et al. (2013). Oxygenated weathering products of Deepwater Horizon oil come from surprising precursors. *Mar. Pollut. Bull.* 75, 140–149. doi: 10.1016/j.marpolbul.2013.07.048
- Haritash, A. K., and Kaushik, C. P. (2009). Biodegradation aspects of Polycyclic Aromatic Hydrocarbons (PAHs): a review. *J. Hazard. Mater.* 169, 1–15. doi: 10.1016/j.jhazmat.2009.03.137
- Harland, C. W., Rabuka, D., Bertozi, C. R., and Parthasarathy, R. (2008). The *Mycobacterium tuberculosis* virulence factor trehalose dimycolate imparts desiccation resistance to model mycobacterial membranes. *Biophys. J.* 94, 4718–4724. doi: 10.1529/biophysj.107.125542
- Hazen, T. C., Dubinsky, E. A., DeSantis, T. Z., Andersen, G. L., Piceno, Y. M., Singh, N., et al. (2010). Deep-Sea oil plume enriches indigenous oil-degrading bacteria. *Science* 330, 204–208. doi: 10.1126/science.1195979
- Hejazi, R. F., and Husain, T. (2004). Landfarm performance under arid conditions. 2. Evaluation of parameters. *Environ. Sci. Technol.* 38, 2457–2469. doi: 10.1021/es026045c
- Horel, A., Mortazavi, B., and Sobecky, P. A. (2012). Responses of microbial community from northern Gulf of Mexico sandy sediments following exposure to Deepwater Horizon crude oil. *Environ. Toxicol. Chem.* 31, 1004–1011. doi: 10.1002/etc.1770
- Juhasz, A. L., Stanley, G. A., and Britz, M. L. (2000). Microbial degradation and detoxification of high molecular weight polycyclic aromatic hydrocarbons by *Stenotrophomonas maltophilia* strain VUN 10,003. *Lett. Appl. Microbiol.* 30, 396–401. doi: 10.1046/j.1472-765x.2000.00733.x
- Kastner, M., Breuer-Jammali, M., and Mahro, B. (1998). Impact of inoculation protocols, salinity, and pH on the degradation of polycyclic aromatic hydrocarbons (PAHs) and survival of PAH-degrading bacteria introduced into soil. *Appl. Environ. Microbiol.* 64, 359–362.
- Khan, A. A., Kim, S. J., Paine, D. D., and Cerniglia, C. E. (2002). Classification of a polycyclic aromatic hydrocarbon-metabolizing bacterium, *Mycobacterium* sp strain PYR-1, as *Mycobacterium vanbaalenii* sp nov. *Int. J. Syst. Evol. Microbiol.* 52, 1997–2002. doi: 10.1099/ijss.0.02163-0
- Kostka, J. E., Prakash, O., Overholt, W. A., Green, S. J., Freyer, G., Canion, A., et al. (2011). Hydrocarbon-degrading bacteria and the bacterial community response in Gulf of Mexico beach sands impacted by the Deepwater Horizon oil spill. *Appl. Environ. Microbiol.* 77, 7962–7974. doi: 10.1128/AEM.05402-11
- Lemelle, K. R., Elango, V., and Pardue, J. H. (2014). Distribution, characterization and exposure of MC252 oil in the supratidal beach environment. *Environ. Toxicol. Chem.* doi: 10.1002/etc.2599. (in press).
- Leys, N. M., Bastiaens, L., Verstraete, W., and Springael, D. (2005). Influence of the carbon/nitrogen/phosphorus ratio on polycyclic aromatic hydrocarbon degradation by *Mycobacterium* and *Sphingomonas* in soil. *Appl. Microbiol. Biotechnol.* 66, 726–736. doi: 10.1007/s00253-004-1766-4
- Liu, Z. F., Liu, J. Q., Zhu, Q. Z., and Wu, W. (2012). The weathering of oil after the Deepwater Horizon oil spill: insights from the chemical composition of the oil from the sea surface, salt marshes and sediments. *Environ. Res. Lett.* 7:035302. doi: 10.1088/1748-9326/7/3/035302
- Michel, J., and Hayes, M. O. (1999). Weathering patterns of oil residues eight years after the Exxon Valdez oil spill. *Mar. Pollut. Bull.* 38, 855–863. doi: 10.1016/S0025-326X(98)00100-3
- Middlebrook, A. M., Murphy, D. M., Ahmadov, R., Atlas, E. L., Bahreini, R., Blake, D. R., et al. (2012). Air quality implications of the Deepwater Horizon oil spill. *Proc. Natl. Acad. Sci. U.S.A.* 109, 20280–20285. doi: 10.1073/pnas.1110052108
- Mohn, W. W., and Stewart, G. R. (2000). Limiting factors for hydrocarbon biodegradation at low temperature in Arctic soils. *Soil Biol. Biochem.* 32, 1161–1172. doi: 10.1016/S0038-0717(00)00032-8
- Monrozier, L. J., Ladd, J. N., Fitzpatrick, R. W., Foster, R. C., and Raupach, M. (1991). Components and microbial biomass content of size fractions in soils of contrasting aggregation. *Geoderma* 50, 37–62. doi: 10.1016/0016-7061(91)90025-O
- Mortazavi, B., Horel, A., Beazley, M. J., and Sobecky, P. A. (2013). Intrinsic rates of petroleum hydrocarbon biodegradation in Gulf of Mexico intertidal sandy sediments and its enhancement by organic substrates. *J. Hazard. Mater.* 244, 537–544. doi: 10.1016/j.jhazmat.2012.10.038
- Nam, K., Kim, J. Y., and Oh, D. I. (2003). Effect of soil aggregation on the biodegradation of phenanthrene aged in soil. *Environ. Pollut.* 121, 147–151. doi: 10.1016/S0269-7491(02)00181-1
- Nemirovskaya, I. A. (2011). Tar balls in Baltic Sea beaches. *Water Resources* 38, 315–323. doi: 10.1134/S0097807811020114
- Nocentini, M., and Pinelli, D. (2001). Biodegradation of PAHs in aggregates of a low permeability soil. *Soil Sediment Contam.* 10, 211–226. doi: 10.1080/20015891109220

- Ortega-Calvo, J. J., and Gschwend, P. M. (2010). Influence of low oxygen tensions and sorption to sediment black carbon on Biodegradation of Pyrene. *Appl. Environ. Microbiol.* 76, 4430–4437. doi: 10.1128/AEM.00461-10
- OSAT-II. (2011). “Summary report for fate and effects of remnant oil remaining in the beach environment,” in *Operational Science and Advisory Team-II, Gulf Coast Incident Management Team*. Report prepared for Lincoln D. Stroh, CAPT, U.S. Coast Guard Federal On-Scene Coordinator Deepwater Horizon MC252, 36 (New Orleans, LA).
- Papizadeh, M., Ardakani, M. R., Motamed, H., Rasouli, I., and Zarei, M. (2011). C-S targeted biodegradation of dibenzothiophene by *Stenotrophomonas sp* NISOC-04. *Appl. Biochem. Biotechnol.* 165, 938–948. doi: 10.1007/s12010-011-9310-3
- Prince, R. C., Elmendorf, D. L., Lute, J. R., Hsu, C. S., Haith, C. E., Senius, J. D., et al. (1994). 17.alpha.(H)-21.beta.(H)-hopane as a conserved internal marker for estimating the biodegradation of crude oil. *Environ. Sci. Technol.* 28, 142–145. doi: 10.1021/es00050a019
- Reddy, C. M., Arey, J. S., Seewald, J. S., Sylva, S. P., Lemkau, K. L., Nelson, R. K., et al. (2012). Composition and fate of gas and oil released to the water column during the Deepwater Horizon oil spill. *Proc. Natl. Acad. Sci. U.S.A.* 109, 20229–20234. doi: 10.1073/pnas.1101242108
- Rodriguez-Blanco, A., Antoine, V., Pelletier, E., Dellile, D., and Ghiglione, F. (2010). Effects of temperature and fertilization on total vs. active bacterial communities exposed to crude and diesel oil pollution in NW Mediterranean Sea. *Environ. Pollut.* 158, 663–673. doi: 10.1016/j.envpol.2009.10.026
- Scow, K. M., and Alexander, M. (1992). Effect of diffusion on the kinetics of biodegradation-experimental results with synthetic aggregates. *Soil Sci. Soc. Am. J.* 56, 128–134. doi: 10.2136/sssaj1992.03615995005600010020x
- Suneel, V., Vethamony, P., Zakaria, M. P., Naik, B. G., and Prasad, K. (2013). Identification of sources of tar balls deposited along the Goa coast, India, using fingerprinting techniques. *Mar. Pollut. Bull.* 70, 81–89. doi: 10.1016/j.marpolbul.2013.02.015
- Tang, Y. J., Carpenter, S. D., Deming, J. W., and Krieger-Brockett, B. (2006). Depth-related influences on biodegradation rates of phenanthrene in polluted marine sediments of Puget Sound, WA. *Mar. Pollut. Bull.* 52, 1431–1440. doi: 10.1016/j.marpolbul.2006.04.009
- Tejeda-Agredano, M. C., Gallego, S., Niqui-Arroyo, J. L., Vila, J., Grifoll, M., and Ortega-Calvo, J. J. (2011). Effect of interface fertilization on biodegradation of polycyclic aromatic hydrocarbons present in nonaqueous-phase liquids. *Environ. Sci. Technol.* 45, 1074–1081. doi: 10.1021/es102418u
- Tibbett, M., George, S. J., Davie, A., Barron, A., Milton, N., and Greenwood, P. F. (2011). Just add water and salt: the optimisation of petrogenic hydrocarbon biodegradation in soils from semi-arid Barrow Island, Western Australia. *Water Air Soil Pollut.* 216, 513–525. doi: 10.1007/s11270-010-0549-z
- Townsend, G. T., Prince, R. C., and Suflita, J. M. (2003). Anaerobic oxidation of crude oil hydrocarbons by the resident microorganisms of a contaminated anoxic Aquifer. *Environ. Sci. Technol.* 37, 5213–5218. doi: 10.1021/es0264495
- Urbano, M., Elango, V., and Pardue, J. H. (2013). Biogeochemical characterization of MC252 oil:sand aggregates on a coastal headland beach. *Mar. Pollut. Bull.* 77, 183–191. doi: 10.1016/j.marpolbul.2013.10.006
- Uribe-Jongbloed, A., and Bishop, P. L. (2007). Comparative study of PAH removal efficiency under absence of molecular oxygen: effect of electron acceptor and hydrodynamic conditions. *J. Environ. Eng. Sci.* 6, 367–376. doi: 10.1139/s06-057
- Uyttebroek, M., Breugelmans, P., Janssen, M., Wattiau, P., Joffe, B., Karlsson, U., et al. (2006). Distribution of the *Mycobacterium* community and polycyclic aromatic hydrocarbons (PAHs) among different size fractions of a long-term PAH-contaminated soil. *Environ. Microbiol.* 8, 836–847. doi: 10.1111/j.1462-2920.2005.00970.x
- Venosa, A. D., Suidan, M. T., Wrenn, B. A., Strohmeier, K. L., Haines, J. R., Eberhart, B. L., et al. (1996). Bioremediation of an experimental oil spill on the shoreline of Delaware Bay. *Environ. Sci. Technol.* 30, 1764–1775. doi: 10.1021/es950754r
- Wang, Z. D., Fingas, M., Blenkinsopp, S., Sergy, G., Landriault, M., Sigouin, L., et al. (1998). Comparison of oil composition changes due to biodegradation and physical weathering in different oils. *J. Chromatogr. A* 809, 89–107. doi: 10.1016/S0021-9673(98)00166-6
- Wick, L. Y., Pasche, N., Bernasconi, S. M., Pelz, O., and Harms, H. (2003). Characterization of multiple-substrate utilization by anthracene-degrading *Mycobacterium frederiksbergense* LB501T. *Appl. Environ. Microbiol.* 69, 6133–6142. doi: 10.1128/AEM.69.10.6133-6142.2003
- Xu, R., and Obbard, J. P. (2003). Effect of nutrient amendments on indigenous hydrocarbon biodegradation in oil-contaminated beach sediments. *J. Environ. Qual.* 32, 1234–1243. doi: 10.2134/jeq2003.1234
- Zhu, L., Chen, Y., Guo, L., and Wang, F. J. (2013). Estimate of dry deposition fluxes of nutrients over the East China Sea: the implication of aerosol ammonium to non-sea-salt sulfate ratio to nutrient deposition of coastal oceans. *Atmos. Environ.* 69, 131–138. doi: 10.1016/j.atmosenv.2012.12.028

**Conflict of Interest Statement:** The authors declare that the research was conducted in the absence of any commercial or financial relationships that could be construed as a potential conflict of interest.

Received: 05 November 2013; accepted: 25 March 2014; published online: 10 April 2014.

Citation: Elango V, Urbano M, Lemelle KR and Pardue JH (2014) Biodegradation of MC252 oil in oil:sand aggregates in a coastal headland beach environment. *Front. Microbiol.* 5:161. doi: 10.3389/fmicb.2014.00161

This article was submitted to Aquatic Microbiology, a section of the journal *Frontiers in Microbiology*.

Copyright © 2014 Elango, Urbano, Lemelle and Pardue. This is an open-access article distributed under the terms of the Creative Commons Attribution License (CC BY). The use, distribution or reproduction in other forums is permitted, provided the original author(s) or licensor are credited and that the original publication in this journal is cited, in accordance with accepted academic practice. No use, distribution or reproduction is permitted which does not comply with these terms.



# The polycyclic aromatic hydrocarbon degradation potential of Gulf of Mexico native coastal microbial communities after the Deepwater Horizon oil spill

**Anthony D. Kappell<sup>1</sup>, Yin Wei<sup>1</sup>, Ryan J. Newton<sup>2</sup>, Joy D. Van Nostrand<sup>3</sup>, Jizhong Zhou<sup>3</sup>, Sandra L. McLellan<sup>2</sup> and Krassimira R. Hristova<sup>1\*</sup>**

<sup>1</sup> Department of Biological Sciences, Marquette University, Milwaukee, WI, USA

<sup>2</sup> School of Freshwater Sciences, Great Lakes WATER Institute, University of Wisconsin-Milwaukee, Milwaukee, WI, USA

<sup>3</sup> Department of Microbiology and Plant Biology, Institute for Environmental Genomics, University of Oklahoma, Norman, OK, USA

## Edited by:

Joel E. Kostka, Georgia Institute of Technology, USA

## Reviewed by:

Zongze Shao, State Oceanic Administration, China

Michail M. Yakimov, CNR-National Research Council, Italy

## \*Correspondence:

Krassimira R. Hristova, Department of Biological Sciences, Marquette University, 530 N. 15th Street, 208 Wehr Life Sciences Building, PO Box 1881, Milwaukee, WI 53201-1881, USA  
e-mail: krassimira.hristova@marquette.edu

The Deepwater Horizon (DWH) blowout resulted in oil transport, including polycyclic aromatic hydrocarbons (PAHs) to the Gulf of Mexico shoreline. The microbial communities of these shorelines are thought to be responsible for the intrinsic degradation of PAHs. To investigate the Gulf Coast beach microbial community response to hydrocarbon exposure, we examined the functional gene diversity, bacterial community composition, and PAH degradation capacity of a heavily oiled and non-oiled beach following the oil exposure. With a non-expression functional gene microarray targeting 539 gene families, we detected 28,748 coding sequences. Of these sequences, 10% were uniquely associated with the severely oil-contaminated beach and 6.0% with the non-oiled beach. There was little variation in the functional genes detected between the two beaches; however the relative abundance of functional genes involved in oil degradation pathways, including polycyclic aromatic hydrocarbons (PAHs), were greater in the oiled beach. The microbial PAH degradation potentials of both beaches, were tested in mesocosms. Mesocosms were constructed in glass columns using sands with native microbial communities, circulated with artificial sea water and challenged with a mixture of PAHs. The low-molecular weight PAHs, fluorene and naphthalene, showed rapid depletion in all mesocosms while the high-molecular weight benzo[ $\alpha$ ]pyrene was not degraded by either microbial community. Both the heavily oiled and the non-impacted coastal communities showed little variation in their biodegradation ability for low molecular weight PAHs. Massively-parallel sequencing of 16S rRNA genes from mesocosm DNA showed that known PAH degraders and genera frequently associated with oil hydrocarbon degradation represented a major portion of the bacterial community. The observed similar response by microbial communities from beaches with a different recent history of oil exposure suggests that Gulf Coast beach communities are primed for PAH degradation.

**Keywords:** Deepwater Horizon, oil spill, microbial community composition, high-throughput sequencing, functional gene arrays, polycyclic aromatic hydrocarbons (PAH), biodegradation, mesocosms

## INTRODUCTION

The destruction of the Deepwater Horizon (DWH) oil rig resulted in the discharge of approximately 4.9 million barrels of light crude oil into Gulf of Mexico marine environments from April 20, 2010 to July 15, 2010, making it the second worst oil spill in US history (Lehr et al., 2010). During the cleanup effort, crude oil along with added dispersants formed more than a 35 km long plume in the Gulf of Mexico that significantly impacted coastal ecosystems, including native microbial community composition (Camilli et al., 2010) with unknown ecological consequences. Significant amounts of oil washed ashore on marshes and beaches in the Gulf of Mexico over a 2- to 3-month period and were subsequently buried underneath layers of sand (Allan et al., 2012), bringing enormous amounts of allochthonous carbon to the beach ecosystems. An estimated  $1.7 \times 10^{11}$  g of C(1)-C(5) hydrocarbons including  $2.1 \times 10^{10}$  g of PAHs were released to the water

column during the spill (Reddy et al., 2012). The low molecular weight PAH, naphthalene was the dominant PAH in the crude oil followed by the low molecular weight PAHs, phenanthrene and fluorene, while the high-molecular weight PAH, chrysene and other PAHs were minor components (Zhanfei et al., 2012). PAHs, particularly high molecular weight compounds, are one of the major contaminant classes of concern in oil spills because many are toxic and/or carcinogenic to humans and wildlife and are often recalcitrant to degradation in environmental media.

Coastal shores protect inland areas from disturbances like hurricanes by buffering wind and wave energy. Additionally, they provide refuge and nesting ground for many species of marine and land animals. Sandy beaches also serve as the primary location of physical interaction between humans and the marine environment with significant impacts upon human health and local and state economies (USEPA, 2004). Permeable sandy sediments

cover large areas of the seafloor in the Gulf of Mexico, including beaches (Huettel and Rusch, 2000). Microbial biofilms cover the sand particles in these coastal ecosystems, and these biofilms harbor phylogenetically and functionally diverse bacteria whose abundances exceed that of the overlying seawater by orders of magnitude (Koster et al., 2005; Hunter et al., 2006; Karnachuk et al., 2006). The permeable sand sediments facilitate porewater exchange, transport of nutrients and removal of waste products for a very active microbial metabolism (Huettel and Rusch, 2000; Rusch et al., 2003).

Sand microbial communities are known to play a major role in the cycling of nutrients in these coastal ecosystems (Hunter et al., 2006; Mills et al., 2008; Huettel et al., 2014), and are likely among the earliest responders to anthropogenic pollution. Microbial communities in the Gulf of Mexico are also thought to be responsible for the intrinsic bioremediation of the crude oil released by the DWH oil spill (Atlas and Hazen, 2011; Chakraborty et al., 2012; Lu et al., 2012). Results from several research groups indicated that hundreds of bacterial taxa can decompose a variety of oil hydrocarbons and rapidly proliferate in the presence of oil in the deep water column (Hazen et al., 2010; Atlas and Hazen, 2011; Lu et al., 2012; Redmond and Valentine, 2012; Valentine et al., 2012; Kimes et al., 2013) but their relative abundance changes as the chemical composition of the oil is modified by the microbial community (Dubinsky et al., 2013). For example, the relative importance of taxa such as uncultivated *Oceanospirillales*, *Pseudomonas*, *Colwellia*, *Cycloclasticus*, *Pseudoalteromonas*, and *Thalassomonas* was controlled by changes in hydrocarbon supply in the water column (Dubinsky et al., 2013). The DWH oil spill dramatically altered not only microbial community composition but also the functional gene structure in the deep sea (Lu et al., 2012). A variety of metabolic genes involved in both aerobic and anaerobic hydrocarbon degradation were highly enriched in the plume compared with outside the plume (Lu et al., 2012). Fewer studies have focused on the impact from increased oil hydrocarbons on the terrestrial microbial communities such as those found in beach sand (Kostka et al., 2011; Newton et al., 2013) and coastal salt marshes (Beazley et al., 2012). In addition, complex hydrocarbon deposition could have major consequences in coastal environments for the entire bacterial community rather than just for those microorganisms capable of using the introduced carbon mixture. Depletion of essential nutrients, such as nitrogen and phosphorus during the hydrocarbon degradation could significantly shift microbial community composition and function.

In this study, we characterized changes in the functional gene composition and abundance of native microbial communities that accompany oil contamination in Gulf beach sands. We also investigated the PAH degradation potential of beach sand microbial communities. To set up comparative analyses, beach sand was collected from a beach in Orange Beach, AL that was severely impacted by oil contamination following the DWH spill and a beach on St. George Island, FL where negligible contamination was detected in the months following the blowout. This allows us to make pre- and post-oil spill comparisons between the communities. Newton et al. (2013) demonstrated the increased abundance of known-oil degraders within the Orange Beach in the

month of June suggesting an accompanying detectable change in the functional gene structure of the community. We investigated the beach sand microbial community functional gene response to hydrocarbon exposure using a functional gene microarray (GeoChip 4.2), targeting 539 gene families. Given that the Gulf of Mexico has a large number of natural hydrocarbon seeps and high petroleum-based vessel traffic (Horel et al., 2012), we hypothesized that the microbial communities of beach sands in this region may have adapted to this exposure. If so, the sand microbial communities from a beach without recent oil contamination and one with recent heavy oiling may have similar hydrocarbon degradation potential and would undergo similar community composition shifts following exposure to PAHs.

## RESULTS AND DISCUSSION

### FUNCTIONAL GENE DIVERSITY

Berm sand from two different sites at St. George and Orange beaches collected at three different months after the DWH blowout were subjected to non-expression functional gene microarray analysis. A total of 28,746 gene variants (between 19,150 and 23,337 persist and time, **Table 1**) representing 23.94% of the 120,054 unique sequences on the GeoChip 4.2 were detected. Functional gene variants are single sequence representatives of a functional gene with different sequences from diverse species or an overlapping sequence among species. The  $\alpha$ -diversity, variation within-community, of functional gene variants was variable across the samples, but no significant differences in diversity indices were observed ( $p > 0.05$ , **Table 1**). This suggests that the presence of oil and its constituents had little effect on the overall functional gene diversity at the two beaches and over time. Collectively, 84% of detected gene variants were shared among the two different beaches and time points, suggesting a large core functional gene group is present among sands in this region of the Gulf of Mexico. Approximately 10% (2762) of all gene variants detected by the array were unique to Orange beach and 6% (1736) of the gene variants were unique to the non-impacted St. George beach, irrespective of the month of sampling. This represents a different resident functional gene community at each beach. Only 1–3% of all gene variants detected were unique to a specific beach and time (**Table 1**) representing a transient functional gene change. These differences in the detection of transient functional gene variants can be related to temporal variation, however, the greatest percentage (2.54%, **Table 1**) of unique gene variants were present during the detectable hydrocarbon sampling of June at Orange beach (Newton et al., 2013). The June sample at Orange beach had a hydrocarbon concentration 1000 times greater than any other sample and was the only sample collected when visible oil was washing ashore (Newton et al., 2013). Fluoranthene, phenanthrene, and pyrene were detected in the Orange beach sand in the month of June at 8.6, 89.4, and  $5.3 \mu\text{g kg}^{-1}$ , respectively. Unknown hydrocarbons with ten or more carbons in a chain ( $\geq 10\text{C}$ ) were detected at  $21.4 \text{ mg kg}^{-1}$ , as well.

### RELATIVE ABUNDANCE OF FUNCTIONAL GENE CATEGORIES

The relative abundance of all functional gene categories was nearly identical across all sampling events at the two beaches and three time points (**Figure 1**). Overall, 27% of the detected gene

**Table 1 | Functional gene variant diversity, similarity, and evenness and percentage of unique and shared genes among samples.**

Microarray analysis site and month	Orange-June	Orange-August	Orange-November	St. George-June	St. George-September	St. George-November
Orange-June	2.54 <sup>a</sup>	72.5	78.54	75.08	74.22	65.56
Orange-August		1.95	73	72.53	68.09	67.99
Orange-November			1.85	76.05	73.2	67.19
St. George-June				0.74	77.26	65.06
St. George-September					1.92	60.84
St. George-November						2.18
S	23337	20831	22737	20793	20992	19150
H'	9.63 ± 0.02	9.50 ± 0.04	9.59 ± 0.02	9.54 ± 0.01	9.53 ± 0.03	9.45 ± 0.02
1/D	8975.7 ± 423.3	7854.2 ± 504.4	8872.6 ± 8.6	8404.0 ± 119.4	8167.4 ± 674.7	7733.1 ± 193.9
J'	0.957 ± 0.002	0.955 ± 0.004	0.956 ± 0.002	0.959 ± 0.001	0.957 ± 0.003	0.959 ± 0.002
E <sub>(1/D)</sub>	0.385 ± 0.018	0.377 ± 0.024	0.390 ± 0.001	0.404 ± 0.006	0.389 ± 0.032	0.404 ± 0.010

S, Number of genes detected; H', Shannon-Weaver diversity index; 1/D, Inverse Simpson diversity index; J', Pielou (Shannon) evenness index; E<sub>(1/D)</sub>, Simpson evenness index.

<sup>a</sup>Numbers in shading indicate the percentage of gene variants detected at that site and time (S) that are unique.

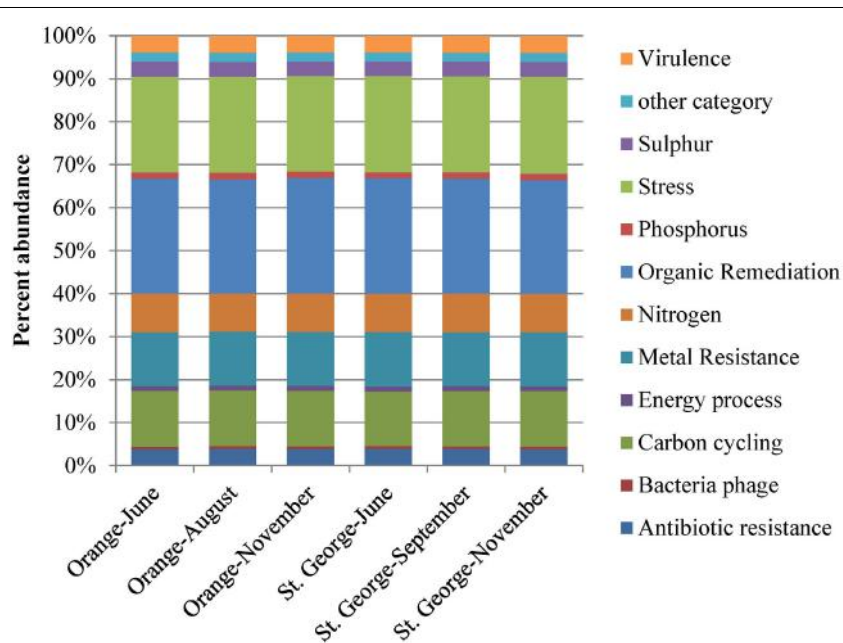


**FIGURE 1 | Percent abundance of all functional gene groups detected by microarray analysis.** The total number of genes detected at each beach sands, St. George or Orange, was used to calculate the relative richness of each gene group. Values were averaged over the two samples from each beach.

variants were for genes involved in organic contaminants degradation; 13% in carbon metabolism; 12.5% in metal resistance; and 9% in nitrogen metabolism.

Of the unique gene variants detected of the residential functional genes (Figure 2) at Orange beach, 29% were involved in organic contaminant degradation, 7% in nitrogen metabolism, 14% in carbon metabolism, 12% in metal resistance, and 18% in survival of abiotic and environmental stress. The increased presence of these genes at the contaminated beach during and after the oiling event suggests that the oil and its constituents triggered small changes in the abundance of organisms carrying hydrocarbon and PAH degradation genes and genes involved

in survival of abiotic and environmental stress. The unique gene variants detected were representatives of functional genes detected at both beach sites. The detection of more unique genes variants at Orange beach compared to St. George beach may be explained by the impact of the oil components on the intrinsic beach community and the addition of gene variants as the pelagic microbial community associated with the contaminated water reaches shore.

#### DIFFERENCES IN THE RELATIVE ABUNDANCE OF FUNCTIONAL GENES

The functional genes (sum of all gene variants detected) showed significantly greater ( $p < 0.05$ ) relative abundance in the June

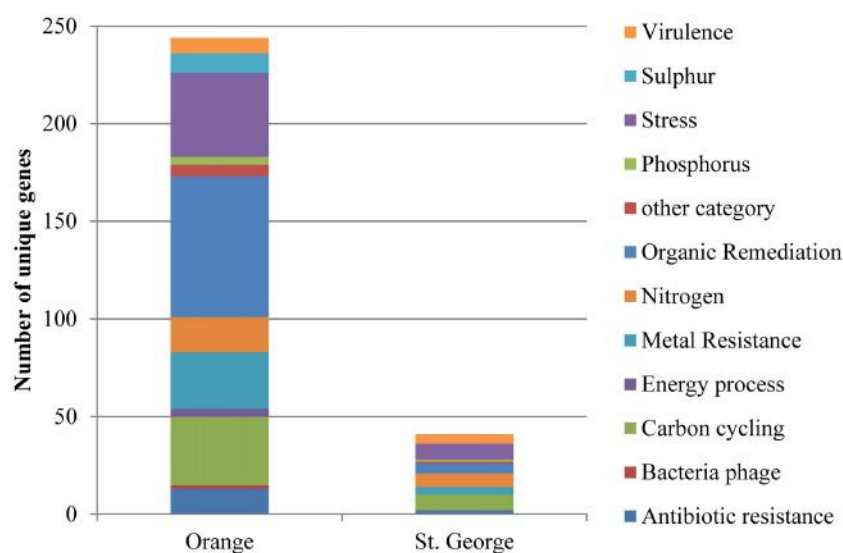


**FIGURE 2 | Number of genes in functional gene groups unique to each beach detected by microarray analysis.** Genes were represented in the beach site when sands were collected at all three time points (June, August or September, and November 2010).

sample at Orange beach than St. George beach (**Table 2**). These differences in abundance maybe directly related to the detection of fluoranthene, phenanthrene, pyrene and  $\geq 10C$  hydrocarbons present at the Orange beach (Newton et al., 2013).

Individual functional genes involved in the degradation pathways for benzoate, xylene, phthalate, toluene, chloroalkane and chloroalkene [**Figure S1**, KEGG pathway database (Kanehisa and Goto, 2000)] were greater in relative abundance in the Orange beach June sample. The majority of differentially detected functional genes in this sample were related to degradation pathways of aromatic hydrocarbons, PAH, and BTEX (benzene, toluene, ethylbenzene, and xylenes) suggesting increased concentration of these compounds following beach oiling. Aromatic hydrocarbons were also detected at Orange beach in the month of June (Newton et al., 2013). Additionally, genes involved in the chloroalkane and chloroalkene pathway were in greater abundance at Orange beach, suggesting the presence and possible accumulation of chlorinated hydrocarbons, feasibly from the degradation of chlorinated aromatics. Methylamine dehydrogenase, which forms formaldehyde from methylamine, was also abundant, indicating the possible accumulation of this single carbon amine from the degradation of more complex hydrocarbons and amino-aromatic compounds. Lu et al. (2012) showed significant increases in genes involved in initial oxidation of hydrocarbons such as *alkB* encoded alkane 1-monoxygenase and the *bbs* gene involved in anaerobic toluene degradation in the oil plume compared to non-plume deep sea waters during the DWH blow-out. In contrast there was no significant difference detected for these genes in our beach sand samples ( $p > 0.05$ ). The lack of significant difference in *alkB* is unexpected as the increase in relative abundance of *Alcanivorax* and other known oil degraders (Newton et al., 2013) would suggest an accompanying detectable increase in the *alkB* gene, in particular the specific probe designed from *Alcanivorax*. This may reflect

possible dissimilarity in sequences that are not represented in the arrayed probes (Zhou and Thompson, 2002). Oligonucleotide based arrays are sensitive to base-pair mismatches and exhibit high hybridization specificity (Cook and Sayler, 2003). This may explain the lack in the extent of change demonstrated in the functional gene array compared to the published changes in phylogeny (Newton et al., 2013). The changes in relative abundance that was detected of functional genes within the community structure indicate shifts in the degradation pathways of microbial community to optimally utilize available hydrocarbons between the initial plume and the hydrocarbons and derivatives that reached the shore.

The increased abundance of genes involved in PAH related degradation pathways in the Orange beach sand community compared to St. George beach suggest an increase in the microbial community members that can take advantage of the greater abundance of hydrocarbons. While the Orange beach microbial community had a greater relative abundance of genes involved in hydrocarbon and PAH degradation, these genes were also present at the non-impacted beach. These results suggest that the native communities found at these beaches have an innate potential for degradation of hydrocarbons and PAHs released during an oil spill.

There was a statistically greater abundance of genes involved in response to nitrogen limitation stress and osmotic stress (**Table 2**) in the heavily oiled beach compared to the non-impacted beach. This indicates the community members responding to hydrocarbons may harbor increased abundance of genes involved in nitrogen limitation and osmotic stress responses. Macro-nutrient limitation including nitrogen is common in oil contaminated communities as the hydrocarbons are utilized causing a decreased organic nitrogen pool (Atlas and Bartha, 1972; Leahy and Colwell, 1990; Toccalino et al., 1993). However, the nitrogen metabolism functional gene group, including nitrogen assimilation and

**Table 2 | Individual genes showing a significant increase ( $p < 0.05$ ) at oil-impacted Orange beach compared to non-impacted St. George beach during the month of June.**

Group	Enzyme	EC	Number <sup>b</sup> detected	Number array	Sum of ratio for gene group on array for June <sup>a</sup>		
					Orange beach		St George beach
					Average <sup>c</sup> ± SD	Average ± SD	P-value
Aromatics (including PAH and BTEX)	akbADF <sup>d</sup>		65	175	32.42 ± 1.44	25.44 ± 0.73	0.025
	Ethyl/benzene dioxygenase ( <i>akbA</i> )	—	1	1	—	—	—
	2-hydroxy-6-oxohepta-2,4-dienoate hydroxylase ( <i>akbD</i> )	3.7.1.9	8	28	—	—	—
	4-hydroxy-2-oxovalerate aldolase ( <i>akbF</i> )	4.1.3.39	46	146	—	—	—
	Arylesterase	3.1.1.2	13	353	119.68 ± 2.49	106.89 ± 1.39	0.023
	Catechol-2,3-dioxygenase	1.13.11.2	336	650	335.48 ± 9.89	297.02 ± 4.17	0.036
	2-halobenzoate dioxygenase	1.14.12.13	33	165	27.97 ± 1.39	19.22 ± 2.46	0.048
	6-hydroxy-D-nicotine oxide	1.5.3.6	13	37	7.04 ± 0.51	3.91 ± 0.20	0.015
	Nitrile hydratase	4.2.1.84	143	263	136.82 ± 5.36	118.70 ± 2.37	0.048
	4,5-dihydroxyphthalate decarboxylase	4.1.1.55	19	43	8.93 ± 0.06	6.93 ± 0.28	0.010
Chloroalkane	4-hydroxybenzoate-3-monoxygenase	1.14.13.2	79	197	73.50 ± 0.00	70.16 ± 0.96	0.038
	Catechol-1,2-dioxygenase	1.13.11.1	82	164	63.21 ± 0.64	53.74 ± 1.86	0.020
	Toulene monooxygenase	1.14.13.7	3	16	1.07 ± 0.03	0.31 ± 0.00	0.010
	Phenol 2-monooxygenase	1.14.13.7	7	9	10.10 ± 0.43	7.82 ± 0.13	0.018
	3-phenylpropanoate dioxygenase	1.14.12.19	32	77	19.83 ± 0.25	15.15 ± 0.60	0.009
Chloroalkene	Quinoprotein methanol dehydrogenase	1.1.2.8	109	199	123.28 ± 2.38	115.65 ± 0.77	0.049
Chloroalkene	Tetrachlorethene reductive dehalogenase	1.97.1.8	58	259	34.18 ± 0.39	28.37 ± 1.66	0.040
Methane Carbon cycling	Methylamine dehydrogenase	1.4.9.1	53	77	57.97 ± 0.45	54.38 ± 0.37	0.013
	Endochitinase	3.2.1.14	30	796	137.11 ± 0.45	182.88 ± 2.20	0.010
	Phosphoenolpyruvate carboxylase	4.1.1.31	381	792	418.34 ± 5.34	367.70 ± 11.29	0.030
	Ribulose-bisphosphate carboxylase	4.1.1.39	138	393	99.08 ± 2.17	87.19 ± 2.48	0.040
Metal Resistance	Zinc ( <i>ZitB/ZntA</i> )	—	221	637	189.27 ± 2.38	168.63 ± 1.23	0.008
Stress	Nitrogen ( <i>glnA/glnR</i> )	—	491	1454	416.13 ± 3.44	381.47 ± 4.21	0.012
	Osmotic ( <i>opuE/proW/V/X</i> )	—	150	457	114.85 ± 0.57	100.91 ± 1.83	0.009
	General ( <i>ObgE</i> )	—	364	1264	288.12 ± 3.93	265.27 ± 3.64	0.026

<sup>a</sup>Average of the sum of the ratio between the gene variant spot fluorescence and average spot fluorescence on the microarray.<sup>b</sup>Total number of gene variants detected (regardless of site) and used to generate the sum.<sup>c</sup>Average of sum from two independent microarrays from samples 100 m apart at same beach.<sup>d</sup>Average of the sum of the ratios of gene groups *akbA*, *akbD*, and *akbF* (shaded in gray).

nitrogen fixation, did not show significant differences ( $p > 0.05$ ) in abundance between the two studied beaches. Functional gene analysis of the DWH deep-sea oil plume observed increased abundance of genes involved in nitrogen assimilation pathways, which was partially accredited to increase of biomass in the water column (Hazen et al., 2010; Lu et al., 2012). However, our results suggest that the community members responding to increased hydrocarbons and PAHs at the beach sands are not nitrogen fixers, but instead dealt with limited nitrogen via other mechanisms.

The greater abundance of osmotic stress genes in Orange beach sand compared to St. George beach could be associated with

the hydrocarbon degrading community, as aromatic compounds have a direct influence on the membrane lipid bilayer, increasing its fluidity and thereby causing an increase in membrane permeability (Sikkema et al., 1994, 1995).

The genes encoding zinc transporters (*zntA* and *zitB*, Table 2) induced in the presence of high metal concentrations showed a greater abundance in the oiled beach. Since *zntA* can be responsible for the transport of zinc, lead and cadmium (Liu et al., 2005), this indicates the oiled community is more suited for responses of high metal concentrations. These metals were detected in oil-impacted waters and salt marshes

(Liu et al., 2012; Joung and Shiller, 2013). It has been suggested that these trace metals increase as lower molecular weight hydrocarbons are degraded (Liu et al., 2012).

Interestingly, the carbon assimilation genes encoding phosphoenolpyruvate carboxylase and RuBisCO were also greater in abundance in the oiled beach (**Table 2**) suggesting an increase in the presence of autotrophic genes. The increase in genes harbored in mixotrophic bacteria might be related to the sensitivity of RuBisCO to oxygen in the oxygen limited and carbon dioxide rich environment. The presence of oil on sediment surface can inhibit the penetration of dissolved oxygen into the sediment and thus inhibit metabolic activity of heterotrophic bacteria utilizing the abundant hydrocarbons (Liu et al., 2012). It is also possible that the mixotrophic bacteria are taking advantage of available hydrocarbons (Subashchandrabose et al., 2013) and thus increasing the abundance of carbon assimilation genes.

While the presence of particular functional genes can be associated with changes in the beach community structure due to oiling, the change in the community composition can be associated with the pelagic microbial community in the contaminated water with already established PAH and hydrocarbon degrading microorganisms as it reaches shore.

Our findings suggest that oil contamination lead to enrichment of bacteria harboring functional genes involved in hydrocarbon degradation and related stress responses within the impacted sand microbial community.

#### DEGRADATION OF A PAH MIXTURE OF NAPHTHALENE, FLUORENE, AND BENZO[ $\alpha$ ]PYRENE

To further explore the intrinsic potential for PAHs degradation by the communities of Orange and St. George beaches, mesocosms utilizing sand from both locations were spiked with a mixture of PAHs. The PAH mixture contained naphthalene and fluorene, which were major PAH components of the source oil from the DWH blowout (Zhanfei et al., 2012), and benzo[ $\alpha$ ]pyrene a highly recalcitrant PAH that can also interfere with the biodegradation of other PAHs (Juhasz and Naidu, 2000). In the presence of the sand microbiome of Orange or St. George beach, naphthalene was quickly removed to undetectable levels by day 8, with significant ( $p < 0.05$ ) concentrations removed by day 2 compared to abiotic degradation controls (**Figure 3**). There was no significant difference ( $p > 0.05$ ) detected between the two beach microbial communities in their degradation potential. The maximum rate of depletion of naphthalene in Orange and St. George beach was  $17.13 \pm 6.88$  and  $14.67 \pm 4.17 \mu\text{g g}^{-1} \text{ day}^{-1}$ , respectively, and was significantly greater ( $p < 0.05$ ) than the abiotic disappearance rate of  $3.77 \pm 0.14 \mu\text{g g}^{-1} \text{ day}^{-1}$ . Measured fluorene concentrations did not show a significant difference ( $p > 0.05$ ) to initial concentrations until day 6 indicating a lag in degradation by the microbial community or inhibition by the presence of initially higher concentrations of naphthalene (**Figure 3**). A significant difference ( $p < 0.05$ ) in fluorene concentrations was observed by day 6 compared to the abiotic control columns. Orange and St. George beach communities were able to degrade fluorene with similar rates at  $8.62 \pm 1.29$  and  $10.57 \pm 3.61 \mu\text{g g}^{-1} \text{ day}^{-1}$ , respectively. The rate of disappearance of fluorene in the abiotic control was

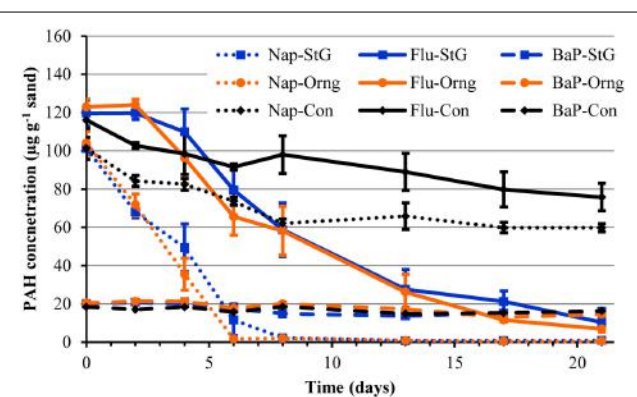


**FIGURE 3 |** Measured PAH concentrations in mesocosm columns containing sand from the oil impacted beach, Orange, and the non-impacted beach, St. George, over time. The sand was spiked with a mixture of  $100 \mu\text{g g}^{-1}$  naphthalene,  $120 \mu\text{g g}^{-1}$  fluorene, and  $20 \mu\text{g g}^{-1}$  benzo[ $\alpha$ ]pyrene prior to column setup. Lines in blue represent St. George (StG) sand mesocosm samples, lines in orange represent Orange (Orng) beach, and black lines represent control abiotic columns (Con). Solid lines represent fluorene (Flu) concentrations, dotted lines represent naphthalene (Nap) concentrations, and the dash line represents benzo[ $\alpha$ ]pyrene (BaP).

$1.49 \pm 0.14 \mu\text{g g}^{-1} \text{ day}^{-1}$ . Benzo[ $\alpha$ ]pyrene was not significantly ( $p > 0.05$ ) degraded in any column during the duration of the measurements.

The results of the mesocosm experiment demonstrate the ability of the sand microbial community to quickly respond to an influx of PAHs such as those found in oil spills. The DWH blowout resulted in water partitioning of the more soluble PAHs during transport of the oil plume to the surface. This partitioning led to deep water plumes composed primarily of methyl-naphthalene and other two ring PAHs while the surface had a larger proportion of three ring PAHs such as fluorene (Diercks et al., 2010). Differential *in situ* degradation rates of PAHs also influence the composition of PAHs eventually impacting and accumulating along the shoreline. Sand collected at Pensacola Beach on September 1, 2010 showed the presence of benzo[ $\alpha$ ]pyrene and fluorene, while naphthalene was not detected (Kostka et al., 2011). At Orange beach in June, fluorene, naphthalene, and benzo[ $\alpha$ ]pyrene were not detected at the sampling sites while these PAHs were detected in other beaches such as those in Mississippi in June and August (Newton et al., 2013). We have shown that although fluorene and naphthalene haven't been detected at Orange and St. George beach in June, August, September, and November 2010 (Newton et al., 2013), sand microbial communities have the potential for the rapid degradation of these chemicals. A similar rapid response to crude oil and diesel fuel additions to mesocosms was found with uncontaminated sand from the Gulf of Mexico, suggesting microbial communities in this region adapt to hydrocarbons, including PAHs, as a result of exposure to natural oil seepages and high petroleum-based vessel traffic (Horel et al., 2012). While benzo[ $\alpha$ ]pyrene is not a common growth substrate for bacteria, experiments have shown that bacteria can degrade benzo[ $\alpha$ ]pyrene when grown on an alternative carbon source (as reviewed in Juhasz and Naidu, 2000).

If the benzo[ $\alpha$ ]pyrene was bioavailable to the microbial community in the sand mesocosms, the available alternative carbon sources may not have been sufficient for co-metabolism of benzo[ $\alpha$ ]pyrene (Juhasz and Naidu, 2000). Alternatively, benzo[ $\alpha$ ]pyrene degrading bacterial species, more rare than low molecular weight PAH degraders, may not have been present in these sand communities (Haritash and Kaushik, 2009). However, this is unlikely due to the presence of known benzo[ $\alpha$ ]pyrene degraders such as *Sphingomonas*, *Mycobacterium*, *Pseudomonas*, and *Burkholderia*; and consortiums such as *Pseudomonas* with *Flavobacterium* (Juhasz and Naidu, 2000) within the mesocosm communities based on the 16S rRNA gene sequences described below. In summary, both beach communities were able to degrade lower molecular weight PAHs to the same extent, indicating the stored potential to degrade PAH contaminants is widespread in the beach sand environment along the Gulf Coast.

## COMMUNITY COMPOSITION IN MESOCOSM COLUMN EXPERIMENTS

The abundance of bacterial 16S rRNA gene sequences revealed little difference between the two beach sand mesocosm microbial community compositions during the PAH depletion mesocosm experiments (Figure 4, Table S1). Sequencing of environmental DNA extracted from the sand mesocosm samples generated over 7.9 million high quality V6 region bacterial rRNA gene tags. Overall, 27 taxa (22 genera and 5 additional unresolved taxa) each constituting  $\geq 1\%$  of the bacterial community were found post acclimation at any time point (days 0, 6, or 13) in either the Orange or St. George mesocosms (averaged over the individual columns; Figure 4). These taxa represented  $\geq 65\%$  of the population within the individual mesocosm community. In contrast these taxa represented  $\leq 25\%$  of the population in the field sand samples (source) used to set up the mesocosms. Although the identity of the taxa in the field and mesocosm communities was similar there were dramatic change in the relative abundances

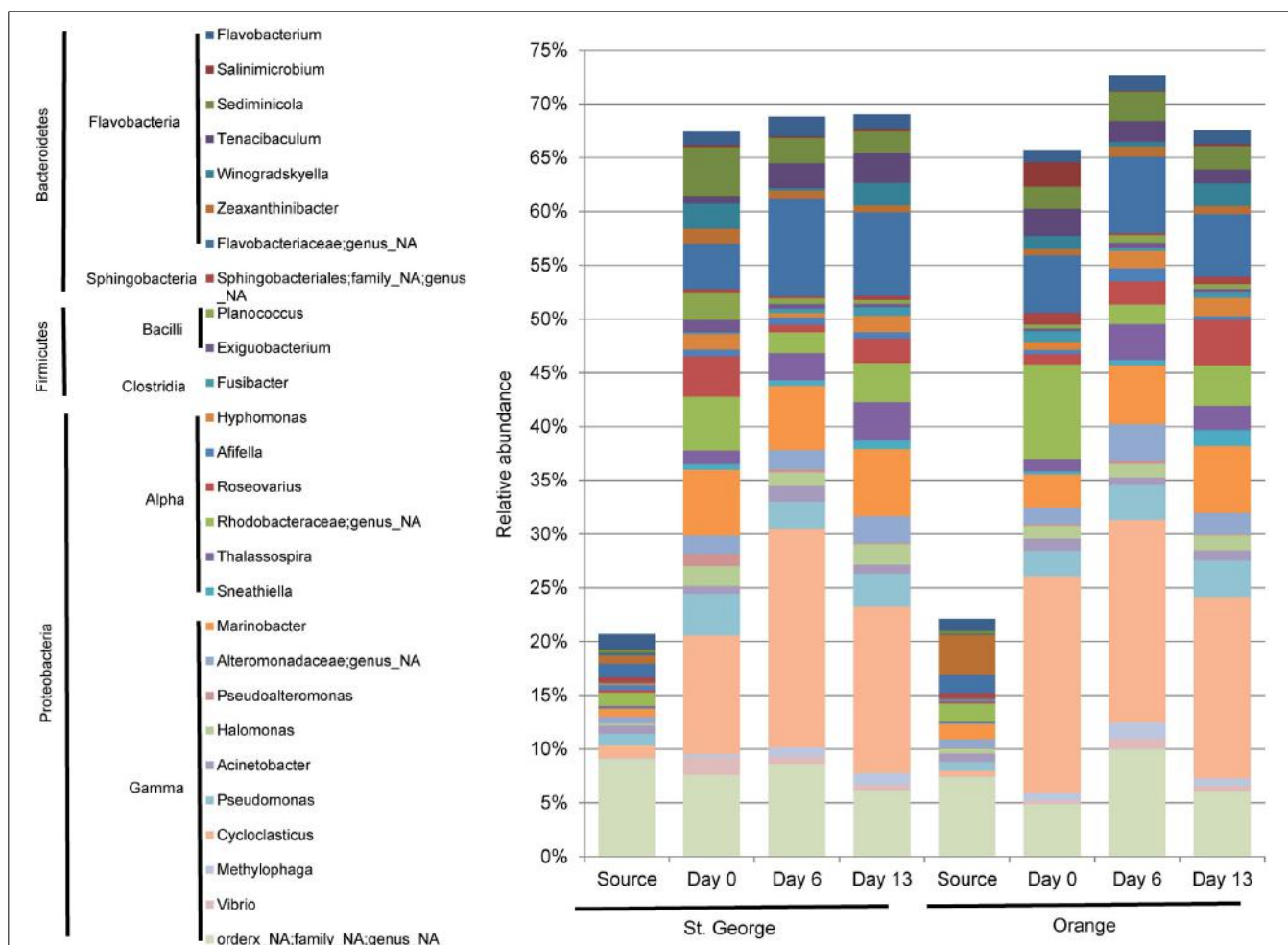


**FIGURE 4 | Taxonomic representation of source and mesocosm column sand samples, assigned from the 16S rRNA gene sequencing data.**

Genera (and un-resolved genera) composing  $\geq 1\%$  of the community at any time (day 0, 6, or 13) within any mesocosm (average of the 2 experimental columns) spiked with PAHs are represented. Source represents the population

determined from the field sand sample, prior to manipulation of the sand for the mesocosm experiments. Day 0 represents approximately 6 h during the assembly of the mesocosm experiments in which the bulk of the sand samples were mixed with PAH containing sand mixture. A genus was considered only if it constituted  $\geq 0.01\%$  of the community from any single sample.

of taxa between the post acclimation, day 0 and the field sample (Source; **Figure 4**). These changes are likely due to positive and negative selection of the taxa during the 6 h time frame of mixing and evaporation of the acetone used to apply the PAHs during the initial assembly of the mesocosms at room temperature. The PAHs spiked within the mesocosms did not show detectable depletion when the sand was sampled after acclimation on day 0 (**Figure 3**).

The core community representing  $\geq 1\%$  of the community in both mesocosm in all three time points (included in **Figure 4**) were identified in the mesocosm samples included representatives of *Flavobacteria*: *Flavobacterium* and *Sediminicola*; *Alphaproteobacteria*: *Thalassospira*; and *Gammaproteobacteria*: *Cycloclasticus*, *Marinobacter*, *Halomonas*, and *Pseudomonas*. With the exception of *Sediminicola*, these genera were reported to be highly associated with oil degradation during the DWH incident (Kostka et al., 2011; Chakraborty et al., 2012; Kimes et al., 2013; Liu and Liu, 2013; Newton et al., 2013). *Sediminicola* was reported as a major member of the microbial community found in the chronically oil and PAH contaminated Liaodong Bay of Bohai Sea, China (Zheng et al., 2014). *Thalassospira* is a known PAH-degrader of fluorene and naphthalene (Kodama et al., 2008) and was associated with oil on the water surface during the DWH blowout (Liu and Liu, 2013). *Cycloclasticus* represented between 15 and 20% of the community in the columns, while only 1.1 and 0.5% in the St. George and Orange beach sands used for the mesocosms, respectively. A similar rapid increase in *Cycloclasticus* under experimental laboratory conditions have been reported previously (Kasai et al., 2002). Studies in marine environments have described *Cycloclasticus* as a primary contributor to PAH degradation (Kasai et al., 2002; Wang et al., 2008;

Jurelevicius et al., 2013) during oil spills (Hazen et al., 2010; Chakraborty et al., 2012; Mason et al., 2012). *Marinobacter* is also well-established in alkane and PAH degradation (Vila et al., 2010). Newton et al. reported also that in the one sample set collected while oil was visibly washing ashore (Orange Beach June) OTUs associated with *Marinobacter* were largely increased in the community. *Pseudomonas* is able to degrade naphthalene in experimental systems and is thought to be involved in the co-metabolization of fluorene (Stringfellow and Aitken, 1995). *Flavobacterium* have been associated with PAH degradation (Trzesicka-Mlynarz and Ward, 1995). Within a mixed culture of *Flavobacterium* sp. and *Pseudomonas* sp., the degradation of benzo[ $\alpha$ ]pyrene was possible (Trzesicka-Mlynarz and Ward, 1995). Despite the enrichment of both, *Flavobacterium* and *Pseudomonas* sp. in our mesocosms, benzo[ $\alpha$ ]pyrene was not degraded in any column during the duration of the measurements suggesting it wasn't bioavailable or longer time is needed for the microorganisms to deplete this pollutant. *Sediminicola* has been associated with oil and PAH contaminated waters (Zheng et al., 2014). The large sequence representation of this core community of known and associated PAH degraders in the mesocosms suggests that biodegradation potential for hydrocarbons, including PAHs, was quickly established in the sand microbial communities prior to detectable degradation of the spiked PAHs.

Eight genera of the community presented in **Figure 4** exhibiting a  $\geq 3$  fold increase in average community percentage between any two time points post acclimation (**Figure 5**) denote a rapidly responsive community. The genera *Afifella*, *Methylophaga*, *Winogradskyella*, *Hyalomonas*, *Roseovarius*, *Tenacibaculum*, *Fusibacter*, and *Sneathiella* showed dynamic changes in relative abundance that may be related to the role they play in

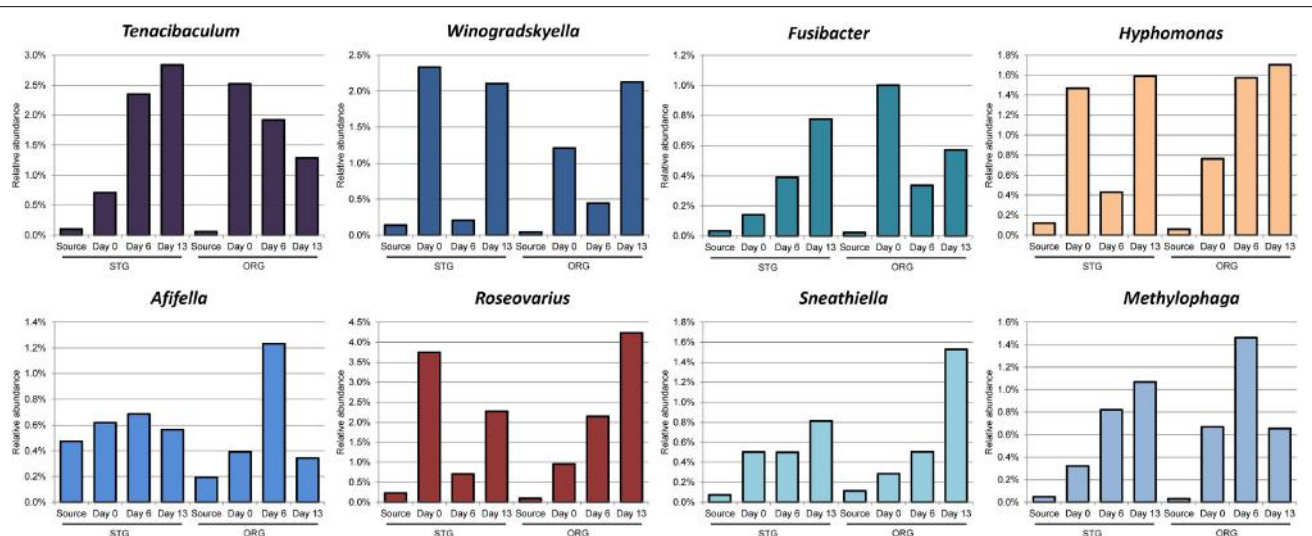


**FIGURE 5 | Bacterial genera enriched within the microbial community in the mesocosm columns.** Only genera demonstrating a  $\geq 3$ -fold increase in relative abundance when compared between any two time points (Days 0, 6, and 13) of at least one sand microbial community (average of 2 replicate mesocosm columns for each beach sand source) and represented in **Figure 4**. Source represents the population

determined from the field sand sample, prior to manipulation of the sand for the mesocosm experiments. Day 0 represents approximately 6 h during the assembly of the mesocosm experiment in which the bulk of the sand samples were mixed with PAH containing sand mixture. Bar graphs in color are for genera abundant above 1% in the community, depicted with the same color as in **Figure 4**.

their respective communities involved in the degradation of naphthalene and fluorene.

*Tenacibaculum* is known to produce bacteriolytic enzymes allowing nutrient recycling, which may account for their increase in abundance (Banning et al., 2010; Dubinsky et al., 2013). *Tenacibaculum* is as yet not associated with direct PAH utilization. *Winogradskyella* was among the core community present in the Gulf of Mexico beach sand following the period of beach oiling from the DWH blowout (Newton et al., 2013) and has been enriched previously with petroleum in microcosms (Zhao et al., 2014). *Fusibacter* species have been associated with oil producing wells (Ravot et al., 1999) and contaminated sites containing chlorinated solvents (Lee et al., 2011). *Fusibacter* prefers anaerobic environments and as yet been determined to be involved in direct degradation of PAHs (Ravot et al., 1999; Lee et al., 2011). *Hyphomonas* abundance has been associated with crude oil added to natural sea-water in microcosms (Coulon et al., 2007). *Hyphomonas* has also been associated with degradation potential of hydrocarbon-contaminated sediments from a harbor in the Tirrenean Sea after the addition of sources of nitrogen and phosphate (Yakimov et al., 2005). *Roseovarius* was one of the genera of numerous Alphaproteobacteria detected in sequences associated with a sample 127 km from the DWH rig (Kimes et al., 2013). *Roseovarius* is also known to be degraders of low molecular weight PAHs (Gallego et al., 2013). *Afifella* is a photosynthetic purple, non-sulfur bacteria that has not be associated with hydrocarbon or PAH degradation (Urdain et al., 2008). *Methylophaga* have been associated with the later phases of the DWH oil spill and has been suggested to be active in the heterotrophic community that was consuming residual cell mass and organic residues (Dubinsky et al., 2013). *Sneathiella* is a halotolerant, aerobic, chemoheterotroph that has not yet been associated with PAH or oil degradation activities (Jordan et al., 2007). Since a number of these genera have been associated with PAH and hydrocarbon degradation communities, their presence may be necessary to support the PAH depletion within the mesocosms and directly impact the ability of other genera to degrade PAHs within the columns.

The presence of the core community with known and associated PAH degraders in all mesocosm columns during the sampling times and their presence during the DWH spill may point to members of these genera as key players in the PAH degradation by the coastal sand microbial community during hydrocarbon degradation. The responsive community which contained associated and yet unassociated PAH degraders in the mesocosm columns may indicate a different involvement of these genera in the degradation of PAHs within the sand communities with different oiling history.

## CONCLUSIONS

Our results indicate that a variety of genes related to hydrocarbons degradation and stress were enriched in response to the oil contamination and associated environmental changes. Specifically, we observed enrichment of metabolic genes involved in the degradation pathways for BTEX, alkanes, alkenes and aromatic hydrocarbons including PAHs. In addition, genes involved in metabolic processes related to osmotic stress and metal

transport showed relative increases most likely related to the oil contamination. However, the relative abundance of the majority of functional gene categories investigated was similar across the two sampled beaches and 5-months separating sampling time points. These results suggest that sand microbial communities are relatively functionally stable and that the hydrocarbon exposure adds a layer of complexity to the system without initiating drastic community change.

The potential of microbial PAH degradation between beaches with a different history of oil contamination was tested in a laboratory column experiment. Upon exposure with a PAH mixture we observed similar biodegradation potential from each beach sand community for the mixture despite of its oiling history. The lower molecular weight PAHs naphthalene and fluorene were depleted with similar rates, while the concentration of benzo[ $\alpha$ ]pyrene remained constant in all mesocosms for the time of incubation. Further study using nutrients and electron donors or acceptors additions is needed to understand if these communities are also primed to degrade recalcitrant pollutants such as benzo[ $\alpha$ ]pyrene and other higher molecular weight PAHs.

The community composition of the PAH degradation in the mesocosms consisted of a core community of known or associated PAH degraders that was consistent among the two sand communities. A responsive community to the PAH addition that showed different shifts in abundance between the two sand mesocosms and may be related to the availability of specific PAHs was also detected. The observed similarity in the ability of the two differently oil impacted microbial communities to degrade PAHs and the presence of a core community containing PAH degraders indicate the wide spread dissemination of PAH degraders on beaches over large distances. This is most likely explained by the large number of natural hydrocarbon seeps and high petroleum-based vessel traffic in this region (Horel et al., 2012) which may select for a PAH and hydrocarbon consortium within the microbial community of the pelagic and coastal waters, as well as, distant beaches these consortiums will eventually reach.

Further study is needed to understand the response of microbial communities not only to change in oil pollutant concentrations but also to stressors such as nutrient starvation, anoxia, and ecological interactions in the Gulf of Mexico coastal sand ecosystems. Experimental mesocosms with stratified conditions to explore the impact of oxygen, electron acceptors, nutrients, and oil pollutant micro-concentration gradients will be particularly useful to address ecological questions under controlled conditions. Combined with meta-omics' technologies this approach provides powerful tools to gain insights into functional networks involved in hydrocarbon degradation in coastal sandy sediments. A global understanding of the impact of oil on indigenous coastal microbial community structures, function, and resilience will help in development of strategies for restoring ecological balance following oil spills in coastal areas.

## MATERIALS AND METHODS

### STUDY SITES AND SAMPLING PROCEDURES

For functional gene microarray analysis, surface sand samples were collected from two beaches in the southeast United States along the Gulf Coast in Alabama, and Florida as described in

(Newton et al., 2013). The beach locations referred to in this study are: Orange beach (Cotton Bayou Beach area in Alabama,  $30^{\circ} 16' 54''$  N,  $87^{\circ} 41' 17''$  W), and St. George (St. George Island, Florida,  $29^{\circ} 41' 22''$  N,  $84^{\circ} 46' 59''$  W). Exposed surface sand (wet intertidal sand located at the high point of wave action on the beach face) was sampled at each beach. For the sand environments, we chose two sampling sites  $\sim$ 100 m apart at each beach location. Samples were collected during five sampling periods: June 13–15, 2010, August 8, 2010, September 20–22, 2010, November 15–18, 2010, and August 15–17, 2011, except for St. George, which we were unable to collect during the August 2010 period. Following collection in the field, the sand samples were stored on ice between 2 and 28 h during the sampling expedition and then on dry ice before being shipped to the lab for further processing. In the lab, sand was stored at  $-80^{\circ}\text{C}$  prior to DNA extraction procedures. Sand for the mesocosm experiments was sampled from Orange beach and St. George in excess of 4 kg during a sampling trip in August 2011 and were stored on ice and then stored at  $4^{\circ}\text{C}$  until use in the mesocosms.

Based on reports by NOAA's cleanup and assessment techniques, Orange beach was classified as heavily oiled following the DWH spill, while St. George had either trace or no oiling and was referred to as a control or un-impacted site in their assessment and in a previous study (Newton et al., 2013). St. George also serves as the no recent oil contamination control beach for all analyses in this study.

#### DNA EXTRACTION

DNA extractions were performed on 5 or 1 g of sand samples essentially as Zhou et al. (1996) described but without CTAB and reduced volumes to scale. Rather than using chlorophorm: isoamyl alcohol, the samples was purified by selective RNA precipitation using 1.5 M ammonium acetate and the Wizard Genomic DNA purification kit (Promega) for protein precipitation, DNA precipitation and DNA rehydration steps. DNA was quantified and checked for quality by NanoDrop spectrophotometry and with 1% agarose gel electrophoresis.

#### MICROBIAL COMMUNITY DNA LABELING, MICROARRAY HYBRIDIZATION AND ANALYSIS

For microarray analysis, 1.5  $\mu\text{g}$  of DNA extracted from 5 g sand sediment was labeled with Cy3 fluorescent dye (GE Healthcare, Piscataway, NJ, USA) by random priming (Wu et al., 2006; Van Nostrand et al., 2009). The labeled DNA was purified, hybridized to GeoChip 4.2, and processed as described in Lu et al. (2012). GeoChip 4.2 is a functional gene array (Hazen et al., 2010; Lu et al., 2012) containing 120,054 distinct probes and covers 200,393 coding sequences in different microbial functional and biogeochemical processes. Spots with signal-to-noise ratios lower than 2 were removed before statistical analysis was performed (He et al., 2010).

All GeoChip hybridization data are available at the Institute for Environmental Genomics, University of Oklahoma (<http://ieg.ou.edu/>). The data was pre-processed to response ratios of each gene variant, which is the ratio of intensity of the variant to the average of all genes on the array. Simpson's, Shannon-Weiner's,

and evenness indices were calculated to access functional gene diversity. ANOVA was used to determine significant differences between the functional microbial communities between the two beach sites and samplings over time. Tukey's test was used for pairwise comparisons. A significance level of  $p < 0.05$  was used for all comparisons (He and Wang, 2011). Total abundance of each gene category or all gene variants representing a functional gene were calculated as the sum of response ratio and compared between the beach locations overtime using ANOVA and Tukey's test for follow-up pairwise comparison.

#### PAH DEGRADATION POTENTIAL OF THE SAND MICROBIAL COMMUNITY

The potential for degradation of PAHs was tested in eight constructed mesocosms, three replicates with native sand communities collected August 2011 for each beach, Orange and St. George, and two abiotic controls. After sampling in the field, the sand was shipped on ice and a stored at  $4^{\circ}\text{C}$ , until used in the mesocosm construction. Glass columns (Chemglass; 7.62 cm inner diameter by 30.5 cm effective length), fitted with fritted glass supports, were filled with sand from Orange beach and St. George beach spiked with a mixture of three low molecular weight PAHs, naphthalene, fluorene, and benzo[ $\alpha$ ]pyrene. Stock concentrations of fluorene, naphthalene, and benzo[ $\alpha$ ]pyrene in acetone was hand mixed into 350 g batches of sand from St. George or Orange beach for 1 min to achieve final concentrations of 100  $\mu\text{g g}^{-1}$  naphthalene, 120  $\mu\text{g g}^{-1}$  fluorene, and 20  $\mu\text{g g}^{-1}$  benzo[ $\alpha$ ]pyrene in the columns. The acetone from PAH mixed sand was allowed to evaporate for 1.5 h at room temperature prior to assembly of the columns. A total of 1.4 kg of sand mixed with PAHs was used to fill each of three glass column replicates for each beach. The time 0 samples were taken approximately 6 h after the initial spike of the first batch of sand which is referred to as the acclimation period. To setup two abiotic control columns, sand from St. George beach was autoclaved to remove the live microbiome prior to addition of PAH as for the other columns. Sodium azide was added to the artificial sea water for the control columns at 0.1%. To all columns, 400 mL of sterile artificial sea water (Kester et al., 1967; Berges et al., 2001) was added and allowed to drain by gravity flow and captured. Filling and draining (400 ml volume) with artificial seawater occurred over 3-h periods. The mesocosms were left filled and drained for 3 h each recreating a 12-h tidal period. The drained sea water was re-circulated to the top of the column by peristaltic pump. Viton tubing (0.32 cm o.d.) was used for all applications that involved contact with effluent water. The columns were operated over a 21 day period at room temperature ( $25 \pm 3^{\circ}\text{C}$ ).

Sand was sampled by sterile metal tubing core from each glass columns at the time points indicated in Figure 4 up to 21 days. For extraction of PAH, a recovery standard of 200  $\mu\text{g}$  phenanthrene-d10 to 10 g of sand sample was used and showed a recovery of 95%. The sand was extracted three times with a total of 10 mL n-hexane. Samples were stored at  $4^{\circ}\text{C}$  until analysis and analyzed within 2 days. PAHs and phenanthrene-d10 was quantified by gas chromatograph analysis using Agilent model 7890A, equipped with flame ionization detector. The GC column

temperature was 55–250°C, programmed at 3°C/min to 75°C hold for 3 min; 5°C min<sup>-1</sup> to 100°C; and 20°C min<sup>-1</sup> to 250°C hold for 60 min. Helium was used as a carrier gas, at a pressure 25 psi. For detector, the flow of hydrogen, air and nitrogen were 30, 400 and 25 mL min<sup>-1</sup>, respectively. Injector and detector temperatures were 250 and 300°C, respectively.

### BACTERIAL 16S RIBOSOMAL GENE TAG SEQUENCING

We amplified bacterial 16S rRNA gene V6 hypervariable regions in our samples according to protocols developed at the Josephine Bay Paul Center at the Marine Biological Laboratory, Woods Hole, MA (Eren et al., 2013; Morrison et al., 2013). For this project sequencing was carried out on 12 mesocosms samples: one each from four mesocosms at three time points: Day 0 after hydrocarbon conditioning (~6 h post-addition), Day 6 and 13. Two mesocosms contained sand from St. George and two contained sand from Orange beach. Once obtained, sequence reads were quality-filtered according to Eren et al. (2013). Additionally, three samples (two sites at St. George and one site at Orange beach) from August 2011, collected at the same location and time as the mesocosm source samples, were sequenced according to the procedures described above. Taxonomy was assigned using GAST (Huse et al., 2008) and the data was uploaded to the Visualization and Analysis of Microbial Population Structures website (VAMPS: <http://vamps.mbl.edu>). The amplification, sequencing, and processing of all 16S rRNA gene community sequence data derived directly from beach sand samples in 2010 is described in (Newton et al., 2013). All mesocosm sequence files described in this study are available at the National Center for Biotechnology Information (NCBI) Sequence Read Archive, Bioproject (PRJNA244096) and for the previously published beach samples (Newton et al., 2013) under Bioproject PRJNA208242. All analyses were performed on averages of the duplicate mesocosms at each time point.

### ACKNOWLEDGMENTS

Funding from Marquette University has supported this work. Partial financial support was provided by the Children's Environmental Health Sciences Core Center at the University of Wisconsin, Milwaukee National Institute of Environmental Health Sciences program, grant ES-004184 to Sandra L. McLellan and to Krassimira R. Hristova. The funders had no role in study design, data collection and analysis, decision to publish, or preparation of the manuscript. The authors would like to thank Dr. Mitch Sogin's group at the Marine Biological Laboratory for the sequencing with specific acknowledgement for Hilary Morrison and Joseph Vineis for the DNA sequence library preparation and data curation.

### AUTHOR CONTRIBUTIONS

Krassimira R. Hristova and Sandra L. McLellan conceived and designed the experiments. Yin Wei performed the experiments. Anthony D. Kappell, Ryan J. Newton, and Joy D. Van Nostrand analyzed the resulting data. Krassimira R. Hristova, Sandra L. McLellan, and Jizhong Zhou contributed materials, reagents, and tools for analysis. The manuscript was prepared by Anthony D. Kappell, Ryan J. Newton, and Krassimira R. Hristova.

### SUPPLEMENTARY MATERIAL

The Supplementary Material for this article can be found online at: <http://www.frontiersin.org/journal/10.3389/fmicb.2014.00205/abstract>

**Table S1 | 16S rRNA gene sequence taxonomical diversity, similarity, and evenness in mesocosms.**

**Figure S1 | Diagram illustrating the inclusive metabolic pathways (based on KEGG Pathway Database) representing the genes involved in PAH and hydrocarbon degradation.** The genes were determined by functional microarray analysis that showed greater abundance in the month of June at Orange beach (heavily oiled) compared to St. George beach (non-impacted) sands. The genes are listed in the same order as in Table 2.

### REFERENCES

- Allan, S. E., Smith, B. W., and Anderson, K. A. (2012). Impact of the deep-water horizon oil spill on bioavailable polycyclic aromatic hydrocarbons in Gulf of Mexico coastal waters. *Environ. Sci. Technol.* 46, 2033–2039. doi: 10.1021/es202942q
- Atlas, R. M., and Bartha, R. (1972). Degradation and mineralization of petroleum in sea water: limitation by nitrogen and phosphorous. *Biotechnol. Bioeng.* 14, 309–318. doi: 10.1002/bit.260140304
- Atlas, R. M., and Hazen, T. C. (2011). Oil biodegradation and bioremediation: a tale of the two worst spills in U.S. history. *Environ. Sci. Technol.* 45, 6709–6715. doi: 10.1021/es2013227
- Banning, E. C., Casciotti, K. L., and Kujawinski, E. B. (2010). Novel strains isolated from a coastal aquifer suggest a predatory role for flavobacteria. *FEMS Microbiol. Ecol.* 73, 254–270. doi: 10.1111/j.1574-6941.2010.00897.x
- Beazley, M. J., Martinez, R. J., Rajan, S., Powell, J., Piceno, Y. M., Tom, L. M., et al. (2012). Microbial community analysis of a coastal salt marsh affected by the Deepwater Horizon oil spill. *PLoS ONE* 7:e41305. doi: 10.1371/annotation/72b08ecf-1e78-4668-a094-c818def0e03f
- Berges, J. A., Franklin, D. J., and Harrison, P. J. (2001). Evolution of an artificial seawater medium: improvements in enriched seawater, artificial water over the last two decades. *J. Phycol.* 37, 1138–1145. doi: 10.1046/j.1529-8817.2001.01052.x
- Camilli, R., Reddy, C. M., Yoerger, D. R., Van Mooy, B. A., Jakuba, M. V., Kinsey, J. C., et al. (2010). Tracking hydrocarbon plume transport and biodegradation at Deepwater Horizon. *Science* 330, 201–204. doi: 10.1126/science.1119523
- Chakraborty, R., Borglin, S. E., Dubinsky, E. A., Andersen, G. L., and Hazen, T. C. (2012). Microbial Response to the MC-252 Oil and Corexit 9500 in the Gulf of Mexico. *Front. Microbiol.* 3:357. doi: 10.3389/fmicb.2012.00357
- Cook, K. L., and Sayler, G. S. (2003). Environmental application of array technology: promise, problems and practicalities. *Curr. Opin. Biotechnol.* 14, 311–318. doi: 10.1016/S0958-1669(03)00057-0
- Coulon, F., McKew, B. A., Osborn, A. M., McGinity, T. J., and Timmis, K. N. (2007). Effects of temperature and biostimulation on oil-degrading microbial communities in temperate estuarine waters. *Environ. Microbiol.* 9, 177–186. doi: 10.1111/j.1462-2920.2006.01126.x
- Diercks, A.-R., Highsmith, R. C., Asper, V. L., Joung, D., Zhou, Z., Guo, L., et al. (2010). Characterization of subsurface polycyclic aromatic hydrocarbons at the Deepwater Horizon site. *Geophys. Res. Lett.* 37, L20602. doi: 10.1029/2010GL045046
- Dubinsky, E. A., Conrad, M. E., Chakraborty, R., Bill, M., Borglin, S. E., Hollibaugh, J. T., et al. (2013). Succession of hydrocarbon-degrading bacteria in the aftermath of the Deepwater Horizon oil spill in the Gulf of Mexico. *Environ. Sci. Technol.* 47, 10860–10867. doi: 10.1021/es401676y
- Eren, A. M., Vineis, J. H., Morrison, H. G., and Sogin, M. L. (2013). A filtering method to generate high quality short reads using Illumina paired-end technology. *PLoS ONE* 8:e66643. doi: 10.1371/journal.pone.0066643
- Gallego, S., Vila, J., Tauler, M., Nieto, J., Breugelmans, P., Springael, D., et al. (2013). Community structure and PAH ring-hydroxylating dioxygenase genes of a marine pyrene-degrading microbial consortium. *Biodegradation* doi: 10.1007/s10532-013-9680-z. [Epub ahead of print].

- Haritash, A., and Kaushik, C. (2009). Biodegradation aspects of polycyclic aromatic hydrocarbons (PAHs): a review. *J. Hazard. Mater.* 169, 1–15. doi: 10.1016/j.hazmat.2009.03.137
- Hazen, T. C., Dubinsky, E. A., DeSantis, T. Z., Andersen, G. L., Piceno, Y. M., Singh, N., et al. (2010). Deep-sea oil plume enriches indigenous oil-degrading bacteria. *Science* 330, 204–208. doi: 10.1126/science.1195979
- He, M., and Wang, W.-X. (2011). Factors affecting the bioaccessibility of methylmercury in several marine fish species. *J. Agric. Food Chem.* 59, 7155–7162. doi: 10.1021/jf201424g
- He, Z., Deng, Y., Van Nostrand, J. D., Tu, Q., Xu, M., Hemme, C. L., et al. (2010). GeoChip 3.0 as a high-throughput tool for analyzing microbial community composition, structure and functional activity. *ISME J.* 4, 1167–1179. doi: 10.1038/ismej.2010.46
- Horel, A., Mortazavi, B., and Sobecky, P. A. (2012). Responses of microbial community from northern Gulf of Mexico sandy sediments following exposure to deepwater horizon crude oil. *Environ. Toxicol. Chem.* 31, 1004–1011. doi: 10.1002/etc.1770
- Huettel, M., Berg, P., and Kostka, J. E. (2014). Benthic exchange and biogeochemical cycling in permeable sediments. *Ann. Rev. Mar. Sci.* 6, 23–51. doi: 10.1146/annurev-marine-051413-012706
- Huettel, M., and Rusch, A. (2000). Transport and degradation of phytoplankton in permeable sediment. *Limnol. Oceanogr.* 45, 534–549. doi: 10.4319/lo.2000.45.3.0534
- Hunter, E. M., Mills, H. J., and Kostka, J. E. (2006). Microbial community diversity associated with carbon and nitrogen cycling in permeable shelf sediments. *Appl. Environ. Microbiol.* 72, 5689–5701. doi: 10.1128/AEM.03007-05
- Huse, S. M., Dethlefsen, L., Huber, J. A., Welch, D. M., Relman, D. A., and Sogin, M. L. (2008). Exploring microbial diversity and taxonomy using SSU rRNA hypervariable tag sequencing. *PLoS Genet.* 4:e1000255. doi: 10.1371/journal.pgen.1000255
- Jordan, E. M., Thompson, F. L., Zhang, X.-H., Li, Y., Vancanneyt, M., Kroppenstedt, R. M., et al. (2007). *Sneathiella chinensis* gen. nov., sp. nov., a novel marine alphaproteobacterium isolated from coastal sediment in Qingdao, China. *Int. J. Syst. Evol. Microbiol.* 57, 114–121. doi: 10.1099/ij.s.0.64478-0
- Joung, D., and Shiller, A. M. (2013). Trace element distributions in the water column near the Deepwater Horizon well blowout. *Environ. Sci. Technol.* 47, 2161–2168. doi: 10.1021/es303167p
- Juhasz, A. L., and Naidu, R. (2000). Bioremediation of high molecular weight polycyclic aromatic hydrocarbons: a review of the microbial degradation of benzo[a]pyrene. *Int. Biodeterior. Biodegradation* 45, 57–88. doi: 10.1016/S0964-8305(00)00052-4
- Jurelevicius, D., Alvarez, V. M., Marques, J. M., de Sousa Lima, L. R. Dias Fde, A., and Seldin, L. (2013). Bacterial community response to petroleum hydrocarbon amendments in freshwater, marine, and hypersaline water-containing microcosms. *Appl. Environ. Microbiol.* 79, 5927–5935. doi: 10.1128/AEM.02251-13
- Kanehisa, M., and Goto, S. (2000). KEGG: kyoto encyclopedia of genes and genomes. *Nucleic Acids Res.* 28, 27–30. doi: 10.1093/nar/28.1.27
- Karnachuk, O. V., Pimenov, N. V., Iusupov, S. K., Frank Iu, A., Puhakka, J. A., and Ivanov, M. V. (2006). [Distribution, diversity, and activity of sulfate-reducing bacteria in the water column in Gek-Gel Lake, Azerbaijan]. *Mikrobiologija* 75, 101–109. doi: 10.1134/S002621706010152
- Kasai, Y., Kishira, H., and Harayama, S. (2002). Bacteria belonging to the genus *Cycloclasticus* play a primary role in the degradation of aromatic hydrocarbons released in a marine environment. *Appl. Environ. Microbiol.* 68, 5625–5633. doi: 10.1128/AEM.68.11.5625-5633.2002
- Kester, D. R., Duedall, I. W., Connors, D. N., and Pytkowicz, R. M. (1967). Preparation of artificial seawater. *Limnol. Oceanogr.* 12, 176–178. doi: 10.4319/lo.1967.12.1.0176
- Kimes, N. E., Callaghan, A. V., Aktas, D. F., Smith, W. L., Sunner, J., Golding, B., et al. (2013). Metagenomic analysis and metabolite profiling of deep-sea sediments from the Gulf of Mexico following the Deepwater Horizon oil spill. *Front. Microbiol.* 4:50. doi: 10.3389/fmicb.2013.00050
- Kodama, Y., Stiknowati, L. I., Ueki, A., Ueki, K., and Watanabe, K. (2008). *Thalassospira tepidiphila* sp. nov., a polycyclic aromatic hydrocarbon-degrading bacterium isolated from seawater. *Int. J. Syst. Evol. Microbiol.* 58, 711–715. doi: 10.1099/ij.s.0.65476-0
- Koster, M., Dahlke, S., and Meyer-Reil, L. A. (2005). Microbial colonization and activity in relation to organic carbon in sediments of hypertrophic coastal waters (Nordrheinische Bodden, Southern Baltic Sea). *Aquat. Microb. Ecol.* 39, 69–83. doi: 10.3354/ame039069
- Kostka, J. E., Prakash, O., Overholt, W. A., Green, S. J., Freyer, G., Canion, A., et al. (2011). Hydrocarbon-degrading bacteria and the bacterial community response in gulf of Mexico beach sands impacted by the deepwater horizon oil spill. *Appl. Environ. Microbiol.* 77, 7962–7974. doi: 10.1128/AEM.05402-11
- Leahy, J. G., and Colwell, R. R. (1990). Microbial degradation of hydrocarbons in the environment. *Microbiol. Rev.* 54, 305–315.
- Lee, J., Lee, T., Löffler, F., and Park, J. (2011). Characterization of microbial community structure and population dynamics of tetrachloroethene-dechlorinating tidal mudflat communities. *Biodegradation* 22, 687–698. doi: 10.1007/s10532-010-9429-x
- Lehr, B., Sky, B., and Possolo, A. (2010). *Oil Budget Calculator Deepwater Horizon*. Washington, DC: National Institute of Standards and Technology, National Oceanic and Atmospheric Administration.
- Liu, J., Stemmler, A. J., Fatima, J., and Mitra, B. (2005). Metal-binding characteristics of the amino-terminal domain of ZntA?: binding of lead is different compared to cadmium and zinc. *Biochemistry* 44, 5159–5167. doi: 10.1021/bi0476275
- Liu, Z., and Liu, J. (2013). Evaluating bacterial community structures in oil collected from the sea surface and sediment in the northern Gulf of Mexico after the Deepwater Horizon oil spill. *Microbiologyopen* 2, 492–504. doi: 10.1002/mbo3.89
- Liu, Z., Liu, J., Zhu, Q., and Wu, W. (2012). The weathering of oil after the Deepwater Horizon oil spill: insights from the chemical composition of the oil from the sea surface, salt marshes and sediments. *Environ. Res. Lett.* 7, 035302. doi: 10.1088/1748-9326/7/3/035302
- Lu, Z., Deng, Y., Van Nostrand, J. D., He, Z., Voordeckers, J., Zhou, A., et al. (2012). Microbial gene functions enriched in the Deepwater Horizon deep-sea oil plume. *ISME J.* 6, 451–460. doi: 10.1038/ismej.2011.91
- Mason, O. U., Hazen, T. C., Borglin, S., Chain, P. S. G., Dubinsky, E. A., Fortney, J. L., et al. (2012). Metagenome, metatranscriptome and single-cell sequencing reveal microbial response to Deepwater Horizon oil spill. *ISME J.* 6, 1715–1727. doi: 10.1038/ismej.2012.59
- Mills, H. J., Hunter, E., Humphrys, M., Kerkhof, L., McGuinness, L., Huettel, M., et al. (2008). Characterization of nitrifying, denitrifying, and overall bacterial communities in permeable marine sediments of the northeastern Gulf of Mexico. *Appl. Environ. Microbiol.* 74, 4440–4453. doi: 10.1128/AEM.02692-07
- Morrison, H. G., Grim, S. L., Vineis, J. H., and Sogin, M. L. (2013). *16S Amplicon Fusion Primers and Protocol For Illumina Platform Sequencing*. Available online at: [http://figshare.com/articles/16S\\_amplicon\\_fusion\\_primers\\_and\\_protocol\\_for\\_Illumina\\_platform\\_sequencing/833944](http://figshare.com/articles/16S_amplicon_fusion_primers_and_protocol_for_Illumina_platform_sequencing/833944)
- Newton, R. J., Huse, S. M., Morrison, H. G., Peake, C. S., Sogin, M. L., and McLellan, S. L. (2013). Shifts in the microbial community composition of gulf coast beaches following beach oiling. *PLoS ONE* 8:e74265. doi: 10.1371/journal.pone.0074265
- Ravot, G., Magot, M., Fardeau, M.-L., Patel, B. K. C., Thomas, P., Garcia, J.-L., et al. (1999). *Fusibacter paucivorans* gen. nov., sp. nov., an anaerobic, thiosulfate-reducing bacterium from an oil-producing well. *Int. J. Syst. Bacteriol.* 49, 1141–1147. doi: 10.1099/00207713-49-3-1141
- Reddy, C. M., Arey, J. S., Seewald, J. S., Sylva, S. P., Lemkau, K. L., Nelson, R. K., et al. (2012). Composition and fate of gas and oil released to the water column during the Deepwater Horizon oil spill. *Proc. Natl. Acad. Sci. U.S.A.* 109, 20229–20234. doi: 10.1073/pnas.1101242108
- Redmond, M. C., and Valentine, D. L. (2012). Natural gas and temperature structured a microbial community response to the Deepwater Horizon oil spill. *Proc. Natl. Acad. Sci. U.S.A.* 109, 20292–20297. doi: 10.1073/pnas.1108756108
- Rusch, A., Huettel, M., Reimers, C. E., Taghon, G. L., and Fuller, C. M. (2003). Activity and distribution of bacterial populations in Middle Atlantic Bight shelf sands. *FEEMS Microbiol. Ecol.* 44, 89–100. doi: 10.1111/j.1574-6941.2003.tb01093.x
- Sikkema, J., de Bont, J. A., and Poolman, B. (1994). Interactions of cyclic hydrocarbons with biological membranes. *J. Biol. Chem.* 269, 8022–8028.
- Sikkema, J., de Bont, J. A., and Poolman, B. (1995). Mechanisms of membrane toxicity of hydrocarbons. *Microbiol. Rev.* 59, 201–222.
- Stringfellow, W. T., and Aitken, M. D. (1995). Competitive metabolism of naphthalene, methylnaphthalenes, and fluorene by phenanthrene-degrading pseudomonads. *Appl. Environ. Microbiol.* 61, 357–362.

- Subashchandrabose, S. R., Ramakrishnan, B., Megharaj, M., Venkateswarlu, K., and Naidu, R. (2013). Mixotrophic cyanobacteria and microalgae as distinctive biological agents for organic pollutant degradation. *Environ. Int.* 51, 59–72. doi: 10.1016/j.envint.2012.10.007
- Toccalino, P. L., Johnson, R. L., and Boone, D. R. (1993). Nitrogen limitation and nitrogen fixation during alkane biodegradation in a sandy soil. *Appl. Environ. Microbiol.* 59, 2977–2983.
- Trzesicka-Mlynarz, D., and Ward, O. (1995). Degradation of polycyclic aromatic hydrocarbons (PAHs) by a mixed culture and its component pure cultures, obtained from PAH-contaminated soil. *Can. J. Microbiol.* 41, 470–476. doi: 10.1139/m95-063
- Urdiaín, M., López-López, A., Gonzalo, C., Busse, H.-J., Langer, S., Kämpfer, P., et al. (2008). Reclassification of *Rhodobium marinum* and *Rhodobium pfennigii* as *Afifella marina* gen. nov. comb. nov. and *Afifella pfennigii* comb. nov., a new genus of photoheterotrophic Alphaproteobacteria and emended descriptions of *Rhodobium*, *Rhodobium orientis* and *Rhodobium gokarnense*. *Syst. Appl. Microbiol.* 31, 339–351. doi: 10.1016/j.syapm.2008.07.002
- USEPA. (2004). *Report to Congress: Impacts and Control of CSOs and SSOs*. Washington, DC: Office of Water.
- Valentine, D. L., Mezic, I., Macesic, S., Crnjacic-Zic, N., Ivic, S., Hogan, P. J., et al. (2012). Dynamic autoinoculation and the microbial ecology of a deep water hydrocarbon eruption. *Proc. Natl. Acad. Sci. U.S.A.* 109, 20286–20291. doi: 10.1073/pnas.1108820109
- Van Nostrand, J. D., Wu, W.-M., Wu, L., Deng, Y., Carley, J., Carroll, S., et al. (2009). GeoChip-based analysis of functional microbial communities during the reoxidation of a bioreduced uranium-contaminated aquifer. *Environ. Microbiol.* 11, 2611–2626. doi: 10.1111/j.1462-2920.2009.01986.x
- Vila, J., Nieto, J. M., Mertens, J., Springael, D., and Grifoll, M. (2010). Microbial community structure of a heavy fuel oil-degrading marine consortium: linking microbial dynamics with polycyclic aromatic hydrocarbon utilization. *FEMS Microbiol. Ecol.* 73, 349–362. doi: 10.1111/j.1574-6941.2010.00902.x
- Wang, B., Lai, Q., Cui, Z., Tan, T., and Shao, Z. (2008). A pyrene-degrading consortium from deep-sea sediment of the West Pacific and its key member Cycloclasticus sp. P1. *Environ. Microbiol.* 10, 1948–1963. doi: 10.1111/j.1462-2920.2008.01611.x
- Wu, L., Liu, X., Schadt, C. W., and Zhou, J. (2006). Microarray-based analysis of subnanogram quantities of microbial community DNAs by using whole-community genome amplification. *Appl. Environ. Microbiol.* 72, 4931–4941. doi: 10.1128/AEM.02738-05
- Yakimov, M. M., Denaro, R., Genovese, M., Cappello, S., D'Auria, G., Chernikova, T. N., et al. (2005). Natural microbial diversity in superficial sediments of Milazzo Harbor (Sicily) and community successions during microcosm enrichment with various hydrocarbons. *Environ. Microbiol.* 7, 1426–1441. doi: 10.1111/j.1462-5822.2005.00829.x
- Zhanfei, L., Jiqing, L., Qingzhi, Z., and Wei, W. (2012). The weathering of oil after the Deepwater Horizon oil spill: insights from the chemical composition of the oil from the sea surface, salt marshes and sediments. *Environ. Res. Lett.* 7:035302. doi: 10.1088/1748-9326/7/3/035302
- Zhao, Y., Chen, M., Bai, J., Li, X., Zulfiqar, F., and Wang, Q. (2014). Response of microbial community to petroleum stress and phosphate dosage in sediments of Jiaozhou Bay, China. *J. Ocean Univ. Chin.* 13, 249–256. doi: 10.1007/s11802-014-2196-2
- Zheng, B., Wang, L., and Liu, L. (2014). Bacterial community structure and its regulating factors in the intertidal sediment along the Liaodong Bay of Bohai Sea, China. *Microbiological Res.* doi: 10.1016/j.micres.2013.09.019. [Epub ahead of print].
- Zhou, J., Bruns, M. A., and Tiedje, J. M. (1996). DNA recovery from soils of diverse composition. *Appl. Environ. Microbiol.* 62, 316–322.
- Zhou, J., and Thompson, D. K. (2002). Challenges in applying microarrays to environmental studies. *Curr. Opin. Biotechnol.* 13, 204–207. doi: 10.1016/S0958-1669(02)00319-1
- Conflict of Interest Statement:** The authors declare that the research was conducted in the absence of any commercial or financial relationships that could be construed as a potential conflict of interest.
- Received:** 10 December 2013; **accepted:** 18 April 2014; **published online:** 09 May 2014. **Citation:** Kappell AD, Wei Y, Newton RJ, Van Nostrand JD, Zhou J, McLellan SL and Hristova KR (2014) The polycyclic aromatic hydrocarbon degradation potential of Gulf of Mexico native coastal microbial communities after the Deepwater Horizon oil spill. *Front. Microbiol.* 5:205. doi: 10.3389/fmicb.2014.00205
- This article was submitted to Aquatic Microbiology, a section of the journal *Frontiers in Microbiology*.
- Copyright © 2014 Kappell, Wei, Newton, Van Nostrand, Zhou, McLellan and Hristova. This is an open-access article distributed under the terms of the Creative Commons Attribution License (CC BY). The use, distribution or reproduction in other forums is permitted, provided the original author(s) or licensor are credited and that the original publication in this journal is cited, in accordance with accepted academic practice. No use, distribution or reproduction is permitted which does not comply with these terms.



# Natural oil slicks fuel surface water microbial activities in the northern Gulf of Mexico

Kai Zier vogel<sup>1\*</sup>, Nigel D'souza<sup>2</sup>, Julia Sweet<sup>3</sup>, Beizhan Yan<sup>4</sup> and Uta Passow<sup>3</sup>

<sup>1</sup> Department of Marine Sciences, University of North Carolina Chapel Hill, Chapel Hill, NC, USA

<sup>2</sup> Lamont-Doherty Earth Observatory, Biology and Paleo Environment, Columbia University, Palisades, NY, USA

<sup>3</sup> Marine Science Institute, University of California Santa Barbara, Santa Barbara, CA, USA

<sup>4</sup> Lamont-Doherty Earth Observatory, Geochemistry, Columbia University, Palisades, NY, USA

## Edited by:

Joel E. Kostka, Georgia Institute of Technology, USA

## Reviewed by:

Gary M. King, Louisiana State University, USA

Ashvini Chauhan, Florida Agricultural and Mechanical University, USA

## \*Correspondence:

Kai Zier vogel, Department of Marine Sciences, University of North Carolina Chapel Hill, 4202N Venable and Murray Halls, CB#3300, Chapel Hill, NC 27599-3300, USA  
e-mail: ziervoge@email.unc.edu

We conducted a series of roller tank incubations with surface seawater from the Green Canyon oil reservoir, northern Gulf of Mexico, amended with either a natural oil slick (GCS-oil) or pristine oil. The goal was to test whether bacterial activities of natural surface water communities facilitate the formation of oil-rich marine snow (oil snow). Although oil snow did not form during any of our experiments, we found specific bacterial metabolic responses to the addition of GCS-oil that profoundly affected carbon cycling within our 4-days incubations. Peptidase and  $\beta$ -glucosidase activities indicative of bacterial enzymatic hydrolysis of peptides and carbohydrates, respectively, were suppressed upon the addition of GCS-oil relative to the non-oil treatment, suggesting that ascending oil and gas initially inhibits bacterial metabolism in surface water. Biodegradation of physically dispersed GCS-oil components, indicated by the degradation of lower molecular weight n-alkanes as well as the rapid transformation of particulate oil-carbon ( $C:N > 40$ ) into the DOC pool, led to the production of carbohydrate- and peptide-rich degradation byproducts and bacterial metabolites such as transparent exopolymer particles (TEP). TEP formation was highest at day 4 in the presence of GCS-oil; in contrast, TEP levels in the non-oil treatment already peaked at day 2. Cell-specific enzymatic activities closely followed TEP concentrations in the presence and absence of GCS-oil. These results demonstrate that the formation of oil slicks and activities of oil-degrading bacteria result in a temporal offset of microbial cycling of organic matter, affecting food web interactions and carbon cycling in surface waters over cold seeps.

**Keywords:** oil slick, Gulf of Mexico, GC600, enzyme activities, carbon cycle, TEP, oil snow

## INTRODUCTION

The northern Gulf of Mexico contains more than 200 hydrocarbon seeps over seafloor oil reservoirs, releasing up to  $1.1 \times 10^8 \text{ L year}^{-1}$  of oil into the water column. The majority of these seeps are located over the Green Canyon oil reservoir  $\sim 200$  miles off the Louisiana coast (MacDonald et al., 2002). Ascending hydrocarbon bubbles in that area rapidly dissolve into the bottom water contributing to the isotopically “old” deep water dissolved organic carbon pool (Wang et al., 2001). Depending on bubble size and upwelling currents, oil bubbles can also reach the surface where they form oil microlayers (hereafter referred to as oil slicks) that can grow up to 10 km in length (MacDonald et al., 2002). Evaporation of the volatile components of the surface oil may be rapid (Solomon et al., 2009). Oil slick compounds that are not subject to immediate evaporation likely undergo further weathering processes at the sea surface (MacDonald et al., 2002). Despite the importance of such processes for carbon fluxes and food web interactions, the fate of oil slick residues is not well understood.

Biological oil weathering facilitated by specialized heterotrophic microbial communities plays a key role in the fate of oil-carbon in the ocean (Head et al., 2006). Oil-degrading bacteria often produce large amounts of exopolymeric substances (EPS) to emulsify crude oil (Gutierrez et al., 2013). Enhanced

production of bacterial EPS in oil-contaminated surface waters during the Deepwater Horizon (DwH) oil spill in the northern Gulf of Mexico in 2010 led to the formation of mucus webs that in turn accelerated the formation of oil-rich marine snow (Passow et al., 2012). After losing their buoyancy, sinking oil snow resulted in the large sedimentation event of surface oil, now known as the “Dirty Blizzard,” representing a major pathway of DwH surface oil to the seafloor (Hollander et al., 2013; Passow, 2013, 2014). In addition to acting as the glue for oil snow, bacterial EPS may also stimulate activities of heterotrophic bacterial communities not directly involved in primary oil degradation (McGenity et al., 2012). We found evidence for such a bacterial oil degradation cascade in roller tank experiments with oil-contaminated surface water from the DwH site (Zier vogel et al., 2012).

Following the procedure of Zier vogel et al. (2012), we conducted a series of roller tank experiments amending surface seawater with oil slick from the Green Canyon area. These experiments examined whether bacterial transformation of oil slick components triggers the formation of oil snow and subsequent sinking of oil-carbon at the investigated site. Given that ascending oil from the Green Canyon reservoir has been characterized as highly biodegraded (Wang et al., 2001; MacDonald et al., 2002), we conducted supplementary experiments with unaltered pristine

oil to acknowledge the role of biological and chemical weathering on the formation of oil snow. We monitored particle formation, dynamics of n-alkanes as well as the particulate and dissolved organic matter pool along with heterotrophic bacterial activities during onboard incubations lasting 4 days. We determined transparent exopolymeric particles (TEP) as a measure for particulate EPS, which often acts as the glue for marine snow (Passow, 2002). To monitor oil snow formation over an extended time period, we also conducted longer term roller tank experiments over 41 days in the home laboratory.

## MATERIALS AND METHODS

### OIL SLICK SAMPLING

An oil slick-seawater sample was taken at the sea surface over a hydrocarbon seep (GC600; 27° 21.79'N, 90° 34.65'W; water depth: 1200 m; **Figure 1**) in September 2012 during the RV Endeavor cruise EN515. A clean HDPE container was carefully lowered from the deck of the vessel into the slick to sample ~5 L of an oil slick-seawater mixture that was then filled into a clean cooler (volume: 25 L) on deck. This was repeated four times to sample a total of about 20 L of the oil slick-seawater mixture. Within minutes after sampling the oil formed a microlayer slick at the surface of the cooler water; ~15 L of the excess seawater underlying the oil slick were then released through the drain plug of the cooler. Aliquots of the remaining 5 L of the oil slick-seawater mixture (hereafter referred to as Green Canyon Slick oil, GCS-oil) were added to the roller tanks, and were used for chemical characterization of the GCS-oil (Characterization of GCS-oil).

### ROLLER TANK INCUBATIONS

#### *Green canyon Oil Experiments (GOE)*

A series of short term, onboard roller tank incubations were initiated shortly after sampling of the GSC-oil (**Table 1**). Acrylic roller tanks (total volume: 1.7 L) were filled with surface seawater that was sampled outside the oil slick at the GC600 site, using Niskin bottles (water depth: 5 m; temperature: 29.5°C; Chlorophyll *a* < 0.2 µg L<sup>-1</sup>). The GOE experiment consisted of four different live treatments, each in triplicate, and one set of killed control tanks containing UV radiated surface seawater. One set of the live treatments contained seawater only, another was supplemented with GCS-oil (1: 43 oil: seawater, v/v). A third and fourth treatment, with and without oil, respectively, additionally contained 10 mL of a particle slurry consisting of planktonic particles collected with an unfixed marine snow trap and *in situ* bottom water. The trap collecting the particle slurry was deployed at 80 m above the seafloor for a period of 6 months at a site ~140 nm to northeast of GC600 (OC26: 28° 44.20'N, 88° 23.23'W; water depth: 1500 m; **Figure 1**) and recovered 3 days before the start of the roller tank incubation. A qualitative microscopical examination of the particles revealed mainly diatom frustules, fecal pellets and clay minerals. The organic matter content of the particle slurry was low (organic matter to dry weight ratio: 2%). As intended, the addition of the particle slurry promoted coagulation and thus aggregate formation in the tanks (hereafter referred to as macro-aggregates).

The tanks were filled to the 1.1 L mark; we deliberately left a headspace that led to the formation of an oil slick at the seawater-headspace interface in the oil treatments. The tanks were incubated on a roller table in the dark at a rotation speed of 2.4 rpm and ambient temperature (~20–25°C) for 4 days. Tanks rotation introduced mildly turbulent water mixing, simulating conditions at the sea surface.

One tank per treatment was sampled prior to the start of the incubation (Day 0) as well as after 2 and 4 days, and analyzed for the parameters described below. Tanks were removed from the roller table and placed upright on the bench for sampling. Samples were carefully collected with a 10 mL glass pipette and filled into a clean glass beaker. Special care was taken to avoid transferring oil from the surface slick to the sample water. In the presence of macro-aggregates >1 mm, two separate subsamples were collected: (1) the water overlying all large particles that had settled to the bottom of the tank (surrounding seawater; SSW), and (2) a slurry of macro-aggregates and a known volume of SSW (aggregate slurry; Agg). All analytical parameters are expressed as a concentration or rate per total tank volume (i.e., 1.1 L), accounting for the smaller total volume of the aggregate slurry relative to the surrounding tank water and making direct comparisons and budgeting possible.

An additional roller tank experiment over 41 days was conducted after returning to the home laboratory to study oil snow formation for an extended time that exceeded the period of oil snow formation during the DWH oil spill (~1 month) (Passow et al., 2012). Two roller tanks were filled with either 800 mL of GC600 surface seawater amended with 80 mL of GCS-oil, or 800 mL surface seawater only. The tanks were incubated on a roller table at a rotation speed of 2.4 rpm at low light (<30 µmol m<sup>-2</sup> s<sup>-1</sup>; 12: 12 h light: dark cycle) and 14°C. Every 1–3 days, the tanks were inspected for macro-aggregates formation without interrupting the rolling motion of the tanks.

#### *Pristine Oil Experiments (POE)*

In addition to the GOE experiments with GCS-oil, we also conducted roller tank incubations with surface seawater and pristine oil onboard the RV Endeavor cruise EN510 in June 2012 as well as in the home laboratory (**Table 1**). The onboard roller tank incubations had surface seawater collected with Niskin bottles at GC600 (27° 21.78'N, 90° 33.88'W; water depth: 5 m; temperature: 28.7°C; Chlorophyll *a* < 0.2 µg L<sup>-1</sup>) either amended with Louisiana crude oil (LA-oil; WP681 from Fisher Scientific) at a ratio of 1: 1100 (v/v) or unamended. Autoclaved surface seawater with and without LA-oil served as killed controls. Incubation time of the onboard Pristine Oil Experiment (POE) was 3 days, and the tanks were incubated under the same conditions and analyzed at day 0 and day 3 for the same parameters as in GOE. Data for day 0 from the oil amended seawater tank is missing.

As for GOE, we conducted a 41-days POE experiment in the home laboratory with two roller tanks filled with 1000 mL of GC600 surface seawater amended with 1 mL of Macondo crude oil (provided by J Short, JWS Consulting LLC, LSU ID 2010158-12, MC-252 Source oil 5/20/10). The tanks were incubated on a roller table under the same conditions as described for the longer

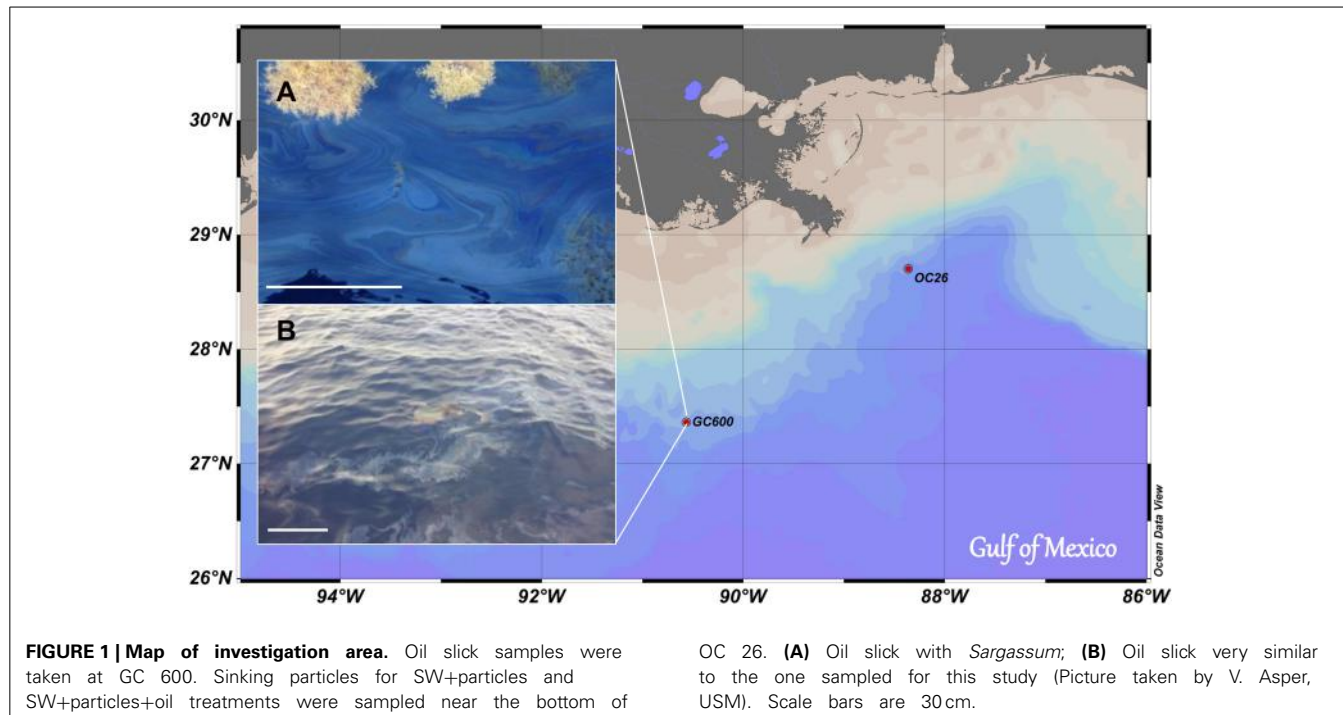


**Table 1 | Experimental set-up of the two onboard roller tank incubations.**

Experiment ID (date; days of incubation)	Treatment ID	Treatment description	Treatment ratios	No of tanks
Green Canyon oil experiment: GOE (September 2012; 4 days)	SW	Visually uncontaminated surface seawater	unaltered	3
	SW+oil	SW amended with Green canyon oil slick (GCS-oil)	25 mL oil slick: 1075 mL SW	3
	SW+particles	SW amended with particles from marine snow camera trap	10 mL particle slurry: 1090 mL SW	3
	SW+particles+oil	SW amended with particles from marine snow camera trap and GCS-oil	25 mL oil slick: 10 mL particle slurry: 1065 mL SW	3
	SW control	UV radiated SW	Unaltered	3
Pristine oil experiment: POE (June 2012; 3 days)	SW	Visually uncontaminated surface seawater	Unaltered	2
	SW+oil	SW amended with Louisiana crude oil (LA-oil)	1 mL oil: 1099 mL SW	1
	SW control	Autoclaved SW	Unaltered	2
	SW control+oil	Autoclaved SW with LA-oil	1 mL oil: 1099 mL control SW	2

term GOE. Every 1–3 days, the tanks were inspected for macro-aggregate formation without interrupting the rolling motion of the tanks.

#### ANALYTICAL METHODS

##### Characterization of GCS-oil

**Hydrocarbon extraction and fractionation.** Oil slick water from the cooler (GCS-oil) as well as roller tank water from the two GCS-oil treatments at day 4 (SW+oil; SW+particles+oil) were

filled into separate 2.5-L amber glass bottles, fixed with Sodium Azide (0.02% final conc.), and stored in the dark at 4°C until extraction. Hydrocarbon extraction was conducted via passage through an Empore C18 solid phase extraction disk installed in a vacuum apparatus after the samples were acidified to a pH of ~2.7 for optimal hydrocarbon adsorption to the pre-conditioned disk. Hydrocarbons were eluted from the disks with a mixture of hexane and acetone at a ratio of 7: 3 (v/v), then passed through an anhydrous Na<sub>2</sub>SO<sub>4</sub> column and solvent-exchanged to hexane

under a steady stream of nitrogen. Samples were centrifuged for 10 min at 10,000 rpm in 2 mL Teflon centrifuge tubes, and the hexane-insoluble fraction was discarded. To purify and separate the aliphatic and aromatic fractions, we performed a fractionation with two silica gel columns; one column was topped with anhydrous  $\text{Na}_2\text{SO}_4$  for the removal of residual water, the other had copper powder for the removal of elemental sulfur. Two elutions were performed on each column, with 15 mL of hexane followed by 15 mL of a 1: 1 mixture of hexane and dichloromethane (v/v). Following column fractionation, the extracts were concentrated under nitrogen and stored at 4°C until further analysis.

**GC × GC analysis.** Fractionated hydrocarbon extracts were analyzed using a Leco comprehensive two-dimensional gas chromatograph—time-of-flight-mass spectrometer (GC × GC-TOF). The samples were injected in splitless mode with the inlet temperature at 300°C. The first-dimension column oven in the GC × GC was held at 60°C for 1 min, then gradually increased at a rate of 1.5–315°C, where it was held for 15 min. The thermal modulator temperature offset was set to 55°C above the first-dimension column (Restek Rx-1MS column, 20 m length, 0.18 mm I.D., 0.18  $\mu\text{m}$  film thickness), and the temperature offset of the secondary column (50% phenyl polysilphenylene-siloxane column, SGE BPX50, 1 m length, 0.1 mm I.D., 0.1  $\mu\text{m}$  film thickness) was set to 30°C above the first-dimension column oven. Helium was used as the carrier gas at a constant flow rate of 1.5 mL  $\text{min}^{-1}$ . The thermal modulator hot jet pulse time was 0.6 s with a 6.9 s cool time between stages. Dried air was used to supply the thermal modulator hot and cold jet gas. The detector signal was sampled at 200 spectra second $^{-1}$ . The transfer line temperature was 310°C, the source temperature was 200°C, and the acquisition voltage was 1677 V. Analytes were quantified for n-alkanes using commercially available standards from Restek Corp. (Bellefonte, PA) and Sigma-Aldrich (St. Louis, MO).

**Oil fluorescence.** During the onboard GOE, we also monitored relative changes in oil fluorescence. Two milliliter of tank water were filled into disposable methacrylate cuvettes and the raw fluorescence signal was measured using the crude oil module (#7200-063; excitation: 365, emission: 410–600) of the Trilogy Laboratory Fluorometer (Turner). The GCS-oil fluorescence signal, expressed as relative fluorescence units (RFU), was corrected with the signal in the unamended seawater treatment that was always considerably lower compared to the oil containing treatments.

#### **Transparent Exopolymer Particles (TEP)**

TEP representing a particulate form of EPS were measured colorimetrically in triplicate samples per tank by filtration of 50–100 mL of tank water onto 0.4  $\mu\text{m}$  polycarbonate filters and subsequent staining with Alcian Blue (Passow and Alldredge, 1995). The dye solution, which complexes carboxyl and half-ester sulfate reactive groups of acidic polysaccharides was calibrated using Gum Xanthan.

#### **Dissolved Organic Carbon (DOC)**

DOC was analyzed in pre-filtered (0.2- $\mu\text{m}$  surfactant free cellulose acetate syringe filters) and acidified (50% phosphoric

acid v/v) samples by high temperature catalytic oxidation using a Shimadzu TOC-5000. DOC was not measured in aggregate slurries. Duplicate samples per tank were injected; instrument settings yielded at least three repeated measurements of each sample.

#### **Particulate Organic Carbon and Nitrogen (POC, PON)**

For POC and PON analysis, duplicate tank water samples of 50–250 mL were vacuum filtered onto pre-combusted GF/F filters. The filters were acidified with 12 M HCl for 12 h to remove inorganic carbon prior to flash combustion to  $\text{CO}_2$  and  $\text{N}_2$  on a Carlo-Erba 1500 Elemental Analyzer, using acetanilide as a standard.

#### **Bacterial abundance**

Ten milliliter of tank water was fixed with formalin immediately after sampling (2% final conc.) and stored for 8 months in the dark at 4°C before the preparation of microscope slides. Prior to slide preparation, samples were pretreated to break up bacterial aggregates and detach bacteria from particles. We used Tween-80 (0.5% final conc.), EDTA (50 mM final conc.), and 10× PBS pH 7.4 (5.26% final conc.), followed by vortex mixing for 10 min. Samples were then sonicated for 3 min in a water bath (adapted from Suter, 2011, and Crump et al., 1998), and stained according to Lunau et al. (2005) as described below. Samples with no macro-aggregates were also subjected to this treatment, and cells numbers counted in selected samples before and after the treatment revealed an increase of 38–152%. Samples used for enumeration of bacterial micro-aggregates were not subject to any physical or chemical treatments prior to staining.

A known volume of each pretreated sample was drawn through a 25 mm diameter 0.2  $\mu\text{m}$  pore, black polycarbonate filter (Millipore, type GTPB) using low vacuum. The filters were transferred to clean microscope slides. Ten microliter of a freshly prepared mounting medium containing 50% glycerol in 1× PBS at pH 7.4, ascorbic acid (1% final conc. v/v), and SYBR green I stain (0.45% final conc. v/v) was placed in the middle of a cover slip (25 mm × 25 mm) and inverted onto the filter. The slide was then placed in the dark at 4°C, until the weight of the cover slip dispensed the stain evenly across the filter. Bacterial cells and micro-aggregates were counted with a Nikon Labophot-2 epifluorescence microscope with blue light excitation at 1000× and 200× magnification respectively. For bacterial cell counts, a minimum of 200 cells were enumerated within a grid of fixed dimensions across each filter. Micro-aggregates were categorized into three distinct size classes (5–40, 40–80, >80  $\mu\text{m}$ ) using an ocular grid. Unless the abundance of micro-aggregates was low, a minimum of 100 aggregates were enumerated within a grid of fixed dimensions across each filter. Bacteria cell counts in tank water samples from the onboard POE were counted by flow cytometry (Accuri C6) using SYBR-GREEN I as a stain.

#### **Bacterial enzymatic activities**

Potential hydrolytic activities of carbohydrate- and peptide-hydrolyzing enzymes were measured using 4-MUF- $\beta$ -D-glucopyranoside and L-leucine-MCA hydrochloride, respectively, as fluorogenic substrate analogs according to

Hoppe (1983). Three mL of tank water were added to triplicate disposable methacrylate cuvettes containing fluorogenic substrate analogs at saturation levels (300  $\mu\text{M}$  for L-leucine-MCA hydrochloride; 333  $\mu\text{M}$  for 4-MUF- $\beta$ -D-glucopyranoside). Cuvettes were incubated under the same conditions as the roller tanks. Fluorescence was measured immediately after sample addition and at two additional time points over the course of 24 h under buffered conditions (20 nM borate buffer; pH 9.2) using a Turner Biosystems TBS-380 fluorometer (excitation/emission channels set to "UV"; 365 nm excitation, 440–470 nm emission). Fluorescence changes were calibrated using standard solutions of 4-methylumbellifereone and 4-methylcoumarin in tank water, and used to calculate hydrolysis rates expressed as cell-specific rates. All of the killed control tanks in GOE and POE showed only minor changes in fluorescence over time possibly due to abiotic substrate hydrolysis. Fluorescence changes in the killed control treatments were used to correct enzymatic hydrolysis rates in the respective live treatments.

## STATISTICAL ANALYSIS

Results of analytical parameters are given as average values  $\pm$  standard deviation. Differences between two average values were analyzed using the Student's *t*-test; differences between three or more average values were assessed using an analysis of variance (One-Way ANOVA) with Tukey HSD *post-hoc* pairwise comparisons of means at the 5% significant level ( $p = 0.05$ ). All statistical analysis was performed in Excel® using the data analysis tool pack.

## RESULTS

### GCS-OIL DYNAMICS DURING ROLLER TANK INCUBATIONS

The C<sub>16</sub>–C<sub>34</sub> components in the initial GCS-oil sample ranged between 3 and 8% of the total n-alkane pool (Figure 2). At the end of both GCS-oil incubations (SW+oil and SW+particles+oil), levels of C<sub>16</sub>–C<sub>21</sub> components decreased by up to one order magnitude compared to the initial sample. All three samples were mostly depleted of <C<sub>15</sub> alkanes, probably due to dissolution during ascending of the oil from the seep.

The initial fluorescence signals in both GCS-oil treatments were on average at 23,072  $\pm$  2538 RFU, decreasing to 50% at day 2 in both treatments. Only 27% and 7% of the initial fluorescence signal were detected at day 4 resulting in a linear decrease in oil fluorescence over time in SW+oil ( $r^2 = 0.99$ ) and SW+particles+oil ( $r^2 = 0.97$ ), respectively.

### FORMATION OF MACRO-AGGREGATES

Macro-aggregate formation was only observed in the presence of the particle slurry during the onboard GOE. By day 4 a single aggregate per tank (diameter:  $\sim 2$  mm) had formed. The presence or absence of GCS-oil had no visible impact on the formation of macro-aggregates. No particles  $> 1$  mm formed in any of the treatments of the longer term GOE, but particles  $< 1$  mm appeared in the presence of GCS-oil at day 19. These particles remained unchanged until the end of the 41 days incubation. No particles of any size were visible in any of the POE experiments.

### TRANSPARENT EXOPOLYMER PARTICLES (TEP)

TEP concentrations in the onboard GOE seawater treatment (SW) doubled between days 0 and 2, followed by a decrease

to initial levels at day 4 [ $F_{(2, 6)} = 6.87, p < 0.05$ ; Table 2]. In contrast TEP remained low until day 2 in the presence of GCS-oil (SW+oil), and subsequently increased by a factor of 4 until the end of the incubation [ $F_{(2, 6)} = 11.5, p < 0.01$ ]. The addition of the particle slurry (SW+particles) led to almost 5 times higher initial TEP concentrations compared to initial SW levels (Student's *t*-test,  $p < 0.05$ ). The amount of TEP in macro-aggregates (Agg), in the presence or absence of GCS-oil, was similar to that in the SSW; at day 4 in the SW+particles treatment, the amount of TEP incorporated in the Agg fraction was lower than in SSW [ $F_{(4, 10)} = 6.7, p < 0.01$ ]. TEP in POE more than doubled during the time course of the non-oil (SW) incubation with similar levels in SW and SW+oil at day 3 [ $F_{(2, 5)} = 38.2, p < 0.001$ ].

### DISSOLVED AND PARTICULATE ORGANIC CARBON (DOC, POC)

DOC concentration in the onboard GOE seawater treatment (SW) increased between days 0 and 2 by a factor of 3, followed by a decrease to initial levels at the end of the incubation [ $F_{(2, 7)} = 1519.9, p < 0.001$ ; Table 2]. DOC in the presence of GCS-oil doubled until day 2, remaining at this high level until day 4 [ $F_{(2, 9)} = 23.6, p < 0.001$ ]. DOC in both particle slurry treatments gradually increased until day 4 [SW+particles:  $F_{(2, 11)} = 9.1, p < 0.005$ ; SW+particles+oil:  $F_{(2, 8)} = 5.9, p < 0.001$ ]. In POE, DOC decreased by a factor of 2 in SW until day 3, reaching similar levels in the presence and absence of LA-oil at day 3 [ $F_{(2, 19)} = 70.7, p < 0.001$ ].

Levels of POC in the GOE seawater tank (SW) more than doubled between days 0 and 2, remaining constant until the end of the incubation [ $F_{(2, 3)} = 117.1, p < 0.001$ ; Table 2]. The addition of GCS-oil led to a 7-fold higher initial POC concentration in SW+oil compared to SW at day 0 (Student's *t*-test,  $p < 0.05$ ). POC in SW+oil gradually decreased until day 4 [ $F_{(2, 3)} = 13.2, p < 0.05$ ]. The particle slurry treatment in the absence of GCS-oil (SW+particles) also had a higher initial POC concentration compared to SW (Student's *t*-test,  $p < 0.05$ ). At day 2, POC concentration in macro-aggregates (Agg) was a factor of 2 higher than in SSW; subsequently POC in SSW slightly increased leading to similar levels in Agg and SSW at the end of the incubation [ $F_{(4, 5)} = 23.1, p < 0.005$ ]. Highest initial POC levels of all four treatments were measured in SW+particles+oil [ $F_{(3, 4)} = 215.1, p < 0.001$ ]. Following macro-aggregate formation, POC in Agg and SSW remained at the same levels at days 2 and 4 [ $F_{(4, 5)} = 50.5, p < 0.001$ ]. POC concentrations in POE increased by factors of 1.5 in SW until day 3; SW+oil at day 3 had 2.5 higher levels of POC compared to the initial SW level (no statistical analysis due to lack of replicates at day 0).

During the GOE experiment, ratios of C: N in SW were statistically indistinguishable from one another, ranging between 6.2 and 8.9 (Table 2). The addition of GCS-oil led to an increase of the C: N ratios by a factor of 4 relative to the non-oil treatments. C: N ratio in SW+oil gradually dropped from 41 at day 0 to 12 at day 4 [ $F_{(2, 3)} = 162.5, p < 0.001$ ]. SW+particles+oil had initial C: N ratios of 34, decreasing until day 2 by a factor of 2.5, and remaining at the same levels in SSW and Agg until the end of the incubation [ $F_{(4, 5)} = 46.8, p < 0.001$ ]. In SW+particles, C: N ratios were low throughout the first 2 days of the incubation,

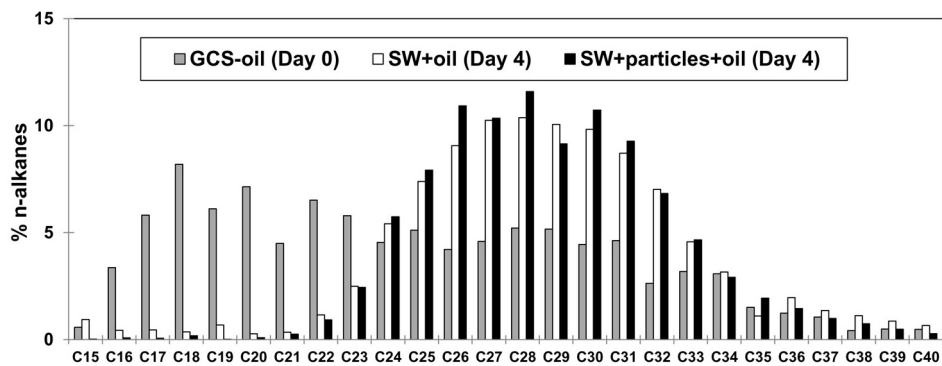


**FIGURE 2 | Chemical characterization of GCS-oil.** Relative distribution of n-alkanes before (Day 0) and after the roller tank incubations (Day 4). Note that all three samples were mostly depleted of <C<sub>15</sub> alkanes, probably due to dissolution during ascending of the oil from the seep.

**Table 2 | Dynamics of the organic carbon pool.**

Experiment		GOE				POE	
Day		0	2	4		0	3
Fraction		SSW	SSW	Agg	SSW	Agg	SSW
TEP	SW	328 ± 397; B	1181 ± 170; A	–	522 ± 274; B	–	478 ± 42; B
	SW+oil	180 ± 42; B	287 ± 151; B	–	1043 ± 385; A	–	n.d.
	SW+particles	1541 ± 21; A	1006 ± 112; B	982 ± 79; B	980 ± 150; B	417 ± 55; C	No exp.
	SW+particles+oil	944 ± 58; A	397 ± 23; B	679 ± 114; AB	387 ± 154; B	523 ± 275; B	No exp.
DOC	SW	1507 ± 7; C	4518 ± 36; A	–	1896 ± 109; B	–	3548 ± 716; A
	SW+oil	1148 ± 66; B	2039 ± 59; A	–	2630 ± 524; A	–	n.d.
	SW+particles	2203 ± 628; B	1818 ± 100; AB	–	3006 ± 109; A	–	No exp.
	SW+particles+oil	1433 ± 30; B	1906 ± 130; AB	–	2816 ± 29; A	–	No exp.
POC	SW	117 ± 6; B	247 ± 6; A	–	241 ± 11; A	–	121#
	SW+oil	867 ± 15; A	595 ± 116; AB	–	356 ± 58; B	–	n.d.
	SW+particles	310 ± 3; AB	172 ± 2; D	383 ± 53; A	227 ± 0.1; CD	297 ± 8; BC	No exp.
	SW+particles+oil	1032 ± 83; A	305 ± 111; B	401 ± 31; B	249 ± 7; B	287 ± 32; B	No exp.
C/N	SW	8.3 ± 0.6; n.s.	8.9 ± 0.9; n.s.	–	6.2 ± 0.4; n.s.	–	10.5#
	SW+oil	40.9 ± 2.5; A	16.2 ± 1.3; B	–	12.1 ± 1.7; B	–	n.d.
	SW+particles	7.7 ± 0.3; BC	6.6 ± 0.1; C	9.5 ± 0.1; B	9 ± 0.8; B	14.3 ± 0.8; A	No exp.
	SW+particles+oil	34.2 ± 3.3; A	13.7 ± 2.8; B	14.1 ± 0.4; B	13.2 ± 0.6; B	12.2 ± 0*; B	No exp.

TEP ( $\mu\text{g GXeq tank}^{-1}$ ), DOC ( $\mu\text{g tank}^{-1}$ ), POC ( $\mu\text{g tank}^{-1}$ ).

SSW, surrounding seawater; Agg, macro-aggregates.

Letters indicate the results of the post-hoc analysis following ANOVA ( $p < 0.05$ ); Concentrations with the same letters are statistically indistinguishable from one another.

n.d. means not determined, no exp. means no experiment.

#single measurement; \*number <0.1.

reaching highest ratios in Agg at day 4 [ $F_{(4, 5)} = 33.9, p < 0.001$ ]. In POE, ratios of C: N were 10.5 and 7.2 in SW at day 0 and day 3, respectively, and 10.6 in SW+oil at day 3.

#### BACTERIAL CELL NUMBERS AND MICRO-AGGREGATE FORMATION

Initial bacterial cell numbers in all four GOE treatments were in the same order of magnitude, ranging between  $2.5 \times 10^8$

$\text{tank}^{-1}$  (SW+particles+oil) and  $5.6 \times 10^8 \text{ tank}^{-1}$  (SW+particles). On day 2, cell numbers in SW and SW+oil were up to 3.5 times higher compared to day 0, thereafter remaining at that higher level in SW (Table 3). In contrast, bacterial numbers in SW+oil decreased to initial levels until day 4. Fewer cells were associated with macro-aggregates compared to SSW in the absence of GCS-oil (SW+particles). Bacterial numbers associated with Agg

**Table 3 | Bacterial abundance and cell-specific enzymatic activities.**

Experiment		GOE				POE	
Day		0	2	4		0	3
Fraction		SSW	SSW	Agg	SSW	Agg	SSW
Bact. cells	SW	4.0	14.1	–	11.7	–	6.4
	SW+oil	3.5	9.9	–	2.5	–	n.d.
	SW+particles	5.6	3.4	1.5	7.4	1.1	No exp.
	SW+particles+oil	2.5	1.8	1.4	1.2	3.9	No exp.
$\beta$ -glu	SW	52 ± 2; C	136 ± 10; A	–	74 ± 25; B	–	6 ± 0*; B
	SW+oil	11 ± 1; C	42 ± 2; B	–	138 ± 6; A	–	n.d.
	SW+particles	55 ± 1; D	165 ± 21; B	212 ± 0; A	45 ± 11; D	102 ± 6; C	No exp.
	SW+particles+oil	27 ± 2; C	113 ± 5; B	257 ± 7; A	96 ± 26; B	119 ± 17; B	No exp.
pep	SW	177 ± 5; B	788 ± 209; A	–	995 ± 34; A	–	26 ± 0.2; C
	SW+oil	102 ± 2; B	150 ± 15; B	–	1749 ± 73; A	–	n.d.
	SW+particles	147 ± 12; E	3051 ± 62; C	10093 ± 125; B	1374 ± 19; D	12872 ± 401; A	No exp.
	SW+particles+oil	173 ± 10; D	1149 ± 35; C	2112 ± 50; B	2465 ± 10; A	1140 ± 17; C	No exp.

Bacterial cells ( $\times 10^8$  tank $^{-1}$ ),  $\beta$ -glucosidase ( $\beta$ -glu, amol cell $^{-1}$  hr $^{-1}$ ), peptidase (pep, amol cell $^{-1}$  hr $^{-1}$ ).

n.d. means not determined, no exp. means no experiment.

\*number <0.1.

in SW+particles+oil treatments were similar (day 2) or higher (day 4) compared to those in the SSW. Bacteria cells in both POE treatments increased by up to one order of magnitude during the 3 days incubation.

Epifluorescence microscopy of samples not subject to physical or chemical dis-aggregation treatments revealed the formation of bacterial micro-aggregates in SW and SW+oil at day 2 (Figure 3). Bacterial micro-aggregates in SW increased in size between days 2 and 4 (Figure 4); in the oil amended tank (SW+oil), micro-aggregates remained smaller at days 2 and 4 compared to SW. In seawater samples amended with particles, we observed yellow fluorescing material that in the presence of GCS-oil appeared to be heavily colonized by bacteria on days 2 and 4 relative to SW+particles (Figures 3K,L).

## BACTERIAL ENZYMATIC ACTIVITIES

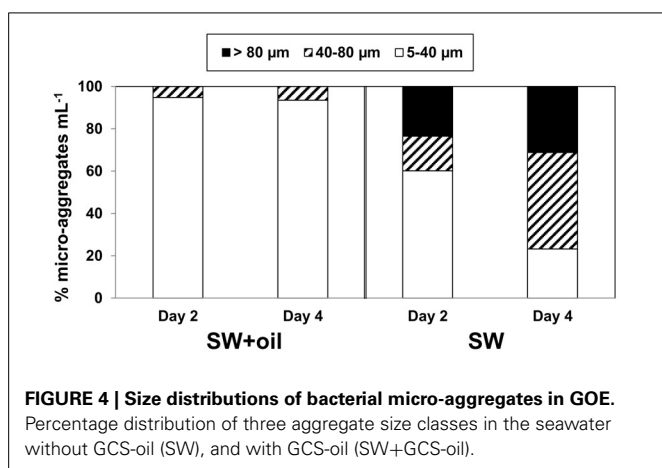
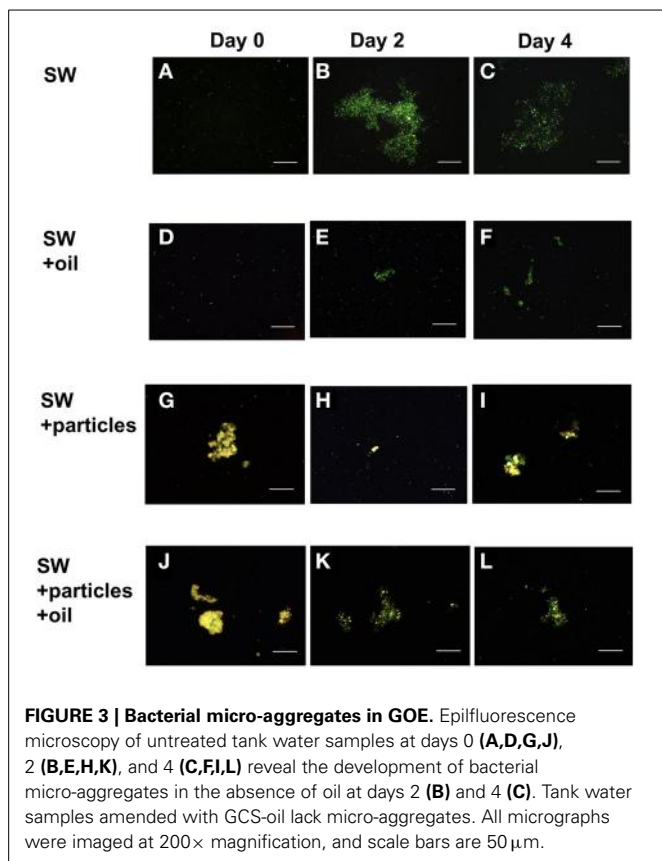
Cell-specific glucosidase activities in the GOE seawater treatment (SW) peaked at day 2 and were lowest at day 0 (Table 3). The addition of GCS-oil lowered the initial cell-specific glucosidase activities in SW+oil by a factor of 5 relative to initial SW levels (Student's *t*-test,  $p < 0.001$ ). Cell-specific glucosidase activity in SW+oil subsequently increased until day 4 [ $F_{(2, 6)} = 842.7$ ,  $p < 0.001$ ]. Macro-aggregate associated activities in both particles treatments (SW+particels, SW+particles+oil) were generally higher compared to the SSW [SW+particels:  $F_{(4, 9)} = 112.2$ ,  $p < 0.001$ ; SW+particles+oil:  $F_{(4, 9)} = 78.3$ ,  $p < 0.001$ ]. Cell-specific glucosidase activities in POE remained constant in the seawater treatment; one order of magnitude higher activities were found in SW+oil compared to the initial SW level [ $F_{(2, 3)} = 11.3$ ,  $p < 0.05$ ].

Cell-specific peptidase activity increased within the first 2 days of the GOE seawater treatment (SW) by a factor of 4.5,

remaining at that level until day 4 (Table 3). The addition of GCS-oil lowered initial cell-specific peptidase activities by a factor of up to 2 in SW+oil compared to SW (Student's *t*-test,  $p < 0.001$ ). Cell-specific peptidase activities in SW+oil remained at the same level between days 0 and 2, and increased by one order of magnitude until the end of the incubation [ $F_{(2, 3)} = 868.4$ ,  $p < 0.001$ ]. The formation of macro-aggregates in the absence of GCS-oil (SW+particles) led to cell-specific peptidase activities in Agg at days 2 and 4 that were one to two orders of magnitude higher compared to SSW [ $F_{(4, 10)} = 26.74$ ,  $p < 0.001$ ]. In contrast cell-specific peptidase activity in Agg in the presence of macro-aggregates and GCS-oil (SW+particles+oil) were one order of magnitude lower compared to Agg in the non-oil treatment. Highest cell-specific peptidase activities in SW+particles+oil were found in SSW at day 4 [ $F_{(4, 10)} = 2904.7$ ,  $p < 0.001$ ]. In POE, cell-specific peptidase activity in SW doubled between days 0 and 2, and peptidase activities in the presence of oil were about 3 times higher compared to SW at day 3 [ $F_{(2, 3)} = 868.4$ ,  $p < 0.001$ ].

## DISCUSSION

Our experiments were designed to test whether oil slick residues from natural oil and gas seeps over the Green Canyon oil reservoir (Figure 1) form oil-rich marine snow. Such oil snow would provide a transport pathway to the sea floor for oil-carbon, similar to the oil snow that formed during the early stages of the DwH oil spill in 2010 (Passow et al., 2012; Ziervogel et al., 2012). The observed macro-aggregates in SW+particles and SW+particles+oil formed due to coagulation of the added particles, and thus differed appreciably from the DwH oil snow that formed as a result of enhanced bacterial mucus production and in the absence of suspended particles (Passow, 2014). Despite



the lack of oil snow formation, the addition of GCS-oil to surface water triggered a specific bacterial metabolic response that affected the timescales of bacterial cycling of carbon in our roller tank incubations.

#### EFFECTS OF GCS-OIL ON CARBON CYCLING IN THE ABSENCE OF MACRO-AGGREGATES

GCS-oil formed a microlayer at the tank water-headspace interface similar in thickness to the one observed in the field (**Figure 1**). The initial oil fluorescence as well as the C: N ratios

of the POM pool in the GCS-oil tanks compared to the non-oil treatments (**Table 2**) indicate that some fraction of the GCS-oil instantly dispersed into the water underneath the surface layer. Turbulent conditions during filling of the GCS-tanks possibly dispersed the oil into  $\mu$ m-sized droplets (e.g. Li and Garrett, 1998). Physically dispersed oil did not affect the DOC pool (**Table 2**), indicating that most of the water soluble fraction of the GCS-oil was removed during its ascent from the seep at 1200 m. This agrees with field observations at Green Canyon seeps, revealing a rapid dissolution of the water soluble fraction of the seep oil into bottom waters (Wang et al., 2001).

Dispersed oil in the tank water was more available to biodegradation compared to the oil slick that persisted until the end of the incubation. The rapid decrease of C: N ratios, POC concentrations, and oil fluorescence accompanied with an increase in DOC in SW+oil (**Table 2**) point to the transformation of oil-carbon into the DOC pool. This transformation was facilitated by heterotrophic bacteria capable of degrading the lower molecular weight n-alkanes of the dispersed oil throughout the GCS-oil incubations (**Figure 2**). Similar biodegradation patterns of n-alkanes were observed during the early stages of the DwH oil spill in the deep-water hydrocarbon plume where C<sub>13</sub>–C<sub>26</sub> n-alkanes had half-lives of 1–6 days (Hazen et al., 2010).

Biodegradation of oil in the ocean often leads to the production of peptide- and carbohydrate-rich organic macromolecules as degradation byproducts (Hazen et al., 2010) and bacterial EPS (Gutierrez et al., 2013). Such metabolic byproducts from primary oil degradation can stimulate activities of non-oil degrading heterotrophic bacterial communities (McGenity et al., 2012). GeoChip analysis of DNA in the deep-water hydrocarbon plume that formed in the early stages of the DwH oil spill revealed high levels of genes associated with the degradation of high molecular weight carbohydrates compared to non-plume associated deep waters (Lu et al., 2012). In addition leucine-aminopeptidase and  $\beta$ -glucosidase activities were elevated in deep waters inside compared to outside the hydrocarbon plume (Ziervogel and Arnosti, in press). Similar to the bacterial dynamics during the DwH oil spill, the here observed patterns of enzyme activities and TEP (used as indicators for bacterial EPS) also point to a bacterial metabolic cascade of primary oil degraders and secondary consumers. Levels of TEP were in the same range in the GCS-oil and the non-oil treatment; however the different temporal development of TEP formation (**Table 2**) points to different bacterial metabolic dynamics in the two treatments. Rapid bacterial growth and metabolism after the start of the non-oil incubation (SW) led to enhanced levels of TEP at day 2. TEP in SW served as the organic network resulting in the formation of bacterial micro-aggregates (**Figures 3B,C**). In contrast, the addition of GCS-oil initially suppressed bacterial metabolism as indicated by the lower enzyme activities at day 0 in the GCS-oil relative to the non-oil treatments (**Table 2**). This partial inhibition of bacterial metabolism in the SW+oil treatment led to lower TEP production in the first 2 days. However, EPS produced by primary oil degraders accumulated throughout the experiment in the GCS-oil treatments, resulting in peak levels of TEP at day 4. The close correlation between TEP and cell-specific enzymatic activities in both treatments (**Figure 5**) underlines the role of TEP as

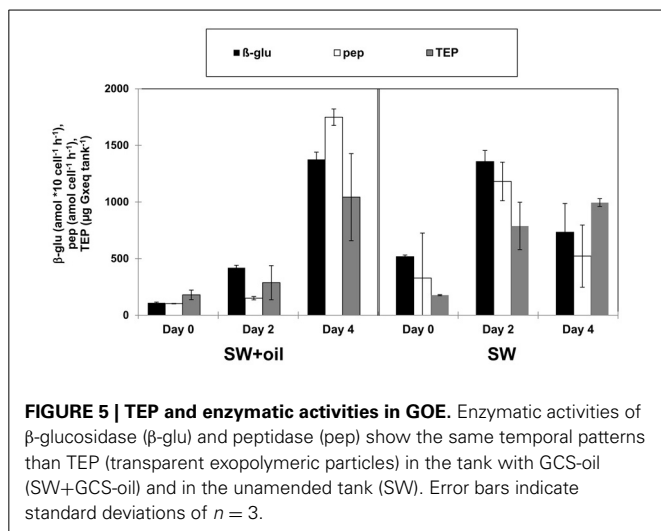


**FIGURE 5 | TEP and enzymatic activities in GOE.** Enzymatic activities of  $\beta$ -glucosidase ( $\beta\text{-glu}$ ) and peptidase (pep) show the same temporal patterns than TEP (transparent exopolymeric particles) in the tank with GCS-oil (SW+GCS-oil) and in the unamended tank (SW). Error bars indicate standard deviations of  $n = 3$ .

an important carbon source for heterotrophic bacteria (Ortega-Retuerta et al., 2010). It also demonstrates the delayed metabolic response of the fraction of the bacterial community not involved in primary oil degradation.

#### EFFECTS OF GCS-OIL ON CARBON CYCLING IN TANK WATER WITH MACRO-AGGREGATES

In addition to TEP formation from bacterial production, TEP was introduced with the particle slurry used for the “+particles” treatments as indicated by initially higher TEP concentrations in SW+particles and SW+particles+oil compared to the non-particle treatments (Table 2). Thus, sticky particles rapidly formed macro-aggregates that were colonized by surface water bacterial communities; it is also possible that bacterial cells attached to the source particles from the marine snow trap were carried over. Bacteria associated with macro-aggregates expressed generally higher enzymatic activities compared to those in SSW (Table 2). Marine aggregates, in general, are hotspots for heterotrophic bacterial activities (Azam, 1998) often expressing higher peptidase compared to  $\beta$ -glucosidase activity (Smith et al., 1992). Cell-specific peptidase activity was particularly enhanced in macro-aggregates in the absence of GCS-oil (SW+particles), suggesting that the presence of oil may have suppressed macro-aggregate associated peptidase activities in SW+particles+oil.

Ratios of C: N and POC levels in the Agg and SSW of the GCS-oil treatment indicate that macro-aggregates did not incorporate significant amounts of dispersed oil (Table 2). Nevertheless, some fraction of the GCS-oil possibly absorbed onto mineral particles in the Agg as well as the SSW fraction of the SW+particles+oil treatment. Given that mineral particles were present in the source slurry, we hypothesize that  $\mu\text{m}$ -sized mineral-oil complexes formed in the tanks with GCS-oil, acting as hotspots for bacterial oil-degraders in SSW. This would explain why the  $\mu\text{m}$ -sized particles in SW+particles+oil appeared to be more colonized by bacteria relative to the ones in the non-oil treatment (Figures 3G–L).

The very similar dynamics of the n-alkane pool in the presence (SW+particles+oil) and absence of particles (SW+oil)

(Figure 2) indicate that the formation of macro-aggregates had no measurable effect on the bioavailability of the dispersed oil within the timecourse of our 4-days incubations. Considering fluxes of the  $C_{16}\text{--}C_{21}$  n-alkanes, [i.e., the biodegraded fraction of the dispersed oil (Figure 2)], we found that 7% of this pool was left in SW+oil at day 4 while only 2% of the  $C_{16}\text{--}C_{21}$  n-alkanes remained in SW+particles+oil at the end of the incubations. This suggests higher rates of oil biodegradation in the presence of macro-aggregates (and mineral-oil complexes in the SSW) at similar total bacterial abundances in the treatments with and without particles. Higher oil biodegradation rates could also explain the greater loss of oil-carbon in SW+particles+oil compared to SW+oil: the addition of GCS-oil led to an increase of 700  $\mu\text{g}$  POC per tank in both treatments (i.e., initial POC in oil treatments subtracted by the respective non-oil treatments). At day 4, 15% of the added oil-carbon was left in SW+oil while only 3% of the oil-carbon was left at the end of the treatment with macro-aggregates.

#### CONCLUSIONS

The lack of oil snow formation in surface seawater over the Green Canyon oil reservoir demonstrates that the fate of oil slick residues stemming from natural deep water seeps in the northern Gulf of Mexico is not driven by sinking oil snow. Fractions of the oil slick, however, may be available for rapid biodegradation, initiating a bacterial metabolic cascade that utilized  $\sim 85\%$  of the oil-carbon within our 4-days incubations. This contrasts with previous studies from the Green Canyon area, suggesting that oil slicks contain highly degraded oil components that had only minor effects on biogeochemical fluxes in the surface ocean (Wang et al., 2001; MacDonald et al., 2002). Moreover higher rates of oil biodegradation can be expected in the presence of macro-aggregates formed by coagulation of suspended particles. Concentrations of suspended particles in northern Gulf of Mexico surface waters increase with decreasing distance to the coast. Thus, in addition to UV radiation (MacDonald et al., 2002), bacterial transformation of oil-carbon should be considered as an important process in the fate of GCS-oil slicks with consequences for microbial food web interactions.

#### ACKNOWLEDGMENTS

We thank the captain and crew of the RV Endeavor as well as chief scientist Joe Montoya (Georgia Tech) for assistance during sampling. Carol Arnosti (UNC) gave invaluable advice during planning of the experiments. Masha Pitiranggon (LDEO) conducted the n-alkane analysis, and Daniel Hoer (UNC) measured DOC. This work was supported by the Gulf of Mexico Research Initiative’s “Ecosystem Impacts of Oil and Gas Inputs to the Gulf” (ECOGIG) program. This is ECOGIG contribution #276 and the data fall under GRIIDC accession numbers “R1.x132.134.0005,” “R1.x132.134.0006,” and “R1.x132.139.0004.”

#### REFERENCES

- Azam, F. (1998). Microbial control of organic carbon flux: the plot thickens. *Science* 280, 694–696. doi: 10.1126/science.280.5364.694
- Crump, B. C., Baross, J. A., and Simenstad, C. A. (1998). Dominance of particle-attached bacteria in the Columbia River estuary, USA. *Aquat. Microb. Ecol.* 14, 7–18. doi: 10.3354/ame014007

- Gutierrez, T., Berry, D., Yang, T., Mishamandani, S., McKay, L., Teske, A., et al. (2013). Role of bacterial exopolymers in the fate of the oil released during the Deepwater Horizon oil spill. *PLoS ONE* 8:e67717. doi: 10.1371/journal.pone.0067717
- Hazen, T. C., Dubinsky, E. A., DeSantis, T. Z., Andersen, G. L., Piceno, Y. M., et al. (2010). Deep-sea oil plume enriches indigenous oil-degrading bacteria. *Science* 330, 204–208. doi: 10.1126/science.1195979
- Head, I. M., Jones, D. M., and Röling, W. F. M. (2006). Marine microorganisms make a meal of oil. *Nat. Rev. Microbiol.* 4, 173–182. doi: 10.1038/nrmicro1348
- Hollander, D. J., Brooks, G. R., Larson, R., Romero, I., Schwing, P., Watson, K., et al. (2013). “Testing the mechanisms of sedimentary oil deposition in the deep-sea,” in *Gulf of Mexico Oil Spill and Ecosystem Science Conference* (New Orleans, LA).
- Hoppe, H. G. (1983). Significance of exoenzymatic activities in the ecology of brackish water - measurements by means of methylumbelliferyl-substrates. *Mar. Ecol. Prog. Ser.* 11, 299–308. doi: 10.3354/meps011299
- Li, M., and Garrett, C. (1998). The relationship between oil droplet size and upper ocean turbulence. *Mar. Pollut. Bull.* 36, 961–970. doi: 10.1016/S0025-326X(98)00096-4
- Lu, Z., Deng, Y., Van Nostrand, J. D., He, Z., Voordeckers, J., Zhou, A., et al. (2012). Microbial gene functions enriched in the Deepwater Horizon deep-sea oil plume. *ISME J.* 6, 451–460 doi: 10.1038/ismej.2011.91
- Lunau, M., Lemke, A., Walther, K., Martens-Habbena, W., and Simon, M. (2005). An improved method for counting bacteria from sediments and turbid environments by epifluorescence microscopy. *Environ. Microbiol.* 7, 961–968. doi: 10.1111/j.1462-2920.2005.00767.x
- MacDonald, I. R., Leifer, I., Sassen, R., Stine, P., Mitchell, R., and Guinasso, N. (2002). Transfer of hydrocarbons from natural seeps to the water column and atmosphere. *Geofluids* 2, 95–107. doi: 10.1046/j.1468-8123.2002.00023.x
- McGenity, T. J., Folwell, B. D., McKew, B. A., and Sanni, G. O. (2012). Marine crude-oil biodegradation: a central role for interspecies interactions. *Aquat. Biosyst.* 8:10. doi: 10.1186/2046-9063-8-10
- Ortega-Retuerta, E., Duarte, C. M., and Reche I. (2010). Significance of bacterial activity for the distribution and dynamics of transparent exopolymer particles in the Mediterranean Sea. *Microb. Ecol.* 59, 808–818. doi: 10.1007/s00248-010-9640-7
- Passow, U. (2002). Transparent exopolymer particles (TEP) in aquatic environments. *Progr. Oceanogr.* 55, 287–333. doi: 10.1016/S0079-6611(02)00138-6
- Passow, U. (2013). “Marine snow as drivers for oil transformation,” in *Gulf of Mexico Oil Spill and Ecosystem Science Conference* (New Orleans, LA).
- Passow, U. (2014). “Formation of oil-associated marine snow: an effective transportation and distribution pathway for spilled oil in marine environments,” in *Gulf of Mexico Oil Spill and Ecosystem Science Conference* (Mobile, AL).
- Passow, U., and Alldredge, A. L. (1995). A dye-binding assay for the spectrophotometric measurement of transparent exopolymer particles (TEP). *Limnol. Oceanogr.* 40, 1326–1335. doi: 10.4319/lo.1995.40.7.1326
- Passow, U., Zier vogel, K., Asper, V., and Diercks, A. (2012). Marine snow formation in the aftermath of the Deepwater Horizon oil spill in the Gulf of Mexico. *Environ. Res. Lett.* 7:035301. doi: 10.1088/1748-9326/7/3/035301
- Smith, D. C., Simon, M., Alldredge, A. L., and Azam, F. (1992). Intense hydrolytic enzyme activity on marine aggregates and implications for rapid particle dissolution. *Nature* 359, 139–142. doi: 10.1038/359139a0
- Solomon, E. A., Kastner, M., MacDonald, I. R., and Leifer, I. (2009). Considerable methane fluxes to the atmosphere from hydrocarbon seeps in the Gulf of Mexico. *Nat. Geosci.* 2, 561–565. doi: 10.1038/ngeo574
- Suter, E. (2011). Particle association of enterococcus and total bacteria in the lower Hudson River estuary, USA. *J. Water Res. Prot.* 3, 715–725. doi: 10.4236/jwarp.2011.310082
- Wang, X. C., Chen, R. F., Whelan, J., and Eglington, L. (2001). Contribution of “old” carbon from natural marine hydrocarbon seeps to sedimentary and dissolved organic carbon pools in the Gulf of Mexico. *Geophys. Res. Lett.* 28, 3313–3316. doi: 10.1029/2001GL013430
- Zier vogel, K., and Arnosti, C. (in press). Enhanced protein and carbohydrate hydrolysis in plume-associated deep waters initially sampled during the early stages of the Deepwater Horizon oil spill. *Deep Sea Res. II*. doi: 10.1016/j.dsr2.2013.09.003i
- Zier vogel, K., McKay, L., Rhodes, B., Osburn, C. L., Dickson-Brown, J., Arnosti, C., et al. (2012). Microbial activities and dissolved organic matter dynamics in oil-contaminated surface seawater from the Deepwater Horizon oil spill site. *PLoS ONE* 7:e34816. doi: 10.1371/journal.pone.0034816

**Conflict of Interest Statement:** The authors declare that the research was conducted in the absence of any commercial or financial relationships that could be construed as a potential conflict of interest.

*Received: 26 November 2013; accepted: 07 April 2014; published online: 08 May 2014.*

*Citation: Zier vogel K, D’souza N, Sweet J, Yan B and Passow U (2014) Natural oil slicks fuel surface water microbial activities in the northern Gulf of Mexico. *Front. Microbiol.* 5:188. doi: 10.3389/fmicb.2014.00188*

*This article was submitted to Aquatic Microbiology, a section of the journal Frontiers in Microbiology.*

*Copyright © 2014 Zier vogel, D’souza, Sweet, Yan and Passow. This is an open-access article distributed under the terms of the Creative Commons Attribution License (CC BY). The use, distribution or reproduction in other forums is permitted, provided the original author(s) or licensor are credited and that the original publication in this journal is cited, in accordance with accepted academic practice. No use, distribution or reproduction is permitted which does not comply with these terms.*



# A survey of deepwater horizon (DWH) oil-degrading bacteria from the Eastern oyster biome and its surrounding environment

Jesse C. Thomas IV<sup>1†</sup>, Denis Wafula<sup>1†</sup>, Ashvini Chauhan<sup>1\*</sup>, Stefan J. Green<sup>2,3</sup>, Richard Gragg<sup>1</sup> and Charles Jagoe<sup>1,4</sup>

<sup>1</sup> Environmental Biotechnology Laboratory, School of the Environment, Florida Agricultural and Mechanical University, Tallahassee, FL, USA

<sup>2</sup> DNA Services Facility, University of Illinois at Chicago, Chicago, IL, USA

<sup>3</sup> Department of Biological Sciences, University of Illinois at Chicago, Chicago, IL, USA

<sup>4</sup> NOAA Environmental Cooperative Science Center, School of the Environment, Florida Agricultural and Mechanical University, Tallahassee, FL, USA

**Edited by:**

Andreas Teske, University of North Carolina at Chapel Hill, USA

**Reviewed by:**

Torsten Thomas, The University of New South Wales, Australia  
Xiang Xiao, Shanghai Jiao Tong University, China

**\*Correspondence:**

Ashvini Chauhan, Environmental Biotechnology Laboratory, School of the Environment, Florida Agricultural and Mechanical University, Suite 305B, FSH Science Research Center, Tallahassee, FL 32307, USA  
e-mail: ashvini.chauhan@famu.edu

**†Present address:**

Jesse C. Thomas, Department of Environmental Health Sciences, University of Georgia, 150 East Green Street, Athens, GA 30602, USA;  
Denis Wafula, College of Pharmacy, The University of New Mexico, Albuquerque, NM 87131, USA

The deepwater horizon (DWH) accident led to the release of an estimated 794,936,474 L of crude oil into the northern Gulf of Mexico over an 85 day period in 2010, resulting in the contamination of the Gulf of Mexico waters, sediments, permeable beach sands, coastal wetlands, and marine life. This study examines the potential response of the Eastern oyster's microbiome to hydrocarbon contamination and compares it with the bacterial community responses observed from the overlaying water column (WC) and the oyster bed sediments. For this purpose, microcosms seeded with DWH crude oil were established and inoculated separately with oyster tissue (OT), mantle fluid (MF), overlaying WC, and sediments (S) collected from Apalachicola Bay, FL, USA. Shifts in the microbial community structure in the amended microcosms was monitored over a 3-month period using automated ribosomal intergenic spacer region analysis, which showed that the microbiome of the OT and MF were more similar to the sediment communities than those present in the overlaying WC. This pattern remained largely consistent, regardless of the concentration of crude oil or the enrichment period. Additionally, 72 oil-degrading bacteria were isolated from the microcosms containing OT, MF, WC, and S and identified using 16S ribosomal RNA gene sequencing and compared by principal component analysis, which clearly showed that the WC isolates were different to those identified from the sediment. Conversely, the OT and MF isolates clustered together; a strong indication that the oyster microbiome is uniquely structured relative to its surrounding environment. When selected isolates from the OT, MF, WC, and S were assessed for their oil-degrading potential, we found that the DWH oil was biodegraded between 12 and 42%, under the existing conditions.

**Keywords:** deepwater horizon oil spill, oyster, bacteria, biodegradation, hydrocarbon

## INTRODUCTION

Since the start of the second industrial revolution, the use of fossil fuels including petroleum hydrocarbons has increased dramatically (Mojib et al., 2011). The world's total oil consumption is expected to rise to over 96.1 million barrels/day by 2015 and up to 113.3 million barrels/day by 2030 [United States Energy Information Administration (US-EIA), 2011a]. As of 2010, the United States alone consumed 19.15 million barrels/day of refined petroleum products and biofuels; which is approximately 22% of the world's total petroleum consumption (United States Energy Information Administration (US-EIA), 2011b). However, despite stimulating growth in areas such as agriculture and transportation, petroleum fuels are a major source of environmental pollution by way of accidental spills, particularly in estuarine and marine ecosystems (Paine et al., 1996; Newman and Unger, 2003).

When coastal ecosystems are impacted by contaminants, important functions (e.g., fishery production, biofiltration) may be affected (Livingston, 1984; Nixon, 1995). Oil spills such as

the 1989 Exxon Valdez accident in Alaska and more recently, the deepwater horizon (DWH) spill illustrate how oil hydrocarbons can cause acute (e.g., lethality) and chronic (e.g., reduced growth and foraging success, reduced fecundity, increased levels of deformities, and abnormal social behavior) impacts to coastal ecosystem services (Peterson, 1991, 2001; Peterson et al., 2003; Hazen et al., 2010; Kostka et al., 2011; Henkel et al., 2012; Whitehead et al., 2012). Assessing impacts of oil spills requires a comprehensive understanding of ecosystem services, including the water filtration capacity and nursery areas that are typically provided by oyster reef habitats (Peterson and Heck, 1999; French McCay et al., 2003).

As of 2000, estuaries in the Gulf of Mexico region contributed 83% of the total Eastern oysters (*Crassostrea virginica*) harvested in the United States (U.S. National Marine Fisheries Service<sup>1</sup>). As a keystone species in the Gulf, oysters and their reef assemblages serve as critical habitat for commercially important seafood, while

<sup>1</sup>www.st.nmfs.gov

also performing critical ecosystem services such as water filtration and sequestration of excess nitrogen (Raj, 2008; Roosi-Snook et al., 2010; Piehler and Smyth, 2011; Grabowski et al., 2012). The value of this habitat, both ecologically and economically, however, may be greatly reduced by pollution, including accidental oil spills.

It should however, be noted that the Gulf of Mexico waters are continuously exposed to a background level of hydrocarbons vented by numerous hydrocarbon seeps, which emit hydrocarbon gas into the overlaying water column (WC) as bubble plumes which are often coated with a thin layer of oil (MacDonald et al., 2002; Leifer and MacDonald, 2003; Solomon et al., 2009). According to some estimates, seepage in the Gulf of Mexico, from over 200 active seeps, contributes oil at a high rate of  $0.4\text{--}1.1 \times 10^8$  L/year (Mitchell et al., 1999). As a corollary, this “natural” oil likely primes the environment continuously, by selectively enriching native microorganisms with the ability to metabolize and mineralize some of this oil. Therefore, it is very likely that a suite of native hydrocarbon-degrading bacteria exist in different niches of the Gulf of Mexico, and as reported previously responded rapidly to the large volume of oil released by the DWH spill (Hazen et al., 2010; Redmond and Valentine, 2012; Dubinsky et al., 2013; Gutierrez et al., 2013).

A significant body of information exists on the pathways and the nature of oil-degrading microbes from a variety of diverse environments, including soils and aquatic ecosystems (Margesin and Schinner, 2001; Aitken et al., 2004; Hamamura et al., 2005; Hazen et al., 2010; Kostka et al., 2011), but virtually nothing is known on the nature and ability of microbes that can degrade oil from the oyster reefs or within the oyster itself. In this report, we have investigated the propensity of a largely understudied ecosystem—the Eastern oyster (*Crassostrea virginica*) microbiome—to degrade the Gulf crude oil. Previous studies have shown that the oyster biome consists of a diverse collection of heterotrophic bacteria that differ from the surrounding seawater in both species composition and abundance (Kueh and Chan, 1985; Pujalte et al., 1999; Campbell and Wright, 2003). Moreover, oyster-associated bacteria often outnumber the bacterial populations present in the WC by several orders of magnitude (Kelly and Dinuzzo, 1985; Mahasneh and Al-Sayed, 1997), most likely due to the oyster’s filter-feeding behavior (Galtsoff, 1964; Haven and Morales-Alamo, 1970; Jorgensen, 1990). Romero et al. (2002) propose two kinds of bacteria found within oysters—autochthonous, which are relatively permanent and remain associated with the oysters and allochthonous, which are passing through the oysters due to the filter-feeding processes. The autochthonous groups are even known to have a strong symbiotic relationship with their bivalve host.

In fact, Colwell and Liston (1960) first suggested the existence of a defined commensal flora in oysters. More recently, the findings of Zurel et al. (2011) have shown that a conserved seasonal association between the Chama-associated oceanospirillales group (CAOG) of bacteria and oysters likely represents a symbiotic association. Trabal et al. (2012) reported a symbiotic host-bacteria relationship during different growth phases of two oyster species—*Crassostrea gigas* and *Crassostrea corteziana*. Such symbionts may assist in the digestion processes, as has been demonstrated in the larvae of *Crassostrea gigas* (Prieur

et al., 1990), and may also supply the bivalve host with vitamins and amino acids that serve as growth factors—as shown in the Pacific vesicomyid clam—*Calyptogena magnifica* found at cold seeps (Newton et al., 2007). Moreover, certain symbiotic bacteria can even protect their host from pathogens by either producing antimicrobial agents, or by growing in high densities that prevents colonization by other strains (Pujalte et al., 1999). More recently, King et al. (2012) used pyrosequencing to reveal substantial differences between stomach and gut microbiomes of oysters from Lake Caillou in Louisiana. These authors found that bacteria belonging to *Chloroflexi*, *Mollicutes*, *Planctomycetes*, and *Spartobacteriia* likely comprise a major core of the oyster stomach microbiome, whereas, *Chloroflexi*, *Firmicutes*, *α-proteobacteria*, and *Verrucomicrobia* were more abundant in the gut.

Despite the existing information on the nature of oyster-associated microbial communities, not much is known on their ability to degrade oil hydrocarbons. Therefore, the purpose of this study was to not only to assess the oyster microbiome, which in itself necessitates further studies because it is a largely understudied microhabitat, but also to enrich, isolate and compare the oil biodegradation efficacy of oyster-associated bacteria.

## MATERIALS AND METHODS

### SITE DESCRIPTION AND SAMPLE COLLECTION

This study was conducted on oysters, water, and sediment (S) samples collected from Dry Bar, the most productive bar, in Apalachicola Bay, Florida ( $29^{\circ} 40.474N$ ,  $085^{\circ} 03.497W$ ). Apalachicola Bay is a relatively pristine estuary, well mixed by freshwater from the Apalachicola-Chattahoochee-Flint (ACF) river system and oceanic Gulf tides (Chauhan et al., 2009). The bay produces 90% of Florida oysters, the third highest catch of shrimp, a rich supply of brown shrimp, scallops, and blue crabs (Livingston, 1984).

Samples for this study were collected on June 14, 2011. Before collecting the environmental samples, physiochemical parameters were measured with a YSI probe, which included salinity (26.5 parts per thousand, ppt), dissolved oxygen (7.2 mg/L), conductivity (45.37 mS), and temperature ( $30.1^{\circ}\text{C}$ ). Oysters were collected using a tong, culled, and 20 adult oysters, of approximately the same size were collected. Additionally, 1 L of water from directly above the oyster bed was collected in a sterile bottle, and approximately 10 g of sediment was collected into a sterile container from below the oyster beds using a sediment grab sampler. All samples were stored on ice and transported to Florida Agricultural and Mechanical University for further processing on the same day samples were collected.

### ENRICHMENT OF OIL-DEGRADING BACTERIA

Oysters were carefully culled and rinsed using sterile 0.85% NaCl to remove debris and shell biofilm. Prior to collection of oyster tissues (OT), mantle fluid (MF) from each oyster was aseptically collected by opening each oyster from the hinge side and aspirating the fluid from the mantle cavity by using sterile syringes fitted with 21 gage needles. By MF, we are referring to the fluid accumulated within the mantle cavity (Pekkarinen, 1997; Sadok et al., 1999). In other words, the liquid within the mantle cavity

enclosed by the valves that bathes the internal tissues including the gills. This is also sometimes called the mantle cavity fluid. Each oyster was then carefully shucked using sterile knives, and OT was then homogenized in pre-sterilized blenders and collected into sterile Falcon tubes (BD Biosciences, San Jose, CA, USA).

Enrichment of oil-degrading bacteria was performed in Bushnell-Haas (BH) medium containing: MgSO<sub>4</sub> 0.2 g/L, CaCl<sub>2</sub> 0.02 g/L, KH<sub>2</sub>PO<sub>4</sub> 1 g/L, (NH<sub>4</sub>)<sub>3</sub>PO<sub>4</sub> 1 g/L, KNO<sub>3</sub> 1 g/L, and FeCl<sub>3</sub> 0.05 g/L, pH 7.1 (Bushnell and Haas, 1941) with a salinity of 3.2 ppt. Even though the measured salinity of the oyster sampling site was higher than that of our enrichment microcosms, the typical salinity of the sampled site is highly dynamic ranging from 3 to 33 ppt, depending on the season and freshwater input from the riverine flows (Livingston et al., 2000). Enrichments contained 100 mL of media and 1% OT, MF, S, or water and supplemented with 0.1% (v/v) or 1% (v/v) of filter-sterilized crude oil that was obtained directly from the source of the Deep Horizon spill site. The oil was provided as the sole source of carbon and energy, and a full characterization of the oil has been reported elsewhere (Kostka et al., 2011). After 1 month of incubation on a rotary shaker at 30°C, 1 mL of enriched sample was transferred into fresh BH media containing 0.5% crude oil and incubation was continued for another month. After the second enrichment, 0.4 mL of sample was serially diluted and plated on BH agar media. Isolated colonies from different environments were streaked onto BH agar media and exposed to oil vapors using filters soaked in 500 μL of crude oil, according to the method of Kleinheinz and Bagley (1997). Those colonies that grew on BH media exposed to oil vapors were re-streaked onto fresh oil-amended liquid media and further purified by a second round on BH-vapor plates.

#### NUCLEIC ACID EXTRACTION AND AUTOMATED RIBOSOMAL INTERGENIC SPACER REGION ANALYSIS

Automated ribosomal intergenic spacer region analysis (ARISA) that employs the bacterial 16S to 23S rRNA intergenic spacer region was used to assess changes in bacterial community structure over the duration of oil-amended enrichments. From the first set (**Figure 1A**) and second set (**Figure 1B**) of oil enrichments established in liquid media, approximately 80 mL of media was collected after filtered through 0.2 μm filter followed by DNA extraction of the filtered biomass using the MOBIO PowerSoil DNA Isolation Kit according to the manufacturer's instructions (MOBIO Laboratories, Carlsbad, CA, USA). The biomass that grew on BH-vapor plates after the second round of enrichment was scraped from the agar surface and resuspended in 10 mL of 0.85% NaCl and centrifuged at 10,000 g for 5 min. The supernatant was decanted and DNA was isolated from the pellet using the MOBIO PowerSoil DNA Isolation Kit. Concentration and quality of DNA was determined using a micro-volume spectrophotometer (NanoDrop Technologies, Wilmington, DE, USA). This constituted the hydrocarbon vapor enrichment (VE) phase.

The fluorescently tagged primers ITSF (5'-GTCGTAAACAAGG-TAGCCGT-3') and ITSReub (5'-GCCAAGGCATCCACC-3') were used to amplify bacterial ITS regions (Cardinale et al., 2004). PCR reactions contained 25 μL of GoTaq Colorless Master Mix

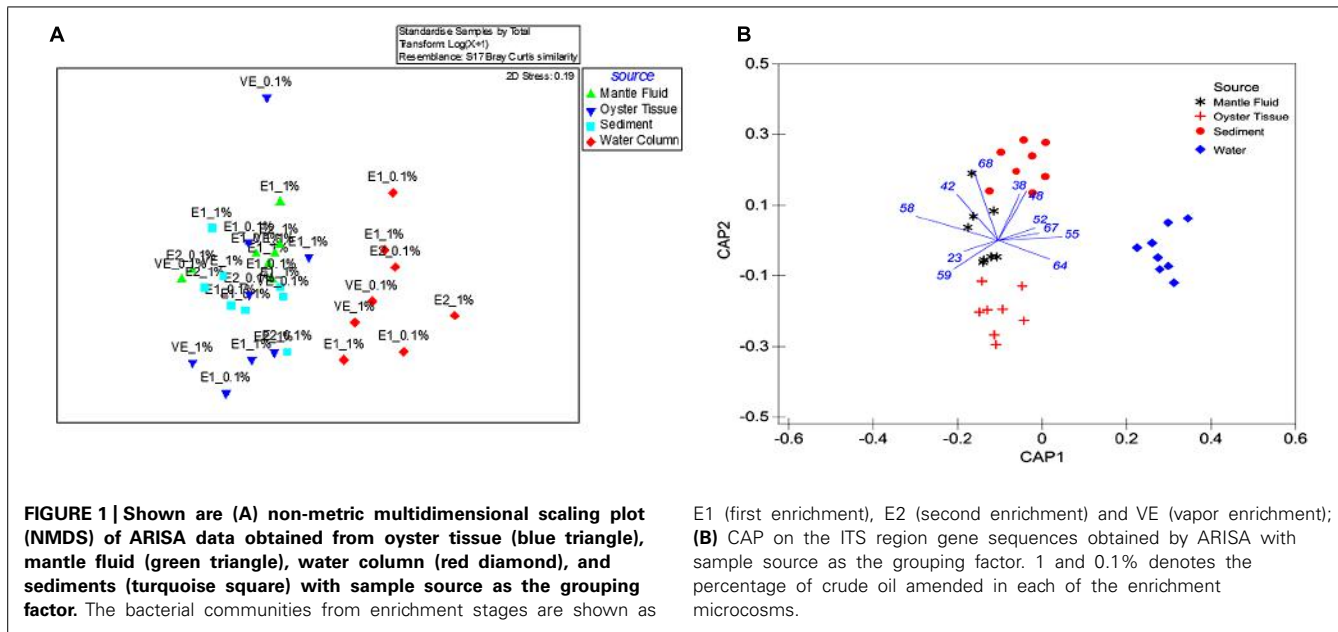
(Promega, Madison, WI, USA), 2 μL of each primer previously diluted to a concentration of 5 pmol, molecular grade water and 50–100 ng of genomic DNA. Thermal cycling conditions consisted of an initial denaturation of 3 min at 94°C, followed by 30 cycles of 45 s at 94°C, 55°C for 1 min, and a final elongation step of 10 min at 72°C. Resulting PCR products were purified using UltraClean PCR clean-up kit according to the manufacturer's protocol (MoBio Laboratories, Carlsbad, CA, USA), quantified, and diluted as stated above. Samples were analyzed by the DNA Services Facility, University of Illinois at Chicago, using an ABI 3730xl capillary electrophoresis system (Life Technologies, Inc., Carlsbad, CA, USA).

After manually examining the electropherogram data and images, background noise thresholds were set to 10 fluorescent units. The resultant peak area data matrix was exported into Microsoft Excel® where a custom script chose peaks that were between 100 and 1000 bp; all peaks within 5 bp were binned to reduce peak calling variation which can occur during sample analysis. Sizing error during ARISA increases with fragment length, and binning or other correction strategies such that any errors associated with run-to-run variability are minimized. Because the ARISA fragments from the samples analyzed in this study ranged approximately between 700 and 1000 bp, we kept the binning threshold at 5 bp (Brown et al., 2005). The data matrix was processed as follows: triplicate runs were averaged to produce a single peak area for each sample, imported into the Primer 6 software suite (version 6.1.10; PRIMER-E, Ivybridge, UK) and normalized using the log (X + 1) pre-treatment function. After transformation, a Bray-Curtis similarity matrix was generated and used as a basis for permutational multivariate analysis of variance (PERMANOVA). Additionally, the data were analyzed using a non-metric multidimensional scaling plot (NMDS), which was compared directly with canonical analysis of principal components (CAP).

#### ISOLATION AND CHARACTERIZATION OF OIL-DEGRADING BACTERIA

From the oil-vapor enriched plates, six colonies from each environment (OT, MF, water, and S), having similar morphologies, were streaked on salt-water yeast extract (SWYE) agar plates consisting of: peptone 10 g/L, yeast extract 3 g/L in 70% artificial seawater, pH 7.1, agar 15 g/L. These isolates were then transferred onto fresh BH agar plates and exposed to crude oil vapors incubated in airtight glass desiccators held at 30°C. After 10 days, colonies that appeared on the crude oil vapor-exposed plates were picked and streaked onto fresh SWYE agar plates. A total of 118 single colonies were re-streaked onto BH agar plates and exposed to oil vapor again so as to obtain axenic isolates. Finally, pure bacterial isolates from the OTs, MF, WC, and S environments were streaked onto SWYE for regular maintenance. For long-term storage, isolates were stored in 15% glycerol, at -80°C.

A direct colony PCR method was used to amplify the 16S rRNA gene from 72 pure isolates obtained from the enrichments. For this, a single colony representing each of the isolated strain was picked using a sterile toothpick and resuspended in a premix of buffer, primers, and taq polymerase. Universal eubacterial primers 1492R and 27F were used for 16S rRNA gene sequencing and subsequent identification of the isolated bacteria as shown previously



(Chauhan et al., 2009). Bacterial 16S rRNA gene sequences were then aligned using Greengenes<sup>2</sup>, aligned using MEGA ver. 6.0 and a phylogenetic tree was constructed using the neighbor-joining distance method with a bootstrap test of 500 replicates (Tamura et al., 2013). The evolutionary distances were computed using the Maximum Composite Likelihood method in the units of the number of base substitutions per site.

#### NUCLEOTIDE SEQUENCE ACCESSION NUMBERS

The partial 16S rRNA gene sequences obtained in this study are available in GenBank under accession numbers JX501343–JX501351.

#### GROWTH KINETICS AND OIL BIODEGRADATION POTENTIAL OF REPRESENTATIVE ISOLATES

Nine isolates were chosen to evaluate growth and oil degradation efficiencies. These particular isolates were chosen because either (1) they were found only in a specific environment, as was the case with *Pseudomonas alcaligenes*, which was isolated only from the S, or (2) they were common between several environments, as was the case with *P. montelii* isolated from S, OT, and MF, respectively.

Briefly, single colonies of the selected isolates were inoculated into 5 mL SWYE media at 30°C overnight. Each of the cultures, in triplicate, was then centrifuged for 5 min at 5,000 × g, rinsed three times with 5 mL of BH media and OD<sub>600</sub> was adjusted to <0.2 using BH media. A Bioscreen C honeycomb plate (Growth Curves USA, NJ, USA) was then inoculated with 350 µL of cell suspension containing 0.75% crude oil, and incubated at 30°C within the Bioscreen C system. To compare growth rates, tests were run without crude oil in BH media containing 0.75% glucose, and control ODs were subtracted from the tests

to assess growth rate of each isolate. Bioscreen C was set to measure OD<sub>450–580</sub> using the wide-band filter at 6 h intervals for 7 days and the doubling time of each isolate was calculated after the completion of the growth experiments, as shown previously (Moat and Foster, 1995).

To estimate the ability of each of the nine isolates to degrade crude oil, a gravimetric method was used (Kostka et al., 2011). Briefly, single colonies of the selected isolates were inoculated into 5 mL SWYE media at 30°C overnight. The cell cultures were centrifuged for 5 min at 5,000 × g. The cell pellet was rinsed three times with 5 mL of BH media until OD<sub>600</sub> was approximately 0.2. Flasks containing 50 mL of BH media were inoculated with 1% (v/v) of actively growing culture, supplemented with 0.75% crude oil and incubated on a rotary shaker at 175 rpm, 30°C for 7 days; after which the residual oil was extracted twice using 50 mL of chloroform. In order to concentrate the remaining oil, the chloroform extract was transferred into pre-weighed glass vials and held in a water bath at 60°C. This caused the chloroform to evaporate leaving behind the residual oil, which was then compared to the initial weight of the amended oil. The average amount of oil lost in the controls (abiotic) was subtracted from the amount of oil lost from the flasks containing the isolates (biotic) to estimate the amount of oil biodegraded by the isolates.

## RESULTS AND DISCUSSION

### COMPARISON OF BACTERIAL COMMUNITY COMPOSITION IN OIL ENRICHED MICROCOSMS

Bacterial communities that could metabolize oil from OTs and MF were compared with those found in the surrounding environment—the overlaying WC and oyster bed S by ARISA of bacterial 16S rRNA genes using a NMDS (**Figure 1A**). The single sampling time performed for this study potentially limits extrapolation of our findings, but at the same time, provides a new perspective on the largely understudied oyster-associated microbiome and directions for future studies.

<sup>2</sup><http://greengenes.lbl.gov/>

Despite that the initial comparison between the bacterial communities in the OT, MF, WC, and S was performed only after being enriched in crude oil for a month, we were still able to detect distinct differences. Specifically, the WC bacteria clustered separately and away from those present in the OTs, MF, and S, respectively (**Figure 1A**). This suggests that the microbiome of OT, MF and S were more similar to each other relative to the WC regardless of the period for which they were enriched in liquid media or exposed to VEs or the concentration of amended oil used in the microcosms (0.1 or 1%). Furthermore, although powerful for visualizing broad patterns, unconstrained ordination methods such as NMDS are known to mask certain patterns among groups dispersed in experimental data (Anderson and Willis, 2003; Anderson and Robinson, 2003). Therefore, a constrained ordination method – the canonical analysis of principal CAP analysis was used, and this demonstrated a significant clustering of bacterial communities selected for oil degradation based on the source environment (**Figure 1B**); this analysis mirrored the NMDS representation such that the WC bacterial communities clustered together and away from the OT microbiome. Furthermore, CAP demonstrated an 87.5% classification rate, and resulted in the discrimination of the MF bacteria which appeared closer to the OT than those that were present in the S.

Moreover, to assess whether the bacterial communities from each of the tested environments (OT, MF, S, and WC) shifted over the course of the enriched time in the presence of crude oil, we performed NMDS using the time of enrichment as the variable factor (E1 = 1; E2 = 2; and VV = 3) on each sampled environment separately (**Figures 2A–D**) or when pooled together regardless of

their origin (**Figure 2E**). This analysis clearly showed that after 1 month of enrichment, communities were still relatively divergent (**Figures 2A–E**). Conversely, during the second and the third enrichment phases, the biodegradative communities became distinctly different suggesting that bacteria had become sufficiently enriched over the course of this study.

A pair wise comparison of data using PERMANOVA showed the same trend as shown by the NMDS analysis, i.e., the OT s ( $P = 0.037$ ) and MF ( $P = 0.012$ ) were more similar to S than the WC ( $P = 0.003$  or less). Unexpectedly, MF and OTs displayed greater similarity with the S than with each other ( $P = 0.0093$ ) and, this pattern of association was consistent, regardless of the concentration of crude oil or time of exposure (data not shown). These findings however, should be interpreted with the caveat that we did not assess the native bacterial communities in a “no-oil” spiked microcosm containing the OT, MF, water, and S, respectively. Despite this limitation in our experimental design, we do provide a preliminary baseline on the response of a largely understudied environment- the oyster microbiome and its response to the addition of oil hydrocarbons, upon which additional studies can be conducted.

#### TAXONOMIC ANALYSIS OF THE OIL-DEGRADING ISOLATES

Taxonomic affiliations of 72 pure bacterial strains isolated from the OT, MF, water, and S environments are summarized in **Tables 1** and **2**. We found a total of 10 different species across the oil-enriched samples with 80% of the isolated strains taxonomically affiliating to the *Pseudomonas* genus, as shown in **Figure 3**. This likely occurred because previous reports have shown that

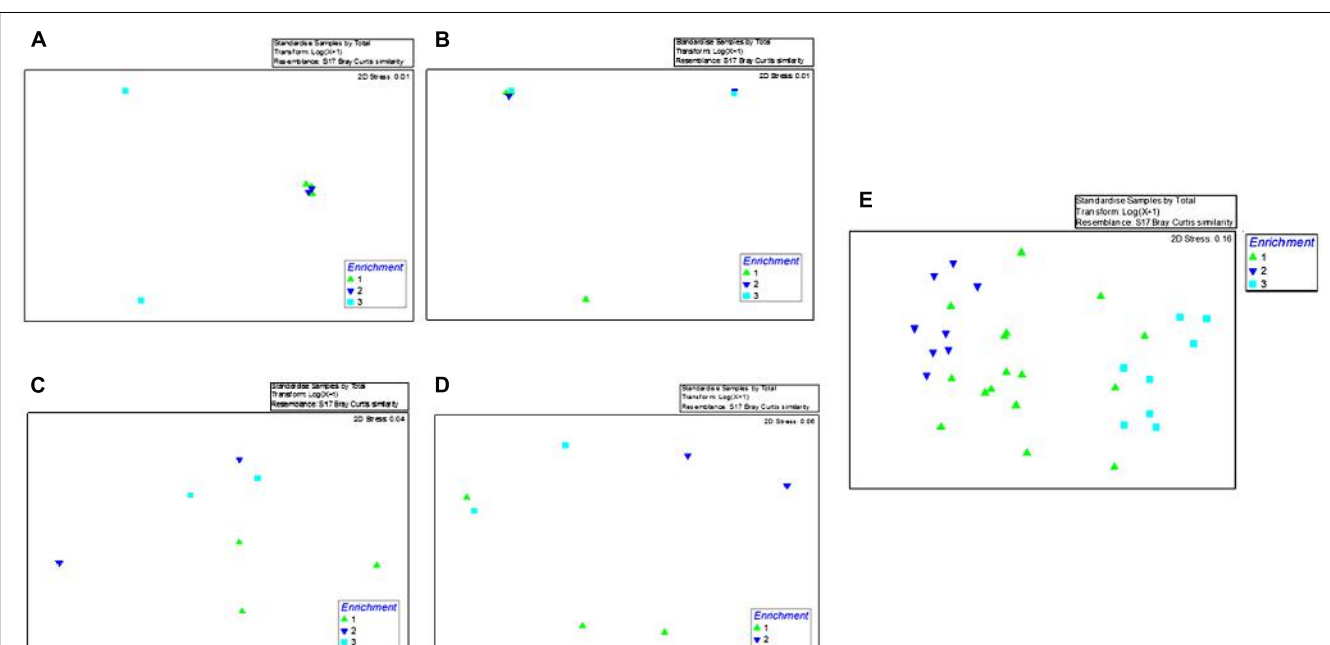


**FIGURE 2 |** Shown are the non-metric multidimensional scaling plot (NMDS) of ARISA data obtained from the first enrichment phase (E1; green triangle), second enrichment phase (E2; blue triangle), and the third enrichment phase (VE; turquoise square) with enrichment time as

**the grouping factor.** Shown in (A–D) are bacterial community profiles within the samples enriched with oyster tissue (A), mantle fluid (B), sediments (C), and water (D), respectively. (E) Shows pooled ARISA data from the oyster tissue, mantle fluid, sediments, and water over the course of this study.

**Table 1 | Summary of oil-degrading bacterial strains isolated from DWH oil-amended microcosms containing oyster tissue (OT), mantle fluid (MF), water column (WC), and sediment (S) samples obtained from Dry Bar, Apalachicola Bay, FL, USA.**

Isolated strains along with their original environment	NCBI match (% identity with nearest neighbor)	Bacterial division of the isolated strains	Accession number of strains chosen for oil degradation assay
Water column: 10*, 26*, 29*, 40*, 41, 44*, 45*, <b>55</b> , 57*, 58, 64*, 67*, 68, 73, 74*, 75*, 76*, 82*, 92*, 99*, 100*, 110*, 115*	<i>Pseudomonas aeruginosa</i> strain PAO1 (99%)/ <i>P. otitidis</i> strain MCC10330 (98%)	γ-Proteobacteria	JX501343
Oyster tissue: 48*, 59*			
Sediment: 1, 3¥, 46, 47¥, 107¥, 108¥	<i>P. monteili</i> strain CIP 104883 (99%)/ <i>P. plecoglossicida</i> strain FPC951 (99%)	γ-Proteobacteria	JX501346
Oyster tissue: 21¥, 88¥			
Mantle fluid: 4, 5¥, 6¥, 8¥, 9¥, 11¥, 15, 16¥, <b>17</b> , 18¥, 19¥, 20, 27¥, 54, 56¥, 77, 78¥, 79, 87, 101¥, 105, 106			
Oyster tissue: <b>69</b> , 104, 116	<i>P. alcaligenes</i>	γ-Proteobacteria	JX501351
Sediment: 51, <b>52</b> , 53	<i>P. pseudoalcaligenes</i> strain Stanier 63 (98%)	γ-Proteobacteria	JX501345
Mantle fluid: <b>28</b>	<i>P. xanthomarina</i> strain KMM 1447 (99%)/ <i>P. stutzeri</i> strain A1501 (99%)	γ-Proteobacteria	JX501347
Oyster tissue: 63, <b>107</b>	<i>P. putida</i> strain F1 (99%)	γ-Proteobacteria	JX501344
Mantle fluid: <b>89</b> , 91, 111, 113, 114	<i>Stenotrophomonas maltophilia</i> strain IAM 12423 (99%)	γ-Proteobacteria	JX501348
Sediment: <b>94</b>	<i>Sphingobium yanoikuyae</i> strain IFO 15102 (99%)	α-Proteobacteria	JX501349
Mantle fluid: <b>109</b>	<i>Microbacterium maritypicum</i> strain MF-C01 (100%)	Actinobacteria	JX501350

\*Denotes strains that taxonomically affiliated with *P. otitidis*.¥ Denotes strains that taxonomically affiliated with *P. plecoglossicida*, respectively.

Strains that appear in bold and underlined text were the ones that were selected for comparing their crude oil degradation propensities. Accession numbers of these nine strains appear in the last column.

**Table 2 | Taxonomic affiliation shown of the 72 oil-degrading bacterial strains that were isolated from DWH oil-amended microcosms containing oyster tissue (OT), mantle fluid (MF), water column (WC), and sediment (S) samples obtained from Dry Bar, Apalachicola Bay, FL, USA.**

Isolated strain affiliation	Oyster tissue	Mantle fluid	Water column	Sediment	Total isolated strains
<i>Pseudomonas monteili</i>	2	22	–	6	30
<i>P. xanthomarina</i>	–	1	–	–	1
<i>P. pseudoalcaligenes</i>	–	–	–	3	3
<i>P. aeruginosa</i>	2	–	23	–	25
<i>P. alcaligenes</i>	3	–	–	–	3
<i>Stenotrophomonas maltophilia</i>	–	6	–	–	6
<i>Sphingobium yanoikuyae</i>	–	–	–	1	1
<i>P. putida</i>	2	–	–	–	2
<i>Microbacterium maritypicum</i>	–	1	–	–	1
Total sequences analyzed	9	30	23	10	72

*Pseudomonas* predominates the oyster microbiome of both raw and retail oysters (Cao et al., 2009). Moreover, it is well-known that pseudomonads grow rapidly in the presence of high concentrations of nutrients (Greene et al., 2000; Rodríguez-Verdugo et al.,

2012), such as those utilized in standard batch enrichments and hence, pseudomonads can easily outcompete other slow-growing bacteria that typically have lower Ks (Monod growth coefficient) and low maximum growth rates.

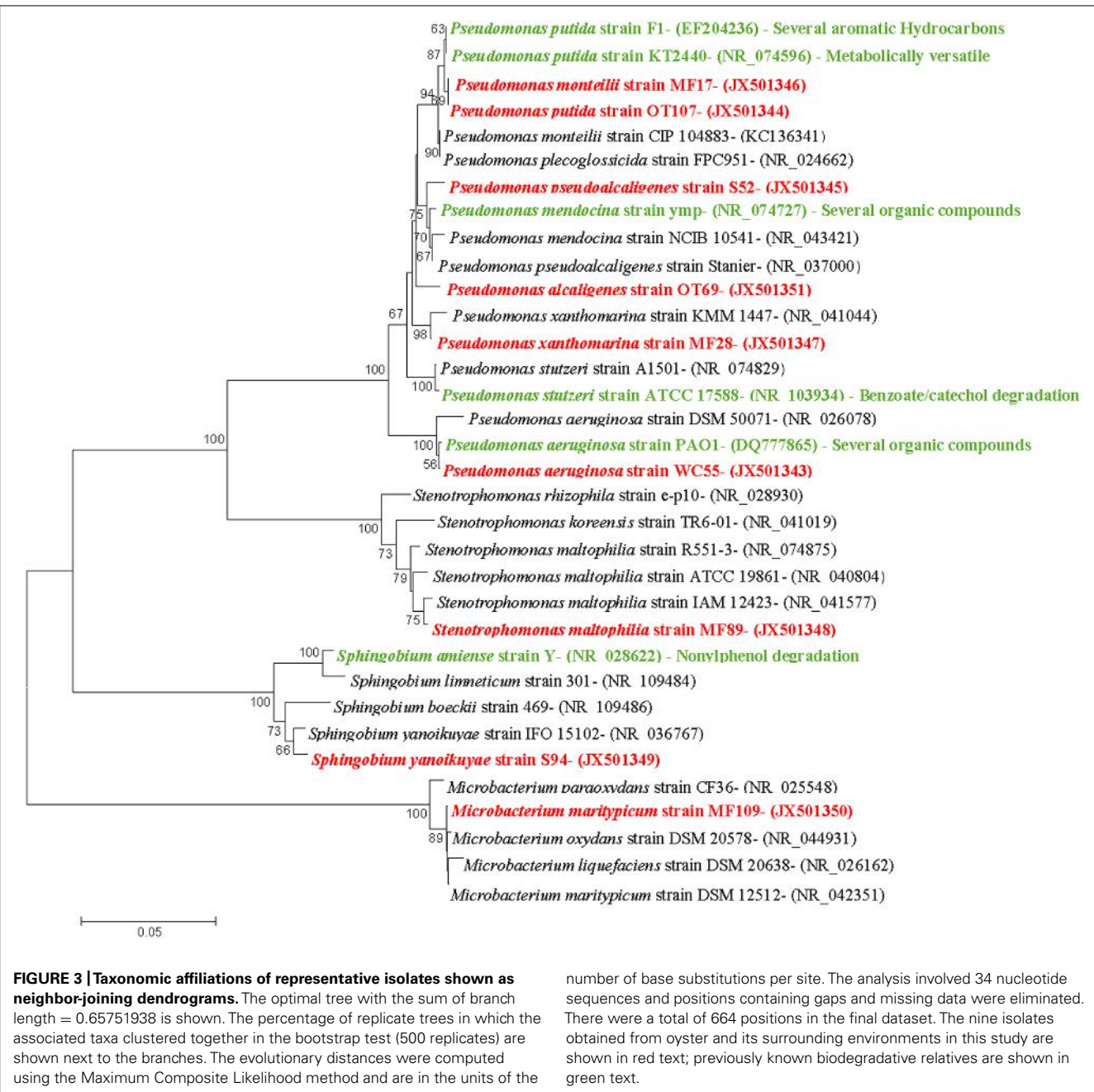


**FIGURE 3 | Taxonomic affiliations of representative isolates shown as neighbor-joining dendograms.** The optimal tree with the sum of branch length = 0.65751938 is shown. The percentage of replicate trees in which the associated taxa clustered together in the bootstrap test (500 replicates) are shown next to the branches. The evolutionary distances were computed using the Maximum Composite Likelihood method and are in the units of the

number of base substitutions per site. The analysis involved 34 nucleotide sequences and positions containing gaps and missing data were eliminated. There were a total of 664 positions in the final dataset. The nine isolates obtained from oyster and its surrounding environments in this study are shown in red text; previously known biodegradative relatives are shown in green text.

Our findings are consistent with several other studies showing that bacteria from the Pseudomonadaceae family respond to degrade the DWH oil. In fact, a group studying the succession of hydrocarbon-degrading bacteria in the aftermath of the DWH oil spill recently reported that unmitigated oil from the wellhead early on in the spill resulted in the highest proportions of n-alkanes and cycloalkanes that corresponded with the predominance of Oceanospirillaceae and *Pseudomonas* (Dubinsky et al., 2013). In another study, 24 bacterial strains isolated from oiled beach sands were shown to comprise of 14 genera but all belonged to Gammaproteobacteria, including the well-known oil degrading bacteria- *Pseudomonas*, *Alcanivorax*,

*Marinobacter*, and *Acinetobacter*, respectively (Kostka et al., 2011). Another group investigating the impact of DWH oil spill on microbial communities in wetland S and seawater samples collected along the Gulf shore recently reported that pyrosequencing based analysis showed 17 bacterial genera with the ability to degrade hydrocarbons, including- *Mycobacterium*, *Novosphingobium*, *Parvibaculum*, *Pseudomonas*, and *Sphingomonas*, in the contaminated S sample (Looper et al., 2013). Thus it appears that the Pseudomonads are a dominant community of hydrocarbon degrading bacteria in the Gulf of Mexico ecosystem, including the oyster microbiome, as shown by this study.

Further taxonomic characterization of the isolated strains revealed that all of WC isolates were  $\geq 98\%$  similar to either the *P. aeruginosa* or *P. otitidis* group, which is a closely related clade in the *Pseudomonas* family (Clark et al., 2006). Isolates from the OTs included *P. alcaligenes*, which are best known for degrading a variety of polycyclic aromatic hydrocarbon (PAH; Peix et al., 2009). In addition, OTs also contained isolates that were  $\geq 98\%$  similar to *P. putida*, as well as two isolates, *P. monteili* and *P. plecoglossicida* that have been placed in the *P. putida* group (Peix et al., 2009); **Figure 3**. Isolates from the MF were found to be  $\geq 98\%$  similar to the *P. monteili*, *P. plecoglossicida* group, however, MF also contained several other bacteria that were not found in the other environments, for example, *P. stutzeri* isolate MF28, which was  $\geq 98\%$  similar to *P. xanthomarina*, a novel bacteria that was originally isolated from marine ascidians (Romanenko et al., 2005). The MF also contained isolates that were  $\geq 98\%$  to *Stenotrophomonas maltophilia*, a common aquatic bacterium (Denton and Kerr, 1998) as well as an actinomycete – *Microbacterium maritypicum* (Takeuchi and Hatano, 1998; Schippers et al., 2005; **Table 1**; **Figure 3**). The S samples led to the isolation of two isolates that were also found in the OT and MF; these displayed  $\geq 98\%$  similarity to *P. plecoglossicida* and *P. monteili*, respectively. However, the S also contained two isolates not found in any of the other surveyed environments- *P. pseudoalcaligenes*, a bacterium in the *P. aeruginosa* group, and *Sphingobium yanoikuya*; an  $\alpha$ -proteobacteria, capable of degrading a range of PAHs (Peix et al., 2009; Schuler et al., 2009).

To compare the 72 bacterial strains isolated from the WC, MF, OT, and S, a UniFrac based analysis was performed using the 16S rRNA sequences obtained in this study (Lozupone et al., 2006). As shown in **Figure 4**, results showed that the oil-degrading bacteria isolated from the OT and MF clustered strongly together on the same axis, however, S and WC bacteria separated out onto different axes. PCA axis 1 accounted for 60.90% of the variability, while PCA axis 2 accounted for 23.10%; together explaining 84% of the variability. Moreover, this data is in line with the ARISA findings, as the OT and MF bacteria in both the enriched samples and the isolated representatives are more similar than those that were present in the overlaying water or the S beds, suggesting the uniqueness of the oyster microbiome. King et al. (2012) recently showed that significant differences exist between stomach and gut microbiomes of the Eastern oyster, *Crassostrea virginica*. However, this and previous studies on the oyster microbiome have not compared the oyster-associated bacterial communities with those of the adjacent WC or S-environments on which the oysters are entirely dependent for their nutrition. Our study, thus, is unique because it provides a comparison of the oyster microbiome to those present in the surrounding oyster reef environment.

#### GROWTH KINETICS OF THE OIL-DEGRADING BACTERIAL ISOLATES

Each of the nine isolates showed good growth over time in both, BH media containing 0.75% glucose or crude oil-spiked microcosms (**Figure 5**); the maximum optical density and doubling times of the isolates during the growth experiments are summarized in **Table 3**. Specifically, the two strains isolated from the

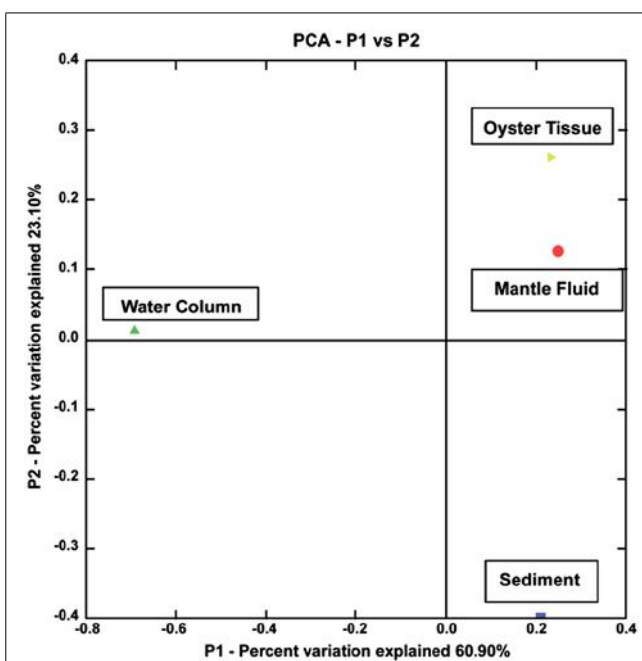


**FIGURE 4 |** Shown is a principal component analysis (PCA) obtained from UniFrac analysis of the 16S rRNA sequences of 72 isolated strains from the oyster tissue (yellow triangle), mantle fluid (red circle), water column (green triangle), and sediment (blue square). The percentages on each of the axes show the percent variation explained by each axes.

OT and MF – *P. alcaligenes* OT69 and *P. xanthomarina* MF28, showed the fastest growth rates, with doubling times between 4.7 and 4.8 h, respectively (**Table 3**). This is most likely because the resident environment of these isolates provides a rich food supply, which facilitates their rapid growth and survival. Conversely, as is expected, the *P. aeruginosa* strain 55 isolated from the oligotrophic WC displayed the slowest doubling time (approximately 22 h), substantially longer than the other isolates (**Figure 5**). It appears that some of the isolated strains possess good catabolic potentials as compared with others reported previously; for example, Subathra et al. (2013) isolated 113 crude oil degrading S bacteria out of which 15 isolates were grown in BH media with 1% crude oil; gravimetric biodegradation loss was found highest at 55% by *P. aeruginosa* I5 isolate after 60 days of incubation. As compared to the previously isolated strain of *P. aeruginosa* I5, the *P. aeruginosa* strain WC55 isolated in this study was found to degrade 42% of Gulf crude oil in just over 7 days (see below), indicating its potent catabolic potential.

Moreover, the growth experiment data was analyzed by one-way ANOVA, which revealed that significant differences ( $P = 0.001$ ) existed between the growth rate of water-associated bacteria and those isolated from the OT, S, and the MF. This again, most likely reflects to the rich array of nutrient sources that are typically encountered in S and the oyster biome.

#### OIL-DEGRADATION ABILITY OF THE ISOLATED BACTERIA

The percentage of crude oil lost abiotically and via microbially mediated mineralization processes is summarized in **Table 3**. *P. aeruginosa* strain WC55, which displayed the slowest doubling

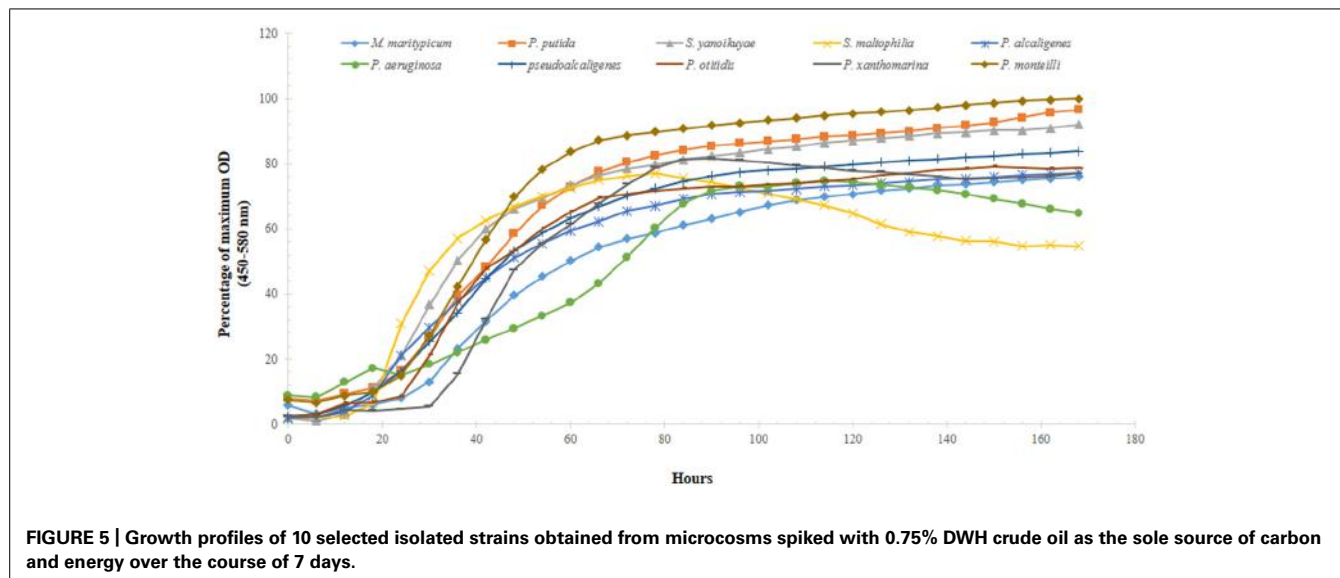


**FIGURE 5 |** Growth profiles of 10 selected isolated strains obtained from microcosms spiked with 0.75% DWH crude oil as the sole source of carbon and energy over the course of 7 days.

**Table 3 |** Growth kinetics and oil degradation abilities of nine selected strains isolated from oyster tissue (OT), mantle fluid (MF), water column (WC), and sediment (S) samples obtained from Dry Bar, Apalachicola Bay, FL, USA.

Isolated strains	Maximum OD <sub>450–580</sub>	Average doubling time (h)	Oil loss (g)	Bacterial oil consumption (%)
Control	NA	NA	26.8 ± 0.6	NA
<i>P. monteili</i> (MF17)	1.2 ± 0.02	8.0 ± 1.3	59 ± 1.6	32.2 ± 1.7
<i>P. xanthomarina</i> (MF28)	1.0 ± 0.01	4.7 ± 0.8	64.1 ± 4.0	37.2 ± 4.07
<i>P. pseudoalcaligenes</i> (S52)	1.0 ± 0.01	8.7 ± 0.5	64.9 ± 10.9	38 ± 10.9
<i>P. aeruginosa</i> (W55)	0.9 ± 0.04	21.9 ± 0.4	69.6 ± 2.7	42.7 ± 2.7
<i>P. alcaligenes</i> (OT69)	0.9 ± 0.03	4.8 ± 0.1	58.1 ± 10.6	31.2 ± 10.7
<i>Stenotrophomonas maltophilia</i> (MF89)	0.9 ± 0.05	5.5 ± 3.7	64.7 ± 3.1	37.8 ± 3.2
<i>Sphingobium yanoikuyae</i> (S94)	1.1 ± 0.01	4.6 ± 1.7	38.9 ± 8.6	12.0 ± 8.6
<i>P. putida</i> (OT107)	1.1 ± 0.06	9.5 ± 1.1	40.2 ± 9.6	13.3 ± 9.6
<i>Microbacterium maritypicum</i> (MF109)	0.9 ± 0.07	7.8 ± 0.8	64.6 ± 1.5	37.8 ± 1.6

time relative to the other isolated strains, showed the highest utilization of crude oil (~42%). It seems likely that this WC - associated bacteria preferentially utilizes hydrocarbon fractions that are most abundant in Gulf crude oil, such as aliphatics C6–C35 (Kostka et al., 2011). Thus, despite of its slow growth, it preferentially and rapidly metabolized the predominant DWH oil fractions. In fact, we recently reported the whole genome sequence of *P. aeruginosa* WC55 compared with other four isolates, namely, *P. alcaligenes* OT69, *P. stutzeri* MF28, *Stenotrophomonas maltophilia* MF89, and *Microbacterium maritypicum* MF109, which confirmed the presence of as many as 958 putative genes for xenobiotic degradation and metabolism in strain WC55, which explains its higher (42%) biodegradation rate of DWH oil relative to other isolates. The other sequenced strains were found to contain lower numbers of putative xenobiotic and metabolism genes, which suggests that *P. aeruginosa* strain WC55 along with *P. alcaligenes* OT69, isolated from the oyster reef WC and OT possess good catabolic versatility (Chauhan et al., 2013).

*P. pseudoalcaligenes*, isolated from the S, achieved slightly higher degradation than *P. aeruginosa* at approximately 45% (Table 3). Several other isolated strains such as, *P. otitidis*, *P. monteili*, *P. alcaligenes*, *Stenotrophomonas maltophilia*, *Microbacterium maritypicum*, and *P. xanthomarina* showed almost similar biodegradation potentials within the range of 32–40%. Surprisingly, under the assay conditions, *P. putida*, which is a well-characterized hydrocarbon-degrader, consumed on an average 50% less oil relative to the other isolates. These oil degradation rates, however, should be interpreted with caution because it remains to be shown whether the isolated oyster-associated microbiota degraded Gulf crude oil individually or that mineralization occurs through assemblages of biodegradative consortia.

## CONCLUSIONS AND ECOLOGICAL IMPACT OF THIS STUDY

Gulf of Mexico oysters are prized for their economic value. Not only are oysters a valuable commodity as seafood; but oyster reefs provide a variety of ecosystem services including critical habitats for commercial fisheries, water filtration, and removal

of excess nutrients from estuarine environments (Raj, 2008; Roosi-Snook et al., 2010; Piehler and Smyth, 2011; Grabowski et al., 2012). The value of this habitat, however, can be greatly reduced by toxic oil discharges, such as those from the 2010 DWH oil spill blowout. Effective response to such large-scale contamination of the marine environments requires a rapid and precise assessment of disturbances caused to the ecosystem such that timely mitigation strategies can be implemented. In this regard, biodegradative bacteria, as those identified from this and previous studies can significantly contribute to degradation of oil contaminants and rehabilitation of the perturbed environments. For example, stimulation of biodegradative communities within an impacted oyster reef ecosystem might be a potential remediation strategy to enhance cleanup and restoration efforts. However, baseline analyses of the oyster microbiome, which remains largely under-studied, are needed to develop successful approaches to problems of contamination of oyster reefs by petroleum and other hydrocarbons.

## ACKNOWLEDGMENTS

Funding for this study was provided by the Woodrow Wilson Foundation Doris Duke Conservation Fellowship. Partial funding was obtained from Department of Defense (DoD) grants W911NF-10-1-0146 and W911NF-10-R-0006; National Science Foundation's Historically Black Colleges and Universities Research Infrastructure for Science and Engineering (HBCU-RISE) initiative grant (No. 0531523); and United States Department of Education's Title III program. This work was also partially supported by cooperative agreement NA06OAR4810164 between NOAA's Educational Partnership Program and the Environmental Cooperative Science Center. We thank Florida State University professors- Dr. Joel Kotska and Dr. Markus Huettel for providing the BP Crude Oil used in this study. We also thank Megan Lamb for help in sample collection.

## REFERENCES

- Aitken, C. M., Jones, D., and Larter, S. (2004). Anaerobic hydrocarbon biodegradation in deep subsurface oil reservoirs. *Nature* 431, 291–294. doi: 10.1038/nature02922
- Anderson, M. J., and Robinson, J. (2003). Generalized discriminant analysis based on distances. *Austr. N. Z. J. Stat.* 45, 301–318. doi: 10.1111/1467-842X.00285
- Anderson, M. J., and Willis, T. J. (2003). Canonical analysis of principal coordinates: a useful method of constrained ordination for ecology. *Ecology* 84, 511–525. doi: 10.1890/0012-9658(2003)084[0511:CAOPCA]2.0.CO;2
- Brown, M. V., Schwalbach, M. S., Hewson, I., and Fuhrman, J. A. (2005). Coupling 16S-ITS rDNA clone libraries and automated ribosomal intergenic spacer analysis to show marine microbial diversity: development and application to a time series. *Environ. Microbiol.* 7, 1466–1479. doi: 10.1111/j.1462-2920.2005.00835.x
- Bushnell, L., and Haas, H. (1941). The utilization of certain hydrocarbons by microorganisms. *J. Bacteriol.* 41, 653–673.
- Campbell, M. S., and Wright, A. C. (2003). Real-time PCR analysis of *Vibrio vulnificus* from oysters. *Appl. Environ. Microbiol.* 69, 7137–7144. doi: 10.1128/AEM.69.12.7137-7144.2003
- Cao, R., Xue, C.-H., Liu, Q., and Xue, Y. (2009). Microbiological, chemical, and sensory assessment of Pacific Oysters (*Crassostrea gigas*) stored at different temperatures. *Czech J. Food Sci.* 27, 102–108.
- Cardinale, M., Brusetti, L., Quatrini, P., Borin, S., Puglia, A. M., Rizzi, A., et al. (2004). Comparison of different primer sets for use in automated ribosomal intergenic spacer analysis of complex bacterial communities. *Appl. Environ. Microbiol.* 70, 6147–6156. doi: 10.1128/AEM.70.10.6147-6156.2004
- Chauhan, A., Cherrier, J., and Williams, H. N. (2009). Impact of sideways and bottom-up control factors on bacterial community succession over a tidal cycle. *Proc. Natl. Acad. Sci. U.S.A.* 106, 4301–4306. doi: 10.1073/pnas.0809671106
- Chauhan, A., Green, S., Pathak, A., Thomas, J., and Venkatraman, R. (2013). Whole-genome sequences of five oyster-associated bacteria show potential for crude oil hydrocarbon degradation. *Genome Announc.* 1, e00802–e00813. doi: 10.1128/genomeA.00802-13
- Clark, L. L., Dajcs, J. J., McLean, C. H., Bartell, J. G., and Stroman, D. W. (2006). *Pseudomonas otitidis* sp. nov., isolated from patients with otic infections. *Int. J. Syst. Evolut. Microbiol.* 56, 709–714. doi: 10.1099/ijss.0.63753-0
- Colwell, R., and Liston, J. (1960). Microbiology of shellfish. Bacteriological study of the natural flora of Pacific oysters (*Crassostrea gigas*). *Appl. Microbiol.* 8, 104–109.
- Denton, M., and Kerr, K. G. (1998). Microbiological and clinical aspects of infection associated with *Stenotrophomonas maltophilia*. *Clin. Microbiol. Rev.* 11, 57–80.
- Dubinsky, E. A., Conrad, M. E., Chakraborty, R., Bill, M., Borglin, S. E., Hollibaugh, J. T., et al. (2013). Succession of hydrocarbon-degrading bacteria in the aftermath of the deepwater horizon oil spill in the gulf of Mexico. *Environ. Sci. Technol.* 47, 10860–10867. doi: 10.1021/es401676y
- French McCay, D. P., Peterson C. H., DeAlteris J. T., Catena J. (2003). Restoration that targets function as opposed to structure: replacing lost bivalve production and filtration. *Mar. Ecol. Prog. Ser.* 264, 197–212. doi: 10.3354/meps264197
- Galtsoff, P. (1964). The American oyster *Crassostrea virginica* Gmelin. *J. Exp. Mar. Biol. Ecol.* 64, 11–28.
- Grabowski, J. H., Brumbaugh, R. D., Conrad, R. F., Keeler, A. G., Opaluch, J. J., Peterson, C. H., et al. (2012). Economic valuation of ecosystem services provided by oyster reefs. *Bioscience* 62, 900–909. doi: 10.1525/bio.2012.62.10.10
- Greene, E. A., Kay, J. G., Jaber, K., Stehmeier, L. G., and Voordouw, G. (2000). Composition of soil microbial communities enriched on a mixture of aromatic hydrocarbons. *Appl. Environ. Microbiol.* 66, 5282–5289. doi: 10.1128/AEM.66.12.5282-5289.2000
- Gutierrez, T., Singleton, D. R., Berry, D., Yang, T., Aitken, M. D., and Teske, A. (2013). Hydrocarbon-degrading bacteria enriched by the Deepwater Horizon oil spill identified by cultivation and DNA-SIP. *ISME J.* 7, 2091–2104. doi: 10.1038/ismej.2013.98
- Hamamura, N., Olson, S. H., Ward, D. M., and Inskeep, W. P. (2005). Diversity and functional analysis of bacterial communities associated with natural hydrocarbon seeps in acidic soils at Rainbow Springs, Yellowstone National Park. *Appl. Environ. Microbiol.* 71, 5943–5950. doi: 10.1128/AEM.71.10.5943-5950.2005
- Haven, D. S., and Morales-Alamo, R. (1970). Filtration of particles from suspension by the American oyster *Crassostrea virginica*. *Biol. Bull.* 139, 248–264. doi: 10.2307/1540081
- Hazen, T. C., Dubinsky, E. A., DeSantis, T. Z., Andersen, G. L., Piceno, Y. M., Singh, N., et al. (2010). Deep-sea oil plume enriches indigenous oil-degrading bacteria. *Science* 330, 204–208. doi: 10.1126/science.1195979
- Henkel, J. R., Sigel, B. J., and Taylor, C. M. (2012). Large-scale impacts of the deepwater horizon oil spill: can local disturbance affect distant ecosystems through migratory shorebirds? *Bioscience* 62, 676–685. doi: 10.1525/bio.2012.62.7.10
- Jorgensen, C. B. (1990). *Bivalve Filter Feeding: Hydrodynamics, Bioenergetics, Physiology and Ecology*. Denmark: Olsen & Olsen.
- Kelly, M. T., and Dinuzzo, A. (1985). Uptake and clearance of *Vibrio vulnificus* from Gulf coast oysters (*Crassostrea virginica*). *Appl. Environ. Microbiol.* 50, 1548–1549.
- King, G. M., Judd, C., Kuske, C. R., and Smith, C. (2012). Analysis of stomach and gut microbiomes of the Eastern oyster (*Crassostrea virginica*) from Coastal Louisiana, USA. *PLoS ONE* 7:e51475. doi: 10.1371/journal.pone.0051475
- Kleinheinz, G., and Bagley, S. (1997). A filter-plate method for the recovery and cultivation of microorganisms utilizing volatile organic compounds. *J. Microbiol. Methods* 29, 139–144. doi: 10.1016/S0167-7012(97)00033-X
- Kostka, J. E., Prakash, O., Overholt, W. A., Green, S. J., Freyer, G., Canion, A., et al. (2011). Hydrocarbon-degrading bacteria and the bacterial community response in Gulf of Mexico beach sands impacted by the Deepwater Horizon oil spill. *Appl. Environ. Microbiol.* 77, 7962–7974. doi: 10.1128/AEM.05402-11
- Kueh, C. S. W., and Chan, K. (1985). Bacteria in bivalve shellfish with special reference to the oyster. *J. Appl. Microbiol.* 59, 41–47. doi: 10.1111/j.1365-2672.1985.tb01773.x

- Leifer, I., and MacDonald, I. (2003). Dynamics of the gas flux from shallow gas hydrate deposits: interactions between oily hydrate bubbles and the oceanic environment. *Earth Planet. Sci. Lett.* 210, 411–424. doi: 10.1016/S0012-821X(03)00173-0
- Livingston, R. J. (1984). *Ecology of the Apalachicola Bay System: An Estuarine Profile*. Tallahassee: Florida State University. doi: 10.5962/bhl.title.4039
- Livingston, R. J., Lewis, F. G., Woodsum, G. C., Niu, X.-F., Galperin, B., Hnuang, W., et al. (2000). Modeling oyster population response to variation in freshwater input. *Estuar. Coast. Shelf Sci.* 50, 655–672. doi: 10.1006/ecss.1999.0597
- Looper, J. K., Cotto, A., Kim, B. Y., Lee, M. K., Liles, M. R., Ní Chadhain, S. M., et al. (2013). Microbial community analysis of Deepwater Horizon oil-spill impacted sites along the Gulf coast using functional and phylogenetic markers. *Environ. Sci. Process. Impacts* 23;15, 2068–2079. doi: 10.1039/c3em00200d
- Lozupone, C., Hamady, M., and Knight, R. (2006). UniFrac—an online tool for comparing microbial community diversity in a phylogenetic context. *BMC Bioinformatics* 7:371. doi: 10.1186/1471-2105-7-371
- MacDonald, I. R., Leifer, I., Sassen, R., Stine, P., Mitchell, R., Guinasso, N. Jr. (2002). Transfer of hydrocarbons from natural seeps to the water column and atmosphere. *Geofluids* 2, 95–107. doi: 10.1046/j.1468-8123.2002.00023.x
- Mahasneh, A. M., and Al-Sayed, H. A. (1997). Seasonal incidence of some heterotrophic aerobic bacteria in Bahrain pelagic and nearshore waters and oysters. *Int. J. Environ. Stud.* 51, 301–312. doi: 10.1080/00207239708711088
- Margesin, R., and Schinner, F. (2001). Biodegradation and bioremediation of hydrocarbons in extreme environments. *Appl. Microbiol. Biotechnol.* 56, 650–663.
- Mitchell, R., MacDonald, I. R., and Kvienvolden, K. A. (1999). Estimation of total hydrocarbon seepage into the Gulf of Mexico based on satellite remote sensing images. *Trans. Am. Geophys. Union* 80(Ocean Sciences Meeting Supplement), OS242.
- Mojib, N., Trevors, J., and Bej, A. (2011). “Microbial biodegradative genes and enzymes in mineralization of non metal pollutants,” in *Microbial Bioremediation of Non-metals*, ed. A. Koukkou (Norfolk: Caister Academic Press), 217–232.
- Moat, A. G., and Foster, J. W. (1995). *Microbial Physiology*, 3rd Edn. New York: John Wiley & Sons, Inc., 96–197.
- Newman, M. C., and Unger, M. A. (2003). *Fundamentals of Ecotoxicology*, 2nd Edn. Boca Raton: Lewis Publisher, 458.
- Newton, I. L., Woyke, T., Auchtung, T. A., Dilly, G. F., Dutton, R. J., Fisher, M. C., et al. (2007). The *Calyptogena magnifica* chemoautotrophic symbiont genome. *Science* 315, 998–1000. doi: 10.1126/science.1138438
- Nixon, S. W. (1995). Coastal marine eutrophication: a definition, social causes, and future concerns. *Ophelia* 41, 199–219. doi: 10.1080/00785236.1995.10422044
- Paine, R. T., Ruesink, J. L., Sun, A., Soulani, E., Wonham, M. J., Harley, C. D. G., et al. (1996). Trouble on oiled waters: lessons from the Exxon Valdez oil spill. *Annu. Rev. Ecol. Syst.* 27, 197–235. doi: 10.1146/annurev.ecolsys.27.1.197
- Peix, A., Ramírez-Bahena, M., and Velázquez, E. (2009). Historical evolution and current status of the taxonomy of genus *Pseudomonas*. *Infect. Genet. Evol.* 9, 1132–1147. doi: 10.1016/j.meegid.2009.08.001
- Pekkarinen, M. (1997). Seasonal changes in calcium and glucose concentrations in different body fluids of *Anodonta anatina* (L) (Bivalvia: Unionidae). *Netherlands J. Zool.* 47, 31–45. doi: 10.1163/156854297X00229
- Peterson, B. J., and Heck, K. L. Jr. (1999). The potential for suspension feeding bivalves to increase seagrass productivity. *J. Exp. Mar. Biol. Ecol.* 240, 37–52. doi: 10.1016/S0022-0981(99)00040-4
- Peterson, C. H. (1991). Intertidal zonation of marine invertebrates in sand and mud. *Am. Sci.* 79, 236–249.
- Peterson, C. H. (2001). The ‘Exxon Valdez’ oil spill in Alaska: acute, indirect and chronic effects on the ecosystem. *Adv. Mar. Biol.* 39, 1–103 doi: 10.1016/S0065-2881(01)39008-9
- Peterson, C. H., Rice, S. D., Short, J. W., Esler, D., Bodkin, J. L., Ballachey, B. E., et al. (2003). Long-term ecosystem response to the Exxon Valdez oil spill. *Science* 302, 2082–2086. doi: 10.1126/science.1084282
- Piehler, M. F., and Smyth, A. R. (2011). Habitat-specific distinctions in estuarine denitrification affect both ecosystem function and services. *Ecosphere* 2. doi: 10.1890/ES10-0008.1
- Prieur, D., Mvel, G., Nicolas, J.-L., Plusquellec, A., and Vigneulle, M. (1990). Interactions between bivalve molluscs and bacteria in the marine environment. *Oceanogr. Mar. Biol. Annu. Rev.* 28, 277–352.
- Pujalte, M. J., Ortigosa, M., Macián, M. C., and Garay, E. (1999). Aerobic and facultative anaerobic heterotrophic bacteria associated to Mediterranean oysters and seawater. *Int. Microbiol.* 2, 259–266.
- Raj, P. S. (2008). Oysters in a new classification of keystone species. *Resonance* 13, 648–654. doi: 10.1007/s12045-008-0071-4
- Redmond, M. C., and Valentine, D. L. (2012). Natural gas, and temperature structured a microbial community response to the Deepwater Horizon oil spill. *Proc. Natl. Acad. Sci. U.S.A.* 109, 20292–20297. doi: 10.1073/pnas.1108756108
- Rodríguez-Verdugo, A., Souza, V., Eguiarte, L. E., and Escalante, A. E. (2012). Diversity across seasons of culturable *Pseudomonas* from a desiccation lagoon in Cuatro Cienegas, Mexico. *Int. J. Microbiol.* 2012, 201389. doi: 10.1155/2012/201389
- Romanenko, L. A., Uchino, M., Falsen, E., Lysenko, A. M., Zhukova, N. V., and Mikhailov, V. V. (2005). *Pseudomonas xanthomarina* sp. nov., a novel bacterium isolated from marine ascidian. *J. Gen. Appl. Microbiol.* 51, 65–71. doi: 10.2323/jgam.51.65
- Romero, J., Garcia-Varela, M., Laclette, J., and Espejo, R. T. (2002). Bacterial 16S rRNA gene analysis revealed that bacteria related to Arcobacter spp. constitute an abundant and common component of the oyster microbiota (*Tiostrea chilensis*). *Microb. Ecol.* 44, 365–371.
- Roosi-Snook, K., Ozbay, G., and Marenghi, F. (2010). Oyster (*Crassostrea virginica*) gardening program for restoration in Delaware’s Inland Bays, USA. *Aquac. Int.* 18, 61–67. doi: 10.1007/s10499-009-9271-5
- Sadok, S., Uglow, R. F., and Haswell, S. J. (1999). Some aspects of nitrogen metabolism in *Mytilus edulis*: effects of aerial exposure. *Mar. Biol.* 135, 297–305. doi: 10.1007/s002270050627
- Schippers, A., Bosecker, K., Spröer, C., and Schumann, P. (2005). *Microbacterium oleivorans* sp. nov. and *Microbacterium hydrocarbonoxydans* sp. nov., novel crude-oil-degrading Gram-positive bacteria. *Int. J. Syst. Evol. Microbiol.* 55, 655–660. doi: 10.1099/ijss.0.63305-0
- Schuler, L., Jouanneau, Y., Ní Chadhain, S. M., Meyer, C., Pouli, M., Zylstra, G. J., et al. (2009). Characterization of a ring-hydroxylating dioxygenase from phenanthrene-degrading *Sphingomonas* sp. strain LH128 able to oxidize benz (a) anthracene. *Appl. Microbiol. Biotechnol.* 83, 465–475. doi: 10.1007/s00253-009-1858-2
- Solomon, E. A., and Kastner, M., and MacDonald, I. R. (2009). Considerable methane fluxes to the atmosphere from hydrocarbon seeps in the Gulf of Mexico. *Nat. Geosci.* 2, 561–565. doi: 10.1038/ngeo574
- Subathra, M. K., Immanuel, G., Suresh, A. H. (2013). Isolation, and identification of hydrocarbon degrading bacteria from Ennore creek. *Bioinformation* 9, 150–157. doi: 10.6026/97320630009150
- Takeuchi, M., and Hatano, K. (1998). Proposal of six new species in the genus *Microbacterium* and transfer of *Flavobacterium marinotypicum* ZoBell and Upham to the genus *Microbacterium* as *Microbacterium marinotypicum* comb. nov. *Int. J. Syst. Bacteriol.* 48, 973–982. doi: 10.1099/00207713-48-3-973
- Tamura, K., Stecher, G., Peterson, D., Filipski, A., and Kumar, S. (2013). MEGA6: molecular evolutionary genetics analysis version 6.0. *Mol. Biol. Evol.* 30, 2725–2729. doi: 10.1093/molbev/mst197
- Trabal, N., Mazón-Suárez, J. M., Vázquez-Juárez, R., Asencio-Valle, F., Morales-Bojórquez, E., and Romero, J. (2012). Molecular analysis of bacterial microbiota associated with oysters (*Crassostrea gigas* and *Crassostrea corteziensis*) in different growth phases at two cultivation sites. *Microb. Ecol.* 64, 555–569. doi: 10.1007/s00248-012-0039-5
- United States Energy Information Administration (US-EIA). (2011a). *How Much Oil Does the United States Consumer Per Year?* Available at: <http://205.254.135.7/tools/faqs/faq.cfm?id=33&t=6>.
- United States Energy Information Administration (US-EIA). (2011b). *Short-Term Energy Outlook*. Available at: <http://www.eia.gov/forecasts/steo/outlook.cfm> (accessed July 12, 2011).
- Whitehead, A., Dubansky, B., Bodinier, C., Garcia, T. I., Miles, S., Pilley, C., et al. (2012). Genomic and physiological footprint of the Deepwater Horizon oil spill on resident marsh fishes. *Proc. Natl. Acad. Sci. U.S.A.* 109, 20298–20302. doi: 10.1073/pnas.1109545108
- Zurel, D., Benayahu, Y., Or, A., Kovacs, A., and Gophna, U. (2011). Composition and dynamics of the gill microbiota of an invasive Indo-Pacific oyster

in the eastern Mediterranean Sea. *Environ. Microbiol.* 13, 1467–1476. doi: 10.1111/j.1462-2920.2011.02448.x

**Conflict of Interest Statement:** The authors declare that the research was conducted in the absence of any commercial or financial relationships that could be construed as a potential conflict of interest.

Received: 21 November 2013; accepted: 20 March 2014; published online: 09 April 2014.

Citation: Thomas JC IV, Wafula D, Chauhan A, Green SJ, Gragg R and Jagoe C (2014) A survey of deepwater horizon (DWH) oil-degrading bacteria from the

Eastern oyster biome and its surrounding environment. *Front. Microbiol.* 5:149. doi: 10.3389/fmicb.2014.00149

This article was submitted to Aquatic Microbiology, a section of the journal Frontiers in Microbiology.

Copyright © 2014 Thomas, Wafula, Chauhan, Green, Gragg and Jagoe. This is an open-access article distributed under the terms of the Creative Commons Attribution License (CC BY). The use, distribution or reproduction in other forums is permitted, provided the original author(s) or licensor are credited and that the original publication in this journal is cited, in accordance with accepted academic practice. No use, distribution or reproduction is permitted which does not comply with these terms.



# Marine coastal sediments microbial hydrocarbon degradation processes: contribution of experimental ecology in the omics'era

**Cristiana Cravo-Laureau and Robert Duran\***

Equipe Environnement et Microbiologie UMR IPREM 5254, Université de Pau et des Pays de l'Adour, Pau, France

**Edited by:**

Ian M. Head, Newcastle University, UK

**Reviewed by:**

Kathleen Scott, University of South Florida, USA

Guang Gao, Nanjing Institute of Geography and Limnology, China

**\*Correspondence:**

Robert Duran, Equipe Environnement et Microbiologie, Université de Pau et des Pays de l'Adour, IPREM UMR CNRS 5254, BP 1155, 64013 Pau Cedex, France  
e-mail: robert.duran@univ-pau.fr

Coastal marine sediments, where important biological processes take place, supply essential ecosystem services. By their location, such ecosystems are particularly exposed to human activities as evidenced by the recent Deepwater Horizon disaster. This catastrophe revealed the importance to better understand the microbial processes involved on hydrocarbon degradation in marine sediments raising strong interests of the scientific community. During the last decade, several studies have shown the key role played by microorganisms in determining the fate of hydrocarbons in oil-polluted sediments but only few have taken into consideration the whole sediment's complexity. Marine coastal sediment ecosystems are characterized by remarkable heterogeneity, owning high biodiversity and are subjected to fluctuations in environmental conditions, especially to important oxygen oscillations due to tides. Thus, for understanding the fate of hydrocarbons in such environments, it is crucial to study microbial activities, taking into account sediment characteristics, physical-chemical factors (electron acceptors, temperature), nutrients, co-metabolites availability as well as sediment's reworking due to bioturbation activities. Key information could be collected from *in situ* studies, which provide an overview of microbial processes, but it is difficult to integrate all parameters involved. Microcosm experiments allow to dissect in-depth some mechanisms involved in hydrocarbon degradation but exclude environmental complexity. To overcome these lacks, strategies have been developed, by creating experiments as close as possible to environmental conditions, for studying natural microbial communities subjected to oil pollution. We present here a review of these approaches, their results and limitation, as well as the promising future of applying "omics" approaches to characterize in-depth microbial communities and metabolic networks involved in hydrocarbon degradation. In addition, we present the main conclusions of our studies in this field.

**Keywords:** **microcosm, mesocosm, molecular ecology, intertidal sediments, experimental ecology, omic's approaches**

## INTRODUCTION

Since Amoco Cadiz oil spill in 1978, many other oil spills such as Exxon Valdez (1989), Erika (1999), Prestige (2002), Deepwater Horizon (DH, 2010) have occurred in marine ecosystems. Such oil spill catastrophes generate a lot of indignation among the human populations, especially in coastal areas where environmental injuries are obvious. Cleanup efforts are urgently implemented in order to mitigate the toxic impact of petroleum compounds on the environment. However, the complete recovery of the ecosystem functioning is difficult to achieve because our knowledge on microbial communities, main actors involved in biodegradation processes, is still limited. The main issues regarding marine oil pollution have been already discussed (for review, see McGenity et al., 2012), and microbial processes involved on hydrocarbon degradation extensively described (Timmis et al., 2010; McGenity, 2014). However coastal marine sediments constitute particular ecosystems, especially intertidal zones where environmental conditions are daily modified according to tide level that in turn drive microbial degradation processes (**Figure 1A**). Although

the impact of petroleum on microbial communities resulting in ecological succession, modifications of microbial populations following the hydrocarbon degradation, has been largely demonstrated (Harayama et al., 2004; Bordenave et al., 2004, 2007; Head et al., 2006; Païssé et al., 2008; Nogales et al., 2011) several scientific ecological questions remains to be solved. Among these questions, the organization of microbial community structures facing the presence of spilled oil, the mechanisms involved in their adaptation conducting to efficient hydrocarbon degradation, the structure/function relationship and the contribution of functional redundancy to microbial community resilience are some of the current burning questions which responses, at the applied point of view, will help to conduct appropriate bioremediation strategies such as bio-augmentation and bio-stimulation. The presence of a pollutant, such as petroleum, in the environment highlights also the importance to address academic concerns in microbial ecology, contributing more generally to the ecological theory. The importance to apply theory in microbial ecology has been emphasized by Prosser et al. (2007), especially for addressing population ecology,

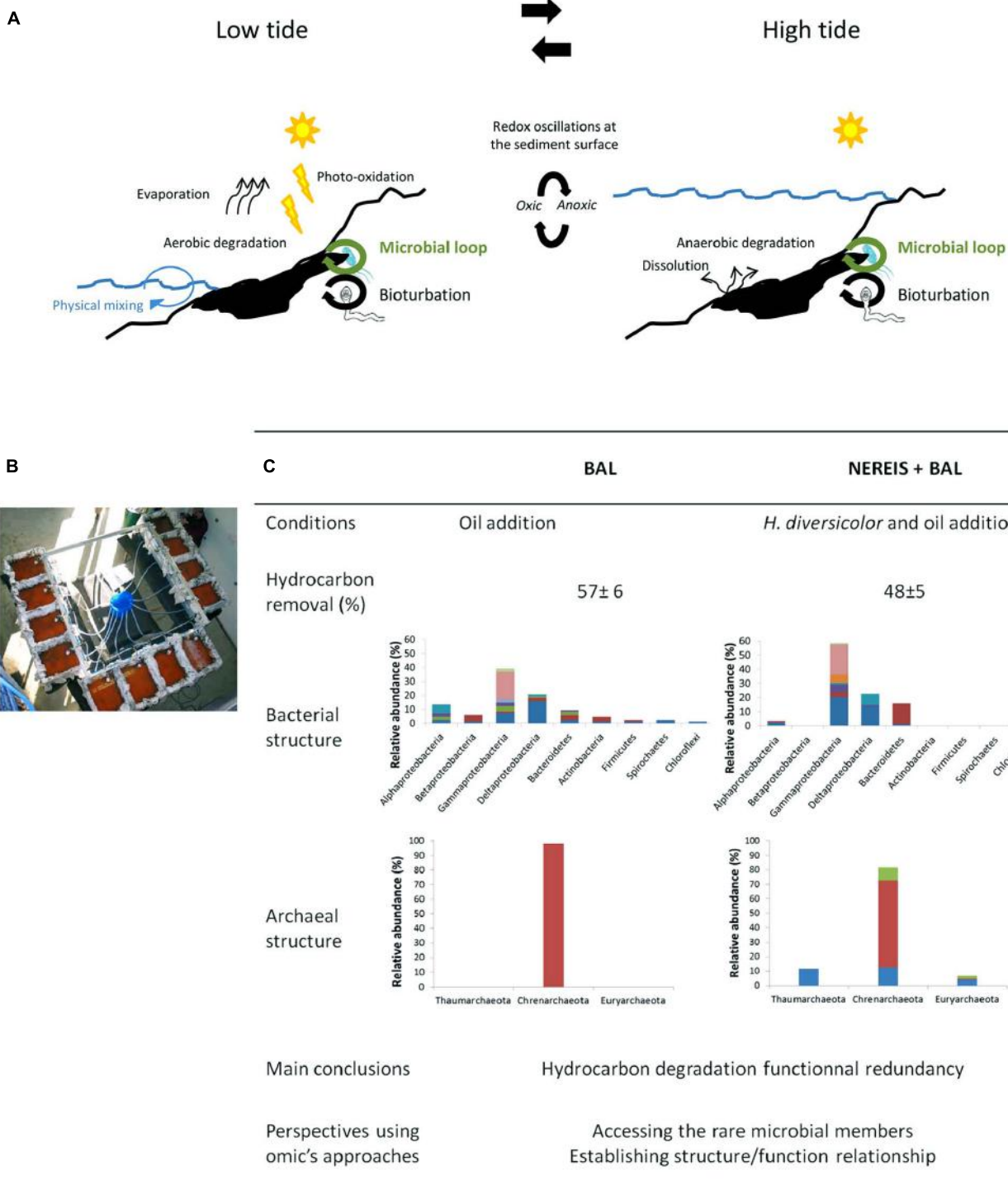


**FIGURE 1 | Mimicking environmental conditions in experimental ecology.** (A) Schematic overview of the main abiotic and biotic mechanisms determining the fate of hydrocarbons in coastal marine sediments according to the tide level. At the intertidal zone, where redox conditions oscillate at the sediments' surface, microbial communities alternate aerobic and anaerobic hydrocarbon degradation processes. Bioturbation processes by macrofauna include sediments reworking, oil burying, and micro-scale oxygen oscillations into the sediments. The microbial loop is controlled by top-down (predation by

grazers and viruses) and bottom-top (nutrients and carbon fluxes) processes. (B) Experimental device used to assess the effect of crude oil on bio-turbated intertidal marine sediments applying tide cycles. (C) Main results and conclusions comparing oil polluted sediments with (NEREIS+BAL) and without *H. diversicolor* addition (BAL) from Stauffert et al. (2013a,b). Bacterial and archaeal communities structures are based on sequences data from 16S rRNA gene transcripts libraries. Colors indicate OTU diversity within each phylum.

micro-organisms interactions, community assembly and the biodiversity-function relationships. Different approaches including *in situ* studies and laboratory experiments have been developed in order to test ecological hypothesis, decipher the role of microbial communities in the ecosystem functioning and understand the microbial behavior in front of a pollution. Microbial experimental systems have been particularly useful to address ecological questions by simplifying microbial systems and allowing experimental controls (see reviews by Jessup et al., 2004, 2005). Combined with the recent advances in meta-omics' technologies that provides powerful tools for analyzing microbial communities, their diversity and their functioning as a whole (for review, see Röling et al., 2010; Liu et al., 2013), such experimental microbial systems are promising approaches to gain new insights on functional networks involved in hydrocarbon degradation processes in marine coastal sediments. We review here the recent progress on the ecology of microbial communities involved on hydrocarbon degradation in marine coastal sediments, attained by both *in situ* and experimental approaches. We present the main conclusions on our work in this field indicating the convenience of using experimental ecology to improve our knowledge in hydrocarbon microbial ecology.

### **IN SITU MICROBIAL ECOLOGY IN COASTAL MARINE POLLUTED SEDIMENTS**

Opening the microbial black box involved in hydrocarbon degradation needs to take into consideration the whole ecosystem. *In situ* studies allow to reach the entire microbial communities in their actual context, considering (biotic and abiotic) ecological interactions. Over the past few years, field studies have been performed in marine sediments addressing the impact of oil on microbial communities, by following their organization and/or by characterizing their composition. In most cases this has been approached by spatial comparisons of contrasting contaminated and uncontaminated sites (El-Tarabily, 2002; Miralles et al., 2007, 2010); or sites with different oil contents (LaMontagne et al., 2004; Dias et al., 2011; Iannelli et al., 2012; Kimes et al., 2013). In this way, following the bacterial diversity of oil-polluted retention basin sediments from the Berre lagoon (France) through nine stations, we have demonstrated that bacterial community structure was associated with the gradient of oil contamination (Païssé et al., 2008). Nevertheless, the adaptation of the bacterial community to oil contamination was not characterized by the dominance of oil-degrading bacteria, but a predominance of bacterial populations associated to the sulfur cycle was observed. Other *in situ* studies have highlighted the presence or the role of sulfur cycle microorganisms in oil-polluted coastal marine sediments, with a focus on sulfate-reducing bacteria (Rosano-Hernandez et al., 2012; Acosta-González et al., 2013). Andrade et al. (2012) suggested that sulfate-reducers constitute a large fraction of the bacteria present in oil-contaminated mangrove sediment. They also demonstrated that abundance of sulfate-reducers decrease with depth and showed greater bacterial abundance and diversity in top layers (0–5 cm) than in deeper layers (below 15 cm). Similarly, Acosta-González et al. (2013), applying culture-dependent and molecular techniques to characterize the bacterial populations after the Prestige oil spill at two sampling times (2004 and

2007), reported the dominance of sulfate-reducing bacteria in oil-polluted sediments. Sulfate reduction was the predominant type of respiration connected to hydrocarbon oxidative capacities, and sulfate-reducing bacteria constituted the prevalent populations (being maximal at 12–15 cm depth). These studies emphasized the ecological importance of sulfate-reducers in oil-polluted marine sediments. Sulfate-reducing microorganisms are known to play a key role in coastal marine ecosystems by recycling the organic matter (Jorgensen, 1982), even after an oil-spill. Acosta-González et al. (2013) also demonstrated that community structure was initially dominated by Gamma and Deltaproteobacteria (2004), while 3 years later, in 2007, the phylum Bacteroidetes was a main component of the community. These results, showing the great plasticity of bacterial community structures and suggesting that they were constantly adapting to the changing environmental factors, highlight the importance to consider the impact of environmental parameters on microorganisms when studying oil degradation in coastal marine sediments. In this way Kostka et al. (2011), considering spatial-temporal variations in oil-contaminated beach ecosystems, showed the selective response of bacterial communities to oil from the DH oil spill. Microbial communities were dominated by members of the Gammaproteobacteria and Alphaproteobacteria, suggested as key players in oil-degradation. These groups are constituted by hydrocarbon-degrading members, the former contributing to the early stages of oil hydrocarbon degradation (oxidizing more reactive components such as *n*-alkanes), and the latter contributing to the later stages of degradation (oxidizing more recalcitrant compounds such as PAHs). In the same way, examining microbial response to DH oil spill in coastal sediments, Horel et al. (2012) showed no seasonal differences in the abundances of total hydrocarbon and alkane degraders in marsh ecosystem with high physical-chemical parameters variations.

Different molecular approaches, mainly involving 16S rRNA gene analyses such as DGGE (LaMontagne et al., 2004; Al-Thukair et al., 2007; Dias et al., 2011; Andrade et al., 2012; Isaac et al., 2013) or T-RFLP (Edlund and Jansson, 2006; Païssé et al., 2008; Iannelli et al., 2012), clone libraries (LaMontagne et al., 2004; Miralles et al., 2007, 2010), and phylo/geochip (Beazley et al., 2012), were used to describe the microbial communities established in oil-polluted coastal environments. More recently, NGS and "omics" approaches have been applied, allowing to in-depth characterization of microbial communities (Kostka et al., 2011).

These studies allowed to assess the complexity of autochthonous microbial communities related to the oil pollution, revealing *in situ* changes in microbial diversity and their selective response to the presence of oil. Nevertheless, *in situ* approaches have many drawbacks since information access on ecophysiology of oil-degrading microorganisms, their activity and degradation pathways remain still limited.

### **EXPERIMENTAL ECOLOGY APPROACHES IN MARINE COASTAL SEDIMENTS STUDIES**

Experimental approaches have been developed to address the ecological role of microbial communities on hydrocarbon mitigation in marine sediments. These approaches have progressed as scientific questions arise with the concomitant advances of

microbial molecular ecology techniques. Enrichment cultures (or slurries), similar approaches to those used for microbial strains isolation, have been used to tackle the impact of crude oil and petroleum hydrocarbon compounds on bacterial communities. Usually, sediments are mixed with a minimal medium (more often artificial sea water) containing crude oil or selected hydrocarbon compounds, and maintained at laboratory under agitation. Following the dynamic modifications of microbial communities in the slurries, fingerprinting techniques and 16S rRNA gene libraries analyses have shown the ecological succession of microbial populations in response to hydrocarbon compounds in pristine deep marine sediments (Cui et al., 2008), mangrove sediments (dos Santos et al., 2011), polluted harbor marine sediments (Wang and Tam, 2011; Dell'Anno et al., 2012; Rocchetti et al., 2012) and anoxic zone of microbial mats (Abed et al., 2011). While such approaches were useful to estimate the microbial degradation capacities of hydrocarbon compounds (Cui et al., 2008; Abed et al., 2011), the efficiency of bioremediation strategies (Dell'Anno et al., 2012) and the early functional response involved on hydrocarbon degradation (Paisse et al., 2011; Païsse et al., 2012), the simplification of the microbial systems present some limitations. Among them, the destruction of the sediments' structure imposes a strong limit to extrapolation to complex systems where microorganisms interact each other and with surrounding organisms according to the structure and stratification of sediments. To overcome these limitations, microcosms maintaining intact the sediment structure have been developed. An elegant example is provided by studies undertaken to determine the impact of crude oil on microbial mats (Bordenave et al., 2004, 2007; Lliros et al., 2008). Microbial mats are vertically stratified structures where microbial populations take place according to micro-gradients of oxygen, sulfur and light at the water-sediment interface. Pieces of microbial mats are maintained in microcosms under diel light-dark cycle (16 h/8 h) to ensure the microbial stratification and then exposed to crude oil. Our studies with microbial mats from Camargue (France) demonstrated, by combining T-RFLP and 16S rRNA (gene and transcript) library analyses, the dynamic changes of microbial communities inhabiting microbial mats in response to *Erika* fuel with concomitant degradation of hydrocarbon compounds (Bordenave et al., 2004) and their resilience after 1 year exposure (Bordenave et al., 2007). Lliros et al. (2008) showed the versatility of such microbial communities by demonstrating that microbial communities had distinct behavior according to the type of crude oil using reconstituted microbial mats from the Ebro delta (Spain) maintained under tidal cycles without renewing water. Microbial mats constitute particular ecosystems relatively easy to maintain in microcosms under their initial stratification because they are ecosystems driven by phototrophic microorganisms that impose a selective pressure. In comparison, marine coastal sediments are more susceptible to the fluctuation of environmental parameters due to tide and waves. Thus, the environmental conditions in which they develop are more difficult to simulate. Experimental systems maintaining sediments with tide simulation such as sediment columns (Röling et al., 2002) and sediments maintained in aquarium (Taketani et al., 2010) allowed to determine the role of nutrients bio-stimulation treatments on

hydrocarbon-degradation efficiency and the impact of crude oil addition on adapted nitrogen fixation populations, respectively. But, because sediments were homogenized prior microcosms setting, these studies simulate mainly chemical-physical environmental parameters without addressing the impact of the other benthic organisms. In order to further maintain sediments as closer as possible to environmental parameters different strategies have been developed. Katayama et al. (2003) maintaining sediments in a tidal flat simulator, with a wave generator and a tide control device, identified oil-susceptible bacteria as bio-indicator of pollution by combining culture-dependent and molecular approaches. Suárez-Suárez et al. (2011) installed mesocosms *in situ* to assess the role of sulfate reducing bacteria in the degradation of Prestige oil. Similarly, Coulon et al. (2012), maintaining intact cores of coastal mudflat sediments in mesocosms under tidal cycles without renewing water, observed the development of phototrophic biofilm playing a crucial role in hydrocarbon degradation. They also demonstrated the negative effect of oil on the benthic macrofauna that in turn allowed the development of phototrophic biofilm (Chronopoulou et al., 2013). This observation highlights the importance to consider sediments as a whole ecosystem where microbial activities involved on hydrocarbon degradation are driven not only by the presence of contaminant but also by biotic and abiotic factors controlling the microbial web functioning. Appropriate experimental ecology approaches would be useful to decipher the mechanisms determining the organization of microbial communities with efficient hydrocarbon degradation capacities. In the next section we present the experimental approach developed in our lab to address the effect of the reworking activity of the benthic macrofauna (bioturbation) in structuring hydrocarbon-degrading microbial communities and the main results obtained.

## MIMICKING ENVIRONMENTAL CONDITIONS IN EXPERIMENTAL ECOLOGY

In intertidal zones, microbial degradation processes are driven by environmental conditions that are daily modified according to tide level (**Figure 1A**). An original microcosm (**Figure 1B**) system maintaining the structure of muddy sediments under tidal cycles was set up ensuring conditions close to those prevailing in the natural environment of coastal marine sediments (Stauffert et al., 2013a). Coastal marine sediments were sampled with a core collector, and transferred while maintaining their integrity into microcosm boxes. Tidal cycles were applied and natural seawater was renewed with each tidal cycle. The experimental design was drawn with the aim to test the hypothesis that the addition of polychaetes stimulates the bioturbation activity which in turn could select a particular microbial community with an increased biodegradation capability. The conditions applied were: (i) CTRL: control condition, (ii) BAL: oil addition, (iii) NEREIS: addition of *Hediste (Nereis) diversicolor* and (iv) NEREIS+BAL, addition of oil and *H. diversicolor*. Oil contamination was performed on the surface (2 cm top layer) after homogenization with sediments (BAL and NEREIS+BAL). *H. diversicolor* was added to the microcosms in order to increase sediments reworking (NEREIS and NEREIS+BAL). By following, over a 9-month period, the petroleum removal, the macrofaunal

reworking activity and the microbial communities' structures and compositions, we demonstrated that the modification of the microbial community structure in mudflat sediments after petroleum addition was dependent on the presence of the added burrowing polychaetes *H. diversicolor* (Stauffert et al., 2013a,b). Contrary to our initial hypothesis, despite that the addition of burrowing organisms stimulated the bioturbation activity and modified the microbial community structure, the overall oil removal capacity was not affected by the addition of polychaetes. For Bacteria (Figure 1C), although both BAL and NEREIS+BAL communities were dominated by Gamma- and Delta-proteobacteria, important differences were observed at the genus level. The BAL community showed more diversity with the presence of minor phyla and a slight increase of Alpha-proteobacteria (Stauffert et al., 2013a). For Archaea (Figure 1B), BAL community was represented only by Crenarchaeota MCG members while NEREIS+BAL community exhibited more diversity (Stauffert et al., 2013b). Thus, from an

initial microbial community two distinct communities showing a similar overall oil removal capacity were obtained. By adding burrowing organisms to sediments maintained near-environmental conditions we were able to manipulate microbial community structure and composition, opening the way for the study of the mechanisms underlying microbial community restructuring after environmental perturbations which includes resistance, resilience, and functional redundancy (Allison and Martiny, 2008). Combining metagenomic and metatranscriptomic analyses with metabolite profiling will provide valuable information to understand the mechanisms underpinning the bacterial communities structuring, particularly the role of the rare microbial members in the establishment of structure/function relationship. Such approach has demonstrated the influence of hydrocarbon compounds on the microbial community inhabiting the deep-sea sediments of the Gulf of Mexico after DH oil spill (Kimes et al., 2013). The application of correlation and co-occurrence analyzes from metagenomics and 16S bar-coding

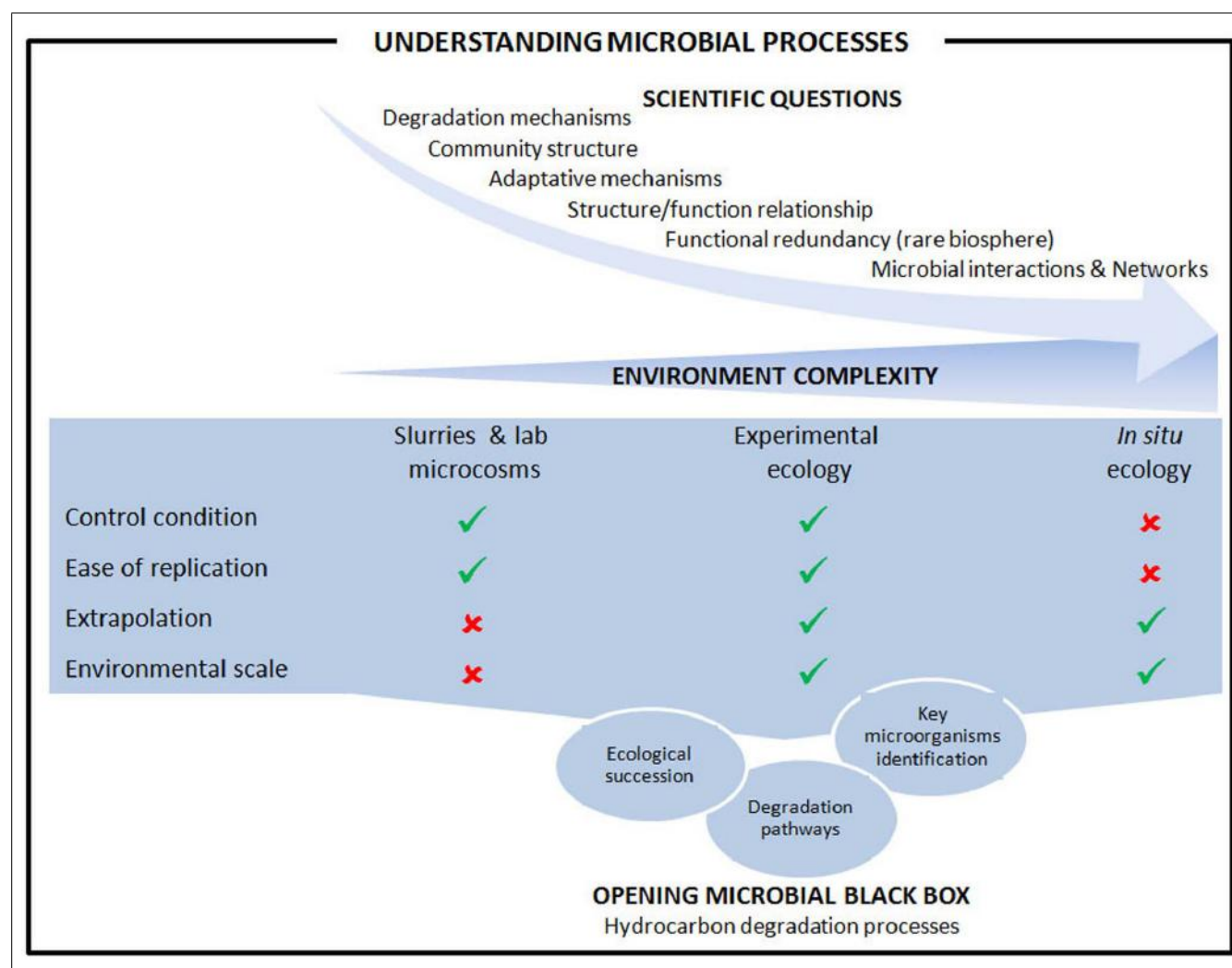


**FIGURE 2 | Understanding microbial processes involved on hydrocarbon degradation in marine coastal sediments.** The general scheme from scientific questions to microbial processes is presented together with the comparison of experimental approaches developed at different environmental complexity.

profiling, that allows to forecast microbial interactions and metabolic networks (Faust and Raes, 2012), to experimental systems may offer the possibility to gain in depth information on how microbial communities behave after a disturbance (Shade et al., 2010; Knight et al., 2012) and define a “core” community ensuring the basal ecosystem functioning. Experimental systems authorize comparative metatranscriptomics approaches (Bordeneave et al., 2009, 2010) that combined with high-throughput sequencing can provide the discovery of novel genes expressed during phytoplankton bloom with the possibility to explore the structure/function relationships (Gilbert et al., 2008). Another example of metatranscriptomic analysis is the identification of a set of genes, including hydrocarbon degradation, stress response and detoxification genes, induced after the environmental disturbance by phenanthrene in soil microcosms (de Menezes et al., 2012). The structure/function relationship can be further elucidated by metaproteomics, enabling the identification of proteins present in the community. The metaproteogenomic approach, that combine metagenomic and metaproteomic analyzes, allowed to describe the metabolism related to naphthalene degradation in soil by comparing four microbial communities maintained in microcosms (Guazzaroni et al., 2013). However, metaproteomics needs further development involving mass spectrometers with high sensitivity to access low abundant proteins (Zarraonaindia et al., 2013). Our microcosm system allows to propose an experimental ecology approach to determine how the fluctuation of environmental parameters, particularly oxygenation and redox oscillations resulting from the biological (bio-turbation) or mechanical (physical-turbation) reworking of the sediment, influence the coupling between bacterial functional groups and their degradation capacities.

## CONCLUDING REMARKS

We reviewed here recent approaches implemented in order to assess microbial processes involved on hydrocarbon degradation in marine coastal sediments. Microbiologists have developed several approaches, including more or less sophisticated experimental systems and *in situ* studies to answer the scientific questions regarding the microbial mechanisms that take place in response to oil and hydrocarbon contaminations. **Figure 2** summarize the main advantage and limitations for the approach considered in addressing the scientific questions. Experimental ecology using experimental systems mimicking as close as possible the environmental conditions combine the advantages of lab controlled systems with the possibility of extrapolation to the real situation found in complex ecosystems. Such approaches offer the opportunity to conduct experiments in replicates, crucial advantage for robust statistical analyses as highlighted by Prosser (2010). The advent of next generation sequencing technologies combined with high-throughput methods assessing functionality (proteomics and metabolomics) has allowed the development of systems biology, a holistic approach to understand complex biological systems. However, because the sediments’ ecology in coastal areas is extremely complex, analysis using system biology tools at different environmental scales would be useful to elucidate microbial hydrocarbon degradation processes.

## ACKNOWLEDGMENTS

This research was funded by the French National Agency (ANR) under the DHYVA (ANR 2006 SEST 09) and DECAPAGE (ANR 2011 CESA 006 01) projects. We would like to thank the CEDRE for the setup of the microcosms and all partners of the DHYVA and DECAPAGE project for their useful discussions. We acknowledge the Regional Platform for Environmental Microbiology PREMICE supported by the Aquitaine Regional Government Council (France).

## REFERENCES

- Abed, R. M. M., Musat, N., Musat, F., and Mußmann, M. (2011). Structure of microbial communities and hydrocarbon-dependent sulfate reduction in the anoxic layer of a polluted microbial mat. *Mar. Pollut. Bull.* 62, 539–546. doi: 10.1016/j.marpolbul.2010.11.030
- Acosta-González, A., Rosselló-Móra, R., and Marqués, S. (2013). Characterization of the anaerobic microbial community in oil-polluted subtidal sediments: aromatic biodegradation potential after the Prestige oil spill. *Environ. Microbiol.* 15, 77–92. doi: 10.1111/j.1462-2920.2012.02782.x
- Allison, S. D., and Martin, J. B. H. (2008). Resistance, resilience, and redundancy in microbial communities. *Proc. Natl. Acad. Sci. U.S.A.* 105, 11512–11519. doi: 10.1073/pnas.0801925105
- Al-Thukair, A. A., Abed, R. M. M., and Mohamed, L. (2007). Microbial community of cyanobacteria mats in the intertidal zone of oil-polluted coast of Saudi Arabia. *Mar. Pollut. Bull.* 54, 173–179. doi: 10.1016/j.marpolbul.2006.08.043
- Andrade, L. L., Leite, D. C. A., Ferreira, E. M., Ferreira, L. Q., Paula, G. R., Maguire, M. J., et al. (2012). Microbial diversity and anaerobic hydrocarbon degradation potential in an oil-contaminated mangrove sediment. *BMC Microbiol.* 12:186. doi: 10.1186/1471-2180-12-186
- Beazley, M. J., Martinez, R. J., Rajan, S., Powell, J., Piceno, Y. M., Tom, L. M., et al. (2012). Microbial community analysis of a coastal salt marsh affected by the deep-water horizon oil spill. *PLoS ONE* 7:e41305. doi: 10.1371/journal.pone.0041305
- Bordenave, S., Fourcans, A., Blanchard, S., Goni-Urriza, M. S., Caumette, P., and Duran, R. (2004). Structure and functional analyses of bacterial communities changes in microbial mats following petroleum exposure. *Ophelia* 58, 195–203. doi: 10.1080/00785236.2004.10410227
- Bordenave, S., Goñi-Urriza, M., Caumette, P., and Duran, R. (2009). Differential display analysis of cdna involved in microbial mats response after heavy fuel oil contamination. *J. Microb. Biochem. Technol.* 1, 1–4. doi: 10.4172/1948-5948.1000001
- Bordenave, S., Goñi-Urriza, M. S., Caumette, P., and Duran, R. (2007). Effects of heavy fuel oil on the bacterial community structure of a pristine microbial mat. *Appl. Environ. Microbiol.* 73, 6089–6097. doi: 10.1128/AEM.01352-07
- Bordenave, S., Goñi-Urriza, M. S., and Duran, R. (2010). “Assessing functionality by differential display and RNA arbitrary PCR,” in *Handbook of Hydrocarbon and Lipid Microbiology*, ed. K. N. Timmis (Heidelberg: Springer-Verlag ), 4051–4061. doi: 10.1007/978-3-540-77587-4\_315
- Chronopoulou, P. M., Fahy, A., Coulon, F., Païssé, S., Goñi Urriza, M., Acuña Alvarez, L., et al. (2013). Impact of a simulated oil spill on benthic phototrophs and nitrogen-fixing bacteria in mudflat mesocosms. *Environ. Microbiol.* 15, 242–252. doi: 10.1111/j.1462-2920.2012.02864.x
- Coulon, F., Chronopoulou, P.-M., Fahy, A., Sandrine, P., Goñi-Urriza, M., Peperzak, L., et al. (2012). Central role of dynamic tidal biofilms dominated by aerobic hydrocarbonoclastic bacteria and diatoms in the biodegradation of hydrocarbons in coastal mudflats. *Appl. Environ. Microbiol.* 78, 3638–3648. doi: 10.1128/AEM.00072-12
- Cui, Z. S., Lai, Q. L., Dong, C. M., and Shao, Z. Z. (2008). Biodiversity of polycyclic aromatic hydrocarbon-degrading bacteria from deep sea sediments of the Middle Atlantic Ridge. *Environ. Microbiol.* 10, 2138–2149. doi: 10.1111/j.1462-2920.2008.01637.x
- Dell’Anno, A., Beolchini, F., Rocchetti, L., Luna, G. M., and Danavaro, R. (2012). High bacterial biodiversity increases degradation performance of hydrocarbons during bioremediation of contaminated harbor marine sediments. *Environ. Pollut.* 167, 85–92. doi: 10.1016/j.envpol.2012.03.043
- de Menezes, A., Clipson, N., and Doyle, E. (2012). Comparative metatranscriptomics reveals widespread community responses during phenanthrene degradation

- in soil. *Environ. Microbiol.* 14, 2577–2588. doi: 10.1111/j.1462-2920.2012.02781.x
- Dias, A. C. F., Dini-Andreote, F., Taketani, R. G., Tsai, S. M., Azevedo, J. L., De Melo, I. S., et al. (2011). Archaeal communities in the sediments of three contrasting mangroves. *J. Soils Sediments* 11, 1466–1476. doi: 10.1007/s11368-011-0423-7
- dos Santos, H. F., Cury, J. C., Do Carmo, F. L., Dos Santos, A. L., Tiedje, J., Van Elsas, J. D., et al. (2011). Mangrove bacterial diversity and the impact of oil contamination revealed by pyrosequencing: bacterial proxies for oil pollution. *PLoS ONE* 6:e16943. doi: 10.1371/journal.pone.0016943
- Edlund, A., and Jansson, J. K. (2006). Changes in active bacterial communities before and after dredging of highly polluted Baltic Sea sediments. *Appl. Environ. Microbiol.* 72, 6800–6807. doi: 10.1128/AEM.00971-06
- El-Tarabily, K. A. (2002). Total microbial activity and microbial composition of a mangrove sediment are reduced by oil pollution at a site in the Arabian Gulf. *Can. J. Microbiol.* 48, 176–182. doi: 10.1139/w01-140
- Faust, K., and Raes, J. (2012). Microbial interactions: from networks to models. *Nat. Rev. Microbiol.* 10, 538–550. doi: 10.1038/nrmicro2832
- Gilbert, J. A., Field, D., Huang, Y., Edwards, R., Li, W. Z., Gilna, P., et al. (2008). Detection of large numbers of novel sequences in the metatranscriptomes of complex marine microbial communities. *PLoS ONE* 3:e3042. doi: 10.1371/journal.pone.0003042
- Guazzaroni, M. E., Herbst, F. A., Lores, I., Tamames, J., Pelaez, A. I., Lopez-Cortes, N., et al. (2013). Metaproteogenomic insights beyond bacterial response to naphthalene exposure and bio-stimulation. *ISME J.* 7, 122–136. doi: 10.1038/ismej.2012.82
- Harayama, S., Kasai, Y., and Hara, A. (2004). Microbial communities in oil-contaminated seawater. *Curr. Opin. Biotechnol.* 15, 205–214. doi: 10.1016/j.copbio.2004.04.002
- Head, I. M., Jones, D. M., and Röling, W. F. (2006). Marine microorganisms make a meal of oil. *Nat. Rev. Microbiol.* 4, 173–182. doi: 10.1038/nrmicro1348
- Horel, A., Mortazavi, B., and Sobecky, P. A. (2012). Seasonal monitoring of hydrocarbon degraders in Alabama marine ecosystems following the deepwater horizon oil spill. *Water Air Soil Poll.* 223, 3145–3154. doi: 10.1007/s11270-012-097-5
- Iannelli, R., Bianchi, V., Macci, C., Peruzzi, E., Chiellini, C., Petroni, G., et al. (2012). Assessment of pollution impact on biological activity and structure of seabed bacterial communities in the Port of Livorno (Italy). *Sci. Total Environ.* 426, 56–64. doi: 10.1016/j.scitotenv.2012.03.033
- Isaac, P., Sanchez, L. A., Bourguignon, N., Cabral, M. E., and Ferrero, M. A. (2013). Indigenous PAH-degrading bacteria from oil-polluted sediments in Caleta Corova, Patagonia Argentina. *Int. Biodeterior. Biodegradation* 82, 207–214. doi: 10.1016/j.ibiod.2013.03.009
- Jessup, C. M., Forde, S. E., and Bohannan, B. J. M. (2005). Microbial experimental systems in ecology. *Adv. Ecol. Res.*, 37, 273–307. doi: 10.1016/S0065-2504(04)37009-1
- Jessup, C. M., Kassen, R., Forde, S. E., Kerr, B., Buckling, A., Rainey, P. B., et al. (2004). Big questions, small worlds: microbial model systems in ecology. *Trends Ecol. Evol.* 19, 189–197. doi: 10.1016/j.tree.2004.01.008
- Jorgensen, B. B. (1982). Mineralization of organic matter in the sea bed[mdash]the role of sulphate reduction. *Nature* 296, 643–645. doi: 10.1038/296643a0
- Katayama, Y., Oura, T., Iizuka, M., Orita, I., Cho, K. J., Chung, I. Y., et al. (2003). Effects of spilled oil on microbial communities in a tidal flat. *Mar. Pollut. Bull.* 47, 85–90. doi: 10.1016/S0025-326X(03)00103-6
- Kimes, N. E., Callaghan, A. V., Aktas, D. F., Smith, W. L., Sunner, J., Golding, B. T., et al. (2013). Metagenomic analysis and metabolite profiling of deep-sea sediments from the Gulf of Mexico following the Deepwater Horizon oil spill. *Front. Microbiol.* 4:50. doi: 10.3389/fmicb.2013.00050
- Knight, R., Jansson, J., Field, D., Fierer, N., Desai, N., Fuhrman, J. A., et al. (2012). Unlocking the potential of metagenomics through replicated experimental design. *Nat. Biotechnol.* 30, 513–520. doi: 10.1038/nbt.2235
- Kostka, J. E., Prakash, O., Overholt, W. A., Green, S. J., Freyer, G., Canion, A., et al. (2011). Hydrocarbon-degrading bacteria and the bacterial community response in gulf of Mexico beach sands impacted by the deepwater horizon oil spill. *Appl. Environ. Microbiol.* 77, 7962–7974. doi: 10.1128/AEM.05402-11
- LaMontagne, M. G., Leifer, I., Bergmann, S., Van De Werfhorst, L. C., and Holden, P. A. (2004). Bacterial diversity in marine hydrocarbon seep sediments. *Environ. Microbiol.* 6, 799–808. doi: 10.1111/j.1462-2920.2004.00613.x
- Liu, D., Hoynes-O'connor, A., and Zhang, F. (2013). Bridging the gap between systems biology and synthetic biology. *Front. Microbiol.* 4:211. doi: 10.3389/fmicb.2013.00211
- Lliros, M., Gaju, N., De Oteyza, T. G., Grimalt, J. O., Esteve, I., and Martinez-Alonso, M. (2008). Microcosm experiments of oil degradation by microbial mats. II. The changes in microbial species. *Sci. Total Environ.* 393, 39–49. doi: 10.1016/j.scitotenv.2007.11.034
- McGenity, T. J. (2014). Hydrocarbon biodegradation in intertidal wetland sediments. *Curr. Opin. Biotechnol.* 27, 46–54. doi: 10.1016/j.copbio.2013.10.010
- McGenity, T. J., Folwell, B. D., Mckew, B., and Sanni, G. O. (2012). Marine crude-oil biodegradation: a central role for interspecies interactions. *Aquat. Biosyst.* 8:10. doi: 10.1186/2046-9063-8-10
- Miralles, G., Acquaviva, M., Bertrand, J. C., and Cuny, P. (2010). Response of an archaeal community from anoxic coastal marine sediments To experimental petroleum contamination. *Aquat. Microb. Ecol.* 59, 25–31. doi: 10.3354/ame01379
- Miralles, G., Nérini, D., Manté, C., Acquaviva, M., Doumenq, P., Michotey, V., et al. (2007). Effects of spilled oil on bacterial communities of Mediterranean coastal anoxic sediments chronically subjected to oil hydrocarbon contamination. *Microb. Ecol.* 54, 646–661. doi: 10.1007/s00248-007-9221-6
- Nogales, B., Lanfranconi, M. P., Piña-Villalonga, J. M., and Bosch, R. (2011). Anthropogenic perturbations in marine microbial communities. *FEMS Microbiol. Rev.* 35, 275–298. doi: 10.1111/j.1574-6976.2010.00248.x
- Paisse, S., Coulon, F., Goñi Urriza, M., Peperzak, L., Mcgenity, T. J., and Duran, R. (2008). Structure of bacterial communities along a hydrocarbon contamination gradient in a coastal sediment. *FEMS Microbiol. Rev.* 66, 295–305. doi: 10.1111/j.1574-6941.2008.00589.x
- Paisse, S., Duran, R., Coulon, F., and Goñi-Urriza, M. (2011). Are alkane hydroxylase genes (alkB) relevant to assess petroleum bioremediation processes in chronically polluted coastal sediments? *Appl. Microbiol. Biotechnol.* 92, 835–844. doi: 10.1007/s00253-011-3381-5
- Paisse, S., Goñi-Urriza, M., Stadler, T., Budzinski, H., and Duran, R. (2012). Ring-hydroxylating dioxygenase (RHD) expression in a microbial community during the early response to oil pollution. *FEMS Microbiol. Ecol.* 80, 77–86. doi: 10.1111/j.1574-6941.2011.01270.x
- Prosser, J. I. (2010). Replicate or lie. *Environ. Microbiol.* 12, 1806–1810. doi: 10.1111/j.1462-2920.2010.02201.x
- Prosser, J. I., Bohannan, B. J. M., Curtis, T. P., Ellis, R. J., Firestone, M. K., Freckleton, R. P., et al. (2007). Essay – the role of ecological theory in microbial ecology. *Nat. Rev. Microbiol.* 5, 384–392. doi: 10.1038/nrmicro1643
- Rocchetti, L., Beolchini, F., Hallberg, K. B., Johnson, D. B., and Dell'anno, A. (2012). Effects of prokaryotic diversity changes on hydrocarbon degradation rates and metal partitioning during bioremediation of contaminated anoxic marine sediments. *Mar. Pollut. Bull.* 64, 1688–1698. doi: 10.1016/j.marpolbul.2012.05.038
- Röling, W. F. M., Ferrer, M., and Golyshin, P. N. (2010). Systems approaches to microbial communities and their functioning. *Curr. Opin. Biotechnol.* 21, 532–538. doi: 10.1016/j.copbio.2010.06.007
- Röling, W. F. M., Milner, M. G., Jones, D. M., Lee, K., Daniel, F., Swanell, R. J. P., et al. (2002). Robust hydrocarbon degradation and dynamics of bacterial communities during nutrient-enhanced oil spill bioremediation. *Appl. Environ. Microbiol.* 68, 5537–5548. doi: 10.1128/AEM.68.11.5537-5548.2002
- Rosano-Hernandez, M. C., Ramirez-Saad, H., and Fernandez-Linares, L. (2012). Petroleum-influenced beach sediments of the Campeche Bank, Mexico: diversity and bacterial community structure assessment. *J. Environ. Manage.* 95, S32–S331. doi: 10.1016/j.jenvman.2011.06.046
- Shade, A., Chiu, C. Y., and Mcmahon, K. D. (2010). Differential bacterial dynamics promote emergent community robustness to lake mixing: an epilimnion to hypolimnion transplant experiment. *Environ. Microbiol.* 12, 455–466. doi: 10.1111/j.1462-2920.2009.02087.x
- Stauffert, M., Cravo-Laureau, C., Jézéquel, R., Barantal, S., Cuny, P., Gilbert, F., et al. (2013a). Impact of oil on bacterial community structure in bioturbated sediments. *PLoS ONE* 8:e65347. doi: 10.1371/journal.pone.0065347
- Stauffert, M., Duran, R., Gassie, C., and Cravo-Laureau, C. (2013b). Response of archaeal communities to oil spill in bioturbated mudflat sediments. *Microb. Ecol.* 1–12. doi: 10.1007/s00248-013-0288-y

- Suárez-Suárez, A., López-López, A., Tovar-Sánchez, A., Yarza, P., Orfila, A., Terrados, J., et al. (2011). Response of sulfate-reducing bacteria to an artificial oil-spill in a coastal marine sediment. *Environ. Microbiol.* 13, 1488–1499. doi: 10.1111/j.1462-2920.2011.02451.x
- Taketani, R. G., Franco, N. O., Rosado, A. S., and Van Elsas, J. D. (2010). Microbial community response to a simulated hydrocarbon spill in mangrove sediments. *J. Microbiol.* 48, 7–15. doi: 10.1007/s12275-009-0147-1
- Timmis, K. N., Mcgenity, T. J., Meer, J. R., and Lorenzo, V. (2010). *Handbook of Hydrocarbon and Lipid Microbiology*. Heidelberg: Springer-Verlag. doi: 10.1007/978-3-540-77587-4
- Wang, Y. F., and Tam, N. F. Y. (2011). Microbial community dynamics and biodegradation of polycyclic aromatic hydrocarbons in polluted marine sediments in Hong Kong. *Mar. Pollut. Bull.* 63, 424–430. doi: 10.1016/j.marpolbul.2011.04.046
- Zarraonaindia, I., Smith, D. P., and Gilbert, J. A. (2013). Beyond the genome: community-level analysis of the microbial world. *Biol. Philos.* 28, 261–282. doi: 10.1007/s10539-012-9357-8

**Conflict of Interest Statement:** The authors declare that the research was conducted in the absence of any commercial or financial relationships that could be construed as a potential conflict of interest.

*Received: 31 October 2013; accepted: 21 January 2014; published online: 12 February 2014.*

*Citation: Cravo-Laureau C and Duran R (2014) Marine coastal sediments microbial hydrocarbon degradation processes: contribution of experimental ecology in the omics'era. *Front. Microbiol.* 5:39. doi: 10.3389/fmicb.2014.00039*

*This article was submitted to Aquatic Microbiology, a section of the journal Frontiers in Microbiology.*

*Copyright © 2014 Cravo-Laureau and Duran. This is an open-access article distributed under the terms of the Creative Commons Attribution License (CC BY). The use, distribution or reproduction in other forums is permitted, provided the original author(s) or licensor are credited and that the original publication in this journal is cited, in accordance with accepted academic practice. No use, distribution or reproduction is permitted which does not comply with these terms.*



# Toward quantitative understanding on microbial community structure and functioning: a modeling-centered approach using degradation of marine oil spills as example

**Wilfred F. M. Röling<sup>1\*</sup> and Peter M. van Bodegom<sup>2</sup>**

<sup>1</sup> Molecular Cell Physiology, Faculty of Earth and Life Sciences, VU University Amsterdam, Amsterdam, Netherlands

<sup>2</sup> Systems Ecology, Department of Ecological Sciences, Faculty of Earth and Life Sciences, VU University Amsterdam, Amsterdam, Netherlands

**Edited by:**

Ian M. Head, Newcastle University, UK

**Reviewed by:**

Byron Crump, Oregon State University, USA

Susannah Green Tringe, Joint Genome Institute, USA

**\*Correspondence:**

Wilfred F. M. Röling, Molecular Cell Physiology, Faculty of Earth and Life Sciences, VU University Amsterdam, Boelelaan 1085, 1081 HV Amsterdam, Netherlands  
e-mail: wilfred.roling@vu.nl

Molecular ecology approaches are rapidly advancing our insights into the microorganisms involved in the degradation of marine oil spills and their metabolic potentials. Yet, many questions remain open: how do oil-degrading microbial communities assemble in terms of functional diversity, species abundances and organization and what are the drivers? How do the functional properties of microorganisms scale to processes at the ecosystem level? How does mass flow among species, and which factors and species control and regulate fluxes, stability and other ecosystem functions? Can generic rules on oil-degradation be derived, and what drivers underlie these rules? How can we engineer oil-degrading microbial communities such that toxic polycyclic aromatic hydrocarbons are degraded faster? These types of questions apply to the field of microbial ecology in general. We outline how recent advances in single-species systems biology might be extended to help answer these questions. We argue that bottom-up mechanistic modeling allows deciphering the respective roles and interactions among microorganisms. In particular constraint-based, metagenome-derived community-scale flux balance analysis appears suited for this goal as it allows calculating degradation-related fluxes based on physiological constraints and growth strategies, without needing detailed kinetic information. We subsequently discuss what is required to make these approaches successful, and identify a need to better understand microbial physiology in order to advance microbial ecology. We advocate the development of databases containing microbial physiological data. Answering the posed questions is far from trivial. Oil-degrading communities are, however, an attractive setting to start testing systems biology-derived models and hypotheses as they are relatively simple in diversity and key activities, with several key players being isolated and a high availability of experimental data and approaches.

**Keywords:** systems biology, flux balance analysis, metagenomics, bottom-up modeling, microbial communities, marine oil spills

## INTRODUCTION: KEY QUESTIONS IN MICROBIAL ECOLOGY AND OIL SPILL BIOREMEDIALTION

Microbes are prime catalysts of environmentally and societally important ecosystem processes, such as the biodegradation of spilled oil. Yet, the large complexity of microbial communities and technical limitations have long prevented the accurate description of microbial communities, let alone establishing the contribution of microorganisms to ecosystem functioning (Fuhrman, 2009). Metagenomics and related microbial ecological approaches are nowadays employed, aiming to answer major questions in microbial ecology:

1. How do microbial communities assemble in terms of functional diversity, species abundances and organization, and what are the drivers of community assembly?
2. How do the functional properties of microorganisms scale to processes at the ecosystem level?

3. How does mass flow between species, and which factors and species control and regulate fluxes, stability and other ecosystem functions?
4. Can generic rules be derived in microbial ecology, what drivers underlie these rules, and do these rules resemble rules in plant and animal ecology?
5. What information is needed for predicting and engineering microbial communities and their functioning?

However, while metagenomic approaches lead to large data sets, the cataloguing of genes itself provides limited insight, and may lead over time to disappointment in microbial ecology and its practitioners (Prosser, 2013). The application of theory from other research areas is needed to provide structure, mechanistic insight and, ultimately, predictive power (Prosser et al., 2007; Raes and Bork, 2008). In this paper, and in contrast to many reviews on individual approaches, we argue for a

novel, bottom-up mathematical framework that combines several existing approaches to better understand microbial communities and their activities. We subsequently indicate what is required to make such framework successful, and identify a need to link microbial physiology to quantitative concepts in order to advance microbial ecology via modeling-based approaches.

We are aware that the job ahead is tremendous and far from trivial. The biodegradation of marine oil spills provides a suitable and realistic starting point to achieve our goals, and also to pose and test specific hypotheses. Many molecular microbial ecology-centered studies have appeared, especially motivated by the 2010 Deepwater Horizon oil spill in the Gulf of Mexico and a desire to know what happened to its microbial communities and their degrading activities (e.g., Camilli et al., 2010; Hazen et al., 2010; Lu et al., 2012; Mason et al., 2012). These studies have provided insights on the major contributing species and their interactions (Head et al., 2006). Upon a spill, microbial biodiversity is strongly reduced, after which oil components are sequentially degraded (Head et al., 2006). First, growth of alkane-degrading specialists occurs, with *Alcanivorax* species contributing up to 90% of cell counts. Next, polycyclic aromatic hydrocarbon (PAH) degrading microorganisms, like *Cycloclasticus*, take over. Conceptual models exist on the importance of nitrogen and phosphorus in oil-biodegradation and on the interactions between functional groups of microorganisms (e.g., Head et al., 2006; **Figure 1**). Several important aspects of the biodegradation of spilled oil are still not well understood: why do certain specialists become dominant during oil-degradation, why are oil compounds sequentially degraded with first the relatively harmless alkanes being removed before the more toxic PAHs are attacked? We hypothesize that multispecies metabolic network-based modeling approaches, as outlined in the next sections, will be able to provide the answers. The obtained insights may subsequently contribute to the design of more effective oil spill bioremediation approaches, and enable the faster removal of toxic PAHs.

## WHY MODEL, AND HOW TO MODEL?

Biology is predominantly non-linear in character, for instance consider the biology text-book examples of Michaelis-Menten enzyme kinetics and Lotka-Volterra prey-predator interactions. The non-linearity in combination with the immense complexity of microbial communities makes it empirically extremely difficult to decipher the respective roles of each player in the provision of community-derived fluxes and community functioning in general, in dynamic environments with varying chemical and physical conditions. These aspects make it obvious that mathematical approaches are needed to ever come close to understanding microbial communities and functioning, and tackle key questions in microbial ecology. Introducing ecological theory has been suggested as one avenue to advance microbial ecology (Prosser et al., 2007), and for instance resource-ratio theory has been applied to oil spill bioremediation (Röling et al., 2002). While extending ecological theory into microbial ecology is undoubtedly very important, a key difference between plants and animals on the one hand and micro-organisms on the other hand is the enormous physiological and biochemical diversity in microorganisms. Thus, we

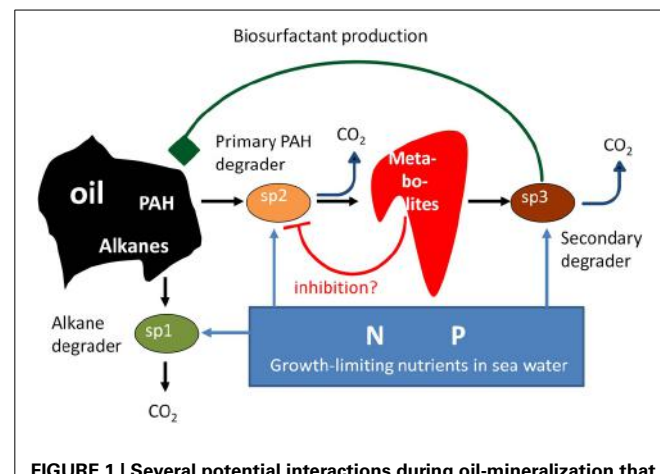


**FIGURE 1 |** Several potential interactions during oil-mineralization that may affect the rate and extent of biodegradation of marine oil spills.

Alkane- and PAH-degrading specialists compete for limiting nutrients in seawater. We extrapolate findings on a benzo[a]pyrene degrading, soil-derived consortium (Kanaly et al., 2002) to marine oil spills (Head et al., 2006) to indicate potential positive mutualistic interactions. The consortium was found to contain a key member (indicated by Sp3) that was unable to degrade the PAH benzo[a]pyrene but excreted factors that aided its degradation and presumably grew on metabolites excreted by other, benzo[a]pyrene-degrading community members (indicated by Sp2).

propose to model within a microbial eco-systems biology context by extending and integrating current systems biology (explained in more detail from Section “What is Needed to Mechanistically Model Complex Communities: The Big Lines” onwards). Systems biology has considerably enhanced insight into the functioning of individual microbial species, and the employed approaches may be adapted and applied to microbial ecology to contribute to improved understanding of microbial community composition and functioning (Röling et al., 2010; Zengler and Palsson, 2012).

Systems biology comprises an iterative cycle of experimentation, data analysis and modeling, hypothesis formulation and testing. Bottom-up systems biology approaches have led to large insights in the functioning of single species by examining the mechanisms through which functional system properties arise in the interactions of components in the system. These approaches require measures on physicochemical and kinetic properties of the components to model system properties (Bruggeman and Westerhoff, 2007). Bottom-up systems biology approaches can direct medicine development (Bakker et al., 2002) and metabolic engineering of microbial strains applied in biotechnological processes (Hoefnagel et al., 2002; Izallalen et al., 2008). We envision that in a similar fashion we will be able to design environmental “medicines”, e.g., the application of process-specific inhibitors, biostimulation with limiting nutrients or bioaugmentation to resolve missing or suboptimal microbial functions.

This contrasts to top-down systems biology approaches, identifying molecular interaction networks on the basis of correlated molecular behavior derived from (meta)genome-wide “omics” studies (Bruggeman and Westerhoff, 2007). The popularity of these approaches coincides with a generally increasing popularity of multivariate statistical approaches in microbial ecology (**Figure 2**; Raes and Bork, 2008). Indeed, they bring the field

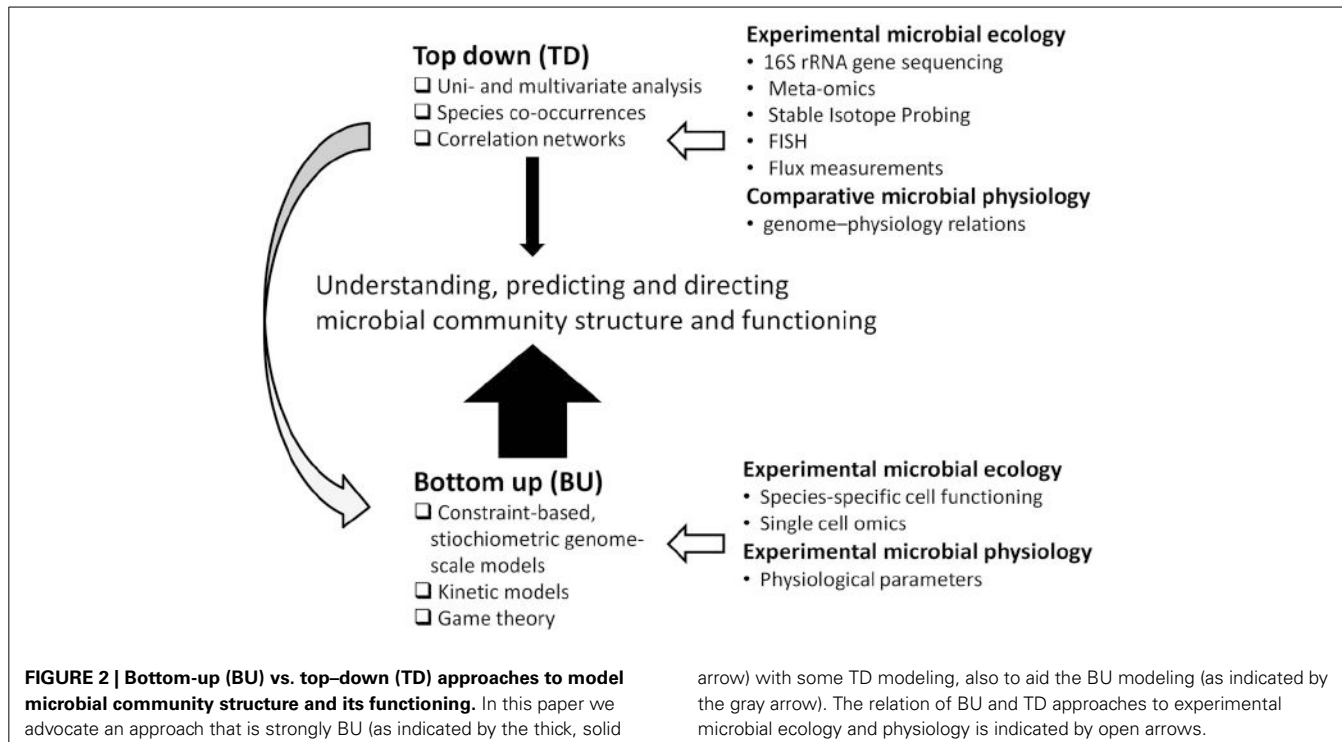


**FIGURE 2 |** Bottom-up (BU) vs. top-down (TD) approaches to model microbial community structure and its functioning. In this paper we advocate an approach that is strongly BU (as indicated by the thick, solid

arrow) with some TD modeling, also to aid the BU modeling (as indicated by the gray arrow). The relation of BU and TD approaches to experimental microbial ecology and physiology is indicated by open arrows.

forward and will do so for the coming time as many microbial systems are still poorly characterized. Yet, such models are phenomenological, and have limited predictive value, while frequently employing relations between properties that are assumed to be linear, even though biology is generally non-linear.

Bottom-up approaches may provide the mechanistic insights required to truly advance microbial ecology in the future. Bottom-up approaches, however, can be parameter-rich and are sensitive to undetermined factors, which are already important drawbacks for modeling single species (Bruggeman and Westerhoff, 2007). These problems are further amplified for complex microbial communities. Thus, there is a need to integrate bottom-up models with top-down approaches for better completeness, and reduce the complexity of the models (Figure 2).

### WHAT IS NEEDED TO MECHANISTICALLY MODEL COMPLEX COMMUNITIES: THE BIG LINES

The abovementioned complexity of microbial communities provides considerable challenges for bottom-up modeling. Clearly, an “abstraction” of reality is needed to understand community structure and functioning. However, a balance (that is, modeling approaches not being too detailed, but also not too simple) is needed to prevent arriving at a dead end, far from the goal of answering major questions in microbial ecology.

A good modeling practice is to start with a relatively simple model, describing a relatively simple community, and then stepwise increase complexity. Modeling and experiments (see Box 1 “Experimental approaches in microbial ecosystems biology”) would need to go hand in hand. Unstructured (that is, well-mixed) simple “communities” consisting of a few interacting species, in a system that is closed (in the sense that no

other species can invade), provide an initial starting point. Later, structure and higher diversity can be introduced, and subsequently dynamics in community structure, by allowing species immigration both in modeling and in experimentation. Biodegradation of marine oil spill provides an excellent starting point for such practice, since often a limited number of microorganisms with specific functions appear to play key roles (e.g., Head et al., 2006; Figure 1). Important representatives of these functional groups have been cultured (Dyksterhouse et al., 1995; Yakimov et al., 1998), allowing for controlled experiments. Furthermore, laboratory experimental designs mimicking beach oil spills have already shown their utility to test hypotheses on oil spill bioremediation (Röling et al., 2002).

The relatively simple modeling approaches should, however, allow for mechanistic insights. For instance, Taffs et al. (2009) constructed a metabolic network to describe community activity by considering the community as a single meta-organism. They connected genes via their inferred metabolites without specifically taking into account that connected genes may have belonged to different species (Taffs et al., 2009). Such boundary-free approaches appear attractive in the current metagenomics era, as generally the exact relationship between a gene and the cell that contained it, is lost in metagenomics. However, when comparing such cell boundary-free models with models that described individual species in a consortium, clear differences were revealed. Boundary-free models suffered from the likelihood of including infeasible reactions and the inability to obtain biomass estimates for individual species (Taffs et al., 2009). Also by simple reasoning one must conclude that some degree of compartmentalization is needed in modeling microbial communities: microbial activities depend on enzyme activities, thus on Michealis-Menten kinetics

**Box 1 | Experimental approaches in microbial ecosystems biology.**

Experiments will be needed to parameterize community models but also to test model-derived hypotheses (**Figure 2**). What one in particular would like to measure is: what activity does a certain species perform in a community, and how fast? With whom does it interact? The current experimental tool box is already quite complete to answer these questions and to reveal how interactions with other species affect a species' metabolism.

Species-specific activities can be quantified by combining Fluorescent *In Situ* Hybridization with the uptake of stable (Musat et al., 2008; Finzi-Hart et al., 2009) or radioactive isotope labeled (Nielsen et al., 2003) or fluorescent substrates (Muller and Nebe-Von-Caron, 2010), or by probe-based capturing of labeled DNA or RNA (Van Mooy et al., 2004; Van Mooy and Devol, 2008). Combinatorial fluorescent labeling and spectral imaging (Valm et al., 2011) can resolve up to 15 phylogenetic target groups at one time by FISH. This approach combined with high throughput flow cytometry with post-sorting analysis hold great promise for the future (Pel et al., 2004; Muller and Nebe-Von-Caron, 2010). Also antibodies can be used to separate species from microbial consortia and to determine species-specific characteristics (Pelz et al., 1999).

Isotopically labeled substrates also enable tracking substrate flow within and between cells. Metabolic flux analysis is the experimental counterpart of FBA to measure realized internal fluxes on basis of measuring external fluxes, mass balancing and reaction stoichiometry. Due to the occurrence of, e.g., cycles or multiple pathways,  $^{13}\text{C}$  Metabolic flux analysis is needed to resolve internal fluxes (Sauer, 2006). Generally, the positional isotope distribution of  $^{13}\text{C}$  in specific amino acids incorporated in cellular protein is determined and the distribution of these so-called isotopomers are fitted to a mathematical model of central metabolism that tracks the flow from  $^{13}\text{C}$  labeled substrate to amino acids to obtain the flux distribution of the species under study. Low internal concentrations currently hamper metabolite-based  $^{13}\text{C}$  flux analysis (Sauer, 2006). In contrast, extracellular products can occur in high concentrations, their isotopomeric analysis enable determining the fluxes through major pathways in human intestinal fermentation of glucose (De Graaf et al., 2010).

Combined with stable isotope probing (SIP), isotopomeric analysis provides information on cross-feeding of metabolites between species (Kovatcheva-Datchary et al., 2009). SIP can also provide information on interactions by predation (Lueders et al., 2006). In SIP an stable isotope-labeled compound is added to an environmental sample and the isotope-labeled biomarkers that are produced in the target organisms are analysed at the community scale (e.g., Pilloni et al., 2011). SIP addressing DNA, rRNA and mRNA provide complementary information on the growth and activity of microorganisms. DNA-based SIP will measure primarily newly formed cells, while RNA-based SIP will address also non-growing microorganisms and is highly dynamic, especially mRNA (Dumont et al., 2011). Jehmlich et al. (Jehmlich et al., 2009) developed a concept for analyzing carbon and nitrogen fluxes in microbial communities by employing protein-based SIP in metabolic labeling experiments with stable isotope labeled substrates.

that relate metabolite concentrations to activities. The intracellular and extracellular concentration of a particular exchangeable metabolite is usually different, suggesting that top-down approaches have limited utility and cell boundaries must be included instead.

“Rules” on microbial cell and community functioning may indicate how one could compartmentalize a complex community and in which detail these compartments should be described. Compartmentalization can be at the level of the individual cell, strain, species, or at a higher level (e.g., functional group). A higher level is preferable, as it minimizes the number of compartments in the model. The observation that a number of *Shewanella* species and *Escherichia coli* were highly similar in growth characteristics (growth rate, fermentation products) and in intracellular fluxes through their major metabolic pathways, led Tang et al. (2009) to introduce the concept of the metabotype. Species with similar metabolic phenotypes are grouped into a metabotype, irrespective of possible differences in their phylogeny. This concept may pave the way to model microbial community functioning on basis of a limited number of compartments describing the different functional types. Spilled oil is degraded by marine microorganisms that are generally specialized in the degradation of either alkanes or PAHs independent of phylogeny (Head et al., 2006), and which may possibly be divided along these lines in metabotypes (**Figure 1**).

The detail in which each compartment is described, must be considered too. Microorganisms respond to their biotic and abiotic environment, and changes therein, by adapting

their biochemistry and physiology. Thus, models should enable simulation of this kinetic flexibility of microorganisms. An empirical Monod equation describing the dependence of growth rate on a single limiting substrate, combined with a fixed-value growth yield and maintenance energy, is frequently used to model microbial growth, but is inadequate for our purpose of understanding growth and activity in environmental settings that are complex and dynamic, such as oil-polluted marine environments. Oil consists of thousands of compounds belonging to a few major classes, such as alkanes and PAHs (Head et al., 2006). While oil is degraded by specialists (**Figure 1**), these specialists can often degrade a range of molecules belonging to a specific class (Dyksterhouse et al., 1995; Yakimov et al., 1998; Schneiker et al., 2006). In addition, oil-degradation is strongly affected by nitrogen and phosphorus limitation (Head et al., 2006; **Figure 1**). Monod equations have limited ability to describe multiple substrate use or changes in type of growth limitation (Kovarova-Kovar and Egli, 1998). Growth yields and maintenance energy requirement are not constant within a single species, but depend on growth conditions (e.g., Van Verseveld et al., 1984; Van Bodegom, 2007).

The other extreme is to consider the complete genetic and metabolic make-up of a species, which seems infeasible since a microbial genome contains thousands of genes, encoding thousands of proteins that can act on thousands of metabolites. For most enzymes, quantitative information, like affinity constants and maximum activities, is limited, and measuring all these parameters is cumbersome, if even feasible. Many genes and

pathways appear to be only expressed and active under a few conditions, or are largely invariant to changes in environmental conditions (e.g., Daran-Lapujade et al., 2007; Tang et al., 2007; Kelk et al., 2012). This suggests that it is possible to reduce compartment complexity in order to determine genome-based metabolic fluxes with a minimal use of kinetic parameters.

Flux-analysis approaches as initially developed in cellular systems biology, like Metabolic Control Analysis (MCA; Kacser et al., 1995) and Hierarchical Regulation Analysis (HRA; Ter Kuile and Westerhoff, 2001; Daran-Lapujade et al., 2007), can contribute to establishing the detail in which a particular compartment needs to be described. MCA and HRA quantify and identify the importance of individual cellular components (e.g., enzymes) and processes (e.g., transcription) for systems-level metabolic fluxes and have aided in establishing how biochemical systems change upon perturbation. These approaches have been extended to analyse metabolic and trophic interactions among species and between species and their abiotic environment (Allison et al., 1993; Getz et al., 2003; Röling, 2007; Röling et al., 2007). For instance, MCA is an advanced sensitivity analysis framework that reveals, computationally or experimentally, how modulation of enzyme activities affects metabolic fluxes and metabolite concentrations in a cell (Kacser et al., 1995). It generates so-called control coefficients that quantitatively indicate the importance of an enzyme for a given process. Control analysis showed that at the cellular level, flux control is often mostly with the transporter (Bakker et al., 1999), and that in anaerobic, organic matter degrading communities, flux control is dominantly with the primary fermenting microorganisms (Röling et al., 2007). These observations suggest that in describing the compartments one should especially focus on uptake kinetics, while in anaerobic organic matter degrading networks the compartment(s) representing primary fermenting microorganisms needs most detail. Also in oil spill degradation several physiological groups of species interact, and the rate of oil-degradation might, for instance, be controlled considerably by biosurfactant-producing community members that live on metabolites excreted by oil component-degrading microorganisms (**Figure 1**).

## FLUX BALANCE ANALYSIS AND MICROBIAL ECOLOGY

Flux balance analysis (FBA) is currently the systems biology approach that appears most suited for the tasks outlined above. FBA is the stoichiometric analysis of a genome-derived metabolic network and allows calculating the possible metabolic flux distributions and other system properties (e.g., biomass yield, growth rate, ability to consume or produce certain chemicals), without requiring detailed kinetic information (Feist et al., 2009; **Figure 3**). To describe which fluxes are possible in a particular condition, physiological constraints (e.g., substrate uptake rates, biomass composition; Section “Deriving Microbial Physiological Parameters for Application in FBA”) and optimization principles (Section “Optimization Principles for Multispecies FBA: Microbial Growth Strategies”; **Figure 3**) are applied. Even when the metabolic network is solely based on gene presence, FBA can provide accurate predictions of system properties of a single species (Feist et al., 2009).

In recent years, FBA approaches have been developed that further aid in more accurately describing the physiology of

individual species. These approaches utilize experimental data on gene expression (Covert et al., 2004; Becker and Palsson, 2008; Shlomi et al., 2008) or implemented theoretical considerations informed by principles from biochemistry and genomics (e.g., Beg et al., 2007; Henry et al., 2007; Chandrasekaran and Price, 2010). Generating metabolic network models, and in particular fine-tuning these models, used to be time consuming but is now considerably aided by high-throughput, internet-based resources (Henry et al., 2010; Boele et al., 2012).

While FBA was initially developed for the analysis of fluxes under steady state conditions, Mahadevan et al. (2002) extended it to dynamic environments, by inserting an FBA model into an ODE (operational differential equation) model. By considering the cell to be in pseudo-steady state at each time point, growth rate and growth yield were calculated at each time point (Mahadevan et al., 2002). Nutrient uptake was described with Michaelis-Menten kinetics to generate dynamics. This dynamic FBA (dFBA) is especially of interest to ecology, since ecosystems are generally dynamic over time and space. dFBA is particularly relevant for marine oil spill biodegradation, since for instance fast growth of *Alcanivorax* occurs within a few days after a spill (Head et al., 2006). dFBA models of microorganisms have been successfully introduced into reactive transport models (Scheibe et al., 2009; Zhuang et al., 2011), which are used in hydrology to describe biogeochemical processes and physical transport processes in detail. Also to describe and understand the growth of key microorganisms on oil spilled on beaches, reactive transport models integrating the supply and removal of nutrients and cells by tidal cycles would be beneficial.

Increasingly, FBA is also applied to describe ecological interactions in simple consortia consisting of two to three species, providing a basis for studying more complex communities (Section “Constructing Metabolite-Based Microbial Interaction Networks”). The first multispecies flux balance analysis was conducted by Stolyar et al. (2007). Reduced metabolic network descriptions of fermenting, hydrogen-producing *Desulfovibrio vulgaris* and hydrogenotrophic *Methanococcus maripaludis* were combined to describe their mutualistic interactions, with the medium as a third compartment through which the species interacted. Several ecologically relevant characteristics, such as flux of metabolites and ratio of the two species, were predicted accurately. It revealed that interspecies transfer of hydrogen was essential in the interaction, while format was not. Competition, and the resulting species ratios, were accurately modeled for iron-reducing *Rhodoferax* and *Geobacter* along the groundwater flow path through an uranium-polluted aquifer, by including simple Michaelis-Menten kinetics to describe nutrient uptake rates that acted as constraints in a dynamic FBA model (Zhuang et al., 2011). The type of limiting nutrient (carbon or nitrogen) determined which species won the competition. Nutrient limitation plays a key role in the degradation of marine oil spills, as do competitive and mutualistic interactions between alkane- and PAH-degraders (Head et al., 2006; **Figure 1**). We hypothesize that by comparing the growth of oil-degrading marine microorganisms, using multispecies, metabolic network-based models that are integrated into reactive transport models in order to take into account nutrient availability and other relevant environmental characteristics, we will be able to decipher

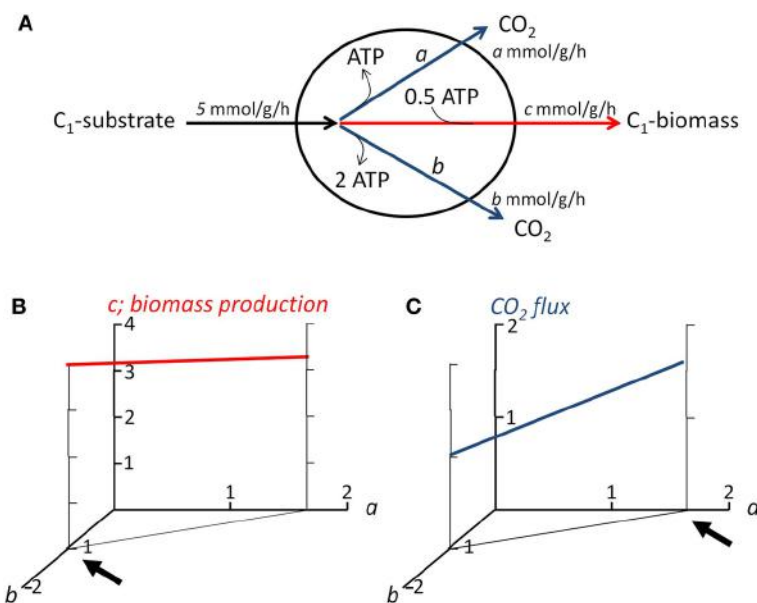


**FIGURE 3 | Demonstration of flux balance analysis and objective functions.** (A) Simplified representation of the metabolism of a microorganism, e.g., an alkane-degrader. The organism is assumed to consume substrate (formulated as C<sub>1</sub>-unit) at a rate of 5 mmol per gram biomass per hour. It grows, at flux *c* (in mmol per gram biomass per hour) by producing offspring from the substrate, which costs 0.5 ATP per C<sub>1</sub>-unit biomass produced. The ATP needed for anabolism can be derived from two catabolic pathways, pathway *a* produces 1 ATP per mole C<sub>1</sub>-substrate consumed, pathway *b* 2 ATP. Two flux balances containing three unknowns (*a*, *b*, and *c*) apply in steady state: 1. the carbon going into the cell, must come out:  $a + b + c = 5$ ; 2. there can be no net

production or consumption of ATP:  $a + 2b - 0.5c = 0$ . As a result, no unique solution is obtained for fluxes *a*, *b*, and *c*, an infinite number of solutions lay along the line  $3a + 5b = 5$ . (B) Relationship between the fluxes through the two catabolic pathways, and associated biomass production. If the objective function of the microorganism is to maximize biomass production, than it should use only pathway *b* for ATP production (indicated by arrow); (C) Relationship between the fluxes through the two catabolic pathways, and associated CO<sub>2</sub> production. If the objective function of the microorganism would be to maximize CO<sub>2</sub> production, than it should use only pathway *a* (indicated by arrow). Thus, the objective functions allow to obtain an unique solution.

why *Alcanivorax* generally dominates and outcompetes other oil-degraders.

While the genomes of several *Alcanivorax* species and other marine microorganisms capable of alkane- or PAH-degradation have been sequenced (Brooijmans et al., 2009), for none of them has an FBA model on their oil-degradation yet been reported. The metabolic network of the PAH-degrading *Mycobacterium vanbaalenii* PYR-1 has a funnel-like topology, in which many peripheral pathways, acting on a wide range of PAHs differing in complexity, converge to a widely conserved central pathway (Kweon et al., 2011). This organization may enhance input diversity with the controlled production of limited outputs, allow for more coordinated regulation, and ensure more efficient metabolic flow with reduced metabolite dissipation (Kweon et al., 2011). The metabolic networks of other marine microorganisms that degrade alkanes or PAHs likely have a similar funnel-like topology (e.g., Schneiker et al., 2006). We expect that FBA models that also consider the costs of protein synthesis, will reveal that diauxic growth by first depleting the smallest and least complex oil compounds enables the fastest growth of an oil-degrader. A consequence might be that after an oil spill the growth of microorganisms that are capable of using a small range of relatively simple alkanes or PAHs is favored over the growth of microorganisms that degrade a wider range that also include the more complex oil compounds, as the latter have to bear the costs for the

genes and proteins required for these activities. The subsequent growth of microorganisms capable of the removal of the more complex and more toxic oil components could then be hampered by the low availability of phosphorous and nitrogen, as most of these nutrients will be contained in the biomass of the pioneering species. Community-level, multispecies FBA will be useful to understand such microbial interactions during oil-degradation and to design new bioremediation strategies.

Community-level FBA reveals fluxes through species (analogous to the fluxes through enzymes within a cell in single species FBA). Conventional multispecies FBA does not provide cell numbers of individual species (again analogous to single species FBA where also the enzyme concentrations mediating the fluxes are not considered), while this is of major interest to microbial ecologists to understand and predict community structure. Recently, a few multispecies FBA approaches have been published that allow for predicting the cell numbers of individual species, for a wide range of microbial interactions (Zomorrodi and Maranas, 2012; Khandelwal et al., 2013).

## CONSTRUCTING METABOLITE-BASED MICROBIAL INTERACTION NETWORKS

So far, multispecies FBA modeling has been applied for up to three species (Taffs et al., 2009) and, unfortunately, no examples are available for oil-degradation yet. This number of interacting

species is still limited, certainly in light of the thousands of species that can occur in just one gram of soil, thus providing a formidable challenge to FBA. High throughput sequencing of phylogenetic marker genes, in particular 16S rRNA genes, nowadays allows to establish relations between species and to construct microbial networks based on correlations between marker-derived species abundances. However, species interrelationships do not inform directly on the nature of these interactions (Faust and Raes, 2012), let alone the type of metabolites involved.

Recently, Langille et al. (2013) described a computational approach to predict the functional composition of a metagenome using 16S rRNA marker gene sequences, under the assumption that phylogeny and function are sufficiently linked. This approach to predict genome content on basis of a 16S rRNA sequence could be integrated into 16S rRNA-gene based microbial interaction networks to predict how the species may metabolically interact. The construction of metabolic networks from experimentally or computationally derived (meta)genome data for FBA itself provides information on the potential interactions between species: the metabolites taken up and produced by a species' network can be predicted (Borenstein et al., 2008; Handorf et al., 2008), allowing for the construction of metabolite-based microbial interaction networks (Borenstein and Feldman, 2009; Röling et al., 2010). Likewise, metagenomics can contribute information on prey-predator interactions, which is challenging in multispecies FBA as predation relates to prey size and prey aggregation behavior (Matz and Kjelleberg, 2005), properties that do not appear from a metabolic network. However, single cell genomics on marine protists revealed which preys they had ingested, and also indicated phage-cell interactions (Yoon et al., 2011). Both protists and phages may affect oil spill biodegradation (Röling et al., 2002; Head et al., 2006).

Also systematic literature mining approaches can enhance our understanding on the organization of microbial interaction networks (Chaffron et al., 2010; Freilich et al., 2010). For instance, a network constructed based on published bacteria co-occurrences showed that this network clustered into species-groups that showed relations between resource competition, metabolic yield and growth rate that correspond to the r/K selection theory (Freilich et al., 2010).

Similar approaches as described above might be applied to marine oil spill degrading microbial communities, by utilizing the many descriptive and empirical studies that have appeared in recent years, especially after the 2010 Deepwater Horizon oil spill (e.g., Camilli et al., 2010; Hazen et al., 2010; Lu et al., 2012; Mason et al., 2012). By combining their data, species-species interactions during different phases of oil spill biodegradation may be inferred to subsequently construct metabolite-based microbial interaction networks which can subsequently be analyzed by multispecies FBA approaches as described in the previous section. By focusing first on key oil-degraders such as *Alcanivorax* and *Cycloclasticus* and their interaction partners (Figure 1), we hypothesize that we can identify species that are either synergistic or antagonistic to degradation of specific classes of oil components and also pinpoint the mechanisms (e.g., metabolic network characteristics) behind these interactions. These species may subsequently be stimulated or inhibited to favor the degradation of relatively more toxic PAHs over alkanes.

## OPTIMIZATION PRINCIPLES FOR MULTISPECIES FBA: MICROBIAL GROWTH STRATEGIES

FBA models are in general underdetermined: the number of variables in the equations to solve is larger than the number of equations themselves, even when constraints such as maximum uptake rates of nutrients and biomass composition are included (Figure 3A). Therefore, FBA uses optimization criteria, or objective functions, to describe a species' physiology. Optimization principle(s) are based on the assumed or determined growth strategies of the organism under study, such as maximization of biomass production. Figures 3B,C demonstrate two different objective functions and their impact on flux distribution over anabolic and catabolic pathways. Often, it is assumed that cells aim to maximize their growth yield (Figure 3B), however this strategy is by no means an universal principle (Schuetz et al., 2007; Schuster et al., 2008). Even a single species can employ different strategies depending on the prevalent growth conditions, such as nutrient scarcity or excess (Schuetz et al., 2007). On basis of <sup>13</sup>C flux analysis of nine bacteria, metabolism was shown to operate close to the so-called Pareto optimal surface of a three-dimensional space defined by competing objectives (biomass yield, ATP yield, minimum sum of absolute fluxes) (Schuetz et al., 2012). Flux states were proposed to evolve under the trade-off of two principles: optimality under one given condition and minimal adjustment between conditions (Schuetz et al., 2012).

The growth strategies of oil-degrading microorganisms, and their dependence on environmental conditions and species identity, are not known. However, we envision that knowledge on growth strategies will be key to understanding and directing the degradation of spilled oil and associated community dynamics. If for instance alkane-degrading microorganisms aim to maximize their biomass production (Figure 3B), a consequence might be that most of the often growth-limiting nitrogen and phosphorus will end up in their biomass (Figure 1). Hence, after alkanes are depleted, little nutrient will be available to enable substantial biomass production of PAH-degrading microorganisms and fast degradation of PAH. If on the other hand alkane-degrading microorganisms aim to maximize CO<sub>2</sub> production from alkanes, for instance as a strategy to avoid that competitors can use these alkanes, less biomass will be formed per molecule alkane degraded (Figure 3C) and more nutrients will be available for growth of PAH-degraders (Figure 1). We expect that by comparing experimental growth in mono- and mixed cultures to FBA models employing different optimization criteria the growth strategies of oil degrading microorganisms will be revealed.

For what cells are optimized in complex, multispecies environments is in fact also not well known. Probabilistic cellular decisions on costs and benefits may be taken at three levels in such environments (Perkins and Swain, 2009): cells firstly have to derive from noisy signals the current and potential future states of their extracellular environment. Second, given those anticipated future states, microbes must weigh the costs and benefits (in terms of fitness and its optimization) of each potential response, at the level of the individual. Finally, the cells must decide in the presence of other (potentially competing or cooperating) decision makers, at the level of the population and the community.

Competition between cells and species in communities may force strategies that appear suboptimal: a strategy with lower fitness in environments without competition, might be successful in environments with competition, an outcome well known from plant ecology too (e.g., Anten and During, 2011; Falster et al., 2012).

Game theory, which studies strategic decision making, can provide a better approach than conventional optimization to study the dynamics and outcome of the development of microbial communities, by capturing evolutionary considerations as affected by interactions between microorganisms (Pfeiffer and Schuster, 2005). The trade-off of growth yield vs. growth rate is an example of such dilemma (Pfeiffer et al., 2001; Kreft and Bonhoeffer, 2005). This trade-off is based on irreversible thermodynamics. Chemotrophic organisms obtain their energy by the degradation of substrates into products with lower free energy. The free energy difference between substrate and product is used for two purposes: ATP production for biomass growth and the thermodynamic driving force of the degradation reaction. Maximal ATP yield would be achieved if the entire free energy difference could be conserved as ATP. However, in that case the reaction would be in thermodynamic equilibrium, and thus rates of substrate degradation and ATP production would be zero. Part of the free energy difference must be used to drive the reaction. The larger this part is, the faster the rate of ATP production but also the lower the yield. High yield is a group-beneficial trait because the economic utilization of a resource benefits all those sharing this (limiting) resource. On the other hand, high growth rate is beneficial for the individual because it allows better competition. Cooperative behavior, resulting in higher yield, was found to outweigh the interest of the individual to grow faster in spatially structured environments, such as biofilms (Pfeiffer et al., 2001).

Evolutionary trade-offs have also impacted metabolic network design, and its regulation. Species inhabiting complex, dynamic environments have metabolic networks in which enzymes have relatively more connections to other enzymes than species living in more constant environments. This makes their networks more robust, but also more costly to maintain and thus less efficient (Morine et al., 2009). Under nutrient scarcity, cheap but less efficient pathways are expressed (Carlson, 2007), in which the length and elemental content of proteins may be adapted to the nutrient limitation (Elser et al., 2011). These metabolic network characteristics appear identifiable from the genome sequence and as such may be incorporated in future multispecies FBA approaches.

The above optimization criteria put emphasis on the fitness of the individual cell and species, as goal in ecosystem development. A framework of ecological network analysis, employing community-level, thermodynamics-motivated flux optimization criteria (Kleidon et al., 2010) has been postulated as alternative theory to describe the goal of ecosystems (Fath, 2004; Ulanowicz et al., 2006; Jørgensen et al., 2007), and has so far mainly been applied to plant and animal ecology, e.g., to predict species distributions (Phillips et al., 2006). Maximum entropy principles have also allowed for predicting species abundances within plant communities (Shipley et al., 2006), although some of its assumptions have been criticized too (e.g., Laughlin et al., 2012). Recently, the utility of multi-level optimization was revealed for purely metabolic models of microbial consortia (Zomorrodi and

Maranas, 2012). An optimization approach was formulated with maximization of the overall biomass as primary, community level-objective function and species-specific biomass maximization as secondary, cellular objective function. This approach allowed for capturing any type of positive or negative interaction, like mutualism, competition and parasitism, and demonstrated the trade-offs between forces driving species and community fitness. It would be interesting to further combine community-level and cell-based optimization approaches in microbial ecology, and oil spill biodegradation in particular, to establish what level of integration is required to describe microbial community functioning.

## DERIVING MICROBIAL PHYSIOLOGICAL PARAMETERS FOR APPLICATION IN FBA

It is essential to be aware that besides information on metabolic pathways and optimization criteria, FBA models also require basic physiological data: a growth-associated maintenance (energy expenditure necessary for non-metabolic activities accompanying biomass synthesis, usually expressed in mmol ATP per gram biomass per hour), growth-rate independent maintenance (or non-growth associated maintenance, the energy needed to maintain the cell in a functional and viable state, without growing), efficiency of respiration [P/e; amount of ATP (P) produced from the movement of an electron (e) through an electron transport chain to an electron acceptor] and biomass composition. Some of these variables might be of less importance in a FBA context than generally conceived. For instance, determining the composition of biomass is tedious, in particular for species within a community, and is highly responsive to changing environmental conditions (e.g., Pramanik and Keasling, 1997, 1998). However, when biomass composition was varied in an *E. coli* FBA model, it had only a minor influence of its modeled growth rate and oxygen uptake rate (Feist et al., 2007). This suggests that biomass composition can be neglected, although it will affect intracellular fluxes (Pramanik and Keasling, 1997, 1998) and trophic interactions (Matz and Kjelleberg, 2005). Similarly, growth-rate independent maintenance energy requirements are tedious to determine and interpret (Van Verseveld et al., 1984). However, *in situ* maintenance energy is much lower than the maintenance energies determined in the laboratory (Morita, 1988), suggesting that growth-rate independent maintenance energy is also not required for modeling, while it may also be estimated from thermodynamic approaches (Tijhuis et al., 1993). The inclusion of growth-associated maintenance, on the other hand, is essential, as microbial metabolism is inefficient: the amount of biomass produced per mole ATP is much less than theoretically possible (Stouthamer, 1973). Westerhoff et al. (1983) described that low thermodynamic efficiencies are optimal for maximum growth, and established a relation between the reduction grade of substrate and efficiency.

FBA models predict growth yields. Given that thermodynamic models more directly predict yield estimates (Vanbriesen, 2002; Roden and Jin, 2011), these estimates may be utilized as additional constraints in FBA. A literature compilation demonstrated a linear relationship between measured microbial growth yield and the free energy of aerobic and anaerobic respiratory and fermentative metabolism of glucose, organic acids, ethanol,

and hydrogen (Rodén and Jin, 2011). An initial prediction of growth yield on basis of thermodynamics may in particular aid fitting P/e ratios from FBA models for respiring microorganisms. Oxidative phosphorylation is generally the major source for ATP in respiring microorganisms, including those active in oil spill degradation, but it is experimentally challenging to quantify its P/e.

Most of the above mentioned physiological parameters would also be needed for other modeling approaches, e.g., kinetic models. Determining these parameters is time-consuming and poses a serious constraint on modeling complex microbial communities in detail, also calling for a more optimal use of the large amount of physiological data collected in the past (see Section “Concluding Remarks”). Paradoxically, top-down approaches (**Figures 2, 4**) may also aid in achieving bottom up-modeling of complex communities: empirical relations may be used to infer physiological parameters or first model activities, and can later on be replaced by more mechanistic descriptions when more insight is obtained. For instance, genome composition and genome-derived metabolic network structure of a microorganism inform on physiological characteristics such as growth rates (Freilich et al., 2009, 2010; Sharp et al., 2010; Vieira-Silva and Rocha, 2010), since they are shaped by the environment in which the microorganism evolved. rRNA operon copy number, tRNA copy number and a composite index of codon usage bias derived from (meta)genome sequence data correlate with maximum growth rate (Sharp et al., 2010; Vieira-Silva and Rocha, 2010). Metabolic variability and co-habitation (or competition) encountered can be derived from genome sequence data, and also correlate with growth rates (Freilich et al., 2009). Such rates, together with principles of biochemistry and genomics (e.g., Beg et al., 2007; Henry et al., 2007; Chandrasekaran and Price, 2010), may be used to constrain FBA models. A quantitative description of substrate uptake rates in multispecies FBA is in particular important for modeling competition and also requires information on substrate affinities. Recently, evidence was obtained that kinetic parameters, such as affinity constants, correlated with the

amino acid composition of enzymes (Zikmanis and Kampenusa, 2012).

## CONCLUDING REMARKS

The road toward understanding and predicting microbial community functioning is clearly still long and will be challenging. Achieving this goal will require a more optimal, integrative use of the enormous amount of data that is already available. Current microbial ecology is strongly dominated by molecular analyses, however the “old” microbial physiology data are still of high value to give further meaning to molecular-based community analysis. Yet, the data are spread over a large number of publications. In biochemistry, kinetic parameters for enzymes, such as turn-over rates, affinity constants, maximum rates have been compiled in the BRENDa database (Schomburg et al., 2013). We advocate establishing a similar database with kinetic parameters of microorganisms, and also containing information on their physiology and ecological characteristics.

Such a database will help to advance microbial ecology in two ways. Firstly, phylogenetic information, as derived from 16S rRNA sequencing or metagenomics, might be linked to the closest relative in such a database to automatically extract its kinetic properties and ease modeling of the ecosystem from which the community data were derived. Secondly, a database with microbial physiology data will facilitate the large-scale correlation of physiological data with genome information (**Figure 4**). This enables deriving “rules” on microbial physiology and ecology (Borenstein et al., 2008; Freilich et al., 2009, 2010), which may aid bottom-up approaches, e.g., to derive the mechanistic reasons behind observed patterns (**Figure 2**).

In addition, more microbial physiological data will be needed, particularly on the impacts of co-cultivation on the physiology of individual species and their interactions. In addition, while microorganisms of industrial and clinical relevance were well-characterized in monocultures in the 1970s to 1990s, advanced culturing methods have now allowed for isolation of species from phyla which were not even described at that time. Comparative

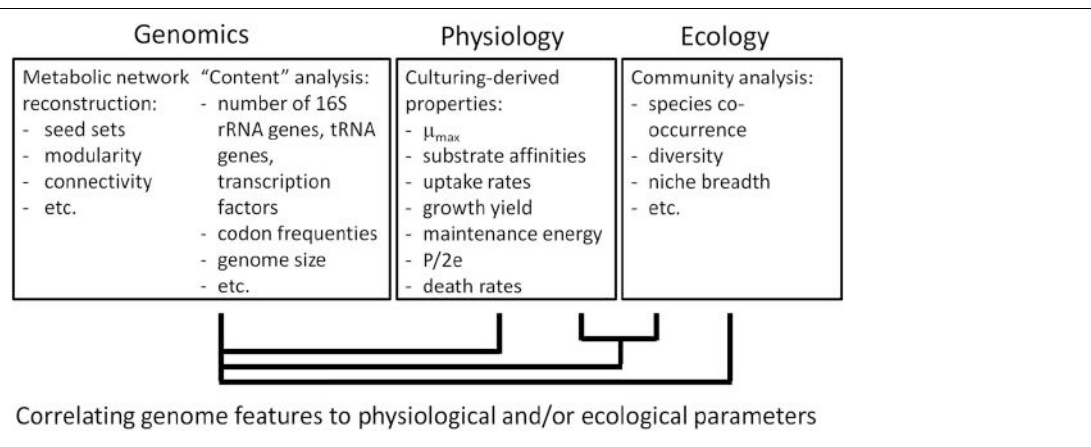


**FIGURE 4 | From genome to physiology and ecology of a species.** The interaction with their environment over evolutionary times has shaped the physiology of microorganisms, which is contained in their genomes. We assume that, in reverse, the genome informs on a species’ physiology and ecology. This

figure indicates how one may derive relationships between genomic information on the one hand and physiological and ecological characteristics on the other hand. These relationships or “rules” will further aid the modeling of microbial communities and functioning by bottom-up approaches.

microbial physiology studies, on novel single species or mixed species cultures, will benefit modeling.

We have provided a synthesis on how approaches currently available can be integrated and extended to computationally derive multispecies, metabolic flux networks from metagenomic data. This integration will contribute to answering key questions in microbial ecology, such as understanding the assembly of microbial communities and their functioning via metabolic interactions. Oil-degrading communities are often simple and dominated by culturable species, providing a suitable, tractable test system. In recent years, an enormous amount of largely descriptive studies on the degradation of marine oil spills has appeared (e.g., Camilli et al., 2010; Hazen et al., 2010; Lu et al., 2012; Mason et al., 2012). This wealth of data can be further analyzed to establish the co-occurrence and dynamic interactions between key microorganisms contributing to oil-degradation. The available genomic information on key isolates (Schneiker et al., 2006) and on non-culturable key players through single cell sequencing (Mason et al., 2012) can be included in the multi-species metabolic models. This modeling, in iteration with well-designed experiments, should substantially enhance our knowledge on the biodegradation of marine oil spills.

## ACKNOWLEDGMENTS

This paper was inspired by the Lorentz Workshop “Microbes in Ecosystems: weaving intracellular processes into microbial networks” held in October 2009 in Leiden, the Netherlands. We thank the participants for their contribution to this workshop, and Frank Bruggeman for commenting on a previous version of this manuscript. The work is supported by the 7th framework project BACSIN of the European Community and project MICROCONTROL in the BE-BASIC programme.

## REFERENCES

- Allison, S. M., Small, J. R., Kacser, H., and Prosser, J. I. (1993). Control analysis of microbial interactions in continuous culture: a simulation study. *J. Gen. Microbiol.* 139, 2309–2317. doi: 10.1099/00221287-139-10-2309
- Anten, N. P. R. and During, H. J. (2011). Is analysing the nitrogen use at the plant canopy level a matter of choosing the right optimization criterion? *Oecologia* 167, 293–303. doi: 10.1007/s00442-011-2011-3
- Bakker, B. M., Assmus, H. E., Bruggeman, F., Haanstra, J. R., Klipp, E., and Westerhoff, H. (2002). Network-based selectivity of antiparasitic inhibitors. *Mol. Biol. Rep.* 29, 1–5. doi: 10.1023/A:1020397513646
- Bakker, B. M., Michels, P. A. M., Opperdoes, F. R., and Westerhoff, H. V. (1999). What controls glycolysis in bloodstream form *Trypanosoma brucei*? *J. Biol. Chem.* 274, 14551–14559. doi: 10.1074/jbc.274.21.14551
- Becker, S. A., and Palsson, B. O. (2008). Context-specific metabolic networks are consistent with experiments. *PLoS Comput. Biol.* 4:e1000082. doi: 10.1371/journal.pcbi.1000082
- Beg, Q. K., Vazquez, A., Ernst, J., De Menezes, M. A., Bar-Joseph, Z., Barabasi, A. L., et al. (2007). Intracellular crowding defines the mode and sequence of substrate uptake by *Escherichia coli* and constrains its metabolic activity. *Proc. Natl. Acad. Sci. U.S.A.* 104, 12663–12668. doi: 10.1073/pnas.0609845104
- Boeleg, J., Olivier, B. G., and Teusink, B. (2012). FAME, the flux analysis and modeling environment. *BMC Syst. Biol.* 6:8. doi: 10.1186/1752-0509-6-8
- Borenstein, E., and Feldman, M. W. (2009). Topological signatures of species interactions in metabolic networks. *J. Comput. Biol.* 16, 191–200. doi: 10.1089/cmb.2008.06TT
- Borenstein, E., Kupiec, M., Feldman, M. W., and Ruppin, E. (2008). Large-scale reconstruction and phylogenetic analysis of metabolic environments. *Proc. Natl. Acad. Sci. U.S.A.* 105, 14482–14487. doi: 10.1073/pnas.0806162105
- Brooijmans, R. J. W., Pastink, M. I., and Siezen, S. J. (2009). Hydrocarbon-degrading bacteria: the oil-spill clean-up crew. *Microb. Biotechnol.* 2, 587–594. doi: 10.1111/j.1751-7915.2009.00151.x
- Bruggeman, F. J., and Westerhoff, H. V. (2007). The nature of systems biology. *Trends Microbiol.* 15, 45–50. doi: 10.1016/j.tim.2006.11.003
- Camilli, R., Reddy, C. M., Yoerger, D. R., Van Mooy, B. A. S., Jakuba, M. V., Kinsey, J. C., et al. (2010). Tracking hydrocarbon plume transport and biodegradation at deepwater horizon. *Science* 330, 201–204. doi: 10.1126/science.1195223
- Carlson, R. P. (2007). Metabolic systems cost-benefit analysis for interpreting network structure and regulation. *Bioinformatics* 23, 1258–1264. doi: 10.1093/bioinformatics/btm082
- Chaffron, S., Rehrauer, H., Pernthaler, J., and Von Mering, C. (2010). A global network of coexisting microbes from environmental and whole-genome sequence data. *Genome Res.* 20, 947–959. doi: 10.1101/gr.104521.109
- Chandrasekaran, S., and Price, N. D. (2010). Probabilistic integrative modeling of genome-scale metabolic and regulatory networks in *Escherichia coli* and *Mycobacterium tuberculosis*. *Proc. Natl. Acad. Sci. U.S.A.* 107, 17845–17850. doi: 10.1073/pnas.1005139107
- Covert, M. W., Knight, E. M., Reed, J. L., Herrgard, M. J., and Palsson, B. O. (2004). Integrating high-throughput and computational data elucidates bacterial networks. *Nature* 429, 92–96. doi: 10.1038/nature02456
- Daran-Lapujade, P., Rossell, S., Van Gulik, W. M., Luttk, M. A. H., De Groot, M. J. L., Slijper, M., et al. (2007). The fluxes through glycolytic enzymes in *Saccharomyces cerevisiae* are predominantly regulated at post-transcriptional levels. *Proc. Natl. Acad. Sci. U.S.A.* 104, 15753–15758. doi: 10.1073/pnas.0707476104
- De Graaf, A. A., Maathuis, A., De Waard, P., Deutz, N. E. P., Dijkema, C., De Vos, W. M., et al. (2010). Profiling human gut bacterial metabolism and its kinetics using [ $^{13}\text{C}$ -U-C13]glucose and NMR. *NMR Biomed.* 23, 2–12. doi: 10.1002/nbm.1418
- Dumont, M. G., Pommerenke, B., Casper, P., and Conrad, R. (2011). DNA-, rRNA- and mRNA-based stable isotope probing of aerobic methanotrophs in lake sediment. *Environ. Microbiol.* 13, 1153–1167. doi: 10.1111/j.1462-2920.2010.02415.x
- Dyksterhouse, S. E., Gray, J. P., Herwig, R. P., Lara, J. C., and Staley, J. T. (1995). *Cycloclasticus pugettii* gen-nov, sp-nov, an aromatic hydrocarbon-degrading bacterium from marine sediments. *Int. J. Syst. Bacteriol.* 45, 116–123. doi: 10.1099/00207713-45-1-116
- Elser, J. J., Acquisti, C., and Kumar, S. (2011). Stoichiogenomics: the evolutionary ecology of macromolecular elemental composition. *Trends Ecol. Evol.* 26, 38–44. doi: 10.1016/j.tree.2010.10.006
- Falster, D. S., Brannstrom, A., Dieckmann, U., and Westoby, M. (2012). Influence of four major plant traits on average height, leaf-area cover net primary productivity, and biomass density in single-species forests: a theoretical investigation. *J. Ecol.* 99, 148–164. doi: 10.1111/j.1365-2745.2010.01735.x
- Fath, B. D. (2004). Distributed control in ecological networks. *Ecol. Model.* 179, 235–245. doi: 10.1016/j.ecolmodel.2004.06.007
- Faust, K., and Raes, J. (2012). Microbial interactions: from networks to models. *Nat. Rev. Microbiol.* 10, 538–550. doi: 10.1038/nrmicro2832
- Feist, A. M., Henry, C. S., Reed, J. L., Krummenacker, M., Joyce, A. R., Karp, P. D., et al. (2007). A genome-scale metabolic reconstruction for *Escherichia coli* K-12 MG1655 that accounts for 1260 ORFs and thermodynamic information. *Mol. Syst. Biol.* 3:121. doi: 10.1038/msb4100155
- Feist, A. M., Herrgard, M. J., Thiele, I., Reed, J. L., and Palsson, B. O. (2009). Reconstruction of biochemical networks in microorganisms. *Nat. Rev. Microbiol.* 7, 129–143. doi: 10.1038/nrmicro1949
- Finzi-Hart, J. A., Pett-Ridge, J., Weber, P. K., Popa, R., Fallon, S. J., Gunderson, T., et al. (2009). Fixation and fate of C and N in the cyanobacterium *Trichodesmium* using nanometer-scale secondary ion mass spectrometry. *Proc. Natl. Acad. Sci. U.S.A.* 106, 6345–6350. doi: 10.1073/pnas.0810547106
- Freilich, S., Kreimer, A., Borenstein, E., Yosef, N., Sharan, R., Gophna, U., et al. (2009). Metabolic-network-driven analysis of bacterial ecological strategies. *Genome Biol.* 10:R61. doi: 10.1186/gb-2009-10-6-r61
- Freilich, S., Kreimer, A., Meilijson, I., Gophna, U., Sharan, R., and Ruppin, E. (2010). The large-scale organization of the bacterial network of ecological co-occurrence interactions. *Nucleic Acids Res.* 38, 3857–3868. doi: 10.1093/nar/gkq118
- Fuhrman, J. A. (2009). Microbial community structure and its functional implications. *Nature* 459, 193–199. doi: 10.1038/nature08058

- Getz, W. M., Westerhoff, H. V., Hofmeyr, J. H. S., and Snoep, J. L. (2003). Control analysis of trophic chains. *Ecol. Model.* 168, 153–171. doi: 10.1016/S0304-3800(03)00208-4
- Handorf, T., Christian, N., Ebenhoh, O., and Kahn, D. (2008). An environmental perspective on metabolism. *J. Theor. Biol.* 252, 530–537. doi: 10.1016/j.jtbi.2007.10.036
- Hazen, T. C., Dubinsky, E. A., Desantis, T. Z., Andersen, G. L., Piceno, Y. M., Singh, N., et al. (2010). Deep-sea oil plume enriches indigenous oil-degrading bacteria. *Science* 330, 204–208. doi: 10.1126/science.1195979
- Head, I. M., Jones, D. M., and Röling, W. F. M. (2006). Marine microorganisms make a meal of oil. *Nat. Rev. Microbiol.* 4, 173–182. doi: 10.1038/nrmicro1348
- Henry, C. S., Broadbelt, L. J., and Hatzimanikatis, V. (2007). Thermodynamics-based metabolic flux analysis. *Bioophys. J.* 92, 1792–1805. doi: 10.1529/biophysj.106.093138
- Henry, C. S., Dejongh, M., Best, A. A., Frybarger, P. M., Lindsay, B., and Stevens, R. L. (2010). High-throughput generation, optimization and analysis of genome-scale metabolic models. *Nat. Biotechnol.* 28, 977–U922. doi: 10.1038/nbt.1672
- Hoefnagel, M. H. N., Starrenburg, M. J. C., Martens, D. E., Hugenholtz, J., Kleerebezem, M., Van Swam, I. I., et al. (2002). Metabolic engineering of lactic acid bacteria, the combined approach: kinetic modelling, metabolic control and experimental analysis. *Microbiology* 148, 1003–1013.
- Izallalen, M., Mahadevan, R., Burgard, A., Postier, B., Didonato, R., Sun, J., et al. (2008). *Geobacter sulfurreducens* strain engineered for increased rates of respiration. *Metab. Eng.* 10, 267–275. doi: 10.1016/j.ymben.2008.06.005
- Jehmlrich, N., Schmidt, F., Taubert, M., Seifert, J., Von Bergen, M., Richnow, H. H., et al. (2009). Comparison of methods for simultaneous identification of bacterial species and determination of metabolic activity by protein-based stable isotope probing (Protein-SIP) experiments. *Rapid Commun. Mass Spectrom.* 23, 1871–1878. doi: 10.1002/rcm.4084
- Jørgensen, S. E., Fath, B., Bastianoni, S., Marques, J., Müller, F., Nielsen, S. N., et al. (eds.). (2007). *A New Ecology: Systems Perspective*. Amsterdam: Elsevier.
- Kacser, H., Burns, J. A., and Fell, D. A. (1995). The control of flux. *Biochem. Soc. Trans.* 23, 341–366.
- Kanaly, R. A., Hayarana, S., and Watanabe, K. (2002). *Rhodanobacter* sp. strain BPC1 in a benzo[a]pyrene-mineralizing bacterial consortium. *Appl. Environ. Microbiol.* 68, 5826–5833. doi: 10.1128/AEM.68.12.5826-5833.2002
- Kelk, S. M., Olivier, B. G., Stougie, L., and Bruggeman, F. J. (2012). Optimal flux spaces of genome-scale stoichiometric models are determined by a few subnetworks. *Sci. Rep.* 2:e580. doi: 10.1038/srep00580
- Khandelwal, R. A., Olivier, B. G., Röling, W. F. M., Teusink, B., and Bruggeman, F. J. (2013). Community flux balance analysis for microbial consortia at balanced growth. *PLoS ONE* 8:10. doi: 10.1371/journal.pone.0064567
- Kleidon, A., Malhi, Y., and Cox, P. M. (2010). Maximum entropy production in environmental and ecological systems. *Philos. Trans. R. Soc. B Biol. Sci.* 365, 1297–1302. doi: 10.1098/rstb.2010.0018
- Kovarova-Kovar, K., and Egli, T. (1998). Growth kinetics of suspended microbial cells: from single-substrate-controlled growth to mixed-substrate kinetics. *Microbiol. Mol. Biol. Rev.* 62, 646–666.
- Kovatcheva-Datchary, P., Egert, M., Maathuis, A., Rajilic-Stojanovic, M., De Graaf, A. A., Smidt, H., et al. (2009). Linking phylogenetic identities of bacteria to starch fermentation in an *in vitro* model of the large intestine by RNA-based stable isotope probing. *Environ. Microbiol.* 11, 914–926. doi: 10.1111/j.1462-2920.2008.01815.x
- Kreft, J. U., and Bonhoeffer, S. (2005). The evolution of groups of cooperating bacteria and the growth rate versus yield trade-off. *Microbiology* 151, 637–641. doi: 10.1099/mic.0.27415-0
- Kweon, O., Kim, S.-J., Holland, R. D., Chen, H., Kim, D.-W., Gao, Y., et al. (2011). Polycyclic aromatic hydrocarbon metabolic network in *Mycobacterium vanbaalenii* PYR-1. *J. Bacteriol.* 193, 4326–4337. doi: 10.1128/JB.00215-11
- Langille, M. G. I., Zaneveld, J., Caporaso, J. G., McDonald, D., Knights, D., Reyes, J. A., et al. (2013). Predictive functional profiling of microbial communities using 16S rRNA marker gene sequences. *Nat. Biotechnol.* 31, 814–821. doi: 10.1038/nbt.2676
- Laughlin, D. C., Joshi, C., van Bodegom, P. M., Bastow, Z. A. and Fule, P. Z. (2012). A predictive model of community assembly that incorporates intraspecific trait variation. *Ecol. Lett.* 15, 1291–1299. doi: 10.1111/j.1461-0248.2012.01852.x
- Lu, Z. M., Deng, Y., Van Nostrand, J. D., He, Z. L., Voordeckers, J., Zhou, A. F., et al. (2012). Microbial gene functions enriched in the Deepwater Horizon deep-sea oil plume. *ISME J.* 6, 451–460. doi: 10.1038/ismej.2011.91
- Lueders, T., Kindler, R., Miltner, A., Friedrich, M. W., and Kaestner, M. (2006). Identification of bacterial micropredators distinctively active in a soil microbial food web. *Appl. Environ. Microbiol.* 72, 5342–5348. doi: 10.1128/AEM.00400-06
- Mahadevan, R., Edwards, J. S., and Doyle, F. J. (2002). Dynamic flux balance analysis of diauxic growth in *Escherichia coli*. *Biophys. J.* 83, 1331–1340. doi: 10.1016/S0006-3495(02)73903-9
- Mason, O. U., Hazen, T. C., Borglin, S., Chain, P. S. G., Dubinsky, E. A., Fortney, J. L., et al. (2012). Metagenome, metatranscriptome and single-cell sequencing reveal microbial response to Deepwater Horizon oil spill. *ISME J.* 6, 1715–1727. doi: 10.1038/ismej.2012.59
- Matz, C., and Kjelleberg, S. (2005). Off the hook—how bacteria survive protozoan grazing. *Trends Microbiol.* 13, 302–307. doi: 10.1016/j.tim.2005.05.009
- Morine, M. J., Gu, H., Myers, R. A., and Bielawski, J. P. (2009). Trade-offs between efficiency and robustness in bacterial metabolic networks are associated with niche breadth. *J. Mol. Evol.* 68, 506–515. doi: 10.1007/s00239-009-9226-5
- Morita, R. Y. (1988). Bioavailability of energy and its relationship to growth and starvation survival in nature. *Can. J. Microbiol.* 34, 436–441. doi: 10.1139/m88-076
- Muller, S., and Nebe-Von-Caron, G. (2010). Functional single-cell analyses: flow cytometry and cell sorting of microbial populations and communities. *FEMS Microbiol. Rev.* 34, 554–587. doi: 10.1111/j.1574-6976.2010.00214.x
- Musat, N., Halm, H., Winterholler, B., Hoppe, P., Peduzzi, S., Hillion, F., et al. (2008). A single-cell view on the ecophysiology of anaerobic phototrophic bacteria. *Proc. Natl. Acad. Sci. U.S.A.* 105, 17861–17866. doi: 10.1073/pnas.0809329105
- Nielsen, J. L., Christensen, D., Kloppenborg, M., and Nielsen, P. H. (2003). Quantification of cell-specific substrate uptake by probe-defined bacteria under *in situ* conditions by microautoradiography and fluorescence *in situ* hybridization. *Environ. Microbiol.* 5, 202–211. doi: 10.1046/j.1462-2920.2003.00402.x
- Pel, R., Floris, V., Gons, H. J., and Hoogveld, H. L. (2004). Linking flow cytometric cell sorting and compound-specific C-13-analysis to determine population-specific isotopic signatures and growth rates in cyanobacteria-dominated lake plankton. *J. Phycol.* 40, 857–866. doi: 10.1111/j.1529-8817.2004.03176.x
- Pelz, O., Tesar, M., Wittich, R. M., Moore, E. R. B., Timmis, K. N., and Abraham, W. R. (1999). Towards elucidation of microbial community metabolic pathways: unravelling the network of carbon sharing in a pollutant-degrading bacterial consortium by immunocapture and isotopic ratio mass spectrometry. *Environ. Microbiol.* 1, 167–174. doi: 10.1046/j.1462-2920.1999.00023.x
- Perkins, T. J., and Swain, P. S. (2009). Strategies for cellular decision-making. *Mol. Syst. Biol.* 5:326. doi: 10.1038/msb.2009.83
- Pfeiffer, T., and Schuster, S. (2005). Game-theoretical approaches to studying the evolution of biochemical systems. *Trends Biochem. Sci.* 30, 20–25. doi: 10.1016/j.tibs.2004.11.006
- Pfeiffer, T., Schuster, S., and Bonhoeffer, S. (2001). Cooperation and competition in the evolution of ATP-producing pathways. *Science* 292, 504–507. doi: 10.1126/science.1058079
- Phillips, S. J., Anderson, R. P., and Schapire, R. E. (2006). Maximum entropy modeling of species geographic distributions. *Ecol. Model.* 190, 231–259. doi: 10.1016/j.ecolmodel.2005.03.026
- Pillonni, G., Von Netzer, F., Engel, M., and Lueders, T. (2011). Electron acceptor-dependent identification of key anaerobic toluene degraders at a tar-oil-contaminated aquifer by Pyro-SIP. *FEMS Microbiol. Ecol.* 78, 165–175. doi: 10.1111/j.1574-6941.2011.01083.x
- Pramanik, J., and Keasling, J. D. (1997). Stoichiometric model of *Escherichia coli* metabolism: incorporation of growth-rate dependent biomass composition and mechanistic energy requirements. *Biotechnol. Bioeng.* 56, 398–421. doi: 10.1002/(SICI)1097-0290(19971120)56:4%3C398::AID-BIT6%3E3.3.CO;2-F
- Pramanik, J., and Keasling, J. D. (1998). Effect of *Escherichia coli* biomass composition on central metabolic fluxes predicted by a stoichiometric model. *Biotechnol. Bioeng.* 60, 230–238.
- Prosser, J. I. (2013). Think before you sequence. *Nature* 494, 41–41.
- Prosser, J. I., Bohannan, B. J. M., Curtis, T. P., Ellis, R. J., Firestone, M. K., Freckleton, R. P., et al. (2007). The role of ecological theory in microbial ecology. *Nat. Rev. Microbiol.* 5, 384–392. doi: 10.1038/nrmicro1643
- Raes, J., and Bork, P. (2008). Molecular eco-systems biology: towards an understanding of community function. *Nat. Rev. Microbiol.* 6, 693–699. doi: 10.1038/nrmicro1935
- Roden, E. E., and Jin, Q. S. (2011). Thermodynamics of microbial growth coupled to metabolism of glucose, ethanol, short-chain organic acids,

- and hydrogen. *Appl. Environ. Microbiol.* 77, 1907–1909. doi: 10.1128/AEM.02425-10
- Röling, W. F. M. (2007). Do microbial numbers count? Quantifying the regulation of biogeochemical fluxes by population size and cellular activity. *FEMS Microbiol. Ecol.* 62, 202–210. doi: 10.1111/j.1574-6941.2007.00350.x
- Röling, W. F. M., Ferrer, M., and Golyshin, P. N. (2010). Systems approaches to microbial communities and their functioning. *Curr. Opin. Biotechnol.* 21, 532–538. doi: 10.1016/j.copbio.2010.06.007
- Röling, W. F. M., Milner, M. G., Jones, D. M., Lee, K., Daniel, F., Swannell, R. J. P., et al. (2002). Robust hydrocarbon degradation and dynamics of bacterial communities during nutrient-enhanced oil spill bioremediation. *Appl. Environ. Microbiol.* 68, 5537–5548. doi: 10.1128/AEM.68.11.5537-5548.2002
- Röling, W. F. M., Van Breukelen, B. M., Bruggeman, F. J., and Westerhoff, H. V. (2007). Ecological control analysis: being(s) in control of mass flux and metabolic concentrations in anaerobic degradation processes. *Environ. Microbiol.* 9, 500–511. doi: 10.1111/j.1462-2920.2006.01167.x
- Sauer, U. (2006). Metabolic networks in motion: C-13-based flux analysis. *Mol. Syst. Biol.* 2, 62. doi: 10.1038/msb4100109
- Scheibe, T. D., Mahadevan, R., Fang, Y., Garg, S., Long, P. E., and Lovley, D. R. (2009). Coupling a genome-scale metabolic model with a reactive transport model to describe *in situ* uranium bioremediation. *Microb. Biotech.* 2, 274–286. doi: 10.1111/j.1751-7915.2009.00087.x
- Schneiker, S., Dos Santos, V., Bartels, D., Bekel, T., Brecht, M., Buhrmester, J., et al. (2006). Genome sequence of the ubiquitous hydrocarbon-degrading marine bacterium *Alcanivorax borkumensis*. *Nat. Biotechnol.* 24, 997–1004. doi: 10.1038/nbt1232
- Schomburg, I., Chang, A., Placzek, S., Sohngen, C., Rother, M., Lang, M., et al. (2013). BRENDA in 2013: integrated reactions, kinetic data, enzyme function data, improved disease classification: new options and contents in BRENDA. *Nucleic Acids Res.* 41, D764–D772. doi: 10.1093/nar/gks1049
- Schuetz, R., Kuepfer, L., and Sauer, U. (2007). Systematic evaluation of objective functions for predicting intracellular fluxes in *Escherichia coli*. *Mol. Syst. Biol.* 3, 119. doi: 10.1038/msb4100162
- Schuetz, R., Zamboni, N., Zampieri, M., Heinemann, M., and Sauer, U. (2012). Multidimensional optimality of microbial metabolism. *Science* 336, 601–604. doi: 10.1126/science.1216882
- Schuster, S., Pfeiffer, T., and Fell, D. A. (2008). Is maximization of molar yield in metabolic networks favoured by evolution? *J. Theor. Biol.* 252, 497–504. doi: 10.1016/j.jtbi.2007.12.008
- Sharp, P. M., Emery, L. R., and Zeng, K. (2010). Forces that influence the evolution of codon bias. *Philos. Trans. R. Soc. B Biol. Sci.* 365, 1203–1212. doi: 10.1098/rstb.2009.0305
- Shipley, B., Vile, D., and Garnier, E. (2006). From plant traits to plant communities: a statistical mechanistic approach to biodiversity. *Science* 314, 812–814. doi: 10.1126/science.1131344
- Shlomi, T., Cabili, M. N., Herrgard, M. J., Palsson, B. O., and Ruppert, E. (2008). Network-based prediction of human tissue-specific metabolism. *Nat. Biotechnol.* 26, 1003–1010. doi: 10.1038/nbt.1487
- Stolyar, S., Van Dien, S., Hillesland, K. L., Pinel, N., Lie, T. J., Leigh, J. A., et al. (2007). Metabolic modeling of a mutualistic microbial community. *Mol. Syst. Biol.* 3, 92. doi: 10.1038/msb4100131
- Stouthamer, A. H. (1973). Theoretical study on amount of atp required for synthesis of microbial cell material. *Antonie Van Leeuwenhoek* 39, 545–565. doi: 10.1007/BF02578899
- Taffs, R., Aston, J. E., Briley, K., Jay, Z., Klatt, C. G., McGlynn, S., et al. (2009). *In silico* approaches to study mass and energy flows in microbial consortia: a syntrophic case study. *BMC Syst. Biol.* 3:114. doi: 10.1186/1752-0509-3-114
- Tang, Y. J., Hwang, J. S., Wemmer, D. E., and Keasling, J. D. (2007). *Shewanella oneidensis* MR-1 fluxome under various oxygen conditions. *Appl. Environ. Microbiol.* 73, 718–729. doi: 10.1128/AEM.01532-06
- Tang, Y. J., Martin, H. G., Dehal, P. S., Deutschbauer, A., Llora, X., Meadows, A., et al. (2009). Metabolic flux analysis of *Shewanella* spp. reveals evolutionary robustness in central carbon metabolism. *Biotech. Bioeng.* 102, 1161–1169. doi: 10.1002/bit.22129
- Ter Kuile, B. H., and Westerhoff, H. V. (2001). Transcriptome meets metabolome: hierarchical and metabolic regulation of the glycolytic pathway. *FEBS Lett.* 500, 169–171. doi: 10.1016/S0014-5793(01)02613-8
- Tijhuis, L., Vanloosdrecht, M. C. M., and Heijnen, J. J. (1993). A thermodynamically based correlation for maintenance gibbs energy-requirements in aerobic and anaerobic chemotropic growth. *Biotechnol. Bioeng.* 42, 509–519. doi: 10.1002/bit.260420415
- Ulanowicz, R. E., Jorgensen, S. E., and Fath, B. D. (2006). Exergy, information and aggradation: an ecosystems reconciliation. *Ecol. Model.* 198, 520–524. doi: 10.1016/j.ecolmodel.2006.06.004
- Valm, A. M., Welch, J. L. M., Rieken, C. W., Hasegawa, Y., Sogin, M. L., Oldenbourg, R., et al. (2011). Systems-level analysis of microbial community organization through combinatorial labeling and spectral imaging. *Proc. Natl. Acad. Sci. U.S.A.* 108, 4152–4157. doi: 10.1073/pnas.1101134108
- Van Bodegom, P. (2007). Microbial maintenance: a critical review on its quantification. *Microb. Ecol.* 53, 513–523. doi: 10.1007/s00248-006-9049-5
- Vanbriesen, J. M. (2002). Evaluation of methods to predict bacterial yield using thermodynamics. *Biodegradation* 13, 171–190. doi: 10.1023/A:1020887214879
- Van Mooy, B. A. S., and Devol, A. H. (2008). Assessing nutrient limitation of *Prochlorococcus* in the North Pacific subtropical gyre by using an RNA capture method. *Limnol. Oceanogr.* 53, 78–88. doi: 10.4319/lo.2008.53.1.0078
- Van Mooy, B. A. S., Devol, A. H., and Keil, R. G. (2004). Quantifying H-3-thymidine incorporation rates by a phylogenetically defined group of marine planktonic bacteria (Bacteriodetes phylum). *Environ. Microbiol.* 6, 1061–1069. doi: 10.1111/j.1462-2920.2004.00636.x
- Van Verseveld, H. W., Chesbro, W. R., Braster, M., and Stouthamer, A. H. (1984). Eubacteria have 3 growth modes keyed to nutrient flow: consequences for the concept of maintenance and maximal growth yield. *Arch. Microbiol.* 137, 176–184. doi: 10.1007/BF00414463
- Vieira-Silva, S., and Rocha, E. P. C. (2010). The systemic imprint of growth and its uses in ecological (Meta) genomics. *PLoS Genet.* 6:e1000808. doi: 10.1371/journal.pgen.1000808
- Westerhoff, H. V., Hellingwerf, K. J., and Vandam, K. (1983). Thermodynamic efficiency of microbial-growth is low but optimal for maximal growth-rate. *Proc. Natl. Acad. Sci. U.S.A.* 80, 305–309. doi: 10.1073/pnas.80.1.305
- Yakimov, M. M., Golyshin, P. N., Lang, S., Moore, E. R. B., Abraham, W. R., Lunsdorf, H., et al. (1998). *Alcanivorax borkumensis* gen. nov., sp. nov., a new, hydrocarbon-degrading and surfactant-producing marine bacterium. *Int. J. Syst. Bacteriol.* 48, 339–348. doi: 10.1099/0020713-48-2-339
- Yoon, H. S., Price, D. C., Stepanauskas, R., Rajah, V. D., Sieracki, M. E., Wilson, W. H., et al. (2011). Single-cell genomics reveals organismal interactions in uncultivated marine protists. *Science* 332, 714–717. doi: 10.1126/science.1203163
- Zengler, K., and Palsson, B. O. (2012). A road map for the development of community systems (CoSy) biology. *Nat. Rev. Microbiol.* 10, 366–372. doi: 10.1038/nrmicro2763
- Zhuang, K., Izallalen, M., Mouser, P., Richter, H., Risso, C., Mahadevan, R., et al. (2011). Genome-scale dynamic modeling of the competition between *Rhodoflexus* and *Geobacter* in anoxic subsurface environments. *ISME J.* 5, 305–316. doi: 10.1038/ismej.2010.117
- Zikmanis, P., and Kampenusa, I. (2012). Relationships between kinetic constants and amino acid composition of enzymes from the yeast *Saccharomyces cerevisiae* glycolysis pathway. *EURASIP J. Bioinform. Syst. Biol.* 1:11. doi: 10.1186/1687-4153-2012-11
- Zomorrodi, A. R., and Maranas, C. D. (2012). OptCom: a multi-level optimization framework for the metabolic modeling and analysis of microbial communities. *PLoS Comput. Biol.* 8:e1002363.. doi: 10.1371/journal.pcbi.1002363
- Conflict of Interest Statement:** The authors declare that the research was conducted in the absence of any commercial or financial relationships that could be construed as a potential conflict of interest.
- Received:** 30 October 2013; **accepted:** 11 March 2014; **published online:** 26 March 2014. **Citation:** Röling WFM and van Bodegom PM (2014) Toward quantitative understanding on microbial community structure and functioning: a modeling-centered approach using degradation of marine oil spills as example. *Front. Microbiol.* 5:125. doi: 10.3389/fmicb.2014.00125
- This article was submitted to Aquatic Microbiology, a section of the journal *Frontiers in Microbiology*.
- Copyright © 2014 Röling and van Bodegom. This is an open-access article distributed under the terms of the Creative Commons Attribution License (CC BY). The use, distribution or reproduction in other forums is permitted, provided the original author(s) or licensor are credited and that the original publication in this journal is cited, in accordance with accepted academic practice. No use, distribution or reproduction is permitted which does not comply with these terms.



# Geomicrobiological linkages between short-chain alkane consumption and sulfate reduction rates in seep sediments

Arpita Bose<sup>1†</sup>, Daniel R. Rogers<sup>1†</sup>, Melissa M. Adams<sup>1</sup>, Samantha B. Joye<sup>2</sup> and Peter R. Girguis<sup>1\*</sup>

<sup>1</sup> Department of Organismic and Evolutionary Biology, Harvard University, Cambridge, MA, USA

<sup>2</sup> Department of Marine Sciences, University of Georgia, Athens, GA, USA

**Edited by:**

Joel E. Kostka, Georgia Institute of Technology, USA

**Reviewed by:**

Laura Lapham, Aarhus University, Denmark

Karsten Zengler, University of California, San Diego, USA

Molly C. Redmond, UNC Charlotte, USA

**\*Correspondence:**

Peter R. Girguis, Biological Laboratories, Department of Organismic and Evolutionary Biology, Harvard University, 16 Divinity Ave., Room 3085, Cambridge, MA 02138, USA  
e-mail: pgirguis@oeb.harvard.edu

<sup>†</sup>These authors have contributed equally to this work.

Marine hydrocarbon seeps are ecosystems that are rich in methane, and, in some cases, short-chain ( $C_2-C_5$ ) and longer alkanes.  $C_2-C_4$  alkanes such as ethane, propane, and butane can be significant components of seeping fluids. Some sulfate-reducing microbes oxidize short-chain alkanes anaerobically, and may play an important role in both the competition for sulfate and the local carbon budget. To better understand the anaerobic oxidation of short-chain *n*-alkanes coupled with sulfate-reduction, hydrocarbon-rich sediments from the Gulf of Mexico (GoM) were amended with artificial, sulfate-replete seawater and one of four *n*-alkanes ( $C_1-C_4$ ) then incubated under strict anaerobic conditions. Measured rates of alkane oxidation and sulfate reduction closely follow stoichiometric predictions that assume the complete oxidation of alkanes to  $CO_2$  (though other sinks for alkane carbon likely exist). Changes in the  $\delta^{13}C$  of all the alkanes in the reactors show enrichment over the course of the incubation, with the  $C_3$  and  $C_4$  incubations showing the greatest enrichment (4.4 and 4.5‰, respectively). The concurrent depletion in the  $\delta^{13}C$  of dissolved inorganic carbon (DIC) implies a transfer of carbon from the alkane to the DIC pool (-3.5 and -6.7‰ for  $C_3$  and  $C_4$  incubations, respectively). Microbial community analyses reveal that certain members of the class Deltaproteobacteria are selectively enriched as the incubations degrade  $C_1-C_4$  alkanes. Phylogenetic analyses indicate that distinct phylotypes are enriched in the ethane reactors, while phylotypes in the propane and butane reactors align with previously identified  $C_3-C_4$  alkane-oxidizing sulfate-reducers. These data further constrain the potential influence of alkane oxidation on sulfate reduction rates (SRRs) in cold hydrocarbon-rich sediments, provide insight into their contribution to local carbon cycling, and illustrate the extent to which short-chain alkanes can serve as electron donors and govern microbial community composition and density.

**Keywords:** short-chain alkanes, methane, ethane, propane, butane, Gulf of Mexico, microbial sulfate reduction,  $C_1-C_4$  hydrocarbons

## INTRODUCTION

Marine hydrocarbon seeps are natural features that support considerable biological diversity and activity (Muyzer and Van Der Kraan, 2008 and references therein). Tectonic activity forms faults that facilitate the release of methane ( $CH_4$ ) and other hydrocarbons from deep subsurface oil and gas deposits, as well as gas hydrates (Muyzer and Van Der Kraan, 2008). Methane is a key constituent of the carbon cycle as it is one of the final products of the microbial degradation of organic matter (Thauer et al., 2008 and references therein), though it can also be produced abiotically through thermochemical and geogenic reactions (Horita and Berndt, 1999).

Because  $CH_4$  is a potent greenhouse gas, there is considerable interest in determining the fate of both biogenic and abiotic methane (for review see Reeburgh, 2007; Thauer et al., 2008). Consequently, microbial methane oxidation under both aerobic and anaerobic conditions has received considerable attention (Thauer et al., 2008 and references therein). The anaerobic oxidation of methane, or AOM, has been the subject of research

for four decades, and much of the work has been focused on identifying the responsible microbes, their distribution, and the biochemistry of AOM. To date, five distinct mechanisms of AOM have been discovered (Callaghan, 2013 and references therein; Haroon et al., 2013). The AOM mechanism most relevant to this study is mediated by microbial consortia of archaea, related to the archaeal anaerobic methane oxidizer group ANME, and bacterial sulfate-reducers of the Desulfosarcinales/*Desulfococcus* (DSS) group (Knittel and Boetius, 2009 and references therein). This microbial consortium mediates coupled AOM and sulfate reduction, though the exact nature of the association is not fully understood (Knittel and Boetius, 2009; Milucka et al., 2012 and references therein).

The study of  $C_2-C_5$  hydrocarbon degradation has lagged behind that of  $CH_4$  in spite of their abundance in some environments. Analogous to methane,  $C_2-C_5$  gases are formed due to thermal cracking of fossilized organic deposits, and  $C_1-C_2$  gases are also produced biologically (Lorant and Behar, 2002; Hinrichs et al., 2006; Jones et al., 2008; Xie et al., 2013). At some

sites, including the Gulf of Cadiz, the Gulf of Mexico (GoM), the Caspian Sea, the Monterey Bay canyon (Lorenson et al., 2002), and the Norwegian continental shelf (Hovland and Thomsen, 1997), C<sub>2</sub>-C<sub>5</sub> hydrocarbons can account for 14–38% of the total gas (see Milkov, 2005 and references therein). In these areas, the oxidation of C<sub>2</sub>-C<sub>5</sub> hydrocarbons may be a significant contributor to the community bioenergetics of marine seeps (Lorenson et al., 2002; Formolo et al., 2004; Sassen et al., 2004; Alain et al., 2006). For example, at GoM cold seeps, sulfate reduction rates (SRRs) are higher than can be accounted for by AOM alone, indicating that sulfate reduction is linked to the oxidation of other organic compounds potentially including short-chain alkanes (Joye et al., 2004; Orcutt et al., 2010; Bowles et al., 2011). The extent of this as well as the influence of short-chain hydrocarbon oxidation on AOM is poorly constrained, but it is possible that C<sub>2</sub>-C<sub>5</sub> hydrocarbon degradation is a significant process that co-occurs with AOM, and may compete for a common oxidant (i.e., SO<sub>4</sub><sup>2-</sup>) (Joye et al., 2004; Orcutt et al., 2010; Bowles et al., 2011).

Recent studies of marine and terrestrial seeps, as well as marine hydrothermal vents, have observed the microbial oxidation of short-chain alkanes coupled to sulfate reduction across a range of temperatures. The microbes, as revealed by phylogenetic analyses of isolates as well as enrichments, align with sulfate reducers within the Deltaproteobacteria and the Firmicutes (Kniemeyer et al., 2007; Savage et al., 2010; Adams et al., 2013; Jaekel et al., 2013). Kniemeyer et al. isolated a bacterium, BuS5, allied to the DSS group within the Deltaproteobacteria that can anaerobically oxidize propane and *n*-butane while reducing sulfate (Kniemeyer et al., 2007). Savage et al. showed that propane and *n*-pentane degrading enrichments from a terrestrial hydrocarbon seep were also dominated by the DSS group (Savage et al., 2010). Jaekel et al. further characterized propane and butane degrading sediment-free enrichments to expand the understanding of the physiology of these microbes (Jaekel et al., 2013). Unlike these previous studies, Adams et al. observed appreciable rates of ethane degradation coupled to sulfate reduction in *ex situ* sediment slurry-based batch reactors with sediments from the Middle Valley hydrothermal vent field (Adams et al., 2013). Collectively, these studies have placed some constraints on the relationship between alkane oxidation and sulfate reduction, though little remains known about the stoichiometric relationship between alkane oxidation—including methane- and sulfate reduction by mixed, natural communities, and their impact on local carbon cycling.

The northern slope of the GoM is an ideal site to study the anaerobic consumption of short-chain alkanes because the sediments lie over hydrocarbon deposits including structure II and H gas hydrates rich in C<sub>1</sub>-C<sub>5</sub> gases (Joye et al., 2004). The sites of hydrocarbon seepage in the GoM are also characterized by the presence of mats dominated by the chemoautotrophic sulfur oxidizing bacterial genus *Beggiatoa* (Joye et al., 2004). The presence of these microbes suggests that H<sub>2</sub>S is available in the environment, which may indicate high advection and seepage rates (Joye et al., 2004). At the northern slope of the GoM, methane is the dominant component of seeping gas (72–96%) with some contribution from short-chain alkanes. The abundance of the short-chain alkanes decreases with chain length

with ethane comprising 2.4–12.4% of the total gas, followed by propane and butane (iC<sub>4</sub> + nC<sub>4</sub>) (1.2–12.6 and 0.3–4.3%, respectively) (Sassen et al., 1998). Stable carbon isotopic properties of the starting materials (*in situ* gas hydrate and chemosynthetic fauna), and the end products (authigenic carbonates) of their degradation are also known (Sassen et al., 2004). Anaerobic microbial oxidation of C<sub>2</sub>-C<sub>5</sub> hydrocarbons has been inferred at the site from the enrichment in the δ<sup>13</sup>C of the residual alkane pools (Sassen et al., 2004). In particular, geochemical measurements reveal a preferential degradation of propane, butane, and pentane (Sassen et al., 2004).

To better understand the role of C<sub>2</sub>-C<sub>5</sub> hydrocarbon degrading organisms in global geochemical cycles, we examined microbially mediated alkane consumption and SRRs, and the effect of alkane consumption on the inorganic carbon pool using sediments collected from a marine hydrocarbon-rich seep in the GoM. Specifically, we conducted a series of experiments in *ex situ* batch reactors to examine: (1) the rate at which microbial communities degrade C<sub>1</sub>-C<sub>4</sub> alkanes; (2) the relationship between alkane degradation and sulfate reduction; (3) the degree to which microbially mediated alkane degradation influences the isotopic signatures of the alkanes and dissolved inorganic carbon (DIC) pools; and (4) how community composition of the GoM sediments are affected by the addition of C<sub>1</sub>-C<sub>4</sub> alkanes. This study advances our understanding by quantifying the potential rates of C<sub>1</sub>-C<sub>4</sub> alkane consumption, sulfate reduction and the possible effects on the local carbon pool at a well-studied marine habitat. Furthermore, we describe the microbial phylotypes that are most abundant during active C<sub>1</sub>-C<sub>4</sub> degradation.

## MATERIALS AND METHODS

### STUDY SITE AND SAMPLE COLLECTION

Sediments were collected from the Garden Banks mud volcano site (GB425) in the northern GoM (27°33.140'N, 92°32.437'W) at 597 m depth, during an expedition with the *R/V Atlantis* and *DSV Alvin* (Dive 4645) in November 2010. Intact sediment cores were recovered with polyvinylchloride core sleeves (20–30 cm height, 6.35 cm ID, 0.32 cm sleeve thickness). Sediment sampling sites were selected based on the presence of chemoautotrophic *Beggiatoa* mats overlying the sediments and the previous detection of alkanes. Retrieved cores were sealed under Argon gas to limit gas exchange with the atmosphere and to prevent reoxidation of sulfide to sulfate, and refrigerated for transport to the laboratory. It is important to note that sulfide reoxidation is very rapid in these sediments, particularly in sediments hosting microbial mats (Bowles et al., 2011). Therefore, it is not surprising that there is no observable sulfate gradient. Hydrogen concentrations at the study site were determined using a “reduction gas analyzer” as described by Orcutt et al. (2005). The *in situ* SRRs were measured shipboard as described previously (Bowles et al., 2011). The bottom water temperature at this study site was 8°C.

### BATCH REACTOR SET-UP AND SAMPLING

Collected sediments were transferred to an anaerobic chamber with a 5% H<sub>2</sub>/75% N<sub>2</sub>/20% CO<sub>2</sub> atmosphere (Coy Laboratory Products, Grass Lake, MI). The sediment core used for this study

was stored for 3 months at 7°C. Sediments were thoroughly mixed, and were then diluted with an equal volume of anaerobic medium with 28 mM sodium sulfate and 2 mM sodium sulfide (Widdel and Bak, 1992). No nitrate or nitrite was added to the medium. The resulting slurry was aliquoted into sterile 200 mL serum bottles and sealed with a butyl rubber stopper under strict anoxic conditions. The serum bottle headspace (100 mL) was flushed and then filled with a single gas at ~69 kPa (concentrations of 40–80 mM, **Figure 1**) of chemically pure (>99% purity) methane, ethane, propane, or butane (Airgas East, Waterford, CT, USA). The solubility at standard conditions (in water) of each gas is as follows: methane (0.9 mM), ethane (1.3 mM), propane (1 mM), and butane (0.8 mM) ([webbook.nist.gov/](http://webbook.nist.gov/)) and exceeds the observed *in situ* concentrations of ~400, 20, 1, and 1 μM, respectively reported below. Excess gas pressure was used to overcome potential issues in isotopic data interpretation as reported for anaerobic propane oxidation previously (Quistad and Valentine, 2011), and to avoid substrate limitation. The control bottles were flushed and filled with chemically pure (>99% purity) nitrogen (N<sub>2</sub>) gas. An initial sample of each gas (except N<sub>2</sub>) was taken for isotopic analyses. The slurry was also subsampled and frozen at -80°C for DNA extraction, sulfide and sulfate quantification.

To test whether alkanes could be oxidized without concomitant sulfate reduction, we use the competitive inhibitor molybdate to inhibit sulfate reduction and monitored the subsequent alkane consumption rates. Briefly, 5 mL of sediment slurry was transferred to 25 mL Balch tubes, in duplicate, per gas amendment, and sealed using a rubber butyl stopper inside an anaerobic chamber. These incubation volumes were used to maximize analyses given the limited sediment volumes. Due to the high sulfate concentration present in these incubations, the effect of changing

the incubation volume should not be detrimental to sulfate reduction. Sodium molybdate was added to each tube to a final concentration of 28 mM (Orcutt et al., 2008). These tubes were then flushed and filled with the appropriate C<sub>1</sub>–C<sub>4</sub> or N<sub>2</sub> gas at ~69 kPa.

All the reactors were incubated at 7°C and the headspace was sampled every 15-days to monitor C<sub>1</sub>–C<sub>4</sub> consumption. After 80 days of incubation, the final gas concentrations were measured, and gas samples were archived in gastight Exetainers (Labco International, Houston, TX, USA) for natural abundance isotopic measurements. Samples were also withdrawn for DIC, DNA, sulfide and sulfate measurement, and preserved by freezing at -80°C in appropriate vials. All sub-samples were collected and measured in triplicate.

## GEOCHEMICAL MEASUREMENTS

C<sub>1</sub>–C<sub>4</sub> alkanes were quantified from the headspace by subsampling a 50 μL aliquot and analyzing alkane concentrations on a gas chromatograph (Hewlett Packard 5890 Series II) equipped with a flame ionization detector and a packed column (RestekRt-XL). Chemically pure alkanes (>99% purity) (Airgas East, Waterford, CT, USA) were used to generate standard curves. To account for potential alkane leakage from the bottles, we set up sediment-free controls and monitored changes in alkane concentration over time. Sediment-free controls showed ~4 ± 1% variation in gas measurements, which represents both the analytical resolution of our measurements and/or modest loss of gas due to leakage or sorption into the stoppers, and is well below the rates of loss observed in the biological treatments (see below). Sulfate concentrations were determined using the QuantiChrom™ Sulfate Assay Kit (BioAssay Systems, Hayward, CA, USA). Sulfide concentrations were measured using a colorimetric assay based on the Cline method (Cline, 1969). Nitrate was measured using the resorcinol method as described previously (Zhang and Fischer, 2006). Nitrite was measured as previously described (Pai et al., 1990).

## MICROBIAL SULFATE REDUCTION RATE MEASUREMENTS

SRRs were measured using a previously described radiotracer method (Fossing and Jorgensen, 1989). Briefly, the slurry incubations were opened under anaerobic conditions and 5 mL subsamples of the enrichments were transferred to a Balch tubes. The tubes were sealed and pressurized as described previously. The Balch tubes were then amended with ca. 10 μL of Na<sup>35</sup>SO<sub>4</sub><sup>2-</sup> (2 μCi) and incubated for 1 day. Following incubation the slurries were shaken and 1 mL of slurry was drawn by syringe into 5 mL of 20% zinc acetate and shaken, effectively trapping H<sub>2</sub><sup>35</sup>S<sub>(aq)</sub> as ZnS<sub>(s)</sub>. The ZnS solution was placed into a 15 mL Falcon tube, and washed three times with a 3% NaCl solution to remove any residual <sup>35</sup>SO<sub>4</sub><sup>2-</sup>. Sulfide was extracted using the hot chromium reduction method (Fossing and Jorgensen, 1989), ultimately trapping sulfide in 20% Zn-acetate. The activity of <sup>35</sup>S was determined by liquid scintillation and SRR were calculated after Fossing and Jorgensen (1989) using Equation 1.

$$\text{SRR} = \left[ \text{SO}_4^{2-} \right] * \frac{1.06}{t} * \frac{a}{(A + a)} \quad (1)$$

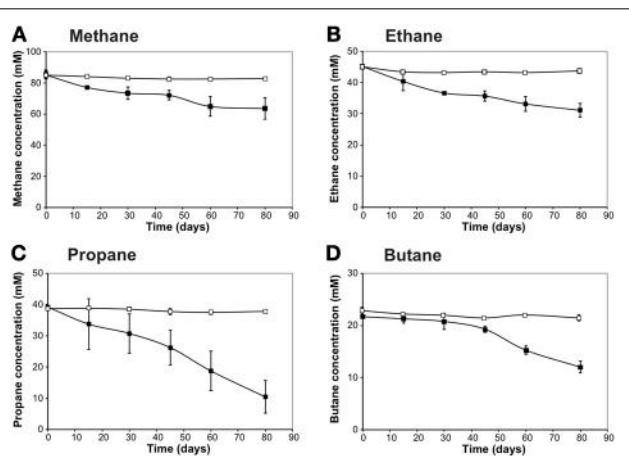


**FIGURE 1 |** Alkane consumption as a function of time by the Gulf of Mexico (GoM) site GB425 (dive 4645 and core 22) incubations. The alkane concentration in the headspace of the sediment incubations was measured using a Hewlett Packard 5890 Series II gas chromatograph equipped with a flame ionization detector, on a Restek Rt-XL Sulfur packed column. **(A)** methane; **(B)** ethane; **(C)** propane; and **(D)** butane. Rates of alkane consumption were calculated using all available time points based on a linear regression.

Where  $[\text{SO}_4^{2-}]$  is the concentration ( $\text{nmol mL}^{-1}$ ) of sulfate incubation,  $a$  is the activity (dpm) of the trapped sulfide, 1.06 is the fractionation factor between the sulfide and sulfate pools,  $A$  is the activity of the sulfate pool, and  $t$  is the incubation time (days). The rates are presented in units of  $\text{nmol S mL}^{-1} \text{ day}^{-1}$ .

## ISOTOPE ANALYSIS

All isotopic analyses were performed at the Stable Isotope Facility at University of California, Davis using a method modified from a previous publication (Atekwana and Krishnamurthy, 1998). For DIC measurements, 1 mL filtered ( $0.2 \mu\text{m}$ ) water samples were collected and injected into evacuated 12 mL septum capped vials (Exetainers, Labco, Houston, TX, USA) containing 1 mL 85% phosphoric acid. The evolved  $\text{CO}_2$  was purged from vials through a double-needle sampler into a helium carrier stream ( $20 \text{ mL min}^{-1}$ ). For high concentration samples, gases were sampled by a six-port rotary valve (Valco, Houston, TX, USA) with a  $100 \mu\text{L}$  loop programmed to switch at the maximum  $\text{CO}_2$  concentration in the helium carrier. For low concentration samples, the entire  $\text{CO}_2$  content was frozen in a trapping loop then released to the GC column. The  $\text{CO}_2$  was passed to the IRMS through a Poroplot Q GC column ( $25 \text{ m} \times 0.32 \text{ mm ID}, 45^\circ\text{C}, 2.5 \text{ mL/min}$ ). A reference  $\text{CO}_2$  peak was used to calculate provisional delta values of the sample  $\text{CO}_2$  peak. Final  $\delta^{13}\text{C}$  values were obtained after adjusting the provisional values such that correct  $\delta^{13}\text{C}$  values for laboratory standards were obtained. Two laboratory standards were analyzed every 10 samples. The laboratory standards are lithium carbonate dissolved in degassed, deionized water, and a deep seawater reference material (both calibrated against NIST 8545).

For isotopic analyses of the  $\text{C}_1$ - $\text{C}_4$  gases, a ThermoScientific PreCon concentration system interfaced to a ThermoScientific Delta V Plus isotope ratio mass spectrometer (ThermoScientific, Bremen, DE) was used as described previously (Yarnes, 2013). Gas samples were purged from Exetainers through a double-needle sampler into a helium carrier stream ( $20 \text{ mL/min}$ ), which is passed through a  $\text{H}_2\text{O}/\text{CO}_2$  scrubber [ $\text{Mg}(\text{ClO}_4)_2$ , Ascarite] and a cold trap cooled by liquid  $\text{N}_2$ . The gas was separated from residual gases by a Rt-Q-BOND GC column ( $30 \text{ m} \times 0.32 \text{ mm} \times 10 \mu\text{m}, 30^\circ\text{C}, 1.5 \text{ mL/min}$ ). After the gas eluted from the separation column, it was either oxidized to  $\text{CO}_2$  by reaction with nickel oxide at  $1000^\circ\text{C}$  ( $\delta^{13}\text{C}$ ), or pyrolyzed in an empty alumina tube heated to  $1350^\circ\text{C}$  ( $\delta^2\text{H}$ ) and subsequently transferred to the IRMS. A pure reference gas ( $\text{CO}_2$  or  $\text{H}_2$ ) was used to calculate provisional delta values of the sample peak. Final  $\delta$ -values are obtained after adjusting the provisional values for changes in linearity and instrumental drift such that correct  $\delta$ -values for laboratory standards were obtained. Laboratory standards were commercially prepared gases diluted in helium or air and were calibrated against NIST 8559, 8560, and 8561.

## DNA EXTRACTION, MASSIVELY PARALLEL SEQUENCING, AND PHYLOGENETIC ANALYSES

Sediment was subsampled under anoxic conditions for  $T_0$  and  $T_f$  for nucleic acid extractions. These samples were flash frozen in liquid  $\text{N}_2$  and stored at  $-80^\circ\text{C}$  until use. DNA was extracted using the PowerSoil® DNA Isolation Kit (MO BIO Laboratories, Inc., Carlsbad, CA, USA) as per the manufacturer's guidelines. The

extracted DNA was subjected to massively parallel sequencing of the 16S ribosomal RNA (rRNA) gene using Roche 454 Titanium™ chemistry and the primer pairs 27F/519R and 340F/806R for the bacterial V1-V3 and archaeal V3-V4 regions, respectively (Dowd et al., 2008; Acosta-Martinez et al., 2010). The resulting sequences were analyzed as previously described, and denoised using the QIIME pipeline (Adams et al., 2013). Phylogenetic analysis was performed as previously described using FastTree(2.1.7) for tree generation with 25 representative sequences (Adams et al., 2013). All sequences generated in this study are deposited with NCBI (accession #SRP032824).

## QUANTITATIVE-PCR

Quantitative PCR (qPCR) was used to determine the abundance of bacterial and archaeal 16S rRNA, *dsrA*, *aprA*, and *mcrA* genes. In addition, qPCR was used to enumerate the abundance of sulfate-reducing prokaryotes by amplifying the adenosine 5'-phosphosulfate [APS] reductase (*aprA*) gene with primers specific to sulfate-reducing bacteria and archaea (Christophersen et al., 2011). Primers specific to the bacterial dissimilatory sulfate reductase (*dsrA*) gene were used to quantify members of sulfate-reducing bacteria (Kondo et al., 2004). We refer to all sulfate-reducing microbes as sulfate-reducing prokaryotes or SRP throughout. Methanogenic archaea were quantified using *mcrA* primers directed specifically toward the methanogenic methyl Coenzyme M reductase encoding gene (Luton et al., 2002; Ver Eecke et al., 2012). Standard curves were constructed by serial dilution of linearized plasmids containing the target gene (Table 1). Quantification was performed in triplicate with the Stratagene MX3005p qPCR System (Agilent Technologies) using the Perfecta SYBR FastMix with low ROX ( $20 \mu\text{L}$  reactions, Quanta Biosciences, Gaithersburg, MD) and specific primers and annealing temperatures (Table 1). The temperature program for all assays was  $94^\circ\text{C}$  for 10 min, 35 cycles of  $94^\circ\text{C}$  for 1 min, the annealing temperature for 1 min (Table 1), extension at  $72^\circ\text{C}$  for 30 s, and fluorescence read after 10 s at  $80^\circ\text{C}$ . Following amplification, dissociation curves were determined across a temperature range of  $55$ - $95^\circ\text{C}$ .  $C_t$ -values for each well were calculated using the manufacturer's software.

## RESULTS

### GEOCHEMICAL CHARACTERISTICS OF SITE GB425

Though the gross geochemistry of this site has been previously described (Joye et al., 2009), here we present the alkane concentrations and other geochemical attributes of the specific sediments used in these studies (Table 2). DIC ranged between 4 and 6 mM, while the observed dissolved organic carbon (DOC) is about 1–3 mM through the sediment depths surveyed. Nitrate and nitrite concentration was 5–40  $\mu\text{M}$  in the upper layers of the sediment. Sulfate, the dominant oxidant, was replete throughout the sediment profile (24–36 mM) and was higher than typical seawater values (28 mM) (Canfield and Farquhar, 2009). *n*-alkanes were observed only between 9 and 15 cm sediment depth. Between the depth ranges of 9–12 and 12–15 cm ethane was observed at 17.22–22.33  $\mu\text{M}$ , propane at 1.45–0.75  $\mu\text{M}$ , butane at 0.74–0.35  $\mu\text{M}$ . Pentane was not observed. Methane concentrations peaked at 425.05  $\mu\text{M}$ , at  $\sim$ 15–18 cm sediment depth (Table 3).

**Table 1 | Primers and Conditions for quantitative PCR assays.**

Process	Target gene	Forward primer (nM)	Reverse primer (nM)	Positive control	Annealing temp in °C (References)
Sulfate reduction	Dissimilatory sulfite reductase	<i>DSR1-F</i> (400) ATCGGNCAKGCTTYCCNTT	<i>DSR-R</i> (600) GTGGMRCGTCAGKRTTGG	<i>Desulfovibrio vulgaris</i>	58°C (Kondo et al., 2004)
Sulfate reduction	Adenosine 5'-phosphosulfate reductase	<i>aps3F</i> (400) TGGCAGATCATGWTYAYGG	<i>aps2R</i> (400) GCGCCGTAACCRTCYTRAA	<i>Desulfovibrio vulgaris</i>	55°C (Christophersen et al., 2011)
Methanogenesis	Methyl CoM reductase	<i>qmcrAFAalt</i> (150) GAR GAC CAC TTY GGH GGT TC	<i>ML-R</i> (200) TTCATTGCRTAGTTWGRTAGTT	<i>Methanosarcina acetivorans</i> , <i>Methanococcus jannaschii</i>	59°C (Luton et al., 2002; Ver Eecke et al., 2012)
Bacteria	16S rRNA	<i>Bact1369F</i> (1000) GTT GGG GCC RCC WCK KCK NAC	<i>Prok1541R</i> (1000) CGGTGAATATGCCCTGC	<i>Arcobacter nitrofigulis</i>	59°C (Suzuki et al., 2001)
Archaea	16S rRNA	<i>Arch349F</i> (500) GYGCASCAGKCGMGAAW	<i>Arch806R</i> (500) GGACTACVSGGTATCTAAT	<i>Ferroplasma acidarmonas</i> Fer1	54°C (Takai and Horikoshi, 2000)

**Table 2 | Geochemical data from site GB425, from which sediments were collected for these analyses in November 2010 (27°33.1887N, 93°32.4449W).**

Depth range (cm)	DIC (mM)	d <sup>13</sup> C-DIC (‰)	Hydrogen (nM)	DOC (mM)	Sulfate (mM)	Sulfide (mM)	Nitrate and Nitrite (mM)	Methane (µM)	pH	Sulfate reduction rate (nmol mL <sup>-1</sup> day <sup>-1</sup> )	Anaerobic methane oxidation (nmol mL <sup>-1</sup> day <sup>-1</sup> )
Overlying water	n.s.	n.s.	n.s.	958	n.s.	n.s.	23.1	n.s.	7.5	n.a.	n.a.
0–3	3.9	−10.0	37.4	2477	24.2	0.6	36.2	122.3	7.5	86 ± 5	0.8 ± 0.3
3–6	4.4	−10.5	242.4	1203	32.3	0.1	5.2	63.0	7.6	344 ± 216	1.6 ± 0.3
6–9	4.2	−12.6	21	1702	32.3	0.6	b.d.l.	378.1	7.9	182	6.8 ± 0.1
9–12	5.1	−19.5	29.8	1.s.	27.9	0.2	b.d.l.	371.9	i.v.	135 ± 22	5.0 ± 2.5
12–15	4.7	−15.2	51.9	1.s.	n.s.	0.8	b.d.l.	413.1	i.v.	n.s.	n.s.
15–18	4.9	−20.1	31.4	1.s.	29.9	0.6	b.d.l.	425.1	8.0	596 ± 8	30.3 ± 7.6
18–21*	5.8	−28.6	38.9	2618	29.1	n.s.	40.6	200.2	i.v.	185 ± 216	7.8 ± 0.5
21–24	6.0	−23.7	39.6	2982	25.0	0.1	b.d.l.	357.7	i.v.	743 ± 340	18.2 ± 10.0
24–27	5.3	−23.3	50.7	1420	35.8	1	b.d.l.	288.8	i.v.	287 ± 120	18.9 ± 0.4
27–30	5.3	−24.4	31.5	1.s.	n.s.	1.2	b.d.l.	203.2	i.v.	n.s.	n.s.

DIC, Dissolved inorganic carbon; DOC, Dissolved organic carbon, n.s., No sample; i.s., Lost sample; i.v., Insufficient volume; b.d.l., Below detection limit; n.a., Not applicable. Rate measurements are mean ± standard error ( $n = 2$ ). \*Data at this depth range appears unreliable.

### C<sub>1</sub>–C<sub>4</sub> ALKANE OXIDATION OCCURS IN BATCH REACTORS

*n*-Alkane consumption began within the first 15 days of the 80-day incubations for C<sub>1</sub>–C<sub>3</sub> gases (defined as >10% consumption compared to  $T_0$ ) (Figure 1). C<sub>4</sub> consumption was only measurable after ~45 days of incubation. The highest % consumption was observed for propane (73 ± 13%) followed by butane (45 ± 5%), ethane (31 ± 6%), and methane (25 ± 6%). The highest rate of consumption was observed for propane (354 ± 37 nmol mL<sup>−1</sup> day<sup>−1</sup>) followed by methane (263 ± 68 nmol cm<sup>−3</sup> day<sup>−1</sup>), ethane (168 ± 5 nmol cm<sup>−3</sup> day<sup>−1</sup>), and butane (125 ± 16 nmol cm<sup>−3</sup> day<sup>−1</sup>) (Figure 2, Table 4). Along with alkane oxidation we also

observed a decline in sulfate concentrations and a concomitant increase in sulfide concentrations (Table 5). Importantly, the sulfide concentrations were below those observed to be inhibitory (16.1 mM) for sulfate-reducing bacteria (Reis et al., 1992).

### SULFATE REDUCTION IS COUPLED TO C<sub>1</sub>–C<sub>4</sub> ALKANE OXIDATION

The addition of each C<sub>1</sub>–C<sub>4</sub> gas increased the SRR over the N<sub>2</sub> control treatment by at least 2-fold (Figure 2). The rates reported from these incubations are comparable to previous reports from GoM non-seep porewaters and sediments (Arvidson et al., 2004; Joye et al., 2004) but lower than those measured shipboard on

freshly collected samples (**Table 2**). While it is impractical to identify the precise cause of this discrepancy, there are a few likely factors that could have contributed to these differences, including (A) natural heterogeneity in the geochemistry and microbial community composition and activity; (B) the process of sediment homogenization prior to incubations, which does not represent

**Table 3 | C<sub>1</sub>-C<sub>5</sub> alkane concentrations in sediments at site GB425, from which sediments were collected for this study in November 2010 (27°33.1887N, 93°32.4449W).**

Depth range (cm)	Methane (μM)	Ethane (μM)	Propane (μM)	n-butane (μM)	Pentane (μM)
9–12	371.94	17.22	1.45	0.74	0.00
12–15	413.12	22.33	0.75	0.35	0.00

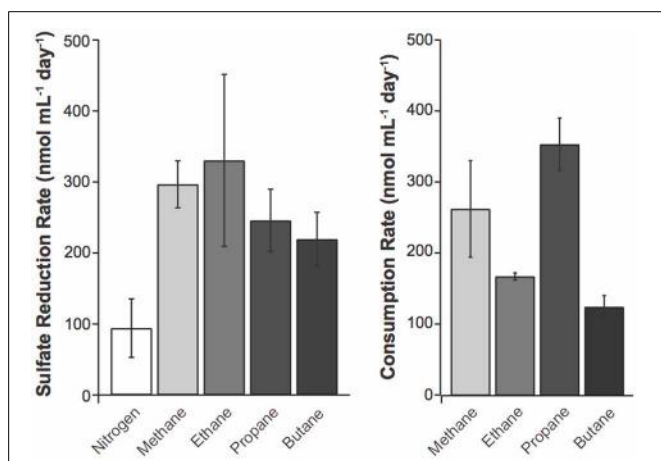


**FIGURE 2 | Potential sulfate reduction rates (SRR) were measured using the  $^{35}\text{SO}_4^{2-}$  radiotracer method (Fossing and Jorgensen, 1989) and consumption rates for C<sub>1</sub>-C<sub>4</sub> alkanes by alkane amended slurries of GoM site GB425 sediments.** The SRR assays were performed for 24 h. Values represent average  $\pm$  standard deviation of triplicate measurements of duplicate incubations. Alkane consumption rates were calculated from a linear regression as in **Figure 1**. Rates of sulfate reduction were calculated as described in the methods.

maximal or minimal rates; and (C) changes in microbial composition and activity during the 3 months of storage. Comparison of SRR in the one-day incubations to C<sub>1</sub>-C<sub>4</sub> alkane oxidation rates (**Table 4**) shows that the addition of methane or any of the four alkanes stimulates SRR over the N<sub>2</sub> control treatment. From the predicted reaction stoichiometry (**Table 6**) both the methane and ethane oxidation rates correspond closely with the observed SRR. In contrast substantially higher levels of propane and butane oxidation were observed than can be supported by sulfate reduction alone. Incubation with molybdate inhibited the oxidation of C<sub>1</sub>-C<sub>4</sub> gases by ~90–97% (**Table 4**), consistent with the direct involvement of sulfate-reducing prokaryotes in alkane oxidation.

### CARBON ISOTOPIC SIGNATURE AND ANALYSES

The  $\delta^{13}\text{C}$  signature of the methane in the headspace did not appreciably change over the course of the incubation period (**Table S1**). This contrasts with the isotopic signatures of the other alkanes. As mentioned, ethane concentration decreased to about 10 mM over the course of the incubation, but the isotopic change in the pool was not significant. The incubations with propane showed the largest decrease in concentration (~30 mM) over the 80-day incubation period. Over this time, the propane pool was enriched by 4.4‰. Finally, incubations with butane resulted in a decrease in the pool size of ~10 mM (1 mmol) and an enrichment in the residual butane pool of 4.5‰.

**Table 5 | Sulfate and sulfide concentrations measured in the initial sediment slurry and at the final time-point.**

	Sulfate concentration (mM)	Sulfide concentration (mM)
Sediment slurry (Initial)	$31.6 \pm 1.2$	$2.3 \pm 0.2$
N <sub>2</sub> control (Final)	$26.4 \pm 1.8$	$8.2 \pm 0.1$
Methane (Final)	$26.1 \pm 6.1$	$9.1 \pm 0.4$
Ethane (Final)	$22.1 \pm 4.0$	$10.4 \pm 1.1$
Propane (Final)	$15.6 \pm 4.1$	$9.5 \pm 1.4$
Butane (Final)	$13.3 \pm 1.2$	$15.4 \pm 3.2$

**Table 4 | Comparing rate of alkane oxidation and sulfate reduction, and the effect of molybdate on alkane oxidation.**

	Rate of alkane consumption (nmol mL⁻¹ day⁻¹)	Rate of alkane consumption with molybdate addition (nmol mL⁻¹ day⁻¹) (%) inhibition)	Total sulfate reduction rate (nmol mL⁻¹ day⁻¹)	Observed ratio using total SRR alkane:SO <sub>4</sub> <sup>2-</sup>	Corrected sulfate reduction rates above the nitrogen control (nmol mL⁻¹ day⁻¹)	Observed ratio using corrected SRR alkane:SO <sub>4</sub> <sup>2-</sup>	Predicted ratio of alkane: SO <sub>4</sub> <sup>2-</sup> from Table 6
Methane	$263 \pm 68$	$29 \pm 1$ (89)	$297 \pm 33$	0.9	$203 \pm 53$	1.3	1
Ethane	$168 \pm 5$	$12 \pm 4$ (93)	$330 \pm 121$	0.51	$236 \pm 127$	0.7	0.57
Propane	$354 \pm 37$	$10 \pm 5$ (97)	$246 \pm 44$	1.4	$152 \pm 60$	2.3	0.4
Butane	$125 \pm 16$	$14 \pm 2$ (89)	$220 \pm 38$	0.57	$125 \pm 56$	1	0.34

Rates of alkane consumption were calculated using all available time points based on a linear regression. Rates of sulfate reduction calculated as described in the methods.

**Table 6 | Gibbs free energy of the anaerobic oxidation of acetate, methane, and alkanes using sulfate as an electron acceptor (conditions shown are at standard temperature and pressure).**

Sulfate reduction process	Reaction	$\Delta G^0$ (kJ/mol $\text{SO}_4^{2-}$ )*	Carbon source: $\text{SO}_4^{2-}$	C: $\text{SO}_4^{2-}$
1 Heterotrophic (acetate)	$\text{SO}_4^{2-} + \text{CH}_3\text{COO}^- \rightarrow 2\text{HCO}_3^- + \text{HS}^-$	-47.7	1:1	2:1
2 Heterotrophic (methane)	$\text{SO}_4^{2-} + \text{CH}_4 \rightarrow \text{HCO}_3^- + \text{HS}^- + \text{H}_2\text{O}$	-33	1:1	1:1
3 Heterotrophic (ethane)	$14\text{SO}_4^{2-} + 8\text{C}_2\text{H}_6 \rightarrow 14\text{HS}^- + 16\text{HCO}_3^- + 8\text{H}_2\text{O} + 2\text{H}^+$	-39.81	8:14	16:14
4 Heterotrophic (propane)	$5\text{SO}_4^{2-} + 2\text{C}_3\text{H}_8 \rightarrow 6\text{HCO}_3^- + 5\text{HS}^- + \text{H}^+ + 2\text{H}_2\text{O}$	-33.06	2:5	6:5
5 Heterotrophic (butane)	$26\text{SO}_4^{2-} + 9\text{C}_4\text{H}_{10} + 4\text{H}_2\text{O} \rightarrow 36\text{HCO}_3^- + 36\text{HS}^- + 26\text{H}^+$	-14	9:26	18:13
6 Autotrophic (with $\text{H}_2$ )	$\text{SO}_4^{2-} + 2\text{HCO}_3^- + 8\text{H}_2 + 2\text{H}^+ \rightarrow \text{CH}_3\text{COO}^- + \text{HS}^- + 8\text{H}_2\text{O}$	-336.5	2:1	2:1

Autotrophic sulfate reduction, in which hydrogen is used to reduce inorganic carbon, is shown for reference.

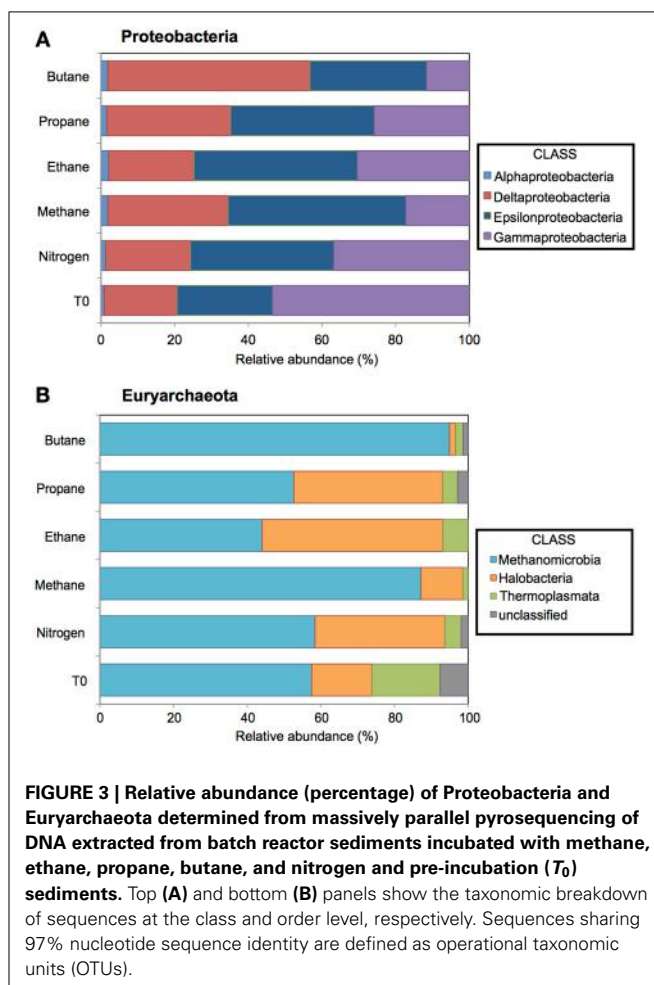
\* $\Delta G^0$  Values reported are those calculated under standard conditions of 1 M concentrations for soluble reactants, 1 atmosphere pressure for gases, 298.15 K temperature at pH 7.0 and are calculated using values from the CRC Handbook for Chemistry and Physics (<http://www.hbcpnetbase.com/>).

## MICROBIAL COMMUNITY ANALYSES

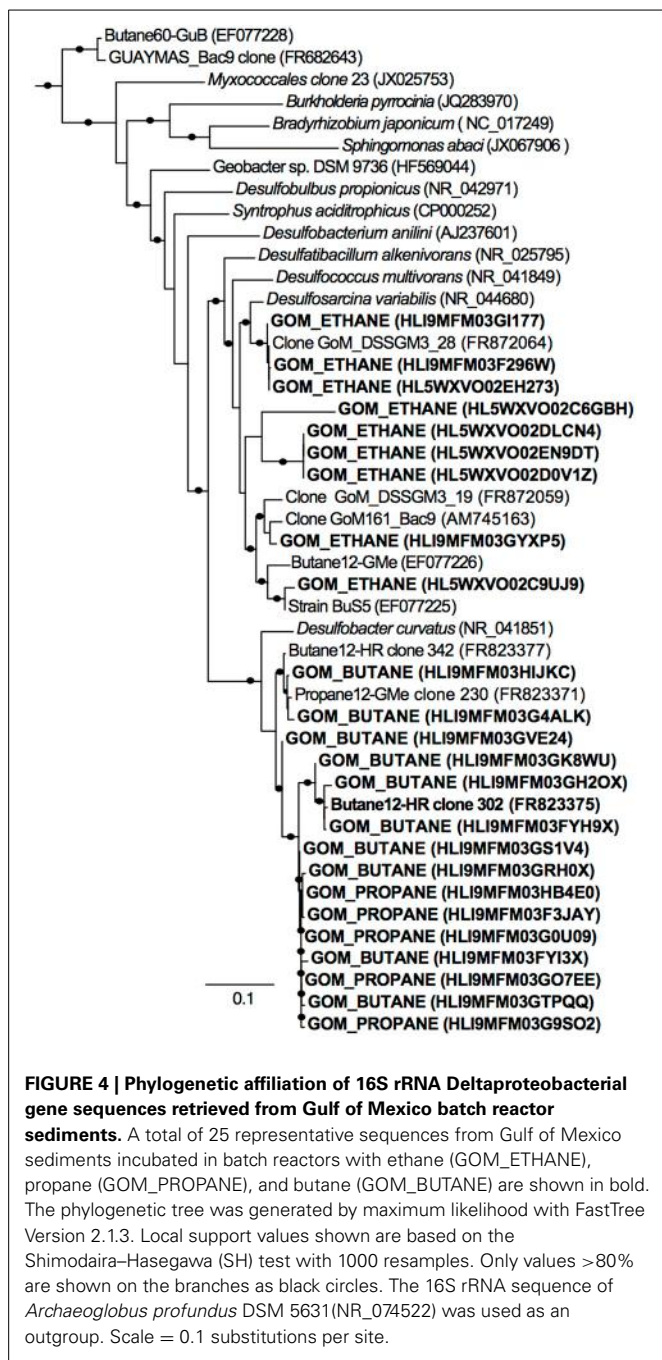
### 454 pyrotag sequencing

A total of 11,725, 17,003, 12,529, 16,208, and 18,015 bacterial sequences were analyzed from sediments incubated with  $\text{N}_2$ , methane, ethane, propane, and butane, respectively, and 12,944 bacterial sequences from the  $T_0$  sediment. There were shifts between the Proteobacterial communities of the alkane batch reactors in comparison to the control and  $T_0$  sediment community (Figure 3A). Among sequences allied to known sulfate-reducing Deltaproteobacteria, there was an increase from the  $T_0$  sequences (~20%) in the  $\text{N}_2$ , methane, ethane, propane, and butane sequence libraries (~23, 32, 23, 33, and 55%, respectively) (Figure 3A). In turn, there was a decrease in the representation of Gammaproteobacteria in the  $\text{N}_2$ , methane, ethane, propane, and butane sequence libraries (~37, 17, 30, 26, and 12%, respectively) from the  $T_0$  sequences (~53%). 16S rRNA gene phylogeny revealed that the ethane reactors harbored a putative SRP community that was distinct from the propane and butane reactors (Figure 4). These sequences comprised the majority (90–95%) of the Deltaproteobacterial community (Figure 4). In the ethane reactor community, the most closely related Deltaproteobacterial 16S rRNA gene sequences (95–99% nucleotide sequence identity) included strain BuS5 (accession no. EF077225), the enrichment culture “Butane12-GMe” (accession no. EF077226), and other SRP clones from sediments retrieved from the GoM (clone GoM\_DSSGM3\_28, accession no. FR872064; clone GoM\_DSSGM3\_19, accession no. FR872059; and clone GoM161\_Bac9, accession no. AM745163) (Kniemeyer et al., 2007; Orcutt et al., 2010; Kleindienst et al., 2012). In contrast, SRP sequences in the propane and butane batch reactor communities were most closely allied to uncultured Deltaproteobacteria clones from propane- and butane-oxidizing enrichments of hydrocarbon seep sediments from the GoM (Propane12-GMe clone 230, accession no. FR823371) and Hydrate Ridge (Butane12-HR clone 302, accession no. FR823377) and Butane12-HR clone 342, accession no. FR823377) (Jaekel et al., 2013).

A total of 18,667, 10,291, 18,545, 12,462, 9743, and 13,233 archaeal sequences were also analyzed from the  $\text{N}_2$ , methane, ethane, propane, and butane batch reactors and  $T_0$  sediments, respectively. There were notable shifts in the sequences allied to the class Methanomicrobia from the initial sediment community



and across the different alkane batch incubations (Figure 3B). Over 58% of sequences were allied to Methanomicrobia in  $T_0$  sediments, increasing to comprise ~87 and 94% of methane and butane sequences. Within the Methanomicrobia, there were also notable changes in sequences identified as phylotypes that mediate AOM. For the putative methane-oxidizing communities, ANME-1 comprised ~40% of the Methanomicrobia in the incubation with methane, but less than 5% of sequences were



allied to ANME-1 in the  $T_0$ ,  $N_2$ , ethane, propane, and butane sediments (Figure S1).

#### Quantitative PCR

qPCR using specific primers for 16S rRNA showed that bacterial 16S rRNA gene abundance was two orders of magnitude higher than archaeal 16S rRNA gene abundance at the start of the incubation (Figures 5A,B). Bacterial abundance was only slightly elevated (less than an order of magnitude) over the  $T_0$  assessment in all treatments at the end of the incubation period with the greatest increase in population observed in the  $N_2$  and

$CH_4$  amendments (~3-fold increase). Addition of alkanes also stimulated bacterial population growth of about 2-fold over the initial population estimates.  $N_2$  and ethane amendments resulted in a 3-fold increase in archaeal populations while propane and butane yielded a 1.5-fold increase. These differences are consistent among treatments. However, 40% of bacterial genomes contain 1–2 copies of rRNA genes, though microbial genomes with as many as 15 copies have been reported (Acinas et al., 2004). Moreover, archaeal genomes are known to harbor between 1 and 5 rRNA gene copies per genome (Acinas et al., 2004). Thus, given these differences, as well as environmental heterogeneity and other factors, the differences presented here likely reflect relative changes in proportion, but the significance of these changes among treatments remains unconstrained.

Estimates of *aprA* gene abundance, a marker for SRP, reveal the highest abundances at the initiation of the incubation and under the  $N_2$  amendments. *aprA* gene abundance after incubation with methane or the tested alkanes show a decrease in abundance, perhaps indicating a shift in community due to incubation effects that is consistent with the decrease in bacterial 16S rRNA gene abundance over the same treatments. Notably, of the alkane additions, propane maintained the largest SRP population followed by ethane, methane and butane treatments (Figure 5IIA).

The 16S rRNA gene phylogeny of SRP is diverse and difficult to capture with specific primers. Accordingly, we employed primers targeting the gene encoding for dissimilatory sulfite reductase (subunit A) with primers that target both Gram-positive and Gram-negative bacterial species of SRP (Kondo et al., 2004). With the exception of the  $N_2$  treatment, the *dsrA* gene abundance is similar across all treatments. The *dsrA* gene abundance in the  $N_2$  treatment is about 3-fold higher than observed in other treatments (Figure 5IIB).

Archaeal *mcrA* gene abundance was highest, and had the greatest standard deviation at the initial sampling. The lowest observed *mcrA* gene abundance occurred in the methane amended samples and concurs with a similar observed decrease in the total archaeal 16S rRNA gene abundance described above. This suggests that the addition of methane adversely affected the natural methanogen population over the course of the incubation (Figure 5IIIa).

#### DISCUSSION

The anaerobic microbial degradation of short-chain alkanes has recently gained attention because microbes mediating these processes may compete for the oxidant pool (sulfate), potentially influencing the rates of AOM (Kniemeyer et al., 2007; Savage et al., 2010; Adams et al., 2013; Jaekel et al., 2013). The data herein reveal that C<sub>1</sub>–C<sub>4</sub> alkane consumption—including anaerobic ethane oxidation—stimulated sulfate reduction. To assess the significance of the determined potential rates of sulfate reduction and *n*-alkane consumption, two points must be addressed: (1) the intrinsic sulfate reduction activity in the GoM sediments used, and (2) the concentrations of the substrates used relative to those measured *in situ*. First, bulk geochemical analyses show that the GoM sediments are rich in organic matter and hydrogen that can support the growth of heterotrophic and autotrophic SRP. At this study site, the DOC concentration was ~1–3 mM and hydrogen was in the nM range. It was therefore critical to account for sulfate

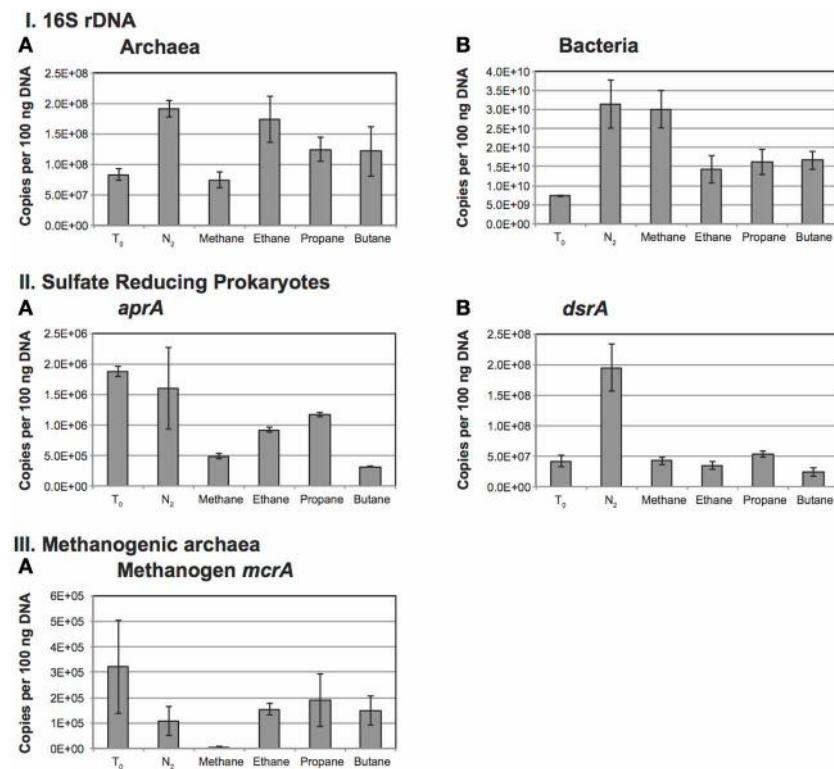


**FIGURE 5 | Abundance of microbes determined using quantitative PCR.** Panel (I) represents the 16S rRNA abundances for A: Bacteria and B: Archaea. Panel (II) represents the abundance of sulfate-reducing bacteria as determined using A: *aprA* and B: *dsrA*. Panel (III) represents the abundance of methanogens as determined using A: *mcrA*.

reduction attributable to endogenous electron donors, which we did by maintaining the native sediments under a N<sub>2</sub> atmosphere. Not surprisingly, these incubations exhibit intrinsic sulfate reduction activity at nearly 100 nmol SO<sub>4</sub><sup>2-</sup> mL<sup>-1</sup> day<sup>-1</sup>. Importantly, the addition of *n*-alkanes increased this baseline sulfate reduction. Second, sulfate concentrations used in the *ex situ* incubations correspond with those measured at various depth ranges at this GoM marine seep (Table 2) and were not limiting (in bulk geochemistry; Table 5) over the course of the incubation. Given that these experiments were conducted at conditions that might favor anaerobic alkane oxidation, e.g., an abundance of one alkane in the gas phase, and a media replete with sulfate, these data provide insight into the relationship between alkane oxidation and sulfate reduction, and represent “potential” rates of *n*-alkane consumption linked to sulfate reduction.

With the aforementioned points in mind, we address the linkage between alkane consumption and sulfate reduction from a few perspectives. First, based on the stoichiometry of each alkane oxidation-sulfate reduction pathway (Table 6) we estimate the contribution of each oxidation pathway to SRR. Second, we use the change in the isotopic signatures of the alkanes and the DIC pool to estimate carbon exchange between the alkane and DIC pools, and compare this carbon mobility with the alkane-oxidation rates (Table S2). Furthermore, we examine the community composition within the enrichments in an effort to elucidate

sulfate-reducing bacteria as determined using A: *aprA* and B: *dsrA*. Panel (III) represents the abundance of methanogens as determined using A: *mcrA*.

community members potentially responsible for alkane oxidation and sulfate reduction (Figures 3–5).

From the stoichiometry of the reaction pathways (Table 6), which assume the alkanes are completely oxidized to HCO<sub>3</sub><sup>-</sup>, and that no alkane-derived carbon is assimilated, the linkage between alkane oxidation and sulfate reduction can be estimated. The methane incubation showed a potential net consumption rate of 263 nmol C mL<sup>-1</sup> day<sup>-1</sup> (Table 4). This coincides with a potential SRR of 297 nmol S mL<sup>-1</sup> day<sup>-1</sup> resulting in a carbon to sulfate ratio of (0.9), consistent with the stoichiometric prediction of C:S of 1. These estimates assume that all the sulfate reduction observed in the incubations is a result of methane oxidation, however, the N<sub>2</sub> control treatments indicate a potential intrinsic SRR of 94 nmol mL<sup>-1</sup> day<sup>-1</sup>. If we assume changes in the community activities between the methane addition and control treatments are negligible, aside from the oxidation of the methane, then we can use the SRR of the control treatment as a background SRR. Correcting for the intrinsic sulfate reduction results in an apparent SRR of 203 nmol mL<sup>-1</sup> day<sup>-1</sup> and an excess methane consumption (a C:S of 1.3, Table 4).

One way in which more carbon may be consumed than predicted from stoichiometry is if the alkane is not completely oxidized to DIC. The shifts in the isotopic composition of the DIC and alkane pools can be used to constrain how much carbon has moved from the alkane pool into the DIC pool and thus establish

if another carbon sink may be important. The moles of carbon from the alkane pool needed to shift the DIC pool from its initial to final composition can be described by:

$$\delta^{13}\text{C-DIC}_{T_f} * [\text{DIC}_{T_0} + \text{Alk}] * V = \delta^{13}\text{C-DIC}_{T_0} * [\text{DIC}_{T_0}] * V + \delta^{13}\text{C-Alk}_{T_0} * [\text{Alk}] * V \quad (2)$$

where  $\delta^{13}\text{C-DIC}$  and  $\delta^{13}\text{C-Alk}$  represents the isotopic signature of the pool,  $[\text{DIC}_{T_0}]$  is the concentration of the initial DIC pool ( $\text{mol CL}^{-1}$ ),  $[\text{Alk}]$  is the alkane carbon oxidized ( $\text{mol CL}^{-1}$ ), and  $V$  is the incubation volume (100 mL). Initial  $[\text{DIC}_{T_0}]$  and  $\delta^{13}\text{C-DIC}_{T_0}$  were calculated as a 1:1 (v:v) mixture of measured values from the media and average values from the pore water (**Table 2**) which comprised the slurry incubations. Using these values the amount of carbon transferred from the initial alkane pool can be estimated. For the methane incubations, this calculation suggests that 2.2 mmols C are transferred from the methane to the DIC pool over the course of the incubation, indicating a rate of methane consumption of  $275 \text{ nmol mL}^{-1} \text{ day}^{-1}$ . This is reasonably consistent with the rate estimates derived from the change in methane concentration over time.

When ethane oxidation is coupled to sulfate reduction, it results in a carbon to sulfate ratio of 8:7 (or 0.57, **Table 6**). The reported oxidation rate of  $168 \text{ nmol ethane mL}^{-1} \text{ day}^{-1}$  (or  $336 \text{ nmol C mL}^{-1} \text{ day}^{-1}$ ) would lead to the consumption of  $294 \text{ nmol SO}_4^{2-} \text{ mL}^{-1} \text{ day}^{-1}$ . This oxidation rate accounts for the majority (89%) of the total estimated sulfate reduction ( $330 \text{ nmol SO}_4^{2-} \text{ mL}^{-1} \text{ day}^{-1}$ ) during the incubation. When SRR are corrected for the potential intrinsic rates, it results in a corrected rate of  $236 \text{ nmol SO}_4^{2-} \text{ mL}^{-1} \text{ day}^{-1}$ . The observed ratio of carbon oxidized to sulfate reduced is 0.7, about 25% more carbon than expected (**Table 4**). Unfortunately, the analytical resolution of the  $\delta^{13}\text{C}$ -ethane precludes estimation of carbon movement among pools (Table S1).

In the case of propane, the estimated SRR increased 2.6-fold over the  $\text{N}_2$  control, with an observed oxidation rate of  $354 \text{ nmol propane mL}^{-1} \text{ day}^{-1}$  (or  $1062 \text{ nmol C mL}^{-1} \text{ day}^{-1}$ ). Given the stoichiometric relationship of 6:5 (**Table 6**), this consumption corresponds to  $885 \text{ nmol SO}_4^{2-} \text{ mL}^{-1} \text{ day}^{-1}$ , a rate 3.6-fold higher than the measured potential SRR ( $246 \text{ nmol S mL}^{-1} \text{ day}^{-1}$ ) (**Table 4**). However, examining the change in the DIC pool, we calculate that 3.9 mmols C (1.3 mmols of propane) moved from the propane pool to the DIC pool (Table S1). This is equivalent to an oxidation rate of  $487 \text{ nmol C mL}^{-1} \text{ day}^{-1}$ , accounting for 46% of the total loss of propane. Thus, there must be another sink for propane (discussed below), implicating the presence of another oxidant, another source of light carbon to the DIC, or both.

Similar to the propane treatment, the butane addition also resulted in higher SRR (2.3-fold) compared to the control treatment. Over the course of the experiment, butane was consumed at a rate of  $125 \text{ nmol butane mL}^{-1} \text{ day}^{-1}$  (or  $500 \text{ nmol C mL}^{-1} \text{ day}^{-1}$ ) (**Table 4**). The corresponding total ( $220 \text{ nmol S mL}^{-1} \text{ day}^{-1}$ ) and corrected SRR ( $125 \text{ nmol S mL}^{-1} \text{ day}^{-1}$ ) can only account for about one-third of the butane consumption (**Table 4**). However, unlike propane, the majority (85%) of the butane

carbon can account for the change in the DIC pool (Table S1). Again it is possible that another sink may exist but identifying such a sink is beyond the scope of these data.

The data above underscore that the rate of oxidation of ethane, propane, and butane cannot be explained solely by the estimated rates of sulfate reduction. Similar observations have been reported by Quistad et al., who noted that the propane loss they observed might be accounted for by abiotic processes such as leakage and dissolution, partial degradation to alcohols or acids, and/or inaccuracy in measurements (Quistad and Valentine, 2011). In our study, however, the observed higher rate of *n*-alkane oxidation may be best explained by (1) utilization of oxidants other than sulfate (e.g.,  $\text{NO}_3^-$ , which is present at site GB425 though not measurable in our reactors; **Table 2**), (2) errors in the estimation of either the oxidation or reduction rates or isotopic assays due to systemic errors, (3) changes in the microbial community or activity of the community over the course of the incubation that were not observable with the sampling design, or (4) the precipitation of (authigenic) carbonate in the batch reactors as has been noted to occur in GoM sediments (Sassen et al., 2004). We address each of these possibilities in detail below.

Nitrate and/or nitrite represent potential alternative oxidants for alkane oxidation, and are present at  $\leq 40 \mu\text{M}$  in the upper layers of Garden Banks sediments. Their concentrations were, however, below our detection limits of  $0.5 \mu\text{M}$  in the sediment slurries at both  $T_0$  and  $T_f$ . Even if one assumes that  $40 \mu\text{M } \text{NO}_3^-$  was present in sediments, it could only produce  $50 \mu\text{M}$  DIC ( $5 \mu\text{mol C}$ ) through complete  $\text{NO}_3^-$  reduction to  $\text{N}_2$ . Thus, nitrate coupled alkane oxidation cannot solely explain the observed discrepancies.

To determine if alkanes were systemically lost via leakage and/or other bottle effects, sediment-free reactors were incubated in parallel, and alkane concentrations were monitored over the course of the incubations. These reactors exhibited  $<5\%$  loss over the course of the incubations, which is markedly lower than our least active biological treatment ( $\text{CH}_4$ ). SRR is known to be sensitive to the incubation time, although sediments—including those from the GoM—are typically incubated for 24 h as was used here (Fossing and Jorgensen, 1989). Moreover, the rates shown here are comparable to previously published rates (Arvidson et al., 2004; Joye et al., 2004). In any case, shorter incubation times might result in higher SRR, and might account for some of the observed excess alkane consumption. Leakage of gas from sample vials (different than the incubation vials) could also affect the isotopic signatures of the alkane pools and could be a source of error resulting in lower precision measurements (though nothing in our data is consistent with this hypothesis).

Shifts in the microbial community could lead to enrichment of acetoclastic methanogens that can use acetate (a possible product of partial propane or butane degradation) to produce methane. Methane has been reported as a potential carbon sink during degradation of higher molecular weight hydrocarbons (Gray et al., 2010). However, in the present study we do not observe any changes in the concentration of the methane produced compared to the  $\text{N}_2$  controls (Table S2). We also do not observe an increase in the total methanogen population in the  $\text{C}_2-\text{C}_4$  amended sediments by qPCR with primers specific for the methanogenic *mcrA*

gene. Thus, methane appears unlikely to be a carbon sink in our experiments.

Finally, precipitation of carbonates may be a sink of carbon within the sediments. The inorganic precipitation of carbonate, known as authigenic carbonate, can occur at the sediment-water interface or within the sediment pore water. Authigenic carbonates are often formed in sediments where increasing alkalinity, typically from sulfate or metal reduction, increases the carbonate saturation state past a saturation threshold causing precipitation of minerals (calcite or aragonite). Sulfate-reduction increases the alkalinity of pore waters by removing hydrogen ion from the local environment in the form of H<sub>2</sub>S and generating bicarbonate concentrations by oxidizing organic carbon. Authigenic carbonates are found throughout the GoM (Roberts and Aharon, 1994; Sassen et al., 2004). Generally, environments such as the GoM with substantial amounts of organic carbon but that hinder aerobic respiration and support alkalinity-increasing processes such as sulfate reduction have the potential to harbor large carbon sinks in the form of authigenic carbonate (Higgins et al., 2009). While inorganic precipitation of carbonates is possible in our incubations, data for the total sedimentary inorganic carbon content is unavailable.

Microbial community analyses via pyrotag sequencing implicate that certain members of the class Deltaproteobacteria are enriched during the batch incubations. Further phylogenetic analyses indicate that the enriched bacteria are closely related to previously enriched/isolated C<sub>3</sub>-C<sub>4</sub> degrading SRP (Kniemeyer et al., 2007; Jaekel et al., 2013), as well as uncultured marine SRP observed in GoM sediments (Orcutt et al., 2010; Kleindienst et al., 2012). The Deltaproteobacterial sequences most enriched in the ethane incubations were closely related to isolate BuS5, and the enrichment culture Butane12-GMe, both of which belong to the DSS cluster (Kniemeyer et al., 2007). Intriguingly, previous studies suggest that BuS5 (degrades propane and *n*-butane) and enrichment Butane12-GMe (degrades *n*-butane) do not degrade ethane (Kniemeyer et al., 2007; Jaekel et al., 2013). Other uncultured DSS cluster members were also identified in the ethane degrading incubations (Kleindienst et al., 2012). Thus, it is possible that SRP closely related to the C<sub>3</sub>-C<sub>4</sub> degrading DSS cluster might be associated with ethane degradation in these incubations, though this hypothesis remains to be tested.

While pyrotag sequencing using 16S rRNA gene data show the phylogenetic structure of the microbial community (and is not quantitative), qPCR analysis helps us to quantitatively assess the functional potential of the microbes in the reactors. Many of the Deltaproteobacteria reduce sulfate using the dissimilatory sulfate reductase or adenosine 5'-phosphosulfate reductase enzymes (encoded by *dsrA* and *aprA* genes, respectively). The qPCR results (both *dsrA* and *aprA* gene abundance) demonstrate that the total number of SRP decrease compared to the T<sub>0</sub> sample and the N<sub>2</sub> control. However, C<sub>2</sub>-C<sub>4</sub> consumption correlates stoichiometrically with SR, and SR rates were higher in the presence of the alkane gases compared to the N<sub>2</sub> control. Collectively, these results indicate that there maybe an enrichment of a specific subset of the SRP community responsible for the consumption of C<sub>2</sub>-C<sub>4</sub>. While lower in abundance than the total SRP in the T<sub>0</sub>

sample or N<sub>2</sub> control, this subset of the community likely exhibits higher specific SR activity.

The data presented here provide insight into alkane oxidation rates in Garden Banks sediments. Like previous studies, these data confirm that the addition of alkanes stimulates sulfate reduction (**Figure 2**, **Table 4**). Notably, the rates of C<sub>2</sub>-C<sub>4</sub> consumption are comparable to CH<sub>4</sub> consumption, though their stoichiometric impacts on the sulfate pool vary. For example, assuming complete oxidation, it is likely that 1, 1.75, 2.5, and 2.8 moles of sulfate are reduced per mole alkane for C<sub>1</sub>-C<sub>4</sub>, respectively. Consequently, the relative effect of C<sub>2</sub>-C<sub>4</sub> oxidation on the sulfate pool is much greater than for methane given the observed similarity in the oxidation rates. Accordingly, alkane oxidation may represent a substantial sink for sulfate in sediments where alkanes are elevated, such as the GoM where they can constitute more than 10% of the total gas pool (Milkov, 2005). This is most likely relevant deeper in the sediments, where alkane concentrations are highest and where sulfate concentrations are lowest. In such scenarios, it is not implausible that C<sub>2</sub>-C<sub>4</sub> oxidation might limit the availability of sulfate for methane oxidation, though this speculation requires further study. The data further constrain carbon exchange between the alkane and DIC pool, and this phenomenon should be considered when interpreting DIC isotope ratios of alkane-replete sediments.

Ethane is the next most abundant short-chain non-methane alkane at our study site (**Table 3**). However, previous studies have reported ethane-driven sulfate reduction at very slow rates by microbial enrichments obtained from a similar location (Kniemeyer et al., 2007). Anaerobic ethane oxidation likely involves a novel mechanism because it requires the activation of a primary carbon, in contrast to butane where secondary carbons are available (Kniemeyer et al., 2007, and references therein). Notably, we observed substantial ethane consumption over the course of these incubations [approximately two orders of magnitude higher than those reported by Kniemeyer et al. (2007), and comparable to the oxidation rates of methane, propane or butane]. The presence of ethane also stimulated sulfate reduction, which implies a relationship between these processes. Our data show anaerobic ethane utilization begins without delay, similar to other alkanes, suggesting that microorganisms are poised for ethane oxidation.

Bulk geochemical and isotopic surveys of alkanes along seeps have been used to imply microbial consumption of short-chain alkanes (Sassen et al., 2004; Orcutt et al., 2005). Our data confirm that short-chain alkanes are oxidized to DIC, likely coupled to sulfate reduction. However, both our alkane consumption rates and the isotopic shifts observed in the DIC pools suggest other sinks may exist. At thermogenic hydrocarbon seeps, these processes may have an important impact on the local carbon and sulfur cycles. The strategies used herein—namely the combination of molecular, geochemical, and isotopic assessments—was leveraged to establish the relationships between anaerobic alkane oxidation and SRRs, carbon flux, microbial activity, and microbial community composition and phylogeny. Future experiments should consider these and previous data to gain further insight into the signatures and mechanisms of these biogeochemical processes

as well as organisms involved in anaerobic short-chain alkane oxidation.

## AUTHOR CONTRIBUTIONS

Arpita Bose, Melissa M. Adams, and Peter R. Girguis designed the research. Melissa M. Adams and Peter R. Girguis directed the *in situ* collections and Samantha B. Joye performed the *in situ* measurements. Arpita Bose and Melissa M. Adams conducted the batch reactor incubations. Arpita Bose and Daniel R. Rogers performed the *ex situ* geochemical analyses. Arpita Bose and Daniel R. Rogers determined the rate of alkane consumption, rate of sulfate reduction, and the molecular analyses. Melissa M. Adams performed the phylogenetic analyses. Arpita Bose and Daniel R. Rogers wrote the manuscript with input from Peter R. Girguis, Melissa M. Adams, and Samantha B. Joye.

## ACKNOWLEDGMENTS

We acknowledge the assistance of the *R/V Atlantis* crews and the pilots and team of the DSV Alvin for enabling the collection of the sediments used in our experiments. We thank Jennifer Delaney for providing assistance with DNA extractions. This research was made possible by a grant from BP/The Gulf of Mexico Research Initiative to the Ecosystem Impacts of Oil and Gas Inputs to the Gulf (ECOGIG) project. Additional support for this research was also provided in part by NSF MCB 0702504 and NASA ASTEP grant 0910169 to Peter R. Girguis and U.S. National Science Foundation (EF-0801741) to Samantha B. Joye. Arpita Bose was a Howard Hughes Medical Institute fellow of the Life Sciences Research Foundation and is currently a L’Oreal USA For Women in Science Fellow.

## SUPPLEMENTARY MATERIAL

The Supplementary Material for this article can be found online at: <http://www.frontiersin.org/journal/10.3389/fmicb.2013.00386/abstract>

## REFERENCES

- Acinas, S. G., Klepac-Ceraj, V., Hunt, D. E., Pharino, C., Ceraj, I., Distel, D. L., et al. (2004). Fine-scale phylogenetic architecture of a complex bacterial community. *Nature* 430, 551–554. doi: 10.1038/nature02649
- Acosta-Martinez, V., Dowd, S. E., Sun, Y., Wester, D., and Allen, V. (2010). Pyrosequencing analysis for characterization of soil bacterial populations as affected by an integrated livestock-cotton production system. *Appl. Soil Ecol.* 45, 13–25. doi: 10.1016/j.apsoil.2010.01.005
- Adams, M. M., Hoarfrost, A. L., Bose, A., Joye, S. B., and Girguis, P. R. (2013). Anaerobic oxidation of short-chain alkanes in hydrothermal sediments: potential influences on sulfur cycling and microbial diversity. *Front. Microbiol.* 4:110. doi: 10.3389/fmicb.2013.00110
- Alain, K., Holler, T., Musat, F., Elvert, M., Treude, T., and Kruger, M. (2006). Microbiological investigation of methane- and hydrocarbon-discharging mud volcanoes in the Carpathian Mountains, Romania. *Environ. Microbiol.* 8, 574–590. doi: 10.1111/j.1462-2920.2005.00922.x
- Arvidson, R. S., Morse, J. W., and Joye, S. B. (2004). The sulfur biogeochemistry of chemosynthetic cold seep communities, Gulf of Mexico, USA. *Mar. Chem.* 87, 97–119. doi: 10.1016/j.marchem.2003.11.004
- Atekwana, E. A., and Krishnamurthy, R. V. (1998). Seasonal variations of dissolved inorganic carbon and delta C-13 of surface waters: application of a modified gas evolution technique. *J. Hydrol.* 205, 265–278. doi: 10.1016/S0022-1694(98)00080-8
- Bowles, M. W., Samarkin, V. A., Bowles, K. M., and Joye, S. B. (2011). Weak coupling between sulfate reduction and the anaerobic oxidation of methane in methane-rich seafloor sediments during *ex situ* incubation. *Geochim. Cosmochim. Acta* 75, 500–519. doi: 10.1016/j.gca.2010.09.043
- Callaghan, A. V. (2013). Enzymes involved in the anaerobic oxidation of n-alkanes: from methane to long-chain paraffins. *Front. Microbiol.* 4:89. doi: 10.3389/fmicb.2013.00089
- Canfield, D. E., and Farquhar, J. (2009). Animal evolution, bioturbation, and the sulfate concentration of the oceans. *Proc. Natl. Acad. Sci. U.S.A.* 106, 8123–8127. doi: 10.1073/pnas.0902037106
- Christophersen, C. T., Morrison, M., and Conlon, M. A. (2011). Overestimation of the abundance of sulfate-reducing bacteria in human feces by quantitative PCR targeting the *Desulfovibrio* 16S rRNA gene. *Appl. Environ. Microbiol.* 77, 3544–3546. doi: 10.1128/AEM.02851-10
- Cline, J. D. (1969). Spectrophotometric determination of hydrogen sulfide in natural waters. *Limnol. Oceanogr.* 14, 454–458. doi: 10.4319/lo.1969.14.3.0454
- Dowd, S. E., Callaway, T. R., Wolcott, R. D., Sun, Y., McKeehan, T., Hagevoort, R. G., et al. (2008). Evaluation of the bacterial diversity in the feces of cattle using 16S rDNA bacterial tag-encoded FLX amplicon pyrosequencing (bTEFAP). *BMC Microbiol.* 8:125. doi: 10.1186/1471-2180-8-125
- Formolo, M. J., Lyons, T. W., Zhang, C. L., Kelley, C., Sassen, R., Horita, J., et al. (2004). Quantifying carbon sources in the formation of authigenic carbonates at gas hydrate sites in the Gulf of Mexico. *Chem. Geol.* 205, 253–264. doi: 10.1016/j.chemgeo.2003.12.021
- Fossing, H., and Jorgensen, B. B. (1989). Measurement of bacterial sulfate reduction in sediments: evaluation of a single-step chromium reduction method. *Biogeochemistry* 8, 205–222. doi: 10.1007/BF00002889
- Gray, N. D., Sherry, A., Hubert, C., Dolfing, J., and Headt, I. M. (2010). “Methanogenic degradation of petroleum hydrocarbons in subsurface environments: remediation, heavy oil formation, and energy recovery,” in *Advances in Applied Microbiology*, Vol. 72, eds A. I. Laskin, S. Sarielani, and G. M. Gadd, (San Diego, CA: Academic Press), 137–161.
- Haroon, M. F., Hu, S., Shi, Y., Imelfort, M., Keller, J., Hugenholtz, P., et al. (2013). Anaerobic oxidation of methane coupled to nitrate reduction in a novel archaeal lineage. *Nature* 500, 567–570. doi: 10.1038/nature12375
- Higgins, J. A., Fischer, W. W., and Schrag, D. P. (2009). Oxygenation of the ocean and sediments: consequences for the seafloor carbonate factory. *Earth Planet. Sci. Lett.* 284, 25–33. doi: 10.1016/j.epsl.2009.03.039
- Hinrichs, K. U., Hayes, J. M., Bach, W., Spivack, A. J., Hmelo, L. R., Holm, N. G., et al. (2006). Biological formation of ethane and propane in the deep marine subsurface. *Proc. Natl. Acad. Sci. U.S.A.* 103, 14684–14689. doi: 10.1073/pnas.0606535103
- Horita, J., and Berndt, M. E. (1999). Abiogenic methane formation and isotopic fractionation under hydrothermal conditions. *Science* 285, 1055–1057. doi: 10.1126/science.285.5430.1055
- Hovland, M., and Thomsen, E. (1997). Cold-water corals - Are they hydrocarbon seep related? *Mar. Geol.* 137, 159–164. doi: 10.1016/S0025-3227(96)00086-2
- Jaekel, U., Musat, N., Adam, B., Kuyper, M., Grundmann, O., and Musat, F. (2013). Anaerobic degradation of propane and butane by sulfate-reducing bacteria enriched from marine hydrocarbon cold seeps. *ISME J.* 7, 885–895. doi: 10.1038/ismej.2012.159
- Jones, D. M., Head, I. M., Gray, N. D., Adams, J. J., Rowan, A. K., Aitken, C. M., et al. (2008). Crude-oil biodegradation via methanogenesis in subsurface petroleum reservoirs. *Nature* 451, 176–180. doi: 10.1038/nature06484
- Joye, S. B., Boetius, A., Orcutt, B. N., Montoya, J. P., Schulz, H. N., Erickson, M. J., et al. (2004). The anaerobic oxidation of methane and sulfate reduction in sediments from Gulf of Mexico cold seeps. *Chem. Geol.* 205, 219–238. doi: 10.1016/j.chemgeo.2003.12.019
- Joye, S. B., Samarkin, V. A., Orcutt, B. N., Macdonald, I. R., Hinrichs, K. U., Elvert, M., et al. (2009). Metabolic variability in seafloor brines revealed by carbon and sulphur dynamics. *Nat. Geosci.* 2, 349–354. doi: 10.1038/ngeo475
- Kleindienst, S., Ramette, A., Amann, R., and Knittel, K. (2012). Distribution and *in situ* abundance of sulfate-reducing bacteria in diverse marine hydrocarbon seep sediments. *Environ. Microbiol.* 14, 2689–2710. doi: 10.1111/j.1462-2920.2012.02832.x

- Kniemeyer, O., Musat, F., Sievert, S. M., Knittel, K., Wilkes, H., Blumenberg, M., et al. (2007). Anaerobic oxidation of short-chain hydrocarbons by marine sulphate-reducing bacteria. *Nature* 449, 898–901. doi: 10.1038/nature06200
- Knittel, K., and Boetius, A. (2009). Anaerobic oxidation of methane: progress with an unknown process. *Annu. Rev. Microbiol.* 63, 311–334. doi: 10.1146/annurev.micro.61.080706.093130
- Kondo, R., Nedwell, D. B., Purdy, K. J., and Silva, S. D. (2004). Detection and enumeration of sulphate-reducing bacteria in estuarine sediments by competitive PCR. *Geomicrobiol. J.* 21, 145–157. doi: 10.1080/01490450490275307
- Lorant, F., and Behar, F. (2002). Late generation of methane from mature kerogens. *Energy Fuels* 16, 412–427. doi: 10.1021/ef010126x
- Lorenson, T. D., Kvvenvolden, K. A., Hostettler, F. D., Rosenbauer, R. J., Orange, D. L., and Martin, J. B. (2002). Hydrocarbon geochemistry of cold seeps from the Monterey Bay National Marine Sanctuary. *Mar. Geol.* 181, 285–304. doi: 10.1016/S0025-3227(01)00272-9
- Luton, P. E., Wayne, J. M., Sharp, R. J., and Riley, P. W. (2002). The *mcrA* gene as an alternative to 16S rRNA in the phylogenetic analysis of methanogen populations in landfill. *Microbiology* 148, 3521–3530.
- Milkov, A. V. (2005). Molecular and stable isotope compositions of natural gas hydrates: a revised global dataset and basic interpretations in the context of geological settings. *Org. Geochem.* 36, 681–702. doi: 10.1016/j.orggeochem.2005.01.010
- Milucka, J., Ferdelman, T. G., Polerecky, L., Franzke, D., Wegener, G., Schmid, M., et al. (2012). Zero-valent sulphur is a key intermediate in marine methane oxidation. *Nature* 491, 541–546. doi: 10.1038/nature11656
- Muyzer, G., and Van Der Kraan, G. M. (2008). Bacteria from hydrocarbon seep areas growing on short-chain alkanes. *Trends Microbiol.* 16, 138–141. doi: 10.1016/j.tim.2008.01.004
- Orcutt, B., Boetius, A., Elvert, M., Samarkin, V., and Joye, S. B. (2005). Molecular biogeochemistry of sulfate reduction, methanogenesis and the anaerobic oxidation of methane at Gulf of Mexico cold seeps. *Geochim. Cosmochim. Acta* 69, 5633–5633. doi: 10.1016/j.gca.2005.04.012
- Orcutt, B., Samarkin, V., Boetius, A., and Joye, S. (2008). On the relationship between methane production and oxidation by anaerobic methanotrophic communities from cold seeps of the Gulf of Mexico. *Environ. Microbiol.* 10, 1108–1117. doi: 10.1111/j.1462-2920.2007.01526.x
- Orcutt, B. N., Joye, S. B., Kleindienst, S., Knittel, K., Ramette, A., Reitz, A., et al. (2010). Impact of natural oil and higher hydrocarbons on microbial diversity, distribution, and activity in Gulf of Mexico cold-seep sediments. *Deep Sea Res. II Top. Stud. Oceanogr.* 57, 2008–2021. doi: 10.1016/j.dsr2.2010.05.014
- Pai, S. C., Yang, C. C., and Riley, J. P. (1990). Formation kinetics of the pink azo dye in the determination of nitrite in natural waters. *Anal. Chim. Acta* 232, 345–349. doi: 10.1016/S0003-2670(00)81252-0
- Quistad, S. D., and Valentine, D. L. (2011). Anaerobic propane oxidation in marine hydrocarbon seep sediments. *Geochim. Cosmochim. Acta* 75, 2159–2169. doi: 10.1016/j.gca.2011.02.001
- Reeburgh, W. S. (2007). Oceanic methane biogeochemistry. *Chem. Rev.* 107, 486–513. doi: 10.1021/cr050362v
- Reis, M. A., Almeida, J. S., Lemos, P. C., and Carrondo, M. J. (1992). Effect of hydrogen sulfide on growth of sulfate-reducing bacteria. *Biotechnol. Bioeng.* 40, 593–600. doi: 10.1002/bit.260400506
- Roberts, H. H., and Aharon, P. (1994). Hydrocarbon-derived carbonate buildups of the northern Gulf of Mexico continental slope: a review of submersible investigations. *Geomar. Lett.* 14, 135–148. doi: 10.1007/BF01203725
- Sassen, R., Macdonald, I. R., Guinasso, N. L., Joye, S., Requejo, A. G., Sweet, S. T., et al. (1998). Bacterial methane oxidation in sea-floor gas hydrate: significance to life in extreme environments. *Geology* 26, 851–854. doi: 10.1130/0091-7613(1998)026<0851:BMOIS>2.3.CO;2
- Sassen, R., Roberts, H. H., Carney, R., Milkov, A. V., Defreitas, D. A., Lanoil, B., et al. (2004). Free hydrocarbon gas, gas hydrate, and authigenic minerals in chemosynthetic communities of the northern Gulf of Mexico continental slope: relation to microbial processes. *Chem. Geol.* 205, 195–217. doi: 10.1016/j.chemgeo.2003.12.032
- Savage, K. N., Krumholz, L. R., Gieg, L. M., Parisi, V. A., Suflita, J. M., Allen, J., et al. (2010). Biodegradation of low-molecular-weight alkanes under mesophilic, sulfate-reducing conditions: metabolic intermediates and community patterns. *FEMS Microbiol. Ecol.* 72, 485–495. doi: 10.1111/j.1574-6941.2010.00866.x
- Suzuki, M. T., Beja, O., Taylor, L. T., and Delong, E. F. (2001). Phylogenetic analysis of ribosomal RNA operons from uncultivated coastal marine bacterioplankton. *Environ. Microbiol.* 3, 323–331. doi: 10.1046/j.1462-2920.2001.00198.x
- Takai, K., and Horikoshi, K. (2000). Rapid detection and quantification of members of the archaeal community by quantitative PCR using fluorogenic probes. *Appl. Environ. Microbiol.* 66, 5066–5072. doi: 10.1128/AEM.66.11.5066-5072.2000
- Thauer, R. K., Kaster, A. K., Seedorf, H., Buckel, W., and Hedderich, R. (2008). Methanogenic archaea: ecologically relevant differences in energy conservation. *Nat. Rev. Microbiol.* 6, 579–591. doi: 10.1038/nrmicro1931
- Ver Eecke, H. C., Butterfield, D. A., Huber, J. A., Lilley, M. D., Olson, E. J., Roe, K. K., et al. (2012). Hydrogen-limited growth of hyperthermophilic methanogens at deep-sea hydrothermal vents. *Proc. Natl. Acad. Sci. U.S.A.* 109, 13674–13679. doi: 10.1073/pnas.1206632109
- Widdel, F., and Bak, F. (1992). “Gram-negative mesophilic sulfate-reducing bacteria,” in *The Prokaryotes, 2nd Edn.* eds A. Balows, H. G. Trüper, M. Dworkin, W. Harder, and K. H. Schleifer (New York, NY: Springer), 3352–3378.
- Xie, S., Lazar, C. S., Lin, Y. S., Teske, A., and Hinrichs, K. U. (2013). Ethane- and propane-producing potential and molecular characterization of an ethanogenic enrichment in an anoxic estuarine sediment. *Org. Geochem.* 59, 37–48. doi: 10.1016/j.orggeochem.2013.03.001
- Yarnes, C. (2013). delta13C and delta2H measurement of methane from ecological and geological sources by gas chromatography/combustion/pyrolysis isotope-ratio mass spectrometry. *Rapid Commun. Mass Spectrom.* 27, 1036–1044. doi: 10.1002/rcm.6549
- Zhang, J.-Z., and Fischer, C. J. (2006). A simplified resorcinol method for direct spectrophotometric determination of nitrate in seawater. *Mar. Chem.* 99, 220–226. doi: 10.1016/j.marchem.2005.09.008
- Conflict of Interest Statement:** The authors declare that the research was conducted in the absence of any commercial or financial relationships that could be construed as a potential conflict of interest.
- Received: 21 September 2013; accepted: 26 November 2013; published online: 12 December 2013.*
- Citation:* Bose A, Rogers DR, Adams MM, Joye SB and Girguis PR (2013) Geomicrobiological linkages between short-chain alkane consumption and sulfate reduction rates in seep sediments. *Front. Microbiol.* 4:386. doi: 10.3389/fmicb.2013.00386
- This article was submitted to Aquatic Microbiology, a section of the journal Frontiers in Microbiology.*
- Copyright © 2013 Bose, Rogers, Adams, Joye and Girguis. This is an open-access article distributed under the terms of the Creative Commons Attribution License (CC BY). The use, distribution or reproduction in other forums is permitted, provided the original author(s) or licensor are credited and that the original publication in this journal is cited, in accordance with accepted academic practice. No use, distribution or reproduction is permitted which does not comply with these terms.*



# Kinetic parameters for nutrient enhanced crude oil biodegradation in intertidal marine sediments

Arvind K. Singh<sup>1,2</sup>, Angela Sherry<sup>1</sup>, Neil D. Gray<sup>1</sup>, D. Martin Jones<sup>1</sup>, Bernard F. J. Bowler<sup>1</sup> and Ian M. Head<sup>1\*</sup>

<sup>1</sup> School of Civil Engineering and Geosciences, Newcastle University, Newcastle upon Tyne, UK

<sup>2</sup> Department of Biochemistry, North – Eastern Hill University, Shillong, Meghalaya, India

**Edited by:**

Joel E. Kostka, Georgia Institute of Technology, USA

**Reviewed by:**

Christoph Aepli, Bigelow Laboratory for Ocean Sciences, USA  
Behzad Mortazavi, University of Alabama, USA  
John H. Pardue, Louisiana State University, USA

**\*Correspondence:**

Ian M. Head, Newcastle University, School of Civil Engineering and Geosciences, Room 3.16, Devonshire Building, Devonshire Terrace, Newcastle-upon-Tyne, NE1 7RU, UK  
e-mail: ian.head@ncl.ac.uk

Availability of inorganic nutrients, particularly nitrogen and phosphorous, is often a primary control on crude oil hydrocarbon degradation in marine systems. Many studies have empirically determined optimum levels of inorganic N and P for stimulation of hydrocarbon degradation. Nevertheless, there is a paucity of information on fundamental kinetic parameters for nutrient enhanced crude oil biodegradation that can be used to model the fate of crude oil in bioremediation programmes that use inorganic nutrient addition to stimulate oil biodegradation. Here we report fundamental kinetic parameters ( $K_s$  and  $q_{max}$ ) for nitrate- and phosphate-stimulated crude oil biodegradation under nutrient limited conditions and with respect to crude oil, under conditions where N and P are not limiting. In the marine sediments studied, crude oil degradation was limited by both N and P availability. In sediments treated with 12.5 mg/g of oil but with no addition of N and P, hydrocarbon degradation rates, assessed on the basis of CO<sub>2</sub> production, were  $1.10 \pm 0.03 \mu\text{mol CO}_2/\text{g wet sediment/day}$  which were comparable to rates of CO<sub>2</sub> production in sediments to which no oil was added ( $1.05 \pm 0.27 \mu\text{mol CO}_2/\text{g wet sediment/day}$ ). When inorganic nitrogen was added alone maximum rates of CO<sub>2</sub> production measured were  $4.25 \pm 0.91 \mu\text{mol CO}_2/\text{g wet sediment/day}$ . However, when the same levels of inorganic nitrogen were added in the presence of 0.5% P w/w of oil ( $1.6 \mu\text{mol P/g wet sediment}$ ) maximum rates of measured CO<sub>2</sub> production increased more than four-fold to  $18.40 \pm 1.04 \mu\text{mol CO}_2/\text{g wet sediment/day}$ .  $K_s$  and  $q_{max}$  estimates for inorganic N (in the form of sodium nitrate) when P was not limiting were  $1.99 \pm 0.86 \mu\text{mol/g wet sediment}$  and  $16.16 \pm 1.28 \mu\text{mol CO}_2/\text{g wet sediment/day}$  respectively. The corresponding values for P were  $63 \pm 95 \text{ nmol/g wet sediment}$  and  $12.05 \pm 1.31 \mu\text{mol CO}_2/\text{g wet sediment/day}$ . The  $q_{max}$  values with respect to N and P were not significantly different ( $P < 0.05$ ). When N and P were not limiting  $K_s$  and  $q_{max}$  for crude oil were  $4.52 \pm 1.51 \text{ mg oil/g wet sediment}$  and  $16.89 \pm 1.25 \mu\text{mol CO}_2/\text{g wet sediment/day}$ . At concentrations of inorganic N above 45  $\mu\text{mol/g wet sediment}$  inhibition of CO<sub>2</sub> production from hydrocarbon degradation was evident. Analysis of bacterial 16S rRNA genes indicated that *Alcanivorax* spp. were selected in these marine sediments with increasing inorganic nutrient concentration, whereas *Cycloclasticus* spp. were more prevalent at lower inorganic nutrient concentrations. These data suggest that simple empirical estimates of the proportion of nutrients added relative to crude oil concentrations may not be sufficient to guarantee successful crude oil bioremediation in oxic beach sediments. The data we present also help define the maximum rates and hence timescales required for bioremediation of beach sediments.

**Keywords:** oil spill, bioremediation, kinetics,  $K_s$ , half saturation constant, maximal rates, *Alcanivorax*, *Cycloclasticus*

## INTRODUCTION

Natural hydrocarbon seeps are quantitatively the largest source of petroleum in marine systems, nevertheless, anthropogenic activities involved in the production transport and use of crude oil and oil products remain important sources of oil pollution (National Research Council, 2003). As a result of the localized release of relatively large quantities of oil, anthropogenic emissions may have effects on local ecosystems that are disproportionate to their

contribution to global budgets of hydrocarbons in the sea. The incidence of major oil spills has decreased by 76% from 787 to 190 during the four decades from 1970 to 2010. In terms of volume this corresponds to a 93% decrease and, excluding the Deepwater Horizon blowout, the total quantity of oil spilt during 2010–2011 (13,000 tonnes from 13 recorded spills) was the lowest so far recorded (ITOPF, 2011). Although such statistics indicate that oil spills are generally declining, major

accidents like the Deepwater Horizon blowout on 20th April 2010 in the Gulf of Mexico are a stark reminder that accidental oil spills remain an important environment hazard. The Deepwater Horizon accident resulted in the world's largest accidental release of crude oil to the sea, releasing an estimated 4.9 million barrels ( $780,000 \text{ m}^3$ ) of light crude oil (OSAT-1, 2010). In offshore regions, the Deepwater Horizon spill had substantial impact on coral communities impacted by the plume from the Macondo well (White et al., 2012). In spite of intensive cleanup efforts, a portion of the spilled Macondo oil drifted to shore and remains trapped in coastal sediments. Concentrations of total petroleum hydrocarbon as high as  $510 \text{ mg g}^{-1}$  sediment were recorded in the surface 2 cm of heavily polluted marsh sediments even 7 months after the spill (Lin and Mendelsohn, 2012).

Crude oils comprise a complex heterogenous mixture of organic and inorganic compounds and broadly contain four groups of compounds; saturated and aromatic hydrocarbons, resins and asphaltenes (Harayama et al., 1999). Whereas lighter fractions evaporate or are degraded microbially, the heavier and more polar crude oil fractions persist due to their slow degradation rates (Walker et al., 1976). Many hydrocarbon degrading organisms are known (Prince, 2005) and in marine environments a number of specialist hydrocarbon degrading taxa are known (Yakimov et al., 2007). Marine saturated hydrocarbon degrading specialists include *Alcanivorax* (Yakimov et al., 1998), *Planococcus* (Engelhardt et al., 2001), *Oleiphilus* (Golyshin et al., 2002), *Oleispira* (Yakimov et al., 2003), *Thalassolituus* (Yakimov et al., 2004). Aromatic hydrocarbon degraders include *Cycloclasticus* spp. which utilize biphenyl, naphthalene, anthracene, phenanthrene, toluene, and benzoate (Dyksterhouse et al., 1995), and *Neptunomonas* which can degrade naphthalene, 2-methylnaphthalene and phenanthrene as sole carbon sources, but are unable to use 2,6-dimethylnaphthalene, 1-methylnaphthalene, biphenyl or ace-naphthene (Hedlund et al., 1999). The chemical complexity of crude oil thus limits the capacity of a single species to degrade only certain components and the combined efforts of mixed bacterial consortia improve hydrocarbon bioremediation in marine environments (Röling et al., 2002; Dell'Anno et al., 2012). However, artificial microbial consortia cannot substitute for highly complex and dynamic indigenous microbial population essential for complete and efficient hydrocarbon degradation (McKew et al., 2007a).

Marine bacteria from the genera *Alcanivorax* and *Cycloclasticus*, have been implicated as key hydrocarbonoclastic agents on a global scale (Maruyama et al., 2003; Cappello et al., 2007). Their abundances and hydrocarbon degradation activity in polluted environments often increases significantly with a concomitant reduction in overall bacterial diversity (MacNaughton et al., 1999; Kasai et al., 2001, 2002a,b; Röling et al., 2002; Cappello et al., 2007; McKew et al., 2007b). A study on bacterial community response in beach sediment impacted by the Deepwater Horizon oil spill demonstrated that *Alcanivorax* spp. became dominant in polluted sediments and responded rapidly in the early stages following oiling (Kostka et al., 2011; Newton et al., 2013).

A 16S rRNA gene, PCR based denaturing gradient gel electrophoresis (DGGE) analysis and qPCR analysis of microbial population in nutrient amended crude oil treated marine sediment plots revealed an increase in number of *Alcanivorax* spp. and simultaneous appearance of *alkB* genes coding for alkane hydroxylase responsible for catabolism of alkanes (Röling et al., 2004; Singh et al., 2011). The success of *Alcanivorax* spp. as alkane degraders in part lies in their ability to use both branched chain and straight chain alkanes efficiently as sources of carbon and energy (Hara et al., 2003). Importantly, although *Alcanivorax borkumensis* SK2 genome has been shown to possess high affinity permeases for nitrate and phosphorus (Schneiker et al., 2006) it has been shown that the nitrate transporter *ntrB* gene and *nirB1* for nitrite reductase are down-regulated in the presence of hexadecane by 3.93- and 6.5-fold respectively (Sabirova et al., 2011). Aromatic hydrocarbon degraders also exhibit a strong positive response to nutrient amendments. Abundance of *Cycloclasticus* spp. in heat treated Arabian light crude oil polluted gravel was shown to increase by 5 orders of magnitude under inorganic nutrient treated conditions and by 2 orders of magnitude under oil contaminated conditions with no nutrients, relative to unoiled sediments without nutrient amendments (Kasai et al., 2002b).

Since *Alcanivorax* spp and *Cycloclasticus* spp. do not compete for organic compounds as carbon sources, their initial abundance, metabolic superiority, and growth rate can be very crucial for determining their emergence, activity and ultimate relative abundance in hydrocarbon polluted environments. While these taxa do not compete directly for carbon and energy sources in oil-polluted environments they do compete for electron acceptors and inorganic nutrients and this may dictate the relative degradation of saturated and aromatic hydrocarbons. Indeed nutrient supply has been shown to have differential effects on rates of aliphatic and aromatic hydrocarbon degradation which has been interpreted in the context of resource ratio theory (Smith et al., 1998). Moreover, there is some evidence that inorganic nutrient availability controls selection of different *Alcanivorax* genotypes (Röling et al., 2002; Head et al., 2006).

Biostimulation efficiently enhances hydrocarbon bioremediation activity (McKew et al., 2007b) and typically saturated hydrocarbon degradation is stimulated initially followed by degradation of aromatic hydrocarbons and polar components respectively (Fusey and Oudot, 1984). In some instances losses of aromatic hydrocarbons before saturated hydrocarbons have been observed (Jones et al., 1983; Cooney et al., 1985). Such differences in hydrocarbon removal patterns could be due to relative growth efficiency of aromatic and aliphatic hydrocarbon degrading organisms under prevailing environmental conditions and their initial abundance. The goal of hydrocarbon bioremediation strategies is to allow degradation activity at maximum rates by providing nutrients in quantities sufficient to support the growth of hydrocarbon degrading organisms and microbial hydrocarbon degradation activity was shown to increase up to  $2.5 \text{ mg N/L}$  ( $0.18 \text{ mM}$ ) beyond which nutrient level does not enhance the rate of degradation (Boufadel et al., 1999). A continuous supply of inorganic nutrient in combination with sand amendments for efficient mass transfer also has been shown to enhance kinetics of

microbial growth, and hydrocarbon degradation (Beolchini et al., 2010).

Although biostimulation of hydrocarbon degradation processes has been studied extensively, there has been very limited attempt to systematically understand the kinetics of nutrient enhanced biodegradation of crude oil and to correlate this with the emergence of specific microbial population in hydrocarbon contaminated marine sediments (Röling et al., 2004; Beolchini et al., 2010). The present study therefore focusses on estimation of kinetic parameters for inorganic nutrient-enhanced hydrocarbon degradation and their effect on the microorganisms responsible.

## MATERIALS AND METHODS

### SAMPLE COLLECTION AND MICROCOISM SET UP

Beach sediment samples consisting of fine sand were collected on 6/11/2009 in sterilized glass bottles (Duran) from a site close to St Mary's Island near Whitley Bay, Newcastle upon Tyne, United Kingdom ( $N 55^{\circ}04' 18''$ ,  $W 01^{\circ}26' 59''$ ). Sediment samples were stored at  $4^{\circ}\text{C}$  for a maximum 24 h prior to the start of the experiments. Oil degrading microcosms comprising beach sediment (10 g), North Sea crude oil (125 mg) and different concentrations of inorganic nutrients (sodium nitrate and potassium dihydrogen phosphate) were prepared in triplicate in serum bottles (114 ml capacity). The oil was weighed directly into the serum bottles, the sediment was added and the nutrient solution was pipetted onto the sediment to give the appropriate levels of nutrients (see "Effect of inorganic nutrient concentration" below). The total volume of nutrient solution added was always made up to 250  $\mu\text{l}$  so that all serum bottles received the same amount of liquid. The sediment, oil and nutrient solution were mixed gently with a glass rod and the microcosms were sealed with butyl rubber stoppers and incubated at  $24^{\circ}\text{C}$  in darkness. Microcosms without nutrient amendment, amended with 250  $\mu\text{l}$  of water served as a control. We monitored oxygen content in the headspace simultaneously with  $\text{CO}_2$  by GC-MS (see below) and in the 6 day incubation period the headspace remained oxic. Our measurements showed that by day 6 the degree of oxygen depletion was  $70.1 \pm 0.1\%$  ( $n = 24$ ) of the initial levels. In long term incubations where greater oxygen consumption occurred with increasing oil degradation, the headspace was replaced with air when oxygen dropped below 15% by volume.

### EFFECT OF INORGANIC NUTRIENT CONCENTRATION ON CRUDE OIL DEGRADATION

Inorganic nutrient treatments were nitrogen alone (0–5% w/w oil), different levels of phosphorus with a constant inorganic nitrogen concentration (0–0.5% P and 3% N w/w oil), or different levels of inorganic nitrogen with constant phosphorus concentration (0–5% N with 0.5% P w/w of oil) all treatments were conducted in triplicate. Control incubations with nutrients and no added oil were also conducted to determine the contribution of indigenous organic carbon to  $\text{CO}_2$  production.

### EFFECT OF CRUDE OIL CONCENTRATION ON OIL DEGRADATION

Microcosms set up as described above were prepared in triplicate with different amounts of oil ranging from 10 to 500 mg of crude oil and 6.25 mg N (44.6  $\mu\text{mole/g}$  sediment) and 0.625 mg

P (2.02  $\mu\text{mole/g}$  sediment). This gives a range of N and P levels ranging from 62.5% N and 6.25% P w/w of oil with 10 mg of oil to 1.25% N and 0.125% P w/w of oil with 500 mg of oil. With 125 mg of oil this is equivalent to 5% N and 0.5% P w/w of oil. The effect of crude oil levels on oil biodegradation was also investigated by treatment with different quantities of crude oil (10–500 mg) but a constant ratio of 5% N and 0.5% P w/w of oil. This was conducted because bioremediation treatments often recommend that a particular mass of inorganic nutrients is supplied relative to the amount of oil present (Swannell et al., 1996). In these treatments the absolute concentration of inorganic nutrients therefore increases with the amount of crude oil present. Thus, experiments treated with a single level of nutrients contained approximately 45  $\mu\text{mol N/g}$  wet sediment, while those that contained a constant ratio of inorganic nutrients relative to the mass of oil had N concentrations ranging from around 3.5–180  $\mu\text{mol N/g}$  wet sediment. If the same amount of nutrient added to the 500 mg oil treatment was added to 125 mg of oil (as used in all other microcosms) this would equate to 20% N and 2% P w/w of oil.

### ESTIMATION OF KINETIC PARAMETERS

Rate data in response to different inorganic nutrient and oil concentrations were fitted to a Monod-type kinetic model ( $q = q_{\max} * [S]/[K_s + [S]]$ ) using non-linear regression implemented in SPSS (IBM SPSS Statistics 19.0.0.1). This was used to derive the model parameters,  $K_s$  (half saturation constant) and  $q_{\max}$  (maximal rates).

### CARBON DIOXIDE MEASUREMENT

Carbon dioxide production as a measure of microbial activity and crude oil degradation was assessed in microcosm headspace samples daily over a period of 6 days using GC-MS. Maximal rates of  $\text{CO}_2$  production were calculated from the steepest part of the  $\text{CO}_2$  accumulation curve which typically followed a lag of 3–4 days (Figure S1). Analysis was performed on a Fisons 8060 GC linked to a Fisons MD 800 MS (electron voltage 70 eV, source temperature  $200^{\circ}\text{C}$ , interface temperature  $150^{\circ}\text{C}$ ). Hundred micro liter of headspace gas was manually injected via a syringe (SGE Analytical Science) under an atmosphere of  $\text{N}_2$  gas. Injection through a manifold which is continuously flushed with  $\text{N}_2$  was used to prevent interference from any ingress of air from the atmosphere during injection. The sample was separated using a HP-PLOT-Q capillary column (30 m  $\times$  0.32 mm). Helium was used as the carrier gas (1 ml/min, 65 kPa, split at 100 ml/min;  $250^{\circ}\text{C}$ ). Data acquisition, integration and quantification were controlled using Xcalibur 1.2 software. A mixture of gases with 10%  $\text{CO}_2$  was used as a standard for calibration. Different volumes of standard gas mix were used to produce a calibration curve which was linear over the range of 1–10%  $\text{CO}_2$ . Percent  $\text{CO}_2$  values were converted to total molar masses for determination of cumulative  $\text{CO}_2$  production.  $R^2$  values for calibration curves ranged from 0.993 to 0.997.

### RESIDUAL OIL EXTRACTION AND ANALYSIS

Petroleum hydrocarbons from the North Sea crude oil treated microcosm sediments were extracted using a mixture of dichloromethane (DCM):methanol (93:7). Prior to extraction

a known quantity of squalane was added in to the sediment as surrogate extraction standard. DCM:methanol (20 ml) was added to the sediment in serum bottle microcosms and stored at room temperature overnight. Microcosms were then sonicated for 1 min and the resulting supernatant was transferred into a flask with this extraction procedure being repeated twice more. The solvent containing the extract was passed through an alumina short column (1 cm bed depth) and then rotary evaporated to dryness before being redissolved in DCM. An aliquot of the organic extract in DCM was evaporated to dryness using a stream of nitrogen gas and solvent exchanged into hexane (200 µl). The total solution was added to a 500 mg/3 ml capacity Isolute® C-18 Solid Phase Extraction (SPE) column prewashed with hexane, and eluted with hexane (5 ml). The eluate was transferred into an autosampler vial and made up to 1 ml with hexane, together with a known amount of heptadecylcyclohexane internal standard. This saturated hydrocarbon fraction was analyzed using an Agilent (HP) 5890 Series II gas chromatograph (GC) fitted with a flame-ionization detector (FID). Samples were injected via split-splitless injector (held at 300°C) using an autosampler. The GC was fitted with a 30 × 0.25 mm fused silica capillary column coated with HP-5 phase (0.25 µm). Hydrogen was used as the carrier gas at a flow rate of 2 ml/min. An initial oven temperature of 50°C was held for 2 min and was then heated to 300°C at 5°C/min., where it was held for 20 min. Data were acquired and processed using Thermo LabSystems Atlas software.

#### DNA EXTRACTION

DNA from 500 mg of frozen microcosm sediment was extracted using a FastDNA® SPIN Kit for Soil (MP Biomedicals™) and a ribolyser (Thermo) according to the manufacturer's instruction. The DNA was eluted in sterilized milliQ water (50 µl) and frozen at -20°C prior to further analysis. The remaining 9.5 g of sediment was used for hydrocarbon extraction and analysis.

#### PRIMER DESIGN

Primers for amplifying 16S rRNA gene fragments from the total bacterial population and *Alcanivorax* spp. were designed using the probe and PCR primer design software tool Primrose (Ashelford et al., 2002) (**Table 1**). For *Alcanivorax*, the forward primer A16SF.493 matched 1606 of 2004048 bacterial sequences in the RDP database release 11, including 1059 of 1108 *Alcanivorax* sequences. The reverse primer A16SR.659 matched 1144 of 2004048 bacterial sequences in the RDP release 11 including 1058

of 1108 *Alcanivorax* sequences. The two primers in combination target 1020 of 2004048 bacterial sequences including 1016 of the 1108 *Alcanivorax* spp. 16S rRNA gene sequences in the database. The inosine-containing primer pair for total bacterial 16S rRNA genes (Gray et al., 2011; Callbeck et al., 2013) targets 855621 of 944469 bacterial sequences with the relevant target region in the RDP database.

#### PCR-AMPLIFICATION OF 16S rRNA GENES

Near full length 16S rRNA gene fragments were amplified using primer pair pA and pH (Edward et al., 1988) as described in Röling et al. (2004). For DGGE analysis, 16S rRNA gene fragments were amplified using primers 2 and 3 (Muyzer et al., 1993) as described previously (Röling et al., 2004). All PCR reactions were conducted using a PC Gene thermal cycler.

#### AGAROSE GEL AND DENATURING GRADIENT GEL ELECTROPHORESIS (DGGE)

Agarose gel electrophoresis of PCR-amplified 16S rRNA gene fragments from *Alcanivorax* spp. was run for 45 min at 80V using a 1.5% (w/v) agarose gel in 1 x TAE buffer. DGGE was conducted at 60°C using a 0.75 mm thick 10% polyacrylamide gel (ratio of acrylamide to bisacrylamide, 37.5:1) with a concentration gradient of 30–55% of denaturant using a Bio-Rad Dcode system. Gels were stained and photographed according to Röling et al. (2004). 100% denaturant comprised 7M Urea and 40% (vol/vol) deionized formamide in TAE buffer. 1 X TAE buffer contained 40 mM Tris-acetate, 1 mM EDTA, pH 8.0). Cloned *Alcanivorax* sp. 16S rRNA genes amplified using primers 2 and 3 (Muyzer et al., 1993) were used as markers for qualitatively identifying DGGE bands related to *Alcanivorax* spp. in DGGE profiles of total bacterial population 16S rRNA genes.

#### 16S rRNA GENE CLONING

DNA extracted from beach sediment as described above, was used to prepare a bacterial 16S rRNA gene clone library from a beach microcosm containing crude oil and treated with 1% N and 0.1% P after 5 days of incubation. The PCR-amplified 16S rRNA gene fragments were cloned with a TOPO® cloning kit (Invitrogen) as per the manufacturer's instructions. The clone libraries were screened for *Alcanivorax* sp 16S rRNA genes using the primer pairs listed in **Table 1**. Cloned *Alcanivorax* 16S rRNA genes were used to prepare standards for qPCR. These primer pairs were also used for detecting the presence of *Alcanivorax* spp. in microcosm sediments treated with different levels of inorganic nutrients.

#### QUANTITATIVE PCR

Quantitative PCR (qPCR) was used to determine the abundance of bacterial 16S rRNA genes using primer pair U1048f and U1371 (Gray et al., 2011; Callbeck et al., 2013), and abundance of *Alcanivorax* 16S rRNA genes was quantified using primer pair A16SF.493 and A16SR.659 (**Table 1**). qPCR was performed in 20 µl of reaction mixture using an iCycler (iQ™5 multicolor, Bio-Rad, Hemel Hempstead, UK) as described in Singh et al. (2011) with the following temperature cycles: one cycle of initial denaturation at 95°C for 7 min followed by 40 cycles of 95°C for 30 s, 61°C for 60 s and 72°C for 40 s. A standard curve for qPCR was prepared by dilution of a PCR-amplified cloned *Alcanivorax*

**Table 1 | Oligonucleotides primers used in qPCR analysis.**

Primer set	Sequence (5'-3')	Target organisms	Primer location
AI 6S F.493	CACCGGCTAATTCGTGC	<i>Alcanivorax</i>	481–498*
AI 6S R.659	ACCGGAAATTCCACCTCC	<i>Alcanivorax</i>	647–664*
U 1048f	GTGITGCAIGGIIGTCGTCA	<i>Bacteria</i>	1048–1068**
U1371	ACGTCITCCICICCTTCCTC	<i>Bacteria</i>	1352–1371**

\*Site on 16S rRNA gene of *Alcanivorax borkumensis* SK2 (S000018396); \*\*Site on *E.coli* 16S rRNA gene.

16S rRNA gene fragment. Standard curves had  $R^2$  values greater than 0.97 and calculated amplification efficiencies ranged from 101 to 113%. The PCR-amplified 16S rRNA gene was gel purified using QIAquick PCR purification kit (Qiagen) and quantified using a nanodrop® ND-1000 spectrophotometer. The number of 16S rRNA gene copies in the undiluted sample was calculated using the formula described by McKew et al. (2007b) and used to prepare a dilution series ranging from  $10^8$  to  $10^0$  target genes per  $\mu\text{l}$ .

## STATISTICAL ANALYSIS

Two sample *t*-tests assuming unequal variances, and single factor ANOVA were performed using Microsoft Excel and non-linear regression for estimation of kinetic parameters was conducted using IBM SPSS Statistics 19.0.0.1.

## RESULTS

### EFFECT OF INORGANIC NUTRIENT CONCENTRATION ON CRUDE OIL DEGRADATION

Microcosms treated with N but without P amendment exhibited stimulation of microbial activity. The activity at 0% N and 0% P ( $1.18 \pm 0.15 \mu\text{mol CO}_2$  produced/g wet sediment/day) was not significantly different from rates of  $\text{CO}_2$  production in sediments treated with no added oil ( $1.05 \pm 0.27 \mu\text{mol CO}_2$ /g wet sediment/day). Activity when inorganic N alone and oil were present was significantly higher. At 0.1% N and 0% P the rate of  $\text{CO}_2$  production was  $2.01 \pm 0.06 \mu\text{mol CO}_2$ /g wet sediment/day (*t*-test;  $P = 0.0095$ ) or with 0.5% N and 0% P  $3.66 \pm 0.05 \mu\text{mol CO}_2$ /g wet sediment/day (*t*-test;  $P = 0.000041$ ). Without P treatment, measured oil degrading activity reached a maximum level at 4% N w/w of oil ( $4.25 \pm 0.91 \mu\text{mol CO}_2$  produced/g wet sediment/day) and at levels of N of 0.5% w/w of oil and above there was no significant difference in the rate of crude oil biodegradation (ANOVA;  $P = 0.750$ ; Figure 1). These data indicated that crude oil degradation was nitrogen limited, but at levels of nitrogen 0.5% w/w of oil and above another factor became limiting.

Microcosms treated with both inorganic N and P showed an enhancement of oil degradation over and above that seen with nitrogen alone (Figure 1). For example  $\text{CO}_2$  production in 0.5% N and 0.5% P treated microcosms ( $9.77 \pm 1.54 \mu\text{mol CO}_2$  produced/g wet sediment/day) was significantly higher than the activity observed with 0.5% N and 0% P ( $3.66 \pm 0.05 \mu\text{mol CO}_2$  produced/g wet sediment/day) (*t*-test;  $P = 0.029$ ). Activity ranged from  $3.41 \pm 0.25 \mu\text{mol CO}_2$  produced/g wet sediment/day at 0% N/0.5% P concentration to  $18.40 \pm 1.04 \mu\text{mol CO}_2$  produced/g wet sediment/day at 5% N/0.5% P but no significant stimulation of oil degradation was seen at N levels greater than 0.5% w/w of oil when P was not limiting (ANOVA;  $P = 0.207$ , Figure 1).

These data were used to estimate half saturation constants and maximal rates using non-linear regression to a Monod-type kinetic model ( $q = q_{\max} \times [S]/K_s + [S]$ ). In sediments with no added P,  $K_s$  and  $q_{\max}$  for inorganic nitrogen was  $0.72 \pm 0.32 \mu\text{mol N/g sediment}$  and  $3.93 \pm 0.22 \mu\text{mol CO}_2$  produced/g wet sediment/day. The  $K_s$  and  $q_{\max}$  for hydrocarbon degradation activity when P was not limiting were  $1.99 \pm 0.87 \mu\text{mol N/g wet sediment}$  and  $16.16 \pm 1.28 \mu\text{mol CO}_2$ /g wet sediment/day

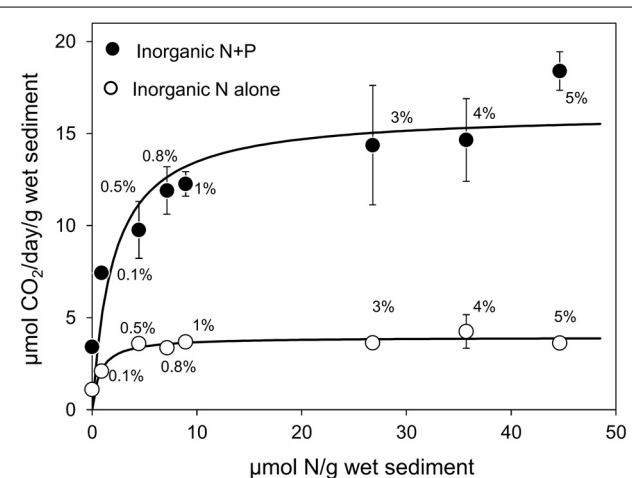


**FIGURE 1 | Effect of inorganic N treatment alone (0–5% N w/w of oil—open circles) or inorganic N (0–5% w/w of oil) with constant P (0.5% w/w of oil) treatment (filled circles) on the rate of  $\text{CO}_2$  production in microcosms containing 10 g beach sediments and 125 mg North Sea crude oil.** Data are plotted as micromoles N/g sediment with the equivalent %N w/w of oil annotated next to each data point. Sodium nitrate and potassium dihydrogen phosphate were used as N and P sources. Each data point represents the average value of three replicates. Where error bars are not seen they are smaller than the symbols. Control incubations with nutrients and no added oil were also conducted to determine the contribution of indigenous organic carbon to  $\text{CO}_2$  production. These typically gave values of  $1.05 \pm 0.27 \mu\text{mol CO}_2$ /g wet sediment/day (see Figure S1).

respectively (Figure 1). The  $K_s$  values for N, with and without P addition, were not statistically significantly different ( $P > 0.05$ ) whereas  $q_{\max}$  when both N and P were provided was significantly (over four times) greater than  $q_{\max}$  when only N was provided ( $P < 0.05$ ).

To systematically determine the level at which P became limiting, microcosms amended with 3% N w/w of oils and different P concentrations were analyzed. With 3% N and 0% P the oil degradation rate was  $3.63 \pm 0.28 \mu\text{mol CO}_2$  produced/g wet sediment/day. This was significantly lower ( $P = 0.04$ ) than rates of  $\text{CO}_2$  production with 3% N and 0.1% P ( $14.37 \pm 3.24 \mu\text{mol CO}_2$  produced/g wet sediment/day; Figure 2). With P ranging from 0.1 to 0.5% rates of  $\text{CO}_2$  production ranged from  $10.56 \pm 1.21 \mu\text{mol CO}_2$  produced/g wet sediment/day to  $13.05 \pm 1.51 \mu\text{mol CO}_2$  produced/g wet sediment/day and there was no significant difference between the 0.1 and 0.5% P treatments (ANOVA;  $P = 0.340$ ).

It was thus clear that P limitation of oil degradation was alleviated above 0.1% P w/w of oil. The  $K_s$  and  $q_{\max}$  values estimated for P were  $63 \pm 95 \text{ nmol/g wet sediment}$  and  $12.05 \pm 1.31 \mu\text{mol CO}_2$ /g wet sediment/day. The  $q_{\max}$  values determined with respect to N (Figure 1) and P (Figure 2) were not statistically significantly different ( $P > 0.05$ ).

### EFFECT OF OIL CONCENTRATION ON CRUDE OIL BIODEGRADATION

Effect of crude oil concentration ranging from 1 mg/g wet sediment to 50 mg/g wet sediment on oil degrading microbial activity

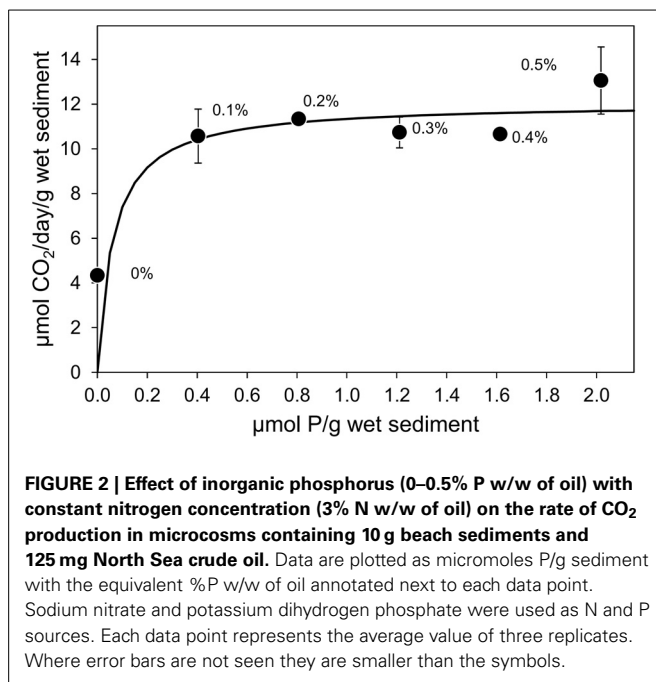


**FIGURE 2 | Effect of inorganic phosphorus (0–0.5% P w/w of oil) with constant nitrogen concentration (3% N w/w of oil) on the rate of CO<sub>2</sub> production in microcosms containing 10 g beach sediments and 125 mg North Sea crude oil.** Data are plotted as micromoles P/g sediment with the equivalent %P w/w of oil annotated next to each data point. Sodium nitrate and potassium dihydrogen phosphate were used as N and P sources. Each data point represents the average value of three replicates. Where error bars are not seen they are smaller than the symbols.

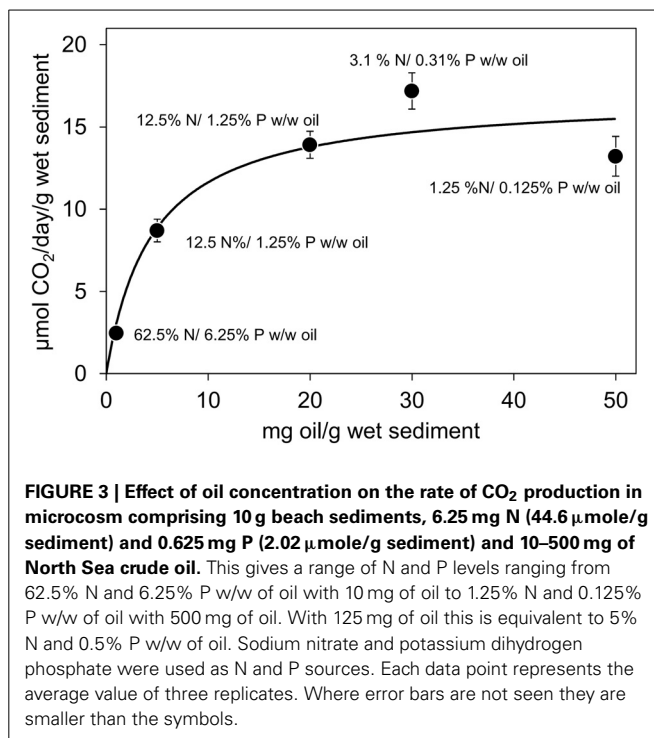


**FIGURE 3 | Effect of oil concentration on the rate of CO<sub>2</sub> production in microcosm comprising 10 g beach sediments, 6.25 mg N (44.6 μmole/g sediment) and 0.625 mg P (2.02 μmole/g sediment) and 10–500 mg of North Sea crude oil.** This gives a range of N and P levels ranging from 62.5% N and 6.25% P w/w of oil with 10 mg of oil to 1.25% N and 0.125% P w/w of oil with 500 mg of oil. With 125 mg of oil this is equivalent to 5% N and 0.5% P w/w of oil. Sodium nitrate and potassium dihydrogen phosphate were used as N and P sources. Each data point represents the average value of three replicates. Where error bars are not seen they are smaller than the symbols.

was investigated. The microcosms were amended either with a single level of inorganic nutrients irrespective of the amount of oil added (0.625 mg N and 0.0625 mg of P per gram of sediment (equivalent to 5% N and 0.5% P w/w of 125 mg of crude oil) or with a constant ratio of 5% N and 0.5% P w/w of crude oil leading to a range of nutrient levels ranging from 0.05 mg N/0.005 mg P to 2.5 mg N/0.25 mg P per gram of sediment equivalent to 20% N/2% P if in total 125 mg of oil rather than 500 mg of oil was present in the microcosms.

Where a single level of inorganic nutrients was provided, the rate of CO<sub>2</sub> evolution increased with increasing quantity of oil between 1 and 20 mg/g sediment (*t*-test:  $P = 0.000003$ ; **Figure 3**). At crude oil concentrations ranging from 20 to 50 mg/g sediment there was no significant difference in the rate of CO<sub>2</sub> production with increasing oil concentration (ANOVA:  $P = 0.08$ ; **Figure 3**). Thus, up to these levels, equivalent to 5% oil by weight of sediment, crude oil was not auto-inhibitory.

When a constant *ratio* of inorganic nutrients was provided with increasing oil concentration, CO<sub>2</sub> production rate decreased when oil levels were greater than 12.5 mg oil/g sediment (**Figure 4**). The CO<sub>2</sub> production rate at 20 mg oil/g sediment ( $10.40 \pm 1.35 \mu\text{mol CO}_2 \text{ produced/g wet sediment/day}$ ) was less than the rate at 12.5 mg oil/g sediment ( $15.59 \pm 2.08 \mu\text{mol CO}_2 \text{ produced/g wet sediment/day}$ ) and with 50 mg oil/g sediment the rates dropped further to  $0.46 \pm 0.04 \mu\text{mol CO}_2 \text{ produced/g wet sediment/day}$ , equivalent to almost a 97% decrease compared to rate at 12.5 mg oil/g sediment. Differences in CO<sub>2</sub> production rates with 12.5 mg oil/g sediment and higher oil concentrations were statistically significant (ANOVA:  $P = 0.00012$ ). The inhibition of oil degrading activity at a lower oil concentration than that seen when inorganic nutrients were added at a single concentration was most likely due to toxicity of the higher absolute amounts of nutrients present in microcosms containing higher

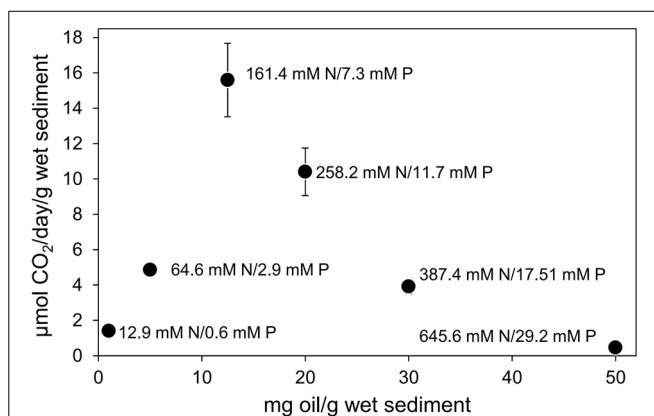


**FIGURE 4 | Effect of oil concentration on the rate of CO<sub>2</sub> production in microcosm comprising 10 g beach sediment and 10–500 mg North Sea crude oil amended with a constant ratio of 5% N and 0.5% P w/w of oil.** Sodium nitrate and potassium dihydrogen phosphate were used as N and P sources. Each point is annotated with the concentration of N and P in millimolar terms, based on the water content of the sediments. Each data point represents the average value of three replicates. Where error bars are not seen they are smaller than the symbols.

levels of oil. If the microcosm containing 50 mg of oil per gram of sediment is considered, the level of nutrients applied would be equivalent to 20% N and 2% P w/w of oil in a treatment containing 12.5 mg oil/g sediment. Indeed a systematic evaluation of the effect of nutrient concentration ranging from 0 to 20% N with 1/10th the P concentration w/w of 125 mg of oil showed that nutrient levels greater than 7% N / 0.7% P w/w of oil (equivalent to 62.5 micromoles N and 2.83 micromoles P/g sediment or

226 mM N/10.2 mM P) resulted in a reduction in CO<sub>2</sub> production rate from oil degradation (**Figure 5**).

### ALKANE DEGRADATION IN MICROCOISM INCUBATIONS

At the end of the 6 day incubation period residual crude oil was extracted from the microcosms treated with 125 mg crude oil and a range of inorganic nutrient concentrations (0%N/0.5%P to 5%N/0.5%P w/w of oil). The saturated hydrocarbon fractions were isolated and the resolved *n*-alkanes, pristane and phytane were quantified. The *nC*<sub>12</sub> to *nC*<sub>32</sub> alkanes present in the oil comprise approximately 10% by weight of the oil and thus the amount of resolved alkanes at the start of the experiment was about 12,500 µg per microcosm in addition volatile hydrocarbons (*nC*<sub>5</sub> to *nC*<sub>10</sub> and benzene and toluene) comprise around 7000 µg per microcosm. Across all treatments the total amount of alkanes measured (the sum of *nC*<sub>12</sub>–*nC*<sub>32</sub>) ranged from 9833 ± 1623 to 12168 ± 628 µg per microcosm. This suggests that a moderate amount of alkane degradation occurred over the 6 day incubation. Indeed, there was no statistically significant difference in the total mass of alkanes recovered, irrespective of the inorganic nutrient amendment (ANOVA: *P* = 0.244). This suggested that the degree of hydrocarbon degradation had been moderate. In addition to losses due to biodegradation some lower molecular weight alkanes may have been lost due to evaporation. Even though the incubations were conducted in sealed serum bottles some evaporative losses may have occurred during sampling the headspace for CO<sub>2</sub>. A systematic analysis of evaporative loss of volatile alkanes in the headspace demonstrated that flushing the headspace with up to 1800 ml of air removed alkanes up to *nC*<sub>9</sub>

to varying degrees, but *nC*<sub>10</sub> was unaffected (**Figure S2**). Alkanes with lower molecular weight than *nC*<sub>12</sub> were lost during the procedure for purification of the saturated hydrocarbon fraction and are not accounted for in our figures.

A more sensitive way to determine *n*-alkane degradation is by measuring the ratio of *n*-alkanes (typically *nC*<sub>17</sub>) relative to the concentration of the more slowly degraded branched alkane, pristane. To assess the degree of degradation of alkanes of different molecular weight we determined *nC*<sub>13</sub>:pristane, *nC*<sub>17</sub>:pristane and *nC*<sub>25</sub>:pristane ratios for all of the treatments (**Figure 6**).

The *nC*<sub>17</sub>:pristane ratio of the starting oil was 1.99 ± 0.01. The range of *nC*<sub>17</sub>:pristane ratios across treatments was relatively small with a maximum value in the 0%N/0.05%P treatment of 1.86 ± 0.04 and the lowest value measured in the 4%N/0.5%P treatment (1.35 ± 0.23). There were significant differences in the *nC*<sub>17</sub>:pristane ratios across all treatments (ANOVA: *P* = 0.036) resulting from lower values measured in treatments from 0.3% N/0.5%P to 5%N/0.5% (1.35 ± 0.23 to 1.64 ± 0.18) compared to the 0%N/0.5%P and 0.1%N/0.5%P treatments (1.86 ± 0.04 and 1.84 ± 0.04). There were no significant differences in the *nC*<sub>17</sub>:pristane ratios between the 0.3%N/0.5%P to 5%N/0.5% treatments (ANOVA: *P* = 0.589). If *nC*<sub>18</sub>:phytane ratios were used the results were essentially the same as obtained with *nC*<sub>17</sub>:pristane ratios. A similar pattern was seen with *nC*<sub>13</sub>:pristane ratios except that all nutrient treatments greater than 0%N/0.5%P gave *nC*<sub>13</sub>:pristane ratios which were statistically indistinguishable (ANOVA: *P* = 0.815) but were significantly different from the 0%N/0.5%P treatment (*P* = 0.018). There was no difference in *nC*<sub>25</sub>:pristane ratios across all treatments (ANOVA: *P* = 0.834). Taken together these data indicate that there was a small degree of degradation of *n*-alkanes and that lower molecular weight alkanes were degraded to a greater degree than higher molecular weight alkanes over the

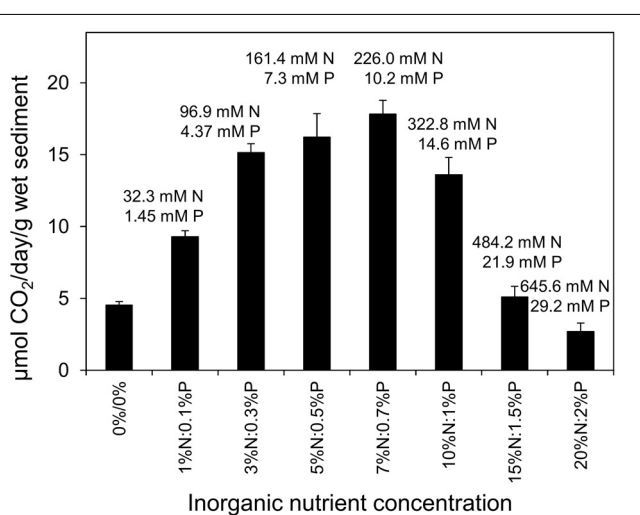


**FIGURE 5 | Effect of inorganic N treatment (0–20% w/w of oil) with 1/10<sup>th</sup> P treatment on the rate of CO<sub>2</sub> production in microcosm comprising 10 g beach sediment and 125 mg North Sea crude oil.**

Sodium nitrate and potassium dihydrogen phosphate were used as N and P sources. For easy cross referencing to **Figure 4**, each point is annotated with the concentration of N and P in millimolar terms, based on the water content of the sediments. Each data point represents average value of three replicates. One percent N by weight of oil is equivalent to approximately 9 micromoles of N per g sediment and 20% N is equivalent to 178 micromoles of N per g sediment.

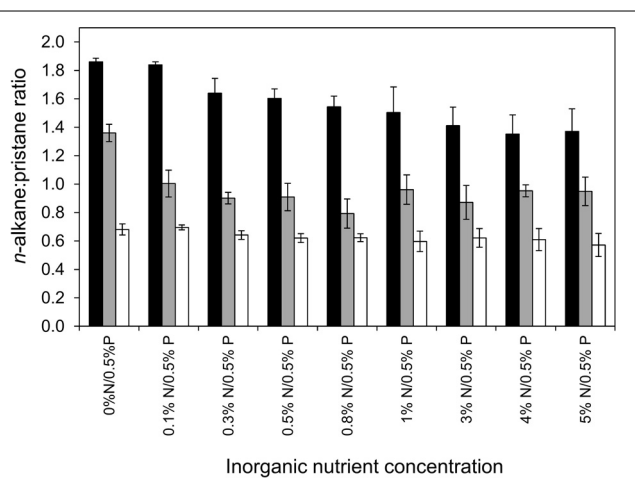


**FIGURE 6 | Effect of inorganic N (0–5%) with constant P (0.5%) treatment w/w of oil on the degradation on *n*-alkane (nC<sub>17</sub>, nC<sub>13</sub>, and nC<sub>25</sub>) to pristane ratios in microcosm comprising 10 g beach sediment and 125 mg North Sea crude oil.** Each data point represents average value of three replicates. nC<sub>17</sub>:pristane black bars, nC<sub>13</sub>:pristane gray bars, nC<sub>25</sub>:pristane white bars.

short 6 day time course of the experiments (**Figure 6**). Estimation of the extent of oil degradation based on a mass balance from the CO<sub>2</sub> produced over the 6 day incubation period, indicated that the CO<sub>2</sub> generated could account for degradation of 6.19 ± 0.02 to 37.28 ± 2.06% of the total mass of *nC<sub>5</sub>*–*nC<sub>32</sub>* alkanes and volatile low molecular weight aromatics (benzene and toluene) initially present, in the 0%N/0.5%P and 5%N/0.5%P treatments respectively. Estimates based on the *nC<sub>17</sub>*:pristane ratio were generally similar and ranged from 6.49 to 32.08%. Notwithstanding differences in the volatility of *nC<sub>13</sub>* and pristane, estimates of degradation based on the *nC<sub>13</sub>*:pristane ratio indicated a greater degree of degradation with a maximum estimated extent of degradation of 49.85%. Discrepancies in these estimates likely reflect the fact that the CO<sub>2</sub> produced integrates degradation of all components of the oil that are being removed whereas the alkane:pristane ratio data provide information on selected compounds which, as a comparison of the *nC<sub>13</sub>*:pristane and *nC<sub>17</sub>*:pristane suggests, are degraded to different degrees over the time course of the experiment.

#### EFFECT OF INORGANIC NUTRIENT AMENDMENT ON BACTERIAL COMMUNITY COMPOSITION

Bacterial communities in microcosms treated with crude oil and different levels of inorganic nutrients were characterized by DGGE analysis of PCR-amplified 16S rRNA genes (**Figure 7**). Following 6 days of incubation a differential response in the bacterial communities to nutrient amendment was observed with bands corresponding to *Cycloclasticus* sp. being detected at lower nutrient concentrations (0–1% N w/w of oil) and *Alcanivorax* spp. becoming much more prevalent at higher nutrient concentrations (**Figure 7**). End-point PCR using *Alcanivorax* specific primers demonstrated that only 20% of samples (3 out of 15) treated with 0.8%N/0.5%P or less harbored detectable *Alcanivorax* whereas in samples treated with 1–5%N/0.5%P, 100% of samples (12 out of 12) harbored detectable *Alcanivorax* 16S rRNA genes. Interestingly all three microcosms treated with 0.5%N/0.5%P contained *Alcanivorax* 16S rRNA genes detectable by end-point PCR while no samples from 0.8%N/0.5% P-treated microcosms contained detectable *Alcanivorax* 16S rRNA genes. The selection of *Alcanivorax* at higher inorganic nutrient concentrations was

consistent with the greater alkane degradation observed in these samples.

Quantification of bacterial 16S rRNA genes by qPCR showed a small, but significant increase in total bacterial abundance relative to nutrient levels (ANOVA: *P* = 0.008). The log bacterial gene abundance was 8.93 ± 0.09/g in sediments treated with 0%N/0.5%P with a maximum value of 10.17 ± 0.18/g sediment treated with 3%N/0.5%P (**Figure 8A**). The differences were due to higher bacterial 16S rRNA gene abundance in microcosms treated with nutrient concentrations greater than 0.3%N/0.5%P and at all nutrient treatments greater than this, there was no significant difference in total bacterial 16S rRNA gene abundance (ANOVA: *P* = 0.14).

Log 16S rRNA gene abundance determined using *Alcanivorax* specific primers ranged from 6.28 ± 0.08/g in sediments treated with 0%N/0.5% P to 8.82 ± 0.52/g, in sediments that received 3% N/0.5% P (**Figure 8B**). There were significant differences in *Alcanivorax* 16S rRNA gene abundance (ANOVA: *P* = 0.014). *Alcanivorax* 16S rRNA gene abundance in microcosms treated with 0.8% N/0.5% P had anomalously low 16S rRNA gene abundance (log abundance, 6.41 ± 0.02/g sediment) and excluding this value which was not significantly different from *Alcanivorax* 16S rRNA gene abundance at all nutrient concentrations less than 0.5% N/0.5% P (ANOVA: *P* = 0.275), showed that at all other nutrient concentrations greater than 0.3% N/0.5% P *Alcanivorax* genes were significantly more abundant than at lower nutrient levels, while there was no difference in abundance in all treatments greater than 0.3% N/0.5% P (ANOVA: *P* = 0.671).

## DISCUSSION

#### KINETICS OF INORGANIC NUTRIENT-STIMULATED CRUDE OIL BIODEGRADATION

Biostimulation with N and P is an effective method for enhancing the rate of oil bioremediation (Atlas and Bartha, 1972, 1973; Bragg et al., 1994; Venosa et al., 1996; Röling et al., 2002; McKew et al., 2007b; Coulon et al., 2007). Early studies of Atlas and Bartha (1972) were the first to demonstrate inorganic N and P-mediated stimulation of crude oil biodegradation and that both N and P amendment were required for oil degradation. Subsequently the feasibility of using oleophilic fertilizer as biostimulating agents

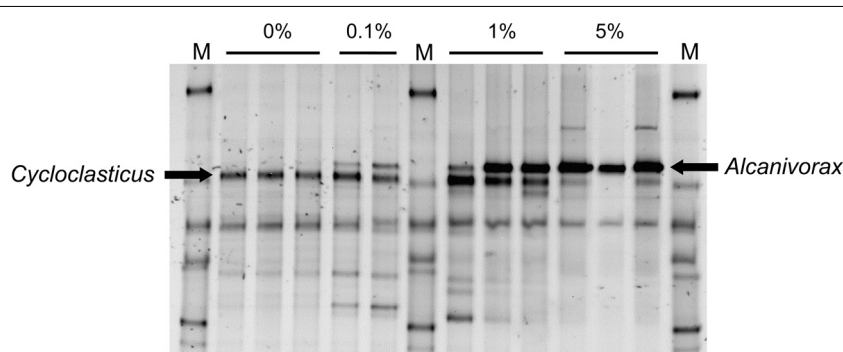


**FIGURE 7 | Denaturing gradient gel electrophoresis of 16S rRNA gene fragments from crude oil and nutrient treated beach microcosms incubated for 6 days.** Fragments corresponding to *Cycloclasticus* spp and

*Alcanivorax* spp. are indicated. All microcosms were treated with 0.5%P w/w of oil and the values above the lanes indicate the percentage of inorganic N added relative to the mass of oil.

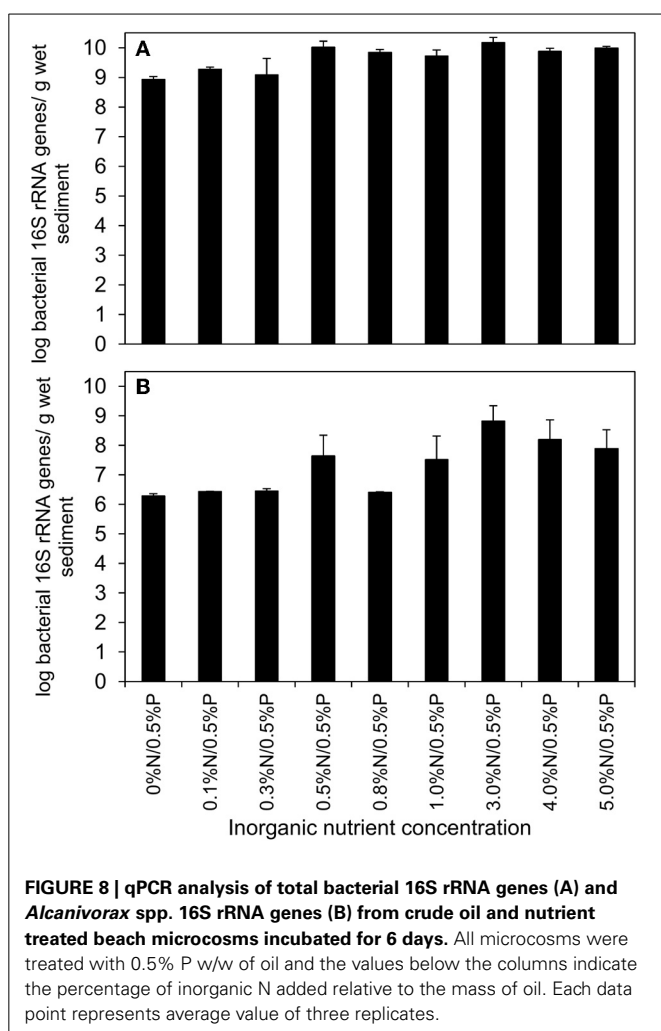


**FIGURE 8 |** qPCR analysis of total bacterial 16S rRNA genes (A) and *Alcanivorax* spp. 16S rRNA genes (B) from crude oil and nutrient treated beach microcosms incubated for 6 days. All microcosms were treated with 0.5% P w/w of oil and the values below the columns indicate the percentage of inorganic N added relative to the mass of oil. Each data point represents average value of three replicates.

was demonstrated (Atlas and Bartha, 1973). The enhancement of hydrocarbon degradation rate with increasing nitrate concentration (Boufadel et al., 1999), and nitrate plus sand amendments (Beolchini et al., 2010) has also been demonstrated. In the study of Beolchini et al. (2010) the sand enhanced biodegradation of high molecular weight aliphatic hydrocarbons and it was suggested that this was effective because it increased the surface area of the solid/liquid interface in the sediment and increased oxygen diffusion and mass transfer. However, these studies did not attempt to systematically analyze the nutrient enhanced kinetic parameters of crude oil biodegradation. Therefore, the focus of the present study was to evaluate the kinetic parameters for crude oil degradation in relation to N and P treatments.

Oil-stimulated CO<sub>2</sub> production rate was used as a proxy for hydrocarbon degradation to determine initial rates in relation to nutrient levels and oil concentration to estimate kinetic parameters that may be useful for modeling crude oil bioremediation programmes for marine beach sediments. N amendment with no added P led to a small but significant stimulation of oil degradation (Figure 1), however when P-limitation was alleviated there was a greater enhancement in the rate of oil degradation up to around 0.8 to 1% N w/w of oil (Figure 1). While  $q_{max}$  values were four-fold higher when both N and P limitation were alleviated

compared to alleviation of N limitation alone, K<sub>s</sub> values for N were similar irrespective of P provision (0.72 ± 0.32 μmol N/g sediment and 1.99 ± 0.87 μmol N/g wet sediment). The water content of the sediments was determined to be 25.16 ± 0.09% ( $n = 3$ ) and 250 μl of nutrient solution was added to each sample (i.e., water content of 2.766 ml per microcosm) and on this basis the K<sub>s</sub> values were converted to molar concentrations. This gave a K<sub>s</sub> value of 2.60 ± 1.16 mM with no P amendment and 7.19 ± 3.14 mM with N and P amendment. This is several orders of magnitude higher than the range of 6.9–122.4 μM reported for heterotrophic bacteria (Reay et al., 1999) and may reflect the fact that the key alkane degraders in the microcosms are *Alcanivorax* sp. which are known to be stimulated during bioremediation treatments and thus may be better adapted to relatively high inorganic nutrient concentrations. The K<sub>s</sub> value for P was much lower at 63 ± 95 nmol/g wet sediment which translates to 227.77 ± 343.46 μM. The mean value obtained is much (orders of magnitude) higher than K<sub>s</sub> values typically reported for phosphate utilization by bacteria and aquatic microbial communities which are usually sub micromolar (Vadstein and Olsen, 1989, 0.013–0.247 μM; Schowanek and Verstraete, 1990, 0.17 μM; Cotner and Wetzel, 1992, 0.019–0.225 μM). This may reflect adaptation of these specialist hydrocarbon-degrading taxa to high nutrient concentrations typical of conditions that are used to promote hydrocarbon bioremediation. Many pure cultures of *Alcanivorax* spp. are available and kinetic analysis with respect to N and P utilization would be highly informative in this regard. It should however, be noted that the error on the estimate of K<sub>s</sub> for phosphate is large (±151%) and indicates that there is a statistical probability that K<sub>s</sub> has a negative value. This is clearly not possible and one would have to conclude that the lower bound must be a small non-zero value. Putting this statistical incongruity to one side the important point is that it is difficult to draw reliable conclusions about the specific kinetic characteristics of the hydrocarbon degrading organisms with respect to inorganic phosphate from these data. Future studies should focus on analysing the response of hydrocarbon degraders to P at sub micromolar levels.

The occurrence of high affinity permeases for inorganic N and P in the genome of *Alcanivorax borkumensis* SK2 (Schneiker et al., 2006) seems to contradict the findings of the present study, however, as far as we are aware these have been annotated largely on the basis of sequences from known permeases and there is no direct evidence available regarding the kinetic of these permeases. Moreover organisms may have different sets of permeases with different affinity for inorganic nutrients allowing them to adapt rapidly to a change from nutrient limited to nutrient replete conditions. However, such conclusions would need, to be supported by detailed proteomic analysis of the response of *Alcanivorax* to growth at different nutrient levels (Sabirova et al., 2006).

#### KINETIC RESPONSE OF CRUDE OIL DEGRADING MICROBIAL COMMUNITIES TO OIL LOADING

Microbial activity generally increases in proportion to an accessible carbon and energy source. However, high concentrations of hydrocarbons have been shown to inhibit oil biodegradation either by causing nutrient or oxygen limitation or through direct toxicity of volatile hydrocarbons (Fusey and Oudot, 1984; Leahy and Colwell, 1990). Therefore, in addition to assessing the kinetics

of hydrocarbon degradation in relation to inorganic nutrient availability we determined the effect of sediment oil loading on biodegradation rates when N and P were not limiting. CO<sub>2</sub> evolution rates increased with increasing oil content from 1 to 50 mg crude oil/g sediment (5% oil by weight; **Figure 3**). This encompasses the range of contamination levels observed following the Exxon Valdez Spill in Prince William Sound, Alaska. The levels of oil in surface sediments in Prince William Sound were highly variable with an average value of  $12.2 \pm 18.6$  mg/g sediment (Bragg et al., 1992). This suggests that effective biodegradation of the labile components of crude oil is likely achievable at oiling levels typically seen in oil spill-affected sediments in the field. Nevertheless, much higher levels of oil contamination (up to 510 mg/g) have been reported following the Deepwater Horizon blow out (Lin and Mendelsohn, 2012). The marsh sediments studied by Lin and Mendelsohn (2012) were from Bay Jimmy within Barataria Bay. Sediments in Barataria bay range from fine sand to coarse silts (most sediment particles in the range 2–5 in the phi scale of Krumbein and Aberdeen, 1937) and Bay Jimmy sediments specifically are organic rich (4.0–16.2% TOC by weight of sediment; Natter et al., 2012). This suggests that oxygen depletion in these sediments may contribute to the relative persistence in these sediments and indeed evidence has been presented that suggests that oiling of these sediments promoted sulfate-reduction (Natter et al., 2012).

The half saturation constant for crude oil in our sediments was estimated to be  $5.83 \pm 1.46$  mg oil/g wet sediment. While this provides a practically useful K<sub>s</sub> value for modeling the kinetics of field scale bioremediation it is not straightforward to compare this with literature values for pure compound and/or pure cultures of microorganisms due to the complexity of the mixture of carbon sources and their low water solubility. If the oil masses are converted to moles of carbon (crude oil is typically 84% carbon by weight) this translates into a K<sub>s</sub> value of  $388 \pm 97$   $\mu\text{mol C/g}$  sediment. We know from oil chemistry data that only a fraction of the alkanes (*n*C<sub>13</sub>–*n*C<sub>17</sub>) were being degraded in the system and in the freshly added oil the mass of *n*C<sub>13</sub>–*n*C<sub>17</sub> was equivalent to about 3% of the total oil mass, giving a K<sub>s</sub> value for the alkanes which were actually being degraded of  $11.64 \mu\text{mol C/g}$  sediment. The low aqueous solubility of alkanes also needs to be considered in this context (e.g., 1.7 nM for hexadecane in seawater at 25°C; Verschueren, 1983). Moreover, aqueous solubility defined under standard physical and chemical conditions may not be truly representative of the situation *in situ*, where biosurfactants may substantially increase the effective aqueous solubility. Nevertheless, the K<sub>s</sub> values reported in terms of mass of sediment would be equivalent to orders of magnitude greater than K<sub>s</sub> values reported for hydrocarbon degradation by pure cultures of bacteria which are in the micromolar or even sub-micromolar range. The toluene degrader *Cycloclasticus oligotrophicus* for example has the lowest known K<sub>s</sub> for an organic substrate (0.014  $\mu\text{M}$ ; Button et al., 1998).

While the kinetic parameters we have estimated will be useful for modeling the fate of the more labile components of crude oil, as these become degraded more persistent fractions of the oil will be degraded more slowly. To address this, studies of partially degraded and heavier oils will be required. Interestingly, it has been reported that nominally labile crude oil hydrocarbons have

persisted in subsurface sediments from Prince William Sound, Alaska, even 16 years after the *Exxon Valdez* oil spill (Short et al., 2007). This persistence could be explained by anoxia reducing the rates of hydrocarbon degradation, though this was discounted by Short et al. (2007) due to high levels of tidal flushing in the sediments. It was however suggested that nutrient availability may have been a factor in the persistence of these hydrocarbons, and perhaps more importantly the formation of water in oil emulsions (mousse), which reduce the surface area of oil available for microbial attack (Short et al., 2007). Subsequent studies however demonstrated that the long term residual oil was biodegradable and that inorganic nutrients and oxygen stimulated its biodegradation (Venosa et al., 2010). These studies emphasize the need to consider more than just microbiological factors when assessing the fate of spilled oil in the field.

### SUPPRESSION OF BIOREMEDIATION BY HIGH LEVELS OF INORGANIC NUTRIENTS

Recommendations for nutrient levels required for crude oil bioremediation are often given in terms of the mass of nutrients required relative to the mass of oil (Röling et al., 2004). Moreover arguments surrounding addition of excessive amounts of nutrients normally relate to avoiding eutrophication of neighboring water bodies (Swannell et al., 1996; Röling et al., 2004). For this reason we determined the response of oil degrading microorganisms to increasing levels of oil in the presence of a constant proportion, but increasing absolute amounts of nutrients. In experiments with increasing oil concentration above 12.5 mg oil/g sediment, marked inhibition of oil degradation was noted (**Figure 4**). This was shown to be a consequence of toxicity of high levels of nutrients rather than an effect of higher levels of oil (**Figure 5**). Converting the added nutrients into an aqueous concentration based on the water content of the sediments indicated that inhibition of oil degradation occurred at sodium nitrate and potassium orthophosphate concentrations of 238 mM nitrate and 10.8 mM phosphate or greater. These absolute concentrations are very high (almost 3 orders of magnitude greater than the K<sub>s</sub> values determined here), but serve to underline the importance of designing treatment strategies on more than a simple mass balance of oil carbon relative to inorganic nutrient levels. It is possible that a similar effect might result from oxygen depletion at higher oil loadings however in the sediment containing 50 mg oil/g of sediment and 5%/0.5% N/P by mass, oxygen was depleted by only  $24.0 \pm 2.8\%$  over the incubation period relative to oxygen levels at the start of the experiment. This compares with the treatment with 12.5 mg oil/g of sediment and 5%/0.5% N/P by mass where oxygen was depleted by  $31.3 \pm 2.8\%$  from the levels at the start of the experiment. Moreover inhibition of oil degradation at 50 mg oil/g of sediment did not occur when lower absolute concentrations of nutrients were provided (**Figure 3**).

### ALKANE DEGRADATION AND GROWTH OF *ALCANIVORAX* IN SHORT TERM INCUBATIONS

Biodegradation of saturated and aromatic hydrocarbons in crude oil contaminated environments has been previously demonstrated (Kasai et al., 2002a,b; Röling et al., 2002; Singh et al., 2011). The lack of detectable degradation of total resolved alkanes in our experiments is consistent with the short incubation

period of the experiments which were designed to determine initial rates of hydrocarbon degradation, not the full extent of degradation possible. Similar experiments conducted over much longer timescales (30–90 days) typically show complete removal of the resolved alkanes. More detailed analysis of hydrocarbon degradation based on ratios of *n*-alkanes to pristane demonstrated that there was modest degradation of lower molecular weight alkanes with increasing inorganic nutrient concentrations (**Figure 6**). This is consistent with the increased rates of CO<sub>2</sub> production and increase in abundance of *Alcanivorax* observed at higher nutrient levels (**Figures 1, 8**).

*Alcanivorax* spp. have been found to be globally significant for *in situ* degradation of straight and branched chain alkanes in marine environments (Dyksterhouse et al., 1995; Yakimov et al., 2005; Head et al., 2006; McKew et al., 2007a,b). A greater decrease in the ratio of *nC*<sub>13</sub>: pristane as compared to *nC*<sub>17</sub>: pristane and *nC*<sub>25</sub>: pristane ratios suggest a preference for degradation of low molecular weight alkanes by the *Alcanivorax* sp. detected in our experiments.

It is also interesting to note that at low nutrient concentrations *Cycloclasticus*-like bacteria were prevalent. These are known aromatic hydrocarbon-degrading bacteria with particularly high substrate affinities which contrasts with *Alcanivorax* which was strongly selected at higher nutrient concentrations (**Figure 7**) consistent with the high K<sub>s</sub> values determined in these experiments. Interestingly despite the significance of inorganic nutrient provision for stimulation of crude oil biodegradation, and the fact that this has been known for several decades, there are relatively few data in the literature on the kinetic parameters for oil degradation with respect to inorganic N or P. This is an important gap in our knowledge of the ecology of hydrocarbon-degrading bacteria and has practical implications for understanding the fate of crude oil in the environment. The present day focus on omics-enabled studies of hydrocarbon-degrading communities would be perfectly complemented by more studies to determine fundamental kinetic and physiological properties of both pure cultures and natural communities of hydrocarbon-degrading bacteria. It will be interesting to note if the high K<sub>s</sub>/low affinity kinetics noted in this study are reflected in the kinetic properties of pure cultures and how they are affected by environmental conditions such as temperature. This kind of information will be essential for incorporation of ecological principles such as resource ratio theory into modeling approaches to better understand the fate of spilled oil (Smith et al., 1998). Both theoretical and experimental approaches to understanding the competitiveness of different hydrocarbon-degrading bacteria under different scenarios would be facilitated by such basic knowledge of the physiology of hydrocarbon degrading bacteria (McKew et al., 2007b). This is an attractive proposition given that many of the key players in marine hydrocarbon degradation are available in culture (Yakimov et al., 2007). In addition genome sequences have been determined for a number of these taxa and it is only a matter of time before many more marine obligate hydrocarbon degrading bacterial genomes are sequenced (Schneiker et al., 2006).

## CONCLUSIONS

The data presented here provide a systematic assessment of key factors that control the biodegradation of crude oil in beach

sediments and provide kinetic parameters that can be used in kinetic modeling of beach oil spill bioremediation. Our results not only confirm that crude oil biodegradation in marine beach sediments is sensitive to the level of inorganic N and P nutrient treatments but that the maximum rates of crude oil biodegradation achievable are approximately 16 μmol C/g sediment/day at the incubation temperature of our experiments (24°C). Half saturation constants for N and P in the form of nitrate and phosphate are high compared to values typically seen in pure cultures of heterotrophic bacteria and underline the importance of maintaining high inorganic nutrient concentrations to accelerate hydrocarbon degradation. The half saturation constants also provide fundamental parameters for future kinetic modeling of bioremediation of beached oil spills. The high nutrient levels that promote crude oil biodegradation also select for specialized alkane degrading bacteria from the genus *Alcanivorax* while selecting against aromatic hydrocarbon degrading bacteria such as *Cycloclasticus* sp. This suggest that by manipulation of nutrient amendments it may be possible to balance aromatic and aliphatic hydrocarbon degradation, albeit at the expense of lower overall rates of biodegradation due to the lower levels of nutrients required to stimulate aromatic hydrocarbon degrading *Cycloclasticus* spp. We also demonstrated that nutrient-enhanced bioremediation is effective only up to a point and care should be taken in oil spill bioremediation, not only to protect against eutrophication by avoiding excessive nutrient loading, but also to avoid inhibition of hydrocarbon degradation at high nutrient levels. Similar analyses on a wider range of sediments will establish if the observations we have made in one beach sediment apply broadly across a range of environments and geographical locations.

## AUTHOR CONTRIBUTIONS

Ian M. Head, Arvind K. Singh, and Neil D. Gray developed the concept and designed experiments; Arvind K. Singh prepared and analyzed microcosm experiments. Arvind K. Singh, Neil D. Gray, and Angela Sherry conducted headspace gas analysis and microbial community analysis. Arvind K. Singh, Bernard F. J. Bowler, and D. Martin Jones were responsible for and conducted crude oil analysis. Data analysis and interpretation was conducted by Arvind K. Singh, Ian M. Head, Angela Sherry, and Neil D. Gray. Arvind K. Singh, and Ian M. Head wrote the manuscript with critical input from Angela Sherry, Neil D. Gray, and D. Martin Jones.

## ACKNOWLEDGMENTS

The financial support from European Commission as Marie Curie Fellowship award to Arvind Singh via the Project BACTOIL (MC-IIF-39431) is gratefully acknowledged. We are also grateful for financial support from the Natural Environment Research Council (Grant NE/E01657X/1 to Ian M. Head, Neil D. Gray, and D. Martin Jones). James Todd is thanked for the supplementary data.

## SUPPLEMENTARY MATERIAL

The Supplementary Material for this article can be found online at: <http://www.frontiersin.org/journal/10.3389/fmicb.2014.00160/abstract>

**Figure S1 | Cumulative CO<sub>2</sub> production in beach sediment microcosms.**

Data from microcosms treated with crude oil plus inorganic nitrogen and phosphorus (black circles), inorganic nitrogen and phosphorus but no oil (gray circles) and killed control microcosms treated with formaldehyde (2% final concentration) and crude oil plus inorganic nitrogen and phosphorus (white circles). Oil treated microcosms contained 10 mg crude oil/g sediment and inorganic nutrient amendments equated to 5% N and 0.5% P by weight of the oil.

**Figure S2 | Effect of headspace flushing on physical removal of volatile saturated hydrocarbons from beach sediment microcosms.**

Concentrations of the individual compounds (C) after flushing the headspace with different volumes of air are presented relative to initial headspace concentration ( $C_0$ ) of the volatile hydrocarbons.

**REFERENCES**

- Ashelford, K. E., Weightman, A. J., and Fry, J. C. (2002). PRIMROSE: a computer program for generating and estimating the phylogenetic range of 16S rRNA oligonucleotide probes and primers in conjunction with the RDP-11 database. *Nucleic Acids Res.* 30, 3481–3489. doi: 10.1093/nar/gkf450
- Atlas, R. M., and Bartha, R. (1972). Degradation and mineralization of petroleum in sea water: limitation by nitrogen and phosphorus. *Biotechnol. Bioeng.* 14, 309–318. doi: 10.1002/bit.260140304
- Atlas, R. M., and Bartha, R. (1973). Stimulated biodegradation of oil slicks using oleophilic fertilizers. *Environ. Sci. Technol.* 7, 538–541. doi: 10.1021/es60078a005
- Beolchini, F., Rocchetti L., Regoli, F., and Dell'Anno, A. (2010). Bioremediation of marine sediments contaminated by hydrocarbons: experimental analysis and kinetic modeling. *J. Hazar Mater.* 182, 403–407. doi: 10.1016/j.jhazmat.2010.06.047
- Boufafel, M. C., Reeser, P., Suidan, M. T., Wrenn, B. A., Cheng, J., Du, X., et al. (1999). Optimal nitrate concentration for the biodegradation of n-heptadecane in a variably saturated sand column. *Environ. Technol.* 20, 191–199. doi: 10.1080/0959332008616808
- Bragg, J. R., Prince, R. C., Harner, E. J., and Atlas, R. M. (1994). Effectiveness of bioremediation for the Exxon Valdez oil spill. *Nature* 368, 413–418. doi: 10.1038/368413a0
- Bragg, J. R., Prince, R. C., Wilkinson, J. B., and Atlas, R. M. (1992). *Bioremediation for Shoreline Cleanup following the 1989 Alaska Oil Spill*. Houston: Exxon Company, 94.
- Button, D. K., Robertson, B. R., Lepp, P. W., and Schmidt, T. M. (1998). A small, dilute-cytoplasm, high-affinity, novel bacterium isolated by extinction culture and having kinetic constants compatible with growth at ambient concentrations of dissolved nutrients in seawater. *Appl. Environ. Microbiol.* 64, 4467–4476.
- Callbeck, C. M., Sherry, A., Hubert, C. R. J., Gray, N. D., Voordouw, G., and Head, I. M. (2013). Improving PCR efficiency for accurate quantification of 16S rRNA genes. *J. Microbiol. Meth.* 93, 148–152 doi: 10.1016/j.mimet.2013.03.010
- Cappello, S., Denaro, R., Genovese, M., Giuliano, L., and Yakimov, M. M. (2007). Predominant growth of *Alcanivorax* during experiments on oil spill bioremediation in mesocosms. *Microbiol. Res.* 162, 185–190. doi: 10.1016/j.mires.2006.05.010
- Cooney, J. J., Silver, S. A., and Bech, E. A. (1985). Factors influencing hydrocarbon degradation in three freshwater lakes. *Microb. Ecol.* 11, 127–137. doi: 10.1007/BF02010485
- Cotner, J. B., and Wetzel, R. G. (1992). Uptake of dissolved inorganic and organic phosphorus compounds by phytoplankton and bacterioplankton. *Limnol. Oceanogr.* 37, 232–243. doi: 10.4319/lo.1992.37.2.0232
- Coulon, F., McKew, B. A., Osborn, A. M., McGenity, T. J., and Timmis, K. N. (2007). Effect of temperature and biostimulation on oil-degrading microbial communities in temperate estuarine waters. *Environ. Microbiol.* 9, 177–186. doi: 10.1111/j.1462-2920.2006.01126.x
- Dell'Anno, A., Beolchini, F., Rocchetti, L., Luna, G. M., and Danovaro, R. (2012). High bacterial biodiversity increases degradation performance of hydrocarbons during bioremediation of contaminated harbor marine sediments. *Environ. Pollut.* 167, 85–92. doi: 10.1016/j.envpol.2012.03.043
- Dyksterhouse, S. E., Gray, J. P., Herwig, R. P., Lara, J. C., and Staley, J. T. (1995). *Cycloclasticus pugetii* gen. nov., sp. Nov., an aromatic hydrocarbon degrading-bacterium from marine sediments. *Int. J. Syst. Bacteriol.* 45, 116–123. doi: 10.1099/00207713-45-1-116
- Edward, U., Rogall, T., Blöcker, H., Emde, M., and Böttger, E. C. (1988). Isolation and complete nucleotide determination of entire genes. Characterisation of a gene coding for 16S ribosomal RNA. *Nucleic Acid Res.* 17, 7843–7853. doi: 10.1093/nar/17.19.7843
- Engelhardt, M. A., Daly, K., Swannell, R. P. J., and Head, I. M. (2001). Isolation and characterization of a novel hydrocarbon- degrading, Gram-positive bacterium, isolated from intertidal beach sediment, and description of *Planococcus alkanoclasticus* sp nov. *J. Appl. Microbiol.* 90, 237–247. doi: 10.1046/j.1365-2672.2001.01241.x
- Fusey, P., and Oudot, J. (1984). Relative influence of physical removal and biodegradation in the depuration of petroleum-contaminated Seashore sediments. *Mar. Pollut. Bull.* 15, 136–141. doi: 10.1016/0025-326X(84)90234-0
- Golyshin, P. N., Chemikova, T. N., Abraham, W. R., Lunsdorf, H., Timmis, K. N., and Yakimov, M. M. (2002). *Oleophilaceae* fam. nov., to include *Oleiphilus messinensis* gen. nov., sp. nov., a novel marine bacterium that obligatory utilizes hydrocarbons. *Int. J. Syst. Evol. Microbiol.* 52, 901–911. doi: 10.1099/ijs.0.01890-0
- Gray, N. D., Sherry, A., Grant, R. J., Rowan, A. K., Hubert, C. R. J., Callbeck, C. M., et al. (2011). The quantitative significance of Syntrophaceae and syntrophic partnerships in methanogenic degradation of crude oil alkanes. *Environ. Microbiol.* 13, 2957–2975. doi: 10.1111/j.1462-2920.2011.02570.x
- Hara, A., Syutsubo, K., and Harayama, S. (2003). *Alcanivorax* which prevails in oil-contaminated seawater exhibits broad substrate specificity for alkane degradation. *Environ. Microbiol.* 5, 746–753. doi: 10.1046/j.1468-2920.2003.00468.x
- Harayama, S., Kishira, H., Kasai, Y., and Syutsubo, K. (1999). Petroleum biodegradation in marine environments. *J. Mol. Microbiol. Biotechnol.* 1, 63–70.
- Head, I. M., Jones, D. M., and Röling, W. F. M. (2006). Marine microorganisms make a meal of oil. *Nat. Rev. Microbiol.* 4, 173–182. doi: 10.1038/nrmicro1348
- Hedlund, B. P., Geiselbrecht, A. D., Bair, T. J., and Staley, J. T. (1999). Polycyclic aromatic hydrocarbon degradation by a new marine bacterium, *Neptunomonas naphthovorans* gen. nov., sp. nov. *Appl. Environ. Microbiol.* 65, 251–259.
- ITOPF. (2011). *Oil Tanker Spill Statistics*. The International Tanker Owners Pollution Federation. Available online at: <http://www.skuld.com/News/News/ITOPF-Oil-Tanker-Spill-Statistics-2011-released/>
- Jones, D. M., Douglas, A. G., Parkes, R. J., Taylor, J., Giger, W., and Schaffner, C. (1983). The recognition of biodegraded petroleum-derived aromatic hydrocarbons in recent marine sediments. *Mar. Pollut. Bull.* 14, 103–108. doi: 10.1016/0025-326X(83)90310-7
- Kasai, Y., Kishira, H., and Harayama, S. (2002b). Bacteria belonging to the genus *Cycloclasticus* play a primary role in the degradation of aromatic hydrocarbons released in a marine environment. *Appl. Environ. Microbiol.* 68, 5625–5633. doi: 10.1128/AEM.68.11.5625-5633.2002
- Kasai, Y., Kishira, H., Sasaki, T., Syutsubo, K., Watanabe, K., and Harayama, S. (2002a). Predominant growth of *Alcanivorax* strains in oil contaminated and nutrient-supplemented sea water. *Environ. Microbiol.* 4, 141–147. doi: 10.1046/j.1462-2920.2002.00275.x
- Kasai, Y., Kishira, H., Syutsubo, K., and Harayama, S. (2001). Molecular detection of marine bacterial populations on beaches contaminated by the Nakhodka tanker oil-spill accident. *Environ. Microbiol.* 3, 246–255. doi: 10.1046/j.1462-2920.2001.00185.x
- Kostka, J. E., Prakash, O., Overholt, W. A., Green, S. J., Freyer, G., Canion, A., et al. (2011). Hydrocarbon-degrading bacteria and the bacterial community response in gulf of mexico beach sands impacted by the deepwater horizon oil spill. *Appl. Environ. Microbiol.* 77, 7962–7974. doi: 10.1128/AEM.05402-11
- Krumbein, W. C., and Aberdeen, E. (1937). The sediments of Barataria Bay. *J. Sed. Petrol.* 7, 3–17. doi: 10.1306/D4268F8B-2B26-11D7-8648000102C1865D
- Leahy, J. G., and Colwell, R. R. (1990). Microbial degradation of hydrocarbons in the environment. *Microbiol. Rev.* 54, 305–315.
- Lin, Q., and Mendelsohn, I. A. (2012). Impacts and recovery of the Deepwater Horizon oil spill on vegetation structure and function of coastal salt marshes in the northern Gulf of Mexico. *Environ. Sci. Technol.* 46, 3737–3743. doi: 10.1021/es203552p
- MacNaughton, S. J., Stephen, J. R., Venosa, A. D., Davis, G. A., Chang, Y. J., and White, D. C. (1999). Microbial population changes during bioremediation of an experimental oil spill. *Appl. Environ. Microbiol.* 65, 3566–3574.
- Maruyama, A., Ishiwata, H., Kitamura, K., Sunamura, M., Fujita, T., Matsuo, M., et al. (2003). Dynamics of microbial populations and strong selection

- for *Cycloclasticus pugetii* following the Nakhodka oil spill. *Microb. Ecol.* 46, 442–453. doi: 10.1007/s00248-002-3010-z
- McKew, B. A., Coulon, F., Osborn, A. M., Timmis, K. N., and McGenity, T. J. (2007a). Determining the identity and roles of oil-metabolizing marine bacteria from the Thames estuary, UK. *Environ. Microbiol.* 9, 165–176. doi: 10.1111/j.1462-2920.2006.01125.x
- McKew, B. A., Coulon, F., Yakimov, M. M., Denaro, R., Genovese, M., Smith, C. J., et al. (2007b). Efficacy of intervention strategies for bioremediation of crude oil in marine ecosystems and effects on indigenous hydrocarbonoclastic bacteria. *Environ. Microbiol.* 9, 1562–1571. doi: 10.1111/j.1462-2920.2007.01277.x
- Muyzer, G., de Waal, E. C., and Uitterlinden, A. G. (1993). Profiling of complex microbial populations by denaturing gradient gel electrophoresis analysis of polymerase chain reaction-amplified genes coding for 16S rRNA. *Appl. Environ. Microbiol.* 59, 695–700.
- National Research Council. (2003). *Oil in the Sea III: Inputs, Fates and Effects*. Washington, DC: National Academic Press.
- Natter, M., Keevan, J., Wang, Y., Keimowitz, A. R., Okeke, B. C., Son, A., et al. (2012). Level and degradation of deepwater horizon spilled oil in coastal marsh sediments and pore-water. *Environ. Sci. Technol.* 46, 5744–5755 doi: 10.1021/es300058w
- Newton, R. J., Huse, S. M., Morrison, H. G., Peake, C. S., Sogin, M. L., and McLellan, S. L. (2013). Shifts in the microbial community composition of gulf coast beaches following beach oiling. *PLoS ONE* 8:e74265. doi:10.1371/journal.pone.0074265
- OSAT-1. (2010). *Summary Report for Sub-Sea and Sub-Surface Oil and Dispersant Detection: Sampling and Monitoring*. Washington, DC: Operational Science Advisory Team (multiagency).
- Prince, R. C. (2005). “The microbiology of marine oil spill bioremediation,” in *Petroleum Microbiology*, eds B. Oliver and M. Magot (Washington, DC: ASM Press), 317–336.
- Reay, D. S., Nedwell, D. B., Priddle, J. and and Ellis-Evans, J. C. (1999). Temperature dependence of inorganic nitrogen uptake: reduced affinity for nitrate at sub-optimal temperatures in both algae and bacteria. *Appl. Environ. Microbiol.* 65, 2577–2584.
- Röling, W. F. M., Milner, M. G., Jones, D. M., Fratipietro, F., Swannell, R. P. J., Daniel, F., et al. (2004). Bacterial community dynamics and hydrocarbon degradation during a field-scale evaluation of bioremediation on a mudflat beach contaminated with buried oil. *Appl. Environ. Microbiol.* 70, 2603–2613. doi: 10.1128/AEM.70.5.2603-2613.2004
- Röling, W. F. M., Milner, M. G., Jones, D. M., Lee, K., Daniel, F., Swannell, R. J. P., et al. (2002). Robust hydrocarbon degradation and dynamics of bacterial communities during nutrient-enriched oil spill bioremediation. *Appl. Environ. Microbiol.* 68, 5537–5548. doi: 10.1128/AEM.68.11.5537-5548.2002
- Sabirova, J. S., Becker, A., Lünsdorf, H., Nicaud, J. M., Timmis, K. N., and Golyshin, P. N. (2011). Transcriptional profiling of the marine oil-degrading bacterium *Alcanivorax borkumensis* during growth on n-alkanes. *FEMS Microbiol. Lett.* 319, 160–168. doi: 10.1111/j.1574-6968.2011.02279.x
- Sabirova, J. S., Ferrer, M., Regenhardt, D., Timmis, K. N., and Golyshin, P. N. (2006). Proteomic insights into metabolic adaptations in *Alcanivorax borkumensis* induced by alkane utilization. *J. Bacteriol.* 188, 3763–3773. doi: 10.1128/JB.00072-06
- Schneiker, S., Martins dos Santos, V. A. P., Bartels, D., Bekel, T., Brecht, M., Buhrmester, J., et al. (2006). Genome sequence of the ubiquitous hydrocarbon-degrading marine bacterium *Alcanivorax borkumensis*. *Nat. Biotechnol.* 24, 997–1004. doi: 10.1038/nbt1232
- Schowanek, D., and Verstraete, W. (1990). Phosphonate utilization by bacteria in the presence of alternative phosphorus sources. *Biodegradation* 1, 43–53. doi: 10.1007/BF00117050
- Short, J. W., Irvine, G. V., Mann, D. H., Maselko, J. M., Pella, J. J., Lindeberg, M. R., et al. (2007). Slightly weathered Exxon Valdez Oil persists in Gulf of Alaska beach sediments after 16 years. *Environ. Sci. Technol.* 41, 1245–1250. doi: 10.1021/es0620033
- Singh, A. K., Sherry, A., Gray, N. D., Jones, D. M., Röling, W. F. M., and Head, I. M. (2011). “Dynamics of *Alcanivorax* spp. in oil-contaminated intertidal beach sediment undergoing bioremediation,” in *Applied Microbiology and Molecular Biology in Oilfield Systems*, eds C. Whitby and T. L. Skovhus (Dordrecht: Springer), 199–209.
- Smith, V. H., Graham, D. W., and Cleland, D. D. (1998). Application of resource-ratio theory to hydrocarbon bioremediation. *Environ. Sci. Technol.* 32, 3386–3395. doi: 10.1021/es9805019
- Swannell, R. P. J., Lee, K., and McDonagh, M. (1996). Field evaluations of marine oil spill bioremediation. *Microbiol. Rev.* 60, 342–365.
- Vadstein, O., and Olsen, Y. (1989). Chemical compositon and phosphate uptake kinetics of limnetic bacterial communities cultured in chemostats under phosphorus limitation. *Limnol. Oceanogr.* 34, 939–946. doi: 10.4319/lo.1989.34.5.0939
- Venosa, A. D., Campo, P., and Suidan, M. T. (2010). Biodegradability of lingering crude oil 19 years after the *Exxon Valdez* oil spill. *Environ. Sci. Technol.* 44, 7613–7621 doi: 10.1021/es101042h
- Venosa, A. D., Suidan, M. T., Wrenn, B. A., Strohmeier, K. L., Haines, J. R., Eberhart, B. L., et al. (1996). Bioremediation of an experimental oil spill on the shoreline of Delaware Bay. *Environ. Sci. Technol.* 30, 1764–1775. doi: 10.1021/es950754r
- Verschueren, K. (1983). *Handbook of Environmental Data of Organic Chemicals*, 2nd Edn. New York, NY: Van Nostrand Reinhold Co.
- Walker, J. D., Colwell, R. R., and Petrakis, L. (1976). Biodegradation rates of components of petroleum. *Can. J. Microbiol.* 22, 1209–1213. doi: 10.1139/m76-179
- White, H. K., Hsing, P. Y., Cho, W., Shank, T. M., Cordes, E. E., Quatrini, A. M., et al. (2012). Impact of the Deepwater Horizon oil spill on a deep-water coral community in the Gulf of Mexico. *Proc. Natl. Acad. Sci. U.S.A.* 109, 20303–20308. doi: 10.1073/pnas.1118029109
- Yakimov, M. M., Denaro, R., Genovese, M., Cappello, S., D'Auria, G., Chernikova, T. N., et al. (2005). Natural microbial diversity in superficial sediments of Milazzo Harbor (Sicily). and community successions during microcosm enrichment with various hydrocarbons. *Environ. Microbiol.* 7, 1426–1441. doi: 10.1111/j.1462-5822.2005.00829.x
- Yakimov, M. M., Giuliano, L., Denaro, R., Grisafi, E., Chernikova, T. N., Abraham, W. R., et al. (2004). *Thalassolitus oleivorans* gen. nov., sp nov., a novel marine bacterium that obligately utilizes hydrocarbons. *Int. J. Syst. Evol. Microbiol.* 54, 141–148. doi: 10.1099/ijss.0.02424-0
- Yakimov, M. M., Giuliano, L., Gentile, G., Crisafi, E., Chemikova, T. N., Abraham, W. R., et al. (2003). *Oleispira Antarctica* gen. nov., sp. nov., a novel hydrocarbonoclastic marine bacterium isolated from Antarctic coastal sea water. *Int. J. Syst. Evol. Microbiol.* 53, 779–785. doi: 10.1099/ijss.0.02366-0
- Yakimov, M. M., Golyshin, P. N., Lang, S., Moore, E. R., Abraham, W. R., Lunsdorf, H., et al. (1998). *Alcanivorax borkumensis* gen. nov., sp. nov., a new hydrocarbon-degrading and surfactant producing marine bacterium. *Int. J. Syst. Bacteriol.* 48, 339–348. doi: 10.1099/00207713-48-2-339
- Yakimov, M. M., Timmis, K. N., and Golyshin, P. N. (2007). Obligate oil-degrading marine bacteria. *Curr. Opin. Biotechnol.* 18, 257–266. doi: 10.1016/j.copbio.2007.04.006

**Conflict of Interest Statement:** The authors declare that the research was conducted in the absence of any commercial or financial relationships that could be construed as a potential conflict of interest.

Received: 07 November 2013; accepted: 25 March 2014; published online: 11 April 2014.

Citation: Singh AK, Sherry A, Gray ND, Jones DM, Bowler BFJ and Head IM (2014) Kinetic parameters for nutrient enhanced crude oil biodegradation in intertidal marine sediments. *Front. Microbiol.* 5:160. doi: 10.3389/fmicb.2014.00160

This article was submitted to Aquatic Microbiology, a section of the journal *Frontiers in Microbiology*.

Copyright © 2014 Singh, Sherry, Gray, Jones, Bowler and Head. This is an open-access article distributed under the terms of the Creative Commons Attribution License (CC BY). The use, distribution or reproduction in other forums is permitted, provided the original author(s) or licensor are credited and that the original publication in this journal is cited, in accordance with accepted academic practice. No use, distribution or reproduction is permitted which does not comply with these terms.



# Volatile hydrocarbons inhibit methanogenic crude oil degradation

Angela Sherry, Russell J. Grant<sup>†</sup>, Carolyn M. Aitken, D. Martin Jones, Ian M. Head \* and Neil D. Gray

School of Civil Engineering and Geosciences, Newcastle University, Newcastle upon Tyne, UK

**Edited by:**

Joel E. Kostka, Georgia Institute of Technology, USA

**Reviewed by:**

Martin Krüger, Federal Institute for Geosciences and Natural Resources (BGR), Germany

Hans H. Richnow, Helmholtz Centre for Environmental Research - UFZ, Germany

**\*Correspondence:**

Ian M. Head, School of Civil Engineering and Geosciences, Newcastle University, Room 3.16, Devonshire Building, Devonshire Terrace, Newcastle-upon-Tyne, NE1 7RU, UK  
e-mail: ian.head@ncl.ac.uk

**†Present address:**

Russell J. Grant, Heslington Hall, University of York, York, UK

Methanogenic degradation of crude oil in subsurface sediments occurs slowly, but without the need for exogenous electron acceptors, is sustained for long periods and has enormous economic and environmental consequences. Here we show that volatile hydrocarbons are inhibitory to methanogenic oil biodegradation by comparing degradation of an artificially weathered crude oil with volatile hydrocarbons removed, with the same oil that was not weathered. Volatile hydrocarbons ( $nC_5-nC_{10}$ , methylcyclohexane, benzene, toluene, and xylenes) were quantified in the headspace of microcosms. Aliphatic ( $n$ -alkanes  $nC_{12}-nC_{34}$ ) and aromatic hydrocarbons (4-methylbiphenyl, 3-methylbiphenyl, 2-methylnaphthalene, 1-methylnaphthalene) were quantified in the total hydrocarbon fraction extracted from the microcosms. 16S rRNA genes from key microorganisms known to play an important role in methanogenic alkane degradation (*Smithella* and *Methanomicrobiales*) were quantified by quantitative PCR. Methane production from degradation of weathered oil in microcosms was rapid ( $1.1 \pm 0.1 \mu\text{mol CH}_4/\text{g sediment/day}$ ) with stoichiometric yields consistent with degradation of heavier  $n$ -alkanes ( $nC_{12}-nC_{34}$ ). For non-weathered oil, degradation rates in microcosms were significantly lower ( $0.4 \pm 0.3 \mu\text{mol CH}_4/\text{g sediment/day}$ ). This indicated that volatile hydrocarbons present in the non-weathered oil inhibit, but do not completely halt, methanogenic alkane biodegradation. These findings are significant with respect to rates of biodegradation of crude oils with abundant volatile hydrocarbons in anoxic, sulphate-depleted subsurface environments, such as contaminated marine sediments which have been entrained below the sulfate-reduction zone, as well as crude oil biodegradation in petroleum reservoirs and contaminated aquifers.

**Keywords:** methanogenic, oil biodegradation, volatile hydrocarbons, non-weathered oil, weathered oil,  $n$ -alkanes

## INTRODUCTION

Hydrocarbons are common in many subsurface environments (Gray et al., 2010) where their degradation to methane by methanogenic microbial consortia is known to occur (Zengler et al., 1999; Anderson and Lovley, 2000; Townsend et al., 2003; Siddique et al., 2006; Gieg et al., 2008, 2010; Jones et al., 2008; Wang et al., 2011). Rates of hydrocarbon degradation are generally lower under anoxic conditions than under oxic conditions (Grishchenkova et al., 2000), and methanogenic hydrocarbon degradation demonstrably supports the lowest rates (Townsend et al., 2003; Jones et al., 2008). For example, during hydrocarbon degradation linked to sulfate reduction lag times are shorter and degradation rates faster in comparison to analogous methanogenic systems (Townsend et al., 2003; Jones et al., 2008; Sherry et al., 2013). This difference is related to the free energy yield of different terminal anaerobic processes. Hexadecane oxidation coupled to sulfate reduction yields  $-556.9 \text{ kJ/mol}$  hexadecane, whereas, methanogenic degradation yields  $-371.8 \text{ kJ/mol}$ . Nevertheless, anaerobic respiratory processes require exogenous electron sinks whereas methanogenesis continues in their absence (Townsend et al., 2003; Gray et al., 2010). Even in hydrocarbon contaminated marine and estuarine sediments initial concentrations of sulfate are likely to be rapidly depleted (Teske,

2010). Accordingly, understanding the controls on methanogenic hydrocarbon degradation is important for assessing the fate of hydrocarbons in anoxic environments. Methanogenic oil degradation is, for instance, most likely responsible for the formation of a large proportion of the world's vast deposits of heavy oil (Head et al., 2003; Townsend et al., 2003; Jones et al., 2008; Gray et al., 2010) and, is an important factor in the natural attenuation of hydrocarbon plumes in contaminated aquifers (Amos et al., 2005; Baedecker et al., 2011). Further, stimulation of methanogenic oil degradation in petroleum reservoirs reaching the end of their normal production lifetime has been proposed as a means to re-pressurize spent reservoirs and recover otherwise stranded residual oil. This process may also offer the opportunity to recover energy from such oils as methane in future unconventional energy recovery strategies (Grishchenkova et al., 2000; Larter et al., 2005; Gieg et al., 2008, 2010; Jones et al., 2008; Mbadinga et al., 2011).

The composition of the crude oil itself may play a critical role in dictating the extent of degradation of oil. For example, in aerobic seawater microcosms the period before the onset of biodegradation for a fresh crude oil was longer than that observed for the same oil that had been pre-weathered (Atlas and Bartha, 1972). Furthermore, when low molecular weight

components were prevented from volatilizing, no biodegradation was observed, suggesting an inhibitory effect of low molecular weight compounds on aerobic oil-degrading microbial consortia (Atlas and Bartha, 1972). Critically, the influence of oil composition on anaerobic oil degradation processes in oil-impacted subsurface systems is currently unknown.

In the present study, anaerobic oil degrading microcosms were either amended with a North Sea crude oil that was artificially weathered to remove volatile aliphatic and aromatic hydrocarbons or amended with the non-weathered oil containing the volatile hydrocarbons. This was done to investigate the inhibitory effects of low molecular weight volatile components of crude oil on the rate and extent of methanogenic oil biodegradation.

## METHODS

### PREPARATION OF METHANOGENIC OIL-DEGRADING MICROCOSMS

Methanogenic microcosms were prepared in glass Wheaton serum bottles (120 ml, VWR Ltd.) and comprised sediment slurry (7 g sediment made up to 100 ml) leaving a headspace of 20 ml. For each microcosm, sediments slurries were prepared with sulfate free carbonate-buffered brackish (7 g/l NaCl) medium (Widdel and Bak, 1992) under anoxic conditions using River Tyne sediment (7 g) as previously described (Jones et al., 2008; Sherry et al., 2009). Subsequently, microcosms were each amended with 250 mg of oil, crimp-sealed and shaken by hand to disperse the oil. Addition of oil was either North Sea crude oil (non-weathered) or North Sea crude oil that was artificially weathered. Weathering was done by incubating non-weathered oil in a glass Petri dish in the air stream of a fume hood at room temperature (0.4 m/s; ~21°C) for 72 h to remove volatile hydrocarbons. Microcosms without oil were prepared to determine the extent of methanogenesis in the absence of crude oil. Control microcosms containing weathered and non-weathered oil were also prepared. The control treatments comprised: 1. addition of bromoethane-sulphonic acid (BES, 10 mM final concentration), an inhibitor of methanogenesis and; 2. microcosms which were subjected to three cycles of autoclaving at 121°C, 20 min followed by incubation at 37°C, for ~17 h. This triple autoclaving approach was adopted to promote germination of bacterial spores present in the sediment. Vegetative cells arising from this treatment were then killed by subsequent autoclaving. All the experimental treatments were prepared in biological triplicate and were incubated statically at room temperature (ca. 21°C), in the dark for a total of 1058 days.

### METHANE PRODUCTION IN MICROCOSMS

Methane in the headspace of microcosms was sampled (0.1 ml) using a nitrogen-flushed, gas-tight, push lock syringe (SGE, Australia). Methane concentrations in samples and standards were determined by gas chromatography with flame ionization detection (GC-FID) using a Carlo Erba 5160 GC fitted with a Chrompak Pora plot Q coated fused silica capillary column (30 m × 0.32 mm) with hydrogen as a carrier gas. The oven (35°C) and injection port (250°C) temperatures were fixed. Methane concentrations were determined periodically with reference to external standard calibrations with a standard gas

(Scientific & Technical Gases Ltd, Newcastle—under—Lyme, UK). After 345 days, prior to headspace gas analysis, a measured volume of gas were removed from the microcosms using a sterile needle and syringe, to release excess pressure produced by gas production during crude oil biodegradation. The volume of gas removed and the concentration of methane was accounted for when calculating the total mass of methane produced in the microcosms.

### QUANTIFICATION OF VOLATILE HYDROCARBONS IN MICROCOSM HEADSPACE

After incubation for 1058 days all microcosms were sacrificed for microbiological and oil chemistry analysis. Prior to sacrificial sampling, volatile hydrocarbons were quantified in headspaces with reference to freshly prepared microcosms comprising North Sea crude oil (250 mg non-weathered oil), distilled water, River Tyne sediment and added deuterated standards ( $n$ C<sub>5</sub>D<sub>12</sub>– $n$ C<sub>10</sub>D<sub>22</sub> alkanes, methylcyclohexane-D-14, benzene-D-6, toluene-D<sub>8</sub>, and *o*-xylene-D-10; Cambridge Isotope Laboratories Inc). All microcosms were equilibrated at 20°C in a heated water bath before headspace sampling. Gas chromatography-mass spectrometry (GC-MS) analysis of the headspace gases/vapors was performed on an Agilent 7890A GC split/split less injector (280°C) linked to an Agilent 5975C MSD. Data acquisition was controlled using Chemstation software, in full scan or in selected ion mode for greater sensitivity. The headspace gas sample (100 µl) was injected manually using an SGE gas tight valve syringe. Separation was performed on an Agilent fused silica capillary column (60 m × 0.25 mm i.d.) HP1-MS phase. The GC temperature programme was 30°C for 5 min, ramped to 80°C at 5°C/min and then to 320°C at 25°C/min. The final temperature was held for 5 min. The carrier gas was helium (flow rate of 1 ml/min, initial pressure of 50 kPa, open split at 50 ml/min). Peaks were identified after comparison of their mass spectra with those from the NIST05 library and from their relative retention times.

### EXTRACTION AND ANALYSIS OF OIL

Aliquots of sediment slurry (90 ml) were used for oil analysis. Quantification standards (squalane and 1,1'-binaphthyl) were added to the sediment slurry which was saponified (refluxed for 1 h with 1 M KOH in methanol) to allow recovery and analysis of the acid metabolite fraction if required for further analysis. The saponified slurry was acidified to pH ~1 using concentrated HCl. The sediment was then removed by Buchner filtration and liquid-liquid solvent extraction with dichloromethane (DCM) was used to obtain the organic solvent soluble fractions. The hydrocarbon fractions from the sediment slurries and from samples of non-weathered and weathered oils were analyzed by GC. Analytical reproducibility for replicate analyses ( $n = 3$ ) of the C<sub>12</sub>–C<sub>34</sub> *n*-alkanes in the oil was <1% relative standard error. To quantify *n*-alkanes, aliquots of the organic extracts were separated using a solid phase extraction (SPE) method to provide a total hydrocarbon fraction (Bennett et al., 1996). Alkanes ( $n$ C<sub>12</sub>– $n$ C<sub>34</sub>) and aromatics were quantified from GC analysis of the total hydrocarbon fractions by measuring peak areas relative to the peak area of the added standards.

## THEORETICAL METHANE YIELD FROM ALKANE DEGRADATION

Theoretical methane yields from the alkanes degraded in the microcosms were derived from the quantity of individual resolved alkanes which were degraded. This was determined by GC analysis of headspace volatile hydrocarbons and solvent extracts from microcosms incubated for 1058 days compared to the oil added at the start of the experiment. The theoretical methane yield was calculated using stoichiometric equations for the methanogenic degradation of each of the alkanes individually. These values were summed to give the total theoretical methane yield from the degraded alkanes (for detailed calculation see Supplementary Methods S1).

## QUANTIFICATION OF *SMITHELLA* AND *METHANOMICROIALES* 16S

### RNA GENES IN METHANOGENIC OIL-DEGRADING MICROCOSMS

DNA extraction from sediment slurry samples (1 ml) was done using a FastDNA Spin Kit for Soil (Q-BIOgene, California, USA) according to the manufacturer's instructions. qPCR assays were performed as previously described using specific primer sets to quantify 16S rRNA gene abundance of total bacteria, *Smithella* spp., hydrogenotrophic methanogens from the order *Methanomicroiales*, facultative acetoclastic methanogens from family *Methanosarcinaceae*, and obligate acetoclastic methanogens from family *Methanosaetaceae* (Gray et al., 2011; Callbeck et al., 2013). All qPCR assays were performed using a CFX96 real-time PCR detection system (Bio-Rad Laboratories Ltd, Hertfordshire, UK). Typically, DNA template (3 µl) and appropriate primers (1 µl at a concentration of 10 pmol µl<sup>-1</sup>) were combined with SsoFast EvaGreen Supermix (Bio-Rad). Reaction conditions included an initial denaturation step at 98°C for 3 min, and 40 subsequent reaction cycles which included denaturation (98°C for 5 s), annealing and elongation (58.5°C for 5 s). Standards containing known amounts of target 16S rRNA genes were prepared by serial 10-fold dilution of PCR amplified 16S rRNA genes which were prepared from cloned genes of known sequence, using vector-specific primers (Gray et al., 2011). DNA template-free negative controls were always conducted. PCR efficiencies for all assays were between 70 and 110% and *R*<sup>2</sup> values for calibration curves were >0.99. Log gene-abundance values for samples all fell within the linear range of the standard calibration.

## STATISTICAL ANALYSIS

Biological and chemical data from experimental microcosms were analyzed by One Way analysis of variance (ANOVA) followed by pairwise comparisons of treatments (Tukey HSD), IBM SPSS statistics 19.

## RESULTS

### METHANE PRODUCTION IN METHANOGENIC OIL DEGRADING MICROCOSMS

Methane production was monitored periodically in microcosms amended with weathered oil and non-weathered oil in comparison with unamended controls, as a proxy for methanogenic biodegradation of the crude oil (Figure 1). For the first 90 days, cumulative methane production was not significantly different in the oil-amended and unamended microcosms (*p* > 0.21). By day 345, all oil amended microcosms had higher methane levels than no oil control microcosms (Figure 1). However, from

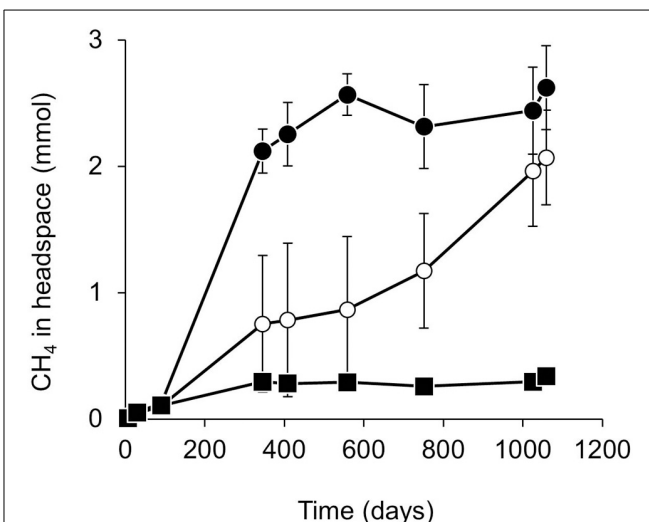


**FIGURE 1 |** Methane production from anaerobic microcosms amended with weathered oil (●), non-weathered oil (○) or prepared without oil (■). Error bars indicate  $\pm 1 \times$  standard error ( $n = 3$  oil amended;  $n = 6$  without oil).

345 to 751 days, the cumulative methane produced in weathered oil-amended microcosms was significantly higher than in microcosms amended with non-weathered oil (*p* < 0.02). By 1058 days the total amount of methane generated in microcosms with weathered and non-weathered oil was similar (*p* = 0.29). In weathered oil microcosms most methane production had occurred by day 345 after which there was little further accumulation of methane which reached a maximum of  $2.7 \pm 0.3$  mmol (Figure 1; *p* > 0.81). Between 90 and 345 days, the rate of methane production was  $1.1 \pm 0.1$  µmol CH<sub>4</sub>/g wet sediment/day. By contrast methane accumulation in the non-weathered oil microcosms occurred at a much lower rate, reaching a maximum of  $2.1 \pm 0.4$  mmol CH<sub>4</sub> after 1058 days of incubation (Figure 1). In this case the rate of methane production between 90 and 345 days was  $0.4 \pm 0.3$  µmol CH<sub>4</sub>/g wet sediment/day. The total amount of methane produced in the no-oil control microcosms reached a maximum of  $0.29 \pm 0.01$  mmol by 345 days equating to a rate of  $0.12 \pm 0.01$  µmol CH<sub>4</sub>/g wet sediment/day. In BES-inhibited microcosms the maximum amount of methane produced was  $0.06 \pm 0.003$  mmol CH<sub>4</sub> in microcosms treated with non-weathered oil and prior to 751 days was  $0.05 \pm 0.01$  mmol CH<sub>4</sub> in microcosms treated with weathered oil. After 751 days CH<sub>4</sub> began to accumulate in two of the BES inhibited weathered oil replicates reaching an average of  $0.78 \pm 0.09$  mmol CH<sub>4</sub> (Supplementary Figure S2). In heat-killed microcosms methane production was consistently very low ( $0.01 \pm 0.001$  mmol CH<sub>4</sub> with non-weathered oil and  $0.01 \pm 0.0002$  mmol CH<sub>4</sub> with weathered oil).

### VOLATILE HYDROCARBONS IN METHANOGENIC OIL DEGRADING MICROCOSMS

The weathering process significantly (*p* < 0.001) depleted the volatile saturated hydrocarbons compared to the non-weathered oil (*n*<sub>C5–C10</sub>, Supplementary Figures S1A,B). By 1058 days, volatile saturated hydrocarbons were present at much higher

levels in heat-killed and BES-treated microcosms containing non-weathered oil, compared to methanogenic oil-degrading microcosms that were not heat killed or inhibited (**Figure 2A**, gray and white bars). In the methanogenic oil degrading microcosms containing non-weathered oil, incubated for 1058 days, the volatile saturated hydrocarbons, with the exception of methylcyclohexane, were present at low concentrations ( $<1.9$  mg/g oil) (**Figure 2A**, black bars;  $p < 0.001$ ). This indicated that the  $nC_5$ – $nC_{10}$  alkanes had been microbially degraded during the incubation period. In microcosms treated with weathered oil and incubated for 1058 days, headspace volatile *n*-alkanes were largely absent in the BES-inhibited and heat-killed microcosms (**Figure 2B**) consistent with the composition of this oil at the start of the experiment (Supplementary Figure S1). Nevertheless all the volatile *n*-alkanes were completely absent in the uninhibited microcosms by 1058 days suggesting that the residual light alkanes i.e.,  $nC_9$  and  $nC_{10}$ , not removed by the weathering treatment were most likely degraded to methane (**Figure 2B**).

By contrast with the *n*-alkanes, the volatile aromatic hydrocarbons (benzene, toluene and xylenes) were present at similar levels in the uninhibited microcosms and in inhibited and heat-killed control microcosms (benzene and toluene  $p \leq 1.00$ ; xylenes  $p \leq 0.99$ ; **Figure 2C**) indicating that none of these aromatic hydrocarbons were degraded under methanogenic conditions. Volatile aromatic hydrocarbons were not present at the end of the incubation period (1058 days) in microcosms treated with

weathered oil (**Figure 2D**) consistent with their absence from the weathered oil (Supplementary Figure S1).

#### BIODEGRADATION OF MODERATELY VOLATILE ALKANES ( $nC_8$ – $nC_{11}$ ) TO METHANE

The moderately-volatile alkanes ( $nC_8$ – $nC_{11}$ ; vapor pressure 1.5–0.05 kPa at 20°C) present in the non-weathered oil and weathered oil treated microcosms were quantified at the beginning and end of the incubation period (0 days and 1058 days; **Figure 3**). At the end of the incubation period, most *n*-alkanes in the non-weathered oil microcosms were severely depleted, with  $nC_8$ – $nC_{11}$  alkanes completely absent (**Figure 3B**). Given their initial high abundance relative to many of the higher molecular weight alkanes this suggests preferential removal of the lighter *n*-alkanes. *n*-alkanes were completely removed in the weathered oil treated microcosms (**Figure 3D**) leaving only the branched chain alkanes pristane and phytane, which are more resistant to biodegradation. The ratio of  $nC_{17}$ :pristane in oil treated microcosms relative to autoclaved controls after 1058 days incubation and oils added at the start of the experiment (Day 0), also indicated that biodegradation of *n*-alkanes had occurred in oil-treated microcosms ( $nC_{17}$ :pristane–Non-weathered oil Day 0,  $1.95 \pm 0.15$ ; heat-killed 1058 days,  $1.98 \pm 0.05$ ; live microcosms 1058 days,  $0.32 \pm 0.32$ ; Weathered oil heat-killed 1058 days,  $1.75 \pm 0.06$ ; live microcosms 1058 days,  $<0.01 \pm 0.00$ ). The  $nC_{17}$ :pristane ratio in the heat-killed control amended with weathered oil was slightly reduced during the incubation period

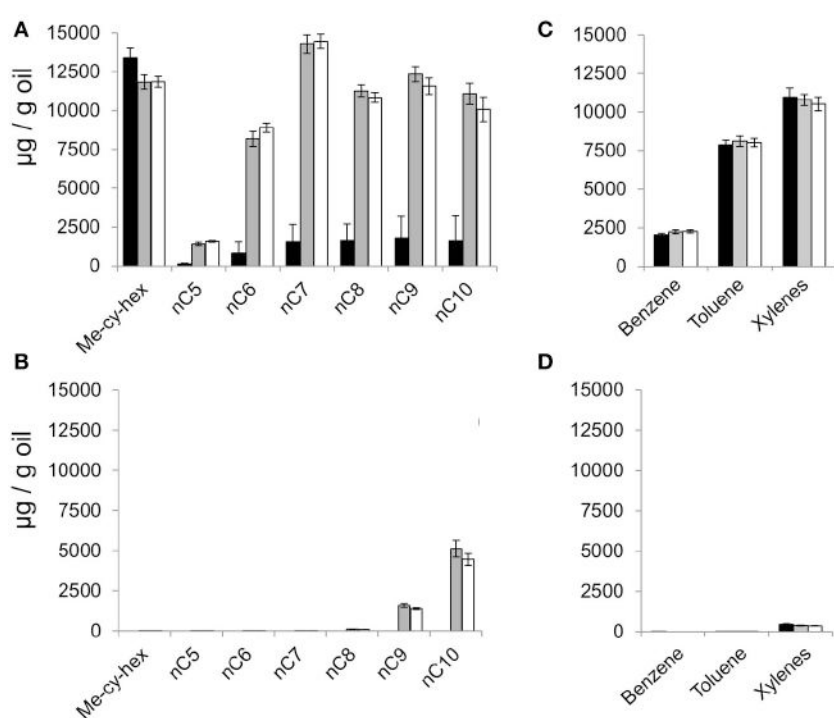


**FIGURE 2 | Headspace volatile hydrocarbons in methanogenic oil-degrading microcosms after 1058 days of incubation.** Headspace saturated hydrocarbons in (A) non-weathered oil and (B) weathered oil treated microcosms. Headspace aromatic hydrocarbons in (C) non-weathered oil and (D) weathered oil treated microcosms. Data from

oil-amended microcosms are represented by black bars, data from oil-amended and BES-inhibited microcosms are shown as gray bars and data from autoclaved, oil-amended microcosms are shown as white bars. Error bars indicate  $\pm 1$  standard error ( $n = 3$ ). Me-cy-hex = methylcyclohexane.

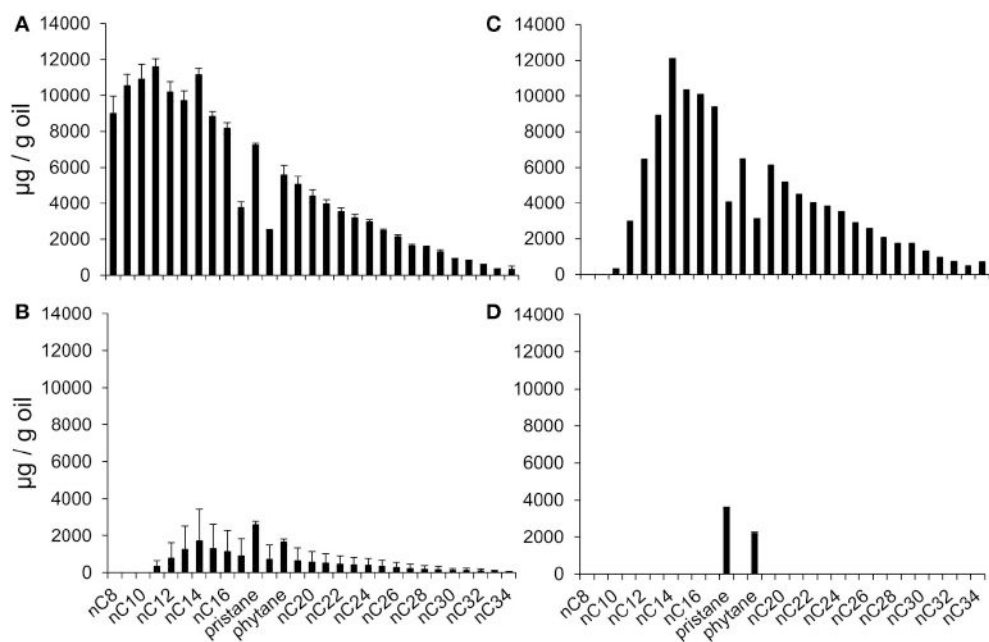


**FIGURE 3 | Saturated hydrocarbons in methanogenic oil-degrading microcosms. (A)** Alkanes in extracts from non-weathered oil treated microcosms at 0 days. **(B)** Alkanes in extracts from non-weathered oil treated

microcosms after 1058 days of incubation. **(C)** Alkanes in extracts from weathered oil treated microcosms at 0 days. **(D)** Alkanes in extracts from weathered oil treated microcosms after 1058 days of incubation.

( $1.75 \pm 0.06$  compared to  $1.95 \pm 0.15$ ,  $p = 0.03$ ) suggesting that the heat-treatment may not have been completely effective in inactivating all of the *n*-alkane degrading bacteria present in the sediment.

#### STOICHIOMETRY OF METHANE PRODUCTION FROM ALKANE DEGRADATION

The theoretical methane yields derived from the observed degradation of the *n*-alkanes in the weathered oil was 1.6 mmoles. This is somewhat less than the average measured methane ( $2.4 \pm 0.3$  mmoles) which was attributable to oil degradation i.e., after subtraction of the methane yield of the no oil controls. However, the *n*-alkanes resolved and quantified by GC and included in this yield estimate, do not constitute the entire complement of degradable alkanes present in the oil (Larter et al., 2012). The theoretical methane yield from *n*-alkanes degraded in the non-weathered oil was 2.2 mmoles which did match with measured maximum methane concentrations in these microcosms ( $2.1 \pm 0.4$  mmol). By contrast, aromatic hydrocarbons such as methyl-naphthalenes and methylbiphenyls were not significantly biodegraded in the experimental microcosms relative to the controls. Typically 4-methylbiphenyl (4-MB) is degraded preferentially to 3-methylbiphenyl (3-MB) and 2-methylnaphthalene (2-MN) is degraded preferentially to 1-methylnaphthalene (1-MN), but the 4-MB/3-MB and 2-MN/1-MN ratios changed little over the period of incubation (Supplementary Table S1).

#### QPCR ANALYSIS OF 16S RRNA GENES (SMITHELLA AND METHANOMICROBIALES)

*Smithella* spp. and methanogens from the order *Methanomicrobiales* are known to be important in methanogenic crude

oil biodegradation in systems similar to those studied here (Jones et al., 2008; Gray et al., 2011). The abundance of 16S rRNA genes from these groups of organisms was therefore quantified in the methanogenic oil degrading microcosms following 1058 days of incubation (Figure 4). Bacteria from the genus *Smithella*, implicated in syntrophic alkane degradation were significantly enriched in both the weathered oil and non-weathered oil amended microcosms relative to no oil controls ( $p < 0.005$ ). 16S rRNA genes from *Smithella* spp. were enriched by  $1.4 \pm 0.3$  and  $2.0 \pm 0.3$  log units in weathered and non-weathered oil containing microcosms respectively, compared with control microcosms with no added oil. Nevertheless, there was not a significant difference between the abundance of 16S rRNA genes in microcosms amended with weathered and non-weathered oil ( $p = 0.197$ ). This is consistent with the observation that similar amounts of methane were produced in both the non-weathered and weathered oil microcosms ( $p = 0.29$ ). In addition, 16S rRNA genes from hydrogenotrophic methanogens of the order *Methanomicrobiales* were significantly enriched in the non-weathered oil and weathered oil amended systems relative to unamended controls ( $1.2 \pm 0.2$  and  $0.9 \pm 0.2$  log units respectively;  $p < 0.006$ ). Again there was not a significant difference between the weathered and non-weathered oil microcosms ( $p = 0.373$ ), consistent with the similar amount of methane produced in both the non-weathered and weathered oil microcosms ( $p = 0.29$ ). Total bacteria, facultative acetoclastic methanogens (Family *Methanosarcinaceae*) and obligate acetoclastic methanogens (Family *Methanosaetaceae*) were also quantified by qPCR. No significant differences were observed between pairwise comparisons of 16S rRNA gene abundances from DNA extracts from microcosms prepared with

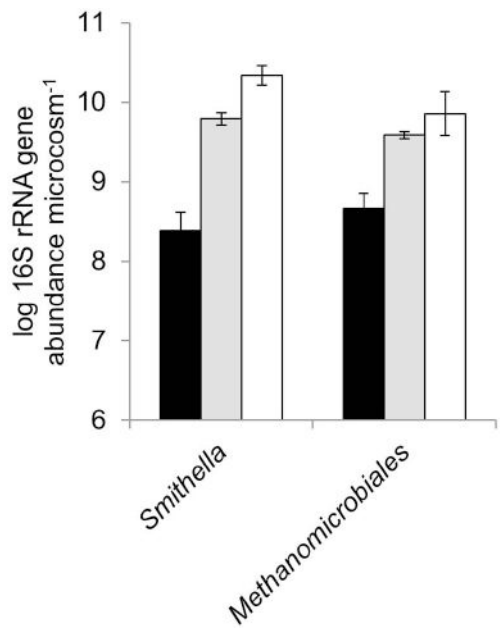


**FIGURE 4 | Log abundance of 16S rRNA genes from *Smithella* spp. and methanogens from the order *Methanomicrobiales* in microcosms amended with weathered oil (gray bars), non-weathered oil (white bars) or prepared without oil (black bars).** All data are from microcosms incubated for 1058 days. The abundance of 16S rRNA genes from *Smithella* spp. and methanogens from the order *Methanomicrobiales* at the start of the incubation was  $7.00 \pm 0.1$  and  $6.91 \pm 0.24$  log 16S rRNA genes/microcosm respectively. Error bars indicate  $\pm 1 \times$  standard error ( $n = 3$ ).

weathered oil, non-weathered oil or prepared without oil for total bacteria ( $p \geq 0.548$ ), family *Methanosaetaceae* ( $p \geq 0.697$ ) or family *Methanomicrobiales* ( $p \geq 0.051$ ) (Supplementary Figure S3).

## DISCUSSION

The inhibitory effect of volatile compounds in crude oil on aerobic hydrocarbon degradation has been known for some time (Atlas and Bartha, 1972; Atlas, 1975). More recent studies suggest that low molecular weight *n*-alkanes, alicyclic alkanes and monoaromatic hydrocarbons may also inhibit anaerobic processes (Chen et al., 2008). Fermentative growth of *Acetobacterium woodii* was completely inhibited by short chain alkanes ( $< C_9$ ), whereas, with increasing chain length, above  $C_9$ , inhibition decreased (Rodriguez Martinez et al., 2008). Toluene has also been shown to inhibit acetoclastic methanogenic activity in anaerobic reactor sludge (Ince et al., 2009) and, BTEX compounds are known to inhibit the anaerobic biodegradation of each other (Dou et al., 2008). Their inhibitory properties are thought to be due to their water solubility which renders them both bioavailable for degradation but at the same time more toxic because the accumulation of such compounds causes the cell membrane to swell and leak causing lysis (Chen et al., 2008; Rodriguez Martinez et al., 2008).

Many laboratory studies have documented methane production from the degradation of crude oil and individual or mixtures of hydrocarbons (Muller, 1957; Zengler et al., 1999; Townsend

et al., 2003; Siddique et al., 2006, 2007; Gieg et al., 2008, 2010; Jones et al., 2008; Wang et al., 2011; Zhou et al., 2012). Methane production profiles from many of these studies share common characteristics including an initial lag phase varying between 3 and 6 months followed by extensive hydrocarbon-driven methane production on time scales of 100's of days. It should be noted that in the first of these studies in the 1950s (Muller, 1957) it was suggested that only "higher alkanes" above  $C_{16}$  were degradable. In fact a very broad range of *n*-alkanes are now known to be utilized by methanogenic consortia (Townsend et al., 2003; Siddique et al., 2006; Jones et al., 2008; Zhou et al., 2012) including those below  $C_{16}$ , and all these *n*-alkanes are removed at faster rates than aromatic oil components (Townsend et al., 2003; Jones et al., 2008). In the current study  $nC_5-nC_{34}$  alkanes were removed without alteration of volatile aromatic hydrocarbons and methylcyclohexane within the time frame of the experiment (Figures 2, 3). Moreover there was no evidence for the removal of higher molecular weight aromatic hydrocarbons such as methylated naphthalenes and methylbiphenyls (Supplementary Table S1). These findings are consistent with patterns observed in subsurface environments such as oil reservoirs where alkane degradation is typically considered to precede the degradation of aromatic compounds (Larter et al., 2012). In in-reservoir degraded oils, removal of  $nC_{6-15}$  *n*-alkanes before  $C_{15+}$  *n*-alkanes is observed (Larter et al., 2012). This is supported by our study of the degradation of the non-weathered oil where the most abundant residual *n*-alkanes were  $nC_{11+}$ , despite higher initial abundance of lighter alkanes (Figure 3B). For these lighter alkanes though, the size defined order of degradation is likely reversed ( $nC_{10} > nC_8 > nC_7 > nC_6$ ) (Siddique et al., 2006) an observation either attributable to the water solubility/hydrophobicity of the compounds whose octanol/water partition coefficients ( $P_{ow}$ ) decrease with decreasing chain length, or due to selective uptake of the more hydrophobic alkanes across cell membranes of *n*-alkane-degrading microorganisms (Siddique et al., 2006).

The persistence of benzene, methylcyclohexane, toluene, and xylene (vapor pressure range from 9.9 to 0.8 kPa at 20°C) but loss of the  $nC_7-nC_{10}$  alkanes (vapor pressure range from 5.3 to 0.1 kPa at 20°C) in the methanogenic non-weathered oil treated microcosms further demonstrates that volatile hydrocarbon removal was biological and not due to evaporation during sampling of headspace. A direct comparison of heptane and methylcyclohexane, for instance, indicates that while they have almost identical vapor pressures (5.3 and 4.9 kPa at 20°C respectively) methylcyclohexane persists while heptane was removed in triplicate microcosms subjected to the same headspace sampling regimen (Figure 2A).

It has been previously suggested that the composition of an oil controls its susceptibility to methanogenic degradation (Muller, 1957) and, specifically, based on a comparison of the degradation of a weathered and unaltered "light paraffinous oil" it was inferred that volatile aromatics are likely inhibitory. In the present study we have now quantified the initial abundances and fates of individual compounds in such oils and clearly shown that methanogenic removal of alkanes proceeded more rapidly when volatile hydrocarbons are absent. Based on our data, light *n*-alkanes, methyl-cyclohexane or aromatic hydrocarbons present

in the non-weathered oil but absent in the weathered oil, can all be implicated in the inhibition, although, it is clear that the light *n*-alkanes were utilized by the methanogenic consortia in our experiments while the light aromatic hydrocarbons were not. This contrasts with the observation that BTEX are effectively degraded under methanogenic conditions in mature fine tailings from oil sands processing facilities where naphtha containing high levels of low molecular weight alkanes and aromatic hydrocarbons are used in upgrading of heavy oil (Siddique et al., 2007). Degradation of aromatics (<sup>13</sup>C-labeled 2-methylnaphthalene) at a rate greater than that for degradation of *n*-alkanes (<sup>13</sup>C-labeled hexadecane) was reported in enrichments prepared with production waters from the Dagang oil field (Jiménez et al., 2012). Interestingly, the study reports that most of the oil from Dagang is heavy oil which was almost completely depleted of *n*-alkanes (92–100% alkane degradation in 8 Dagang oils), therefore the microorganisms in production waters from the Dagang oil field which were used as inoculum in microcosm experiments may already have been pre-enriched for aromatic hydrocarbon degraders in the reservoir and therefore show a more rapid degradation of aromatic hydrocarbons (2-methylnaphthalene) than alkanes (n-hexadecane). Furthermore, some of the enrichments were reported to have received additions of 2 mM sulfate (Jiménez et al., 2012), and it has been shown previously that under sulfate-reducing conditions the extent of aromatic hydrocarbon degradation (3-methylbiphenyl) is greater when sulfate is present than under methanogenic conditions (Jones et al., 2008).

*Smithella* and *Methanomicrobiales* were significantly enriched in both the weathered oil and non-weathered oil amended microcosms relative to controls with no oil addition after 1058 days (Figure 4), supporting previous research that they play an important role in alkane biodegradation (Jones et al., 2008; Gray et al., 2011). No differences were observed between the abundance of *Smithella* and *Methanomicrobiales* in weathered oil amended microcosms compared to non-weathered oil amended microcosms suggesting that weathering of the oil does not adversely affect the microbiology of oil biodegradation after prolonged periods of >1000 days. In agreement with data from (Jones et al., 2008), the 16S rRNA gene abundances of facultative (*Methanosaetaceae*) and obligate acetoclastic methanogens (*Methanosaetaceae*) were lower than hydrogenotrophic methanogens (*Methanomicrobiales*) in the oil-amended microcosms.

## IMPLICATIONS FOR ANAEROBIC BIOREMEDIALATION AND ENERGY RECOVERY TECHNOLOGIES

In surface oil spills which are common throughout the world, knowledge of the composition of an oil, its distribution in the environment and, the specific local environmental risks associated with a spill can inform remediation strategies (Atlas and Bragg, 2009; Atlas and Hazen, 2011). Monitored natural attenuation (MNA) is a risk based approach where the likelihood that a sensitive receptor will be impacted by a contaminant spill is assessed on the basis of natural biodegradation rates and other factors such as contaminant transport. Under oxic conditions rates of crude oil degradation in marine sediments can be enhanced by the application of fertilizers and dispersants, strategies that have been used for large oil spills such as the Exxon

Valdez and the Deepwater Horizon (Atlas and Hazen, 2011). The release of petroleum components into anaerobic subsurface environments is also common throughout the world arising from natural releases, leaks, or deliberate disposal to soils, marine and freshwater sediments and aquifers. MNA is an accepted option for management of such contaminated environments (Parisi et al., 2009; Feisthauer et al., 2012; Naidu et al., 2012); indeed microbially mediated natural attenuation is likely even more important in the subsurface because processes such as evaporative loss and photooxidation are respectively either limited or entirely absent. It has been shown that methanogenic degradation of crude oil hydrocarbons can be significant in polluted subsurface environments (e.g., the Weißbandt-Gölzau and Bemidji aquifers) and further that release of methane from this process leads to the depletion of other electron acceptors as a result of anaerobic and aerobic methane oxidation (Amos et al., 2005; Feisthauer et al., 2010, 2012). Indeed the wide distribution of methanogenic petroleum hydrocarbon degradation capacity in both shallow and deep subsurface environments suggests that this process will be important after the depletion of other electron acceptors, especially if, as has been suggested, methanogenic consortia are more tolerant to higher concentrations of hydrocarbon contaminants compared to microorganisms using other electron acceptors, such as sulphate-reducing bacteria (Baker et al., 2012).

Despite the documented importance of methanogenic oil degradation in subsurface environments we have shown that hydrocarbon degradation in methanogenic crude oil impacted environments may be impeded by some components of the crude oil. Oils with higher levels of volatile hydrocarbons will be more inhibitory to oil-degrading microbial consortia than weathered oils with little or no volatiles and this inhibition will consequently reduce the rate of contaminant biodegradation. It is therefore important that the presence of volatile hydrocarbons is taken into account when MNA is applied for the management of contaminant plumes in anoxic environments.

In addition to remediation, methanogenic petroleum hydrocarbon degradation offers the potential to enhance energy recovery from stranded oil in petroleum reservoirs as methane (Grishchenkova et al., 2000; Gieg et al., 2008, 2010; Jones et al., 2008). This might be achieved by stimulation of indigenous methanogenic oil-degrading communities or specific methanogenic oil-degrading consortia. Based on the data presented here it appears that the chemical composition of a crude oil or other hydrocarbon mixtures may have marked effects on oil degradation to methane. Thus oils with higher levels of volatile hydrocarbons in environments where no alternative mechanisms of volatile hydrocarbon loss are possible, may be less amenable to rapid anaerobic conversion to methane. Determination of the isotopic composition of methane in the incubations would potentially have been valuable to this study, as used previously in a hydrocarbon-degrading methanogenic enrichment culture (Morris et al., 2012) and in the assessment of *in situ* processes in hydrocarbon contaminated aquifers (Feisthauer et al., 2010, 2012). Future work should quantitatively determine the absolute and relative inhibitory effects of individual light hydrocarbons or defined mixtures to allow accurate prediction of timescales of subsurface methanogenic oil biodegradation under natural and engineered conditions.

## IMPLICATIONS FOR THE DYNAMICS OF PETROLEUM RESERVOIR DEGRADATION AND HEAVY OIL FORMATION

In petroleum reservoirs, oil composition is controlled by a complex interplay of geological factors i.e., source rock variation, thermal maturity, oil expulsion and migration and the balance between oil degradation and fresh oil charge (Larter et al., 2005, 2012; Adams et al., 2006). This complexity gives rise to oils which have different absolute amounts and relative distributions of saturated and aromatic hydrocarbons, resins and asphaltenes. For deep subsurface petroleum accumulations putatively inhibitory volatile compounds can often only be removed by water washing or biodegradation and thus conditions conducive to petroleum biodegradation and water washing (reservoir temperatures less than 80–90°C; presence of nutrients and an extensive oil-water contact zone Head et al., 2003) may enhance the removal of potentially inhibitory compounds and thus accelerate biodegradation. In the context of water washing it is also worth noting that the volatile hydrocarbons have lower octanol water partition coefficients than higher molecular weight hydrocarbons.

From the current study, it can be inferred that the onset and subsequent rates of methanogenic hydrocarbon degradation will be dependent in part on the initial concentration of volatile hydrocarbons in reservoir oil, as well as on the availability of nutrients, water, and transport/diffusion rates. Oils with high concentrations of light *n*-alkanes and aromatic hydrocarbons would retard degradation of all other compound classes. In this study it seems that much of the volatile hydrocarbon component is eventually degraded in the non-weathered oil (**Figure 2A**) and this is likely to occur much more slowly under reservoir conditions. Indeed *in situ* rates of oil degradation inferred from reservoir field data indicate that in reservoir degradation rates are substantially lower (first order rate constants of  $10^{-6}$ – $10^{-7}$  year $^{-1}$ ) than the rates measured in laboratory incubations (Larter et al., 2003). Thus if all rates are scaled to in-reservoir degradation timescales, then a difference in lag phase between a weathered and a non-weathered oil may well be significant. Furthermore, in-reservoir oil degradation typically occurs on similar time-scales to oil charging and mixing (Larter et al., 2012) thus inhibitory compounds may be constantly replenished during continuous charging and mixing resulting in a subtle control on the rate of in-reservoir oil biodegradation.

The discovery of the inhibitory effects of volatile hydrocarbons on methanogenic crude oil biodegradation is also relevant to the “biostatic hypothesis” (Sunde and Torsvik, 2005). The biostatic hypothesis is based on the observation that, despite being replete with appropriate electron donors, electron acceptors and nutrients, samples from petroleum reservoirs do not exhibit souring attributable to the activity of sulfate-reducing bacteria unless they have been degassed or diluted (Sunde and Torsvik, 2005). It is possible that the inhibition of microbial activity by volatile hydrocarbons that we observed in this study may at least, in part, explain the apparent biostatic nature of some petroleum reservoirs.

To our knowledge this is the first systematic evaluation of the inhibition of methanogenic biodegradation of crude oil by volatile hydrocarbons. The geochemical and microbiological findings have implications for understanding rates of in-reservoir oil biodegradation and the formation of heavy oil. The presence

of volatile hydrocarbons should also be considered when monitored natural attenuation or biostimulation is applied for the management of hydrocarbon plumes in contaminated anoxic environments. Furthermore, knowledge of the chemical composition of a crude oil may serve to enhance energy recovery from stranded oil as methane, in petroleum reservoirs.

## AUTHOR CONTRIBUTIONS

Ian M. Head, D. Martin Jones, and Neil D. Gray developed the concept and designed experiments; Angela Sherry prepared and analyzed microcosm experiments. Angela Sherry and Russell J. Grant conducted molecular microbiology and analyzed data with Neil D. Gray; Data interpretation was conducted by Neil D. Gray, Angela Sherry, and Ian M. Head; Carolyn M. Aitken performed oil geochemistry and analyzed the data together with D. Martin Jones; Angela Sherry, Neil D. Gray, and Ian M. Head wrote the manuscript.

## ACKNOWLEDGMENTS

The authors would like to thank James A. Todd for analysis of volatile hydrocarbons in non-weathered and weathered oils. The authors are grateful for the financial support provided by the Natural Environment Research Council (Grant NE/E01657X/1 to Ian M. Head, Neil D. Gray and D. Martin Jones).

## SUPPLEMENTARY MATERIAL

The Supplementary Material for this article can be found online at: <http://journal.frontiersin.org/Journal/10.3389/fmicb.2014.00131/abstract>

## REFERENCES

- Adams, J. J., Riediger, C., Fowler, M., and Larter, S. R. (2006). Thermal controls on biodegradation around the Peace River tar sands: paleopasteurization to the west. *J. Geochem. Explor.* 89, 1–4. doi: 10.1016/j.gexplo.2005.11.004
- Amos, R. T., Mayer, K. U., Bekins, B. A., Delin, G. N., and Williams, R. L. (2005). Use of dissolved and vapor-phase gases to investigate methanogenic degradation of petroleum hydrocarbon contamination in the subsurface. *Water Resour. Res.* 41, 1–15. doi: 10.1029/2004WR003433
- Anderson, R. T., and Lovley, D. R. (2000). Biogeochemistry–hexadecane decay by methanogenesis. *Nature* 404, 722–723. doi: 10.1038/3501270
- Atlas, R. M. (1975). Effects of temperature and crude oil composition on petroleum biodegradation. *Appl. Microbiol.* 30, 396–403.
- Atlas, R. M., and Bartha, R. (1972). Biodegradation of petroleum in seawater at low temperatures. *Can. J. Microbiol.* 18, 1851–1855. doi: 10.1139/m72-289
- Atlas, R. M., and Bragg, J. (2009). Bioremediation of marine oil spills: when and when not – the Exxon Valdez experience. *Microb. Biotechnol.* 2, 213–221. doi: 10.1111/j.1751-7915.2008.00079.x
- Atlas, R. M., and Hazen, T. C. (2011). Oil biodegradation and bioremediation: a tale of the two worst spills in U.S. history. *Environ. Sci. Technol.* 45, 6709–6715. doi: 10.1021/es2013227
- Baedecker, M. J., Eganhouse, R. P., Bekins, B. A., and Delin, G. N. (2011). Loss of volatile hydrocarbons from an LNAPL oil source. *J. Contam. Hydrol.* 126, 140–152. doi: 10.1016/j.jconhyd.2011.06.006
- Baker, K. M., Bottrell, S. H., Thornton, S. F., Peel, K. E., and Spence, M. J. (2012). Effect of contaminant concentration on *in situ* bacterial sulfate reduction and methanogenesis in phenol-contaminated groundwater. *Appl. Geochem.* 27, 2010–2018. doi: 10.1016/j.apgeochem.2012.05.010
- Bennett, B., Bowler, B. F. J., and Larter, S. R. (1996). Determination of C0-C3 alkylphenols in crude oils and waters. *Anal. Chem.* 68, 3697–3702. doi: 10.1021/ac960299x
- Callbeck, C. M., Sherry, A., Hubert, C. R. J., Gray, N. D., Voordouw, G., and Head, I. M. (2013). Improving PCR efficiency for accurate quantification of 16S rRNA genes. *J. Microbiol. Methods* 93, 148–152. doi: 10.1016/j.mimet.2013.03.010

- Chen, Y., Cheng, J. J., and Creamer, K. S. (2008). Inhibition of anaerobic digestion process: a review. *Bioresour. Technol.* 99, 4044–4064. doi: 10.1016/j.biortech.2007.01.057
- Dou, J., Liu, X., and Hu, Z. (2008). Substrate interactions during anaerobic biodegradation of BTEX by the mixed cultures under nitrate reducing conditions. *J. Hazard. Mater.* 158, 264–272. doi: 10.1016/j.jhazmat.2008.01.075
- Feisthauer, S., Seidel, M., Bombach, P., Traube, S., Knöller, K., Wange, M., et al. (2012). Characterization of the relationship between microbial degradation processes at a hydrocarbon contaminated site using isotopic methods. *J. Contam. Hydrol.* 133, 17–29. doi: 10.1016/j.jconhyd.2012.03.001
- Feisthauer, S., Siegert, M., Seidel, M., Richnow, H. H., Zengler, K., Gründger, F., et al. (2010). Isotopic fingerprinting of methane and CO<sub>2</sub> formation from aliphatic and aromatic hydrocarbons. *Org. Geochem.* 41, 482–490. doi: 10.1016/j.orggeochem.2010.01.003
- Gieg, L. M., Davidova, I. A., Duncan, K. E., and Suflita, J. M. (2010). Methanogenesis, sulfate reduction and crude oil biodegradation in hot Alaskan oilfields. *Environ. Microbiol.* 12, 3074–3086. doi: 10.1111/j.1462-2920.2010.02282.x
- Gieg, L. M., Duncan, K. E., and Suflita, J. M. (2008). Bioenergy production via microbial conversion of residual oil to natural gas. *Appl. Environ. Microbiol.* 74, 3022–3029. doi: 10.1128/AEM.00119-08
- Gray, N. D., Sherry, A., Grant, R. J., Rowan, A. K., Hubert, C. R., Callbeck, C. M., et al. (2011). The quantitative significance of Syntrophaceae and syntrophic partnerships in methanogenic degradation of crude oil alkanes. *Environ. Microbiol.* 13, 2957–2975. doi: 10.1111/j.1462-2920.2011.02570.x
- Gray, N. D., Sherry, A., Hubert, C., Dolfing, J., and Head, I. M. (2010). Methanogenic degradation of petroleum hydrocarbons in subsurface environments: remediation, heavy oil formation, and energy recovery. *Adv. Appl. Microbiol.* 72, 137–161. doi: 10.1016/S0065-2164(10)72005-0
- Grishchenkova, V. G., Townsend, R. T., McDonald, T. J., Autenrieth, R. L., Bonner, J. S., and Boronin, A. M. (2000). Degradation of petroleum hydrocarbons by facultative anaerobic bacteria under aerobic and anaerobic conditions. *Process Biochem.* 35, 889–896. doi: 10.1016/S0032-9592(99)00145-4
- Head, I. M., Jones, D. M., and Larter, S. R. (2003). Biological activity in the deep subsurface and the origin of heavy oil. *Nature* 426, 344–352. doi: 10.1038/nature02134
- Ince, O., Kolukirik, M., Cetecioglu, Z., Eyice, O., Inceoglu, O., and Ince, B. (2009). Toluene inhibition on an anaerobic reactor sludge in terms of potential activity and composition of acetoclastic methanogens. *J. Environ. Sci. Heal. A. Tox. Hazard. Subst. Environ. Eng.* 44, 1551–1556. doi: 10.1080/10934520903263470
- Jiménez, N., Morris, B. E. L., Cai, M., Gründger, F., Yao, J., Richnow, H. H., et al. (2012). Evidence for *in situ* methanogenic oil degradation in the Dagang oil field. *Org. Geochem.* 52, 44–54. doi: 10.1016/j.orggeochem.2012.08.009
- Jones, D. M., Head, I. M., Gray, N. D., Adams, J. J., Rowan, A. K., Aitken, C. M., et al. (2008). Crude oil biodegradation via methanogenesis in subsurface petroleum reservoirs. *Nature* 451, 176–180. doi: 10.1038/nature06484
- Larter, S., Huang, H., Adams, J., Bennett, B., and Snowdon, L. R. (2012). A practical biodegradation scale for use in reservoir geochemical studies of biodegraded oils. *Org. Geochem.* 45, 66–76. doi: 10.1016/j.orggeochem.2012.01.007
- Larter, S. R., Head, I. M., Huang, H., Bennett, B., Jones, M., Aplin, A. C., et al., (2005). “Biodegradation, gas destruction and methane generation in deep subsurface petroleum reservoirs: an overview. Petroleum geology: North-West Europe and Global Perspectives,” in *Proceedings of 6th Geology Conference, Geological Society* (London), 633–639.
- Larter, S., Wilhelms, A., Head, I., Koopmans, M., Aplin, A., Di Primio, R., et al. (2003). The controls on the composition of biodegraded oils in the deep subsurface—part 1: biodegradation rates in petroleum reservoirs. *Org. Geochem.* 34, 601–613. doi: 10.1016/S0146-6380(02)00240-1
- Mbadinga, S. M., Wang, L.-Y., Zhou, L., Liu, J.-F., Gu, J.-D., and Mu, B.-Z. (2011). Microbial communities involved in anaerobic degradation of alkanes. *Int. Biodeter. Biodegr.* 65, 1–13. doi: 10.1016/j.ibiod.2010.11.009
- Morris, B. E. L., Herbst, F.-A., Bastida, F., Seifert, J., von Bergen, M., Richnow, H.-H., et al. (2012). Microbial interactions during residual oil and n-fatty acid metabolism by a methanogenic consortium. *Environ. Microbiol. Rep.* 4, 297–306. doi: 10.1111/j.1758-2229.2012.00333.x
- Muller, F. M. (1957). On methane fermentation of higher alkanes. A. Van Leeuw. *J. Microb.* 23, 369–384. doi: 10.1007/BF02545890
- Naidu, R., Nandy, S., Megharaj, M., Kumar, R. P., Chadalavada, S., Chen, Z., et al. (2012). Monitored natural attenuation of a long-term petroleum hydrocarbon contaminated sites: a case study. *Biodegradation* 23, 881–895. doi: 10.1007/s10532-012-9580-7
- Parisi, V. A., Brubaker, G. A., Zenker, M. J., Prince, R. C., Gieg, L. M., Da Silva, M. L. B., et al. (2009). Field metabolomics and laboratory assessments of anaerobic intrinsic bioremediation of hydrocarbons at a petroleum-contaminated site. *Microb. Biotechnol.* 2, 202–212. doi: 10.1111/j.1751-7915.2009.00077.x
- Rodriguez Martinez, M. F., Kelessidou, N., Law, Z., Gardiner, J., and Stephens, G. (2008). Effect of solvents on obligately anaerobic bacteria. *Anaerobe* 14, 55–60. doi: 10.1016/j.anaerobe.2007.09.006
- Sherry, A., Gray, N. D., Aitken, C. M., and Dolfing, J. (2009). “Chapter 42: Microbial oil degradation under methanogenic conditions,” in *Handbook of Hydrocarbon and Lipid Microbiology*, Vol. 5, ed K. N. Timmis (Heidelberg: Springer), 3905–3918.
- Sherry, A., Gray, N. D., Ditchfield, A. K., Aitken, C. M., Jones, D. M., Röling, W. F. M., et al. (2013). Anaerobic biodegradation of crude oil under sulphate-reducing conditions leads to only modest enrichment of recognized sulphate-reducing taxa. *Int. Biodeter. Biodegr.* 81, 105–113. doi: 10.1016/j.ibiod.2012.04.009
- Siddique, T., Fedorak, P. M., and Foght, J. M. (2006). Biodegradation of short-chain n-alkanes in oil sands tailings under methanogenic conditions. *Environ. Sci. Technol.* 40, 5459–5464. doi: 10.1021/es060993m
- Siddique, T., Fedorak, P. M., MacKinnon, M. D., and Foght, J. M. (2007). Metabolism of BTEX and naphtha compounds to methane in oil sands tailings. *Environ. Sci. Technol.* 41, 2350–2356. doi: 10.1021/es062852q
- Sunde, E., and Torsvik, T. (2005). “Microbial control of hydrogen sulfide production in oil reservoirs,” in *Petroleum Microbiology*, eds B. Ollivier and M. Magot (Washington, DC: ASM Press), 201–213.
- Teske, A. (2010). “Chapter 43: Sulfate-reducing and methanogenic hydrocarbon-oxidizing microbial communities in the marine environment,” in *Handbook of Hydrocarbon and Lipid Microbiology*, ed K. N. Timmis (Heidelberg: Springer), 2203–2223. doi: 10.1007/978-3-540-77587-4\_160
- Townsend, G. T., Prince, R. C., and Suflita, J. M. (2003). Anaerobic oxidation of crude oil hydrocarbons by the resident microorganisms of a contaminated anoxic aquifer. *Environ. Sci. Technol.* 37, 5213–5218. doi: 10.1021/es0264495
- Wang, L.-Y., Gao, C.-X., Mbadinga, S. M., Zhou, L., Liu, J.-F., Gu, J.-D., et al. (2011). Characterization of an alkane-degrading methanogenic enrichment culture from production water of an oil reservoir after 274 days of incubation. *Int. Biodeter. Biodegr.* 65, 444–450. doi: 10.1016/j.ibiod.2010.12.010
- Widdel, F., and Bak, W. (1992). “Gram-negative mesophilic sulfate-reducing bacteria,” in *The Prokaryotes*, Vol. 4, eds A. Balows, H. G. Trüper, M. Dworkin, W. Harder, K.-H. Schleifer (Verlag, NY: Springer), 3352–3379. doi: 10.1007/978-1-4757-2191-1\_21
- Zengler, K., Richnow, H. H., Rossello-Mora, R., Michaelis, W., and Widdel, F. (1999). Methane formation from long-chain alkanes by anaerobic microorganisms. *Nature* 401, 266–269. doi: 10.1038/45777
- Zhou, L., Li, K.-P., Mbadinga, S. M., Yang, S.-Z., Gu, J.-D., and Mu, B.-Z. (2012). Analyses of n-alkanes degrading community dynamics of a high-temperature methanogenic consortium enriched from production water of a petroleum reservoir by a combination of molecular techniques. *Ecotoxicology* 6, 1680–1691. doi: 10.1007/s10646-012-0949-5

**Conflict of Interest Statement:** The authors declare that the research was conducted in the absence of any commercial or financial relationships that could be construed as a potential conflict of interest.

**Received:** 15 October 2013; **accepted:** 13 March 2014; **published online:** 03 April 2014. **Citation:** Sherry A, Grant RJ, Aitken CM, Jones DM, Head IM and Gray ND (2014) Volatile hydrocarbons inhibit methanogenic crude oil degradation. *Front. Microbiol.* 5:131. doi: 10.3389/fmicb.2014.00131

This article was submitted to Aquatic Microbiology, a section of the journal *Frontiers in Microbiology*.

Copyright © 2014 Sherry, Grant, Aitken, Jones, Head and Gray. This is an open-access article distributed under the terms of the Creative Commons Attribution License (CC BY). The use, distribution or reproduction in other forums is permitted, provided the original author(s) or licensor are credited and that the original publication in this journal is cited, in accordance with accepted academic practice. No use, distribution or reproduction is permitted which does not comply with these terms.



# Effective bioremediation strategy for rapid *in situ* cleanup of anoxic marine sediments in mesocosm oil spill simulation

Maria Genovese<sup>1†</sup>, Francesca Crisafi<sup>1†</sup>, Renata Denaro<sup>1</sup>, Simone Cappello<sup>1</sup>, Daniela Russo<sup>1,2</sup>, Rosario Calogero<sup>1</sup>, Santina Santisi<sup>1,2</sup>, Maurizio Catalfamo<sup>1</sup>, Alfonso Modica<sup>3</sup>, Francesco Smedile<sup>1</sup>, Lucrezia Genovese<sup>1</sup>, Peter N. Golyshin<sup>4</sup>, Laura Giuliano<sup>1,5</sup> and Michail M. Yakimov<sup>1\*</sup>

<sup>1</sup> Institute for Coastal Marine Environment, CNR, Messina, Italy

<sup>2</sup> Department of Biological and Environmental Sciences, University of Messina, Messina, Italy

<sup>3</sup> Environmental Laboratory, Syndial SpA, Priolo Gargallo, Italy

<sup>4</sup> Environmental Genomics, School of Biological Sciences, Bangor University, Bangor, UK

<sup>5</sup> Mediterranean Science Commission, Monaco, Monaco

## Edited by:

Ian M. Head, Newcastle University, UK

## Reviewed by:

Kathleen Scott, University of South Florida, USA

Anne Bernhard, Connecticut College, USA

## \*Correspondence:

Michail M. Yakimov, Institute for Coastal Marine Environment, CNR, Spianata S. Raineri, 86, 98122 Messina, Italy  
e-mail: michail.yakimov@iamc.cnr.it

<sup>†</sup>These authors have contributed equally to this work.

The purpose of present study was the simulation of an oil spill accompanied by burial of significant amount of petroleum hydrocarbons (PHs) in coastal sediments. Approximately 1000 kg of sediments collected in Messina harbor were spiked with Bunker C furnace fuel oil (6500 ppm). The rapid consumption of oxygen by aerobic heterotrophs created highly reduced conditions in the sediments with subsequent recession of biodegradation rates. As follows, after 3 months of ageing, the anaerobic sediments did not exhibit any significant levels of biodegradation and more than 80% of added Bunker C fuel oil remained buried. Anaerobic microbial community exhibited a strong enrichment in sulfate-reducing PHs-degrading and PHs-associated *Deltaproteobacteria*. As an effective bioremediation strategy to clean up these contaminated sediments, we applied a Modular Slurry System (MSS) allowing the containment of sediments and their physical–chemical treatment, e.g., aeration. Aeration for 3 months has increased the removal of main PHs contaminants up to 98%. As revealed by CARD-FISH, qPCR, and 16S rRNA gene clone library analyses, addition of Bunker C fuel oil initially affected the activity of autochthonous aerobic obligate marine hydrocarbonoclastic bacteria (OMHCB), and after 1 month more than the third of microbial population was represented by *Alcanivorax*-, *Cycloclasticus*-, and *Marinobacter*-related organisms. In the end of the experiment, the microbial community composition has returned to a status typically observed in pristine marine ecosystems with no detectable OMHCB present. Eco-toxicological bioassay revealed that the toxicity of sediments after treatment was substantially decreased. Thus, our studies demonstrated that petroleum-contaminated anaerobic marine sediments could efficiently be cleaned through an *in situ* oxygenation which stimulates their self-cleaning potential due to reawakening of allochthonous aerobic OMHCB.

**Keywords:** marine anoxic sediments, crude oil pollution, hydrocarbonoclastic bacteria, *in situ* bioremediation, aerated slurry system

## INTRODUCTION

The worldwide production of crude oil and natural gas is at the peak, with an estimated worldwide production of 89 million barrels per day in 2011 (International Energy Agency, <http://omrpublic.iea.org/>). Approximately, a half of this amount is transported by the sea (Gertler et al., 2010). As follows, worldwide marine coastal areas are exposed to the oil spills occurring as a result of accidents or illegal practices (Psarros et al., 2010). The release of thousands of tons of petroleum hydrocarbons (PHs) affects the marine environment and causes severe ecological and economical damage. For example, only the pollution resulting from the tanker washing or ballast water has been estimated to contribute about 2 million tons per year worldwide (Ferraro et al., 2007; Gertler et al., 2010). The recent spillage of 780,000 m<sup>3</sup> of

oil into the Gulf of Mexico proved again that human activities might cause a contamination without precedents. This accident presented a huge challenge to existing oil spill treatment methods, and current technologies were not able to cope with the size and nature of the Deepwater Horizon oil spill. Therefore, there is an urgent demand for development and optimization of bioremediation techniques that can play a central role in marine oil spill response contingency plans.

One of the most important issues in bioremediation is the application (or stimulation) of autochthonous hydrocarbon-degrading microbial populations. Some marine gammaproteobacteria have a high affinity toward PHs. Species such as *Alcanivorax borkumensis* (Yakimov et al., 1998), *Cycloclasticus pugetii* (Dyksterhouse et al., 1995), *Oleispira antarctica* (Yakimov

et al., 2003), *Oleiphilus messinensis* (Golyshin et al., 2002), and *Thalassolituus oleivorans* (Yakimov et al., 2004) constitute a distinct group of obligate marine hydrocarbon-degrading bacteria (OMHCB). Following a sudden oil spill event, these organisms outcompete most of the naturally occurring oligotrophic marine microorganisms (Hara et al., 2003; Yakimov et al., 2007). Growing on PHs, aerobic OMHCB use oxygen not only as the terminal electron acceptor for respiratory energy conservation, but also as an indispensable reactant in the PHs activation mechanism. Thus, the stimulation of the OMHCBs degradation activity in the contaminated site can significantly improve the self-cleaning potential. Unfortunately, due to metabolic requirements of the OMHCBs, this type of bioremediation is restricted to either seawater column or superficial sediments. Due to a high biological oxygen demand and its slow diffusion into marine sediments, these compartments below the surface are typically highly reduced (Engelen and Cypionka, 2009). The realization that activated oxygen is used to overcome the chemical sluggishness of hydrocarbons has for some decades favored the view that hydrocarbons are not biodegradable under anoxic conditions (Widdel and Rabus, 2001). Although recently, a number of strictly anaerobic microorganisms have been shown to utilize PHs as growth substrates, this process is extremely slow compared to aerobic degradation and can not be considered as rapid bioremediation scenario.

The aim of this study was to monitor both immediate and long-term responses of indigenous microbial consortia to a simulated oil spill and during bioremediation treatment. Keeping in mind that the decontamination of PHs-polluted anoxic sediments is a very sluggish process, the stimulation of indigenous aerobic OMHCBs was performed by the *in situ* aeration of sediments within a modular slurry system (MSS) to avoid the contamination of the surrounding aquifer. The succession of microbial community and efficacy of petroleum biodegradation in both untreated

(anoxic) external and aerated internal sediments was monitored during 3 months after contamination. Additionally, the toxicity of sediments was controlled by application of Microtox® and amphipods *Corophium orientale* eco-toxicological bioassays.

## MATERIALS AND METHODS

### EXPERIMENTAL MESOCOSM

The experiment was carried out in rectangular tank of  $3.75\text{ m}^3$  capacity (166 cm long, 150 cm deep, 150 cm wide). This reservoir was filled with ca. 2000 l of seawater taken directly from the harbor of Messina ( $38^{\circ}11'42.58''\text{N}$   $15^{\circ}34'25.19''\text{E}$ ). Prior to use, the seawater was filtered through a  $200\text{ }\mu\text{m}$  nylon mesh to remove large metazoans and detritus. Approximately 1000 kg of sandy sediments were collected at the same place and artificially contaminated with Bunker C furnace fuel oil (6500 ppm) to simulate the oil spill accident. Temperature inside the mesocosm was maintained about  $20 \pm 1^{\circ}\text{C}$  for all experimental period. Mesocosm has continuously received seawater at the flow rate of  $11\text{ min}^{-1}$ . The MSS used in mesocosm experiment is shown on **Figure 1**. The MSS was developed especially for *in situ* aeration ( $201\text{ min}^{-1}$ ) of polluted sediments without their removal from contaminated side to avoid the re-contamination of adjacent aquifer. The reactor was inserted into the sediment. Sediment directly beneath the MSS were treated by the reactor, and those sediments outside of it were undisturbed and served as a control. All experimentations have been conducted for 3 months. To monitor the succession of microbial population and the efficiency of petroleum degradation, 1.5–2.0 kg of sediments (up to 10 kg in total) were sampled on fixed days ( $T_0$ ,  $T_1$ ,  $T_{29}$ , and  $T_{90}$ ) at six different points inside and outside the MSS. Additionally, measurements of the biochemical oxygen demand ( $\text{BOD}_5$ ), reduction potential ( $E_h$ ), and eco-toxicological assays (Microtox® and *Corophium orientale* mortality test) were monitored. The  $E_h$  of sediment was measured by a Waterproof CyberScan PCD 650

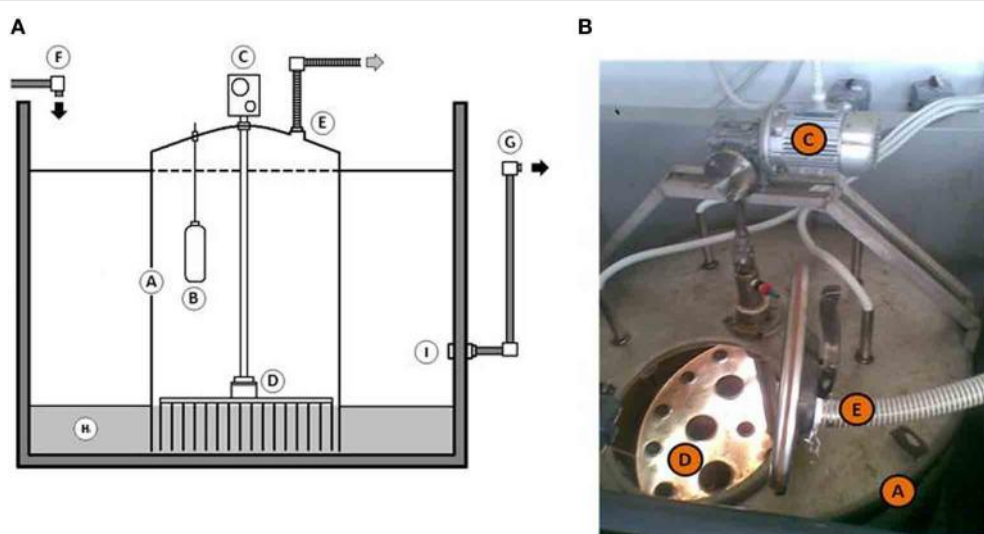


**FIGURE 1 | (A,B)** Schematic representation (A) and detail (B) of "Modular Slurry System" used throughout this study. Abbreviation used: A, Modular Slurry System; B, temperature controller; C, external air pump;

D, steel plate with needles to supply an oxygen into deep sediments; E, exhaust tube; F, seawater inlet; G, seawater outlet; H, contaminated sediments; I, overflow regulation system.

multiparameter (Eutech Instruments) according to the manufacturer's instructions at aforementioned time intervals. BOD<sub>5</sub> was measured using a BOD sensor (VELP Scientifica) after 5 days of incubation in accordance with the manufacturer's instructions.

### ANALYSIS OF PETROLEUM HYDROCARBONS

Efficiency of petroleum degradation was estimated by the analysis of total extracted and resolved hydrocarbons (TERHC). At the fixed time points, TERCH were extracted from sediments following the 3550C EPA (Environmental Protection Agency) procedure. Briefly, 500 ml mixture of CH<sub>2</sub>Cl<sub>2</sub>:CH<sub>3</sub>COCH<sub>3</sub> (1:1, vol/vol) was added to 1000 g of pooled and dried either internal or external sediments, collected from six different sites (see above). Mixture was sonicated for 2 min in ultrasound bath (Branson 1200 Ultrasonic Cleaner, Branson USA). Samples were further shaken at 150 rpm for 30 min, centrifuged for 10 min at 5000 × g and supernatant was passed through a ceramic column filled with anhydrous Na<sub>2</sub>SO<sub>4</sub> (Sigma-Aldrich, Milan). Same treatment of pooled and dried sediments was repeated with 500 ml of CH<sub>2</sub>Cl<sub>2</sub> and the obtained extracts were combined and volatilized to the dryness. Residues were re-suspended in CH<sub>2</sub>Cl<sub>2</sub> prior the gas chromatography (GC) analysis (Rocchetti et al., 2011). All measures were performed using a Master GC DANI Instruments (Development ANalytical Instruments), equipped with SSL injector and FID detector. Sample (1 µl) was injected in splitless mode at 330°C. The analytical column was a Restek Rxi-5 Sil MS with Integra-Guard, 30 m × 0.25 mm (ID × 0.25 µm film thickness). Helium carrier gas was maintained at a constant flow of 1.5 ml min<sup>-1</sup>. TERCH were calculated using the mean response factors of *n*-alkanes, i.e., individual *n*-alkane concentrations from *n*-C<sub>15</sub> to *n*-C<sub>40</sub>, pristane and phytane were calculated for each sample. To estimate the biodegradation of aliphatic fraction, the evaluation indices *n*-C<sub>17</sub>/pristane and *n*-C<sub>18</sub>/phytane were selected for this study. The amount of analyzed TERCH was expressed as ppm (part per million) or mg kg<sup>-1</sup>.

### ECOTOXICOLOGICAL ASSAYS

The Microtox® luminescence assay was performed on sediment pore water. Sub-samples of sediment were centrifuged (5000 × g for 45 min, 4°C) and filtered (0.45 µm nitrate cellulose membrane) to remove the fine suspended particles and maintained at 4°C until used in assays. Microtox® toxicity tests were conducted according to the standard procedures EN12457 with the following modifications. As far as the Solid Phase Test deals with fine particles that affected the bioluminescence of bacteria (Bulich et al., 1992; Benton et al., 1995; Ringwood et al., 1997), each experimental sediment sample was compared with a reference sediment sample with the same granulometry, collected from a pristine site. Toxicities were reported as effective concentration of toxicant resulting in a 50% decrease in bioluminescence (EC<sub>50</sub>). EC<sub>50</sub> with 95% of confidence intervals were calculated following the procedures outlined in the Microtox® System Operating Manual (Microtox, 1982). Amphipods *Corophium orientale* were delivered from CIBM (Livorno, Italy). The animals were used following the procedure reported by Onorati et al. (1999). Briefly, the juveniles and young adults, which passed through 1000 µm and retained by 710 µm mesh sieve, were selected for ecotoxicology

experiments. The test was carried out inside 2.5-l glass flasks containing approximately 2 cm layer of sediments and filled with 1000 ml of filtered seawater. The seawater was aerated and kept at a constant temperature (16 ± 2°C). Flasks were illuminated during 12 h daily by a lamp system consisted of six tubes (36W, 120 cm). One hundred amphipods were randomly selected and introduced into each flask. No food was added to the test and control chambers. At the end of exposition (10 days), amount of survived organisms were counted. Missing amphipods were assumed as dead animals. The sensitivity of the populations was estimated as a fraction of dead organisms to the initial amount of added amphipods. All the experiments were replicated twice.

### TOTAL RNA EXTRACTION, REVERSE TRANSCRIPTION-PCR (RT-PCR) AND 16S rRNA CLONE LIBRARIES

Total RNA was extracted from sediment sample (5 g) using the FastRNA® Pro soil direct Kit (MP Biomedicals™) as previously described (Roussel et al., 2009). Extracted RNA from three different samples was pooled and further converted to cDNA using First-Strand cDNA Synthesis SuperScript™ II Reverse Transcriptase (Life Technologies). RT reaction mixtures (20 µl) contained 1 µl the random hexamer primer mix (Bioline), 30 ng of RNA, 1 µl 10 mM dNTPs (Gibco, Invitrogen Co., Carlsbad, CA) and sterile distilled water (14 µl). After heating to 65°C for 5 min, and incubate on ice for 1 min, the mixture was supplemented with 4 µl of 5 × First-Strand Buffer, 1 µl of DTT and 1 µl of SuperScript™. The mixture was shaken and incubated at 50°C for 30 min. Finally, SuperScript™ enzyme was inactivated by heating at 70°C for 15 min. 16S rRNA genes were amplified from total cDNA using the universal primers (530F [5'-GTGCCAGCMGCCGCGG-3'] and 1492R [5'-TACGGYTACCTTGTTACGACT-3']) (Lane, 1991). The PCR was performed in 50 µl mixture (total volume) containing 1× solution Q (Qiagen), 1× Qiagen reaction buffer, 1 µM of each forward and reverse primer, 10 µM dNTPs (Gibco, Invitrogen Co.), 2.0 ml (50–100 ng) of template and 2.0 U of Qiagen Taq Polymerase (Qiagen). The reaction (3 min hot-start at 95°C; 1 min at 94°C, 1 min at 50°C, 2 min at 72°C, 30 cycles; final extension 10 min at 72°C) was performed with GeneAmp 5700 (PE Applied Biosystems). The quality of amplification products was checked by agarose electrophoresis and purified using Qiaquick Gel Extraction kit (Qiagen). Purified 16S crDNA amplicons were further cloned into the pGEM T-easy Vector II (Promega), transformed into *E. coli* DH10β cells and subsequently amplified with primers, specific for the pGEM T-easy vector (M13F (5'-TGTAAAACGACGGCCAGT-3') and M13R (5'-TCACACAGGAAACAGCTATGAC-3')). Positive products were purified and sequenced by Macrogen (Amsterdam, The Netherlands). Sequences were checked for possible chimeric origin using Pintail 1.1 software (Ashelford et al., 2005). For the 16S rRNA gene sequences, initial alignment of amplified sequences and close relatives identified with BLAST (Altschul et al., 1997) were performed using the SILVA alignment tool (Pruesse et al., 2007) and manually aligned with ARB (Ludwig et al., 2004). After alignment, the neighbor-joining algorithm of ARB package was used to generate the phylogenetic trees based on distance analysis for 16S rRNA genes. The robustness of inferred topologies

was verified by bootstrap re-sampling analysis, using the same distance model (1000 replicates).

#### ENUMERATION OF CELLS BY CARD-FISH

The catalyzed reporter deposition fluorescence *in situ* hybridization (CARD-FISH) was performed using the protocol of Pernthaler et al. (2002) with some modifications. Briefly, 5 g of pooled sediment samples were fixed with formaldehyde (2% v/v final concentrations) and left for 12 h at 4°C. Fixed sediment samples were further incubated for at least 15 min with Tween 80 (final concentration, 1 mg l<sup>-1</sup>) and then sonicated during 20 min in an Ultrasonic cleaner (Branson 1200, Milan) for the bacterial dispersion (Kuwae and Hosokawa, 1999). Supernatant samples were then filtered onto polycarbonate membrane filters (type GTTP; pore size, 0.2 µm; diameter, 2.5 cm; Sartorius, Göttingen, Germany). Filters for CARD-FISH counts were embedded in low-melting point agarose (0.1% wt/vol, Sigma-Aldrich, Milan), dried at 37°C for 20 min, and dehydrated with 95% ethanol. Embedded cells were permeabilized by 1 h of exposition with solution A (10 mg ml<sup>-1</sup> of lysozyme (Sigma-Aldrich, Milan); 0.5 M EDTA, 0.1 M Tris-HCl [pH 8.0]) followed by the 30 min-long incubation with achromopeptidase (60 U ml<sup>-1</sup>; 0.01 M NaCl, 0.01 M Tris-HCl [pH 8.0]) at 37°C. Filters were cut in sections and hybridized with 5'-horseradish peroxidase (HRP)-labeled oligonucleotide probes as described by Pernthaler et al. (2002). Probes used in this work are listed in Table 1. After the hybridization and amplification steps, slides were examined using a epifluorescence with Axioplan 2 Imaging (Zeiss; Carl Zeiss Inc., Thornwood, NY) microscope. All results were expressed as number of cells per gram of sediment.

#### DETERMINATION OF CELL NUMBERS BY QUANTITATIVE PCR (qPCR)

qPCR method was employed to determine the relative cell densities of *Alcanivorax*, *Marinobacter*, and *Cycloclasticus* in the sediment samples. Primers used through this study are listed in

**Table 2.** Primers were based on the sequences of *Alcanivorax* alkane hydroxylase gene (*alkB2*), *Marinobacter* alkane hydroxylase gene (*alkB*), and *Cycloclasticus* aromatic ring-hydroxylating dioxygenase (*phnA*) gene. Primers for *alkB2* and *phnA* genes were previously designed and validated for qPCR elsewhere (McKew et al., 2007; Gray et al., 2011). The primers specific for the *alkB* gene of *Marinobacter* were designed through this study using Primer Express software Primer Express software, version 2.0 (Applied Biosystems, Foster City, Calif.) with reference to the *Marinobacter hydrocarbonoclasticus* (FO203363).

Total DNA was extracted from 2.0 g of sediment samples collected at selected time scales from three different points inside the MSS by using a Bio101 FastDNA SPIN kit as described by the manufacturer (Bio101, Inc., Vista, Calif.). Extracted DNA was dissolved in 50 µl of TE buffer (10 mM Tris-HCl, 1 mM EDTA [pH 7.5]) and quantified using a NanoDrop ND-1000 spectrophotometer (Celbio). The quality of the extracted DNA was analyzed by electrophoresis on a 1.0% agarose gel. The qPCR was performed with absolute quantification method in an ABI Prism 7300 Real-time PCR System (Applied Biosystems) in a total volume of 25 µl, consisting 12.5 µl of SYBR green master mix, 200 nM of each primers, and 50 ng of template DNA. The volume of each reaction was adjusted to 25 µl by adding DNase-free water. The cycling parameters for the qPCR amplification were as follows: an initial denaturation step at 95°C for 10 min, followed by 45 cycles of denaturation at 95°C for 15 s and annealing/elongation at 60°C for 60 s. A dissociation step was added to check for primer-dimer formation. A tenfold serial dilution series of genomic DNA ranging from 10 to 10<sup>8</sup> copies per reaction was used in triplicate to create the standard curve for quantification. Serial dilutions were prepared once for each target and used for real-time quantification. From the slope of each curve, PCR amplification efficiency was calculated as it described elsewhere (Rasmussen, 2001). Obtained slope values, (-3.17 for *alkB2*, -3.29 for *alkB*, and -3.37 for *phnA*) fell within the optimal

**Table 1 | CARD-FISH specific probes used in the present study.**

Probe	Sequence (5' to 3') of probe	FA (%)	Source
Eub338	GCTGCCTCCCGTAGGAGT	35	Amann et al., 1990
<i>Marinobacter</i> sp.	ATGCTTAGGAATCTGCCAGTAGTG	20	Karner and Fuhrman, 1997
<i>Cycloclasticus</i> sp.	GGAAACCCGCCAACAGT	20	Karner and Fuhrman, 1997
<i>Alcanivorax</i> sp.	CGACGCGAGCTCATCCATCA	20	Karner and Fuhrman, 1997

FA: percentage of formamide in hybridization buffer.

**Table 2 | qPCR primers used in the present study.**

Gene	Forward Reverse	Organism	Amplification efficiency (E)	Source
<i>alkB2</i>	CGCCGTGTGAATGACAAGGG CGACGCTTGGCGTAAGCATG	<i>Alcanivorax</i>	99.6%	McKew et al., 2007
<i>alkB</i>	TCCCTTGGTATGGCGCAGTT ACGATCCTGTTCAAGCCGAG	<i>Marinobacter</i>	97.3%	This study
<i>phnA</i>	CGTTGTGCGCATAAAGGTGCGG CTTGCCCTTCATACCCGCC	<i>Cycloclasticus</i>	96.2%	McKew et al., 2007

range corresponding to an efficiency of 99.6, 97.3, and 96.2%, respectively. Amplicon numbers were quantified against the standard curve using automatic analysis settings for the Ct values and baseline settings. Detected target genes were converted to cell density in sediments (cells gram<sup>-1</sup>) assuming that all three genes present as a single copy per genome.

## STATISTICAL ANALYSIS

For statistical analyses, clones from each 16S crDNA library were separately considered to define phylotypes, or operational taxonomic units (OTUs) at cutoff of either 95 or 97% of sequence identity (Kemp and Aller, 2004). Clustering of sequences was performed using Dotur program (Schloss and Handelsman, 2005). Various parameters for each clone library, such as diversity index, rarefaction analysis, taxa, total clones, singletons, Shannon dominance, equitability, Simpson and chao2 were calculated by PAST version 2.17c (<http://folk.uio.no/ohammer/past>; Hammer et al., 2001). Coverage values given as  $C = 1 - (n_1/N)$ , where  $n_1$  is the number of clones which occurred only once in the library of N clones (Good, 1953), were calculated to determine how efficient clone libraries described the complexity of original bacterial community. The Primer 6 ecological software package developed by the Plymouth Marine Laboratory (Clarke and Gorley, 2006) was employed to perform the Hierarchical Cluster Analysis (HCA) (Clarke, 1993). We applied HCA on microbial biodiversity and Bray-Curtis similarity on relative abundance matrix of the OTUs detected at different sampling time. Significant difference of the microbial assemblages derived from both treated and control samples at the different sampling times was detected via the *P*-test significance and principal coordinates analysis (PCoA) using UniFrac program (<http://bmf.colorado.edu/unifrac/index.psp>, last access: 24 July 2008) (Lozupone et al., 2007). Differences in cell number per gram of sediment detected by DAPI, CARD, and qPCR between different samples was examined by analysis of variance (ANOVA) on ranks (Holm\_Sidak method). Relative importance of each treatment group was investigated by Multiple Comparisons vs. Control Group comparison test. Calculations were carried out using SigmaStat software for Windows, ver.

3.1 (Copyright 1992–1995; Jandel Corporation). Differences were considered significant at  $P < 0.05$ .

## NUCLEOTIDE SEQUENCE ACCESSION NUMBERS

To avoid the submission of identical sequences obtained among 411 analyzed clones, only 98 distinguishing 16S rRNA gene sequences have been deposited in the DDBJ/EMBL/GenBank databases under accession numbers KF896304-KF896401.

## RESULTS

### GEOCHEMICAL PROPERTIES OF THE SEDIMENTS

Oxygen consumption in the external superficial sediments (0–5 cm) was monitored during all 3 months of experimentation. These values were compared with BOD in the internal MSS sediments taken at the beginning ( $T_0$ ), after 1 day ( $T_1$ ), 1 month ( $T_{29}$ ), and after 3 months ( $T_{90}$ ) of experimentation (Figure 2). Sediments outside of the MSS exhibited constant BOD rates of approximately 2.5 mg O<sub>2</sub> day<sup>-1</sup> kg<sup>-1</sup> during all period of experimentation, whereas the aerated sediments inside of the MSS demonstrated a progressive increment of oxygen consumption. Maximum of oxygen demand (16.0 mg O<sub>2</sub> day<sup>-1</sup> kg<sup>-1</sup>) was obtained at  $T_{29}$  and afterwards the BOD values tended to diminish, reaching 10.0 mg O<sub>2</sub> day<sup>-1</sup> kg<sup>-1</sup> at the end of experiment. Outside the MSS, the amendment of the Bunker C furnace fuel oil turned initially oxygenated ( $T_0$ ,  $E_h = 77 \pm 4$  mV) sediments into highly reduced ones (Figure 3). The external sediments below 5 cm became oxygen-depleted already within 1 day after spiking, obviously due to the active respiration of aerobic heterotrophic microorganisms. The reduction potential of external sediments decreased continuously during the experiment and after 3 months reached the  $E_h$  values of –345 mV in the deepest layers. In contrary, inside the MSS the sediments remained aerobic during all period of bioremediation effort.

### HYDROCARBON ANALYSIS

Before the addition of 6500 ppm of Bunker C fuel oil into the mesocosm, the total hydrocarbon concentration in the original Messina harbor sediments was estimated at the level of 120 ppm.

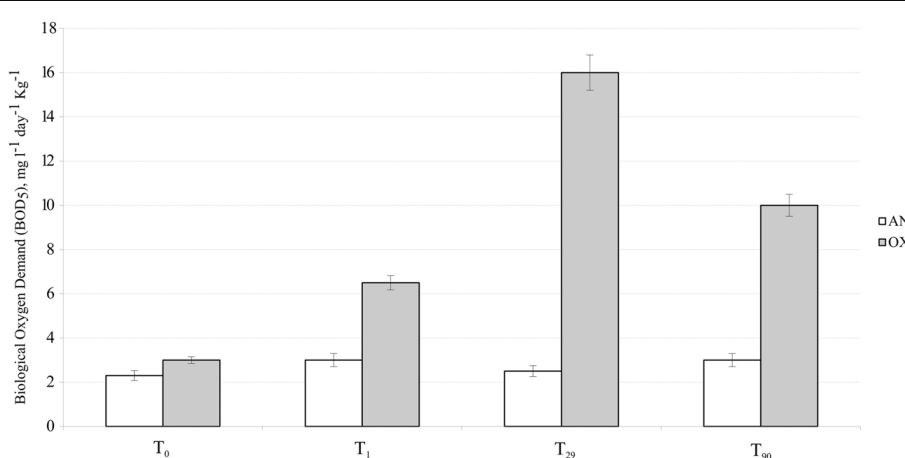
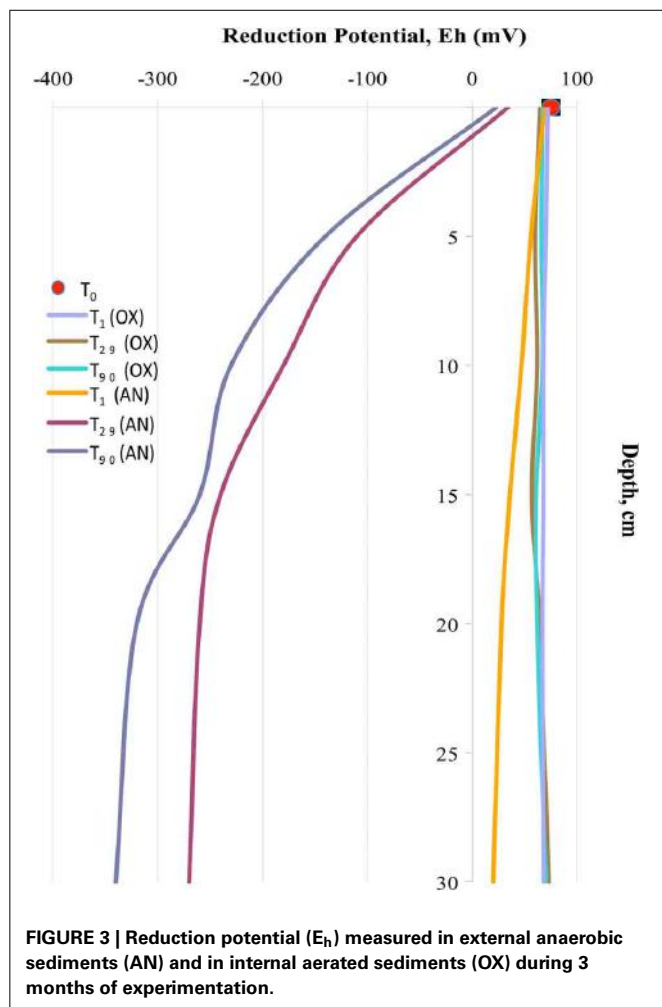


**FIGURE 2 | Dynamic of oxygen consumption (BOD values) measured in MSS external (untreated) superficial sediments (white bars) and internal sediments (gray bars).** Error bar indicates the standard deviation of triplicate measurements.



The PHs fingerprint analysis showed a clear dominance of alkyl-aromatic derivatives (97%) over aliphatic hydrocarbons (3%) (data not shown). Once Bunker C fuel oil was added to the sediments, the TERHC fraction mass balance was shifted toward the dominance of aliphatic and naphthenic hydrocarbons (70%) over aromatics (30%). The degree of the Bunker C fuel oil degradation in both, aerated MSS and in the untreated anoxic sediments was examined at the end of experiment ( $T_{90}$ ). The concentration of PHs, especially aliphatic hydrocarbons was normalized using the pristane/phytane ratio, and the values obtained in triplicate subsamples were averaged. In the aerated internal MSS sediments, the total degradation of Bunker C fuel oil TERHC fraction was  $97.7 \pm 0.9\%$ . In contrast, external anoxic sediments contained more than  $81.8 \pm 1.2\%$  of initially added Bunker C fuel oil. Additionally, we performed the gravimetric analysis of total extracted hydrophobic fraction (TEHF) in the sediments. The TEHF values inside the MSS accounted for  $780 \pm 80 \text{ mg kg}^{-1}$  dry sediment weight, whereas in concordance with extremely slow biodegradation rates under anaerobic conditions, the external sediments contained more than  $5400 \pm 120 \text{ mg kg}^{-1}$  of hydrophobic material. As shown in subsequent section, TEH fraction seems to be primarily responsible for the observed toxicity of Bunker C fuel oil.

## ECOTOXICOLOGICAL ANALYSIS

According to standard guidelines of Italian Institute for Environmental Protection and Research (ISPRA, 2013), ecotoxicological analysis of hydrocarbon-contaminated sediments were carried out using the Microtox® luminescence and amphipod *Corophium orientale* bioassays. Eventual decrease in Microtox® bioluminescence was measured on sediment pore water, whereas the rate of amphipods mortality was tested by direct exposition of *C. orientale* with the petroleum-contaminated sediments during 10 days. Following the EN12457 protocol, we combined the sediment pore water with sterile seawater in both 1:2 and 1:10 ratios (vol/vol) and no significant level of bioluminescence decay has been observed. As it reported in EN12457 protocol, Microtox® bioluminescent assay tested on sediment pore water typically exhibits an underestimated sensitivity against highly hydrophobic contaminants, such as PHs. This is mainly due to both extremely low solubility of these compounds in water and an almost irreversible adsorption to a sedimentary matrix. Corresponding to the standardized protocol described by Onorati et al. (1999), the toxicological analysis of the sediments was performed with amphipods *C. orientale*. Addition of Bunker C fuel oil to the sediments ( $T_0$ ) caused the mortality in almost all organisms ( $98 \pm 2\%$ ). The petroleum-contaminated external sediments remained highly toxic during all 3 months of experimentation with mortality indices exceeding 90% (Figure 4). At the same time, the toxicity of polluted internal MSS sediments dropped almost twice after 1 month of aeration ( $T_{29}$ ) and continued to decrease till the end of bioremediation treatment, approaching the vitality of 62% of amphipods exposed to  $T_{90}$  sediments. This indicated that the internal MSS sediment at  $T_{90}$  was significantly less toxic than their external counterpart.

## DIVERSITY AND SUCCESSION OF BACTERIAL COMMUNITIES DURING BIOREMEDIATION AND NATURAL SEDIMENT AGEING

To monitor the succession of metabolically active microbial communities during the bioremediation treatment, five 16S rRNA transcript libraries were established. 450 clones from these libraries were randomly selected and analyzed. Among those, 411 sequences were included into phylogenetic analysis ( $T_0$ , 96 clones;  $T_1$ , 83 clones;  $T_{29}$ , 80 clones;  $T_{90}$ , 90 clones and  $T_{90OUT}$ , 62 clones). The majority of native  $T_0$  clones were affiliated with the *Gammaproteobacteria* (51%), followed by the *Alphaproteobacteria* (22%). Other proteobacteria, belonging to microaerophilic and anaerobic *Epsilon-* and *Delta-**proteobacteria* were also present, although in significantly lower numbers (6 and 2% of all clones analyzed, respectively). Remaining fraction of  $T_0$  microbial community consisted of the members of *Cyanobacteria* (7%), *Chloroflexi* (5%), *Verrucomicrobia* (3%), and *Bacteroidetes* (2%) (Figure 5). At the level of the Class, the derived from members of *Gammaproteobacteria* were predominant in all analyzed MSS internal sediments, with percentage ranging from 73 to 88%. There was a 50%-reduction of *Alphaproteobacteria* observed during first month of sediment treatment (decrease from 22 to 11%). Further on, their numbers returned to the initial ( $T_0$ ) values by the end of experiment. No *Delta-**proteobacteria*-related organisms were detected in the internal MSS sediments throughout the experiment. A completely different scenario was

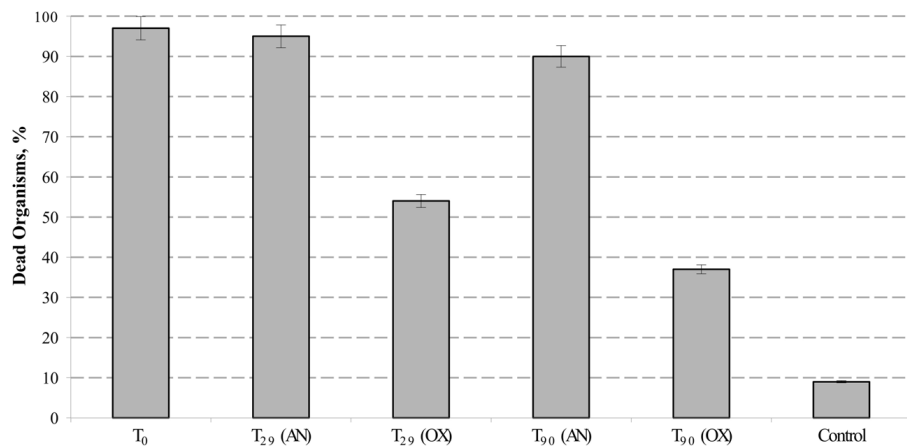


**FIGURE 4 | Mortality of *Corophium orientale* organisms in polluted (AN), treated (OX), and control (native) sediments.** Error bar indicates the standard deviation of duplicate measurements.

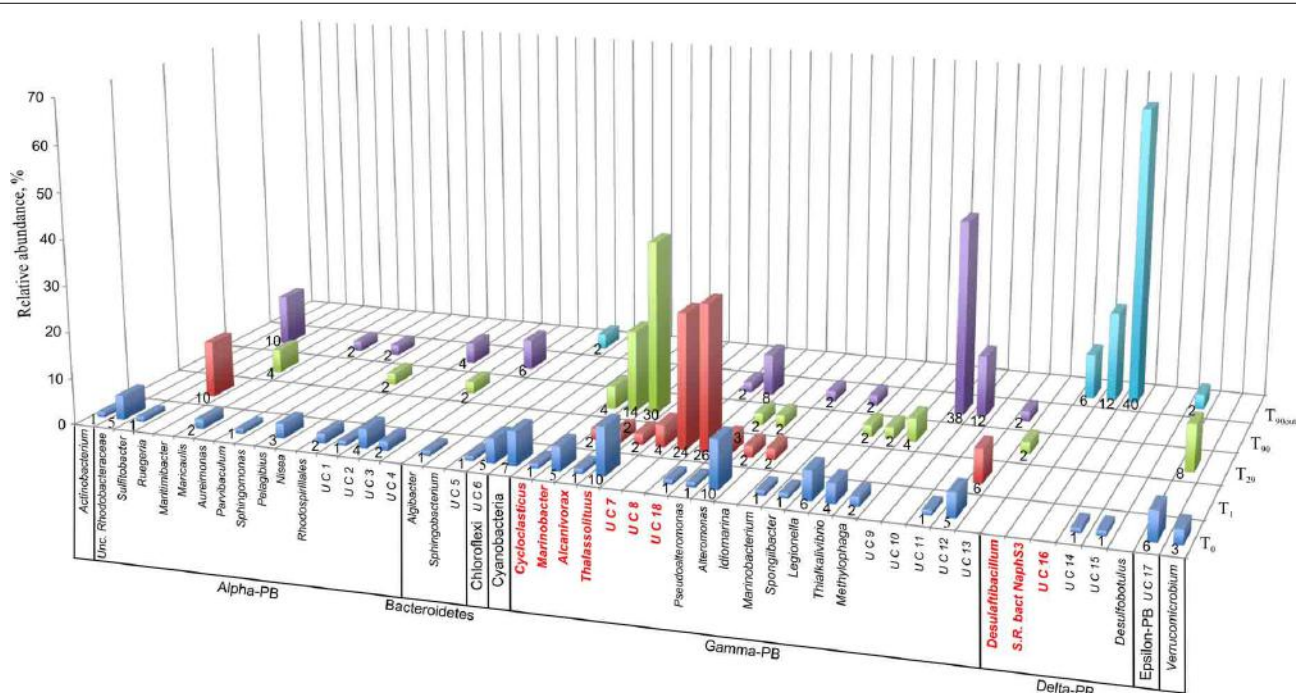
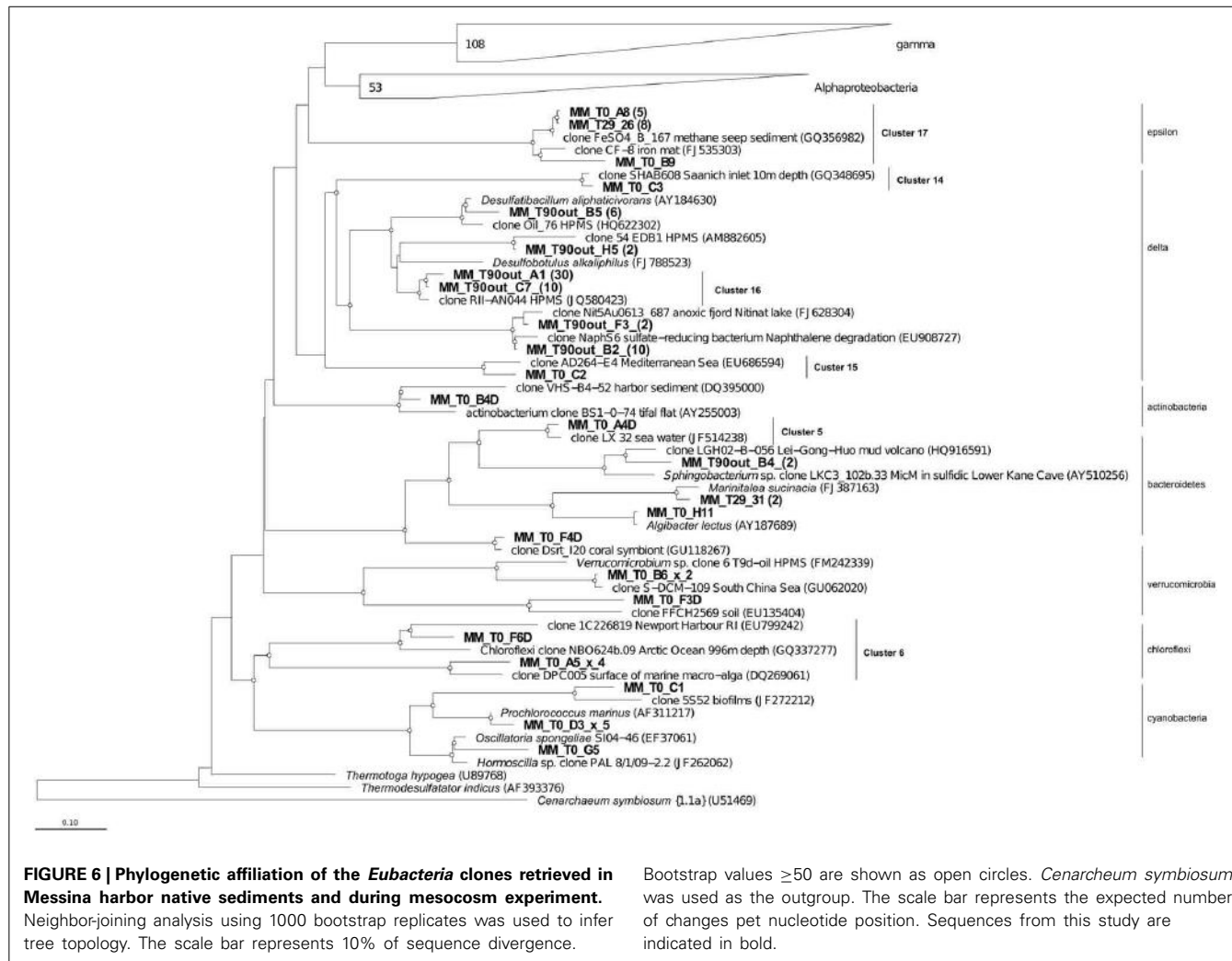


**FIGURE 5 | Dendrogram representation of taxonomic analysis of 16S crDNA clones retrieved from five libraries.** The numbers at the base of columns represent the percentage of clones in corresponding libraries.

Abbreviations used: PB, *Proteobacteria* divisions; UC, Unaffiliated cluster. Bacterial groups involved in, or associated to, hydrocarbon degradation are marked in bold and red.

observed regarding the succession of microbial community thriving in the external anoxic sediments. As we mentioned above, after loading the Bunker C fuel oil, the sediments became highly reduced within a short period of time and were inhabited mainly by the members of *Delta proteobacteria* (96.8%). The analysis of 16S rRNA transcripts from T<sub>90</sub>OUT clone library revealed a notable prevalence of hydrocarbon-degrading or hydrocarbon contamination-associated *Delta proteobacteria* (90.3%). In particular, almost two-thirds of all clones (40 out of 62 clones

analyzed) were closely related to the uncultured bacterium RII-AN044 found in anoxic polluted sediments after the Prestige oil spill (Acosta González et al., 2013). More than 16% of clones revealed >98% of similarity to the delta-proteobacterium NaphS6, capable of naphthalene and 2-methylnaphthalene degradation (Wilkes et al., 2008). Almost 10% of T<sub>90</sub>OUT clones were closely related to the *n*-alkanes- and *n*-alkenes-degrading strain *Desulfatibacillus aliphaticivorans* (Cravo-Laureau et al., 2004) (Figure 6).



In accordance with the type of the contaminant load, the majority of analyzed clones had highest Blastn homologies with sequences related to PH-degrading or petroleum contamination-associated organisms belonging to the *Gamma*-, *Alpha*- and *Delta*proteobacteria (Figures 6–8). At the genus and species level, more than 10% of initial microbial population was attributed to obligate marine hydrocarbonoclastic bacteria *Thalassolituus oleivorans* (Yakimov et al., 2004). This organism seemed to be sensitive to Bunker C fuel oil, since its abundance decreased to 2% after 1 day of oil exposition and disappeared afterwards. Three other OMHCB belonging to genera *Alcanivorax*, *Cycloclasticus*, and *Marinobacter* demonstrated similar dynamics, i.e., being in relative minority in the beginning of the experiment, they became predominant in T<sub>29</sub> microbial community and disappeared in the T<sub>90</sub> library (Figure 5). Noteworthy, the addition of Bunker C fuel oil to sediments drastically changed the structure of T<sub>1</sub> microbial community and the proportion of aforementioned *Gammaproteobacteria*-related OMHCB decreased threefold compared with the initial population. In contrast, previously undetected organisms related to dinoflagellate-associated *Rugeria* sp. and to three deep-branching clusters of

*Gammaproteobacteria* accounted for 77% of all analyzed T<sub>1</sub> clones. Having only 16S rRNA gene sequences at our disposal, we cannot state that these uncultured organisms were involved in biodegradation activity, but they definitely possessed a remarkable resilience to the toxicity of Bunker C fuel oil (Païssé et al., 2008, 2010).

Additionally to 16S rRNA-based analysis, the diversity and succession of both, total bacterial population and hydrocarbon-degrading bacteria, was assessed through the combined application of CARD-FISH and qPCR. Using the *Eubacteria*-specific probe Eub338, the concentration of CARD-positive cells at the beginning of experiment was estimated at  $2.98 \pm 0.17 \times 10^6$  cells  $\text{gram}^{-1}$  (Table 3). Their numbers decreased by 20% within 1 day after the oil spill simulation ( $P < 0.001$ ,  $n = 10$ ) and reached initial values at the end of experiment ( $2.79 \pm 0.12 \times 10^6$  cells  $\text{gram}^{-1}$ ). Noteworthy, a tenfold increase in the number of CARD-positive cells ( $2.95 \pm 0.11 \times 10^7$  cells  $\text{gram}^{-1}$ ) was detected after 29 days of oil spill, which fully corresponded to the observed dynamics of the BOD and clone libraries' values (Figure 2). Before the oil spill simulation (T<sub>0</sub>), the fraction of *Alcanivorax*-related cells, detected with the CARD-FISH

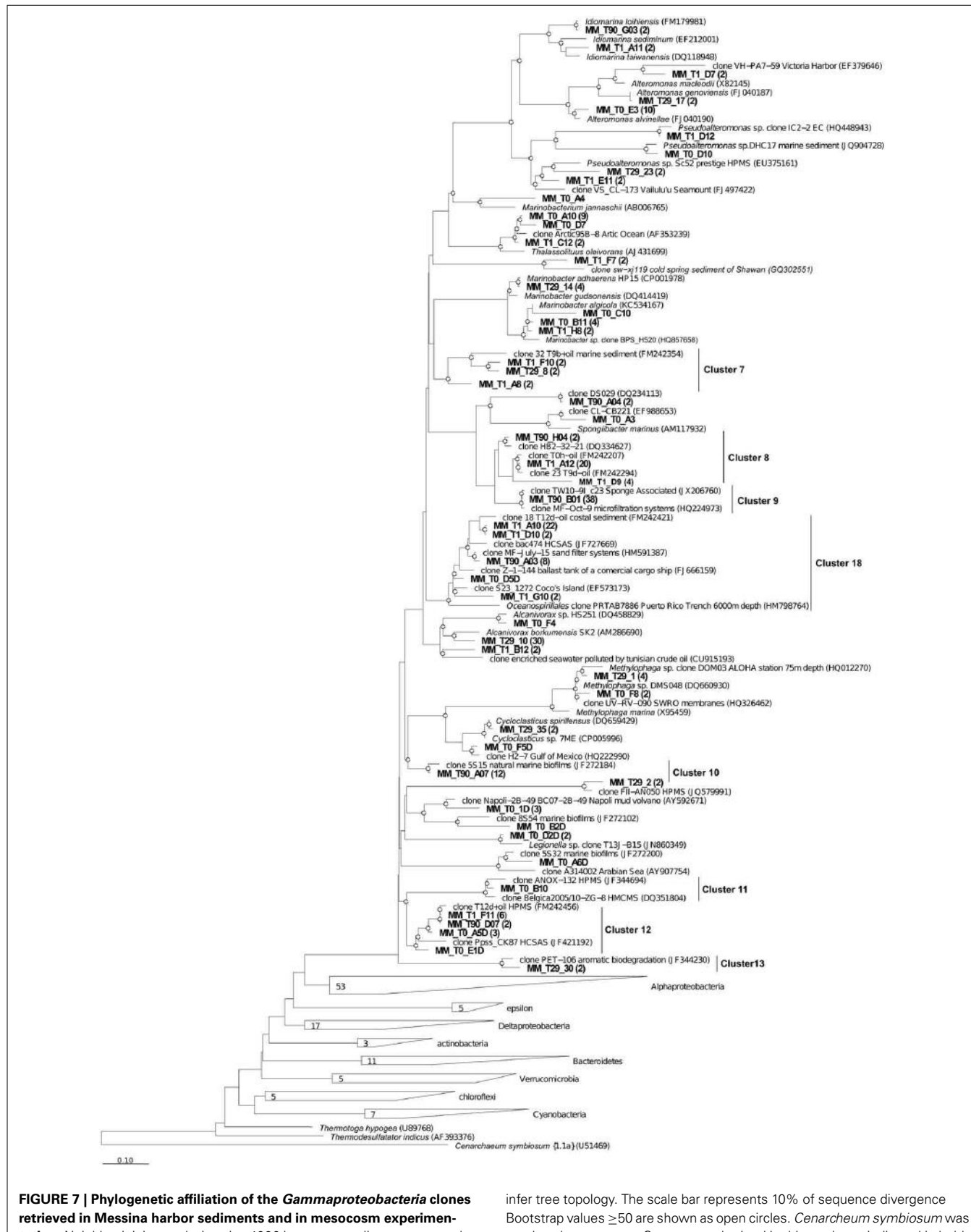
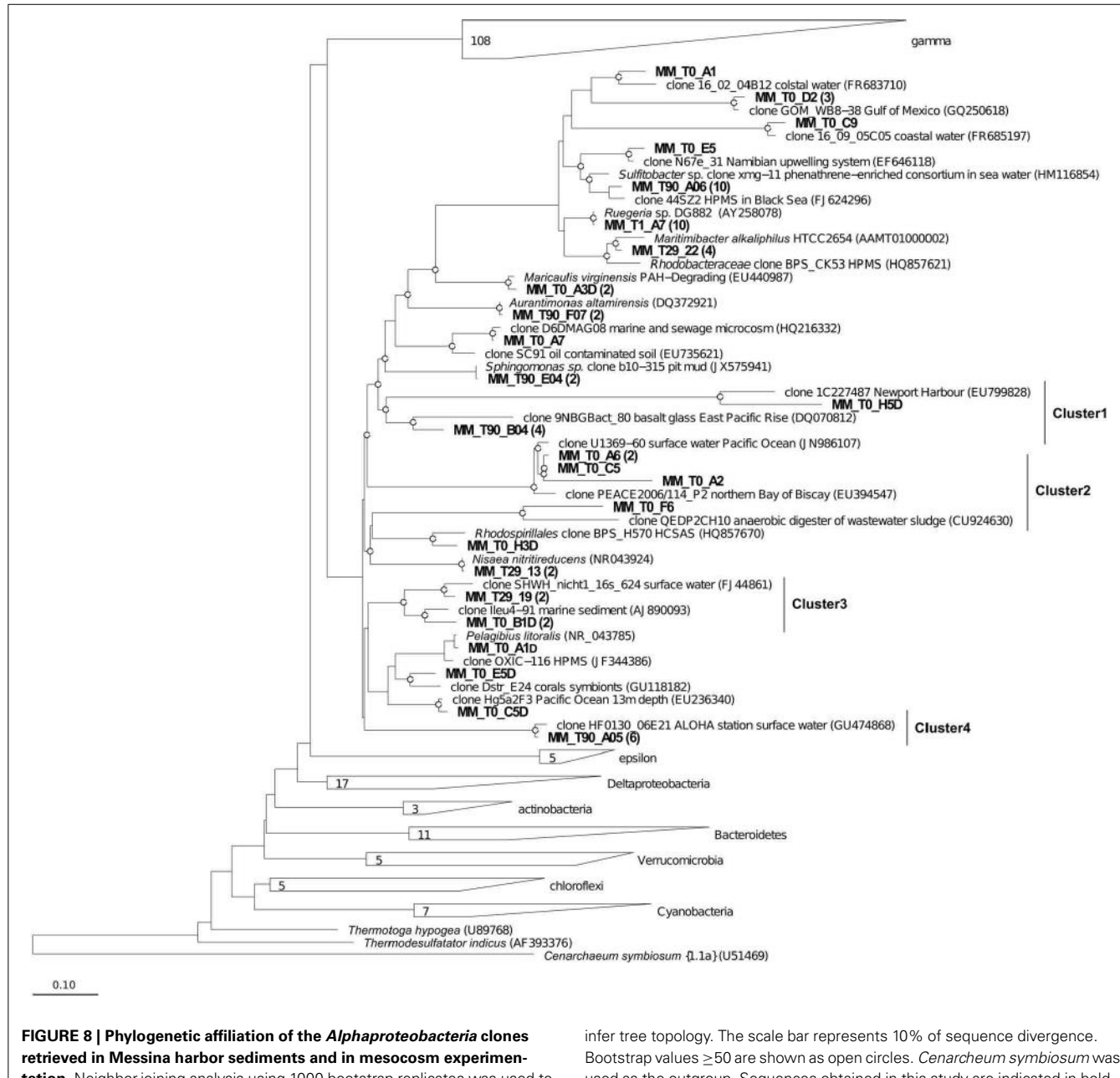


**FIGURE 7 | Phylogenetic affiliation of the *Gammaproteobacteria* clones retrieved in Messina harbor sediments and in mesocosm experimentation.** Neighbor-joining analysis using 1000 bootstrap replicates was used to infer tree topology. The scale bar represents 10% of sequence divergence. Bootstrap values  $\geq 50$  are shown as open circles. *Cenarcheum symbiosum* was used as the out-group. Sequences obtained in this study are indicated in bold.

infer tree topology. The scale bar represents 10% of sequence divergence. Bootstrap values  $\geq 50$  are shown as open circles. *Cenarcheum symbiosum* was used as the out-group. Sequences obtained in this study are indicated in bold.



genus-specific probe, accounted for 7.7% of all Eub338-positive cells. After the addition of Bunker C fuel oil, their abundance increased within 1 month up to 27.5%. According to the analysis of 16S crDNA clone libraries, *Alcanivorax* became extinct in microbial community thriving in the MSS internal sediments at the end of experiment. Dynamics of the *Marinobacter*-related bacteria was comparable with that of *Alcanivorax* population, with the only exception that the *Marinobacter* cells decreased their abundance by 44% at  $T_1$ , likely due to the higher sensitivity to the load of fuel oil. Compared to an initial density, their population increased twofold at  $T_{29}$ , from  $4.5 \pm 0.2$  to  $9.0 \pm 0.1 \times 10^5$  cells  $g^{-1}$ . Although due to the overwhelming growth of *Alcanivorax*,

the relative abundance of *Marinobacter* during bioremediation experiment has never exceeded its initial values (15.2% of all Eub338-stained cells at  $T_0$ ) and at  $T_{29}$  (corresponding to the maximum of cell density in MSS) accounted for only 3% of total microbial community. Bacteria stained with *Cycloclasticus*-specific CARD-FISH probe, initially present in mesocosm sediments at concentration of  $1.14 \pm 0.15 \times 10^5$  cells  $gram^{-1}$ , were not detected at  $T_1$ , whereas their concentration increased four times after 1 month of the oil spill simulation. Similarly to the dynamics of *Alcanivorax*, neither *Marinobacter*, nor *Cycloclasticus* were present in the MSS microbial community at the end of experiment.

Succession of hydrocarbon-degrading bacteria during the sediment bioremediation was additionally quantified by qPCR. Based on the a priori higher sensitivity of qPCR approach, obtained numbers were slightly higher than those from taxon-specific CARD-FISH data. Nevertheless, obtained results remarkably corroborated with CARD-FISH counts and the general trend in *Alcanivorax*, *Marinobacter*, and *Cycloclasticus* dynamics was identical (Table 3). None of these hydrocarbon-degrading bacteria were detected by qPCR at the end of experiment.

### STATISTICAL ANALYSIS OF BACTERIAL DIVERSITY

As it shown in Table 4, the diversity index and coverage values have been calculated for each 16S rRNA transcript library. Based on sequence similarity threshold for OTU definition  $\geq 97\%$  (Rosselló-Mora and Amann, 2001), a total of 93 different OTUs were discerned. The rarefaction analysis did not demonstrate the saturation in any library (data not shown), however, the coverage values varying between 0.64 ( $T_0$  library) and 0.92 ( $T_{90OUT}$  library) indicated that a satisfactory overview on bacterial community was obtained. As reflected by the high values of Simpson, Shannon and the number of missing species provided by Chao-2, the highest bacterial diversity was observed in original sediments ( $T_0$ ). Bacterial biodiversity was drastically affected by Bunker C fuel oil addition, decreasing the Simpson, Shannon and Equitability values, due to strong selection for both petroleum contamination-resilient and hydrocarbon-degrading bacteria (Harayama et al., 1999; Kasai et al., 2001, 2002; Syutsubo et al., 2001). Dominance index reached the highest value at  $T_{29}$  and  $T_{90}$ . After 1 month of aeration, the microbial population of the internal MSS sediments was dominated by OMHCBS, whereas at the end of experiment, the dominant Cluster 9 of the *Gammaproteobacteria* accounted for 42% of all  $T_{90}$  clones. This cluster consists of organisms recovered from pristine seawater and marine sediments. As mentioned above, the microbial community of anaerobic external sediments  $T_{90OUT}$  was totally different compared with aerated internal sediments. Both fuel oil contamination and rapid development of anaerobiosis have selected a very specialized and poorly diverse microbial population (5 OTUs; Dominance 0.44; Coverage 91%). These data were confirmed by the HCA and UniFrac PCoA analyses. At the end of the experiment, the microbial communities thriving in the

MSS external ( $T_{90OUT}$ ) and the internal ( $T_{90}$ ) sediments were significantly different from each other ( $P1 = 50.85\%$  and  $P2 = 31.39\%$ ). Noteworthy, both applied statistical analyses confirmed that comparing with OMHCB-enriched  $T_{29}$  population, the  $T_{90}$  microbial community was more similar to those recovered from early stages of the experiment ( $T_0$  and  $T_1$  libraries) (Figure 9). This finding indirectly hints at the process of self-recovery of petroleum-contaminated sediments, which was confirmed by GC analysis of the contaminated sediments in and outside the MSS.

### DISCUSSION

The influence of the massive Bunker C fuel oil load upon the microbial population of coastal sediments collected in Messina harbor and their recovery was investigated during 3 months in the mesocosms experiment. These sediments chronically polluted with alkynaphthalenes were chosen since the autochthonous microbial community is likely adapted to the steady presence of PHs and consequently may exhibit a higher biodegradation ability than those from pristine environments (Païssé et al., 2008, 2010). Accordingly, the fraction of the OMHCB genera *Alcanivorax*, *Cycloclasticus*, *Marinobacter* and *Thalassolituus*, usually imperceptible in pristine marine environments (Yakimov et al., 2007), accounted for a fifth part of the native microbial community of Messina harbor sediments. To simulate accidental oil spill we spiked 1000 kg sandy sediments with Bunker C fuel oil (6500 mg

**Table 4 | Diversity indices calculated for the five clone libraries created at different time of aeration and sediment ageing.**

Diversity index	$T_0$	$T_1$	$T_{29}$	$T_{90}$	$T_{90OUT}$
Taxa/(OTUs)_S	46	16	14	12	5
Number of clones	96	83	80	90	62
Dominance_D	0.04	0.15	0.22	0.24	0.44
Simpson_1-D	0.96	0.85	0.78	0.76	0.55
Shannon_H	3.5	2.31	2.08	1.89	1.09
Equitability_J	0.91	0.84	0.78	0.76	0.68
Chao-2	104.1	16	14	12	5
Singletomes	31	1	0	0	0
Doubletones	7	10	8	6	2
Coverage	0.64	0.74	0.77	0.87	0.92

**Table 3 | CARD-FISH and qPCR cell number quantification in the MSS internal sediment during the bioremediation treatment.**

Method	Probe/primers	Cell numbers, $10^5 \times g$ sediments $^{-1} \pm SD$			
		$T_0$	$T_1$	$T_{29}$	$T_{90}$
CARD-FISH	<i>Eubacteria</i>	$29.8 \pm 1.7$	$23.6 \pm 1.5$	$295.0 \pm 11.0$	$27.9 \pm 1.2$
	<i>Alcanivorax</i> sp.	$2.3 \pm 0.1$	$3.1 \pm 0.2$	$81.0 \pm 1.3$	ND
	<i>Marinobacter</i> sp.	$4.5 \pm 0.2$	$2.6 \pm 0.1$	$9.0 \pm 0.1$	ND
	<i>Cycloclasticus</i> sp.	$1.2 \pm 0.2$	ND	$4.9 \pm 0.1$	ND
qPCR*	<i>alkB2</i>	$5.17 \pm 0.17$	$4.73 \pm 0.18$	$94.60 \pm 3.80$	ND
	<i>alkB</i>	$7.90 \pm 0.23$	$3.50 \pm 0.20$	$15.30 \pm 2.00$	ND
	<i>phnA</i>	$2.10 \pm 0.16$	$3.78 \pm 0.12 \times 10^{-3}$	$7.13 \pm 0.28$	ND

\*These values mean the average number of cells detected in triplicate from three individual subsamples of sediments collected in different parts of MSS.

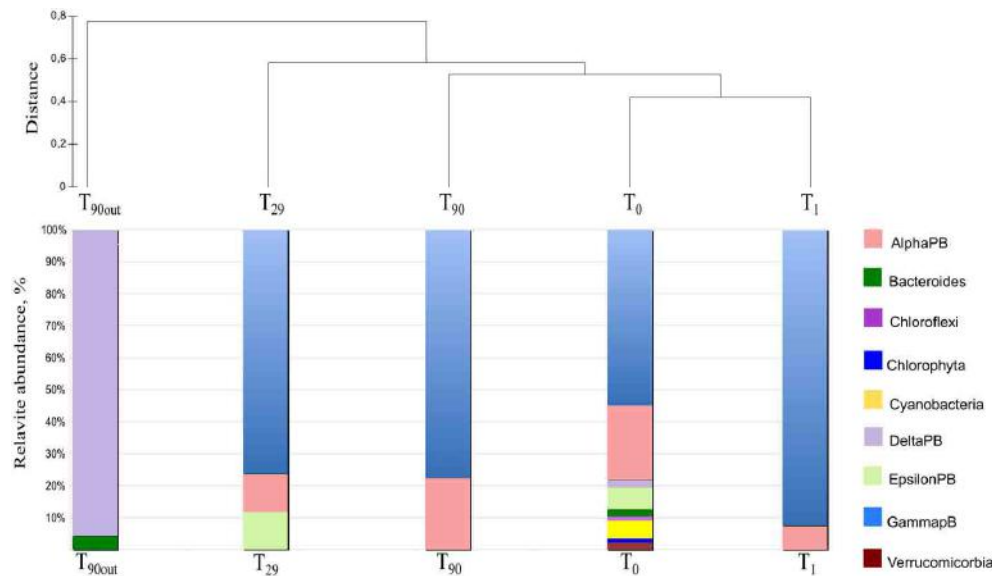


**FIGURE 9 | Dendrogram of microbial biodiversity and similarity analysis of the 16S rRNA transcripts detected at different sampling time and treatment.** The UPGMA cluster analysis was

obtained by using group average clustering from Euclidean distance on relative abundance matrix of OTUs detected in the analyzed libraries.

$\text{kg}^{-1}$ ). This type of heavy fuel oil is frequently used by the cargo and tanker ships and is generally more complex in composition and impurities than distilled fuels. Bunker C fuel oil includes about 25% polycyclic aromatic, 15% aliphatic, 45% naphthenic and 15% non-hydrocarbon compounds (Clark et al., 1990). As it generally observed, after the oil spill reaches a shoreline, the oil burial is the main mechanism of the pollution dispersal. This results in intense oiling of subsurface sediments and consequent reduction in oxygen concentration due to initial activation of aerobic hydrocarbon-degrading microorganisms (Albaiges et al., 2006; Acosta González et al., 2013). Once  $\text{O}_2$  concentration drops to zero, the degradation rates of both aliphatic and aromatic PHs decrease significantly. According with this observation, the oil cleanup was very marginal, and  $>80\%$  of initially added Bunker C fuel oil was extracted from the anaerobic external sediments after 3 months of oil spill simulation. At the end of experiment, analysis of microbial community of the MSS external sediments revealed the overwhelming dominance of the *Delta*proteobacteria.

The stimulation of autochthonous bacteria to tackle the pollution in contaminated environment is widely used in the remediation of aerobic sites (Harayama et al., 2004). However, this technology is hardly applicable to oxygen-depleted marine sediments. Additionally, due to high probability of contaminant spreading while removing, the application of *ex-situ* remediation technologies is severely limited. To initiate the self-cleaning process in sediments driven by indigenous aerobic OMHCB, we used *in situ* aeration of polluted anoxic sediments in specially designed MSS. It is generally assumed, that petroleum contamination induced drastic changes in the bacterial community structure associated with a decrease of diversity (Grötschel et al., 2002; Röling et al., 2002; Yakimov et al., 2005, 2007; Head et al., 2006; Bordenave et al., 2007). These changes were referred

to both toxic effect of PHs and a strong selection toward highly specialized hydrocarbon-degrading microorganisms (Harayama et al., 1999; Kasai et al., 2001; Grötschel et al., 2002; Yakimov et al., 2005, 2007). Accordingly, the most drastic shifts in the MSS bacterial community dynamic was observed at the beginning and after 1 month of the oil spill. As revealed by 16S crDNA clone library analysis, more than a half of MSS microbial population at T<sub>29</sub>, belonged to *Alcanivorax* (43%), *Cycloclasticus* (7%) and *Marinobacter* (5%), the genera of OMHCB, known to play a pivotal role in petroleum degradation in marine environments (Harayama et al., 1999; Röling et al., 2002, 2004; Yakimov et al., 2007). Noteworthy, the dominance of these OMHCB genera was confirmed by both CARD-FISH and qPCR analyses. At the end of the treatment, the level of TERHC degradation in the MSS internal sediments was almost 98%, and the resulting microbial community was characterized by an almost complete extinction of OMHCBs. Both HCA and UniFrac PCoA statistic analyses of the OTUs abundance matrix indicated that the structure of T<sub>90</sub> microbial community was more similar to initial microbial community structures. As a consequence of successful bioremediation, the *Corophium orientale* eco-toxicological bioassay revealed that toxicity of the MSS internal sediments was substantially lower compared with the untreated external sediments. Thus, to the best of our knowledge, our studies for the first time demonstrated that petroleum-contaminated anaerobic marine sediments could be efficiently recovered by their capping and *in situ* aeration, thus stimulating the self-cleaning potential due to reawakening of residing aerobic OMHCBs.

## ACKNOWLEDGMENTS

This work was funded by the European Community Projects ULIXES (FP7-KBBE-2010-4 Project 266473 “Unravelling and

exploiting Mediterranean Sea microbial diversity and ecology for xenobiotics' and pollutants' clean-up") and KILL-SPILL (FP7-KBBE-2012.3.5-01-4 Project 312139 "Integrated Biotechnological Solutions for Combating Marine Oil Spills"). We would like to thank all partners of these projects for their useful discussions.

## REFERENCES

- Acosta González, A., Rosselló Móra, R., and Marqués, S. (2013). Characterization of the anaerobic microbial community in oil polluted subtidal sediments: aromatic biodegradation potential after the Prestige oil spill. *Environ. Microbiol.* 15, 77–92. doi: 10.1111/j.1462-2920.2012.02782.x
- Albaiges, J., Morales-nin, B., and Villas, F. (2006). The Prestige oil spill: a scientific response. *Mar. Pollut. Bull.* 53, 205–207. doi: 10.1016/j.marpolbul.2006.03.012
- Altschul, S. F., Madden, T. L., Schaffer, A. A., Zhang, J., Zhang, Z., Miller, W., et al. (1997). Gapped BLAST and PSI-BLAST: a new generation of protein database search programs. *Nucleic Acids Res.* 25, 3389–3402. doi: 10.1093/nar/25.17.3389
- Amann, R. I., Krumholz, L., and Stahl, D. A. (1990). Fluorescent-oligonucleotide probing of whole cells for determinative, phylogenetic, and environmental studies in microbiology. *J. Bacteriol.* 172, 762–770.
- Ashelford, K. E., Chuzhanova, N. A., Fry, J. C., Jones, A. J., and Weightman, A. J. (2005). At least 1 in 20 16S rRNA sequence records currently held in public repositories is estimated to contain substantial anomalies. *Appl. Environ. Microbiol.* 71, 7724–773. doi: 10.1128/AEM.71.12.7724-7736.2005
- Benton, M. J., Malott, M. L., Knight, S. S., Cooper, C. M., and Benson, W. H. (1995). Influence of sediment composition on apparent toxicity in a solid phase test using bioluminescent bacteria. *Environ. Toxicol. Chem.* 14, 411–414. doi: 10.1002/etc.5620140309
- Bordenave, S., Goñi-Urriza, M. S., Caumette, P., and Duran, R. (2007). Effects of heavy fuel oil on the bacterial community structure of a pristine microbial mat. *Appl. Environ. Microbiol.* 73, 6089–6097. doi: 10.1128/AEM.01352-07
- Bulich, A. A., Greene, M. W., and Underwood, S. R. (1992). "Measurement of soil and sediment toxicity to bioluminescent bacteria when in direct contact for a fixed time period," in *Memorias de Water Environment Federation, 65th Annual Conference and Exposition* (Nueva Orleans, Louisiana), 53–64.
- Clark, R. N., King, T. V. V., Klejwa, M., Swayze, G., and Vergo, N. (1990). High spectral resolution reflectance spectroscopy of minerals. *J. Geophys. Res.* 95, 12653–12680. doi: 10.1029/JB095iB08p12653
- Clarke, K. R. (1993). Non parametric multivariate analyses of changes in community structure. *Aust. J. Ecol.* 18, 117–143. doi: 10.1111/j.1442-9993.1993.tb00438.x
- Clarke, K. R., and Gorley, R. N. (2006). *PRIMER v6. User Manual and Tutorial*. Plymouth: PRIMER-E.
- Cravo-Laureau, C., Matheron, R., Cayol, J. L., Joulian, C., and Hirschler-Réa, A. (2004). *Desulfatibacillum aliphaticivorans* gen. nov., sp. nov., an n-alkane-and n-alkene-degrading, sulfate-reducing bacterium. *Int. J. Syst. Evol. Microbiol.* 54, 77–83. doi: 10.1099/ijss.0.027170-0
- Dyksterhouse, S. E., Gray, J. P., Herwig, R. P., Lara, J. C., and Staley, J. T. (1995). *Cycloclasticus pugettii* gen. nov., sp. nov., an aromatic hydrocarbon-degrading bacterium from marine sediments. *Int. J. Syst. Bacteriol.* 45, 116–123. doi: 10.1099/0020713-45-1-116
- Engelen, B., and Cypionka, H. (2009). The subsurface of tidal-flat sediments as a model for the deep biosphere. *Ocean Dynam.* 59, 385–391. doi: 10.1007/s10236-008-0166
- Ferraro, G., Bernardini, A., David, M., Meyer-Roux, S., Muellenhoff, O., Perkovic, M., et al. (2007). Towards an operational use of space imagery for oil pollution monitoring in the Mediterranean basin: a demonstration in the Adriatic Sea. *Mar. Pollut. Bull.* 54, 403–422. doi: 10.1016/j.marpolbul.2006.11.022
- Gertler, C., Yakimov, M. M., Malpass, M. C., and Golyshin, P. N. (2010). "Shipping-related accidental and deliberate release into the environment," in *Handbook of Hydrocarbon and Lipid Microbiology*, ed. K. N. Timmis (Berlin, Heidelberg: Springer), 243–256. doi: 10.1007/978-3-540-77587-4\_16
- Golyshin, P. N., Chernikova, T. N., Abraham, W. R., Lünsdorf, H., Timmis, K. N., and Yakimov, M. M. (2002). *Oleophilaceae* fam. nov., to include *Oleophilus messinensis* gen. nov., sp nov., a novel marine bacterium that obligately utilizes hydrocarbons. *Int. J. Syst. Evol. Microbiol.* 52, 901–911. doi: 10.1099/ijss.0.01890-0
- Good, I. J. (1953). The population frequencies of species and the estimation of population parameters. *Biometrika* 40, 237–264. doi: 10.2307/2333344
- Gray, S. B., Classen, A. T., Kardol, P., Yermakov, Z., and Miller, R. M. (2011). Multiple climate change factors interact to alter soil microbial community structure in an old-field ecosystem. *Soil Sci. Soc. Am. J.* 75, 2217–2226. doi: 10.2136/sssaj2011.0135
- Grötzschel, S., Köster, J., Abed, R. M. M., and De Beer, D. (2002). Degradation of petroleum model compounds immobilized on clay by a hypersaline microbial mat. *Biodegradation* 13, 273–283. doi: 10.1023/A:1021263009377
- Hammer, Ø., Harper, D. A. T., and Ryan, P. D. (2001). PAST: palaeontological statistics software package for education and data analysis. *Palaeontol. Electron.* 4, 9.
- Hara, A., Syutsubo, K., and Harayama, S. (2003). *Alcanivorax* which prevails in oil-contaminated seawater exhibits broad substrate specificity for alkane degradation. *Environ. Microbiol.* 5, 746–753. doi: 10.1046/j.1468-2920.2003.00468.x
- Harayama, S., Kasai, Y., and Hara, A. (2004). Microbial communities in oil-contaminated seawater. *Curr. Opin. Biotechnol.* 15, 205–214. doi: 10.1016/j.copbio.2004.04.002
- Harayama, S., Kishira, H., Kasai, Y., and Shutsubo, K. (1999). Petroleum biodegradation in marine environments. *J. Mol. Microbiol. Biotechnol.* 1, 63–70.
- Head, I. M., Jones, D. M., and Röling, W. F. (2006). Marine microorganisms make a meal of oil. *Nat. Rev. Microbiol.* 4, 173–182. doi: 10.1038/nrmicro1348
- ISPRA. (2013). "Batterie di saggi ecotossicologici per sedimenti e acque interne," in *Manuali di Ecotossicologia*, eds ISPRA-settore editoria. ISBN: 978-88-448-0607-1.
- Karner, M. B., and Fuhrman, J. (1997). Determination of active marine bacterioplankton: a comparison of universal 16S rRNA probes, autoradiography, and nucleoid staining. *Appl. Environ. Microbiol.* 63, 1208–1213.
- Kasai, Y., Kishira, H., Sasaki, T., Syutsubo, K., Watanabe, K., and Harayama, S. (2002). Predominant growth of *Alcanivorax* strains in oil contaminated and nutrient supplemented seawater. *Environ. Microbiol.* 4, 141–147. doi: 10.1046/j.1462-2920.2002.00275.x
- Kasai, Y., Kishira, H., Syutsubo, K., and Harayama, S. (2001). Molecular detection of marine bacterial populations on beaches contaminated by the Nakhodka tanker oil spill accident. *Environ. Microbiol.* 3, 246–255. doi: 10.1046/j.1462-2920.2001.00185.x
- Kemp, P. F., and Aller, J. Y. (2004). Bacterial diversity in aquatic and other environments: what 16S rDNA libraries can tell us. *FEMS Microbiol. Ecol.* 47, 161–177. doi: 10.1016/S0168-6496(03)00257-5
- Kuwae, T., and Hosokawa, Y. (1999). Determination of the abundance and biovolume of bacteria in sediments by dual staining with 4',6-diamidino-2-phenylindole and acridine orange: relationship to dispersion treatment and sediment characteristics. *Appl. Environ. Microbiol.* 65, 3407–3412.
- Lane, D. J. (1991). "16/23S rRNA sequencing," in *Nucleic Acid Techniques in Bacterial Systematics*, eds E. Stackebrandt and M. Goodfellow (New York, NY: Wiley), 115–175.
- Lozupone, C. A., Hamady, M., Kelley, S. T., and Knight, R. (2007). Quantitative and qualitative  $\beta$  diversity measures lead to different insights into factors that structure microbial communities. *Appl. Environ. Microbiol.* 73, 1576–1585. doi: 10.1128/AEM.01996-06
- Ludwig, W., Strunk, O., Westram, R., Richter, L., Meier, H., Yadhukumar, et al. (2004). ARB: a software environment for sequence data. *Nucleic Acids Res.* 32, 1363–1371. doi: 10.1093/nar/gkh293
- McKew, B.A., Coulon, F., Yakimov, M. M., Denaro, R., Genovese, M., Smith, C. J., et al. (2007). Efficacy of intervention strategies for bioremediation of crude oil in marine systems and effects on indigenous hydrocarbonoclastic bacteria. *Environ. Microbiol.* 9, 1562–1571. doi: 10.1111/j.1462-2920.2007.01277.x
- Microtox System Operating Manual. (1982). *Microbics Operations*. Carlsbad, CA: Beckman Instruments, Inc.
- Onorati, F., Bigongiari, N., Pellegrini, D., and Giuliani, S. (1999). The suitability of *Corophium orientale* (Crustacea, Amphipoda) in harbour sediment toxicity bioassessment. *Aquat. Ecosys. Health Manage.* 2, 465–473. doi: 10.1016/S1463-4988(99)00030-5
- Païssé, S., Coulon, F., Goñi-Urriza, M., Peperzak, L., McGinity, T. J., and Duran, R. (2008). Structure of bacterial communities along a hydrocarbon contamination gradient in a coastal sediment. *FEMS Microbiol. Ecol.* 66, 295–305. doi: 10.1111/j.1574-6941.2008.00589
- Païssé, S., Goñi-Urriza, M., Coulon, F., and Duran, R. (2010). How a bacterial community originating from a contaminated coastal sediment responds to an oil input. *Microb. Ecol.* 60, 394–405. doi: 10.1007/s00248-010-9721-7
- Pernthaler, A., Pernthaler, J., and Amann, R. (2002). Fluorescence *in situ* hybridization and catalyzed reporter deposition for the identification of marine

- bacteria. *Appl. Environ. Microbiol.* 68, 3094–3101. doi: 10.1128/AEM.68.6.3094-3101.2002
- Pruesse, E., Quast, C., Knittel, K., Fuchs, B. M., Ludwig, W. G., Peplies, J., et al. (2007). SILVA: a comprehensive online resource for quality checked and aligned ribosomal RNA sequence data compatible with ARB. *Nucleic Acids Res.* 35, 7188–7196. doi: 10.1093/nar/gkm864
- Psarros, G., Skjøng, R., and Eide, M. S. (2010). Under-reporting of maritime accidents. *Accid. Anal. Prev.* 42, 619–625. doi: 10.1016/j.aap.2009.10.008
- Rasmussen, R. (2001). “Quantification on the LightCycler,” in *Rapid Cycle Real-Time PCR, Methods and Applications*, eds S. Meuer, C. Wittwer, and K. Nakagawara (Heidelberg: Springer Press), 21–34. doi: 10.1007/978-3-642-59524-0\_3
- Ringwood, A. H., DeLorenzo, M. E., Ross, P. E., and Holland, A. F. (1997). Interpretation of Microtox® solid phase toxicity tests: the effects of sediment composition. *Environ. Toxicol. Chem.* 16, 1135–1140. doi: 10.1002/etc.5620160607
- Rocchetti, L., Beolchini, F., Ciani, M., and Dell’Anno, A. (2011). Improvement of bioremediation performance for the degradation of petroleum hydrocarbons in contaminated sediments. *Appl. Environ. Soil Sci.* 2011:319657. doi: 10.1155/2011/319657
- Röling, W. F., Milner, M. G., Jones, D. M., Fratipietro, F., Swannell, R. P., Daniel, F., et al. (2004). Bacterial community dynamics and hydrocarbon degradation during a field-scale evaluation of bioremediation on a mudflat beach contaminated with buried oil. *Appl. Environ. Microbiol.* 70, 2603–2613. doi: 10.1128/AEM.70.5.2603-2613.2004
- Röling, W. F., Milner, M. G., Jones, D. M., Lee, K., Daniel, F., Swannell, R. P., et al. (2002). Robust hydrocarbon degradation and dynamics of bacterial communities during nutrient-enhanced oil spill bioremediation. *Appl. Environ. Microbiol.* 68, 5537–5548. doi: 10.1128/AEM.68.11.5537-5548.2002
- Rosselló-Mora, R., and Amann, R. (2001). The species concept for prokaryotes. *FEMS Microbiol. Rev.* 25, 39–67. doi: 10.1016/S0168-6445(00)00040-1
- Roussel, E. G., Sauvadet, A. L., Allard, J., Chaduteau, C., Richard, P., Cambon Bonavita, M. A., et al. (2009). Active archaeal methane cycling communities associated with gassy subsurface sediments of marennes-oléron bay (France) *Science* 320, 1046. doi: 10.1126/science.1154545
- Schloss, P. D., and Handelsman, J. (2005). Introducing DOTUR, a computer program for defining operational taxonomic units and estimating species richness. *Appl. Environ. Microbiol.* 71, 1501–1506. doi: 10.1128/AEM.71.3.1501-1506.2005
- Syutsubo, K., Sinthurat, N., Ohashi, A., and Harada, H. (2001). Population dynamics of anaerobic microbial consortia in thermophilic granular sludge in response to feed composition change. *Water Sci. Technol.* 43, 59–66.
- Widdel, F., and Rabus, R. (2001). Anaerobic biodegradation of saturated and aromatic hydrocarbons. *Curr. Opin. Biotech.* 12, 259–276. doi: 10.1016/S0958-1669(00)00209
- Wilkes, H., Vieth, A., and Elias, R. (2008). Constraints on the quantitative assessment of in-reservoir biodegradation using compound-specific stable carbon isotopes. *Org. Geochem.* 39, 1215–1221. doi: 10.1016/j.orggeochem.2008.02.013
- Yakimov, M. M., Denaro, R., Genovese, M., Cappello, S., D’Auria, G., Chernikova, T. N., et al. (2005). Natural microbial diversity in superficial sediments of Milazzo Harbor (Sicily) and community successions during microcosm enrichment with various hydrocarbons. *Environ. Microbiol.* 7, 1426–1441. doi: 10.1111/j.1462-5822.2005.00829.x
- Yakimov, M. M., Giuliano, L., Denaro, R., Crisafi, E., Chernikova, T. N., Abraham, W. R., et al. (2004). *Thalassolituus oleivorans* gen. nov., sp. nov., a novel marine bacterium that obligately utilizes hydrocarbons. *Int. J. Syst. Evol. Microbiol.* 54, 141–148. doi: 10.1099/ijss.0.02424-0
- Yakimov, M. M., Giuliano, L., Gentile, G., Crisafi, E., Chernikova, T. N., Abraham, W. R., et al. (2003). *Oleispira antarctica* gen. nov., sp. nov., a novel hydrocarbon-oclastic marine bacterium isolated from Antarctic coastal sea water. *Int. J. Syst. Evol. Microbiol.* 53, 779–785. doi: 10.1099/ijss.0.02366-0
- Yakimov, M. M., Golyshin, P. N., Lang, S., Moore, E. R. B., Abraham, W. R., Lünsdorf, H., et al. (1998). *Alcanivorax borkumensis* gen. nov., sp. nov., a new, hydrocarbon-degrading and surfactant-producing marine bacterium. *Int. J. Syst. Bacteriol.* 48, 339–348. doi: 10.1099/00207713-48-2-339
- Yakimov, M. M., Timmis, K. N., and Golyshin, P. N. (2007). Obligate oil-degrading marine bacteria. *Curr. Opin. Biotech.* 18, 257–266. doi: 10.1016/j.copbio.2007.04.006
- Conflict of Interest Statement:** The authors declare that the research was conducted in the absence of any commercial or financial relationships that could be construed as a potential conflict of interest.
- Received:** 02 December 2013; **accepted:** 25 March 2014; **published online:** 14 April 2014.
- Citation:** Genovese M, Crisafi F, Denaro R, Cappello S, Russo D, Calogero R, Santisi S, Catalfamo M, Modica A, Smedile F, Genovese L, Golyshin PN, Giuliano L and Yakimov MM (2014) Effective bioremediation strategy for rapid *in situ* cleanup of anoxic marine sediments in mesocosm oil spill simulation. *Front. Microbiol.* 5:162. doi: 10.3389/fmicb.2014.00162
- This article was submitted to Aquatic Microbiology, a section of the journal *Frontiers in Microbiology*.
- Copyright © 2014 Genovese, Crisafi, Denaro, Cappello, Russo, Calogero, Santisi, Catalfamo, Modica, Smedile, Genovese, Golyshin, Giuliano and Yakimov. This is an open-access article distributed under the terms of the Creative Commons Attribution License (CC BY). The use, distribution or reproduction in other forums is permitted, provided the original author(s) or licensor are credited and that the original publication in this journal is cited, in accordance with accepted academic practice. No use, distribution or reproduction is permitted which does not comply with these terms.



# Anaerobic hydrocarbon and fatty acid metabolism by syntrophic bacteria and their impact on carbon steel corrosion

Christopher N. Lyles<sup>1</sup>, Huynh M. Le<sup>1</sup>, William Howard Beasley<sup>2</sup>, Michael J. McInerney<sup>1</sup> and Joseph M. Suflita<sup>1\*</sup>

<sup>1</sup> Department of Microbiology and Plant Biology, Institute for Energy and the Environment, and the OU Biocorrosion Center, University of Oklahoma, Norman, OK, USA

<sup>2</sup> Howard Live Oak, LLC, Norman, OK, USA

**Edited by:**

Andreas Teske, University of North Carolina at Chapel Hill, USA

**Reviewed by:**

Jason B. Sylvan, University of Southern California, USA

Shawn R. Campagna, University of Tennessee, Knoxville, USA

**\*Correspondence:**

Joseph M. Suflita, Department of Microbiology and Plant Biology, OU Biocorrosion Center, University of Oklahoma, 770 Van Vleet Oval, Norman, OK 73019, USA  
e-mail: jsuflita@ou.edu

The microbial metabolism of hydrocarbons is increasingly associated with the corrosion of carbon steel in sulfate-rich marine waters. However, how such transformations influence metal biocorrosion in the absence of an electron acceptor is not fully recognized. We grew a marine alkane-utilizing, sulfate-reducing bacterium, *Desulfoglaeba alkanexedens*, with either sulfate or *Methanospirillum hungatei* as electron acceptors, and tested the ability of the cultures to catalyze metal corrosion. Axenically, *D. alkanexedens* had a higher instantaneous corrosion rate and produced more pits in carbon steel coupons than when the same organism was grown in syntrophic co-culture with the methanogen. Since anaerobic hydrocarbon biodegradation pathways converge on fatty acid intermediates, the corrosive ability of a known fatty acid-oxidizing syntrophic bacterium, *Syntrophus aciditrophicus* was compared when grown in pure culture or in co-culture with a H<sub>2</sub>-utilizing sulfate-reducing bacterium (*Desulfovibrio* sp., strain G11) or a methanogen (*M. hungatei*). The instantaneous corrosion rates in the cultures were not substantially different, but the syntrophic, sulfate-reducing co-culture produced more pits in coupons than other combinations of microorganisms. Lactate-grown cultures of strain G11 had higher instantaneous corrosion rates and coupon pitting compared to the same organism cultured with hydrogen as an electron donor. Thus, if sulfate is available as an electron acceptor, the same microbial assemblages produce sulfide and low molecular weight organic acids that exacerbated biocorrosion. Despite these trends, a surprisingly high degree of variation was encountered with the corrosion assessments. Differences in biomass, initial substrate concentration, rates of microbial activity or the degree of end product formation did not account for the variations. We are forced to ascribe such differences to the metallurgical properties of the coupons.

**Keywords:** syntropy, biocorrosion, microbiologically influenced corrosion (MIC), hydrocarbon degradation, fatty acid oxidation

## INTRODUCTION

Anaerobic hydrocarbon biodegradation is metabolically coupled with the consumption of a variety of terminal electron acceptors (for recent reviews see, Callaghan, 2013; Heider and Schühle, 2013). It is essential to understand the underlying geochemical settings for such bioconversions in order to reliably assess the attendant environmental consequences. Arguably, the greatest impact of this metabolism is manifest in sulfate-laden environments where petroleum metabolism may be coupled with sulfide production. Aside from the destruction of the hydrocarbons *per se*, the formation of sulfide has several important consequences including health and safety concerns (Reiffenstein et al., 1992), reservoir souring (Jenneman et al., 1986; McInerney et al., 1996; Nemati et al., 2001; Hubert and Voordouw, 2007), and metal biocorrosion (Hamilton, 1985). Not surprisingly, these problems are most acute in marine environments where sulfate-reducing bacterial communities thrive in petroleum deposits,

hydrocarbon seeps, petroleum hydrothermal sediments, methane hydrates, oil field equipment, and in hydrocarbon-contaminated sediments (Teske, 2010). Moreover, in offshore and near coastal drilling operations where seawater is injected into petroleum reservoirs to maintain oil field formation pressures, efforts are regularly made to remove sulfate from seawater in order to control the deleterious consequences of scale deposits as well as to minimize microbial sulfate reduction, reservoir souring, and sulfide-induced metal corrosion (Bader, 2007). When exogenous electron acceptors are limiting, anaerobic hydrocarbon mineralization can still proceed and result in the formation of methane (Dolfing et al., 2008; Gieg et al., 2008; Jones et al., 2008; Heider and Schühle, 2013). In fact, methanogenic enrichments and isolates are regularly obtained from hydrocarbon-rich marine ecosystems (Teske, 2010), even though these organisms are not known to directly utilize petroleum components. Rather, acetoclastic and hydrogenotrophic methanogens catalyze the terminal

mineralization steps as members of thermodynamically-based hydrocarbonoclastic syntrophic microbial assemblages of varying complexity (Dolfing et al., 2008; Gieg et al., 2008; Jones et al., 2008). The consequences of methanogenic hydrocarbon metabolism minimally include the overall diminution in the quality of petroleum reserves (Head et al., 2010), and the formation of methane a powerful greenhouse gas (Blake and Rowland, 1988). The other end product of this bioconversion, carbon dioxide, can potentially alter the *in situ* mineralization pathways in petrolierous reservoirs. If carbon dioxide is in a high enough concentration, acetoclastic methanogenesis may become a dominant process and increase the rate of methane production and sequestration of carbon dioxide (Mayumi et al., 2013).

Thus, the complete mineralization of hydrocarbons under anaerobic conditions, like the biodegradation of other complex forms of organic matter, can be initiated or accomplished by specialized microbial isolates that can couple this metabolism to the consumption of exogenous electron acceptors or enter into complex syntrophic partnerships. Such bioconversions often result in the transient formation of fatty acid metabolites (e.g., acetate, propionate, butyrate, and benzoate) that have been postulated as intermediates of anaerobic hydrocarbon metabolism under both methanogenic and sulfate-reducing conditions (Cozzarelli et al., 1994; Van Stempvoort et al., 2007, 2009; Struchtemeyer et al., 2011). In syntrophic partnerships, it is well known that non-methanogens, such as hydrogen/formate-utilizing, sulfate-reducing bacteria (SRB), can fulfill the role of the terminal electron-accepting microorganism (Hopkins et al., 1995; Warikoo et al., 1996; Jackson et al., 1999). Conversely, a syntrophic association with methanogens can also be realized even in environments with high sulfate concentrations (Struchtemeyer et al., 2011).

The role of SRB and methanogens as agents of metal corrosion, when grown as pure cultures or as members of syntrophic consortia, is not fully appreciated. These organisms have been implicated in the corrosion of metal via direct electron transfer from zero-valent iron under electron donor-limited conditions (Dinh et al., 2004; Uchiyama et al., 2010; Enning et al., 2012; Enning and Garrelfs, 2014). Additionally, when electron donors are sufficient, the inorganic and organic compounds produced during metabolism (e.g., hydrogen, fatty acids, carbon dioxide, and sulfides) have frequently been associated with metal biocorrosion (King and Miller, 1971; King and Wakerley, 1972; King et al., 1973a,b; Crolet et al., 1999; Hedges and McVeigh, 1999; Garsany et al., 2003; Kermani and Morshed, 2003; Suflita et al., 2008).

Given the diverse modes of existence for the requisite microorganisms, we used defined incubations of both pure and co-culture syntrophic bacteria to examine their impact on carbon steel biocorrosion. More specifically, we evaluated a known hydrocarbon-degrading bacterium, *Desulfoglaeba alkanexedens* strain ALDC (Davidova et al., 2006), grown with sulfate or syntrophically in co-culture with a methanogen as the electron acceptor. *D. alkanexedens* strain ALDC is a marine alkane-degrading, sulfate-reducing bacterium, that can completely oxidize C<sub>6</sub>–C<sub>12</sub> *n*-alkanes via the fumarate addition pathway. The bacterium can also syntrophically degrade the same suite of aliphatic hydrocarbons in a sulfate-free medium when

co-cultured with the hydrogen/formate-consuming methanogen, *Methanospirillum hungatei* strain JF-1 (Ferry et al., 1974). We also evaluated biocorrosion with a known fatty acid-oxidizing syntrophic bacterium, *Syntrophus aciditrophicus* strain SB (Hopkins et al., 1995; Jackson et al., 1999), grown as a pure culture or with either a hydrogen/formate-utilizing methanogen or SRB as the electron-accepting microorganism. *S. aciditrophicus* strain SB, metabolizes various saturated and unsaturated fatty acids, methyl esters of butyrate and hexanoate, benzoate, and alicyclic acids when grown in co-culture with a hydrogen/formate-consuming microorganism (Mouttaki et al., 2007) including the methanogen *M. hungatei* strain JF-1 or the SRB *Desulfovibrio* sp. strain G11 (McInerney et al., 1979). Its use of a primary sodium pump to create a chemostatic potential and to synthesize ATP using a sodium gradient mimics the bioenergetic scheme of many marine microorganisms (McInerney et al., 2007). Similarly, *M. hungatei* strain JF-1 also has the capacity to produce and use sodium gradients (Anderson et al., 2009). *S. aciditrophicus* strain SB can also be grown as a pure culture on crotonate whereupon it produces acetate, cyclohexane carboxylate, and benzoate as metabolic end products (Mouttaki et al., 2007). Lastly, all pure cultures were individually evaluated for their ability to corrode metal coupons. Our results suggest that the corrosion of carbon steel was generally more evident when anaerobic microbial metabolism was linked to sulfate reduction rather than methanogenesis. However, a greater than expected standard deviation in corrosivity was measured in replicate incubations. After controlling and monitoring the biological and chemical characteristics of the incubations, we are forced to attribute the variability to presumed compositional differences in the metal used for the construction of the coupons.

## MATERIALS AND METHODS

### ELECTROCHEMICAL CELL CONSTRUCTION

Electrochemical cells were made from culture bottles (100 ml; Figure S1) fitted with rubber stoppers that were modified to hold a graphite counter electrode and a Luggin probe filled with 1 M potassium chloride (KCl) solution containing a saturated calomel reference electrode (Gamry Instruments, Warminster, PA; Figure S2). The working electrode was a 1020 carbon steel coupon (Alabama Specialty Products, Munford, AL) with dimensions of 0.95 cm diameter × 1.27 cm and a surface area of 4.5 cm<sup>2</sup>. The metal was prepared using the specifications detailed in ASTM Standard A576-90b (2006), and consisted of the elemental components listed in Table S1 according to the manufacturer (above). A wire was attached to the coupon using rosin core solder and the entire assembly was sealed with epoxy resin (Figure S3). The working electrode assembly was then washed with acetone and methanol, before being sterilized by immersion for 30 min in a 70% ethanol bath. The ethanol was evaporated with an open flame, and the coupon was dried under nitrogen and handled aseptically. Sterile electrochemical probes (Figure S2) were placed in the incubations (Figure S4) while inside a well-working anaerobic chamber (N<sub>2</sub>:H<sub>2</sub> 95:5%), and linear polarization resistance (LPR) curves were recorded every 5 min for a 30 min period using computer controlled potentiostats (model 600, Gamry Instruments, Warminster, PA). The potential was swept ± 10 mV

above and below the corrosion potential ( $E_{corr}$ ) at a rate of 0.125 mV/s. Tafel slope regions were used to extrapolate resistance polarization ( $R_p$ ) values within  $\pm 5$  mV of the  $E_{corr}$ . The instantaneous corrosion rate is derived by taking the inverse of the resistance polarization ( $1/R_p$ ;  $\text{ohms}^{-1} \text{cm}^{-2}$ ). The LPR measurement was taken intermittently based on the metabolic activity measured within anaerobic incubations (below). Thus, the  $1/R_p$  curves reflect various points along the curve shown in **Figure 1**. A  $1/R_p$  value for each time point was selected based on the mean distribution of six LPR curves within the 30 min measurement period. Finally, instantaneous corrosion rates were generalized as low [ $<0.0254$  millimeter per year (mmpy)], moderate (0.0254–0.127 mmpy), or high (0.127–0.508 mmpy) based on the  $1/R_p$  logarithmic value (**Figure 1**).

#### CULTIVATION OF THE HYDROCARBON-DEGRADING BACTERIUM

The mineral medium was prepared as previously described (McInerney et al., 1979), except rumen fluid and sulfate were omitted. The medium was amended with 10 ml/L of a trace metal and vitamin solution (Tanner, 2002), 0.0001% solution of resazurin as a redox indicator, sodium bicarbonate (24 mM), and 10 ml/L of a 2.5% solution of cysteine sulfide used as a reductant. The medium was dispensed into the electrochemical cells (50 ml) and inoculated with 20% transfers for the *D. alkanexedens* strain ALDC or *M. hungatei* strain JF-1 pure culture incubations or 10% transfers of each microorganism for the co-culture incubations. The mineral medium was the same for all axenic cultures or co-cultures, but the substrate, sulfate concentration, and headspace gas composition were adjusted for different incubation conditions (**Table 1**). The headspace for the axenic cultures of *M. hungatei* strain JF-1 was monitored and exchanged every 14 days to resupply H<sub>2</sub>/CO<sub>2</sub> to support the hydrogenotrophic growth of the methanogen. Strict anaerobic conditions were maintained throughout the 44 days incubation period. Triplicate cultures were incubated at 32°C and monitored

for corrosion with the potentiostats every 26 days after moving the cultures inside the anaerobic chamber. After each LPR measurement, the culture bottles were resealed and the headspace exchanged to the appropriate atmosphere.

#### CULTIVATION OF THE FATTY ACID-OXIDIZING SYNTROPH

A basal medium was prepared as previously described (Tanner, 2002), and was amended with 10 ml/L trace metal and vitamin solution (Tanner, 2002), a 0.0001% solution of resazurin as a redox indicator, sodium bicarbonate (24 mM), and 20 ml/L of a 2.5% solution of cysteine sulfide used as a reductant. The medium was dispensed into the electrochemical cells (50 ml) and inoculated with 20% transfers of *S. aciditrophicus* strain SB or *Desulfovibrio* sp. strain G11 pure cultures, or 10% transfers of each of the microorganisms for the syntrophic co-culture incubations. The basal medium was the same for all cultures and co-cultures, but the substrate, sulfate concentration, and headspace atmosphere were adjusted depending on the desired incubation condition (**Table 2**). The headspace in autotrophically grown *Desulfovibrio* sp. strain G11 incubations was exchanged daily to resupply H<sub>2</sub>/CO<sub>2</sub> to support the growth of this microorganism. Cultures were incubated in triplicate while medium controls were in duplicate. Incubations were held at 32°C and monitored electrochemically for the instantaneous corrosion rate as described above, every 7 days (experiment 1) or 28 days (experiment 2) after placing the cultures inside the anaerobic chamber. After each LPR measurement, the culture bottles were resealed and the headspace exchanged to the original atmosphere.

#### SPENT MEDIUM EXPERIMENTS

The corrosivity of the basal medium (Tanner, 2002) was assessed after amendment with various fatty acids with concentrations of crotonate and lactate ranging from 0 to 20 mM, as well as acetate ranging from 0 to 40 mM. These compounds were exogenously amended to mimic the concentration of substrates and end products produced by a crotonate grown co-culture of *S. aciditrophicus* strain SB and *Desulfovibrio* sp. strain G11 and lactate metabolism by a pure culture of *Desulfovibrio* sp. strain G11. Acetate was amended at a ratio of 2:1 for crotonate metabolism and 1:1 for

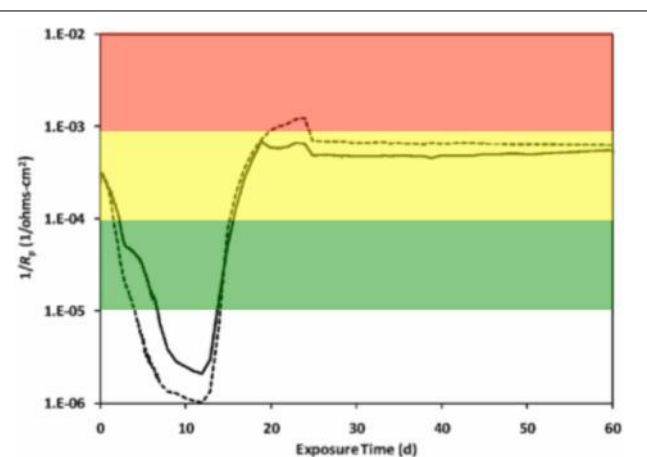


**FIGURE 1 |** An instantaneous corrosion rate ( $1/R_p$ ) curve adapted from

Aktas et al. (2010). The basic shape of the curve represents the corrosion of C1020 metal over time.  $1/R_p =$  (■)  $10^{-5} \text{ ohms}^{-1} \text{ cm}^{-2}$ ,  $<0.0254 \text{ mmpy}$ ; (■)  $10^{-4} \text{ ohms}^{-1} \text{ cm}^{-2}$ ,  $0.0254\text{--}0.127 \text{ mmpy}$ ; (■)  $10^{-3} \text{ ohms}^{-1} \text{ cm}^{-2}$ ,  $0.127\text{--}0.508 \text{ mmpy}$ .

**Table 1 |** Substrate, sulfate, and headspace amendments for hydrocarbon degrading incubations.

Axenic or co-culture incubations	Substrate	Sulfate (mM)	Headspace atmosphere
<i>D. alkanexedens</i> ALDC	1 ml n-decane	20	138 kPa N <sub>2</sub> /CO <sub>2</sub> (80:20)
<i>M. hungatei</i> JF-1	H <sub>2</sub> /CO <sub>2</sub> (138 kPa in ~40 mls of headspace)	–	138 kPa H <sub>2</sub> /CO <sub>2</sub> (5:95)
<i>D. alkanexedens</i> ALDC + <i>M. hungatei</i> JF-1	1 ml n-decane	–	138 kPa N <sub>2</sub> /CO <sub>2</sub> (80:20)
Uninoculated medium control	1 ml n-decane	20	138 kPa H <sub>2</sub> /CO <sub>2</sub> (80:20)

“–”No amendment.

**Table 2 | Substrate, sulfate, and headspace amendments for fatty acid oxidizing incubations.**

Axenic or co-culture incubations	Substrate	Sulfate (mM)	Headspace atmosphere
<i>S. aciditrophicus</i> SB	20 mM crotonate	–	138 kPa N <sub>2</sub> /CO <sub>2</sub> (80:20)
<i>S. aciditrophicus</i> SB + <i>Desulfovibrio</i> sp. G11	20 mM crotonate	20	138 kPa N <sub>2</sub> /CO <sub>2</sub> (80:20)
<i>S. aciditrophicus</i> SB + <i>M. hungatei</i> JF-1	20 mM crotonate	–	138 kPa N <sub>2</sub> /CO <sub>2</sub> (80:20)
<i>Desulfovibrio</i> sp. G11 (heterotrophic)	20 mM lactate	20	138 kPa N <sub>2</sub> /CO <sub>2</sub> (80:20)
<i>Desulfovibrio</i> sp. G11 (autotrophic)	H <sub>2</sub> /CO <sub>2</sub> (138 kPa in ~40 mls of headspace)	20	138 kPa H <sub>2</sub> /CO <sub>2</sub> (5:95)
<i>Desulfovibrio</i> sp. G11 (autotrophic)	H <sub>2</sub> from metal surface	20	138 kPa N <sub>2</sub> /CO <sub>2</sub> (80:20)
Uninoculated medium control	20 mM crotonate	–	138 kPa N <sub>2</sub> /CO <sub>2</sub> (80:20)
Uninoculated medium control	20 mM lactate	20	138 kPa N <sub>2</sub> /CO <sub>2</sub> (80:20)
Uninoculated medium control	–	20	138 kPa H <sub>2</sub> /CO <sub>2</sub> or 138 kPa N <sub>2</sub> /CO <sub>2</sub>

“–,” No amendment.

lactate metabolism. To represent sulfide production within the uninoculated incubations, sodium sulfide was amended at 10 and 20 mM concentrations. The pH for all incubations was ~7.0. The incubation conditions are described in **Table 3**. Duplicate uninoculated incubations were held at 32°C and monitored electrochemically every 17 days inside the anaerobic chamber as described above.

## PROFILOMETRY

At the end of the incubation, the coupons were recovered and localized corrosion damage was assessed with light profilometry (PS50 profilometer, Nanovea, Irvine, CA). The coupons were acid-cleaned to remove corrosion deposits according to ASTM Standard A576-90b (2006). The initial surface profiling of coupons was conducted by a cooperating external laboratory (Phillips 66, Bartlesville, OK, USA). However, a model PS50 profilometer (Nanovea, Irvine, CA) was eventually acquired for this purpose. Only the flat surface of the cylindrical coupons were analyzed for localized pitting evaluations. Line scans were run at a data acquisition rate of 2000 Hz using a 300 μm optical pen at a 3.0 μm step size. All surface analysis was performed using 3D analysis software (Ultra v6.2 Nanovea, Irvine, CA). Pitting was defined as damage that was 20 μm below the mean surface plane and at least a 20 μm in diameter. These experimental parameters were chosen based on the distribution of collected points across all coupons analyzed. Surface damage was also assessed by comparing histograms for each coupon.

**Table 3 | Uninoculated medium controls containing various concentrations of fatty acids and sulfide amended to represent crotonate metabolism by *S. aciditrophicus* strain SB or lactate metabolism by *Desulfovibrio* sp. strain G11.**

Crotonate metabolism	Lactate metabolism
20 mM crotonate	20 mM lactate
10 mM crotonate + 20 mM acetate + 10 mM sulfide	10 mM lactate + 10 mM acetate + 10 mM sulfide
0 mM crotonate + 40 mM acetate + 20 mM sulfide	0 mM lactate + 20 mM acetate + 20 mM sulfide
No amendment medium control	No amendment medium control

Each histogram consists of 2501 points collected from the profilometer. The *y* value indicates the depth (μm) of the points while the *x* value is the percentage of points at that particular depth.

## STATISTICAL METHODS

All statistical analyses were done using R (The R Foundation for statistical computing). Treatment means were estimated by a Bayesian multilevel model that accounted for the dependencies among the 2501 points from each coupon. Using the MCMCglmm package (Hadfield, 2010) and vague priors, eight parallel MCMC chains were run for 10,000 iterations after burn-in; the largest *R* was less than 1.001. Our primary model produced point and error estimates consistent with a frequentist multi-level model (using the lme4 package; Bates, 2010) and with a frequentist ANOVA (that considered only the mean of each coupon). Coupons not scanned at the University of Oklahoma were excluded from the analysis since a different profilometry protocol was employed and the resulting histograms were not comparable. In addition, a medium control coupon was similarly excluded since it had a damaged area on its surface (but no pits matching the experimental parameters were evident). To be entirely transparent, a comparison of the datasets with and without the outliers is depicted in the supplemental information (see Figure S21). To facilitate reproducibility, the code and profilometry data are available at <https://github.com/LiveOak/LylesCarbonSteelCorrosion>.

## ANALYTICAL METHODS

Crotonate loss was measured by HPLC (Dionex model IC-3000, Sunnyvale, CA) using an Alltech Prevail™ organic acid column (250 × 4.6 mm, particle size 5 μM; Grace, Deerfield, IL) and UV absorbance detector (Dionex model AD25, Sunnyvale, CA). The gradient pump was operated at a flow rate of 1.0 ml/min and mixed a mobile phase consisting of 60% (vol/vol) KH<sub>2</sub>PO<sub>4</sub> (25 mM, pH 2.5) and 40% acetonitrile. The UV absorbance detector was set to 254 nm. Sulfate depletion was analyzed by ion chromatography (Dionex model IC-1000, Sunnyvale, CA) and has been previously described in Lyles et al. (2013). Methane production was monitored by gas chromatography (Packard model 427, Downers Grove, Ill.) and has been previously described in Gieg et al. (2008).

## RESULTS

### ANAEROBIC HYDROCARBON BIODEGRADATION AND THE CORROSION OF CARBON STEEL

There are many important ecological consequences associated with anaerobic hydrocarbon biodegradation in the environment. We used pure cultures and defined co-cultures to investigate the impact of this metabolism on one of the most important ecological consequences, the biocorrosion of carbon steel. *D. alkanexedens* strain ALDC and *M. hungatei* strain JF-1 were cultured axenically and as a syntrophic partner in the presence of carbon steel coupons. Coupon damage was assessed by periodically measuring the instantaneous corrosion rate during the course of the experiment and by surface profilometry at the end of the incubation period (**Table 4**).

After 44 days of incubation, *D. alkanexedens* strain ALDC cultured on *n*-decane reduced sulfate at a rate of  $0.060 \pm 0.014 \text{ mM SO}_4 \cdot \text{day}^{-1}$  (Figure S5) and produced an instantaneous corrosion rate of  $7.8 \times 10^{-3} \pm 8.3 \times 10^{-4} \text{ ohms}^{-1} \text{ cm}^{-2}$  ( $\sim 0.381 \text{ mmpp}$ ; **Figure 2**). Approximately 18% of the

*n*-decane was oxidized during the incubation period based on the amount of sulfate reduced within the incubation (data not shown). When *D. alkanexedens* strain ALDC and *M. hungatei* strain JF-1 were co-cultured on the same hydrocarbon, an average of  $62.0 \pm 22.5 \mu\text{mole}$  methane (Figure S6) was produced, suggesting that  $\sim 0.2\%$  of the parent hydrocarbon was utilized by the co-culture. The instantaneous corrosion rate for the co-culture was  $7.0 \times 10^{-4} \pm 4.3 \times 10^{-4} \text{ ohms}^{-1} \text{ cm}^{-2}$  ( $\sim 0.0508 \text{ mmpp}$ ; **Figure 2**). Pure cultures of *M. hungatei* strain JF-1 cultured hydrogenotrophically ( $\text{H}_2/\text{CO}_2$ ) produced  $\sim 1500 \pm 700 \mu\text{mole}$  methane over the initial 24 days incubation but the rate decreased with each headspace exchange over the entire incubation (Figure S7). The pure methanogen exhibited an instantaneous corrosion rate of  $6.56 \times 10^{-5} \pm 4.4 \times 10^{-5} \text{ ohms}^{-1} \text{ cm}^{-2}$  ( $< 0.0254 \text{ mmpp}$ ); a value that was even lower than the comparable rate determination in the uninoculated control ( $1.01 \times 10^{-4} \pm 4.48 \times 10^{-5} \text{ ohms}^{-1} \text{ cm}^{-2}$ ;  $< 0.0254 \text{ mmpp}$ ).

When profilometry was used to assess localized corrosion in the coupons, differences between replicate incubations were evident (**Table 4**; Figure S8). One coupon replicate in the *D.*

**Table 4 |** The number of pits and the instantaneous corrosion rates for replicates of the hydrocarbon and fatty acid oxidizing cultures as well as the spent medium incubations.

Incubation condition (substrate amendment)	Number of pits + instantaneous corrosion rate ( $1/R_p$ )										
	Experiment 1			Experiment 2							
	Replicate 1	Replicate 2	Replicate 3	Replicate 1	Replicate 2	Replicate 3					
<b>HYDROCARBON DEGRADING CULTURES</b>											
<i>D. alkanexedens</i> ALDC ( <i>n</i> -decane)	ND		259		ND		—	—	—	—	—
<i>D. alkanexedens</i> ALDC + <i>M. hungatei</i> JF-1 ( <i>n</i> -decane)	64	3		ND	—	—	—	—	—	—	—
<i>M. hungatei</i> JF-1 ( $\text{H}_2/\text{CO}_2$ )	2	—	—	—	—	—	—	—	—	—	—
Uninoculated basal medium ( <i>n</i> -decane)	50		—	—	—	—	—	—	—	—	—
<b>FATTY ACID OXIDIZING CULTURES</b>											
<i>S. aciditrophicus</i> SB (crotonate)	1		ND		1		ND		ND		ND
<i>S. aciditrophicus</i> SB + <i>M. hungatei</i> JF-1 (crotonate)	88		ND	ND	—	—	—	—	—	—	—
<i>S. aciditrophicus</i> SB + <i>Desulfovibrio</i> sp. G11 (crotonate)	36	37	32	158	3	32	32		32		32
<i>Desulfovibrio</i> sp. G11 (lactate)	ND	23	12	ND	ND	ND	ND	ND	ND	ND	ND
<i>Desulfovibrio</i> sp. G11 ( $\text{H}_2/\text{CO}_2$ )	ND		ND	ND	ND	ND	ND	ND	ND	ND	ND
<i>Desulfovibrio</i> sp. G11 (H <sub>2</sub> from metal surface)	ND	ND	ND	1	ND	ND	ND	ND	ND*	ND*	
Uninoculated basal medium (crotonate)	ND	45	—	ND	ND	ND	ND	ND	—	—	—
Uninoculated basal medium (lactate)	—	—	—	ND	—	—	—	—	—	—	—
Uninoculated basal medium ( $\text{H}_2/\text{CO}_2$ )	ND			ND		ND	ND	—	—	—	—
<b>SPENT MEDIUM INCUBATIONS</b>											
20 mM crotonate	ND		ND		—	—	—	—	—	—	—
10 mM crotonate + 20 mM acetate + 10 mM sulfide	ND		ND	—	—	—	—	—	—	—	—
0 mM crotonate + 40 mM acetate + 20 mM sulfide	ND	ND	—	—	—	—	—	—	—	—	—
20 mM lactate	ND		ND	—	—	—	—	—	—	—	—
10 mM lactate + 10 mM acetate + 10 mM sulfide	ND		ND	—	—	—	—	—	—	—	—
0 mM lactate + 20 mM acetate + 20 mM sulfide	ND		ND	—	—	—	—	—	—	—	—
Unamended basal medium control	ND	ND	—	—	—	—	—	—	—	—	—

ND, Not detectable.

—, Replicate not done or data not available.

\*The metal had pitting on the side but could not be quantified by the profilometer.

$1/R_p =$   $10^{-5} \text{ ohms}^{-1} \text{ cm}^{-2}$ ,  $< 0.0254 \text{ mmpp}$ ;  $10^{-4} \text{ ohms}^{-1} \text{ cm}^{-2}$ ,  $0.0254-0.127 \text{ mmpp}$ ;  $10^{-3} \text{ ohms}^{-1} \text{ cm}^{-2}$ ,  $0.127-0.508 \text{ mmpp}$ .

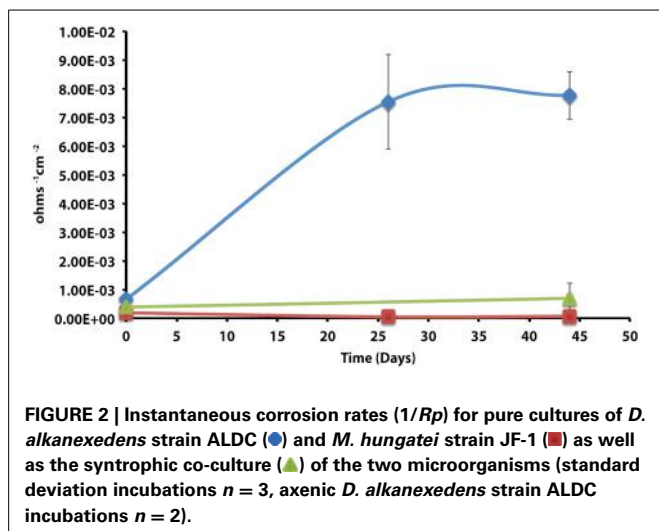


**FIGURE 2 |** Instantaneous corrosion rates ( $1/R_p$ ) for pure cultures of *D. alkanexedens* strain ALDC (●) and *M. hungatei* strain JF-1 (■) as well as the syntrophic co-culture (▲) of the two microorganisms (standard deviation incubations  $n = 3$ , axenic *D. alkanexedens* strain ALDC incubations  $n = 2$ ).

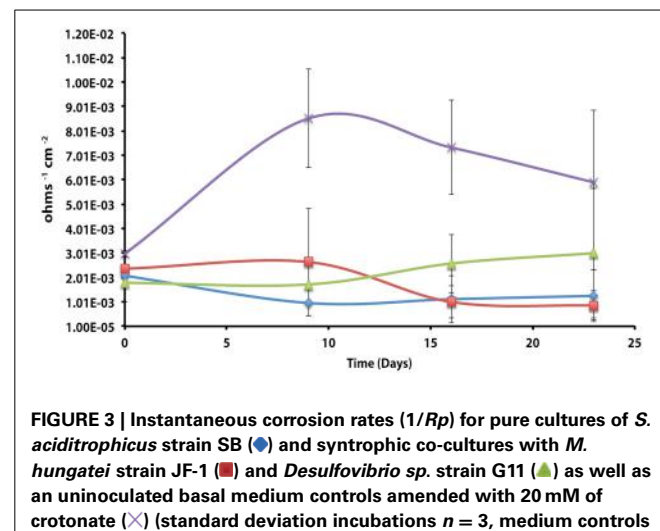


**FIGURE 3 |** Instantaneous corrosion rates ( $1/R_p$ ) for pure cultures of *S. aciditrophicus* strain SB (●) and syntrophic co-cultures with *M. hungatei* strain JF-1 (■) and *Desulfovibrio* sp. strain G11 (▲) as well as an uninoculated basal medium controls amended with 20 mM of crotonate (×) (standard deviation incubations  $n = 3$ , medium controls  $n = 2$ ).

*alkanexedens* strain ALDC incubation exhibited substantial pitting (259 pits) while pits were not evident on the other replicate coupon despite similar sulfate reduction (Figure S5) and instantaneous corrosion rates (Figure 2). Pitting was not as severe for coupon replicates incubated in the syntrophic co-culture. That is, 66 pits were counted on replicate one, 3 pits on replicate two, and 0 pits on replicate three. The pure culture incubation of *M. hungatei* strain JF-1 and the uninoculated control had 2 and 50 pits, respectively.

#### ANAEROBIC FATTY ACID BIODEGRADATION AND THE CORROSION OF CARBON STEEL

The corrosion potential of the fatty acid-oxidizing syntroph, *S. aciditrophicus* strain SB, was evaluated in a similar manner by growing the bacterium, as a pure culture or in defined co-culture with *M. hungatei* strain JF-1 or *Desulfovibrio* sp. strain G11 (Table 4; Figure 3). The instantaneous corrosion rates were not substantially different between the pure culture of *S. aciditrophicus* strain SB and co-cultures *M. hungatei* strain JF-1 or *Desulfovibrio* sp. strain G11. However, localized corrosion increased when *S. aciditrophicus* strain SB was co-cultured with *Desulfovibrio* sp. strain G11 compared to when the syntroph was grown as a pure culture or when it was coupled with the methanogen (Table 4). Additionally, localized corrosion was also evident when coupons were exposed to pure cultures of *Desulfovibrio* sp. strain G11 grown in lactate-amended incubations with sulfate as the electron acceptor.

The instantaneous corrosion rates for pure cultures of *S. aciditrophicus* strain SB and related co-cultures are compared in Figure 3. Incubations containing axenic cultures of *S. aciditrophicus* strain SB were found to produce an instantaneous corrosion rate of  $1.12 \times 10^{-3} \pm 9.65 \times 10^{-4}$  ohms<sup>-1</sup> cm<sup>-2</sup> ( $\sim 0.0762$  mmpp). In co-culture with *M. hungatei* strain JF-1,  $15.65 \pm 7.16$  μmole methane was produced over the 16 days incubation period (Figure S9), and the instantaneous corrosion rate was  $2.64 \times 10^{-3} \pm 2.91 \times 10^{-3}$  ohms<sup>-1</sup> cm<sup>-2</sup> ( $\sim 0.178$  mmpp). When co-cultured with *Desulfovibrio* sp.

strain G11, the sulfate reduction rate was  $0.34 \pm 0.08$  mM SO<sub>4</sub>•day<sup>-1</sup> (Figure S10), and the instantaneous corrosion rate was  $2.6 \times 10^{-3} \pm 1.19 \times 10^{-3}$  ohms<sup>-1</sup> cm<sup>-2</sup> ( $\sim 0.1524$  mmpp). Uninoculated basal medium controls amended with 20 mM of crotonate had an instantaneous corrosion rate of  $7.33 \times 10^{-3} \pm 2.01 \times 10^{-3}$  ohms<sup>-1</sup> cm<sup>-2</sup> ( $\sim 0.4318$  mmpp). In all incubations containing *S. aciditrophicus* strain SB, crotonate was not detected by HPLC after 14 days of incubation (Figure S11). Additionally, the large standard deviations observed between  $1/R_p$  values (Figure 3) associated with incubations of *S. aciditrophicus* strain SB and related co-cultures suggest that there is no difference in instantaneous corrosion rates, despite the formation of different metabolic end products (i.e., sulfide, methane, acetate) within each of the various incubation conditions.

Axenic incubations of *Desulfovibrio* sp. strain G11 cultured in the same media but amended with 20 mM of lactate produced an instantaneous corrosion rate of  $1.5 \times 10^{-3} \pm 6.0 \times 10^{-4}$  ohms<sup>-1</sup> cm<sup>-2</sup> ( $\sim 0.089$  mmpp; Figure 4). These incubations reduced sulfate at a rate of  $2.00 \pm 0.1$  mM SO<sub>4</sub>•day<sup>-1</sup> (Figure S10). The uninoculated media control containing 20 mM of lactate produced an instantaneous corrosion rate of  $3.2 \times 10^{-3} \pm 6.0 \times 10^{-4}$  ohms<sup>-1</sup> cm<sup>-2</sup> ( $\sim 0.1778$  mmpp; Figure 4). Thus, there is no significant difference for the instantaneous corrosion rates between *Desulfovibrio* sp. strain G11 and uninoculated control incubations. Additionally, when *Desulfovibrio* sp. strain G11 was cultured autotrophically with 138 kPa overpressure of H<sub>2</sub>/CO<sub>2</sub> in the headspace as well as from hydrogen emanating from the metal surface, the sulfate reduction rate was  $0.79 \pm 0.04$  mM SO<sub>4</sub>•day<sup>-1</sup> and  $0.35 \pm 0.10$  mM SO<sub>4</sub>•day<sup>-1</sup>, respectively (Figure S10). In all replicates of autotrophically-grown cultures of this microorganism, the instantaneous corrosion rates (Figure 5) ranged between  $5.17 \times 10^{-5} \pm 4.70 \times 10^{-5}$  and  $5.51 \times 10^{-5} \pm 3.51 \times 10^{-5}$  ohms<sup>-1</sup> cm<sup>-2</sup> ( $< 0.0208$  mmpp), which is lower than the uninoculated controls containing either 138 kPa of H<sub>2</sub>/CO<sub>2</sub> or N<sub>2</sub>/CO<sub>2</sub> in the headspace ( $1.02 \times 10^{-4} \pm 1.13 \times 10^{-4}$  ohms<sup>-1</sup> cm<sup>-2</sup>).

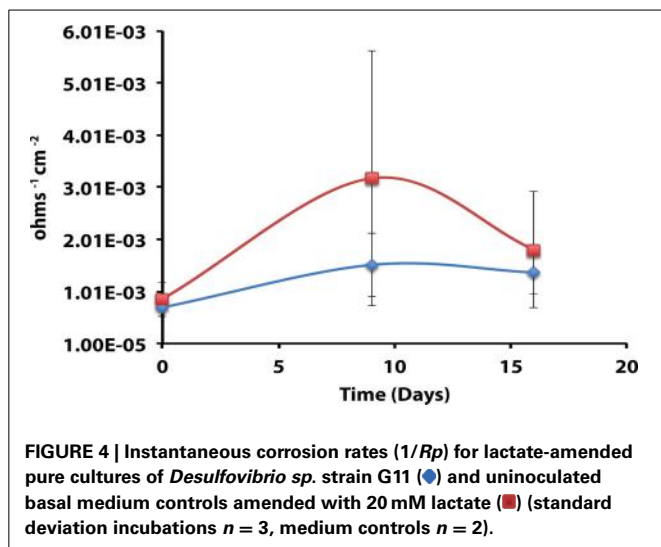


**FIGURE 4 |** Instantaneous corrosion rates ( $1/R_p$ ) for lactate-amended pure cultures of *Desulfovibrio* sp. strain G11 (●) and uninoculated basal medium controls amended with 20 mM lactate (■) (standard deviation incubations  $n = 3$ , medium controls  $n = 2$ ).

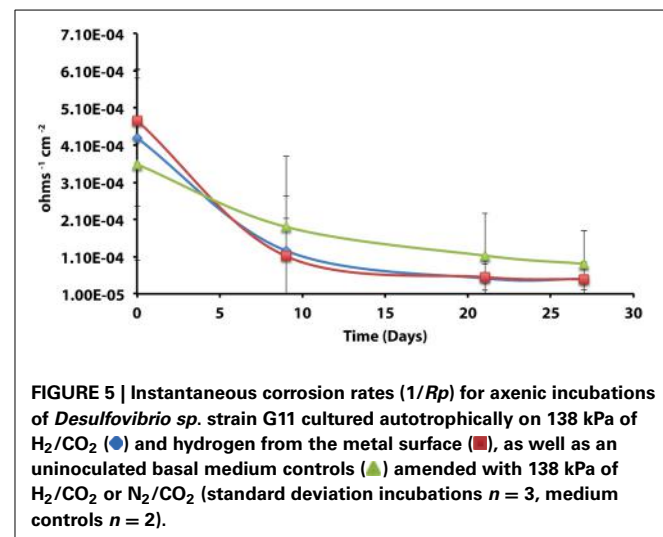


**FIGURE 5 |** Instantaneous corrosion rates ( $1/R_p$ ) for axenic incubations of *Desulfovibrio* sp. strain G11 cultured autotrophically on 138 kPa of  $\text{H}_2/\text{CO}_2$  (●) and hydrogen from the metal surface (■), as well as an uninoculated basal medium controls (▲) amended with 138 kPa of  $\text{H}_2/\text{CO}_2$  or  $\text{N}_2/\text{CO}_2$  (standard deviation incubations  $n = 3$ , medium controls  $n = 2$ ).

Carbon steel coupons were assessed for localized corrosion using profilometry, and the numbers of pits counted from surface profiles (Figure S12) are compared in **Table 4** (experiment 1). Even though pure cultures of *S. aciditrophicus* strain SB produced instantaneous corrosion rates of  $10^{-3}$  and  $10^{-4}$ , only 2 pits were identified on the metal surface. When *S. aciditrophicus* strain SB was co-cultured with *Desulfovibrio* sp. strain G11, an average of  $35 \pm 2.6$  pits were identified across the three replicates. Finally, when *S. aciditrophicus* strain SB was co-cultured with *M. hungatei* strain JF-1, one replicate produced 88 pits, while the other replicates had no detectable pits. When coupons were exposed to pure cultures of *Desulfovibrio* sp. strain G11 grown on lactate, replicate one had no pits, but replicates two and three had 23 and 12 pits, respectively. No pits were detected on coupons analyzed from incubations containing *Desulfovibrio* sp. strain G11 cultured under autotrophic conditions. Additionally, exposure to uninoculated medium amended with 20 mM crotonate caused one out of two metal samples to produce 45 pits.

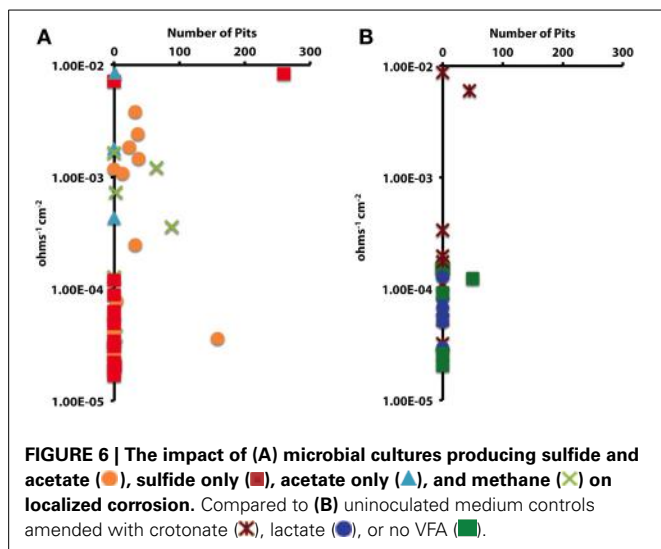
Given the unexpectedly high level of variability encountered, the same experiments were repeated with the same degree of replication. With few exceptions, the instantaneous corrosion rates were largely in the  $10^{-5}$  ohms<sup>-1</sup> cm<sup>-2</sup> range (**Table 4** experiment 2; Figure S13), and pitting was mainly associated with the *S. aciditrophicus* strain SB and *Desulfovibrio* sp. strain G11 co-cultures (**Table 4** experiment 2; Figure S14). *S. aciditrophicus* strain SB alone or in co-culture with *Desulfovibrio* sp. strain G11 metabolized  $\sim 2$  mM crotonate over the 30 days incubation (Figure S15), and the co-culture incubation reduced sulfate at  $0.30 \pm 0.08$  mM  $\text{SO}_4^{2-}\text{day}^{-1}$  (Figure S16). For comparison, *Desulfovibrio* sp. strain G11 cultured with lactate,  $\text{H}_2/\text{CO}_2$  overpressure, or hydrogen emanating from the coupon reduced sulfate at  $1.08 \pm 0.006$ ,  $0.36 \pm 0.06$ , and  $0.16 \pm 0.09$  mM  $\text{SO}_4^{2-}\text{day}^{-1}$ , respectively (Figure S15). Thus, even though similar sulfate reduction rates were measured between cultures and co-cultures from experiment 1, the instantaneous corrosion rates as well as localized corrosion were substantially less within these repeat incubations (**Table 4**).

## CORROSIVITY OF SPENT MEDIA

The apparent corrosivity of uninoculated controls (**Table 4**) caused us to question the role of parent substrates and metabolic end products in exacerbating coupon damage. This prompted an experiment wherein acetate and sulfide were exogenously added to the sterile basal medium to simulate the concentration of these substances following the metabolism of crotonate by a co-culture of *S. aciditrophicus* strain SB and *Desulfovibrio* sp. strain G11. The same thing was done to simulate the products acetate and sulfide associated with lactate metabolism by *Desulfovibrio* sp. strain G11. These incubation conditions were chosen because localized corrosion was consistently associated with the production of acetate and sulfide. The results indicated that instantaneous corrosion rates typically ranged between  $10^{-4}$  and  $10^{-5}$  ohms<sup>-1</sup> cm<sup>-2</sup>, and pitting was not detected on any of the metal surfaces (**Table 4**; Figures S17–S20).

## STATISTICAL TESTS

In order to determine whether statistical differences existed between the various experimental treatments, incubations were grouped according to end product production. These treatment groups included: sulfide only, sulfide and acetate, acetate only, methane, and uninoculated media controls. The treatment groups were then assessed by plotting the number of pits vs. the instantaneous corrosion rates for the individual microbial incubations (**Figure 6A**), and then compared to the uninoculated media controls (**Figure 6B**). The results suggested that when sulfide and acetate were produced as end products, corrosion was elevated relative to other microbial incubations as well as to the media controls (**Figure 6**). To further examine these differences, the surface damage for each coupon was compared using a Bayesian multilevel model. **Figure 7** displays the 63 histograms of points collected from the profilometer (i.e., one histogram for each coupon) separated into the five treatment groups. A histogram that is concentrated near the top of a panel (e.g.,  $-5 \mu\text{m}$ ) indicates less surface damage than a histogram concentrated closer to the bottom (e.g.,  $-20 \mu\text{m}$ ). A value of  $0 \mu\text{m}$  represents the highest point on the coupon's surface. The histograms are



skewed down, indicating that the depth of the (numerous) points are greater than the height of the (infrequent) peaks. The results indicated that incubations producing both sulfide and acetate as end products was the only treatment group that corroded significantly more than the media controls ( $p = 0.016$ ); typically the mean surface damage for these coupons was 2.2  $\mu\text{m}$  deeper than the uninoculated media controls.

## DISCUSSION

Anaerobic hydrocarbon degradation is an important ecological process within petroleum-laden environments, and one potential consequence of this metabolic activity is the sulfide-induced corrosion of carbon steel. However, the inherent complexity of the natural environment often makes it difficult to ascertain the biotic and abiotic factors that substantially influence biocorrosion. Our approach was to investigate this process in a more defined manner. That is, biocorrosion can be viewed as the interaction between electron donors of interest, a specific inoculum, the prevailing environmental conditions, and the composition of the metal (Suflita et al., 2013). Thus, we used defined microbial systems wherein the biological interactions with the electron donors were known and the metabolic end products could be reasonably anticipated. More specifically, we explored the impact of sulfate as an electron acceptor on metal biocorrosion in defined microbial assemblages and compared the damage to coupons when the same organisms were cultivated as syntrophic partnerships.

The corrosivity of the alkane-degrading, sulfate-reducing bacterium *D. alkanexedens* strain ALDC was previously assessed and was found to produce higher instantaneous corrosion rates and more pits compared to an uninoculated medium control containing 20 mM sulfide (Suflita et al., 2013). Presumably, the production of sulfide by *D. alkanexedens* strain ALDC from *n*-decane oxidation was responsible for the increase in instantaneous corrosion rate and localized corrosion. In this study, when axenic incubations of *D. alkanexedens* strain ALDC were cultured on *n*-decane under sulfate-reducing conditions, instantaneous corrosion rates were  $\sim 10$  times higher than comparable pure cultures

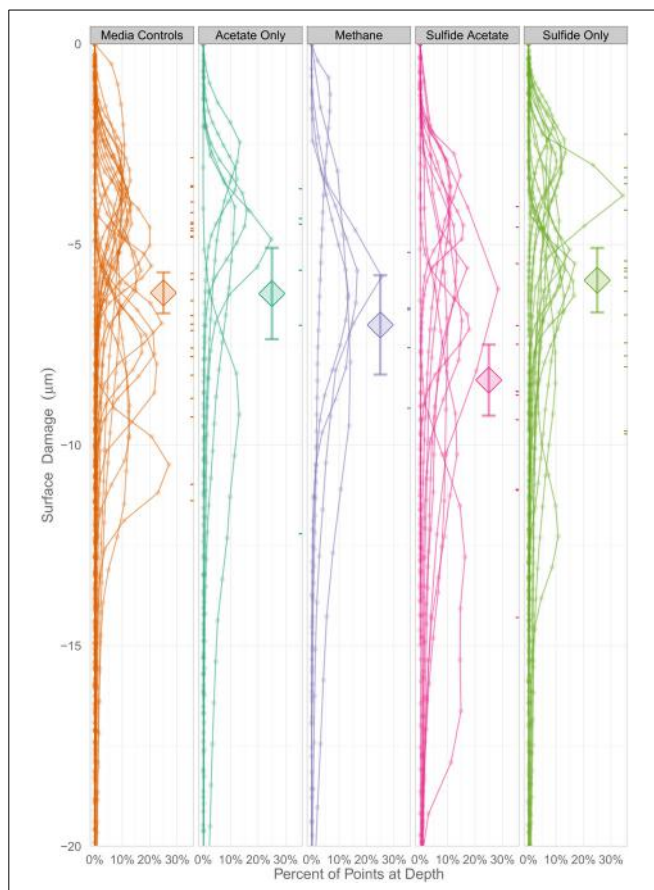


**FIGURE 7 |** A Bayesian multilevel model comparing the mean surface damage for treatment groups as well as individual coupons. The diamonds indicate a treatment group's mean depth, and the tick marks on the right side of the columns indicate an individual coupon's mean depth. The error bars mark the 16 and 84% percentiles of each treatment's posterior distribution, which corresponds to the asymptotic 68% coverage of a  $\pm 1$  standard error band, but is allowed to be asymmetric.

of *M. hungatei* strain JF-1 grown on  $\text{H}_2/\text{CO}_2$  or in a co-culture of the two microorganisms (Figure 2). Pitting also decreased when coupons were incubated with *M. hungatei* strain JF-1 alone or with the co-culture (Table 4; Figure S8). The biological replicates of *D. alkanexedens* strain ALDC pure culture incubations had similar sulfate reduction and instantaneous corrosion rates (Figure 2; Figure S5); however, despite these similarities, the replicate incubations had a high variability in the number of pits observed on the individual coupons (Table 4). This result suggests that the coupons were differentially pitting even though the replicate incubations were biologically and chemically similar. Variability in localized corrosion was also observed in both the co-culture and the uninoculated control incubations, in which a single replicate produced pits under the respective incubation conditions (Table 4). This result suggested that pitting was not specifically a function of sulfide production, as this end product was not produced in either incubation. Nevertheless, coupon pitting under methanogenic conditions as well as with uninoculated controls was a relatively rare occurrence compared to incubations under sulfate-reducing conditions (Figures 6, 7; Figure S21).

Previous research has suggested that the acetate concentration can exacerbate carbon steel corrosion by multiple mechanisms (Crolet et al., 1999; Hedges and McVeigh, 1999; Garsany et al., 2003; Suflita et al., 2008). At less than circumneutral pH values, at least some fraction of the acetate will exist as acetic acid and cause direct damage to metal surfaces. Therefore, it may be that *S. aciditrophicus* strain SB can contribute to corrosion through the production of acetate from the metabolism of fatty acids as a pure culture or when in syntrophic partnership. However, the instantaneous corrosion rates were not significantly different between axenic cultures of *S. aciditrophicus* strain SB and co-culture incubations with *M. hungatei* strain JF-1 or *Desulfovibrio* sp. strain G11 (Figure 3). However, when the coupons were subject to profilometric analysis, pitting was largely restricted to co-culture incubations of *S. aciditrophicus* strain SB and *Desulfovibrio* sp. strain G11 (Table 4 experiment 1; Figure S12). When *S. aciditrophicus* strain SB and *Desulfovibrio* sp. strain G11 co-culture incubations were repeated, instantaneous corrosion rates were substantially slower (Table 4 experiment 2; Figure S13), but pits were identified on all metal samples from the incubations (Table 4 experiment 2; Figure S14). Despite the 18 mM difference in crotonate metabolism between the experiments (Figures S11, S15), the *S. aciditrophicus* strain SB and *Desulfovibrio* sp. strain G11 co-culture was the only incubation condition that produced localized corrosion in all six replicates. The results suggest that corrosion is likely increased due to the production of both acetate and sulfide during the metabolism of crotonate under sulfate-reducing conditions.

The impact of lactate-grown *Desulfovibrio* sp. strain G11 on metal corrosion was similarly evaluated. This organism incompletely oxidizes lactate to acetate and uses sulfate as an external electron acceptor. Thus, if localized corrosion is at least a function of both acetate and sulfide production, pitting would be expected on the metal coupons. In fact, the results are largely consistent with this contention in that pitting occurred on metal surfaces in two of three replicate incubations (Table 4 experiment 1; Figure S12). Nevertheless, when these incubations were repeated, the instantaneous corrosion rates were substantially lower and no pits were evident by profilometry (Table 4 experiment 2; Figure S14) even though similar rates of sulfate reduction were measured between the two experiments (Figures S10, S16). The variability in pitting behavior between replicate incubations and repeat experiments that exhibited similar rates of substrate utilization and metabolic end product formation is enigmatic. Since the biological activity and the resulting chemistry is both defined and controlled, we are forced to attribute the variability to incubation components we could not adjust. More specifically, we presume the variations can somehow be attributed to differences in the composition of the carbon steel coupons. However, according to the bulk analysis by the manufacturer, the coupons were compositionally similar (Table S1).

To exemplify, autotrophically cultured *Desulfovibrio* sp. strain G11 cultures are able to reduce sulfate at different rates depending on whether the coupon itself served as a hydrogen source or if the electron donor was supplied exogenously. In the latter case, the sulfate reduction rate was comparable to the co-culture of this organism with *S. aciditrophicus* strain SB (Figures S10,

S16). However, corrosion measures were substantially less with the pure culture relative to the co-culture, thus implicating acetate as a confounding factor in sulfide-induced corrosion. (Table 4 experiments 1 and 2). The only exception is one replicate from experiment two (Table 4), which produced an instantaneous corrosion rate of  $10^{-3}$  ohms $^{-1}$  cm $^{-2}$  and had pitting on the side of the coupon (data not shown). Thus, only one metal coupon out of twelve substantially corroded upon exposure to autotrophically-grown *Desulfovibrio* sp. strain G11. Considering the relatively small amount of sulfide produced in these incubations ( $\sim$ 2 mM), the lack of acetate production, and the relatively consistent levels of coupon corrosion, differences in the corrosion behavior of a single replicate also point to potential differences in the coupons themselves.

Methanogens such as *Methanobacterium thermoautotrophicum* (Lorowitz et al., 1992) and *Methanococcus maripaludis* strain KA1 (Uchiyama et al., 2010) have been previously described to stimulate corrosion by either scavenging hydrogen or direct electron utilization from the surface of the metal coupons, respectively. *M. hungatei* strain JF-1 has not been reported to utilize either of these corrosion mechanisms, and when the metal was the only source of hydrogen in the incubation, methane production, instantaneous corrosion rates, and pitting were all negligible (data not shown) over the incubation period. Additionally, incubations of *M. hungatei* strain JF-1 amended with 138 kPa of H<sub>2</sub>/CO<sub>2</sub> did not exacerbate corrosion on any metal sample (Table 4). However, *M. hungatei* strain JF-1 was associated with corrosion within two incubations. The first was in co-culture with *D. alkanexedens* strain ALDC (Table 4, replicate 1, 64 pits; Figure S8), and the second was in co-culture with *S. aciditrophicus* strain SB (Table 4 experiment 1, replicate 1, 88 pits; Figure S12). Considering methane production was similar between replicate incubations (Figures S6, S9), the lack of sulfide production, and that pits were not detected on any other metal samples, the corrosion of these particular coupons are also attributed to the variability in the elemental composition of the metal sample.

Uninoculated media controls containing crotonate and lactate occasionally produced higher instantaneous corrosion rates (Figures 2, 3) than the corresponding inoculated incubations, and one replicate of a crotonate exposed coupon was found to have 45 pits at the end of the incubation (Table 4 experiment 1; Figure S12). Thus, we concluded that the potential for metal corrosion due to exposure to various fatty acids could be important considering that formate, acetate, propionate, butyrate, and benzoate have all been detected in oil reservoirs with concentrations exceeding 20 mM (Magot et al., 2000). However, when comparable uninoculated controls were specifically evaluated, corrosion was found to be negligible (Table 4 experiment 2). Additionally, corrosion was not stimulated on metal samples that were exposed to uninoculated incubations amended with crotonate, lactate, acetate and sulfide to represent the spent medium of *S. aciditrophicus* strain SB and *Desulfovibrio* sp. strain G11 co-cultures as well as lactate-amended *Desulfovibrio* sp. strain G11 pure cultures (Table 4; Figures S17–S20). Thus, the differences between our initial observations and subsequent experimentation (Table 4) also seem to be a function of the variable nature of the coupons, despite identical manufacturer bulk analyses.

Biocorrosion experiments exhibited high standard deviations for instantaneous corrosion rates and pitting for metal samples that was independent of inoculum type, biomass levels, initial substrate concentration, rates of microbial activity, or the degree of end product formation. Eliminating these factors as major contributors to the measured variability, forces us to attribute the large standard deviations to inconsistencies in the individual metal coupon samples. The bulk analysis of the metal from the manufacturer does not lend credence to this suggestion. However, low grade carbon steel is known to contain manganese sulfide inclusions (MnS) that are sites for pitting initiation and pit propagation (Vuillemin et al., 2003; Avci et al., 2013). The density of these submicron sized inclusions on carbon steel is typically thousands per square millimeter (Avci et al., 2013). It is unknown if the inclusions are evenly (randomly) distributed in metal or if they are clustered (heterogeneous) to any degree. It also seems clear that some inclusions are more susceptible as sites of pit initiation than others (Wranglen, 1974; Davis, 2013). Thus, both the distribution and the reactivity of inclusion bodies within a metal sample could substantially influence corrosion processes and help explain why seemingly similar metal samples may behave differently in corrosion experiments.

There was generally no agreement between instantaneous corrosion rates and the number of pits; that is localized corrosion did not always occur on coupons with higher ( $10^{-3}$  ohms $^{-1}$  cm $^{-2}$ )  $1/R_p$  values (Table 4; Figure 6). Electrochemical measurements, such as LPR, are considered highly sensitive and accurate (<0.5% error; Jones, 1996) for monitoring generalized corrosion, and profilometry can detect and quantify pits on a micron-scale. However, considering these methods were not always in agreement, other corrosion analyses would seem pertinent (e.g., weight loss, total iron determinations, manganese loss). Additionally, by differentially focusing our analysis on bulk fluids, the findings may not reflect reactions occurring in a biofilm on the metal surface. Localized metabolic activities in microbial biofilms, particularly the production of organic acids, can cause the pH to substantially decrease at the metal surface (Vroom et al., 1999). These points notwithstanding, our results generally show that localized corrosion was elevated when coupons were exposed to sulfide-producing cultures relative to methanogenic cultures or to uninoculated controls (Figures 6, 7; Figure S21).

The major implications of this work are that the anaerobic biodegradation of hydrocarbons or associated fatty acid intermediates linked to sulfate reduction can have important consequences with respect to the biocorrosion of carbon steel. That is, when sulfate is available as an electron acceptor, microbial assemblages will produce sulfide and low molecular weight organic acids that generally increase the corrosion of carbon steel. However, when the same organisms are in sulfate-limited environments and forced to live a syntrophic existence with a methanogen, biocorrosion is substantially reduced. These trends must be considered fairly general with more specific inferences being somewhat masked by the surprisingly high degree of variability associated with the corrosion assessments. Since the biological and chemical characteristics of the incubations were controlled, we were forced to attribute the high variability to differences with the metal samples themselves.

## AUTHOR CONTRIBUTIONS

All authors contributed equally to this work. Christopher N. Lyles was responsible for designing electrochemical and profilometry analyses to assess the corrosion of metal coupons, as well as data analysis, interpretation of results, and drafting the manuscript. Huynh M. Le cultured the microorganisms and also contributed to data analysis and interpretation. William Howard Beasley provided the statistical analyses. Michael J. McInerney critically revised the manuscript as well as provided much needed insight into a variety of aspects surrounding syntrophic microorganisms. Joseph M. Suflita is the corresponding author and has overseen all aspects of this project for both scientific accuracy and integrity.

## ACKNOWLEDGMENTS

This work was supported by a grant (Award No. N0001408WX20857) from the Office of Naval Research. We would also like to thank Karen Cloke of Phillips 66 for her assistance with the profilometry analysis.

## SUPPLEMENTARY MATERIAL

The Supplementary Material for this article can be found online at: <http://www.frontiersin.org/journal/10.3389/fmicb.2014.00114/abstract>

## REFERENCES

- Aktas, D. E., Lee, J. S., Little, B. J., Ray, R. I., Davidova, I. A., Lyles, C. N., et al. (2010). Anaerobic metabolism of biodiesel and its impact on metal corrosion. *Energy Fuels* 24, 2924–2928. doi: 10.1021/ef100084j
- Anderson, I., Ulrich, L. E., Lupa, B., Susanti, D., Porat, I., Hooper, S. D., et al. (2009). Genomic characterization of methanomicrobiales reveals three classes of methanogens. *PLOS ONE* 4:e5797. doi: 10.1371/journal.pone.0005797
- ASTM Standard A576-90b. (2006) (reapproved 2012). “Standard practice for preparing, cleaning, and evaluating corrosion test specimens,” in *Corrosion of Metals; Wear and Erosion* (West Conshohocken, PA: ASTM International).
- Avci, R., Davis, B. H., Wolfenden, M. L., Beech, I. B., Lucas, K., and Paul, D. (2013). Mechanism of MnS-mediated pit initiation and propagation in carbon steel in an anaerobic sulfidogenic media. *Corros. Sci.* 76, 267–274. doi: 10.1016/j.corsci.2013.06.049
- Bader, M. S. H. (2007). Sulfate removal technologies for oil fields seawater injection operations. *J. Pet. Sci. Eng.* 55, 93–110. doi: 10.1016/j.petrol.2006.04.010
- Bates, D. M. (2010). *lme4: Mixed-Effects Modeling with R*. Available online at: <http://lme4.r-forge.r-project.org/lMMwR/lrgprt.pdf>
- Blake, D., and Rowland, F. (1988). Continuing worldwide increase in tropospheric methane, 1978 to 1987. *Science* 239, 1129–1131. doi: 10.1126/science.239.4844.1129
- Callaghan, A. V. (2013). Enzymes involved in the anaerobic oxidation of n-alkanes: from methane to long-chain paraffins. *Front. Microbiol.* 4:89. doi: 10.3389/fmicb.2013.00089
- Cozzarelli, I. M., Baedecker, M. J., Eganhouse, R. P., and Goerlitz, D. F. (1994). The geochemical evolution of low-molecular-weight organic acids derived from the degradation of petroleum contaminants in groundwater. *Geochim. Cosmochim. Acta* 58, 863–877. doi: 10.1016/0016-7037(94)90511-8
- Crolet, J. L., Dugstad, A. L., and Thevenot, N. L. (1999). Role of free acetic acid on the CO<sub>2</sub> corrosion of steels. *Corrosion* 1–16.
- Davidova, I. A., Duncan, K. E., Choi, O. K., and Suflita, J. M. (2006). *Desulfoglaeba alkanexedens* gen. nov., sp. nov., an n-alkane-degrading, sulfate-reducing bacterium. *Int. J. Syst. Evol. Microbiol.* 56, 2737–2742. doi: 10.1099/ijs.0.64398-0
- Davis, B. H. (2013). *Anaerobic Pitting Corrosion of Carbon Steel in Marine Sulfidogenic Environment*. M.Sc. thesis, Physics Department, Montana State University, 156.
- Dinh, H. T., Kuever, J., Mußmann, M., Hassel, A. W., Stratmann, M., and Widdel, F. (2004). Iron corrosion by novel anaerobic microorganisms. *Nature* 427, 829–832. doi: 10.1038/nature02321

- Dolfing, J., Larter, S. R., and Head, I. M. (2008). Thermodynamic constraints on methanogenic crude oil biodegradation. *ISME J.* 2, 442–452. doi: 10.1038/ismej.2007.111
- Enning, D., and Garrels, J. (2014). Corrosion of iron by sulfate-reducing bacteria: new views of an old problem. *Appl. Environ. Microbiol.* 80, 1226–1236. doi: 10.1128/AEM.02848-13
- Enning, D., Venzlaff, H., Garrels, J., Dinh, H. T., Meyer, V., Mayrhofer, K., et al. (2012). Marine sulfate-reducing bacteria cause serious corrosion of iron under electroconductive biogenic mineral crust. *Environ. Microbiol.* 14, 1772–1787. doi: 10.1111/j.1462-2920.2012.02778.x
- Ferry, J. G., Smith, P. H., and Wolfe, R. S. (1974). Methanospirillum, a new genus of methanogenic bacteria, and characterization of *Methanospirillum hungati* sp. nov. *Int. J. Syst. Bacteriol.* 24, 465–469. doi: 10.1099/00207713-24-4-465
- Garsany, Y., Pletcher, D., and Hedges, B. (2003). “The role of acetate in CO<sub>2</sub> corrosion of carbon steel: studies related to oilfield conditions,” in *Corrosion 1–15. NACE International, Paper no. 03324* (Houston, TX).
- Gieg, L. M., Duncan, K. E., and Suflita, J. M. (2008). Bioenergy production via microbial conversion of residual oil to natural gas. *Appl. Environ. Microbiol.* 74, 3022–3029. doi: 10.1128/AEM.00119-08
- Hadfield, J. D. (2010). MCMC methods for multi-response generalized linear mixed models: the MCMCpack R package. *J. Stat. Softw.* 33, 1–22.
- Hamilton, W. A. (1985). Sulphate-reducing bacteria and anaerobic corrosion. *Annu. Rev. Microbiol.* 39, 195–217. doi: 10.1146/annurev.mi.39.100185.001211
- Head, I. M., Aitken, C. M., and Group, P. R. (2010). “Hydrocarbon degradation in petroleum reservoirs,” in *Handbook of Hydrocarbon and Lipid Microbiology*, ed. K. N. Timmis (Berlin; Heidelberg: Springer Berlin Heidelberg), 3098–3107.
- Hedges, B., and McVeigh, L. (1999). “The role of acetate in CO<sub>2</sub> corrosion: the double whammy,” in *Corrosion 1–18. NACE International, Paper no. 21* (Houston, TX).
- Heider, J., and Schühle, K. (2013). “Anaerobic biodegradation of hydrocarbons including methane,” in *The Prokaryotes*, eds E. Rosenberg, E. F. DeLong, S. Lory, E. Stackebrandt, and F. Thompson (Berlin; Heidelberg: Springer Berlin Heidelberg), 605–634.
- Hopkins, B. T., McInerney, M. J., and Warikoo, V. (1995). Evidence for anaerobic syntrophic benzoate degradation threshold and isolation of the syntrophic benzoate degrader. *Appl. Environ. Microbiol.* 61, 526–530.
- Hubert, C., and Voordouw, G. (2007). Oil field souring control by nitrate-reducing *Sulfurospirillum* spp. that outcompete sulfate-reducing bacteria for organic electron donors. *Appl. Environ. Microbiol.* 73, 2644–2652. doi: 10.1128/AEM.02332-06
- Jackson, B., Bhupathiraju, V., Tanner, R., Woese, C., and McInerney, M. (1999). *Syntrophus aciditrophicus* sp. nov., a new anaerobic bacterium that degrades fatty acids and benzoate in syntrophic association with hydrogen-using microorganisms. *Arch. Microbiol.* 171, 107–114. doi: 10.1007/s00203050685
- Jenneman, G. E., McInerney, M. J., and Knapp, R. M. (1986). Effect of nitrate on biogenic sulfide production. *Appl. Environ. Microbiol.* 51, 1205–1211.
- Jones, D. A. (1996). “Chapter 3: Electrochemical kinetics of corrosion,” in *Principles and Preventions of Corrosion 2nd edn*, eds B. Stenquist, R. Kernan, and P. Daly (Upper Saddle River, NJ: Prentice Hall), 75–115.
- Jones, D. M., Head, I. M., Gray, N. D., Adams, J. J., Rowan, A. K., Aitken, C. M., et al. (2008). Crude-oil biodegradation via methanogenesis in subsurface petroleum reservoirs. *Nature* 451, 176–180. doi: 10.1038/nature06484
- Kermani, M. B., and Morshed, A. (2003). Carbon dioxide corrosion in oil and gas production—a compendium. *Corrosion* 59, 659–683. doi: 10.5006/1.3277596
- King, R. A., and Miller, J. D. A. (1971). Corrosion by sulphate-reducing bacteria. *Nature* 233, 491–492. doi: 10.1038/233491a0
- King, R. A., Miller, J. D. A., and Smith, J. S. (1973a). Corrosion of mild steel by iron sulphides. *Br. Corros. J.* 8, 137–141. doi: 10.1179/000705973798322251
- King, R. A., Miller, J. D. A., and Wakerley, D. S. (1973b). Corrosion of mild steel in cultures of sulphate-reducing bacteria—effect of changing the soluble iron concentration during growth. *Br. Corros. J.* 8, 89–93. doi: 10.1179/bcj.1973.8.2.89
- King, R. A., and Wakerley, D. S. (1972). Corrosion of mild steel by ferrous sulphide. *Br. Corros. J.* 8, 41–45. doi: 10.1179/000705973798322521
- Lorowitz, W. H., Nagle, D. P., and Tanner, R. S. (1992). Anaerobic oxidation of elemental metals coupled to methanogenesis by *Methanobacterium thermoautotrophicum*. *Environ. Sci. Technol.* 26, 1606–1610. doi: 10.1021/es00032a018
- Lyles, C. N., Aktas, D. F., Duncan, K. E., Callaghan, A. V., Stevenson, B. S., and Suflita, J. M. (2013). Impact of organosulfur content on diesel fuel stability and implications for carbon steel corrosion. *Environ. Sci. Technol.* 47, 6052–6062. doi: 10.1021/es4006702
- Magot, M., Ollivier, B., and Patel, B. K. (2000). Microbiology of petroleum reservoirs. *Antonie Van Leeuwenhoek* 77, 103–116. doi: 10.1023/A:1002434330514
- Mayumi, D., Dolfing, J., Sakata, S., Maeda, H., Miyagawa, Y., Ikarashi, M., et al. (2013). Carbon dioxide concentration dictates alternative methanogenic pathways in oil reservoirs. *Nat. Commun.* 4, 1–6. doi: 10.1038/ncomms2998
- McInerney, M., Bryant, M., and Pfennig, N. (1979). Anaerobic bacterium that degrades fatty acids in syntrophic association with methanogens. *Arch. Microbiol.* 122, 129–135. doi: 10.1007/BF00411351
- McInerney, M. J., Rohlin, L., Mouttaki, H., Kim, U., Krupp, R. S., Rios-Hernandez, L., et al. (2007). The genome of *Syntrophus aciditrophicus*: life at the thermodynamic limit of microbial growth. *Proc. Natl. Acad. Sci. U.S.A.* 104, 7600–7605. doi: 10.1073/pnas.0610456104
- McInerney, M. J., Wofford, N. Q., and Sublette, K. L. (1996). Microbial control of hydrogen sulfide production in a porous medium. *Appl. Biochem. Biotechnol.* 57–58, 933–944. doi: 10.1007/BF02941774
- Mouttaki, H., Nanny, M. A., and McInerney, M. J. (2007). Cyclohexane carboxylate and benzoate formation from crotonate in *Syntrophus aciditrophicus*. *Appl. Environ. Microbiol.* 73, 930–938. doi: 10.1128/AEM.02227-06
- Nemati, M., Jenneman, G. E., and Voordouw, G. (2001). Impact of nitrate-mediated microbial control of souring in oil reservoirs on the extent of corrosion. *Biotechnol. Prog.* 17, 852–859. doi: 10.1021/bp010084v
- Reiffenstein, R. J., Hulbert, W. C., and Roth, S. H. (1992). Toxicology of hydrogen sulfide. *Annu. Rev. Pharmacol. Toxicol.* 32, 109–134. doi: 10.1146/annurev.pa.32.040192.000545
- Struchtemeyer, C. G., Duncan, K. E., and McInerney, M. J. (2011). Evidence for syntrophic butyrate metabolism under sulfate-reducing conditions in a hydrocarbon-contaminated aquifer. *FEMS Microbiol. Ecol.* 76, 289–300. doi: 10.1111/j.1574-6941.2011.01046.x
- Suflita, J. M., Lyles, C. N., Aktas, D. F., and Sunner, J. (2013). “Chapter 16: Biocorrosion issues associated with ultra low sulfur diesel and biofuel blends,” in *Understanding Biocorrosion: Fundamentals and Applications* (Woodhead Publishing), (in press).
- Suflita, J. M., Phelps, T. J., and Little, B. (2008). Carbon dioxide corrosion and acetate: a hypothesis on the influence of microorganisms. *Corrosion* 64, 854–859. doi: 10.5006/1.3279919
- Tanner, R. S. (2002). “Cultivation of bacteria and fungi,” in *Manual of Environmental Microbiology*, eds R. L. Crawford, G. R. Knudsen, M. J. McInerney, and L. D. Stetzenback (Washington, DC: ASM Press), 62–70.
- Teske, A. (2010). “Sulfate-reducing and methanogenic hydrocarbon-oxidizing microbial communities in the marine environment,” in *Handbook of Hydrocarbon and Lipid Microbiology*, ed K. N. Timmis (Berlin; Heidelberg: Springer Berlin Heidelberg), 2204–2216.
- Uchiyama, T., Ito, K., Mori, K., Tsurumaru, H., and Harayama, S. (2010). Iron-corroding methanogen isolated from a crude-oil storage tank. *Appl. Environ. Microbiol.* 76, 1783–1788. doi: 10.1128/AEM.00668-09
- Van Stempvoort, D. R., Armstrong, J., and Mayer, B. (2007). Seasonal recharge and replenishment of sulfate associated with biodegradation of a hydrocarbon plume. *Ground Water Monit. R.* 27, 110–121. doi: 10.1111/j.1745-6592.2007.00168.x
- Van Stempvoort, D. R., Millar, K., and Lawrence, J. R. (2009). Accumulation of short-chain fatty acids in an aquitard linked to anaerobic biodegradation of petroleum hydrocarbons. *Appl. Geochem.* 24, 77–85. doi: 10.1016/j.apgeochem.2008.11.004
- Vroom, J. M., De Grauw, K. J., Gerritsen, H. C., Bradshaw, D. J., Marsh, P. D., Watson, G. K., et al. (1999). Depth penetration and detection of pH gradients in biofilms by two-photon excitation microscopy. *Appl. Environ. Microbiol.* 65, 3502–3511.
- Vuillemin, B., Philippe, X., Oltra, R., Vignal, V., Coudreuse, L., Dufour, L. C., et al. (2003). SVET, AFM and AES study of pitting corrosion initiated on MnS inclusions by microinjection. *Corros. Sci.* 45, 1143–1159. doi: 10.1016/S0010-938X(02)00222-6

- Warikoo, V., McInerney, M. J., Robinson, J. A., and Suflita, J. M. (1996). Interspecies acetate transfer influences the extent of anaerobic benzoate degradation by syntrophic consortia. *Appl. Environ. Microbiol.* 62, 26–32.
- Wranglen, G. (1974). Pitting and sulphide inclusions in steel. *Corros. Sci.* 14, 331–349. doi: 10.1016/S0010-938X(74)80047-8

**Conflict of Interest Statement:** The authors declare that the research was conducted in the absence of any commercial or financial relationships that could be construed as a potential conflict of interest.

*Received: 09 November 2013; paper pending published: 13 January 2014; accepted: 07 March 2014; published online: 01 April 2014.*

*Citation:* Lyles CN, Le HM, Beasley WH, McInerney MJ and Suflita JM (2014) Anaerobic hydrocarbon and fatty acid metabolism by syntrophic bacteria and their impact on carbon steel corrosion. *Front. Microbiol.* 5:114. doi: 10.3389/fmicb.2014.00114

*This article was submitted to Aquatic Microbiology, a section of the journal Frontiers in Microbiology.*

*Copyright © 2014 Lyles, Le, Beasley, McInerney and Suflita. This is an open-access article distributed under the terms of the Creative Commons Attribution License (CC BY). The use, distribution or reproduction in other forums is permitted, provided the original author(s) or licensor are credited and that the original publication in this journal is cited, in accordance with accepted academic practice. No use, distribution or reproduction is permitted which does not comply with these terms.*



# DNA-based stable isotope probing coupled with cultivation methods implicates *Methylophaga* in hydrocarbon degradation

Sara Mishamandani<sup>1</sup>, Tony Gutierrez<sup>1,2\*</sup> and Michael D. Aitken<sup>1</sup>

<sup>1</sup> Department of Environmental Sciences and Engineering, Gillings School of Global Public Health, University of North Carolina, Chapel Hill, NC, USA

<sup>2</sup> Centre for Marine Biodiversity and Biotechnology, School of Life Sciences, Heriot-Watt University, Edinburgh, UK

**Edited by:**

Andreas Teske, University of North Carolina at Chapel Hill, USA

**Reviewed by:**

Kathleen Scott, University of South Florida, USA

Molly C. Redmond, University of North Carolina at Charlotte, USA

**\*Correspondence:**

Tony Gutierrez, School of Life Sciences, Heriot-Watt University, John Muir building, Edinburgh EH14 4AS, UK

e-mail: tony.gutierrez@hw.ac.uk

Marine hydrocarbon-degrading bacteria perform a fundamental role in the oxidation and ultimate removal of crude oil and its petrochemical derivatives in coastal and open ocean environments. Those with an almost exclusive ability to utilize hydrocarbons as a sole carbon and energy source have been found confined to just a few genera. Here we used stable isotope probing (SIP), a valuable tool to link the phylogeny and function of targeted microbial groups, to investigate hydrocarbon-degrading bacteria in coastal North Carolina sea water (Beaufort Inlet, USA) with uniformly labeled [<sup>13</sup>C]*n*-hexadecane. The dominant sequences in clone libraries constructed from <sup>13</sup>C-enriched bacterial DNA (from *n*-hexadecane enrichments) were identified to belong to the genus *Alcanivorax*, with  $\leq 98\%$  sequence identity to the closest type strain—thus representing a putative novel phylogenetic taxon within this genus. Unexpectedly, we also identified <sup>13</sup>C-enriched sequences in heavy DNA fractions that were affiliated to the genus *Methylophaga*. This is a contentious group since, though some of its members have been proposed to degrade hydrocarbons, substantive evidence has not previously confirmed this. We used quantitative PCR primers targeting the 16S rRNA gene of the SIP-identified *Alcanivorax* and *Methylophaga* to determine their abundance in incubations amended with unlabeled *n*-hexadecane. Both showed substantial increases in gene copy number during the experiments. Subsequently, we isolated a strain representing the SIP-identified *Methylophaga* sequences (99.9% 16S rRNA gene sequence identity) and used it to show, for the first time, direct evidence of hydrocarbon degradation by a cultured *Methylophaga* sp. This study demonstrates the value of coupling SIP with cultivation methods to identify and expand on the known diversity of hydrocarbon-degrading bacteria in the marine environment.

**Keywords:** hydrocarbon degradation, stable isotope probing, *Methylophaga*, *Alcanivorax*, *n*-hexadecane, marine environment

## INTRODUCTION

Hydrocarbon-degrading bacteria comprise an important component to the total microbial diversity in the marine environment, contributing significantly to the degradation and ultimate removal of hydrocarbons from the marine water column and sediment. Considering the enormous volumes of hydrocarbons that enter the oceans each year through natural seepage, anthropogenic activities and other sources, the fact that the sea surface is not covered in a layer of oil is largely due to the presence and activities of these types of bacteria. Species of hydrocarbon-degrading bacteria, belonging to over 20 genera and distributed across some of the major bacterial Classes (*Alpha*-, *Beta*- and *Gammaproteobacteria*; *Actinomycetes*; *Flexibacter-Cytophaga-Bacteroides*), have been isolated and described (Floodgate, 1995; Head and Swannell, 1999; Head et al., 2006; Yakimov et al., 2007). To our knowledge, the marine environment is the only place where we find bacteria with the ability to utilize hydrocarbons almost exclusively as a sole source of carbon and energy.

So-called “hydrocarbon specialists”, or “obligate oil-degraders”, these organisms are ubiquitous in the ocean, often found at  $<0.1\%$  abundance of the total microbial community in seawater, and becoming strongly selected for and increasing to levels constituting up to 90% of the total microbial community upon exposure to crude oil or its refined petrochemical products (Röling et al., 2002, 2004; Teira et al., 2007). This hydrocarbon-elicited bloom in microbial-expressed hydrocarbon catabolizing potential is one of the ocean’s inherent mechanisms to keeping the total load of hydrocarbons to background levels, in-turn helping to mitigate the potential detrimental effects that these chemical pollutants can pose to marine life.

Whilst our knowledge on the diversity of hydrocarbon-degrading bacteria in the ocean has progressed, it is far from complete, and novel taxa continue to be discovered. One bacterial genus that has proven contentious with respect to whether any of its members might be capable of degrading hydrocarbons is *Methylophaga*. Members of this genus are strictly aerobic and

moderately halophilic, belonging to the *Piscirickettsiaceae* family in the *Gammaproteobacteria*, and exhibit an exclusive requirement for C<sub>1</sub> sources (methanol, methylamine, dimethylsulfide) as sole growth substrates, with the exception of some species that are also capable of utilizing fructose (Janvier and Grimont, 1995). A few studies have reported the enrichment of *Methylophaga* spp. in oil-contaminated field samples and in laboratory experiments with oil (Röling et al., 2002; Yakimov et al., 2005; Coulon et al., 2007), but whether those organisms could degrade hydrocarbons was not addressed in those studies. Recently, Vila et al. (2010) isolated a *Methylophaga* species, designated strain AF3, from a beach impacted by the *Prestige* oil spill and showed it to grow in a synthetic seawater medium amended with high molecular weight polycyclic aromatic hydrocarbons (PAHs). However, since the medium was also amended with nutritionally-rich Luria-Bertani medium, the assumption that strain AF3 could grow on PAHs was unsubstantiated. Hence, compelling evidence showing a *Methylophaga* species to degrade hydrocarbons remains lacking.

One method that circumvents the requirement to isolate microorganisms in order to assess their metabolic and physiological characteristics is stable isotope probing (SIP). This method has been used successfully on environmental samples to identify a target microbial group(s) based on their ability to perform a specific metabolic process, thereby being able to link the phylogenetic identity of an organism to its function (Dumont and Murrell, 2005). An added advantage of this technique is its ability to identify target members of a microbial community that are not amenable to cultivation in the laboratory. In this study, we investigated hydrocarbon-degrading bacteria in surface seawater on the North Carolina coast using DNA-based SIP with uniformly labeled [<sup>13</sup>C]n-hexadecane and identified *Alcanivorax* and several other taxa, including *Methylophaga*, in the isolated <sup>13</sup>C-labeled “heavy” DNA. We subsequently isolated a strain representing this SIP-identified *Methylophaga*, designated strain SM14, which was found capable of growing on n-hexadecane as a sole source of carbon and energy. This work, which couples DNA-SIP with cultivation-based methods, for the first time reveals direct evidence implicating a *Methylophaga* species with the ability to utilize a hydrocarbon as a growth substrate.

## MATERIALS AND METHODS

### FIELD SAMPLE

During a field trip 1 mile offshore from the Beaufort Inlet (34° 33.42' N, 76° 51.06' W), North Carolina, USA on 27 August 2010, ca. 20 L of surface seawater was collected into pre-autoclaved polypropylene (Nalgene) bottles and stored at 4°C. On the following day, ca. 18 L of the water sample was filtered through 0.2-μm Nucleopore filters and the retained biomass resuspended in ONR7a medium (Dyksterhouse et al., 1995) to a total volume of ca. 100 ml to act as the inoculum for use in enrichment, mineralization, degradation and SIP experiments (described below).

### SIP INCUBATIONS

SIP incubations were performed as described previously (Gutierrez et al., 2013). Briefly, 16 125-ml autoclaved glass screw-top Erlenmeyer flasks with caps lined with aluminum foil to

prevent the adsorption of hydrocarbons were prepared. Each flask contained 15 ml of ONR7a medium, 1mg of labeled (<sup>14</sup>C or <sup>13</sup>C) and/or unlabeled n-hexadecane, and 5 ml of inoculum. [U-<sup>13</sup>C] n-hexadecane was obtained from Sigma-Aldrich (United States). For SIP, duplicate flasks were prepared with 1 mg of [U-<sup>13</sup>C] n-hexadecane, and a second set of duplicates was prepared with 1mg of the unlabeled counterpart. To determine the endpoint of each SIP experiment, the mineralization of [U-<sup>14</sup>C] n-hexadecane was measured in triplicate flasks by liquid scintillation counting of <sup>14</sup>CO<sub>2</sub> trapped in KOH-soaked filter paper over time, as described below. An additional set of triplicate flasks was used to monitor the disappearance of unlabeled n-hexadecane by gas chromatography–mass spectrometry (GC–MS). Samples were taken periodically from these flasks for DNA extraction and subsequent measurement of the abundance of target organisms (by qPCR as described below) identified through SIP. Triplicate flasks of acid-killed controls (pH ≤ 2) containing unlabeled n-hexadecane were prepared by adding 85% phosphoric acid (ca. 0.7 ml per flask). All flasks were incubated on an orbital shaker (250 rpm; 21°C) in the dark. At the endpoint of each SIP incubation—defined as the time when the extent of mineralization of the <sup>14</sup>C-labeled n-hexadecane began to approach an asymptote—whole DNA from the total volume in the paired flasks amended with the [U-<sup>13</sup>C] n-hexadecane and the corresponding paired set with unlabeled n-hexadecane was extracted using the method of Tillet and Neilan (2000).

To monitor the mineralization of [U-<sup>14</sup>C] n-hexadecane, each triplicate flask contained the <sup>14</sup>C-labeled compound to 20,000 dpm and 2.5 mg of unlabeled n-hexadecane. Killed controls (in triplicate) were also prepared by adding 85% phosphoric acid to pH ≤ 2 prior to inoculation. For the CO<sub>2</sub> trap, a sterile glass test tube (12 × 75 mm) containing a piece of filter paper saturated with 60 μl of 2 M KOH was inserted into each flask. The filter paper from each flask was removed daily and the captured <sup>14</sup>C from any <sup>14</sup>CO<sub>2</sub> respired was counted on a Packard (Meriden, CT, USA) Tri-Carb liquid scintillation analyser (model 1900TR). The KOH-saturated filter paper from each flask was replaced at each sampling point for the course of the experiment. The percentage of <sup>14</sup>C mineralized for [U-<sup>14</sup>C] n-hexadecane was calculated by subtracting the triplicate values for the acidified controls from those of the experimental and then dividing by the total dpm of <sup>14</sup>C added.

### CsCl GRADIENT ULTRACENTRIFUGATION AND IDENTIFICATION OF <sup>13</sup>C-ENRICHED DNA

To separate <sup>13</sup>C-enriched and unenriched DNA, total extracted DNA from each sample was added to cesium chloride (CsCl) solutions (1.72 g ml<sup>-1</sup>) for isopycnic ultracentrifugation and gradient fractionation, as previously described (Jones et al., 2011). As an internal standard for unlabeled DNA, 5 μl of purified *Escherichia coli* DNA (ca. 40 ng ml<sup>-1</sup>) was added and mixed into each tube prior to ultracentrifugation. Each fraction was then analyzed by denaturing gradient gel electrophoresis (DGGE) to visualize the separation of DNA. For this, PCR amplification of each fraction was carried out with primers 63f-GC (Marchesi et al., 1998) and 517r (Muyzer et al., 1993) using a PCR program as described by Yu and Morrison (2004). PCR

products were confirmed on a 1.5% (w/v) agarose gel alongside a HindIII DNA ladder (Invitrogen, Carlsbad, CA, USA). DGGE was performed using 6.5% acrylamide gels containing a denaturant range of 30–60%. After electrophoresis for 16 h at 60°C and 60 V, gels were stained with ethidium bromide (1:25,000 dilution; 15 min). Gel images were captured and visualized using the GNU Image Manipulation Program (GIMP; version 2.6.8).

#### 16S rRNA GENE LIBRARIES OF $^{13}\text{C}$ -ENRICHED DNA

16S rRNA clone libraries, each comprising 96 clones, were prepared from combined fractions containing the  $^{13}\text{C}$ -enriched DNA from each of the duplicate SIP incubations. For this, the general eubacterial primers 27f and 1492r were used for amplification of the 16S rRNA gene and then partially sequenced using primer 27f (Wilmotte et al., 1993) at the Beckman Coulter Genomics sequencing facility (Danvers, MA, USA). The  $^{13}\text{C}$ -enriched heavy DNA fractions were selected based on the DGGE evidence, as discussed below. After excluding vector sequences, poor-quality reads and chimeras, clone sequences were grouped into operational taxonomic units (OTUs) based on applying a 97% sequence identity cutoff. The complete linkage clustering and dereplicate tools available at the Pyrosequencing Pipeline tool of RDP-II (Cole et al., 2009) were used to select representative sequences for dominant OTUs identified in each of the libraries. Near-complete 16S rRNA gene sequences for the represented sequences were obtained at the University of North Carolina-Chapel Hill Genome Analysis Facility. Sequencher 4.8 (Gene Codes Corp., Ann Arbor, MI, USA) was used to edit and assemble these sequences, and the BLASTn search program and RDP-II (Maidak et al., 1999) were used to check for close relatives and phylogenetic affiliation.

#### REAL-TIME QUANTITATIVE PCR

To quantify sequences in the dominant OTUs, primers for real-time quantitative PCR (qPCR) were developed using the Probe Design and Probe Match tools of ARB, as previously described (Gutierrez et al., 2011). The Probe Check tool of RDP-II was used to confirm primer specificity, and the optimal annealing temperature of each primer pair was determined using an Eppendorf (Hauppauge, NY, USA) or Applied Biosystems (Foster City, CA, USA) Mastercycler gradient thermal cycler. The template for these reactions, and for the construction of respective standard curves for qPCR, was either a plasmid containing a representative sequence that had been linearized using PstI (New England BioLabs, Ipswich, MA, USA), or a PCR amplicon of the 16S rRNA gene, and purified using the QIAquick nucleotide removal kit (Qiagen, Valencia, CA, USA). The primer pairs, their optimal annealing temperature, amplification efficiency (Pfaffl, 2001), detection limit and RDP hits are shown in Table 1. To confirm the fractions from the DGGE profiles that corresponded to unlabeled DNA, *E. coli* primers ECP79f (5'-GAAGCTTGCTTCTTGCT-3') and ECR620r (5'-GAGCCCGGGATTCACA-3') were used to quantify the abundance of the *E. coli* 16S rRNA genes in each fraction. An annealing temperature of 55°C was used for the qPCR program employing these primers (Sabat et al., 2000).

Purified DNA from time-series incubations with unlabeled hydrocarbon was quantified using a NanoDrop ND-3300 fluorospectrometer (Thermo, Waltham, MA, USA) and the Quant-iT Picogreen double-stranded DNA (dsDNA) kit (Invitrogen). As duplicates of the separated  $^{12}\text{C}$ - and  $^{13}\text{C}$ -labeled incubations for each of the three SIP incubations displayed similar distributions of DNA in the fractions, as well as similar DGGE profiles, only the replicate incubation whose fractions contained the highest total amount of DNA was used for further analyses. SIP-identified sequences were quantified in each separated SIP fraction using at least duplicate reactions by qPCR, as described previously (Singleton et al., 2006). Single reactions were performed on each triplicate DNA extraction (from triplicate samples) from the time series containing unlabeled hydrocarbon.

#### ISOLATION AND DEGRADATION EXPERIMENTS

The detection of *Methylophaga* sequences in the heavy DNA clone library from SIP prompted us to isolate these organisms in order to further verify their potential to degrade hydrocarbons. For this, a fresh inoculum was prepared (as described above) from the same batch of North Carolina surface seawater and used to inoculate three 250-ml Erlenmeyer flasks, each containing 50 ml of ONR7a medium amended with methanol supplied via the vapor phase, as previously described (Paje et al., 1997). Methanol, as the sole carbon and energy source, was used in order to preferentially enrich for methylotrophs. After 1-week incubation (250 rpm; 21°C) in the dark, samples (50 µl) from each flask were streaked directly onto ONR7a agar plates and stored in a desiccator containing a small beaker containing ca. 50 ml of methanol. Colonies displaying distinct colonial morphologies were picked and subcultured onto fresh ONR7a agar medium (amended with methanol via the vapor phase) until pure cultures were obtained and stored in glycerol (30% v/v) at –80°C. One isolate, designated strain SM14, was selected for further study.

The potential of strain SM14 to grow on *n*-hexadecane as the sole carbon and energy source was determined in acid-washed (0.1 N HCl) 250-ml autoclaved glass screw-top Schott bottles with caps lined with aluminum foil to prevent the adsorption of hydrocarbons. Each bottle contained 50 ml of ONR7a medium and 1 mg of unlabeled *n*-hexadecane (>99% purity). One set of triplicate bottles was inoculated with strain SM14 cells that had been washed several times with sterile ONR7a broth. Uninoculated controls, acid-killed controls and bottles that were inoculated, but without any added *n*-hexadecane, were also prepared. All incubations were conducted in triplicate and incubated in the dark with shaking (150 rpm) at 25°C. Growth was monitored spectrophotometrically by taking triplicate measurements of the culture medium periodically at an optical density of 600 nm. Concentrations of *n*-hexadecane were measured by gas chromatography (GC). For this, triplicate samples (1 ml) were taken at each time point and extracted with 2 ml of ethyl acetate (EA). Heptanone, as internal standard, was added to each of the non-aqueous EA extracts prior to injection (3 µl) into a Hewlett Packard 5890 series II GC equipped with an Equity 1 (Supelco) column (60 m × 0.32 mm i.d.) and a flame ionization detector. The operating conditions were as follows: column temperature initially 60°C for 1 min, then 60–250°C at 18°C/min, followed

**Table 1 | Quantitative PCR primers developed and used in this study.**

Target OTU	Primer name	Primer sequence (5' → 3')	T <sub>M</sub> (°C) <sup>a</sup>	qPCR standard <sup>b</sup>	Amplicon length	Amp. Eff. <sup>c</sup>	Detect. limit <sup>d</sup>	RDP hits <sup>e</sup>
1	Alc-411	CSKGGAGTACTTGACGT	58	HEX19	195	1.82	5	21
	Alc-604r	CTGCACTCTAGCYGCCA						448(6)
4	Met-126f	GGGATCTGCCTGACAGTGGG	60	HEX76	90	1.63	1	88
	Met-214r	GGTTCATCTGTCAGCGTGAG						96(83)

<sup>a</sup>Empirically determined PCR annealing temperature.

<sup>b</sup>Representative clone sequences used to generate standard curves. Names are as in **Figures 3, 5**.

<sup>c</sup>Amp. Eff., amplification efficiency (Pfaffl, 2001) with OTU-specific primers.

<sup>d</sup>Detection limit of each qPCR assay expressed as number of 16S rRNA gene copies per milliliter of culture.

<sup>e</sup>Number of sequences returned by the Ribosomal Database Project II release 10.18 (Cole et al., 2009)(excluding sequences from this study) with no mismatches to primer pairs. Values in parentheses are the total hits that each pair of primers target.

by holding at 250°C for 18.5 min; injector temperature at 300°C; detector temperature at 310°C; and carrier gas He (1.0 ml min<sup>-1</sup>).

### PHYLOGENETIC TREE

The 16S rRNA sequences of the isolated strain and SIP-identified representative sequences were aligned using CLUSTAL\_X (Thompson et al., 1994) with close relatives as determined by RDP and BLASTn searches of GenBank. A neighbor-joining tree was constructed with bootstrapped replication (1000 times) and *Escherichia coli* 0157:H7 (AY513502) was used as an outgroup.

### NUCLEOTIDE SEQUENCE ACCESSION NUMBERS

The following accession numbers were submitted to GenBank for <sup>13</sup>C-enriched DNA from SIP experiment with *n*-hexadecane: *Alcanivorax* sp. clone HEX19 (KF875698) and *Methylophaga* sp. clone HEX76 (KF790924). The accession number for *Methylophaga* sp. strain SM14 is KF790925.

## RESULTS

### INCUBATIONS WITH LABELED AND UNLABELED *n*-HEXADECANE

During the SIP experiment, incubations containing unlabeled or <sup>14</sup>C-labeled *n*-hexadecane were run in parallel to measure, respectively, for the disappearance and mineralization of this hydrocarbon. As shown in **Figure 1**, complete removal of *n*-hexadecane occurred by day 5, whereas mineralization of <sup>14</sup>C associated with *n*-hexadecane continued up until day 7. The endpoint selected for the extraction of DNA from the <sup>13</sup>C incubations was 7 days, which corresponded to slowing of the mineralization rate for the *n*-hexadecane. The DNA extracts (from each of the duplicate <sup>13</sup>C incubations) was subjected to isopycnic ultracentrifugation to isolate the <sup>13</sup>C-enriched “heavy” DNA for subsequent analysis.

### DNA GRADIENT ULTRACENTRIFUGATION AND IDENTIFICATION OF LABELED 16S rRNA GENES

DGGE analysis of the fractions from the SIP incubations showed clear evidence of isotopic enrichment of DNA in [<sup>13</sup>C]*n*-hexadecane incubations, separation of <sup>13</sup>C-labeled and unlabeled DNA, and different banding patterns between the <sup>13</sup>C-enriched and unenriched DNA fractions (**Figure 2**). For the <sup>13</sup>C incubations shown in **Figure 2**, fractions 7–10 were combined and used to construct the 16S rRNA gene clone library. Fractions from the duplicate gradient (i.e., of the duplicate <sup>13</sup>C incubation) were

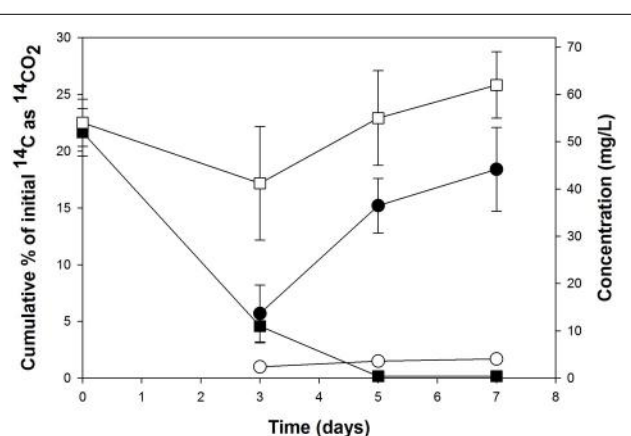


**FIGURE 1 | Cumulative <sup>14</sup>CO<sub>2</sub> recovered from incubations with [<sup>14</sup>C]*n*-hexadecane (circles) and disappearance of *n*-hexadecane as measured by GC-MS (squares) by the North Carolina surface seawater field sample.** The endpoint for this SIP incubation was determined to be 7 days. Each data point is the mean ± standard deviation from triplicate incubations. Filled symbols represent live cultures (non-acid treated); open symbols represent acid-inhibited controls. Some error bars are smaller than the symbol.

combined and similarly manipulated (data not shown). After excluding vector sequences, poor sequence reads, chimeras, and singleton sequences, the clone library constructed from pooled <sup>13</sup>C-enriched DNA comprised 85 sequences. **Table 2** shows the OTU representation in the clone library together with the phylogenetic affiliation based on a BLASTn search in GenBank. Of the 85 sequences, 5 OTUs were identified based on a >97% sequence identity cutoff. OTU-1 (71 sequences) comprised the majority (84%) of the 85 sequences and was found affiliated to the genus *Alcanivorax*. OTU-2 (4 sequences) and OTU-5 (4 sequences) were affiliated to the genus *Marinobacter* and shared 95% sequence identity. OTU-3 (3 sequences) and OTU-4 (3 sequences) were, respectively, affiliated to *Oleibacter* and *Methylophaga*. All other OTUs in the clone library were represented by single sequences and are presented in **Supplementary Table 1**.

Primers for qPCR were designed targeting the 16S rRNA gene of the most dominant SIP-identified group, *Alcanivorax* OTU-1 (**Table 1**), in order to quantify this group in the “heavy” DNA

from the SIP incubations (**Figure 2**) and in incubations with unlabeled *n*-hexadecane to confirm its enrichment (**Figure 3**). As shown in **Figure 2**, qPCR detection of this group was largely confined to the “heavy” DNA (fractions 7–10), thus confirming its enrichment of the  $^{13}\text{C}$  label from [ $^{13}\text{C}$ ]*n*-hexadecane. By day 5 in the unlabeled incubations (**Figure 3**), the gene copy number of this group increased by ca. 5 orders of magnitude, coinciding with the disappearance and mineralization of the *n*-hexadecane (**Figure 1**). This increase in gene copy number also coincided with

an increase in the total concentration of DNA as indicator of cell growth. The observed significant increase in the 16S rRNA gene copy number of this organism by day 5 coupled with its growth (total DNA as proxy), the disappearance and mineralization of the *n*-hexadecane, and appearance of respective 16S rRNA genes in only the most heavily  $^{13}\text{C}$ -enriched DNA fractions (**Figure 2**) of incubations containing the  $^{13}\text{C}$ -labeled substrate, strongly supports the enrichment of this *Alcanivorax* on the *n*-hexadecane as a growth substrate.

A similar approach was used to confirm the apparent enrichment of *Methylophaga* OTU-4 in the clone library constructed from  $^{13}\text{C}$ -enriched DNA (**Table 2**) and link this organism to the degradation of *n*-hexadecane. As shown in **Figure 2**, 13% of total *Methylophaga* genes were confined to the “heavy” DNA (fractions 7–10) compared to 56% in the “light” DNA (fractions 16–19), thus indicating partial enrichment of this organism in the  $^{13}\text{C}$ -enriched DNA. **Figure 3** shows that the gene copy number of this group increased by ca. 3 orders of magnitude by day 3,

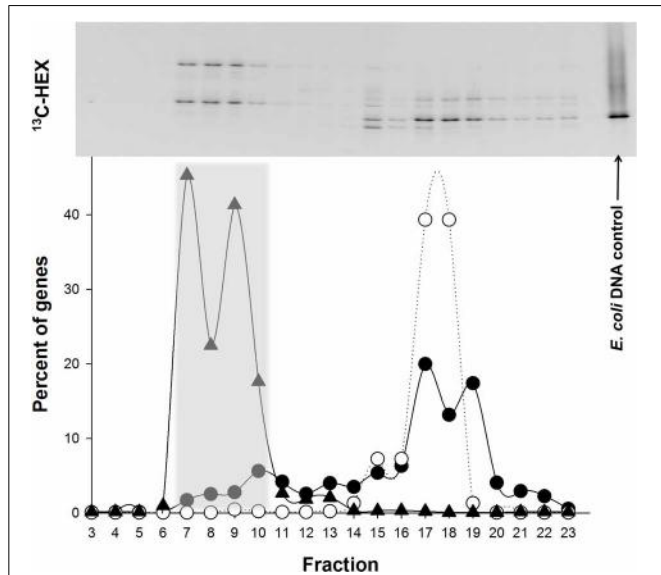


**FIGURE 2 | Distribution of the “heavy” and “light” DNA in separated SIP fractions.** (Top) DGGE image of bacterial PCR products from separated [ $^{13}\text{C}$ ]*n*-hexadecane fractions, with decreasing densities from left to right. The position of unlabeled *E. coli* DNA, which was used as an internal control in the isopycnic centrifugation, is shown on the right. (Bottom) Distribution of qPCR-quantified 16S rRNA gene sequences is shown below the DGGE image for *Alcanivorax* (triangles) and *Methylophaga* (solid circles) in fractions from the [ $^{13}\text{C}$ ]*n*-hexadecane incubations. The distribution of qPCR-quantified 16S rRNA gene sequences for *E. coli* is also shown (open circles) in fractions from the  $^{13}\text{C}$  incubation. Gene copies in a fraction are presented as a percentage of the total genes quantified in the displayed range of fractions. Data points are aligned with equivalent fractions of the DGGE image.

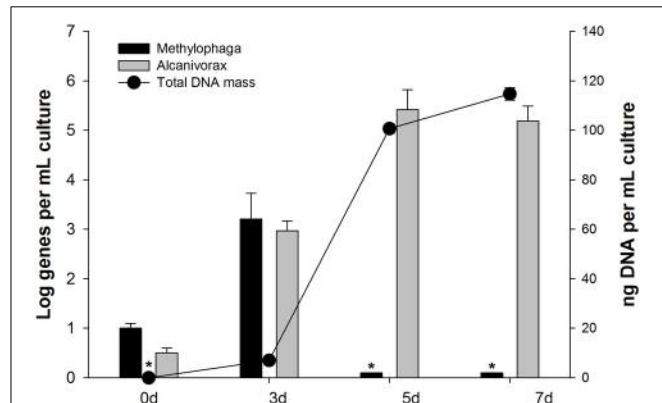


**FIGURE 3 | Abundance of *Alcanivorax* and *Methylophaga* 16S rRNA genes during incubation with unlabeled *n*-hexadecane.** Bars are the mean  $\pm$  standard deviations of results from triplicate qPCRs measuring the abundance of group-specific 16S rRNA genes. Circles are the mean  $\pm$  standard deviations of triplicate measurements of the total mass of DNA per sample. Bars or data points with asterisks represent numbers with one or more readings below the quantification limit of the assay and are presented as the largest possible value for that point.

**Table 2 | SIP-identified sequences in the clone library constructed from  $^{13}\text{C}$ -enriched DNA<sup>a</sup>.**

OUT no.	Rep. seq. <sup>b</sup>	Closest BLASTn match <sup>c</sup>	Accession no.	Clones in library (%) <sup>d</sup>
1	HEX19	<i>Alcanivorax jadensis</i> (98%)	AJ001150	71
2	HEX85	<i>Marinobacter lipolyticus</i> (97%)	AY147906	4
3	HEX49	<i>Oleibacter marinus</i> (99%)	AB435650	3
4	HEX76	<i>Methylophaga thiooxydans</i> (97%)	DQ660915	3
5	HEX17	<i>Marinobacter flavimaris</i> (100%)	AY517632	4

<sup>a</sup>HEX, SIP with [ $^{13}\text{C}$ ]*n*-hexadecane.

<sup>b</sup>Representative sequence for each OTU. Singleton sequences are listed in **Supplementary Table 1**.

<sup>c</sup>Results are to the closest type strain; percentage similarity shown in parentheses.

<sup>d</sup>Total number of sequences in  $^{13}\text{C}$ -enriched DNA clone library from the *n*-hexadecane SIP incubation was 85. A 97% cut-off was used to classify sequences to an OTU.

which coincided with ca. 80% disappearance of the *n*-hexadecane, 6% of  $^{14}\text{C}$  mineralized (as  $^{14}\text{CO}_2$ ) of initial  $^{14}\text{C}$  (as  $^{14}\text{C}$ -labeled *n*-hexadecane) and increase in total DNA concentration (as indicator of growth). At days 5 and 7, the gene copy number of this organism declined to reflect initial numbers (<0.5 Log genes per mL of culture).

#### GROWTH ON AND DEGRADATION OF *n*-HEXADECANE BY *METHYLOPHAGA* SP. STRAIN SM14

Enrichment experiments using the North Carolina field sample as inoculum and with methanol as the sole carbon and energy source yielded two isolates, designated strain SM13 and strain SM14. Both strains were found affiliated to the genus *Methylophaga* based on sequencing of their 16S rRNA gene—they shared 94% sequence identity between them. Strain SM13 proved difficult to maintain in laboratory culture as it eventually ceased to grow upon subsequent subculturing and was therefore no longer used for further experimentation. On the other hand, strain SM14 yielded small (0.05–0.15 mm) off-white colonies after 2 weeks incubation on ONR7a agar amended with Na-pyruvate as the sole carbon and energy source (not shown). The strain also grew well in ONR7a broth amended with Na-pyruvate or methanol. Evidence of the strain's ability to grow on *n*-hexadecane as a sole carbon and energy source is shown in **Figure 4**. At an initial *n*-hexadecane concentration of 0.002% (v/v), the strain reached a low cell density of ca. 0.015 at 600 nm. However, growth coincided with the disappearance of the *n*-hexadecane, which was indicative that the hydrocarbon was being degraded by the strain and utilized as a carbon source for growth. No growth was measured in uninoculated controls, or in inoculated incubations in the absence of any added *n*-hexadecane. Cultures amended with higher concentrations of *n*-hexadecane yielded higher cell densities (results not shown). Evidence that this was a pure culture of *Methylophaga* strain SM14 was confirmed by 16S rRNA gene sequencing of DNA isolated from cell pellets collected toward the end of these growth experiments.

#### PHYLOGENETIC ANALYSIS

The near-complete 16S rRNA gene sequence of the major SIP-identified OTUs and *Methylophaga* strain SM14 were used to construct a phylogenetic tree with related sequences from GenBank (**Figure 5**). The representative sequence for *Alcanivorax* identified from incubations with  $^{13}\text{C}$ -hexadecane (HEX19; OTU-1) shared highest 16S rRNA sequence identity (98%) with *Alcanivorax jadensis* T9 $^T$  (Fernandez-Martinez et al., 2003)—previously (*Fundibacter*) *jadensis* that had been isolated from intertidal sediment collected from the German North Sea coast (Bruns and Berthe-Corti, 1999); second highest sequence identity (97%) was with *Alcanivorax borkumensis* SK2 $^T$  that was isolated from seawater/sediment samples collected near the Isle of Borkum in the North Sea (Yakimov et al., 1998).

The 16S rRNA sequence of *Methylophaga* strain SM14 shared 99.9% identity with SIP clone HEX76 (*Methylophaga* OTU-4). Highest sequence identity for both SM14 and clone HEX76 was found with two uncultured *Methylophaga* clones, DOM03 and DOM14 (97.5% similarity), identified associated with marine dissolved organic matter (DOM) (McCarren et al., 2010). Highest

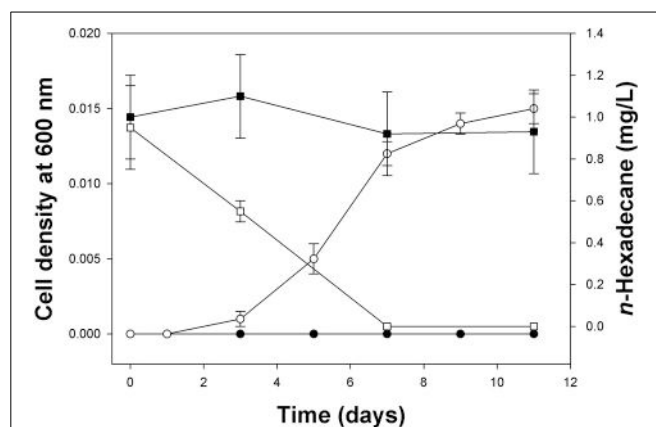
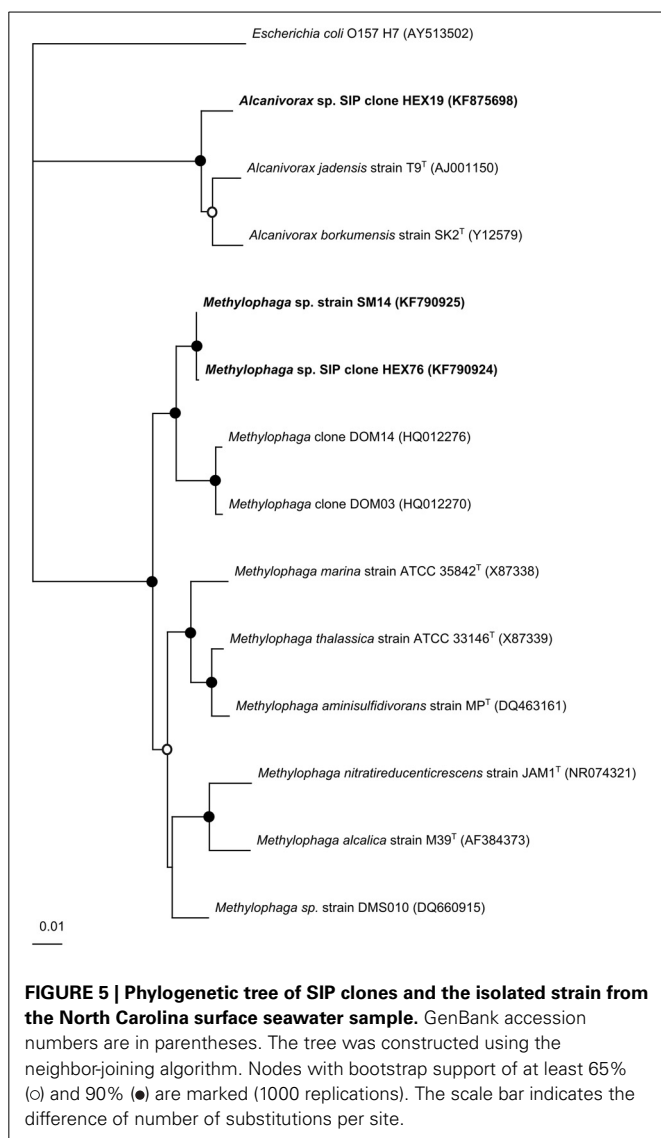


**FIGURE 4 | Growth of *Methylophaga* sp. strain SM14 on *n*-hexadecane (0.002% v/v) as the sole carbon and energy source and disappearance of the *n*-hexadecane as measured by GC.** Each data point is the mean  $\pm$  standard deviation from triplicate incubations. Open symbols represent live cultures (non-acid treated); filled symbols represent acid-inhibited controls. Circles and squares are cell density and GC measurements, respectively. Some error bars are smaller than the symbol.

sequence identity of SM14 and HEX76 to type strains was with *M. thiooxydans* DMS010 $^T$  (97.1%) isolated from an enrichment culture of the coccolithophorid *Emiliana huxleyi* with dimethylsulfide (Schäfer, 2007; Boden et al., 2010), whereas they shared  $\leq$ 95% to other *Methylophaga* type strains. To further clarify the phylogenetic identity of strain SM14, tree construction was also performed with the neighbor-joining, maximum parsimony, and maximum likelihood methods. In all cases, the position of strain SM14 always grouped to the genus *Methylophaga*.

#### DISCUSSION

SIP has proven useful for linking the phylogenetic identity of microorganisms with a metabolic function. However, careful attention must be employed in its design and execution in order for it to yield interpretable, unambiguous results. One of the main challenges in SIP is obtaining sufficient incorporation of the  $^{13}\text{C}$  into biomass, which in the case for DNA-SIP, its enrichment into DNA. Whilst the extent of labeling can be increased with longer incubation times, this can lead to the  $^{13}\text{C}$  becoming distributed among other members of the microbial community—i.e., that are not necessarily directly capable of metabolizing the isotopically-labeled substrate—by cross-feeding on  $^{13}\text{C}$ -labeled metabolic byproducts, intermediates, or dead cells (Leuders et al., 2004). To avert this, we had set up several  $^{12}\text{C}$  and  $^{14}\text{C}$  incubations that ran in parallel to the  $^{13}\text{C}$  incubations in order to tractably measure for the degradation (by GC-MS) and mineralization (by scintillation counts) of the *n*-hexadecane to help guide our selection of the point at which to terminate the  $^{13}\text{C}$  incubations (endpoint of experiment) whereby sufficient  $^{13}\text{C}$  incorporation had been achieved with minimal cross-feeding. The absence of a heavy DNA band in the  $^{12}\text{C}$  controls (not shown) and the distinct bimodal distribution between  $^{13}\text{C}$  and  $^{12}\text{C}$  DNA bands on DGGE confirmed the incorporation of the label from  $[^{13}\text{C}]n$ -hexadecane by a subgroup of the total microbial community.



Based on the clone libraries constructed from  $^{13}\text{C}$ -enriched DNA, the main consumers of the  $[^{13}\text{C}]n$ -hexadecane were affiliated with *Alcanivorax*—a group of cosmopolitan bacteria that utilize petroleum oil hydrocarbons almost exclusively as a preferred carbon and energy source. Since this SIP-identified *Alcanivorax*, represented by OTU-1 (clone HEX19), was found with  $\geq 2\%$  16S rRNA sequence difference to closely related type strains, it is likely to represent a new phylogenetic taxon within this genus. Further confirmation for the enrichment of this *Alcanivorax* OTU and its dominant role in the degradation of the *n*-hexadecane was provided by qPCR which revealed a dramatic increase in the abundance of the 16S rRNA gene copy number for these organisms in the unlabeled incubations (Figure 3). In addition, since growth of these organisms coincided with disappearance of the *n*-hexadecane, and appearance of their 16S rRNA genes in only the most heavily enriched  $^{13}\text{C}$ -DNA fractions, suggests that their presence in the clone libraries constructed from heavy DNA was unlikely due to cross-feeding. Other possible contributors

to the consumption of the  $[^{13}\text{C}]n$ -hexadecane during SIP were *Marinobacter* and *Oleibacter*, as several sequences (3–9% of the total clone library) were found affiliated with these genera in the libraries constructed from heavy DNA—members of these genera are commonly found enriched during oil spills in marine waters and can play a major role in the degradation of aliphatic hydrocarbons, such as *n*-hexadecane.

Intriguingly, several sequences affiliated to *Methylophaga* were also identified in the heavy DNA clone libraries (ca. 4% of the total clone library), and since this SIP-identified *Methylophaga* (represented by OTU-4) was found with  $\geq 3\%$  16S rRNA sequence difference to closely related type strains, it is likely to represent a new phylogenetic taxon within this genus. To our knowledge, this represents the first identification of *Methylophaga* by SIP targeting hydrocarbon degraders using a  $^{13}\text{C}$ -labeled hydrocarbon. Based on the presence of these organisms in the heavy DNA fractions (Figure 2) and increased abundance of their 16S rRNA gene copy number by day 3 in the unlabeled incubations—which coincided with the disappearance and mineralization of the *n*-hexadecane—these results supported the contribution of the respective newly identified *Methylophaga* (OTU-4) to the degradation of the hydrocarbon. We are unable at the present time to explain why the initial increase in their gene copy number was, by day 5, subsequently followed by a regression in their abundance to below detection limits. We observed similar results during a crude oil enrichment experiment in which pyrosequencing was used to analyse the bacterial community response associated with the marine diatom *Skeletonema costatum* to reveal an initial and distinctive bloom in *Methylophaga* (unpublished results). As the SIP experiment was designed to minimize the possibility of cross-feeding, and the various analyses performed (i.e., DNA quantification, qPCR of target genes, etc) support the enrichment of *Methylophaga* on the *n*-hexadecane as a growth substrate within at least the first 3 days of the experiment, it is highly unlikely that any *Methylophaga* DNA had migrated into the heavy fractions during isopycnic ultracentrifugation unless it was enriched with  $^{13}\text{C}$ . This is further supported by the fact that no single sequence of the internal standard (unlabeled *E. coli* DNA) was detected in the heavy fractions and clone libraries constructed from the heavy DNA. It is more likely, in fact, that *Methylophaga* sequences were underrepresented in  $^{13}\text{C}$ -enriched DNA clone libraries because the SIP experiment was terminated (day 7) after the apparent peak in growth of *Methylophaga* occurred (day 3; Figure 3).

In order to further validate whether the SIP-identified *Methylophaga* (OTU-4) were capable of utilizing *n*-hexadecane as a sole carbon and energy source, we isolated a member of this genus, *Methylophaga* strain SM14, that shared 99.9% 16S rRNA gene sequence identity to the representative sequence for this OTU (i.e., SIP clone HEX76) and directly demonstrated its ability to grow on and degrade *n*-hexadecane as a sole carbon and energy source (Figure 4). Collectively, our results present compelling evidence to implicate, for this first time, a novel member of the genus *Methylophaga* in hydrocarbon degradation, hence expanding the substrate spectrum for certain members of this genus beyond solely utilizing C1 carbon sources—with the exception of a few species able to also utilize fructose.

The discovery of hydrocarbon-degrading *Methylophaga* has important implications to assessing their role in the fate of the oil that entered the Gulf of Mexico during the Deepwater Horizon spill. During the active phase of the spill (April 20 to July 15), methylotrophic bacteria (incl. *Methylophaga*) were not detected near the leaky wellhead (Hazen et al., 2010; Valentine et al., 2010; Yang et al., 2014), whereas these organisms were reported to account for at least 5% of the total bacterial community after the spill—i.e., Kessler et al. (2011) reported 5–36% in Sep. 2010; Yang et al. (2014) report 0.23–6% and 2% in Sep. 2010 and Oct. 2010, respectively. However, a recent report by Dubinsky et al. (2013) which analyzed the microbial community composition of plume waters during June and August 2010—a time period not covered in these earlier reports—describes the start of a *Methylophaga* enrichment in plume waters during late June that appeared to be sustained until late August. Furthermore, transcriptional analysis by Rivers et al. (2013) of water column samples collected during the active phase of the spill (May 26 to June 3, 2010) revealed that *Methylophaga* were in a heightened state of metabolic activity within the plume relative to non-plume waters. Kessler et al. (2011) postulated that methylotrophs, such as *Methylophaga*, had contributed to the consumption of the methane released during the spill. However, such organisms are not recognized for carrying out the oxidation, or being capable of growing on, methane as a carbon and energy source. Hence, their potential to have consumed the methane remains contentious in the absence of substantive evidence to support this. Our results from SIP and with strain SM14 herein provide evidence to reassess the possibility that a subset of the *Methylophaga* community in the Gulf of Mexico, specifically those with hydrocarbon-degrading potential, may have contributed to the degradation of some components of the oil (e.g., saturated hydrocarbons). Dubinsky et al. (2013) measured higher-than-background levels of BTEX, cyclo-alkanes and *n*-alkanes in plume waters during the *Methylophaga*-enrichment phase in late June that, hence, might have acted as potential carbon and energy sources for these organisms. We hypothesize that the apparent enrichment of these organisms, albeit ephemerally, during the latter phase of the spill may have been in part associated with the potential for some members of this genus to degrade hydrocarbons.

## AUTHOR CONTRIBUTIONS

Sara Mishamandani, Tony Gutierrez, and Michael D. Aitken contributed to the design of the work and its interpretation. Sara Mishamandani and Tony Gutierrez produced all of the data and, together with Michael D. Aitken, drafted and critically revised the manuscript and approved the final version for publication.

## ACKNOWLEDGMENTS

We thank Frank Schwartz for providing us the opportunity to take samples during a field trip offshore the NC coast, and Janelle Fleming for additional assistance with our sampling needs. This work was supported by a Marie Curie International Outgoing Fellowship (PIOF-GA-2008-220129) within the 7th European Community Framework Programme. Partial support was also provided through the US National Institute of Environmental Health Sciences, grant 5 P42ES005948. Sara Mishamandani was

supported by a Summer Undergraduate Research Fellowship from the Office for Undergraduate Research at the University of North Carolina at Chapel Hill and by the Kimball King Undergraduate Research Fund administered by the UNC Honors Office. We also thank Scott Hauswirth for assistance with the GC-MS analysis at UNC Chapel Hill, James MacKinlay for assistance with the GC analysis at Heriot-Watt, David Singleton for assistance with qPCR, and Kirk Semple for providing [ $1-^{14}\text{C}$ ]*n*-hexadecane. Finally, we would like to also thank the two reviewers for their valuable comments during the preparation of the manuscript.

## SUPPLEMENTARY MATERIAL

The Supplementary Material for this article can be found online at: <http://www.frontiersin.org/journal/10.3389/fmich.2014.00076/abstract>

**Supplementary Table 1 |** Singleton 16S rRNA gene sequences recovered from the heavy DNA clone library<sup>a</sup>.

## REFERENCES

- Boden, R., Kelly, D. P., Murrell, J. C., and Schäfer, H. (2010). Oxidation of dimethylsulfide to tetrathionate by *Methylophaga thiooxidans* sp. nov.: a new link in the sulphur cycle. *Environ. Microbiol.* 12, 2688–2699. doi: 10.1111/j.1462-2920.2010.02238.x
- Bruns, A., and Berthe-Corti, L. (1999). *Fundibacter jadensis* gen. nov., sp. nov., a new slightly halophilic bacterium, isolated from intertidal sediment. *Int. J. Syst. Bacteriol.* 49, 441–448. doi: 10.1099/00207713-49-2-441
- Cole, J. R., Wang, Q., Cardenas, E., Fish, J., Chai, B., Farris, R. J. et al. (2009). The ribosomal database project: improved alignments and new tools for rRNA analysis. *Nucleic Acids Res.* 37, D141–D145. doi: 10.1093/nar/gkn879
- Coulon, F., McKew, B. A., Osborn, A. M., McGenity, T. J., and Timmis, K. N. (2007). Effects of temperature and biostimulation on oil-degrading microbial communities in temperate estuarine waters. *Environ. Microbiol.* 9, 177–186. doi: 10.1111/j.1462-2920.2006.01126.x
- Dubinsky, E. A., Conrad, M. E., Chakraborty, R., Bill, M., Borglin, S. E., Hollibaugh, J. T., et al. (2013). Succession of hydrocarbon-degrading bacteria in the aftermath of the Deepwater Horizon oil spill in the Gulf of Mexico. *Environ. Sci. Technol.* 47, 10860–10867. doi: 10.1021/es401676y
- Dumont, M., and Murrell, J. (2005). Stable isotope probing – linking microbial identity to function. *Nat. Rev. Microbiol.* 3, 499–504. doi: 10.1038/nrmicro1162
- Dyksterhouse, S. E., Gray, J. P., Herwig, R. P., Cano Lara, J., and Staley, J. T. (1995). *Cycloclasticus pugetii* gen. nov., sp. nov., an aromatic hydrocarbon-degrading bacterium from marine sediments. *Int. J. Syst. Bacteriol.* 45, 116–123. doi: 10.1099/00207713-45-1-116
- Fernandez-Martinez, J., Pujalte, M. J., Garcia-Martinez, J., Mata, M., Garay, E., and Rodriguez-Valera, F. (2003). Description of *Alcanivorax venustensis* sp. nov. and reclassification of *Fundibacter jadensis* DSM 12178<sup>T</sup> (Bruns and Berthe-Corti 1999) as *Alcanivorax jadensis* comb. nov., members of the amended genus *Alcanivorax*. *Int. J. Syst. Evol. Microbiol.* 53, 331–338. doi: 10.1099/ijss.0.01923-0
- Floodgate, G. D. (1995). Some environmental aspects of marine hydrocarbon bacteriology. *Aquat. Microb. Ecol.* 9, 3–11. doi: 10.3354/ame009003
- Gutierrez, T., Singleton, D. R., Aitken, M. D., and Semple, K. T. (2011). Stable-isotope probing of an algal bloom identifies uncultivated members of the *Rhodobacteraceae* associated with low molecular-weight PAH degradation. *Appl. Environ. Microbiol.* 77, 7856–7860. doi: 10.1128/AEM.06200-11
- Gutierrez, T., Singleton, D. R., Berry, D., Yang, T., Aitken, M. D., and Teske, A. (2013). Hydrocarbon-degrading bacteria enriched by the Deepwater Horizon oil spill identified by cultivation and DNA-SIP. *ISME J.* 7, 2091–2104. doi: 10.1038/ismej.2013.98
- Hazen, T. C., Dubinsky, E. A., DeSantis, T. Z., Andersen, G. L., Piceno, Y. M., Singh, N., et al. (2010). Deep-sea oil plume enriches indigenous oil-degrading bacteria. *Science* 330, 204–208. doi: 10.1126/science.1195979
- Head, I. M., Jones, D. M., and Röling, W. F. (2006). Marine microorganisms make a meal of oil. *Nat. Rev. Microbiol.* 4, 173–182. doi: 10.1038/nrmicro1348

- Head, I. M., and Swannell, R. P. J. (1999). Bioremediation of petroleum hydrocarbon contaminants in marine habitats. *Curr. Opin. Biotech.* 10, 234–239. doi: 10.1016/S0958-1669(99)80041-X
- Janvier, M., and Grimont, P. A. D. (1995). The genus *Methylophaga*, a new line of descent within phylogenetic branch  $\gamma$  of *Proteobacteria*. *Res. Microbiol.* 146, 543–550. doi: 10.1016/0923-2508(96)80560-2
- Jones, M. D., Singleton, D. R., Sun, W., and Aitken, M. D. (2011). Multiple DNA extractions coupled with stable-isotope probing of anthracene-degrading bacteria in contaminated soil. *Appl. Environ. Microbiol.* 77, 2984–2991. doi: 10.1128/AEM.01942-10
- Kessler, J. D., Valentine, D. L., Redmond, M. C., Du, M., Chan, E. W., Mendes, S. D., et al. (2011). A persistent oxygen anomaly reveals the fate of spilled methane in the deep Gulf of Mexico. *Science* 331, 312–315. doi: 10.1126/science.1199697
- Leuders, T., Wagner, B., Claus, P., and Friedrich, M. (2004). Stable isotope probing of rRNA and DNA reveals a dynamic methylotroph community and trophic interactions with fungi and protozoa in oxic rice field soil. *Environ. Microbiol.* 6, 60–72. doi: 10.1046/j.1462-2920.2003.00535.x
- Maidak, B. L., Cole, J. R., Parker, C. T. Jr., Garrity, G. M., Larsen, N., Li, B., et al. (1999). A new version of the RDP (Ribosomal Database Project). *Nucleic Acids Res.* 27, 171–173. doi: 10.1093/nar/27.1.171
- Marchesi, J. R., Sato, T., Weightman, A. J., Martin, T. A., Fry, J. C., Hiom, S. J., et al. (1998). Design and evaluation of useful bacterium-specific PCR primers that amplify genes coding for bacterial 16S rRNA. *Appl. Environ. Microbiol.* 64, 795–799.
- McCarren, J., Becker, J. W., Repeta, D. J., Shi, Y., Young, C. R., Malmstrom, R. R., et al. (2010). Microbial community transcriptomes reveal microbes and metabolic pathways associated with dissolved organic matter turnover in the sea. *Proc. Natl. Acad. Sci. U.S.A.* 107, 16420–16427. doi: 10.1073/pnas.1010732107
- Muyzer, G., de Waal, E. C., and Uitterlinden, A. G. (1993). Profiling of complex microbial populations by denaturing gradient gel electrophoresis analysis of polymerase chain reaction-amplified genes coding for 16S rRNA. *Appl. Environ. Microbiol.* 59, 695–700.
- Paje, M. L., Neilan, B., and Couperwhite, I. (1997). A *Rhodococcus* species that thrives on medium saturated with liquid benzene. *Microbiology* 143, 2975–2981. doi: 10.1099/00221287-143-9-2975
- Pfaffl, M. W. (2001). A new mathematical model for relative quantification in real-time RT-PCR. *Nucleic Acids Res.* 29, 2002–2007. doi: 10.1093/nar/29.9.e45
- Rivers, A. R., Sharma, S., Tringe, S. G., Martin, J., Joye, S. B., and Moran, M. A. (2013). Transcriptional response of bathypelagic marine bacterioplankton to the Deepwater Horizon oil spill. *ISME J.* 7, 2315–2329. doi: 10.1038/ismej.2013.129
- Röling, W. F. M., Milner, M. G., Jones, D. M., Fratipietro, F., Swannell, R. P. J., Daniel, F., et al. (2004). Bacterial community dynamics and hydrocarbon degradation during a field-scale evaluation of bioremediation on a mudflat beach contaminated with buried oil. *Appl. Environ. Microbiol.* 70, 2603–2613. doi: 10.1128/AEM.70.5.2603-2613.2004
- Röling, W. F. M., Milner, M. G., Martin Jones, D., Lee, K., Daniel, F., Swannell, R. J. P., et al. (2002). Robust hydrocarbon degradation and dynamics of bacterial communities during nutrient-enhanced oil spill bioremediation. *App. Environ. Microbiol.* 68, 5537–5548. doi: 10.1128/AEM.68.11.5537-5548.2002
- Sabat, G., Rose, P., Hickey, W. J., and Harkin, J. M. (2000). Selective and sensitive method for PCR amplification of *Escherichia coli* 16S rRNA genes in soil. *Appl. Environ. Microbiol.* 66, 844–849. doi: 10.1128/AEM.66.2.844-849.2000
- Schäfer, H. (2007). Isolation of *Methylophaga* spp. from marine dimethylsulfide-degrading enrichment cultures and identification of polypeptides induced during growth on dimethylsulfide. *Appl. Environ. Microbiol.* 73, 2580–2591. doi: 10.1128/AEM.02074-06
- Singleton, D. R., Sangaiah, R., Gold, A., Ball, L. M., and Aitken, M. D. (2006). Identification and quantification of uncultivated *Proteobacteria* associated with pyrene degradation in a bioreactor treating PAH-contaminated soil. *Environ. Microbiol.* 8, 1736–1745. doi: 10.1111/j.1462-2920.2006.01112.x
- Teira, E., Lekunberri, I., Gasol, J. M., Nieto-Cid, M., Alvarez-Salgado, X. A., and Figueiras, F. G. (2007). Dynamics of the hydrocarbon-degrading *Cycloclasticus* bacteria during mesocosm-simulated oil spills. *Environ. Microbiol.* 9, 2551–2562. doi: 10.1111/j.1462-2920.2007.01373.x
- Thompson, J. D., Higgins, D. G., and Gibson, T. J. (1994). CLUSTAL\_X: improving the sensitivity of progressive multiple sequence alignment through sequence weighting, position-specific gap penalties and weight matrix choice. *Nucleic Acids Res.* 22, 4673–4680. doi: 10.1093/nar/22.22.4673
- Tillet, D., and Neilan, B. A. (2000). Xanthogenate nucleic acid isolation from cultured and environmental cyanobacteria. *J. Phycol.* 36, 251–258. doi: 10.1046/j.1529-8817.2000.99079.x
- Valentine, D. L., Kessler, J. D., Redmond, M. C., Mendes, S. D., Heintz, M. B., Farwell, C., et al. (2010). Propane respiration jump-starts microbial response to a deep oil spill. *Science* 330, 208–211. doi: 10.1126/science.1196830
- Vila, J., Nieto, J. M., Mertens, J., Springael, D., and Grifoll, M. (2010). Microbial community structure of a heavy fuel oil-degrading marine consortium: linking microbial dynamics with polycyclic aromatic hydrocarbon utilization. *FEMS Microbiol. Ecol.* 73, 349–362. doi: 10.1111/j.1574-6941.2010.00902.x
- Wilmette, A., van der Auwera, G., and De Wachter, R. (1993). Structure of the 16S ribosomal RNA of the thermophilic cyanobacterium *Chlorogloeoopsis HTF* (*Mastigocladus laminosus* HTF) strain PCC7518, and phylogenetic analysis. *FEMS Microbiol. Lett.* 317, 96–100. doi: 10.1016/0014-5793(93)81499-P
- Yakimov, M. M., Denaro, R., Genovese, M., Cappello, S., D'Auria, G., Chernikova, T. N., et al. (2005). Natural microbial diversity in superficial sediments of Milazzo Harbor (Sicily) and community successions during microcosm enrichment with various hydrocarbons. *Environ. Microbiol.* 7, 1426–1441. doi: 10.1111/j.1462-5822.2005.00829.x
- Yakimov, M. M., Golyshin, P. N., Lang, S., Moore, E. R. B., Abraham, W.-R., Lönsdorf, H., et al. (1998). *Alcanivorax borkumensis* gen. nov., sp. nov., a new, hydrocarbon-degrading and surfactant-producing marine bacterium. *Int. J. Syst. Bacteriol.* 48, 339–348. doi: 10.1099/00207713-48-2-339
- Yakimov, M. M., Timmis, K. N., and Golyshin, P. N. (2007). Obligate oil-degrading marine bacteria. *Curr. Opin. Biotech.* 18, 257–266. doi: 10.1016/j.copbio.2007.04.006
- Yang, T., Nigro, L. M., Gutierrez, T., D'Ambrosio, L., Joye, S. B., Highsmith, R., et al. (2014). Pulsed blooms and persistent oil-degrading bacterial populations in the water column during and after the Deepwater Horizon blowout. *Deep-Sea Res. II*. doi: 10.1016/j.dsr2.2014.01.014. (in press).
- Yu, Z., and Morrison, M. (2004). Comparisons of different hypervariable regions of *rrs* genes for use in fingerprinting of microbial communities by PCR-denaturing gradient gel electrophoresis. *Appl. Environ. Microbiol.* 70, 4800–4806. doi: 10.1128/AEM.70.8.4800-4806.2004
- Conflict of Interest Statement:** The authors declare that the research was conducted in the absence of any commercial or financial relationships that could be construed as a potential conflict of interest.
- Received:** 20 November 2013; **paper pending published:** 22 January 2014; **accepted:** 11 February 2014; **published online:** 27 February 2014.
- Citation:** Mishamandani S, Gutierrez T and Aitken MD (2014) DNA-based stable isotope probing coupled with cultivation methods implicates *Methylophaga* in hydrocarbon degradation. *Front. Microbiol.* 5:76. doi: 10.3389/fmicb.2014.00076
- This article was submitted to Aquatic Microbiology, a section of the journal *Frontiers in Microbiology*.
- Copyright © 2014 Mishamandani, Gutierrez and Aitken. This is an open-access article distributed under the terms of the Creative Commons Attribution License (CC BY). The use, distribution or reproduction in other forums is permitted, provided the original author(s) or licensor are credited and that the original publication in this journal is cited, in accordance with accepted academic practice. No use, distribution or reproduction is permitted which does not comply with these terms.



# Evaluation of the biodegradation of Alaska North Slope oil in microcosms using the biodegradation model BIOB

Jagadish Torlapati<sup>1</sup> and Michel C. Boufadel<sup>2\*</sup>

<sup>1</sup> Center for Natural Resources Development and Protection, New Jersey Institute of Technology, Newark, NJ, USA

<sup>2</sup> Department of Civil and Environmental Engineering, Center for Natural Resources Development and Protection, New Jersey Institute of Technology, Newark, NJ, USA

**Edited by:**

Joel E. Kostka, Georgia Institute of Technology, USA

**Reviewed by:**

Roger C. Prince, ExxonMobil Biomedical Sciences, Inc., USA

Robert Duran, Université de Pau et des Pays de l'Adour, France

**\*Correspondence:**

Michel C. Boufadel, Center for Natural Resources Development and Protection, New Jersey Institute of Technology, Faculty Memorial Hall 213, 323 MLK Blvd, Newark, NJ 07102, USA  
e-mail: boufadel@gmail.com

We present the details of a numerical model, BIOB that is capable of simulating the biodegradation of oil entrapped in the sediment. The model uses Monod kinetics to simulate the growth of bacteria in the presence of nutrients and the subsequent consumption of hydrocarbons. The model was used to simulate experimental results of Exxon Valdez oil biodegradation in laboratory columns (Venosa et al., 2010). In that study, samples were collected from three different islands: Eleanor Island (EL107), Knight Island (KN114A), and Smith Island (SM006B), and placed in laboratory microcosms for a duration of 168 days to investigate oil bioremediation through natural attenuation and nutrient amendment. The kinetic parameters of the BIOB model were estimated by fitting to the experimental data using a parameter estimation tool based on Genetic Algorithms (GA). The parameter values of EL107 and KN114A were similar whereas those of SM006B were different from the two other sites; in particular biomass growth at SM006B was four times slower than at the other two islands. Grain size analysis from each site revealed that the specific surface area per unit mass of sediment was considerably lower at SM006B, which suggest that the surface area of sediments is a key control parameter for microbial growth in sediments. Comparison of the BIOB results with exponential decay curves fitted to the data indicated that BIOB provided better fit for KN114A and SM006B in nutrient amended treatments, and for EL107 and KN114A in natural attenuation. In particular, BIOB was able to capture the initial slow biodegradation due to the lag phase in microbial growth. Sensitivity analyses revealed that oil biodegradation at all three locations were sensitive to nutrient concentration whereas SM006B was sensitive to initial biomass concentration due to its slow growth rate. Analyses were also performed to compare the half-lives of individual compounds with that of the overall polycyclic aromatic hydrocarbons (PAHs).

**Keywords:** oil spill, biodegradation, numerical modeling

## INTRODUCTION

The Exxon Valdez oil spill (EVOS) of 1989 in Prince William Sound (PWS) resulted in the contamination of approximately 2000 km of shoreline within the Gulf of Alaska (Bragg et al., 1994). The more recent Deepwater Horizon oil spill contaminated over 1600 km of shoreline within the Gulf of Mexico (Barron, 2012; Lubchenco et al., 2012). Removal of oil spilled in the environment requires approaches that are both effective and environmentally safe, and one of the techniques is bioremediation, which relies on augmenting the natural biodegradation rate of oil (Atlas, 1995; Vogel, 1996; Xu and Obbard, 2004; Cunliffe and Kertesz, 2006; Karamalidis et al., 2010).

Bioremediation can be studied by conducting laboratory scale experiments (Boufadel et al., 1999; Sabaté et al., 2004; Chen et al., 2008; Tian et al., 2008; Beolchini et al., 2010; Lors et al., 2012) or field scale experiments. Boufadel et al. (1999) evaluated the nitrate concentration required for maximum biodegradation of n-heptadecane in sand columns with monitored oxygen consumption and carbon dioxide production. They reported that the maximum biodegradation occurs at a concentration of

2.5 mg nitrate-N/L. They also speculated nitrogen recycling by biomass when the influent nitrate concentration was zero. This occurred by lysing (break apart) of cells to provide nutrients that other cells could use for growth and biodegradation. Wrenn et al. (2006) studied the effects of nutrient source and supply in crude oil biodegradation. They observed that the extent and rate of oil biodegradation remain unchanged regardless of whether the nutrient supply was intermittent or continuous. Desai et al. (2008) investigated the biodegradation kinetics of individual components and PAHs and their studies indicated that the prediction of natural or enhanced biodegradation of PAHs cannot be based on single compound kinetics as this assumption would overestimate the rate of disappearance, and does not account for the inhibition due to competitive interactions between the compounds.

Venosa et al. (2010) conducted laboratory experiments to study the biodegradation of 19 year old lingering weathered oil in PWS due to EVOS at three different islands. They observed that the most weathered oil was the most biodegradable. The experimental results obtained from laboratory scale experiments could

be used to gain a better understanding of the kinetic processes involved in biodegradation by the use of numerical models.

Numerical models have been routinely used by researchers to predict the results. Essaid et al. (2003) used the US Geological Survey (USGS) solute transport and biodegradation code BIOMOC coupled with the USGS universal inverse modeling code UCODE to quantify the BTEX dissolution and biodegradation at a site located in Bemidji, MN. Vilcáez et al. (2013) developed a numerical model for the biodegradation of oil droplets as opposed to dissolved oil, and it was applied to estimate the time scale of biodegradation of Deepwater Horizon oil spill in Gulf of Mexico. The model revealed that small oil droplets biodegraded faster due to their larger surface area per unit mass. Herold et al. (2011) modeled the enhanced bioremediation of ground-water contaminated by acenaphthene, methylbenzofurans, and dimethylbenzofurans. The calibrated model was used to explore the feasibility and efficiency of remediation scenarios. It was observed from their simulations that even with several simplifications made in conceptualization, they were able to demonstrate the ability of their model to detect key processes needed for an effective remediation scheme. Geng et al. (2013) developed a mathematical model to simulate the biodegradation of residual hydrocarbon in a variably-saturated sand column. They estimated the biodegradation kinetic parameters by fitting the model to experimental data of oxygen, CO<sub>2</sub> and residual mass of heptadecane obtained from two columns. They were also able to predict accurately the biodegradation for three other columns using the same parameters.

The goal of this study is to present a numerical model, BIOB which is capable of simulating the biodegradation of oil entrapped in the sediments, and to estimate its parameters using the experimental results from Venosa et al. (2010). The estimated parameters will be used to predict biodegradation under different environmental conditions. A parameter estimation tool based on Genetic Algorithm (GA) is employed to automatically conducting the fitting. Finally, the sensitivity of the model prediction to the kinetic parameters of the BIOB model is evaluated.

## BIODEGRADATION OF EXXON VALDEZ OIL IN MICROCOSMS

Venosa et al. (2010) conducted laboratory experiments to test the biodegradability of 19 year old lingering oil due to the 1989 EVOS in Alaska, USA. They assessed whether or not oil weathered more than 70% could undergo further biodegradation. Oil weathering could occur as a result of its physical (e.g., evaporation, dissolution, washout), chemical (e.g., photooxidation), or microbial (e.g., biodegradation) processes. Oil weathering by biodegradation can be distinguished from the other processes by using biomarkers (e.g., hopane) to normalize the measured oil concentration. Biomarkers are compounds that biodegrade very slowly within the time frame of interest and have been used to evaluate the effectiveness of biodegradation (Bragg et al., 1994; Venosa et al., 1996). In Venosa et al. (2010), the PAH concentrations were normalized using hopane. The degree of weathering is calculated by comparing the constitution of the weathered oil with the fresh oil. Samples were collected from three different sites of Eleanor Island (EL107), Knight Island (KN114A), and Smith Island (SM006B) whose respective mass weathering indices

(MWI) were 30, 76, and 60%. These samples of oil-contaminated sediment were collected from each site by digging up to 10–40 cm below the surface. The volume of each sample was about 50 L and the collected samples were used for microcosm experiments at the University of Cincinnati. Seawater samples from each island were also collected for natural attenuation experiments.

The collected samples were then used for experiments to study (a) natural attenuation, the biodegradation due to the nutrients naturally present in seawater/sediment and (b) nutrient-amended treatment, where nutrients were added to the samples and the concentrations of the nutrients were maintained by adding 10 mg/L of KNO<sub>3</sub> to ensure no nutrient limitation occurs (Venosa et al., 1996; Boufadel et al., 1999; Du et al., 1999). Each microcosm contained 800 mL volume of mixed sediment weighing approximately 1.5 kg with glass beads of diameter 2 and 3 mm at the top and bottom of the sediment to prevent sediment fines from exiting the unit. A peristaltic pump was used to withdraw seawater from the bottom of the microcosms at a flow rate of 2 mL/min to an overhead reservoir. The overhead reservoir worked by a siphon mechanism and the seawater is released to the natural attenuation microcosms every 4 h. Samples were collected at 0, 14, 28, 56, 112, and 168 days and the temperature during the experimental study was similar to the conditions in PWS which was 15°C.

The sediments from each microcosm were analyzed for hydrocarbons using gas chromatography/mass spectrometry (GC/MS). The Total Kjeldahl Nitrogen (TKN) was measured using the Hach method (Hach et al., 1985). The results obtained from these experimental analyses indicated that there was significant biodegradation in the nutrient-amended samples, even when the MWI was high. The experimental results were fitted by Venosa et al. (2010) using a first-order decay model. Their model showed that the highest biodegradation rate occurred in the most weathered oil (KN114A). The experimental results also showed that natural attenuation (non-nutrient amended microcosms) resulted in significant oil biodegradation although the biodegradation rates were lower compared to the nutrient-amended microcosms. This shows that supplying nutrients to the contaminated sediment increased the biodegradation potential in the microcosms and thereby this could be used to significantly increase the biodegradation rates of PAHs at the contaminated sites.

## METHODS

### NUMERICAL MODEL

The numerical model, BIOB, uses Monod kinetics to simulate the biodegradation of hydrocarbon entrapped between the sediments. It also simulates the growth of bacterial biomass in the presence of nutrients. The decay of hydrocarbon can be mathematically expressed as follows (Geng et al., 2014):

$$\frac{dS}{dt} = -\frac{\mu}{Y_X} X \quad (1)$$

Where S is the concentration of the polycyclic aromatic hydrocarbons (PAHs) (mg S/kg sediment), X is the concentration of the biomass (mg X/kg sediment), Y<sub>X</sub> is the biomass yield coefficient

for growth on the hydrocarbon (mg X/mg S) and  $\mu$  is the growth rate of the biomass ( $\text{day}^{-1}$ ) given by Geng et al. (2014):

$$\mu = \mu_{\max} \left(1 - \frac{X}{X_{\max}}\right) \frac{S}{K_S + S} \frac{N}{K_N + N} \quad (2)$$

Where  $\mu_{\max}$  is the maximum growth rate ( $\text{day}^{-1}$ ),  $X_{\max}$  is the maximum allowable microbial concentration (mg X/kg sediment),  $K_S$  is the half saturation concentration of PAH (mg S/kg sediment),  $N$  is the nitrogen-based nutrient concentration (nitrate+nitrite+ammonia) (mg-N/L of pore water), and  $K_N$  is the half-saturation concentration for nitrogen consumption (mg-N/L of pore water). The term  $\left(1 - \frac{X}{X_{\max}}\right)$  was introduced by Geng et al. (2014) to account for the decrease in biomass accumulation when the microbial concentration approaches its maximum value. Geng et al. (2014) also included an expression for hopane removal due to physical processes in Equation 1. However, it was noted in Venosa et al. (2010) study that hopane concentration remained constant throughout the experiment and hence this term was made equal to zero for the purpose of this study. This suggests that the hydrocarbon decay in the microcosms occurred due to the biodegradation process and not due to abiotic processes such as leaching or washout. BIOB also includes equations to solve for the consumption of nutrients,  $O_2$  and the production of  $CO_2$  levels. Typically,  $O_2$  consumption and  $CO_2$  production could be used to evaluate the microbial growth. Experimentally, the microbial concentration can be estimated using MPN (most probable number) (Alexander, 1965) or qPCR (quantitative polymerase chain reaction) which is used to quantify a specific targeted DNA (Heid et al., 1996; Smith and Osborn, 2009). In the Venosa et al. (2010) study, the nutrients,  $O_2$  and  $CO_2$  levels were not measured in the experiments and they were always present in excess, and hence these equations were not considered in the current model. The complete set of equations used in the BIOB model is presented in Supplementary Material (Appendix A1).

The biomass growth can be expressed mathematically as follows (Geng et al., 2014):

$$\frac{dX}{dt} = (\mu - k_d) X \quad (3)$$

Where  $k_d$  is the endogenous biomass decay rate ( $\text{day}^{-1}$ ).

**Table 1 | Parameters estimated by the model using individual datasets.**

Parameter	Units	Lower	Upper	Estimated value (EL107)	Estimated value	Estimated value	Literature values
		bound	bound		(KN114A)	(SM006B)	
$X_{\max}$	mg X/kg sediment	0	2	0.34	1.27	1.04	0.63 (Geng et al., 2014)
$X_0$	mg X/kg sediment	0	0.5	1.4E-03	3.00E-3	2.46E-3	4.8E-7–4.8E-3 (Köpke et al., 2005)
$\mu_{\max}$	$\text{day}^{-1}$	0.01	10	3.41	3.34	1.35	1.8–9.6 (Nicol et al., 1994)
$k_d$	$\text{day}^{-1}$	0.05	0.5	0.38	0.28	0.29	0.05–0.76 (Essaid et al., 1995)
$Y_X$	mg X/mg S	0.001	4	0.28	0.27	0.19	0.01–1.33 (Essaid et al., 1995)
$K_S$	mg S/mg hopane	0.5	500	51.8	43.8	40.2	
$K_N$	mg of N/L of solution	0.02	5	1.56	1.55	1.77	0.1 (Essaid and Bekins, 1997)

$X_0$  is the initial biomass concentration.

The model can be solved for the concentration of biomass and PAH at different times by numerically solving the Equations (1) through (3) using an ordinary differential equation (ODE) solver. BIOB uses a Runge–Kutta Fehlberg adaptive time-stepping scheme to solve the equations (Chapra and Canale, 1998).

#### INVERSE PROBLEM—PARAMETER ESTIMATION

The Monod kinetic model requires several parameters that define the system. Therefore, we need to estimate these model parameters before it were modeled using BIOB. Since no microbial concentration was presented in the study, the maximum microbial concentration ( $X_{\max}$ ) and the initial microbial concentration ( $X$ ) were also estimated. Therefore, a total of seven parameters were estimated using a parameter estimation tool based on a mathematical tool known as GA (Torlapati, 2013). It should be noted that the GA is only used for estimating the different parameters that are being used in BIOB (Equations 1–3). **Table 1** shows the seven parameters that were estimated along with their higher and lower bounds. The general procedure of a GA is described below.

The six key steps involved in a traditional GA are: encoding, population generation, selection, crossover, mutation, and termination (Holland, 1975). The GA starts with a randomly-generated initial set of solutions (also known as chromosomes) between the higher and lower bounds set by the user and this is called the initial population. A solution is a randomly generated parameter between the higher and lower bound set by the user that will be used to calculate the objective function. These randomly generated solutions or chromosomes are used to calculate the fitness of the population using the objective function. The objective function value is assigned as the fitness for each chromosome and it is used to assess its ability to survive the current generation. For a minimization problem, a lower value of fitness is desirable. Based on this fitness value, two parents are selected using a selection process. The selected parents undergo a crossover, where the genetic information is exchanged between the parents using a crossover function. Since the genetic information is transferred to the subsequent generation of children, it is always preferable to choose individuals with better fitness in the selection process. It is also possible that an offspring generated from the crossover of the parents could undergo a mutation operation governed by a mutation probability. The fitness of the offspring is calculated and is combined with the entire population. The individuals with poor

fitness are removed from the population (death) at the end of the generation. There are several strategies available for the discarding bad solutions, and for implementing the process of encoding, selection, crossover, and mutation. Further details about the GA are available in Torlapati (2013). The specific methods used in this study are discussed in section Results.

### PARAMETER SENSITIVITY

The sensitivity of the model output to the parameter estimates were evaluated using the following approach. The covariance matrix,  $V_x$ , of the parameters was evaluated according to the equation (Bard, 1974):

$$V_x = \sigma^2 H^{-1} \quad (4)$$

Where  $H$  is the Hessian matrix whose terms are the second derivative of the objective function with respect to the parameters. The variance of errors,  $\sigma^2$ , can be estimated by Bard (1974):

$$\sigma^2 = \frac{F}{n - p} \quad (5)$$

Where  $F$  is the value of the objective function at the optimum,  $n$  is the number of observations and  $p$  is number of estimated parameters.

### RESULTS

Bioavailability of oil to the degrading microbial communities is an important phenomenon since the biodegradation occurs at the oil-water interface for hydrocarbons with low solubility (Johnsen et al., 2005). Since experimental data was used to calibrate the parameters for the model, the rate of biodegradation for oil with low bioavailability will be lower compared to a location with higher bioavailability. The experimental dataset from the nutrient amended experiments was used to estimate the kinetic parameters required for BIOB. For the inverse problem, an initial population size of 48 was used. This means that 48 random solutions were generated for each parameter between the higher and lower bound given in **Table 1**. This is to ensure that the estimated parameters do not exceed values observed in the literature. The initial population size determines the solution space in which the GA searches for the parameters. A low initial population might not provide a wide range of solutions and we might be stuck in a local minimum whereas a higher population increases the computational time. It was observed from our simulations that the results did not improve beyond the population size of 48 and hence a population size of 48 was used for all parameter estimation simulations. The number of generations used in our parameter estimation model was 300. The initial hopane-normalized PAH concentrations were (Venosa et al., 2010) 72.65, 44.68, and 58.68 mg/mg hopane for EL107, KN114A, and SM006B, respectively. The concentration of nitrogen (N) in Equation 2 was set to 10 mg/L for the complete duration of 168 days since Venosa et al. (2010) study ensured that there was sufficient nutrient concentration available for nutrient-amended experiments. The input data for the parameter estimation model was experimental data obtained from the study. Since the experiments were performed

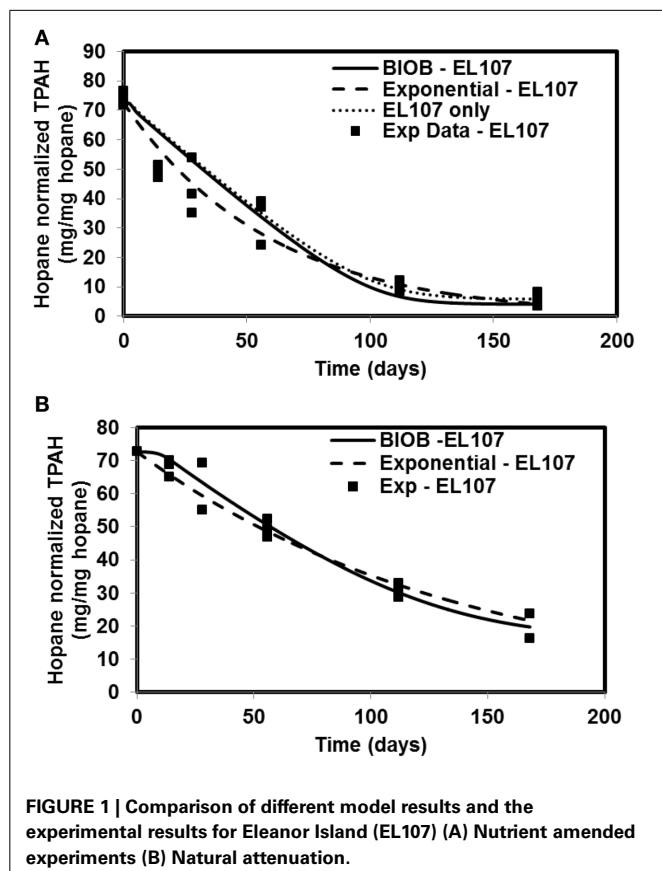
in triplicates, the average value was obtained at each sample measurement and was provided as an input to the GA. The “fitness” of each solution was then evaluated by calculating the error (difference) between the model concentration and the observed (input) experimental concentration that was provided. This error was normalized by the observed concentration at the corresponding time, and the normalized error was squared, added for all the experimental data, and assigned as fitness for that population. The objective of the GA was to minimize this weighted least squares (WLS) by genetic recombination of the solutions generated in the initial population. This was continued for 300 generations and the solution with the best fitness at the end of the simulation was used for the final parameters. All the simulations were performed on Intel Core i7 desktop computer with 8 cores and a total clock speed of 3.40 GHz. The time step used for all the simulations was 3 h.

Initially, the parameter estimation tool was run with the nutrient amended experimental data for all three islands provided as simultaneous input. The estimated parameters over-predicted the biodegradation for the SM006B dataset. Therefore, the parameters were estimated for each island dataset separately, and the fit improved greatly. The parameters estimated for individual island datasets are presented in **Table 1**. The estimated parameters that were obtained for each island dataset were compared against each other and it was observed that the EL107 and KN114A datasets had similar parameters. Hence, the parameter estimation tool was run again with the experimental data from the both the islands provided as input to obtain the common solution for these two datasets. The estimated parameters are provided in **Table 2** along with the parameters estimated for SM006B. Note that the best fit parameters presented in **Table 2** also include the standard deviation for each parameter and the details of these calculations are presented in section Sensitivity Analysis. Subsequently, the best-fit parameters obtained for the nutrient amended experiments (**Table 2**) were used to estimate the nutrient concentration in the natural attenuation experiments. The natural attenuation microcosms were supplied with seawater collected from each site every 4 h to provide reaeration of the seawater and gentle mixing. The purpose of the parameter estimation tool was to estimate the naturally present nutrients (N) in the seawater that were utilized for biodegradation. The concentrations of nitrogen for natural attenuation estimated by the parameter estimation tool were 0.56, 0.79, and 2.21 mg/L for EL107, KN114A, and SM006B, respectively. The concentration of nutrients in SM006B location was about three to four times higher than the other two locations.

The time-varying hopane-normalized PAH concentrations for three islands (both nutrient amended experiments and natural attenuation) of EL107, KN114A, and SM006B with the parameters obtained from the GA for the nutrient amended treatments are shown in **Figures 1–3**, respectively. Details about the performance of parameter estimation tool with increasing generations are presented in Supplementary Material (Appendix A2). Comparisons in these Figures were made against the experimental data collected at different days and the exponential fit. The comparisons were also made against the individually estimated parameters for EL107 (**Figure 1A**) and KN114A (**Figure 2A**) locations. It can be observed from these Figures that the results from

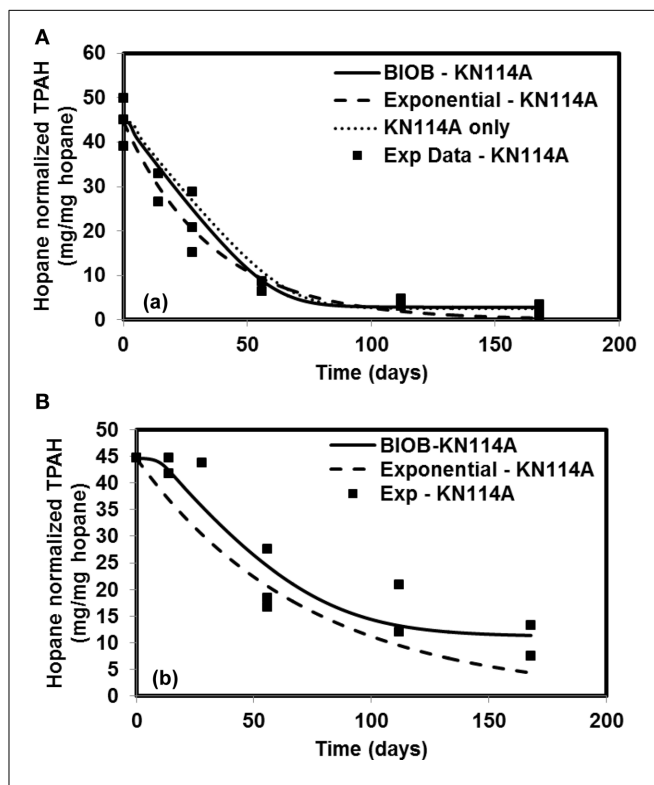
**Table 2 | Parameters estimated in the model and their best-fit value.**

Parameter	Units	Lower bound	Upper bound	Estimated value (EL107 and KN114A)	Estimated value (SM006B)	Literature values
$X_{\max}$	mg X/kg sediment	0	2	$0.40 \pm 0.0601^a$ $1.18 \pm 0.0601^b$	$1.04 \pm 0.033$	0.63 (Geng et al., 2014)
$X_0$	mg X/kg sediment	0	0.5	$1.45E-03 \pm 1.87^a$ $4.34E-03 \pm 1.87^b$	$2.46E-03 \pm 0.76$	$4.8E-7$ – $4.8E-3$ (Köpke et al., 2005)
$\mu_{\max}$	day <sup>-1</sup>	0.01	10	$5.12 \pm 0.063$	$1.35 \pm 0.013$	1.6–6.4 (Nicol et al., 1994)
$k_d$	day <sup>-1</sup>	0.05	0.5	$0.32 \pm 0.072$	$0.29 \pm 0.018$	0.05–0.76 (Essaid et al., 1995)
$Y_X$	mg X/mg S	0.001	4	$0.28 \pm 0.058$	$0.19 \pm 0.029$	0.01–1.33 (Essaid et al., 1995)
$K_S$	mg S/mg hopane	0.5	500	$56.9 \pm 0.076$	$40.2 \pm 0.023$	
$K_N$	mg of N/L of solution	0.02	5	$1.63 \pm 0.48$	$1.77 \pm 0.094$	0.1 (Essaid and Bekins, 1997)

<sup>a</sup>EL107.<sup>b</sup>KN114A. $X_0$  is the initial biomass concentration.**FIGURE 1 | Comparison of different model results and the experimental results for Eleanor Island (EL107) (A) Nutrient amended experiments (B) Natural attenuation.**

the model simulations predicted the experimental results well. It can also be observed from the Figures that the results from the combined data parameter estimates and the individual island data parameter estimates are similar.

It can be observed from **Table 2** that the biomass growth rate ( $\mu_{\max}$ ) for SM006B location is four times lower compared to the other two islands. However, the values of biomass decay rate ( $k_d$ ) and half saturation constant for nitrogen consumption ( $K_N$ ) are similar for all three locations. This suggests that the

**FIGURE 2 | Comparison of model results and the experimental results for Knight Island (KN114A) (A) Nutrient amended experiments (B) Natural attenuation.**

biodegradation kinetics was different at the SM006B location. The differences in biodegradation kinetics could be due to the fact that the interfacial area between the oil and water may have been a limiting factor in SM006B (Geng et al., 2013). The composition of the oil could also be different as the presence of heavier PAH compounds could reduce the overall biodegradation rate. To check for the possible limitation of interfacial area, the specific surface area per unit mass was evaluated for each of the islands by using the grain size distribution obtained from the literature. The

average diameter of the sediment was 4.2 mm (Li and Boufadel, 2010), 7 mm (Xia et al., 2010), and 9.4 mm (Xia and Boufadel, 2011) for Eleanor Island (EL056C), Knight Island (KN114A), and Smith Island (SM006B), respectively. The grain size distribution of Eleanor Island presented in this study is not from a same beach as was used in the Venosa et al. (2010) study. The value was used as a representative sample for this study as a qualitative analysis. The grain size distribution can be used to calculate the specific surface area per mass of sediment ( $A_S$ ) as follows (Geng et al., 2013):

$$A_S = \frac{6}{\varphi d_{avg} \rho_{sediment}} \quad (6)$$

Where  $\varphi$  is the shape factor,  $d_{avg}$  is the average grain size, and  $\rho_{sediment}$  is the density of sediment.

It can be observed from Equation 6 that the specific surface area per unit mass is inversely proportional to average grain size. It was assumed that all the particles are spherical for simplicity and the value of shape factor was taken equal to 1.0. The specific surface area calculated using the above equation for EL107, KN114A, and SM006B was 0.86, 0.52, and 0.39 m<sup>2</sup>/kg, respectively. This indicates that the specific surface area per mass of sediment was lower in the SM006B location than the other two locations and could be one of the reasons for low interfacial area between oil and water and hence low biodegradation rates. This is reflected in the low values of growth rate ( $\mu_{max}$ ) and maximum biomass

accumulation values (as observed in **Table 2**) for the SM006B location.

In order to compare the goodness of fit for the exponential fit and BIOB, the objective function (WLS) was evaluated. The comparison of objective function values for BIOB and exponential fit are presented in **Table 3**. A lower value of the objective function indicates that the model results are closer to the experimental data. Therefore, for nutrient amended experiments, BIOB provided a better fit than the exponential fit for KN114A and SM006B datasets and the exponential fit is marginally better for EL107 dataset. For the natural attenuation experiments, BIOB provided a better fit for EL107 and KN114A whereas the exponential fit provided a marginally better fit for SM006B. BIOB's prediction for SM006B in the nutrient amended experiments is also more intuitive as there is a slight lag before the actual biodegradation begins whereas the exponential fit indicates an immediate biodegradation. This is not accurate because the biomass requires some time to grow before they are able to biodegrade the PAHs and this observation is consistent with the experimental data and hence a better fit than the exponential model as shown by the objective function values.

## SENSITIVITY ANALYSIS

The sensitivity analyses were performed only for the nutrient amended experiments as the only parameter that was estimated in natural attenuation experiments was nutrient concentration and we present the sensitivity to nutrient concentration in a section Sensitivity to Nutrient Concentration. Based on the Equation 5, the variance of errors ( $\sigma^2$ ) at the optimum was 0.038 for EL107 and KN114A, and 0.0017 for SM006B for the nutrient amended experiments.

The sensitivity of the parameter estimates was checked by varying each parameter between -20 and +50% of its original value while the other parameters were kept the same and the fitness was re-evaluated with the deviated parameters. **Figures 4A,B** show the results from analyses for EL107 and KN114A, and SM006B, respectively. It can be observed from **Figure 4A** (EL107 and KN114A) that the model is not sensitive to parameters  $K_N$  and the initial biomass concentration ( $X$ ). The model is sensitive to yield coefficient ( $Y_X$ ), biomass decay rate ( $k_d$ ), half saturation constant ( $K_S$ ), maximum allowable biomass concentration ( $X_{max}$ ) and

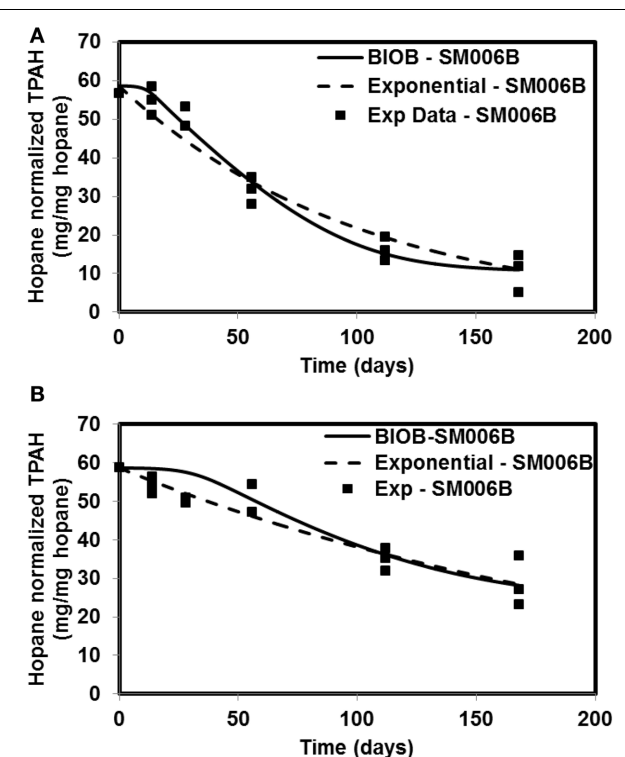


**FIGURE 3 | Comparison of model results and the experimental results for Smith Island (SM006B) (A) Nutrient amended experiments (B) Natural attenuation.**

**Table 3 | Comparison of the objective function values between the BIOB and Exponential models.**

	BIOB	Exponential
EL107 <sup>a</sup>	0.3	0.15
KN114A <sup>a</sup>	0.28	0.97
SM006B <sup>a</sup>	0.014	0.06
EL107 <sup>b</sup>	0.002	0.013
KN114A <sup>b</sup>	0.11	0.63
SM006B <sup>b</sup>	0.029	0.012

<sup>a</sup>Nutrient amended treatment.

<sup>b</sup>Natural attenuation.

Lower value of objective function is preferred because it indicates that the model results are closer to the experimental results.

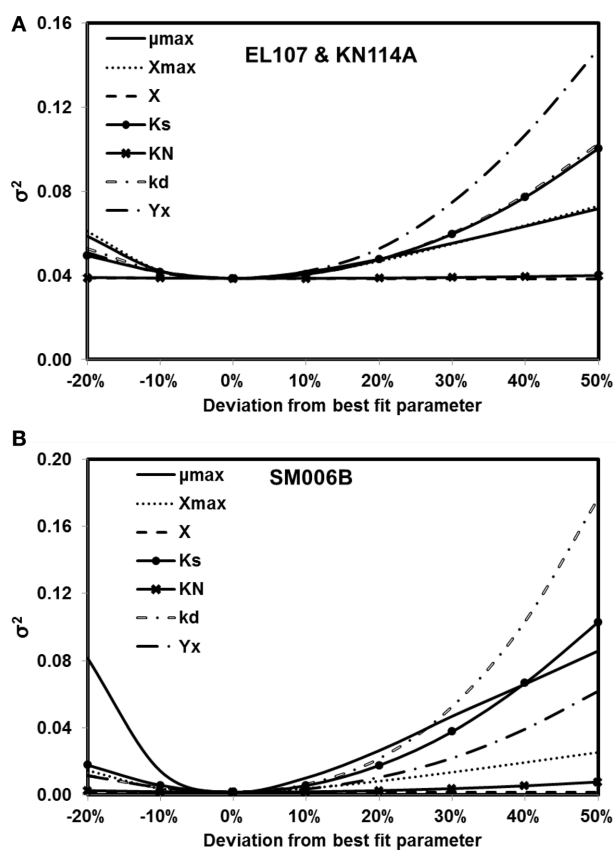


**FIGURE 4 | Sensitivity analysis for kinetic parameter estimates for (A) EL107 and KN114A (B) SM006B.** Note that the minimum value of the variance of errors is at 0% deviation (i.e., estimated parameters).

biomass growth rate ( $\mu_{\max}$ ). In **Figure 4B** (SM006B), the model is not sensitive to the initial biomass concentration ( $X$ ), slightly sensitive to half saturation constant of nitrogen ( $K_N$ ), moderately sensitive to the parameter  $X_{\max}$ , and  $Y_X$ , and highly sensitive to the parameters  $K_s$ ,  $\mu_{\max}$ , and  $k_d$ . The difference in sensitivities for the two systems as shown in **Figures 4A,B** indicates that the biodegradation kinetics of SM006B is indeed different from the remaining datasets. The sensitive parameters are different for each system and one needs to pay attention to these differences when employing a field scale bioremediation process. Researchers who use parameter estimation tools to estimate bioremediation parameters should pay attention to the highly sensitive parameters as small variations can change the fitness values significantly. Finally, it can be observed that the minimum value of the fitness function was obtained at 0% deviation and this shows the robustness of the search algorithm.

To quantify the findings from **Figures 4A,B**, the covariance matrix,  $V_x$ , of the parameters was evaluated according to the Equation 4. To estimate the values of the Hessian matrix ( $H$  in Equation 5), a quadratic function can be fitted to the objective function vs. deviation from the best fit parameter (as shown in **Figures 4A,B**) and the second derivative of this fitted quadratic function was calculated. For the sake of simplicity, only the diagonal values of the Hessian matrix were evaluated for this

study. The standard deviation values evaluated from the covariance matrix for each parameter are presented in **Table 2** along with the best fit parameters. The value of standard deviation is large for some parameters like initial biomass concentration and half saturation constant for nitrogen consumption. This is due to low curvature of the objective function for these parameters and this indicates the low sensitivity to these parameters. Also the standard deviation values were quite small for the rest of the parameters and there was no overlap between the two systems except for  $K_N$  and  $k_d$  values. This further validates the hypothesis that the biodegradation kinetics of SM006B was indeed different from the other two islands.

#### SENSITIVITY TO NUTRIENT CONCENTRATION

Nutrient concentration is an important parameter in biodegradation, as it has been observed by several researchers that the nitrate concentration should be about 2–10 mg/L for near maximum biodegradation rate (Atlas and Bartha, 1972; Atlas, 1981; Boufadel et al., 1999; Du et al., 1999; Wrenn et al., 2006). The nutrient concentration for the base case scenario was 10 mg/L. Simulations were performed with different nutrient concentrations between 0.1 and 10 mg/L for EL107 and KN114A locations whereas for the SM006B location, the nutrient concentration was varied between 1 and 10 mg/L. The results are presented in **Figures 5A–C** for EL107, KN114A, and SM006B datasets, respectively. It can be observed from the Figures that for all datasets that, as the nutrient concentration decreases, the biodegradation rate continues to decrease. **Table 4** reports the predicted PAH concentrations as a percentage of the initial concentration at 168 days for various nutrient concentrations for all sites. As the nutrient concentration increases, the PAH concentration at 168 days becomes smaller. For EL107 and KN114A, the concentration was affected by small increase in the nutrient concentrations for values less than 1.0 mg-N/L. Such was not the case for SM006B, where nutrient concentrations less than 1.0 mg-N/L had no effect on oil biodegradation. For this reason, the lowest nutrient value for SM006B in **Table 4** was 1.0 mg-N/L, and such a value resulted in 99.2% of the initial PAH concentration remaining at 168 days. This might provide a partial explanation of the slow biodegradation of oil in the beaches of Smith Island, including SM006B.

#### SENSITIVITY TO INITIAL BIOMASS CONCENTRATION

Different scenarios were chosen in addition to the base case scenario to study the sensitivity of the system to the initial biomass concentration. The initial biomass concentrations for the base case were 1.5E-3, 4.34E-03, and 2.46E-03 mg X/kg of sediments for EL107, KN114A, and SM006B, respectively. The order of magnitude of the initial biomass concentration was increased 10-fold and decreased 100, 10,000-fold for EL107, KN114A, and SM006B datasets. The results from these simulations are presented in **Figures 6A–C** for EL107, KN114A, and SM006B locations, respectively. It can be observed from the **Figure 6A** (EL107) and **Figure 6B** (KN114A) that the model is not very sensitive to the initial biomass concentration after the first few days. This may be due to a high nutrient concentration and a relatively high growth rate of the bacteria in EL107 and KN114A locations. This allows the bacteria to grow rapidly and reach the

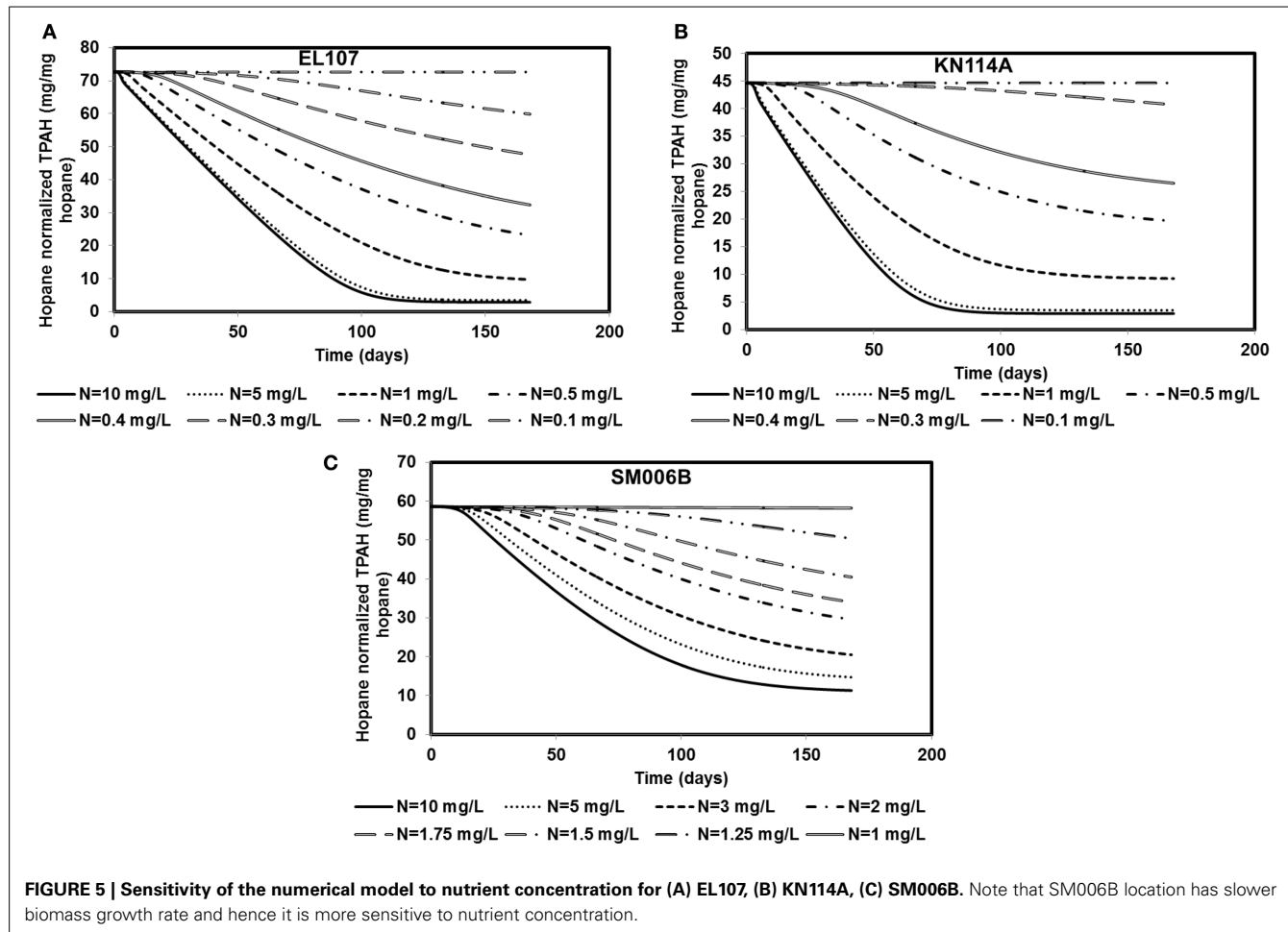


**Table 4 | PAH concentrations as percentage of the initial concentrations for different nutrient concentrations at  $t = 168$  days.**

	PAH concentration (mg/mg hopane)		PAH concentration (mg/mg hopane)	
	EL107		KN114A	
	Initial PAH concentration	72.65	Initial PAH concentration	58.68
Nutrient concentration (mg-N/L)	Percent of initial concentration		Nutrient concentration (mg-N/L)	Percent of initial concentration
0.1	100	99.9	1.00	99.2
0.2	82	99.8	1.25	86
0.3	66	91	1.50	69
0.4	44	59	1.75	58
0.5	32	44	2.00	50
1.0	13	21	3.00	35
5.0	5	8	5.00	25
10.0	4	6	10.00	19

Percentages are rounded.

maximum allowable concentration in the system. As a result, the oil biodegradation is not adversely impacted after the initial phase in EL107 and KN114A locations. The final hydrocarbon concentration after the 168 day experiment was similar for all initial biomass concentrations for both these locations. However, for the

SM006B location (Figure 6C), the initial lag before biodegradation continued to increase as the initial biomass concentration was decreased. This is due to the fact that biomass growth rate is slower and hence the biomass takes longer to grow. There was a decrease in the PAH biodegradation by 14 and 20% when the

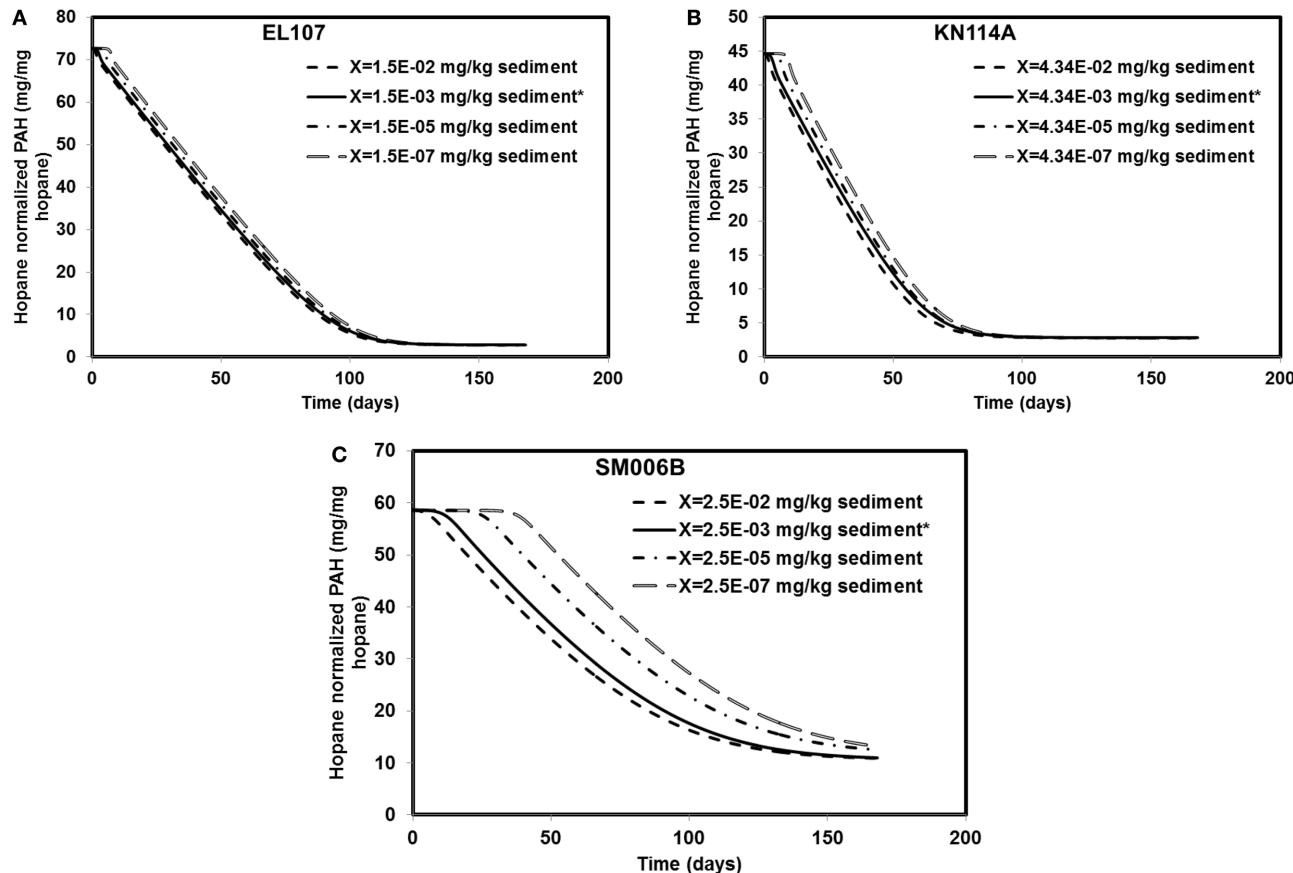


**FIGURE 6 | Sensitivity of the numerical model to biomass concentration for (A) EL107, (B) KN114A, (C) SM006B.** Note that X represents the initial biomass concentration. \* in the legend indicates the base case scenario.

biomass concentration was decreased by 100 and 10,000-fold. There was no difference in the final PAH concentration when the biomass concentration was increased 10-fold. Therefore, a low initial biomass concentration does not affect the overall biodegradation rate in EL107 and KN114A case due to its faster biomass growth rate whereas the initial biomass concentration seems to play a significant role in the SM006B case when it was decreased. This suggests that the biodegradation kinetics was not limited by the initial biomass concentration as the biodegradation happens almost immediately in the case of EL107 and KN114A (Figure 3A). This further supports the hypothesis that the interfacial area between oil and water plays a significant role in bioremediation than initial biomass concentration.

## DISCUSSION

To compare the biodegradation rate of the polycyclic aromatic compounds (PAHs) with the biodegradation rate of individual compounds, we identified the compound with first-order decay rate similar to that of the PAHs for each location as reported by Venosa et al. (2010). This compound was designated as the representative compound which means that the rate of biodegradation of PAH is representative of the biodegradation rate of the identified compound. The first-order biodegradation rates were 0.017,

0.0294, and 0.0099 day<sup>-1</sup> for nutrient amended experiments and 0.0072, 0.0138, and 0.0043 day<sup>-1</sup> for natural attenuation experiments of EL107, KN114A, and SM006B, respectively. Half-life ( $t_{1/2}$ ) was evaluated from the first order decay rates (k) as follows:

$$t_{1/2} = \frac{\ln 2}{k} \quad (7)$$

**Table 5** shows the names of the representative compounds and their respective half-life values for nutrient amended experiments. The first-order decay rates for the hopane-normalized individual compounds are available in the supplementary information of Venosa et al. (2010) and Equation 7 was used to evaluate the half-life values. These values are reported in **Table 5** for nutrient-amended experiments. In addition to the representative compound, the slowest and fastest biodegradable compounds are also identified for each island. **Table 5** also shows the fastest and slowest biodegradable compounds for each island along with their half-life values. **Table 6** provides the names and half-life values of the representative compounds as well the fastest and slowest compound for the natural attenuation experiments.

The parameters in **Tables 5, 6** are used to plot the temporal variation of the concentration of hydrocarbon for

**Table 5 | Comparison of biodegradation rates for nutrient-amended experiments.**

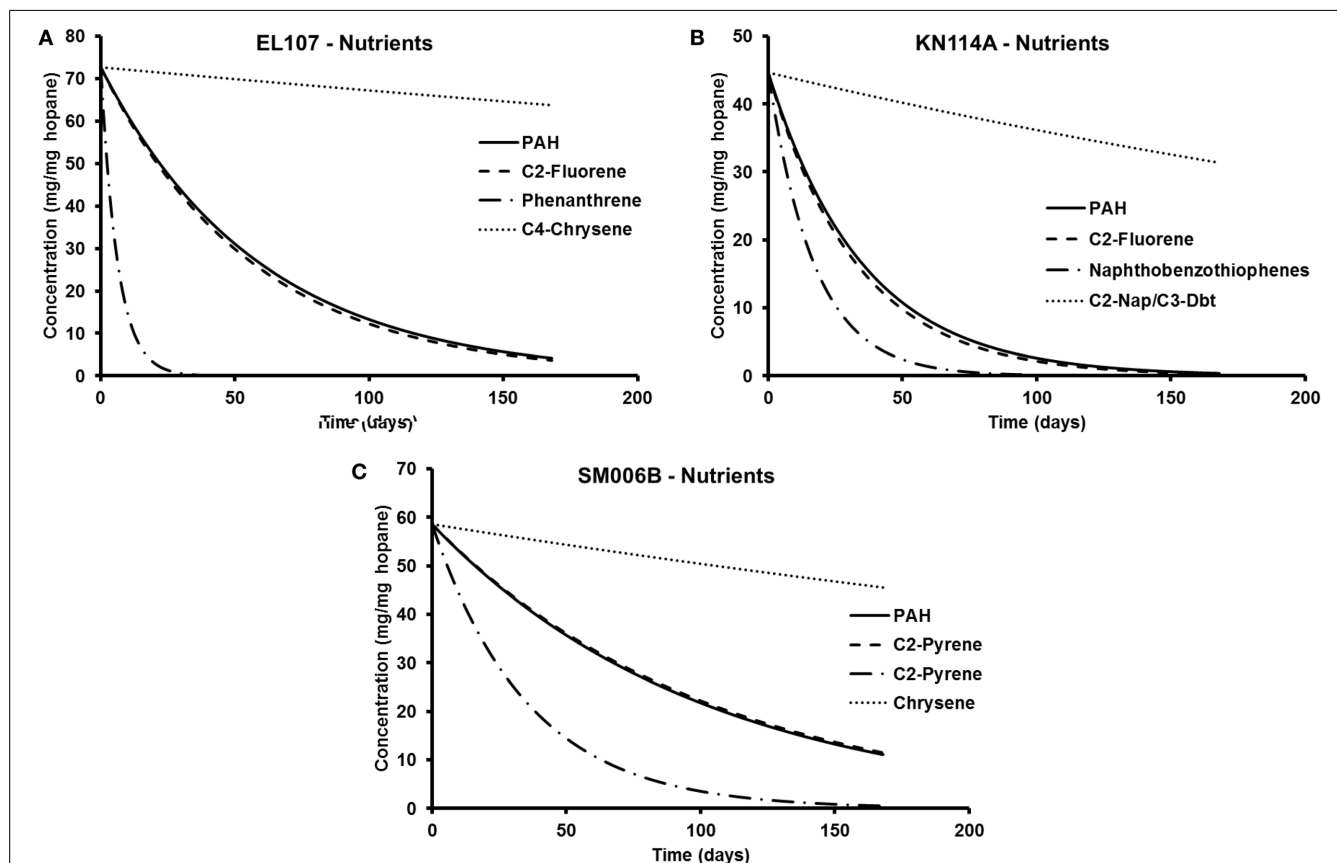
Island	PAH half life	Representative compound (Venosa et al., 2010)	Half life (Venosa et al., 2010)	Fastest compound	Half life (Venosa et al., 2010)	Slowest compound	Half life (Venosa et al., 2010)
EL107	40.8	C2-Fluorene	38.9	Phenanthrene	4.3	C4-Chrysene	888.7
KN114A	24.4	NBT	22.9	C1-Fluorene	11.9	C4-Chrysene	330.1
SM006B	70.0	C2-Nap/C3-DBT	71.5	DBT	24.8	C4-Chrysene	462.1

C2-Nap represents C2-Naphthalenes, NBT—Naphthobenzo-thiophenes, and DBT represents Dibenzothiophene. All units for half-life values are in days.

**Table 6 | Comparison of biodegradation rates for natural attenuation experiments.**

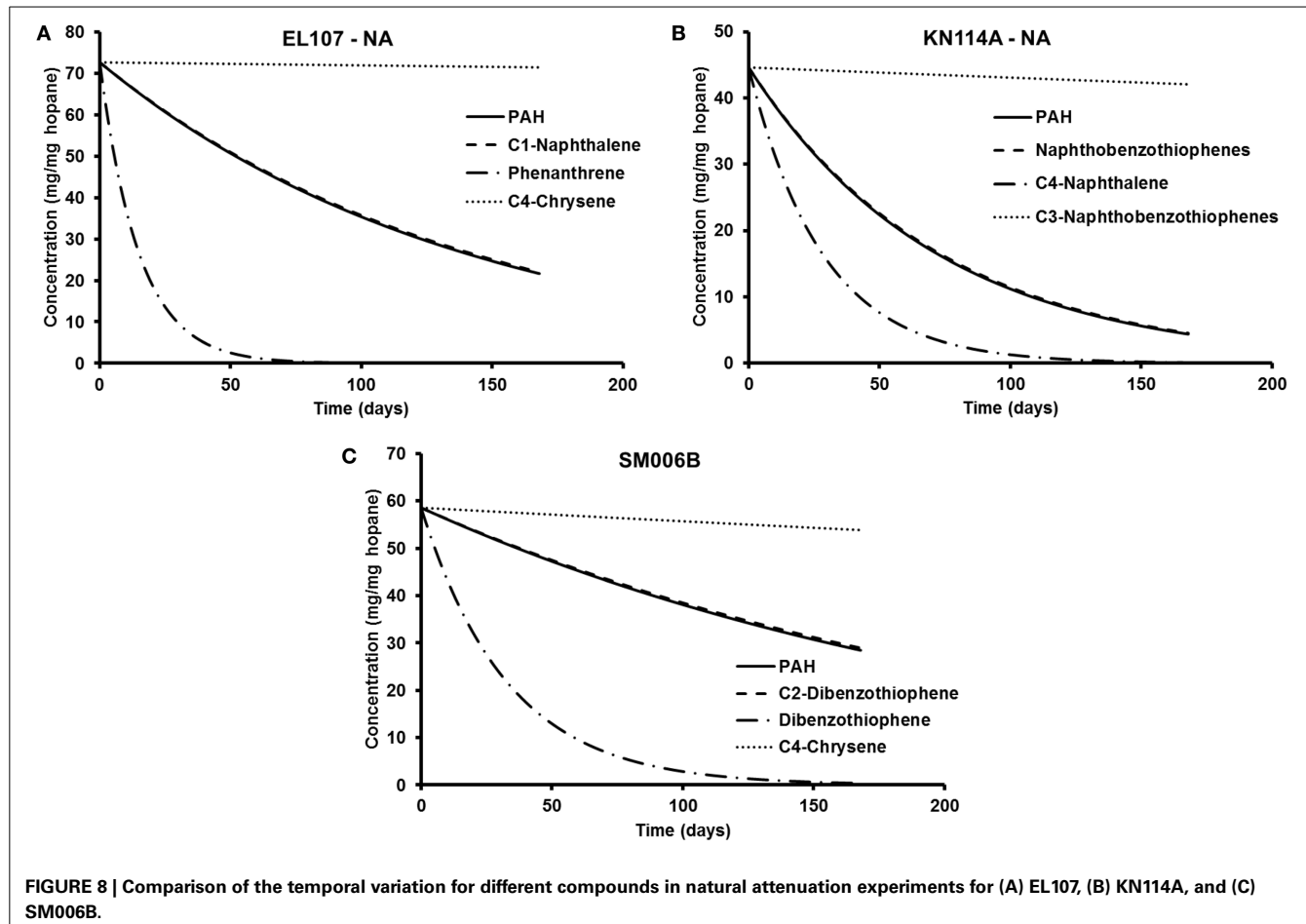
Island	PAH half life (Venosa et al., 2010)	Representative compound (Venosa et al., 2010)	Half life (Venosa et al., 2010)	Fastest compound	Half life (Venosa et al., 2010)	Slowest compound	Half life (Venosa et al., 2010)
EL107	96.3	C1-Naphthalene	97.6	Phenanthrene	10.3	C4-Chrysene	6931.5
KN114A	50.2	NBT	51.0	C4-Naphthalene	19.6	C3-NBT	1980.4
SM006B	161.2	C2-DBT	165.0	DBT	23.0	C4-Chrysene	1386.3

NBT—Naphthobenzo-thiophenes and DBT represents Dibenzothiophene. All units for half-life values are in days.

**FIGURE 7 | Comparison of the temporal variation for different compounds in nutrient-amended experiments for (A) EL107, (B) KN114A, and (C) SM006B.**

each island. It was assumed that the respective compounds have the same concentration as the initial PAH concentration at that island to allow for easy comparison. The results from the simulations are shown in Figures 7A–C for EL107,

KN114A, and SM006B, respectively, for the nutrients amended experiments and Figures 8A–C show simulation results for natural attenuation experiments for EL107, KN114A, and SM006B, respectively. It can be observed from the Figures



that the biodegradation rates vary vastly between different compounds.

We have also compared the number of compounds with biodegradation rate higher and lower than the representative compound for that island. For the nutrient-amended experiments, there were 10 compounds biodegrading at higher rate than the representative compound for all islands whereas there were 17, 11, and 13 compounds biodegrading at lower rate than the representative compound for EL107, KN114A, and SM006B Islands, respectively. Similarly, for the natural attenuation experiments there were 11, 9, and 9 compounds biodegrading at higher rate than the representative compound for EL107, KN114A, and SM006B, respectively, whereas there were 16, 12, and 15 compounds biodegrading at lower rate than the representative compound for EL107, KN114A, and SM006B Islands, respectively.

The weighted rates at each site were evaluated by multiplying the initial concentration of the compound with its rate and this summation was divided by the concentration of the PAH at the site. These weighted rates were used to compute the half-life using Equation 7 and comparison between the half-life computed using exponential curve fitted data and weighted half-lives are shown in Table 7. It can be observed from the Table that the weighted half-lives for each site are lower than the half-lives computed from the exponential curve fitted data. It should also be noted that BIOB

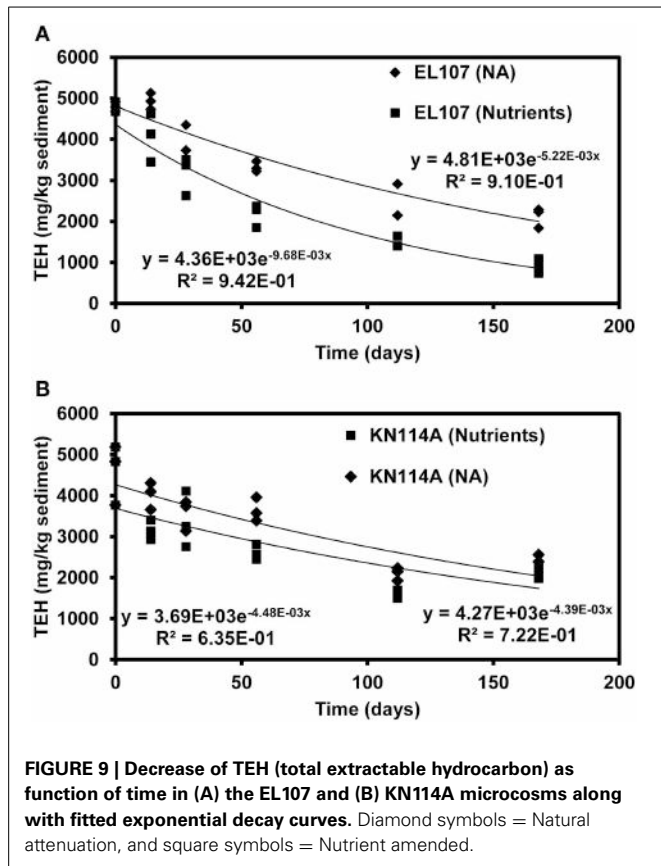
**Table 7 | Comparison of the half-lives between the weighted and fitted decay rates.**

	Weight half-life (days)	Fitted half-life (days)
EL107—Nutrients	25.26	40.77
KN114A—Nutrients	20.06	24.41
SM006B—Nutrients	60.93	70.01
EL107—NA	57.81	96.27
KN114A—NA	36.64	50.23
SM006B—NA	140.26	161.20

NA represents natural attenuation.

is capable of estimating the biodegradation of individual hydrocarbons where information about these compounds such as the concentrations of the hydrocarbon and the microbes capable of biodegrading that hydrocarbon are available. In Equations 1 and 2, the term  $S$  will represent the concentration of the hydrocarbon instead of the PAH concentration if we use BIOB to estimate the biodegradation of individual compounds.

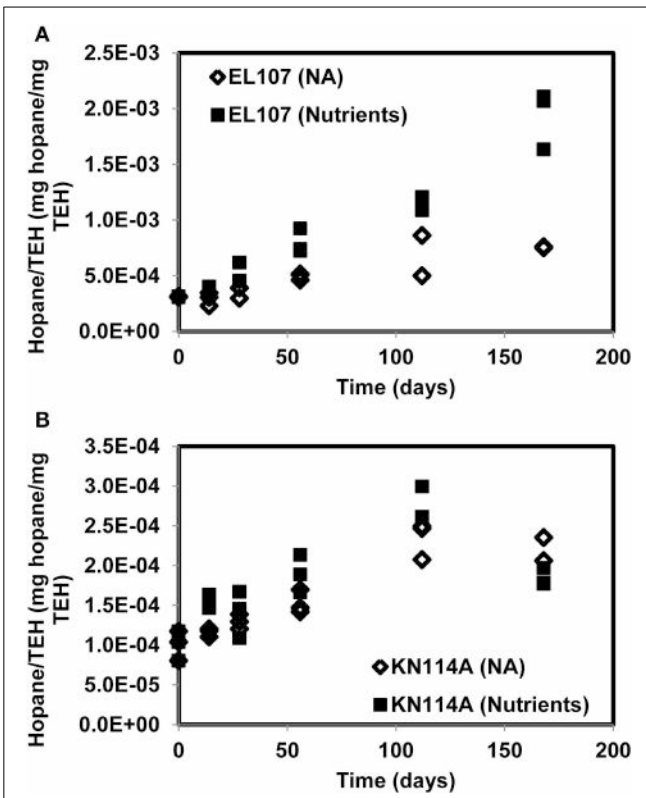
Figures 9A, B report the concentration of total extractable hydrocarbon (TEH) as function of time in the microcosms of EL107 and KN114A, respectively. Simple exponential decays were fitted to illustrate the decreasing behavior. The Natural



Attenuation data for EL107 (Figure 9) show a lag in the decrease of TEH with time, similar to that observed for the hopane-normalized PAH concentration for EL107 (Figure 2B), which suggests that the lag is due to biotic factors, namely the initial phase of microbial growth (or microbial acclimation period). For KN114A, the decrease is more or less immediate for both data sets (Figure 10), but a sudden drop in the TEH concentration occurs at 120 days for all microcosms. We have considered and ruled out any possibility for this decrease, which occurred for both Natural attenuation and nutrient amended microcosms. We believe these data points do not represent correct results, but they don't invalidate the overall trend of decrease with time.

Figure 10 reports the concentration of hopane normalized by the total mass of TEH for EL107 and KN114A. The increase with time reflects the biodegradation of compounds less resistant to biodegradation than hopane. For KN114A, the decrease between 120 and 180 days reflect the low TEH values at 112 days (Figure 9B). The sudden decrease cannot be due to the biodegradation of hopane, because although hopane does biodegrade, its time scale of biodegradation is longer than a few weeks, more on the order of years (Atlas and Bragg, 2007).

Figures 11A, B report the PAH concentration normalized by the concentration of TEH as function of time for (A) EL107 and (B) KN114A. Fitted straight lines were obtained to determine if there is a correlation between the biodegradation of PAH and that of TEH. For EL107, a low  $R^2$  was noted along with a small slope,



which suggests that the biodegradation of PAH is not directly related to the biodegradation of TEH. We think this has to do also with the variability of the TEH at 112 days. However, the high  $R^2$  for KN114A suggests a strong linear relation between the biodegradation of PAH and that of TEH. At face value, Figure 11 suggests that tracking the biodegradation of PAHs is not sufficient to infer the biodegradation of the rest of the compounds (i.e., TEH).

It should also be noted that the seawater that was renewed to the microcosms was recirculated to the reservoir that supplies the seawater to the microcosms. Therefore, in case of oil leaching, it would probably be replenished to the microcosms when the seawater is renewed. The leaching of oil is also not mentioned in Venosa et al. (2010) and the hopane concentration remains fairly constant throughout the length of the experiment which means the removal of oil due to physical processes was limited. Therefore, we did not account for leaching in the model.

## CONCLUSIONS

In this study, the biodegradation model BIOB was used to simulate the experimental data from nutrient amended and the natural attenuation treatments from Venosa et al. (2010) study. The kinetic parameters required for the BIOB were estimated using a parameter estimation tool based on GA. It was observed from the estimated parameters that the SM006B location had relatively

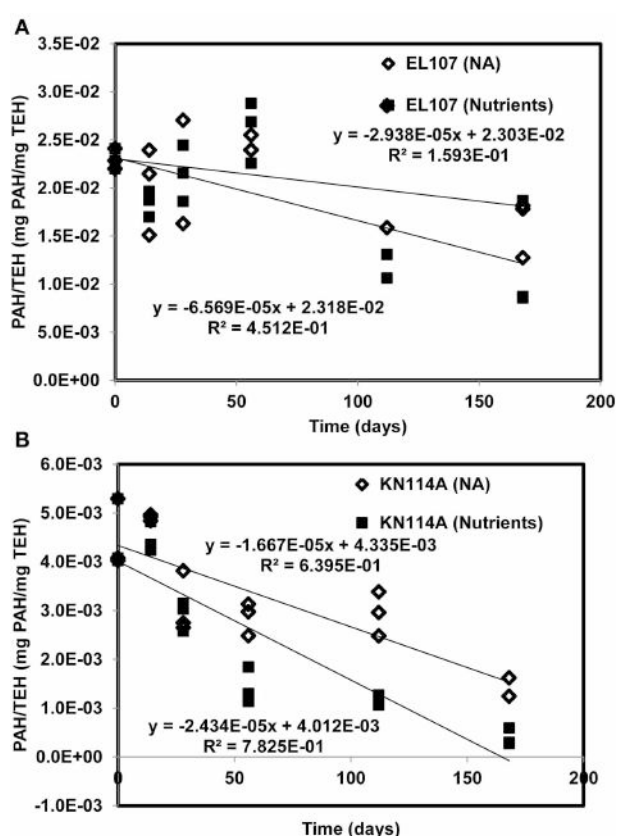


**FIGURE 11 | PAH concentration normalized by the concentration of total extractable hydrocarbon (TEH) as function of time for (A) EL107 and (B) KN114A.** Fitted straight lines were obtained to determine if there is a correlation between the biodegradation of PAH and that of TEH.

slower biodegradation rate compared to the other two locations. Grain size analysis from each site revealed that the specific surface area per unit mass of sediment was considerably lower at SM006B, which suggests that the surface area of sediments is a key control parameter for microbial growth in sediments. Subsequently, the best-fit parameters obtained from the nutrient amended experiments were used to estimate the nutrient concentration for the natural attenuation experiments. The estimated parameters were able to predict the experimental results well for all the datasets. In comparison with the exponential decay model, the results from BIOB showed better goodness of fit for KN114A and SM006B datasets while the fit for EL107 dataset for nutrient amended experiments was relatively similar for both exponential decay and BIOB. For natural attenuation treatment, the exponential fit provided a better fit for the SM006B dataset whereas BIOB provided a better fit for EL107 and KN114A datasets. In particular, BIOB was able to capture the initial slow biodegradation due to the lag phase in microbial growth. In addition, the exponential fit does not account for the limitation of nutrients and has no predictive capabilities whereas the parameters estimated for BIOB are still valid at different nutrient concentrations. Therefore, BIOB can be used to predict the bioremediation scenarios at the site.

It was observed from our sensitivity analyses that the initial biomass concentration and the half saturation coefficient of nitrate were not sensitive parameters for EL107 and KN114A locations whereas the biomass growth rate, biomass decay rate, yield coefficient, half-saturation constant for hopane-normalized PAH, maximum allowable biomass were the most sensitive parameters. For the SM006B location, the system was highly sensitive to biomass decay rate, biomass growth rate, half saturation constant for hopane-normalized PAH, yield coefficient and slightly sensitive to maximum allowable biomass concentration and half-saturation constant for nitrogen, and insensitive to small changes in initial biomass concentration. In addition, when the sensitivity analyses were performed on the nutrient concentration, SM006B location was more sensitive to small changes than EL107 and KN114A locations due to the slow biomass growth rate. Even though the nutrient concentration was a sensitive parameter, there was no significant difference in concentration trends for the nutrient concentrations of 5 and 10 mg of N/L in EL107 and KN114A locations. Also, the initial biomass concentration had much lower effects on the final PAH concentration after 168 days in EL107 and KN114A locations than in the SM006B location. The high nutrient concentration allowed for a rapid biomass growth and thus, the PAH biodegradation was not substantially affected after the initial few days in the EL107 and KN114A location whereas in the SM006B location, when the initial biomass concentration was decreased by several orders of magnitude, the biomass required several days before the biomass concentration was sufficient enough to cause hydrocarbon decay. Therefore, it can be concluded that the initial biomass concentration affects oil biodegradation significantly during the initial phase of the biodegradation process. Comparisons were also made to study the biodegradation decay rates of individual compounds against the decay rate of the PAH. It was observed that the weighted average of the individual decay rates was greater than the decay rate of the PAH. In conclusion, we determine that the Monod kinetic model, BIOB is a useful tool that can be used to predict the extent of biodegradation in laboratory scale experiments and in marine environments such as beaches where the oil is entrapped within sediments with no significant transport or dissolution.

## ACKNOWLEDGMENTS

This work was supported by Exxon Valdez Oil Spill Trustee Council under Project No. 11100836. However, it doesn't reflect the views of the Council, and no official endorsement should be inferred. Input from Dr. Yves Robert Personna is greatly appreciated.

## SUPPLEMENTARY MATERIAL

The Supplementary Material for this article can be found online at: <http://www.frontiersin.org/journal/10.3389/fmich.2014.00212/abstract>

## REFERENCES

- Alexander, M. (1965). "Most-probable-number method for microbial populations," in *Methods of Soil Analysis. Part 2. Chemical and Microbiological Properties*, ed A. G. Norman (Madison, WI: American Society of Agronomy, Soil Science Society of America), 1467–1472.

- Atlas, R., and Bragg, J. (2007). "Assessing the long-term weathering of petroleum on shorelines: uses of conserved components for calibrating loss and bioremediation potential," in *Arctic and Marine Oilspill Program Technical Seminar* (Canada), 263–289.
- Atlas, R. M. (1981). Microbial degradation of petroleum hydrocarbons: an environmental perspective. *Microbiol. Rev.* 45, 180–209.
- Atlas, R. M. (1995). Petroleum biodegradation and oil spill bioremediation. *Mar. Pollut. Bull.* 31, 178–182. doi: 10.1016/0025-326X(95)00113-2
- Atlas, R. M., and Bartha, R. (1972). Degradation and mineralization of petroleum in sea water: limitation by nitrogen and phosphorous. *Biotechnol. Bioeng.* 14, 309–318. doi: 10.1002/bit.260140304
- Bard, Y. (1974). *Nonlinear Parameter Estimation*. New York, NY: Academic Press.
- Barron, M. G. (2012). Ecological impacts of the deepwater horizon oil spill: implications for immunotoxicity. *Toxicol. Pathol.* 40, 315–320. doi: 10.1177/0192623311428474
- Beolchini, F., Rocchetti, L., Regoli, F., and Dell'Anno, A. (2010). Bioremediation of marine sediments contaminated by hydrocarbons: experimental analysis and kinetic modeling. *J. Hazard. Mater.* 182, 403–407. doi: 10.1016/j.jhazmat.2010.06.047
- Boufadel, M., Reeser, P., Suidan, M., Wrenn, B., Cheng, J., Du, X., et al. (1999). Optimal nitrate concentration for the biodegradation of n-heptadecane in a variably-saturated sand column. *Environ. Technol.* 20, 191–199. doi: 10.1080/0959332008616808
- Bragg, J. R., Prince, R. C., Harner, E. J., and Atlas, R. M. (1994). Effectiveness of bioremediation for the Exxon Valdez oil spill. *Nature* 368, 413–418. doi: 10.1038/368413a0
- Chapra, S. C., and Canale, R. P. (1998). *Numerical Methods for Engineers: With Programming and Software Applications*. Boston, MA: WCB/McGraw-Hill.
- Chen, J., Wong, M., Wong, Y., and Tam, N. F. (2008). Multi-factors on biodegradation kinetics of polycyclic aromatic hydrocarbons (PAHs) by *Sphingomonas* sp. a bacterial strain isolated from mangrove sediment. *Mar. Pollut. Bull.* 57, 695–702. doi: 10.1016/j.marpolbul.2008.03.013
- Cunliffe, M., and Kertesz, M. A. (2006). Effect of *Sphingobium yanoikuya* B1 inoculation on bacterial community dynamics and polycyclic aromatic hydrocarbon degradation in aged and freshly PAH-contaminated soils. *Environ. Pollut.* 144, 228–237. doi: 10.1016/j.envpol.2005.12.026
- Desai, A. M., Autenrieth, R. L., Dimitriou-Christidis, P., and McDonald, T. J. (2008). Biodegradation kinetics of select polycyclic aromatic hydrocarbon (PAH) mixtures by *Sphingomonas paucimobilis* EPA505. *Biodegradation* 19, 223–233. doi: 10.1007/s10532-007-9129-3
- Du, X., Reeser, P., Suidan, M. T., Huang, T., Moteleb, M., Boufadel, M. C., et al. (1999). "Optimum nitrogen concentration supporting maximum crude oil biodegradation in microcosms," in *International Oil Spill Conference* (Seattle, WA: American Petroleum Institute), 485–488. doi: 10.7901/2169-3358-1999-1-485
- Essaid, H. I., and Bekins, B. A. (1997). *BIOMOC, a Multispecies Solute-Transport Model With Biodegradation*. Menlo Park, CA: US Department of the Interior, US Geological Survey.
- Essaid, H. I., Bekins, B. A., Godsy, E. M., Warren, E., Baedecker, M. J., and Cozzarelli, I. M. (1995). Simulation of aerobic and anaerobic biodegradation processes at a crude oil spill site. *Water Resour. Res.* 31, 3309–3327. doi: 10.1029/95WR02567
- Essaid, H. I., Cozzarelli, I. M., Eganhouse, R. P., Herkelrath, W. N., Bekins, B. A., and Delin, G. N. (2003). Inverse modeling of BTEX dissolution and biodegradation at the Bemidji, MN crude-oil spill site. *J. Contam. Hydrol.* 67, 269–299. doi: 10.1016/S0169-7722(03)00034-2
- Geng, X., Boufadel, M. C., Personna, Y., Lee, K., and Tsao, D. (2014). BioB: a mathematical model for the biodegradation of low solubility hydrocarbons. *Mar. Pollut. Bull.* doi: 10.1016/j.marpolbul.2014.04.007. [Epub ahead of print].
- Geng, X., Boufadel, M. C., and Wrenn, B. (2013). Mathematical modeling of the biodegradation of residual hydrocarbon in a variably-saturated sand column. *Biodegradation* 24, 153–163. doi: 10.1007/s10532-012-9566-5
- Hach, C. C., Brayton, S. V., and Kopelove, A. B. (1985). A powerful Kjeldahl nitrogen method using peroxymonosulfuric acid. *J. Agric. Food Chem.* 33, 1117–1123. doi: 10.1021/jf00066a025
- Heid, C. A., Stevens, J., Livak, K. J., and Williams, P. M. (1996). Real time quantitative PCR. *Genome Res.* 6, 986–994. doi: 10.1101/gr.6.10.986
- Herold, M., Greskowiak, J., Ptak, T., and Prommer, H. (2011). Modelling of an enhanced PAH attenuation experiment and associated biogeochemical changes at a former gasworks site in southern Germany. *J. Contam. Hydrol.* 119, 99–112. doi: 10.1016/j.jconhyd.2010.09.012
- Holland, J. H. (1975). *Adaptation in Natural and Artificial Systems: An Introductory Analysis With Applications to Biology, Control, and Artificial Intelligence*. Ann Arbor, MI: U Michigan Press.
- Johnsen, A. R., Wick, L. Y., and Harms, H. (2005). Principles of microbial PAH-degradation in soil. *Environ. Pollut.* 133, 71–84. doi: 10.1016/j.envpol.2004.04.015
- Karamalidis, A., Evangelou, A., Karabika, E., Koukkou, A., Drainas, C., and Voudrias, E. (2010). Laboratory scale bioremediation of petroleum-contaminated soil by indigenous microorganisms and added *Pseudomonas aeruginosa* strain Spet. *Bioresour. Technol.* 101, 6545–6552. doi: 10.1016/j.biortech.2010.03.055
- Köpke, B., Wilms, R., Engelen, B., Cypionka, H., and Sass, H. (2005). Microbial diversity in coastal subsurface sediments: a cultivation approach using various electron acceptors and substrate gradients. *Appl. Environ. Microbiol.* 71, 7819–7830. doi: 10.1128/AEM.71.12.7819-7830.2005
- Li, H., and Boufadel, M. C. (2010). Long-term persistence of oil from the Exxon Valdez spill in two-layer beaches. *Nat. Geosci.* 3, 96–99. doi: 10.1038/ngeo749
- Lors, C., Damidot, D., Ponge, J.-F., and Périé, F. (2012). Comparison of a bioremediation process of PAHs in a PAH-contaminated soil at field and laboratory scales. *Environ. Pollut.* 165, 11–17. doi: 10.1016/j.envpol.2012.02.004
- Lubchenco, J., McNutt, M. K., Dreyfus, G., Murawski, S. A., Kennedy, D. M., Anastas, P. T., et al. (2012). Science in support of the deep-water horizon response. *Proc. Natl. Acad. Sci.* 109, 20212–20221. doi: 10.1073/pnas.1204729109
- Nicol, J. P., Wise, W. R., Molz, F. J., and Benefield, L. D. (1994). Modeling biodegradation of residual petroleum in a saturated porous column. *Water Resour. Res.* 30, 3313–3325. doi: 10.1029/94WR01879
- Sabaté, J., Vinas, M., and Solanas, A. (2004). Laboratory-scale bioremediation experiments on hydrocarbon-contaminated soils. *Int. Biodeterior. Biodegrad.* 54, 19–25. doi: 10.1016/j.ibiod.2003.12.002
- Smith, C. J., and Osborn, A. M. (2009). Advantages and limitations of quantitative PCR (Q-PCR)-based approaches in microbial ecology. *FEMS Microbiol. Ecol.* 67, 6–20. doi: 10.1111/j.1574-6941.2008.00629.x
- Tian, Y., Liu, H. J., Zheng, T. L., Kwon, K. K., Kim, S. J., and Yan, C. L. (2008). PAHs contamination and bacterial communities in mangrove surface sediments of the Jiulong River Estuary, China. *Mar. Pollut. Bull.* 57, 707–715. doi: 10.1016/j.marpolbul.2008.03.011
- Torlapati, J. (2013). *Development and Application of One Dimensional Multi-component Reactive Transport Models*. Alabama: Auburn University.
- Venosa, A. D., Campo, P., and Suidan, M. T. (2010). Biodegradability of lingering crude oil 19 years after the Exxon Valdez oil spill. *Environ. Sci. Technol.* 44, 7613–7621. doi: 10.1021/es101042h
- Venosa, A. D., Suidan, M. T., Wrenn, B. A., Strohmeier, K. L., Haines, J. R., Eberhart, B. L., et al. (1996). Bioremediation of an experimental oil spill on the shoreline of Delaware Bay. *Environ. Sci. Technol.* 30, 1764–1775. doi: 10.1021/es950754r
- Vilcáz, J., Li, L., and Hubbard, S. S. (2013). A new model for the biodegradation kinetics of oil droplets: application to the Deepwater Horizon oil spill in the Gulf of Mexico. *Geochem. Trans.* 14, 4. doi: 10.1186/1467-4866-14-4
- Vogel, T. M. (1996). Bioaugmentation as a soil bioremediation approach. *Curr. Opin. Biotechnol.* 7, 311–316. doi: 10.1016/S0958-1669(96)80036-X
- Wrenn, B., Sarnecki, K., Kohar, E., Lee, K., and Venosa, A. (2006). Effects of nutrient source and supply on crude oil biodegradation in continuous-flow beach microcosms. *J. Environ. Eng.* 132, 75–84. doi: 10.1061/(ASCE)0733-9372(2006)132:1(75)
- Xia, Y., and Boufadel, M. C. (2011). Beach geomorphic factors for the persistence of subsurface oil from the Exxon Valdez spill in

- Alaska. *Environ. Monit. Assess.* 183, 5–21. doi: 10.1007/s10661-011-1902-4
- Xia, Y., Li, H., Boufadel, M. C., and Sharifi, Y. (2010). Hydrodynamic factors affecting the persistence of the Exxon Valdez oil in a shallow bedrock beach. *Water Resour. Res.* 46, W10528. doi: 10.1029/2010WR009179
- Xu, R., and Obbard, J. P. (2004). Biodegradation of polycyclic aromatic hydrocarbons in oil-contaminated beach sediments treated with nutrient amendments. *J. Environ. Qual.* 33, 861–867. doi: 10.2134/jeq2004.0861

**Conflict of Interest Statement:** The authors declare that the research was conducted in the absence of any commercial or financial relationships that could be construed as a potential conflict of interest.

Received: 14 January 2014; accepted: 22 April 2014; published online: 14 May 2014.  
Citation: Torlapati J and Boufadel MC (2014) Evaluation of the biodegradation of Alaska North Slope oil in microcosms using the biodegradation model BIOB. *Front. Microbiol.* 5:212. doi: 10.3389/fmicb.2014.00212

This article was submitted to Aquatic Microbiology, a section of the journal Frontiers in Microbiology.

Copyright © 2014 Torlapati and Boufadel. This is an open-access article distributed under the terms of the Creative Commons Attribution License (CC BY). The use, distribution or reproduction in other forums is permitted, provided the original author(s) or licensor are credited and that the original publication in this journal is cited, in accordance with accepted academic practice. No use, distribution or reproduction is permitted which does not comply with these terms.